SAN/1108-8/1

CENTRAL RECEIVER SOLAR THERMAL POWER SYSTEM, PHASE 1: CDRL ITEM 2, PILOT PLANT PRELIMINARY DESIGN REPORT

Volume 2. System Description and System Analysis

STMPO # 078
EXTRA Q.C.D.

By
Raymon W. Hallet, Jr.
Robert L. Gervais

October 1977
Date Published

Work Performed Under Contract No. EY-76-C-03-1108

McDonnell Douglas Astronautics Company
Huntington Beach, California

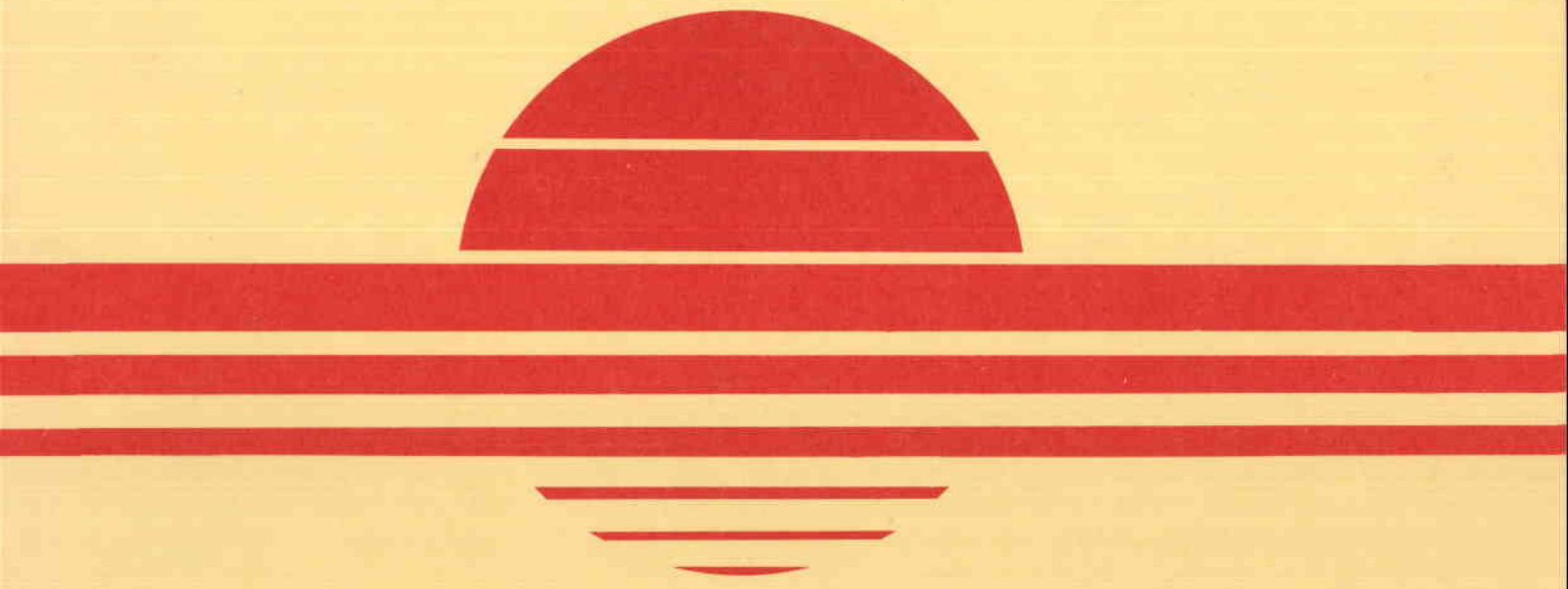

U.S. Department of Energy

Solar Energy

NOTICE

SAN/1108-8/1
Distribution Category UC-62

CENTRAL RECEIVER SOLAR THERMAL POWER SYSTEM PHASE 1

CDRL ITEM 2
Pilot Plant
Preliminary Design Report

VOLUME II
System Description and System Analysis

Raymon W. Hallet, Jr. and Robert L. Gervais

MCDONNELL DOUGLAS ASTRONAUTICS COMPANY
5301 Bolsa Avenue
Huntington Beach, California 92647

Date Published – October 1977

Prepared for the U.S. Department of Energy
Under Contract No. EY-76-C-03-1108

PREFACE

This report is submitted by the McDonnell Douglas Astronautics Company to the Department of Energy under Contract EY-76-C-03-1108 as the final documentation of CDRL Item 2. This Preliminary Design Report summarizes the analyses, design, test, production, planning, and cost efforts performed between 1 July 1975 and 1 May 1977. The report is submitted in seven volumes, as follows:

Volume I, Executive Overview

Volume II, System Description and System Analysis

Volume III, Book 1, Collector Subsystem

Book 2, Collector Subsystem

Volume IV, Receiver Subsystem

Volume V, Thermal Storage Subsystem

Volume VI, Electrical Power Generation/Master Control Subsystems and Balance of Plant

Volume VII, Book 1, Pilot Plant Cost and Commercial Plant Cost and Performance

Book 2, Pilot Plant Cost and Commercial Plant Cost and Performance

Specific efforts performed by the members of the MDAC team were as follows:

- McDonnell Douglas Astronautics Company
  Commercial System Summary
  System Integration
  Collector Subsystem Analysis and Design
  Thermal Storage Subsystem Integration

- Rocketdyne Division of Rockwell International
  Receiver Assembly Analysis and Design
  Thermal Storage Unit Analysis and Design

- Stearns-Roger, Inc.
  Tower and Riser/Downcomer Analysis and Design
  Electrical Power Generation Subsystem Analysis and Design

- University of Houston
  Collector Field Optimization

- Sheldahl, Inc.
  Heliostat Reflective Surface Development

- West Associates
  Utility Consultation on Pilot Plant and Commercial System Concepts

CONTENTS

Section 1
INTRODUCTION

The major efforts which have been part of this contract for a preliminary design of a 10-MW Central Receiver Solar Thermal Power System have involved the early development of a preliminary baseline design, a series of Subsystem Research Experiments (SRE) to verify the initial design concepts, and the meshing of the early design with experimental data to produce the final preliminary design. Throughout these activities an active system analysis and integration effort has been maintained to provide direction and focus to the various program efforts. These activities have included the transformation of initial program requirements into a preliminary system design, the evolution of subsystem requirements which lay the foundation for subsystem design and test activity, and the overseeing of the final preliminary design effort to ensure that the subsystems are operationally compatible and capable of producing electricity at the lowest possible cost per unit of energy. Volume II of the Preliminary Design Report presents the results of the overall system effort that went on during this contract. The effort is assumed to include not only the total system definition and design but also all subsystem interactions.

1.1 PROGRAM GOALS

The major goal of the program has been to develop a preliminary design of a 10-MWe central receiver Pilot Plant system capable of providing technical verification of an anticipated cost-effective Commercial system design. In addition, economic data acquired during the Pilot Plant effort would be useful in predicting early Commercial system costs as well as giving direction to major cost-reduction efforts.

To achieve that goal, it was first necessary to define a technically and operationally sound Commercial system design that is consistent with design guidelines and restrictions imposed by the Department of Energy.

Within that framework, several design approaches were possible. Through a properly directed system analysis effort, key system and intersubsystem trade studies were carried out to identify the most cost-effective design approach for the Commercial system. In many cases, as are discussed later in this volume, high performance on an individual subsystem level was compromised in order to produce the most cost-effective integrated system. This result clearly indicated the possible flaw that can arise in designing a subsystem on the basis of individual performance only without regard for the resulting cost implications and its interactions with the rest of the system elements.

With the conceptual definition of the Commercial system to serve as the starting point, the previously expressed program goal of defining a representative Pilot Plant was then possible. In general, the approach used in defining the overall Pilot Plant as well as the various subsystems was to duplicate or represent as closely as possible any critical parameters of the Commercial system which could possible lead to a question of the technical soundness of the Commercial system design or the designs of any of the subsystems. In general, the parameters represented issues pertaining to the integrated operation of the system, the operation of the subsystems over their anticipated operational ranges, and issues related to the geometrical aspects within the collector field and between the collector field and receiver. In addition, because of the cost sensitivity of the collector field on the Commercial system, the desire to employ full-size Commercial heliostats to gain manufacturing and operational experience was an overriding concern in developing the Pilot Plant design.

1.2 PROGRAM METHODOLOGY

The overall program methodology which has served to guide the system analysis and integration effort and provide a starting point for the subsystem design and test activities is shown in Figure 1-1. Starting with a series of program inputs which include Department of Energy, utility, and self-imposed constraints, along with representative environmental conditions, an initial Commercial system definition was developed. From this definition, a series of verification requirements were established which combined with other Pilot Plant design objectives and guidelines to form a set of Pilot Plant design requirements. Alternate approaches to Pilot Plant design were

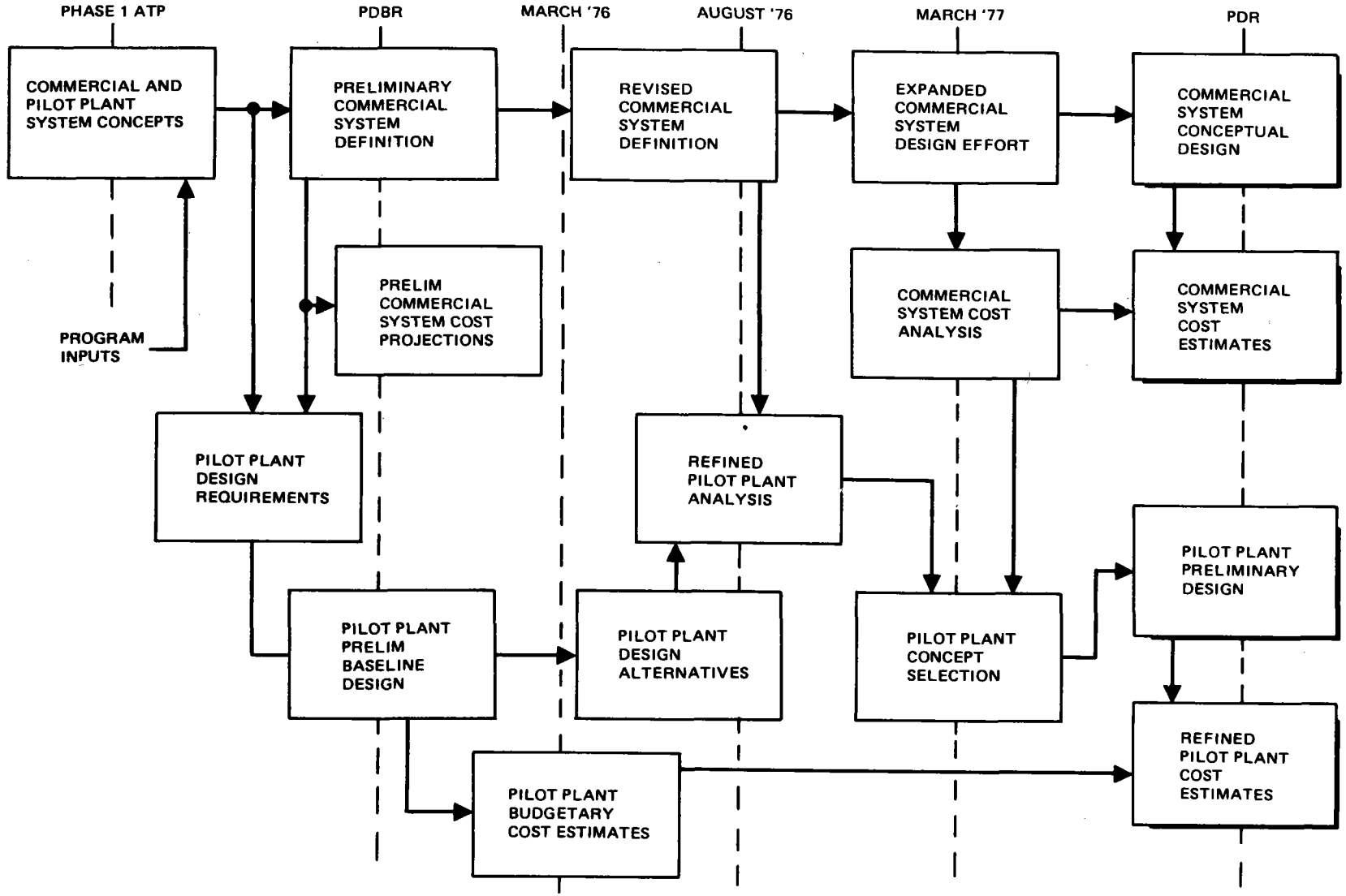

Figure 1-1. System Definition Network

considered which satisfied the defined requirements. Simultaneous to the Pilot Plant design effort, the Commercial system design was being revised as necessary to provide additional focus for the Pilot Plant design effort. Based on inputs from both the Pilot Plant design effort and the revised Commercial system definition effort, a refined Pilot Plant analysis was carried out which introduced the selection criteria and resulted in the selection of the preferred approach to Pilot Plant design. Subsequently, a design freeze was initiated which led to the Pilot Plant preliminary design and system cost analysis efforts which represent major outputs of the current contract. Parallel to the Pilot Plant activity, the Commercial system design was undergoing further expansion as necessary to support the Commercial system cost analysis effort which serves as a second major output of this contract.

In developing the designs of both the Pilot Plant and the Commercial systems, and for various subsystems, an effort was maintained at all times to employ a multidiscipline design approach. In addition to drawing heavily on system analysis and technology experts, design efforts included active participation personnel in from system effectiveness, manufacturing, safety, quality assurance, logistics, planning, fiscal management, and pricing.

1.3 COMMERCIAL SYSTEM SUMMARY

The principal task in developing the Commercial system definition was to transform a series of Department of Energy requirements and design guidelines into an operationally sound, cost-effective system design. In arriving at the cost-effective system design (i.e., minimum mills/kW-hr configuration), an effort was made to include considerations of both initial investment and the anticipated operational costs. The actual design evolved through a series of high-level cost and performance trade studies which resulted in a conceptual system definition and a series of subsystem requirements, design constraints, and interface conditions. Subsystem design efforts in turn worked toward the establishment of cost effective designs within the constraints imposed by the overall system definition.

1.3.1 Requirements

Generalized design guidelines have been established by the Department of Energy for the Commercial system in addition to a specific set of performance

requirements. It was established that the system will be designed on the basis of established water-steam turbine equipment and will derive its power for turbine operation exclusively from collected solar energy. This philosophy rules out the design of a hybrid system in which a solar receiver and a fossil-fueled boiler are operated in a parallel or series-parallel configuration. As a result, a thermal storage subsystem must be included in the design to absorb the operational transients in available power and provide extended generating capacity during periods when the sun is not available. The system will also be designed to use wet cooling although it is recognized that dry cooling will be mandatory once initial commercial penetration is made. Finally, the system must be designed to be compatible with extended operational periods in a desert environment.

Specific Commercial system performance requirements are tabulated in Table 1-1, along with an indication of the source. In general, those labeled "MDAC" were developed as a result of trade studies carried out by MDAC to provide additional design resolution. The 100-MWe net capacity requirement from receiver steam and the corresponding 70-MWe power level from the thermal storage represent minimum Commercial-size modular capacity. The indicated values of solar multiple and hours of storage were developed by MDAC as a result of an economic trade study which treated collectable power, storage capacity, turbine power demand and spillage, for a stand-alone Commercial system. The hot-startup requirement, as indicated in the table, is intended to be as short as possible within the practical limits of the turbine equipment.

Since the operation of the system is closely coupled with the local environment, a summary of the major environmental and site-related requirements is presented in Table 1-2. For the most part, these requirements have been established from existing wind, ambient temperature, and seismic data.

1.3.2 System Characteristics

A conceptual description of the overall baseline system including the five major subelements is shown in Figure 1-2. The collector and receiver subsystems were designed primarily from energy collection considerations. These considerations led to the selection of 360-deg collector field which uses to the greatest extent possible the effective ground area in the vicinity of

Table 1-1

COMMERCIAL SYSTEM REQUIREMENTS

		Source
Design Point Power Level		
• From Receiver (Best sun angle 950 w/m^2 insolation)	100-MWe Net	DoE
• From Thermal Storage	70-MWe Net	DoE
Solar Multiple $\equiv \frac{\text{maximum power collected}}{\text{design point power to turbine}}$	1.7	MDAC
Hours of Storage	6	MDAC
System Startup Times		
• Hot	20 Minutes*	DoE
• Cold	6 Hours	DoE
Plant Availability (Exclusive of sunshine)	90%	DoE
Operational Lifetime (With normal maintenance)	30 Years	DoE

*Minimize within practical limits

Table 1-2

MAJOR ENVIRONMENTAL AND SITE-RELATED REQUIREMENTS

		Source
Temperature		
• Design Point	28°C (82.6°F) Dry Bulb	DoE
	23°C (74°F) Wet Bulb	DoE
• Survive	-30°C to +50°C (-20°F to +120°F)	DoE
Wind Condition		
• Maximum Operational with Gusts	16 m/s (36 mph)	MDAC
• Maximum Survival		
Sustained (Tower only)	40 m/s (90 mph)	MDAC
With Gusts (Other Subsystems)	40 m/s (90 mph)	DoE
Seismological	Seismic Zone 3	DoE
	NRC Reg. Guide 1.60 Response Spectrum	DoE
	OBS - 0.165 hor. "G" SSS - 0.333 hor. "G"	MDAC
Soil Conditions	Barstow Data	DoE

the tower. The external single-pass-to-superheat receiver was design to be compatible with the 360-deg collector field. The external design results in a relatively short tower because the redirected energy must merely strike the side of the receiver instead of passing through an aperature with a limited field of view. In addition, the single-pass design has a low thermal mass as well as a low structural mass which ensures compatibility with the transient solar environment in which it must operate and permits the use of reasonable tower designs even in seismically active areas. The thermal storage subsystem uses the thermocline or temperature stratification method for storage where both hot and cold fluids are contained in the same tank simultaneously.

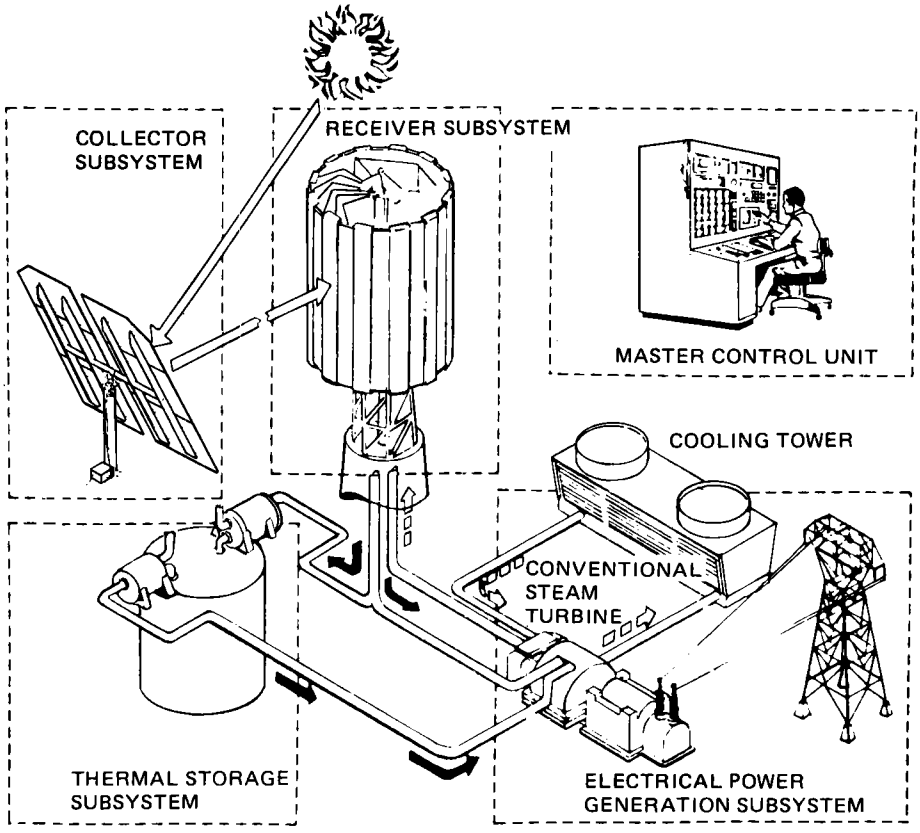

Figure 1-2. Central Receiver Baseline Concept

The storage media is a low-cost mixture of Caloria HT-43 and rock. The approach results in an extremely inexpensive storage system which is capable of producing moderate temperature steam for turbine operation. In addition, the thermal storage subsystem can be operated in its charging and discharging mode simultaneously. The turbine, generator, and heat-rejection equipment are all commercially available items which require no development for solar-electric applications.

The principal characteristics of the overall system and major subsystems are summarized in Figure 1-3 and Table 1-3. In evolving this system design, which is compatible with the previously specified requirements, a continual effort was made to develop a system which had the lowest cost of energy on an annual basis even through the absolute performance level of many of the subsystems was significantly compromised. This situation was acceptable because of the significant cost implications involved in achieving higher performance for many of the subsystems. A discussion of several of these key cost and performance trade studies is presented in the next section.

The overall system design illustrated in Figure 1-3 and summarized in Table 1-3 consists of a 100-MWe single-tower module with an energy collection solar multiple of 1.7. The tower location and field trim were defined to maximize the annual energy collection per unit of investment. The heliostat layout, which is in a radial stagger arrangement, has a packing fraction which varies from ~45% near the central exclusion to ~13% along the northern perimeter with an average field coverage density of ~23%.

The receiver can provide various steam conditions to the rest of the system through a simple control temperature set point adjustment. This permits the receiver to be operated in a manner which is most compatible with the overall system operating mode. The two outlet steam conditions defined in Table 1-3 correspond to conditions where the receiver powers the turbine directly (rated steam) and when all receiver power flows to thermal storage (derated steam). The advantage of the two steam condition approach is that the steam temperature can be maintained at as low a condition as possible while still satisfying the temperature requirements of the equipment it supplies. This results in minimizing receiver surface temperature and thereby reducing receiver heat loss.

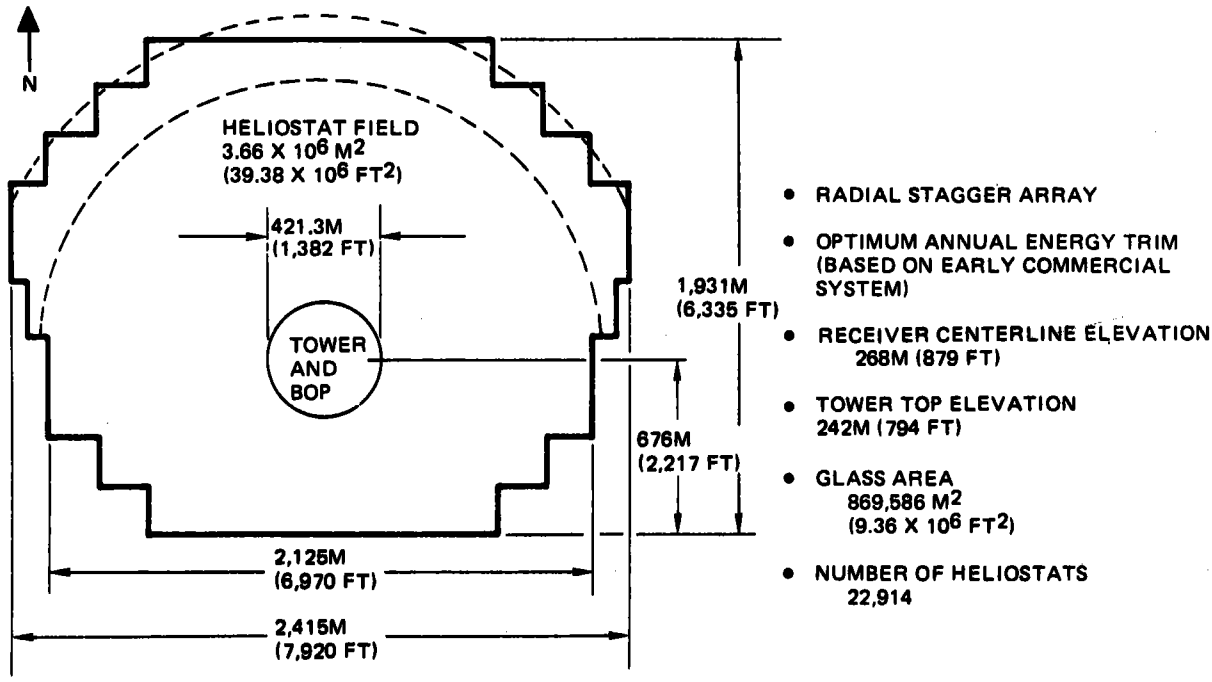

Figure 1-3. Commercial System Field Layout

Table 1-3

COMMERCIAL SYSTEM CHARACTERISTICS

Module Size		
• Capacity	100 MWe	
• Solar Multiple (Equinox noon)	1.7	
Receiver Configuration	External, single-pass-to-superheat	
Receiver Size		
• Diameter	17m	(56 ft)
• Height	25.5m	(84 ft)
Receiver Steam Conditions (Outlet)		
• Pressure	11.1 MPa	(1615 psia)
• Temperature		
Rated Steam	516°C	(960°F)
Derated Steam	368°C	(694°F)
Thermal Storage Media	Caloria HT-43 + Rock	
Method of Storage	"Single" tank (thermocline)	
Thermal Storage Capacity	6 Hours	
Thermal Storage Temperature Range	232° to 316°C (450° to 600°F)	
Turbine Configuration	Tandem-Compound, Double-Flow, Automatic Admission, Industrial Turbine	
Turbine Steam Conditions (Inlet)		
• Throttle Steam	510°C (950°F)	
	10.1 MPa (1465 psia)	
• Admission Steam	296°C (565°F)	
	2.52 MPa (365 psia)	
Heat Rejection	Wet cooling towers	

The thermal storage subystem which employs the Caloria plus rock mixture is designed to provide 6 hr of extended turbine operation by releasing sensible heat over the temperature range of 316° to 232°C (600°-450°F). The Caloria plus rock mixture used in a single-tank thermocline storage mode represents the most cost-effective approach to large-scale storage. The fact that turbine cycle performance is compromised because of the moderate temperature steam available from the storage subsystem is far outweighed by the cost impact necessary to achieve higher-temperature storage and thereby higher cycle efficiency when operating from storage steam. The effect is discussed in greater detail in the next section. The subsystem itself is capable of accepting excess receiver steam above that required for the turbine, producing a steady-state source of turbine steam while accepting highly transient input energy from the receiver, and developing a steam flow which can be used to supplement receiver flow through the turbine.

The turbine selected for the system is a commercially available automatic admission industrial turbine with the admission port being designed to be compatible with steam conditions available from thermal storage.

1.3.3 System Design Evolution

The system design, as well as the conceptual definition of the various subsystems, emerged as a result of a series of cost and performance trade studies. For the most part, these studies can be subdivided into two general categories: those related to optical energy transfer and those related to the water/steam loop. The first of these categories include the collector/receiver configuration and collector field module size. The latter category treats the approach to thermal storage, the definition of the overall steam conditions, and overall water/steam loop complexity. Due to the highly interactive nature of the parameters involved in each of these categories, the trade studies, in general, are complex and not easily separable into discrete study packages. However, for the purposes of current discussion, the studies have been simplified into discrete study areas and are summarized in the following paragraphs.

1.3.3.1 Collector Field/Receiver Configuration and Module Size

The overall goal of this set of studies was to define the configuration and module size which leads to the lowest cost of energy on an annual basis.

The studies treated all of the cost and performance aspects of the energy collection portion of the system, which includes the collector field(s), receiver(s), tower(s), and the water/steam piping. From the collector field standpoint, the critical performance issues include size and angular limitations imposed by the receiver, cosine effects, blocking and shadowing, and heliostat focusing and tracking accuracy required. The critical receiver parameters include size and weight, quantity, complexity, surface absorptivity, radiation/convection losses, availability, and thermal response. Tower considerations which are reflected almost exclusively in cost impacts include height, strength required for receiver support, and quantity. Piping network parameters include run lengths, heat loss, and pressure drop.

The conclusions developed as a result of the MDAC study effort indicated that an external receiver with a 360-deg collector field is the most cost-effective approach to system design. This means that the poorer average collector field performance associated with a partial southern field layout and the higher heat losses associated with the external receiver are more than offset by the ability to use fewer, shorter towers with lighter loads to support. Also, the full 360-deg collector field allows a larger number of heliostats to be placed reasonably close to the receiver. This is particularly important if atmospheric attenuation factors and beam-dispersion effects are included for remote heliostats. Also, from the standpoint of thermal responsiveness, it is desirable to have a receiver which is compatible with the highly transient nature of the incident solar radiation. For this reason, a multiple panel single-pass-to-superheat approach was selected. The low thermal mass and the external nature of the panels permits rapid cooldown and ease of maintenance, which results in higher availability levels than would be experienced with a recirculating cavity-type receiver.

From the standpoint of module size, single- and multiple-module approaches were considered as alternatives for commercial (100 MWe) system design. The results of a study comparing 1, 3, and 10 modules are shown in Figure 1-4. The study was based on a total field size necessary to provide a 1.7 solar multiple. Implicit in the analysis are the assumptions of identical receiver performance in all cases (normally the smaller units would have a

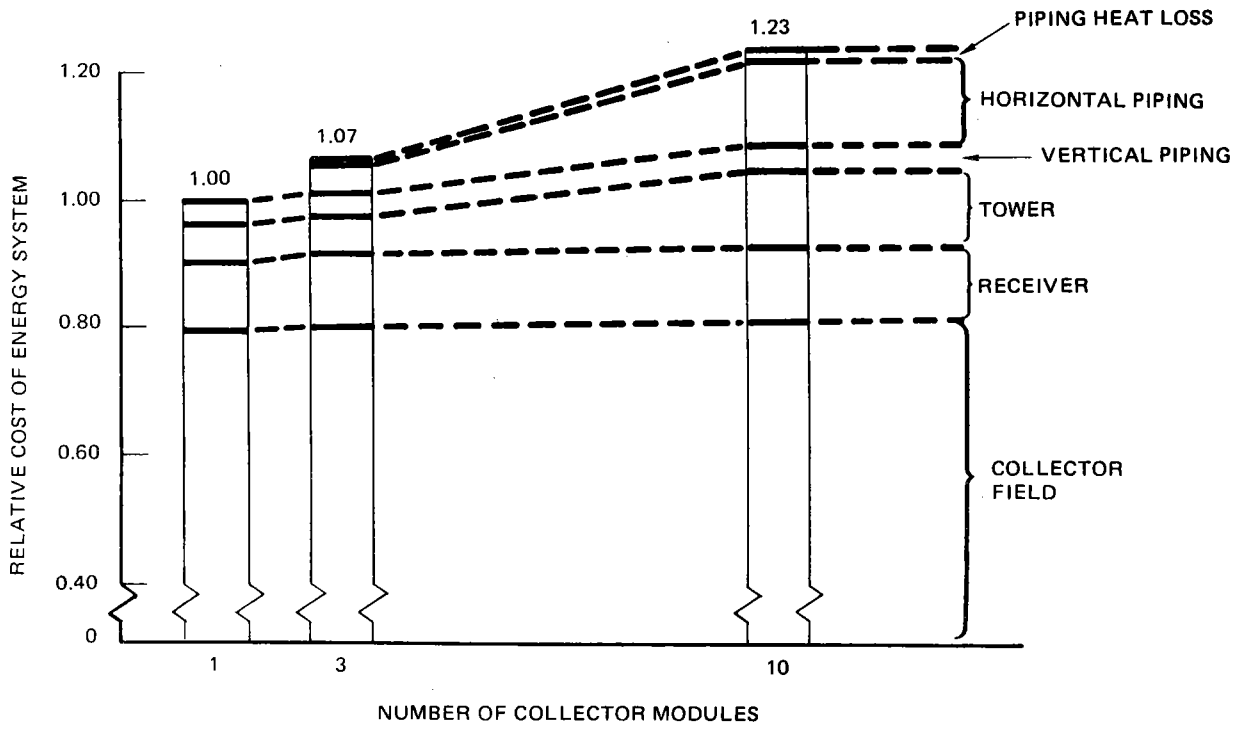

Figure 1-4. Impact of Multiple Modules on Cost (506 MW Peak Absorbed Power)

lower performance), geometrically identical collector fields, and negligible pressure drop in the interconnecting piping. The increase in relative cost as more smaller modules are assumed is due primarily to the addition of a fairly expensive horizontal piping network, which experiences heat loss over a 24-hr period, and an increase in tower cost associated with building many shorter towers as opposed to building a single larger tower. If the piping pressure drop effects were considered, the multiple-tower approaches would suffer additional penalties.

1.3.3.2 Water/Steam Loop Design

The subsystems which combine to form the water/steam loop include the receiver, thermal storage, and balance of plant. As in the case of the collector field/receiver design, the overall goal in defining these subsystems is to minimize the cost per unit energy produced. In addition, because these systems are closely coupled to form the water/steam loop, care must be exercised to develop designs which are operationally compatible from a temperature, pressure, and flow rate standpoint.

The starting point for the design of these subsystems is the Department of Energy requirement to use existing steam turbine designs. The requirements imposed on the turbine are: (1) have at least a 100-MWe rating, (2) be capable of nonreheat cycle, (3) be capable of rapid daily startup, and (4) be capable of separate or simultaneous operation from two steam sources (receiver and thermal storage). A survey of existing turbines capable of satisfying these conditions quickly narrows to a 100-MWe industrial turbine manufactured by General Electric. The inlet steam temperature may be specified at any level between 482° and 538°C (900° and 1,000°F), while the pressure may be specified somewhere in the range of 8.72-10.1 MPa (1,265-1,465 psia). From a cycle efficiency standpoint, which has significant leverage on sizing the rest of the system, it is desirable to operate at as high a pressure and temperature level as possible. This has resulted in the selection of a pressure level of 10.1 MPa (1,465 psia) at the turbine inlet as the design point condition. To ensure that the bulk temperature levels in the receiver and piping network do not exceed 538°C (1,000°F) on a steady basis, a design point turbine inlet temperature of 510°C (950°F) has been selected.

With the turbine inlet condition set, the receiver and thermal storage must be designed to be compatible to the greatest extent possible with these conditions. From the receiver standpoint, small variations in the design point pressure and temperature level produce only minor effects on receiver cost and performance. Therefore, the receiver can be designed to directly match the turbine inlet steam conditions (adding some temperature and pressure for piping losses).

Of the three subsystems which make up the water/steam loop, the design of the thermal storage subsystem plays a critical role in influencing system cost and performance. The critical issue which must be investigated involves the trade between a moderate-temperature (low-cost) storage approach, which compromises turbine cycle efficiency against the significantly more expensive high-temperature options capable of producing higher temperature steam and thus higher cycle efficiency. The results of a trade study carried out to evaluate this design issue are shown in Figure 1-5. The horizontal bars on the figure show the relative cost of adding an increment of electrical energy and thereby combine all the critical cost and performance issues into a single evaluation parameter. The first case represents the baseline Caloria plus rock storage approach which employs the thermocline principle of stratified hot- and cold-temperature layers in a common storage tank. Also shown is the temperature level of the steam which can be produced by the storage media. The remaining cases shown are designed to produce higher temperature steam by using multiple stages and Hitec as the high-temperature storage fluid. In viewing these results, it is seen that for all but Case 3, the incremental cost per unit energy increases because the increased cost associated with adding the high-temperature capability far outweighs the increased electrical output resulting from higher cycle efficiency. Only for the case (3) where both the Caloria and Hitec tanks are filled with rock material is it economically justified to adopt the multifluid (temperature) storage approach. Due to the current lack of information pertaining to the operation of Hitec-rock systems in a thermocline mode and system operational complexity introduced with the use of multiple storage loops, the lowest cost per unit energy approach was not adopted as the baseline design. However, continued experimental work should be carried out in that area.

CASE	THERMAL STORAGE STEAM TEMP (°C)	(°F)	COST OF ANNUAL ENERGY OUTPUT INCREMENT (¢/KWHe)
1. CALORIA/ROCK (BASELINE)	299	570	1.0
2. CALORIA/ROCK PLUS HITEC	400	(750)	1.2
3. CALORIA/ROCK PLUS HITEC/ROCK	400	(750)	0.65
4. ALL LIQUID (CALORIA, HITEC)	400	(750)	2.49
5. ALL HITEC/ROCK	400	(750)	3.14

Figure 1-5. Comparison of Thermal Storage Concepts

1.3.4 System Operation and Control

To ensure the successful operation and control of the solar electric system, it is envisioned that a master control subsystem will be a vital part of the overall system design. The heart of the master control will be a computerized control capable of assisting an operator in starting and running the system. It is felt that this capability will be necessary due to the unorthodox nature in which solar power plants will operate. Conventional plants maintain close control over their firing rate which is one of their critical control parameters. The solar plant on the other hand must continually react to uncontrolled changes in input power. This reactive method of operation requires that a control capability exist which minimizes any lag time. It is also important that the system be brought up on a daily basis as rapidly as possible in order to maximize the energy production capability without compromising the lifetime of critical components. In addition, the master control and related computer capability will play a vital role in providing a predictive capability for the system which can be affected by a wide variety of environmental factors.

1.4 PILOT PLANT SYSTEM

As previously stated, the purpose of the Pilot Plant is to provide a technical verification of the Commercial system and an early indication of system economics. The first task in designing a Pilot Plant is to determine the extent of the verification required along with the potential cost impact. In general, three broad levels of Commercial system simulation are possible. In order of increasing complexity or cost, they are: (1) an operational simulation where representative subsystems are operated in an integrated fashion without regard for subsystem scalability, (2) the operational verification of subsystems which replicate anticipated commercial subsystems in size, operating conditions, or geometry, and (3) the operational verification of a system whose subsystems are scaled versions of their commercial counterparts, while the relative sizes between the subsystems are also preserved. This latter approach to verification includes such factors as duplicating the Commercial system solar multiple and hours of storage.

In reviewing the three approaches, it is felt that the first method, although the least expensive, involves significant compromise in many areas of interest. For example, a unique collector field and receiver configuration independent

of the Commercial system could be used for verification. Although this approach would provide a great deal of valuable operational information, many details related to the similar collector field or receiver would be omitted.

The third approach, on the other hand, represents an overkill of the verification activity by requiring that the relative sizes of the subsystems be maintained at their commercial levels. This would mean that a solar multiple of 1.7 and a 6-hr storage capacity would be required. It would seem difficult to justify the significantly larger cost increase in the Pilot Plant that would be necessary to satisfy such an approach.

The proper compromise for the Pilot Plant design appears to be to employ the second method, where subystems which are scaled versions of the Commercial subsystems are operated in an integrated manner while such factors as size and geometry are preserved. This includes the 360-deg nature of the collector field and receiver, the relative tower height (heliostat look angles), spacing within the collector field, and the use of full-size heliostats. As a result of this philosophy, an effort has been made throughout the design of the Pilot Plant to develop a system design which closely resembles the ultimate Commercial system on a subsystem basis while satisfying all imposed requirements.

1.4.1 Requirements

A summary of the principal performance requirements for the Pilot Plant is presented in Table 1-4. With the exception of the value for solar multiple which is a characteristic of the MDAC system, the requirements are all imposed by the Department of Energy. The principal difference in the sizing condition between the Pilot Plant and Commercial system is that the Pilot Plant is sized for 2 PM on the worst cosine day (Winter solstice). The Commercial system is sized for noon on the best field cosine day (equinox). The specified levels for electrical power production from receiver and thermal storage steam along with the indicated hours of storage represent practical compromise between the full Commercial system and levels which are so small that scaling up to Commercial-size systems is impossible. Additional requirements related to the design environment are identical to those specified for the Commercial system in Table 1-2.

Table 1-4

PILOT PLANT SYSTEM REQUIREMENTS

Design Point Power Level (Net)	
• From Receiver (2 PM day of worst sun angle, 950 W/m^2 insolation level)	10 MWe
• From Thermal Storage	7 MWe
Solar Multiple	1.1
Hours of Storage	3
System Startup Time	
• Hot	20 Minutes (or as fast as practical)
• Cold	6 Hours
Plant Availability (Exclusive of Sunshine)	90%
Operational Lifetime (With Normal Maintenance)	30 Years

1.4.2 System Definition

The first step in defining the Pilot Plant system is to focus on the key aspects of the Commercial system which will require prior technical verification. In addition to the issue of overall system operation, the areas requiring technical verification, in general, are related to the collector, receiver, and thermal storage subsystems which are unique to a solar plant. Once these issues have been defined, a natural flowdown of requirements to the Pilot Plant is established which supplement those specified in Section 1.4.1 to provide the necessary design, performance, and operational information for the Pilot Plant design.

From the collector subsystem standpoint, it is desirable to preserve both the full-size Commercial heliostats and the overall collector field geometry. By using Commercial heliostats, it is possible to verify the heliostat design, gain manufacturing experience, and develop operational and life data on the

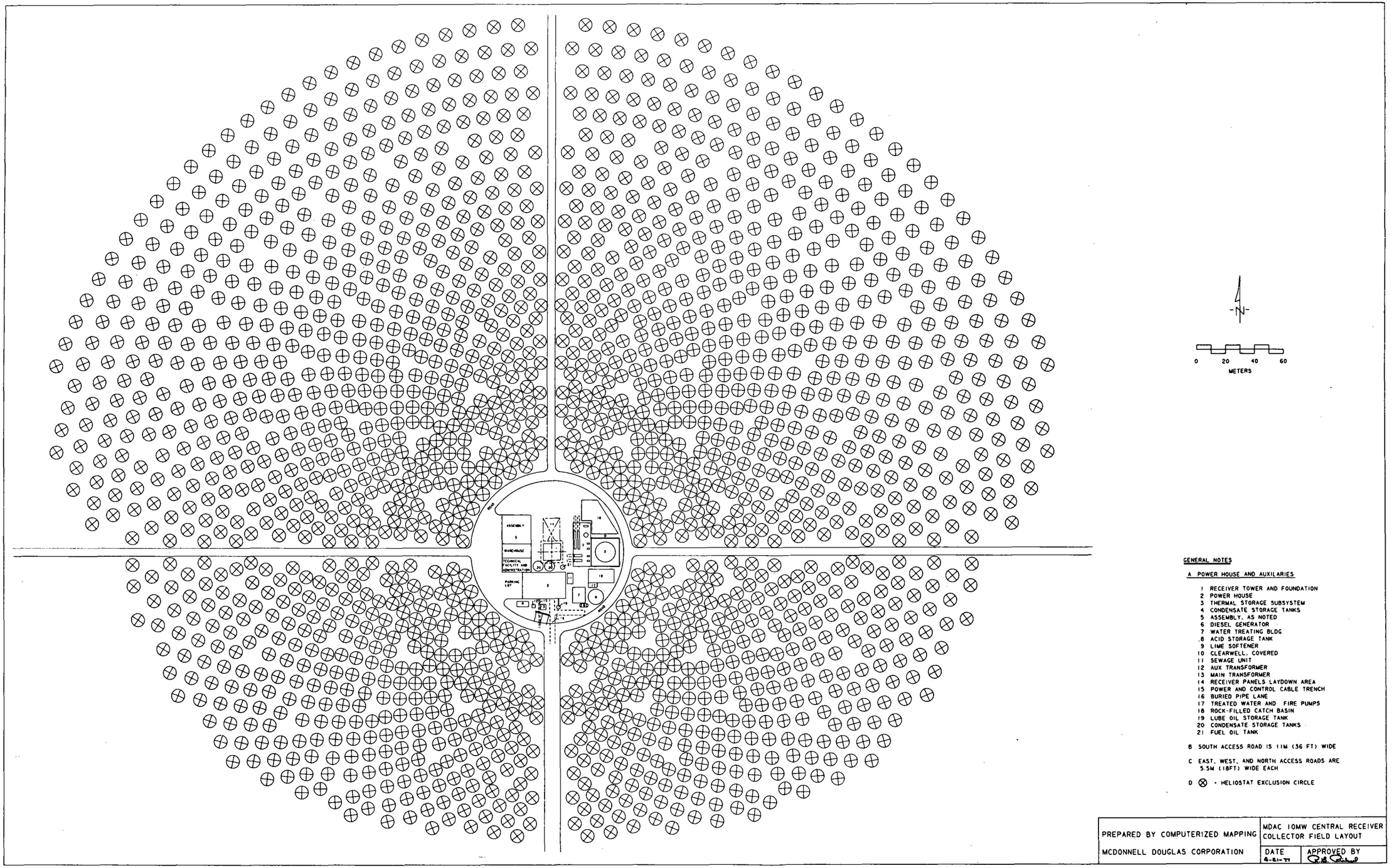

Figure 1-6. MDAC 10-MW Central Receiver Collector Field Layout

Commercial heliostat design. By preserving the collector field geometry and relative heliostat spacing, it is possible to gain information on aerodynamic and optical interactions as well as installation and maintenance experience on closely packed heliostat arrays. In addition, by preserving field geometry, the heliostats are verified for all possible operational tracking angles.

For the receiver, it is desirable to preserve a high degree of similarity to the Commercial design in key areas such as materials, tube sizes, and panel designs. To maintain a thermal environment in the tubes which is similar to that anticipated for the Commercial receiver, constraints must be established for the heat flux distribution over the surface. This translates directly into constraints on receiver size and heliostat aim strategies.

The major verification objectives related to thermal storage involve the operation of the thermocline within the tank, long-term Caloria stability, and rock/tank structural interaction. In addition, a verification of a controlled charging and discharging process as it interacts with the other system elements is also required.

A summary description of the baseline Pilot Plant design which was developed to satisfy all the allocated and imposed requirements is presented in Figures 1-6 and 1-7 and Table 1-5. The collector field layout shown in Figure 1-6 is intended to approximate the radial stagger heliostat arrangement of the Commercial system. It is composed of 1,760 heliostats on 32 circular arcs with the inner 19 forming complete circles. To facilitate access, the continuous arcs have been broken by quadrant roads. A summary of collector field sizing data is contained in the first part of Table 1-5.

The water/steam loop schematic, shown in Figure 1-7, depicts the major elements of the receiver, thermal storage, and balance of plant equipment. The receiver, schematically shown in the upper left corner, is composed of 6 preheat panels followed by 18 parallel single-pass-to-superheat panels. During startup and shutdown, receiver outlet flow is diverted to the receiver flash tank to ensure that no water is passed to the rest of the system through the main steam downcomer. The thermal storage subsystem shown in the upper right corner is composed of the thermal storage heater, which is used

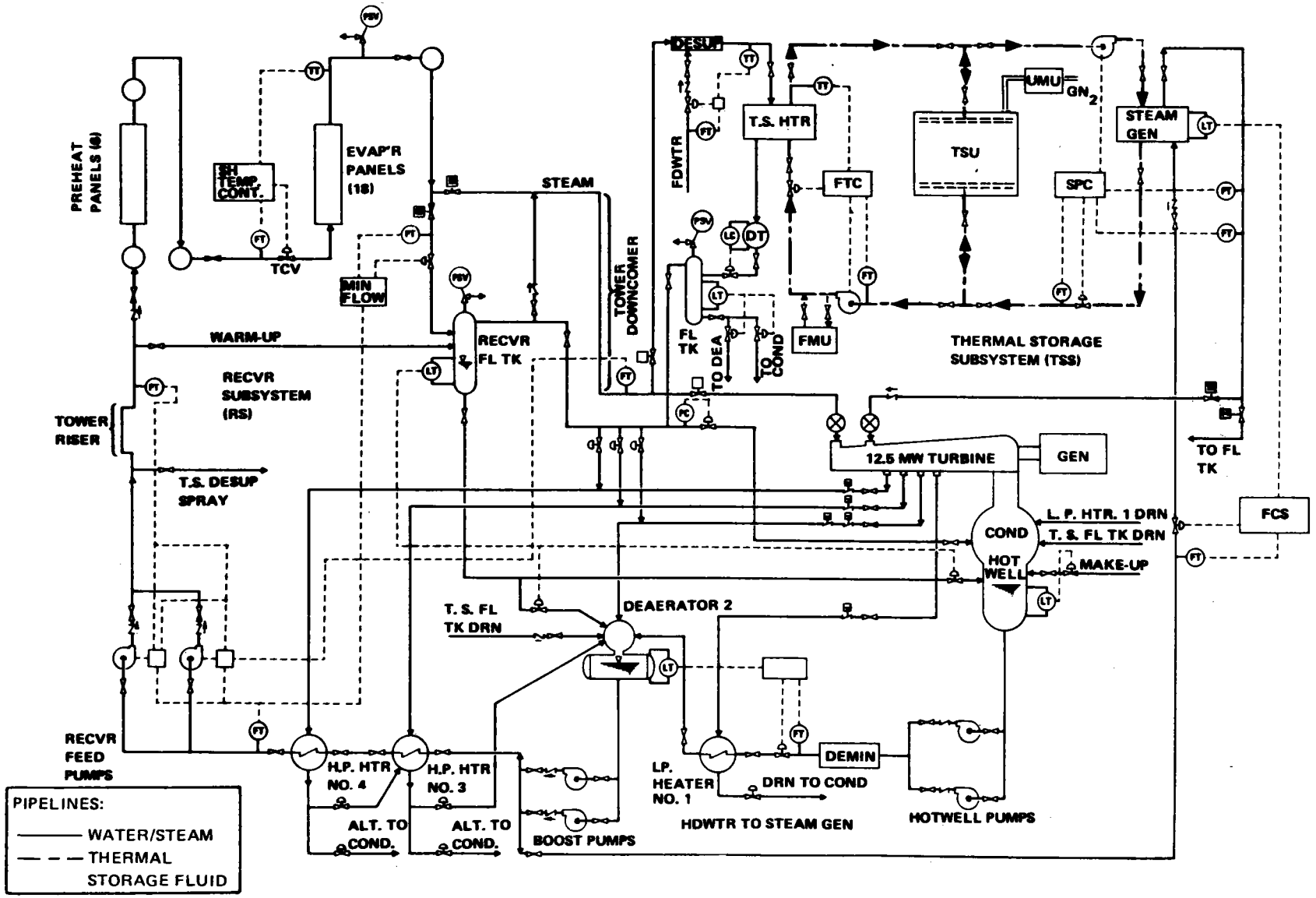

Figure 1-7. Overall Pilot Plant Schematic

Table 1-5

PILOT PLANT SYSTEM AND SUBSYSTEM LEVEL CHARACTERISTICS

Collector Field Size (Excluding Tower Exclusion)	0.29×10^6 m^2 (3.12×10^6 ft^2)
Number of Heliostats	1760
Heliostat Arrangement	Radial Stagger (Continuous Arcs)
Receiver Centerline Elevation	80m (262 ft)
Receiver Size	
• Diameter	7m (23 ft)
• Height	12.5m (41 ft)
Receiver Steam Conditions	
• Pressure	10.45 MPa (1515 psia)
• Temperature	
Rated Steam	516°C (960°F)
Derated Steam	349°C (660°F)
Thermal Storage Temperature Range	219° to 302°C (425° to 575°F)
Turbine Steam Conditions	
• Throttle Steam	510°C (950°F) 10.1 MPa (1,465 psia)
• Admission Steam	274°C (525°F) 2.65 MPa (385 psia)

to charge system by condensing receiver steam; a thermal storage unit (TSU), which contains the Caloria/rock mixture; and the steam generator, which is used to generate turbine admission steam by extracting energy from the high-temperature side of the TSU. The turbine and balance of plant equipment shown in the bottom of the figure consists of a 12.5-MW automatic admission industrial turbine and four extraction heaters. The turbine is capable of operating exclusively from either receiver steam using the first port or thermal storage using the downstream admission port. In addition, simultaneous operation from both steam sources is possible. In all cases, total turbine flow is limited by the maximum flow capability of the last stage. A summary of the pertinent design conditions for the receiver, thermal storage, and turbine are shown in Table 1-5.

Section 2
DATA LISTS

This section presents a concise response to the "Data List" items requested by Sandia for both the Commercial and Pilot Plant systems. The information is presented as briefly as possible with references being made to more complete discussions in other sections. Because the primary thrust of the current contract effort has been to develop a Pilot Plant design, some of the detailed information requested for the Commercial system exceeds the scope of the design effort carried out for that system. In most cases, however, efforts have been made to provide estimates of the Commercial system design and performance parameters in compliance with the request.

2.1 COMMERCIAL SYSTEM

2.1.1 Plant Design Characteristics

Design characteristics of interest include all of the pertinent design, performance, and operational information necessary to completely describe the system.

2.1.1.1 Plant Schematics

The overall Commercial system schematic which treats both the water/steam and Caloria fluid loops is shown in Figure 2-1. Included are the major elements of the receiver (upper left) and the thermal storage (upper right) subsystems, as well as the balance of plant equipment (bottom half). Figures 2-2 through 2-7 illustrate the flow paths associated with the six basic system operating modes. A detailed discussion of the Commercial system operating modes is in Section 3.7.1.

2.1.1.2 Physical Characteristics

The overall characteristics of the Commercial system collector field and pertinent collector field and receiver design information are shown in Figure 2-8. Additional information pertaining to the receiver dimensions, storage material, operating temperatures and pressures, etc is presented in Table 2-1.

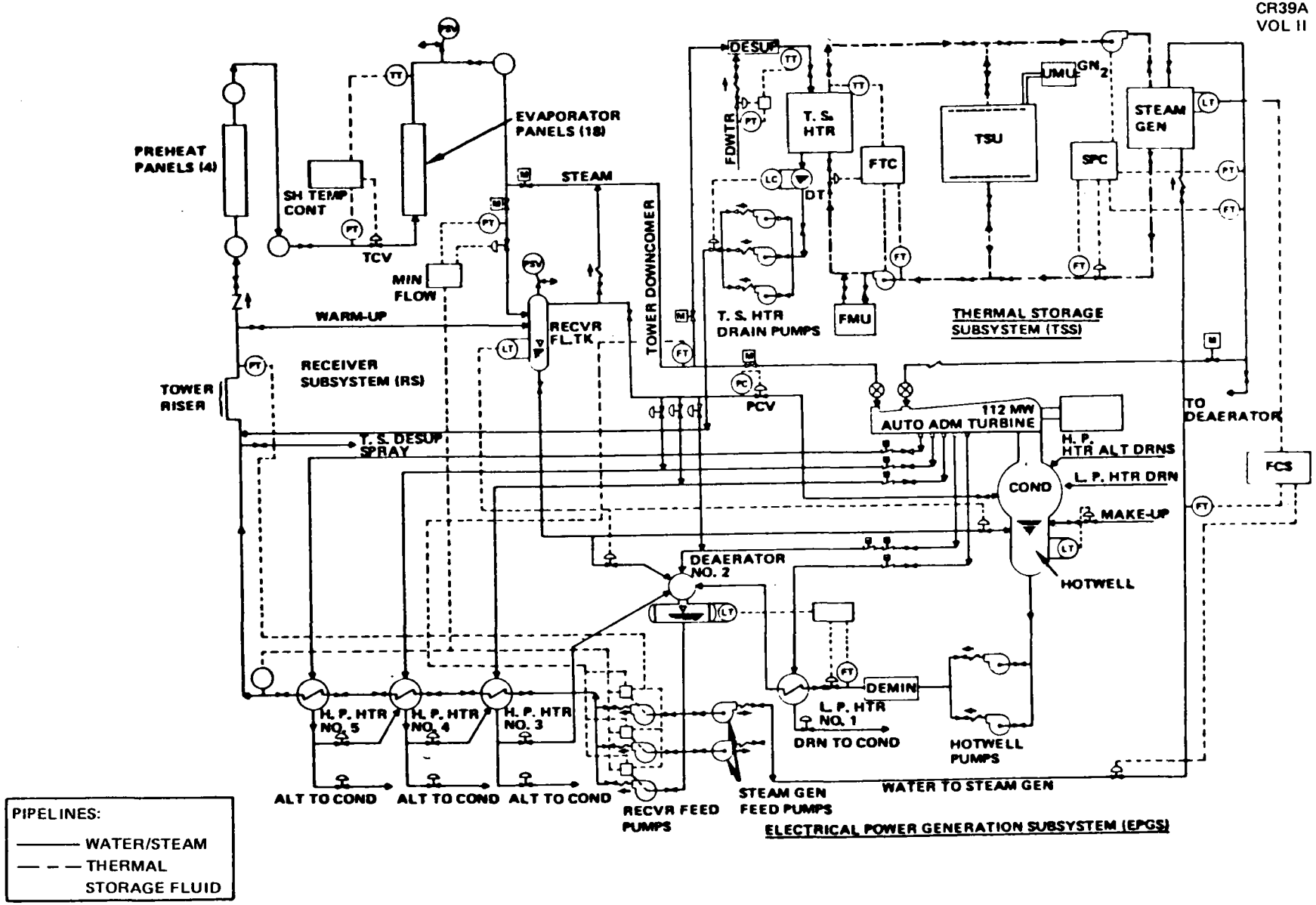

Figure 2-1. Overall Commercial System Schematic

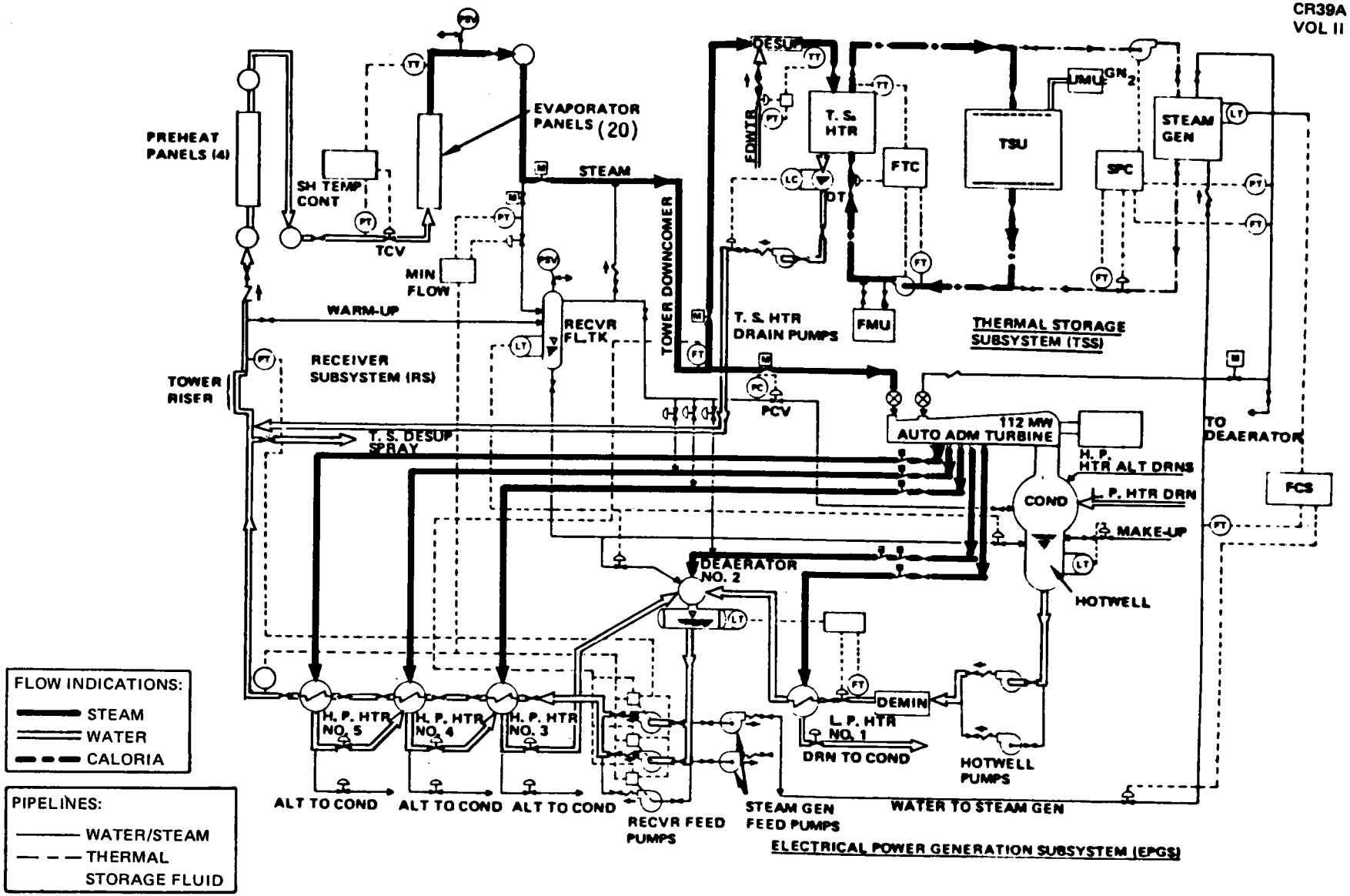

Figure 2-2. Normal Solar Operation (Commercial System)

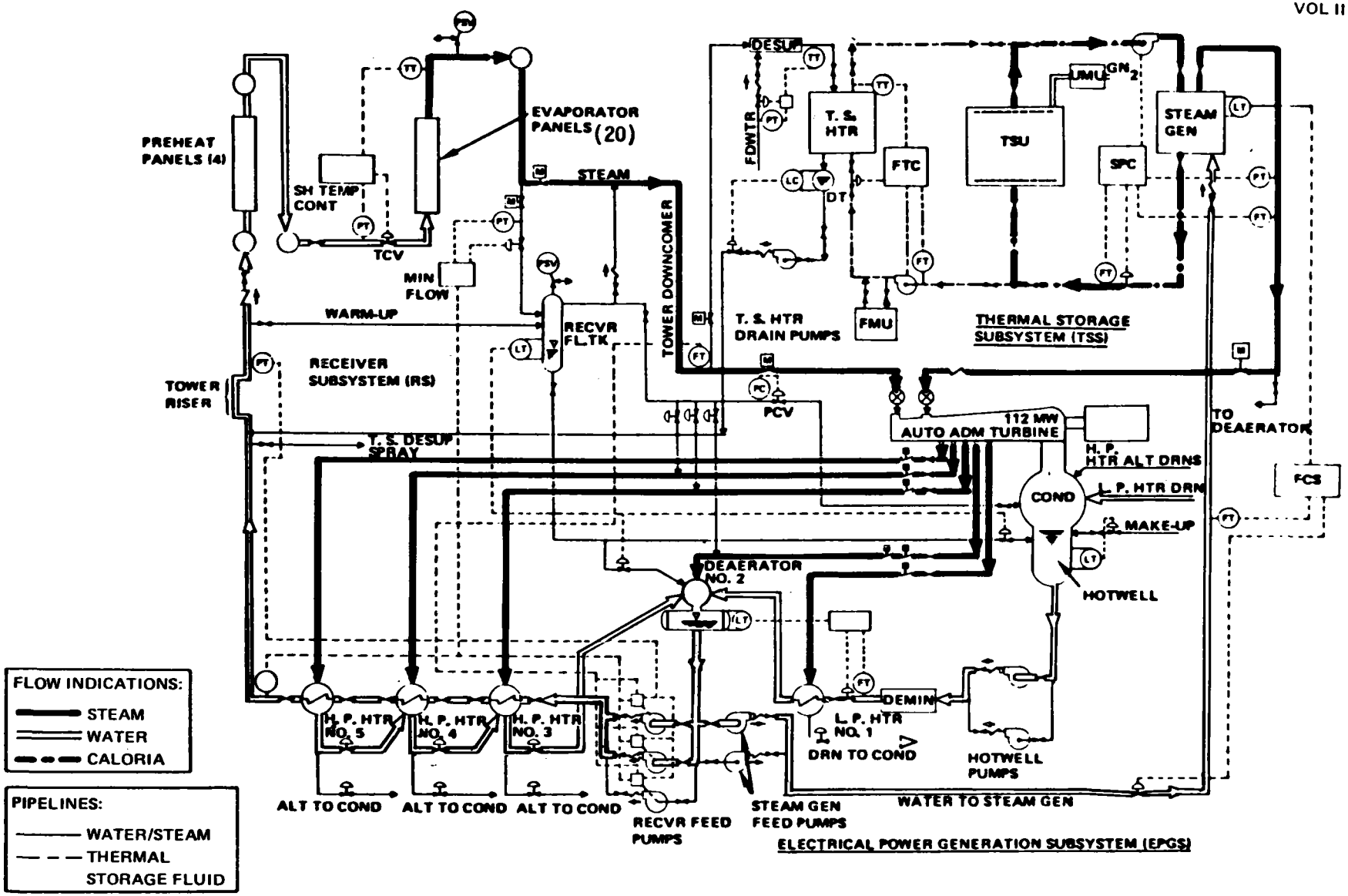

Figure 2-3. Low Solar Power Operation (Commercial System)

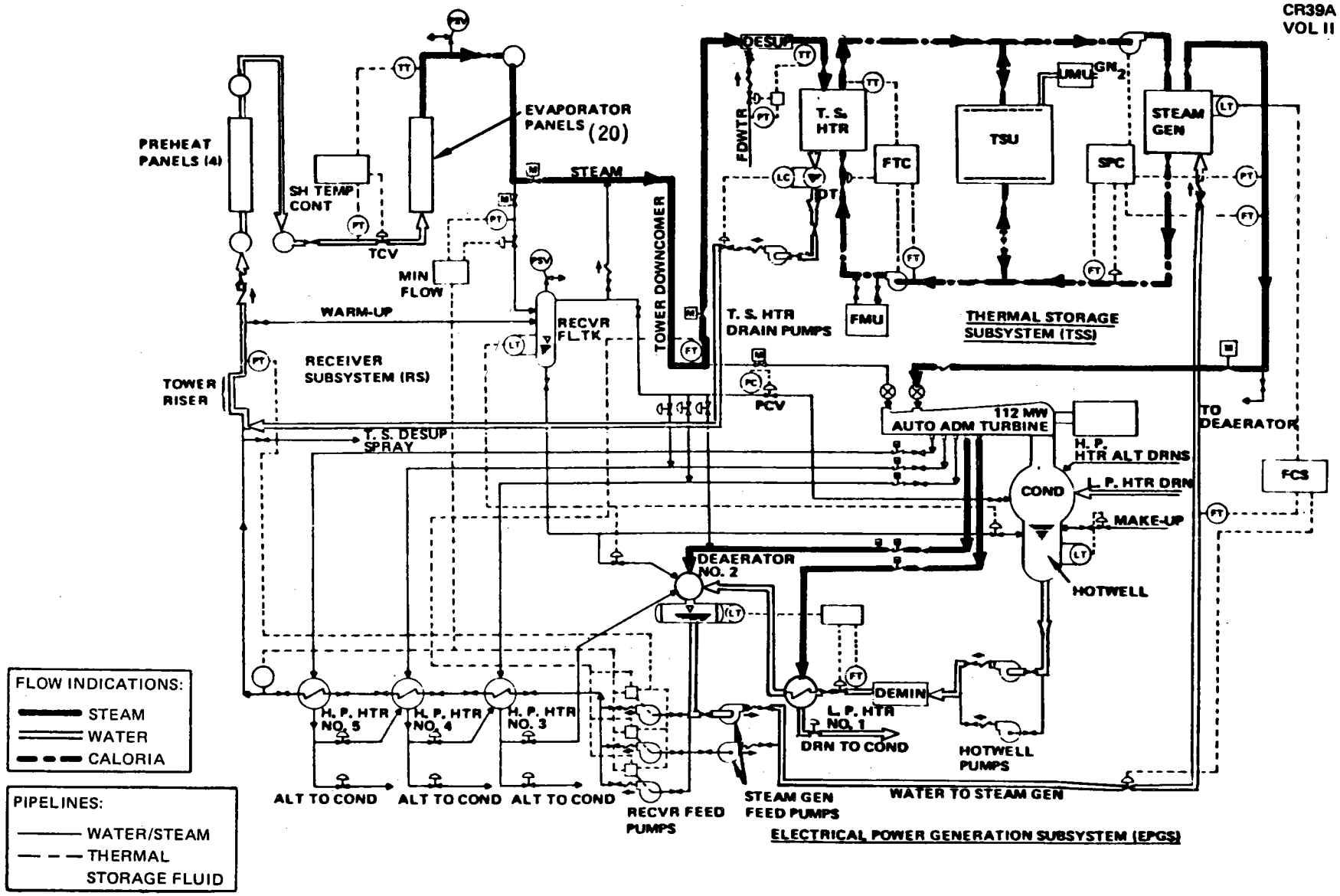

Figure 2-4. Intermittent Cloud Operation (Commercial System)

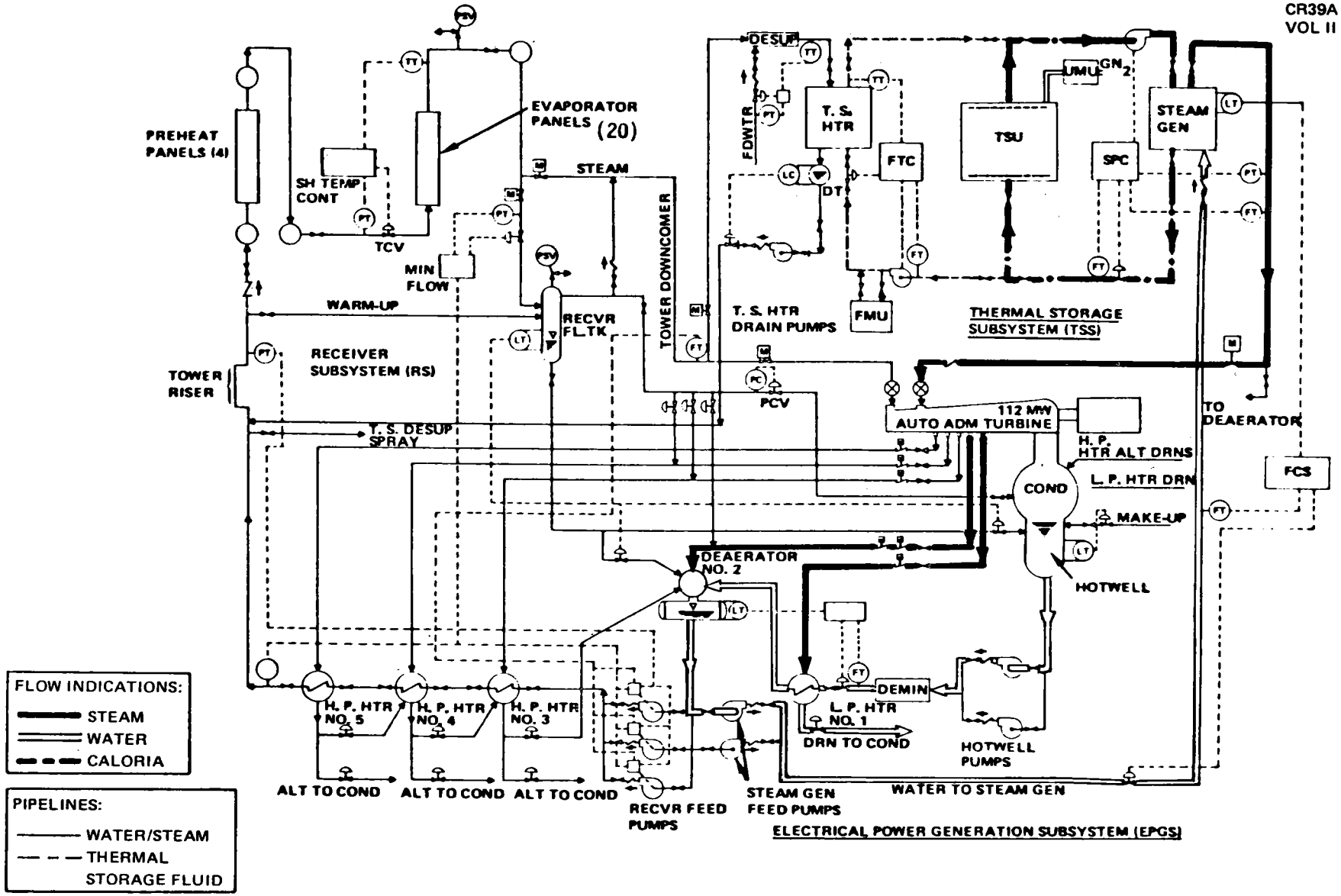

Figure 2-5. Extended Operation (Commercial System)

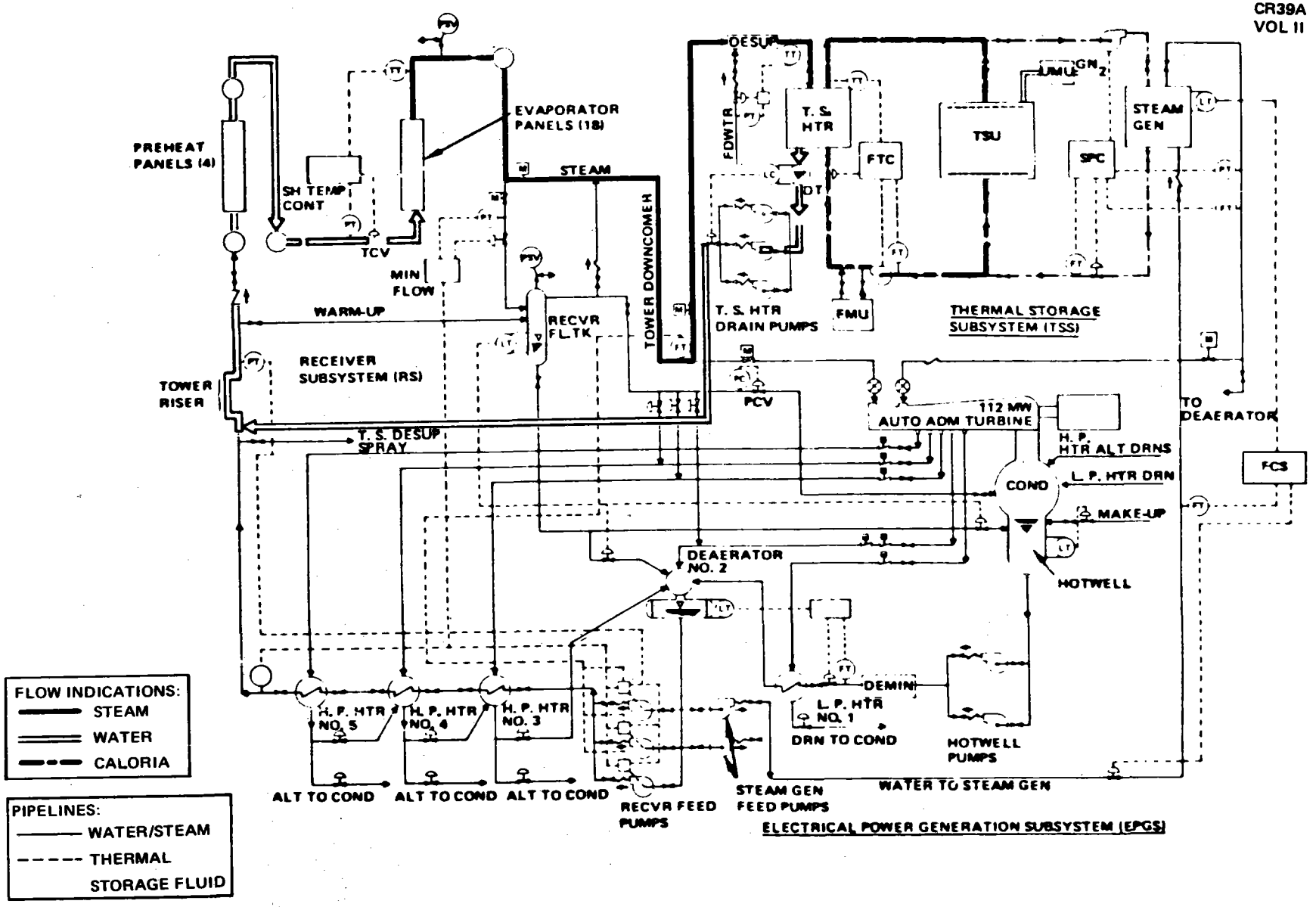

Figure 2-6. Charging of Thermal Storage Only (Commercial System)

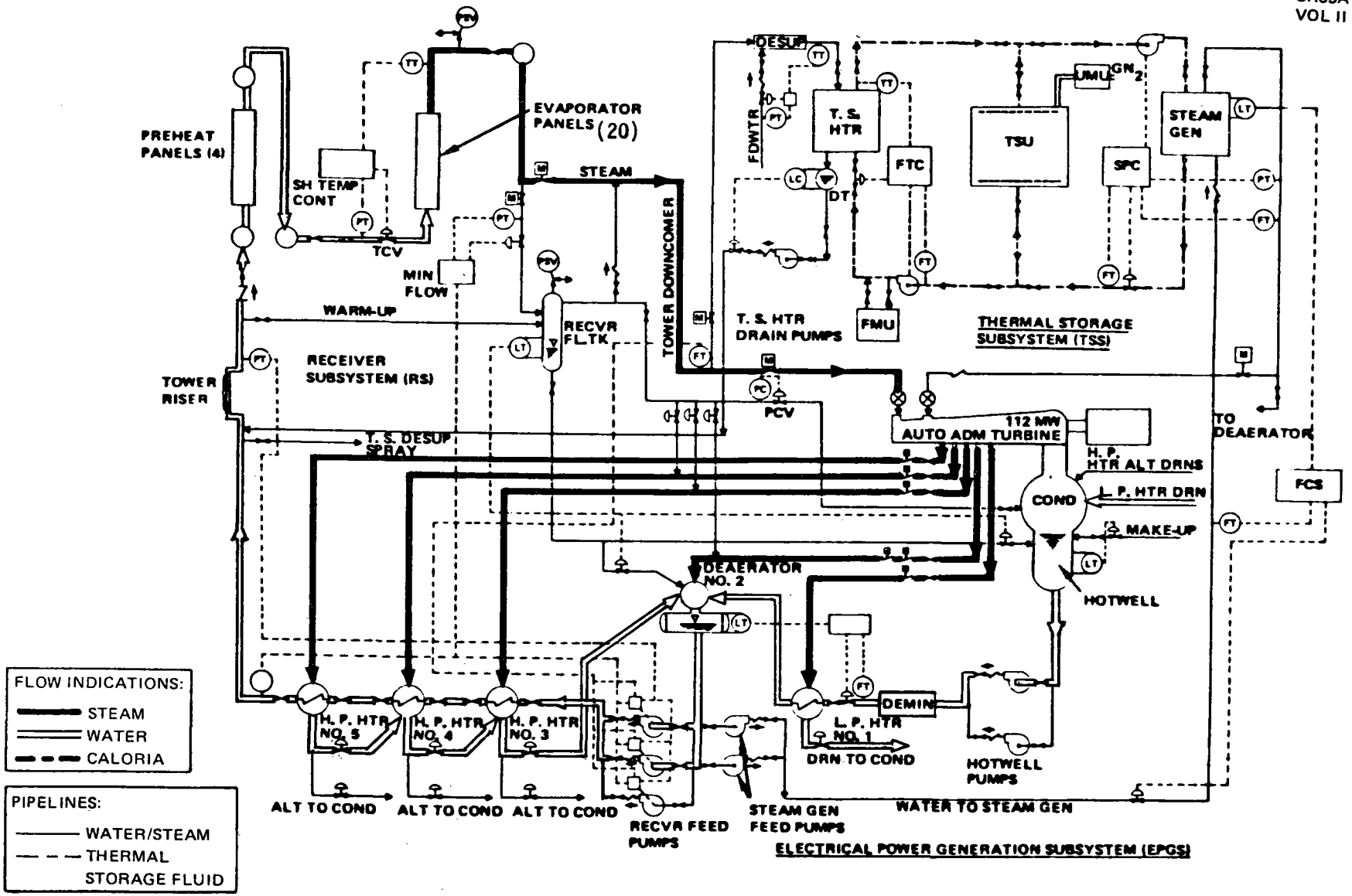

Figure 2-7. Fully Charged Thermal Storage (Commercial System)

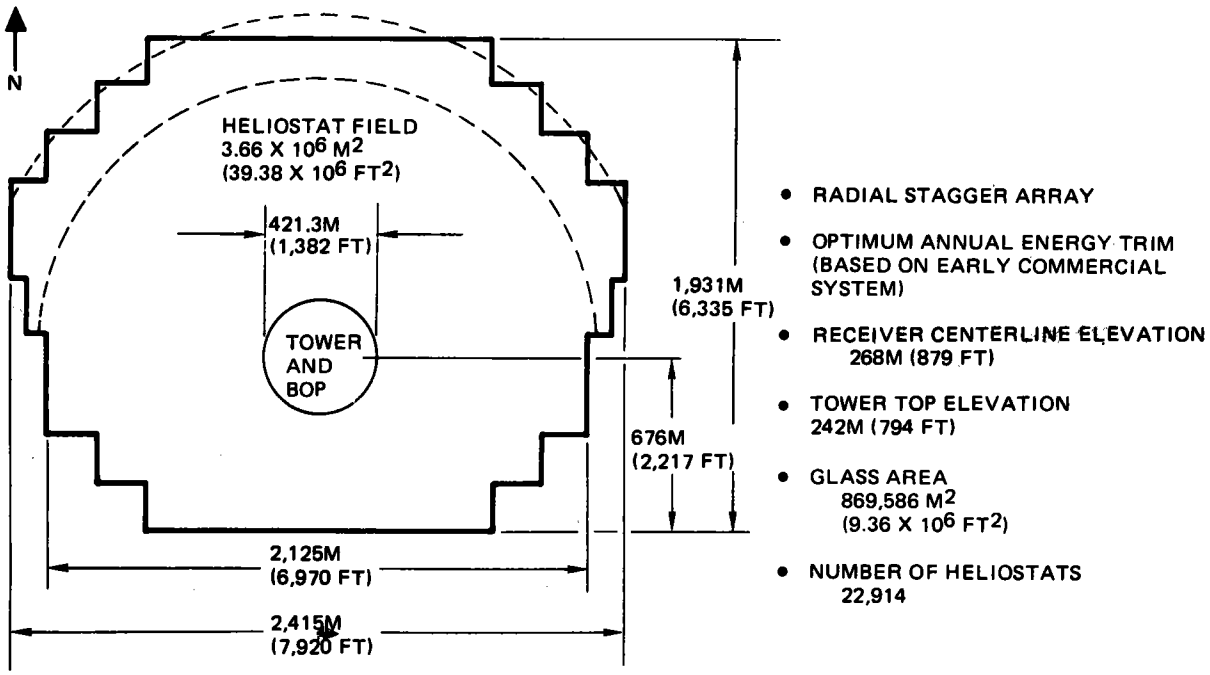

Figure 2-8. Commercial System Field Layout

Table 2-1

COMMERCIAL SYSTEM CHARACTERISTICS

Module Size	
• Capacity	100 MW
• Solar Multiple (equinox noon)	1.7
Receiver Configuration	External, single-pass-to-superheat
Receiver Size	
• Diameter	17m (56 ft)
• Height	25.5m (84 ft)
Receiver Steam Conditions	
• Pressure	11.1 MPa (1,615 psia)
• Temperature	
Rated Steam	516°C (960°F)
Derated Steam	368°C (694°F)
Thermal Storage Media	Caloria HT-43 + Rock
Method of Storage	"Single" tank (thermocline)
Thermal Storage Capacity	6 Hours
Thermal Storage Temperature Range	232° to 316°C (450° to 600°F)
Turbine Configuration	Tandem-Compound, Double-Flow, Automatic Admission, Industrial Turbine
Turbine Steam Conditions	
• Throttle Steam	510°C (950°F) 10.1 MPa (1465 psia)
• Admission Steam	296°C (565°F) 2.52 MPa (365 psia)
Heat Rejection	Wet cooling towers

2.1.1.3 System Waterfall Charts

A detailed breakdown of the Commercial system performance is presented in a waterfall format for both the equinox noon design point and on an annual average basis in Figure 2-9 and 2-10. Included in each figure is a detailed tabulation of the appropriate step-by-step efficiencies. In each case, a total of 810 MW of thermal power is assumed to strike the heliostat surfaces if they are oriented normal to the incident sunlight. Implicit in this value is a conservative heliostat outage assumption of ~ 2%. If the full field of 22, 914 heliostats were operational, the solar power striking the heliostats oriented normal to the sun would be 826. 1 MW. This would require a corresponding adjustment in the waterfall levels shown. It should also be noted that in determining overall system efficiency, care must be exercised to subtract out the power flow to thermal storage before any overall efficiency level is calculated based on the power levels shown.

2.1.1.4 Subsystem Characteristics

The nominal subsystem characteristics and corresponding maximum and minimum conditions in general fall into two categories: those related to the optical portion of the system, and those related to the fluid loop components. The heliostats which make up the collector subsystem are designed to effectively track the sun at solar elevation angles in excess of 10°. Since local shadowing at certain locations within the collector field can obscure the heliostat sensor mirror at low sun elevation angles, sensor controlled tracking will be impossible for those affected heliostats. In those portions of the field, a selective heliostat activation procedure will be employed such as bringing on every other one. In this way, an early and effective quantity of thermal power can be redirected toward the receiver, thus facilitating receiver startup.

The maximum and minimum operating ranges for the subsystems which interface with the water/steam or Caloria loops can, in general, be expressed as a range of flow rate or power level that is permitted while critical temperature and pressure conditions are constant. Following this approach, the nominal operating conditions for the receiver, thermal storage, and turbine are defined in Table 2-2; typical ranges for the various subsystems are tabulated in Table 2-3 by flow rate and power level, assuming that the stated pressure and temperature conditions are maintained.

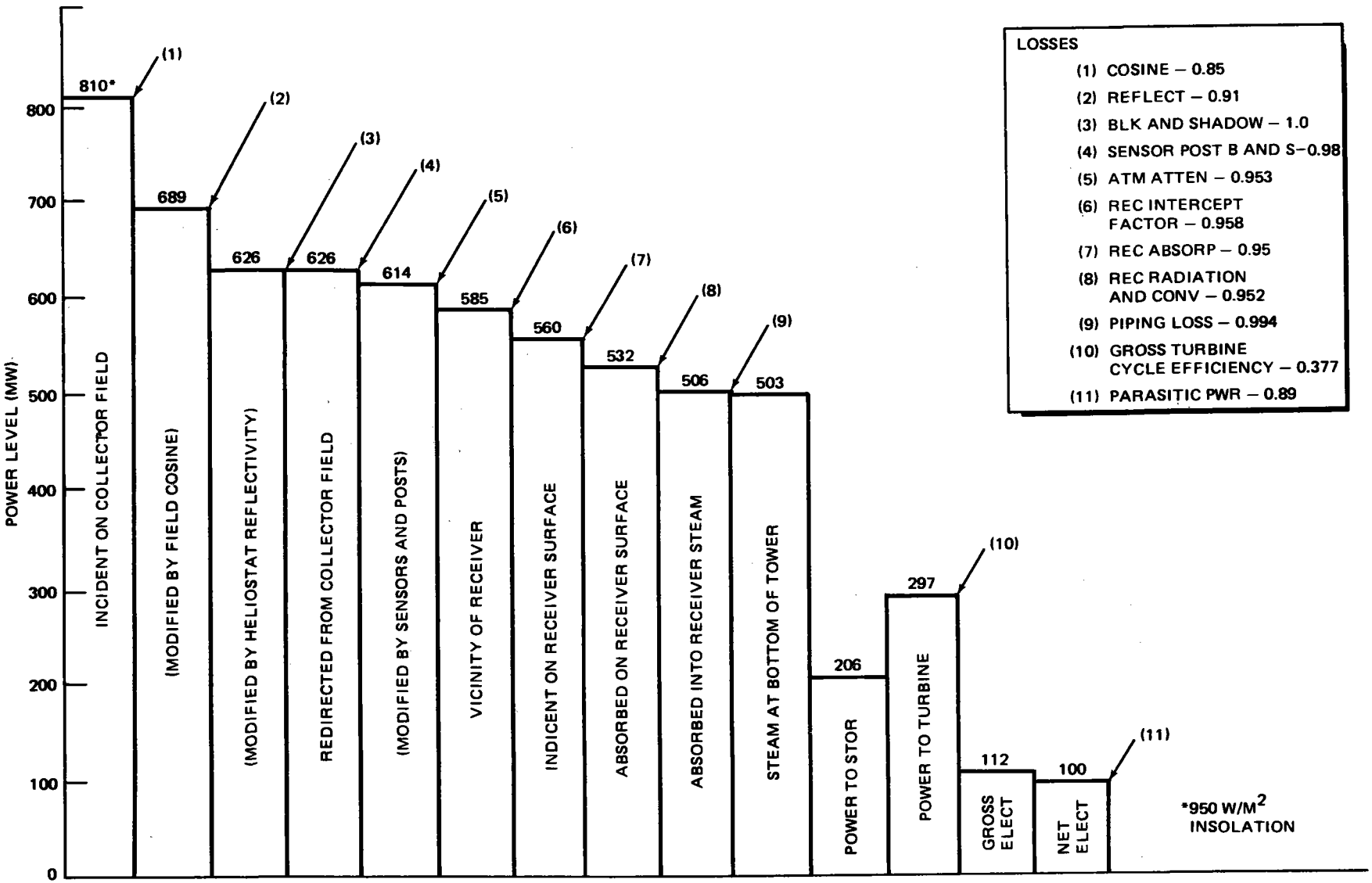

Figure 2-9. Commercial System Power Flow (Equinox Noon)

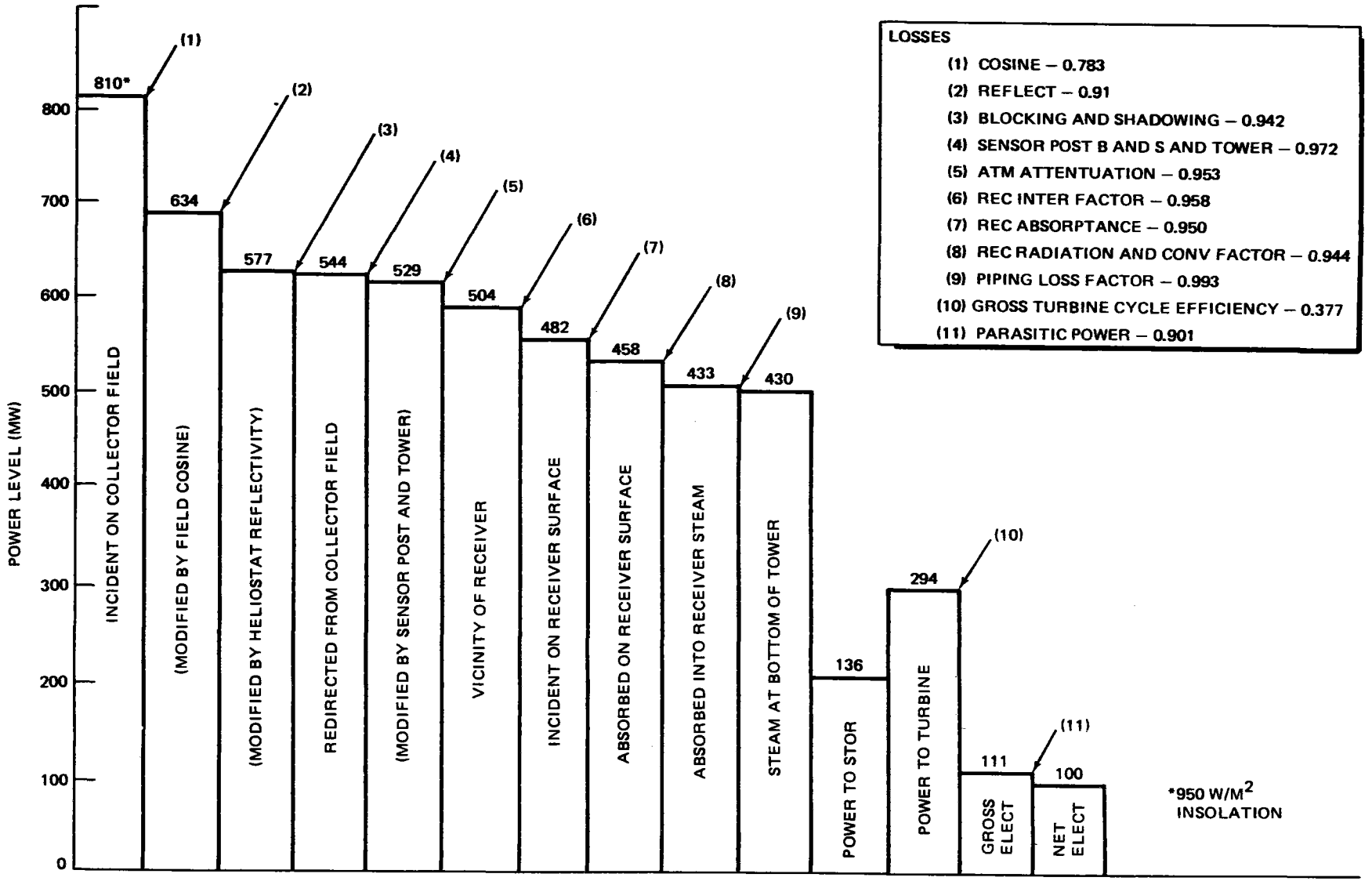

Figure 2-10. Commercial System Power Flow (Annual Average)

Table 2-2

COMMERCIAL SUBSYSTEM NOMINAL OPERATING CONDITIONS

Subsystem	Temperature °C (°F)	Pressure MPa (psia)	Flow Rate Kg/sec (lb/hr)	Power Level MW (Btu/hr)
Receiver				
• Rated Steam	516 (960)	11.1 (1,615)	213.0 (1.687×10^6)	506.4 (1.73×10^9)
• Derated Steam	368 (694)	11.1 (1,615)	135.9* (1.08×10^6)	254.2 (0.868×10^9)
Thermal Storage				
• Charging Steam at Heat Exchanger	360 (680)	10.1 (1,465)	135.9 (1.08×10^6)	255 (0.870×10^9)
• Discharge Steam Leaving Steam Generator	299 (570)	2.72 (395)	114.3 (0.906×10^6)	284 (0.969×10^9)
Turbine				
• Throttle Steam	510 (950)	10.1 (1,465)	121.3 (0.960×10^6)	297 (1.01×10^6)
• Admission Steam	296 (565)	2.52 (365)	114.3 (0.906×10^6)	284 (0.969×10^9)

*Limited by Sandia constraint on thermal storage charging rate

Table 2-3

COMMERCIAL SUBSYSTEM OPERATING RANGES

Subsystem	Temperature °C (°F)	Pressure MPa (psia)	Flow Rate Kg/sec (10^6 lb/hr)	Power Level MW (10^9 Btu/hr)
Receiver				
• Rated Steam	516 (960)	10.2 - 11.1 (1,485 - 1,615)	34.0** - 213.0 (0.269 - 1.687)	92.4** - 506.4 (0.32 - 1.73)
• Derated Steam	368 (694)	10.2 - 11.1 (1,485 - 1,615)	34.0** - 135.9* (0.269 - 1.08)	63.7** - 254.2* (0.217 - 0.868)
Thermal Storage				
• Charging Steam at Heat Exchanger	360 (680)	10.1 (1,465)	6.7** - 135.9 (0.053 - 1.08)	12.5** - 255* (0.043 - 0.870)
• Discharge Steam Leaving Steam Generator	299 (570)	2.72 (395)	12.6** - 114.3 (0.100 - 0.906)	31.4** - 284 (0.107 - 0.969)
Turbine				
• Throttle Steam	510 (950)	10.1 (1,465)	34.0** - 121.3 (0.269 - 0.960)	92.4** - 297 (0.32 - 1.01)
• Admission Steam Only	296 (565)	2.52 (365)	12.6** - 114.3 (0.100 - 0.906)	31.4** - 284 (0.107 - 0.969)

*Limited by Sandia constraint on thermal storage charging rate
**Approximate values

2.1.1.5 Subsystem Efficiencies

The efficiency variation for the collector subsystem is shown in Figure 2-11 for various sun azimuth and elevation angles. Implicit in this data are the following assumptions:

- Heliostat reflectivity = 1.0.
- Receiver interception factor = 0.958
- Sensor post blocking and shadowing factor = 0.98
- Atmospheric attenuation factor = 1.0

Collector subsystem efficiency at other values of heliostat reflectivity can be determined by multiplying the indicated efficiency by the actual reflectivity.

The receiver efficiency defined as the power absorbed into the steam divided by the incident power is summarized as follows:

Time	Incident Power	Absorbed Power	Efficiency
Equinox Noon	560	506.4	0.904
Minimum Rated Steam	118	92.4	0.783
Annual Average	482	433	0.898

Assumptions made in arriving at these values include an absorptivity of 0.95, an emissivity of 0.89, a wind speed of 3.5 m/s (8 mph), and an ambient temperature of 23°C (74°F). Since neither forced nor free convection dominates, a root sum squares addition of the two heat loss components was applied. Under the temperature and wind conditions defined above, 0.92% of the incident power would be lost because of convection.

The thermal storage subsystem has a volumetric efficiency defined as the ratio of extractable energy to total energy in the tank of 90%. The subsystem has an energy recovery efficiency of 98% which is defined as the ratio of extractable energy to charging energy.

The gross cycle efficiency for the turbine is shown in Figure 2-12 as a function of turbine flow rate for both receiver and thermal storage steam operation. A wet cooled condenser is assumed with a turbine back pressure of 6.35 cm Hg (2.5 in Hg).

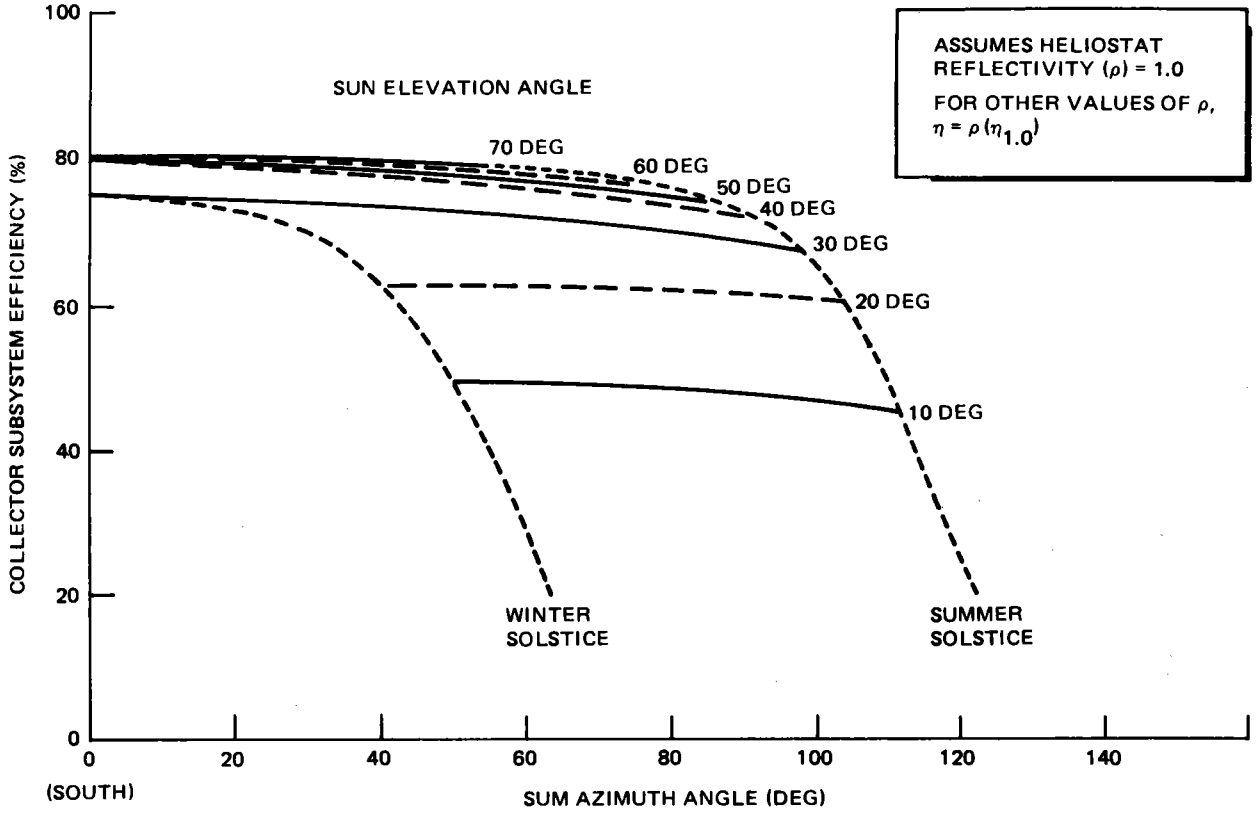

Figure 2-11. Collector Field Performance

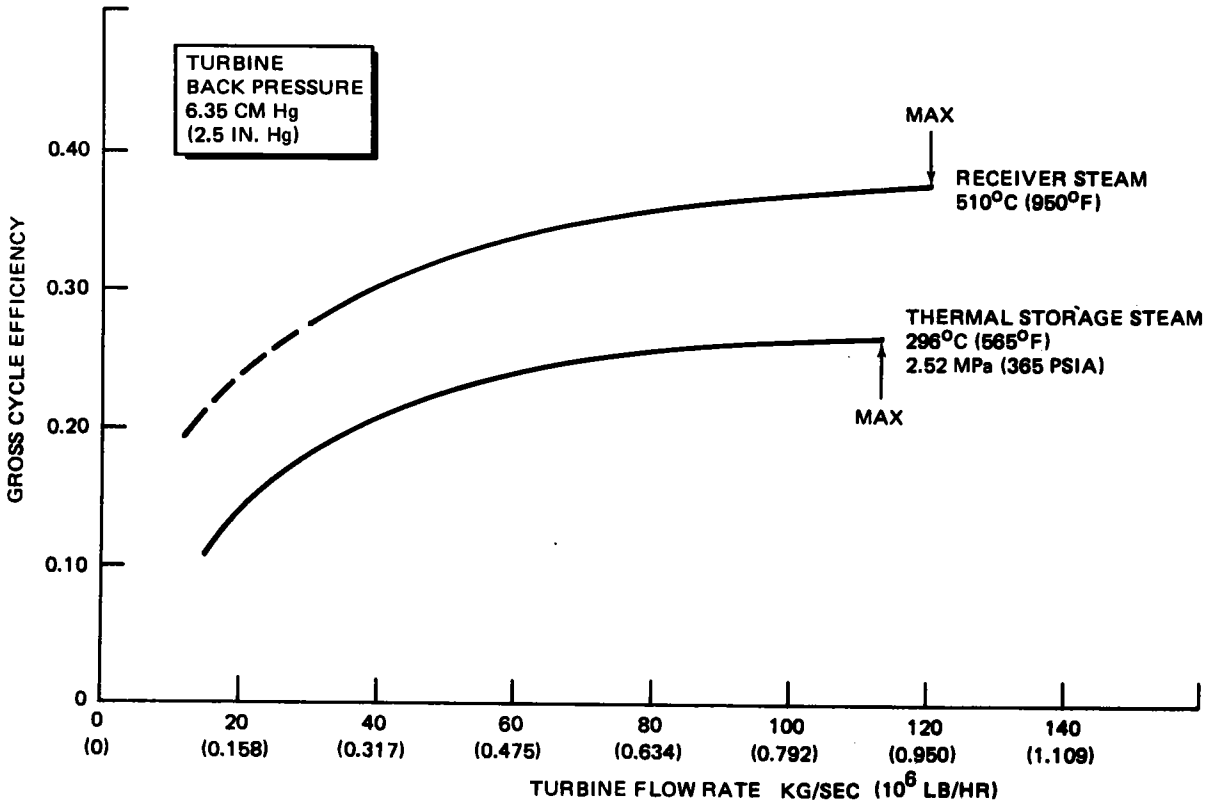

Figure 2-12. Impact of Flow Rate on Turbine Cycle Efficiency (Commercial Turbine)

2.1.1.6 Auxiliary Power Requirements

A summary of the total Commercial system auxiliary power requirement is contained in the following tabulation for four different conditions. A detailed breakdown of this data is contained in Section 3.5.5.

	Auxiliary Power Requirements (kW)
• Equinox Noon (Design Point)	12,000
• Evening Operation from Thermal Storage	6,100
• Emergency Power	1,483 (AC)
	50 (DC)
• Nighttime Standby	685

2.1.2 Design Rationale and Evolution

(See Section 3.2)

2.1.3 Annual Energy Calculations

Annual energy calculations were carried out for the Commercial system for several different insolation models. The simplest analysis assumed a constant insolation level of 950 W/m^2 throughout the year. The system was assumed to have a solar multiple of 1.7 with 6-hr storage capability. The assumption was made that the collector field was activated at a 10-deg sun elevation angle and by a 15-deg sun elevation angle, the receiver had reached a derated steam condition at which time all energy could be diverted to storage. At the time when the calculation was made, it was assumed that the threshold for rated steam operation from the receiver was 50% of maximum design flow. At this point, the turbine would be completing the starting and loading phase. An accounting of the energy collection for the various days of the year is shown in Table 2-4, along with an indication of the quantity flowing directly to the turbine, that going to storage, and that portion lost because of over-collection (rate of energy collection exceeds the capability of the turbine and thermal storage unit to accommodate the energy flow). Assuming a net cycle efficiency of 33.7%, which includes the influence of plant parasitic loads, a net annual electrical production of 423,000 MWH would be anticipated. This calculation also assumed that the system were down 35 days per year due to cloudiness or maintenance requirements.

Table 2-4

SYSTEM PERFORMANCE SUMMARY

SOLAR MULTIPLE = 1.7, 6-HR STORAGE

Day	Total Collection Capability (MWHt)	Direct Turbine Operation (100 MWe)		Excess Energy (MWHt)	Energy to Storage (MWHt)	Period of Operation From Storage 70 MWe (Hr)	Spillage	
		Required Energy (MWHt)	Period (Hr)				MWHt	(%)
Jun 21	5,290	3,485	11.7	1,805	1,757	6.0	48	0.9
May 21/ Jul 21	5,202	3,396	11.4	1,806	1,757	6.0	49	0.9
Apr 21/ Aug 21	4,905	3,158	10.6	1,747	1,747	5.96	0	0
Equinox	4,422	2,860	9.6	1,562	1,562	5.33	0	0
Feb 21/ Oct 21	3,731	2,443	8.2	1,288	1,288	4.40	0	0
Jan 21/ Nov 21	3,122	2,115	7.1	1,007	1,007	3.44	0	0
Dec 21	2,832	1,966	6.6	866	866	2.96	0	0

Since these calculations were developed, changes in the receiver operating requirements as well as changes in receiver design will allow rated receiver steam to be maintained down to 16% of maximum design flow. This would permit the turbine to experience a slightly longer operating day using receiver steam exclusively. This would result in a slight increase in the anticipated energy output.

2.1.4 Transient Plant Operation

(See Section 3.7)

2.1.5 Plant Control

The approach to plant control for the Commercial system is essentially identical to that defined for the Pilot Plant, with the differences arising in the number of hardware items being controlled. The principal feature of the selected approach to plant control is the full complement of manual and computer-aided controls which provide maximum flexibility to the operator or test engineers. A more detailed discussion of the elements of the overall plant control and the master control part of plant control is in Volume II, Section 2.2.5, and Volume VI, Section 6.

2.1.6 Plant Safety Considerations

The plant safety considerations for the Commercial system are identical to those of Pilot Plant. They are discussed in Section 4.10.3.

2.2 PILOT PLANT SYSTEM

2.2.1 Plant Design Characteristics

The plant design characteristics of interest include all of the pertinent design, performance, and operational information necessary to characterize the Pilot Plant system.

2.2.1.1 Plant Schematics

The overall Pilot Plant system schematic which treats both the water/steam and Caloria fluid loops is shown in Figure 2-13. Included in the schematic are the major elements of the receiver (top left corner), the thermal storage

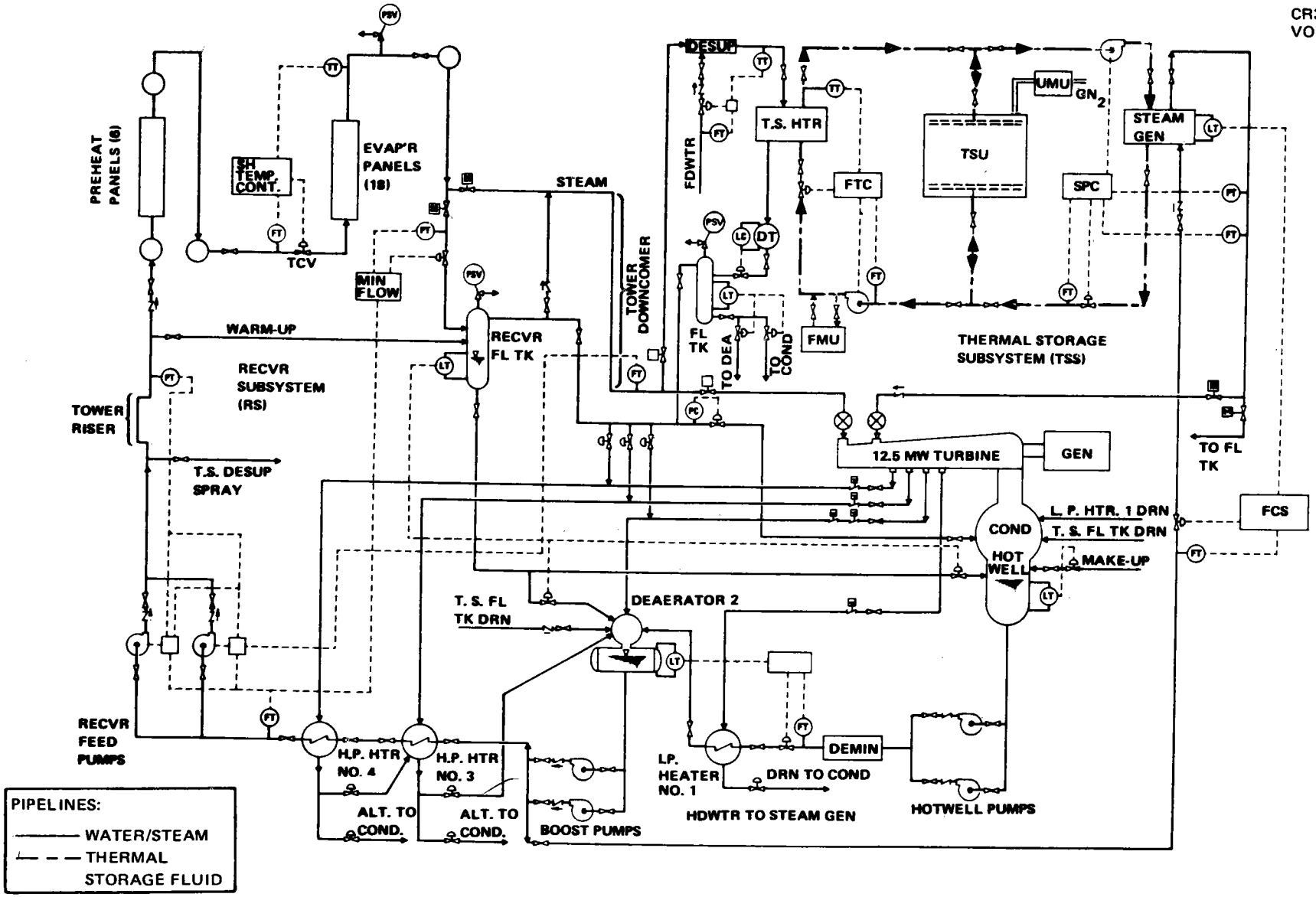

Figure 2-13. Overall Pilot Plant System Schematic

subsystem (top right corner), and the balance of plant equipment (bottom half of figure) which are similar to the corresponding subsystems of the Commercial system. Figures 2-14 through 2-19 illustrate the flow paths associated with the six basic system operating modes previously defined for the Commercial system. A more detailed discussion of the Pilot Plant operating modes is in Section 4.6.1.

2.2.1.2 Physical Characteristics

The overall characteristics of the Pilot Plant collector field were presented in Figure 1-5; a summary of other pertinent subsystem characteristics are in Table 1-4.

2.2.1.3 Waterfall Chart

A detailed breakdown of the Pilot Plant system performance is presented in a waterfall format for the Winter 2 PM design point, for equinox noon, and on an annual average basis in Figures 2-20 through 2-22. Included on each figure is a detailed tabulation of the appropriate step-by-step efficiencies. In each case presented, a total of 61.4 MW of thermal power is assumed to strike the heliostat surfaces when they are orientated normal to the incident sunlight. Implicit in this value is a conservative heliostat outage rate assumption and relocation penalty of 3.2%. If all available heliostats were oriented normal to the sun, the solar power striking the glass surfaces would be 63.5 MWt. If this power were available, a corresponding adjustment would have to be made in the various waterfall levels shown.

2.2.1.4 Subsystem Characteristics

As in the case of the Commercial system, the Pilot Plant subsystem characteristics can be subdivided into those related to the collector field and those related to the water/steam and Caloria loops. The heliostats which make up the collector field will be identical in design and operation to those anticipated for the Commercial system. They will be capable of effectively tracking the sun at solar elevation angles in excess of 10 deg. Since local shadowing at certain locations within the collector field will obscure the heliostat sensor mirror at low sun elevation angles, sensor-controlled tracking will be impossible for those affected heliostats. In those portions of the field, a selective heliostat activation procedure would be employed, such as bringing

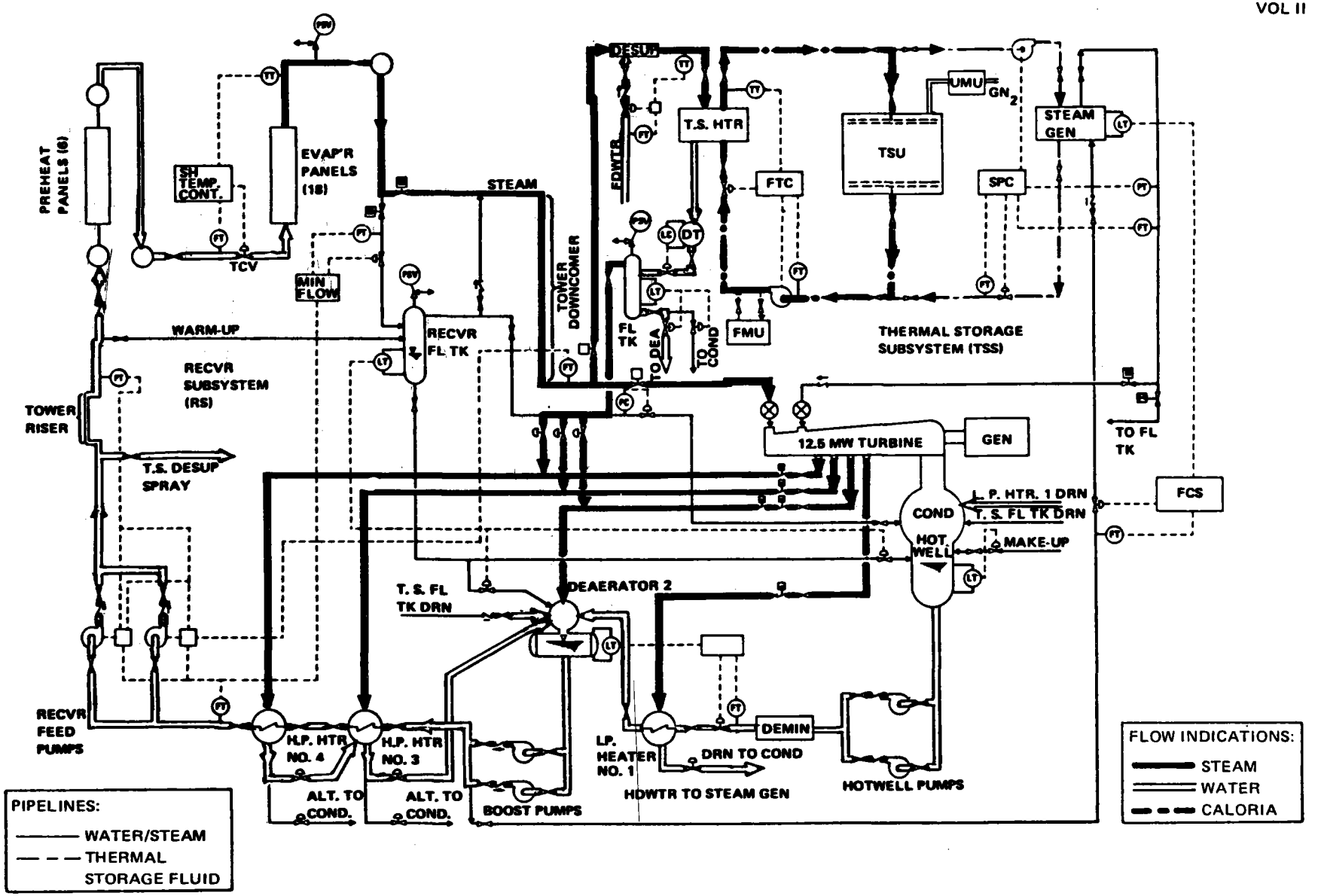

Figure 2-14. Normal Solar Operation (Pilot Plant)

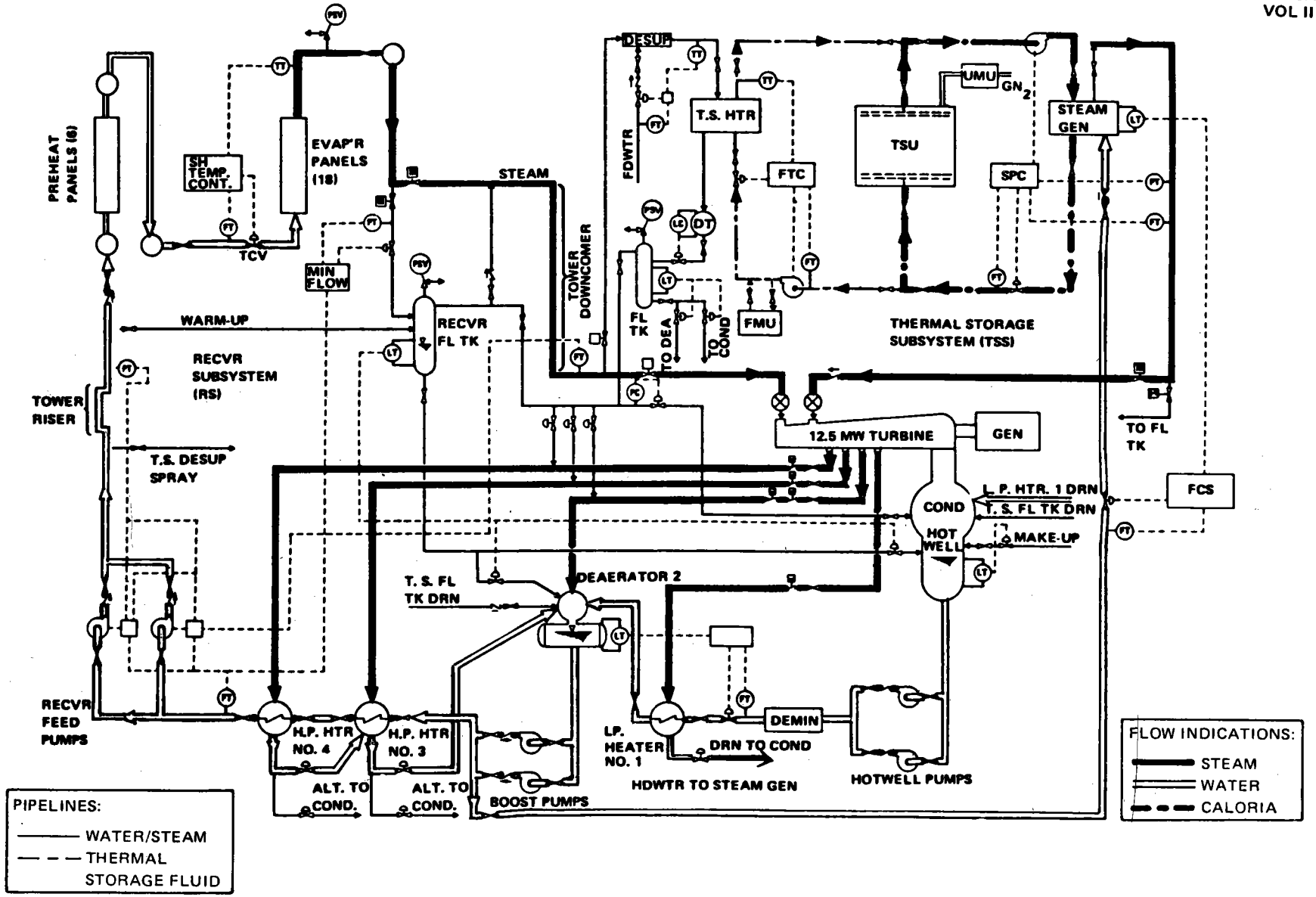

Figure 2-15. Low Solar Power Operation (Pilot Plant)

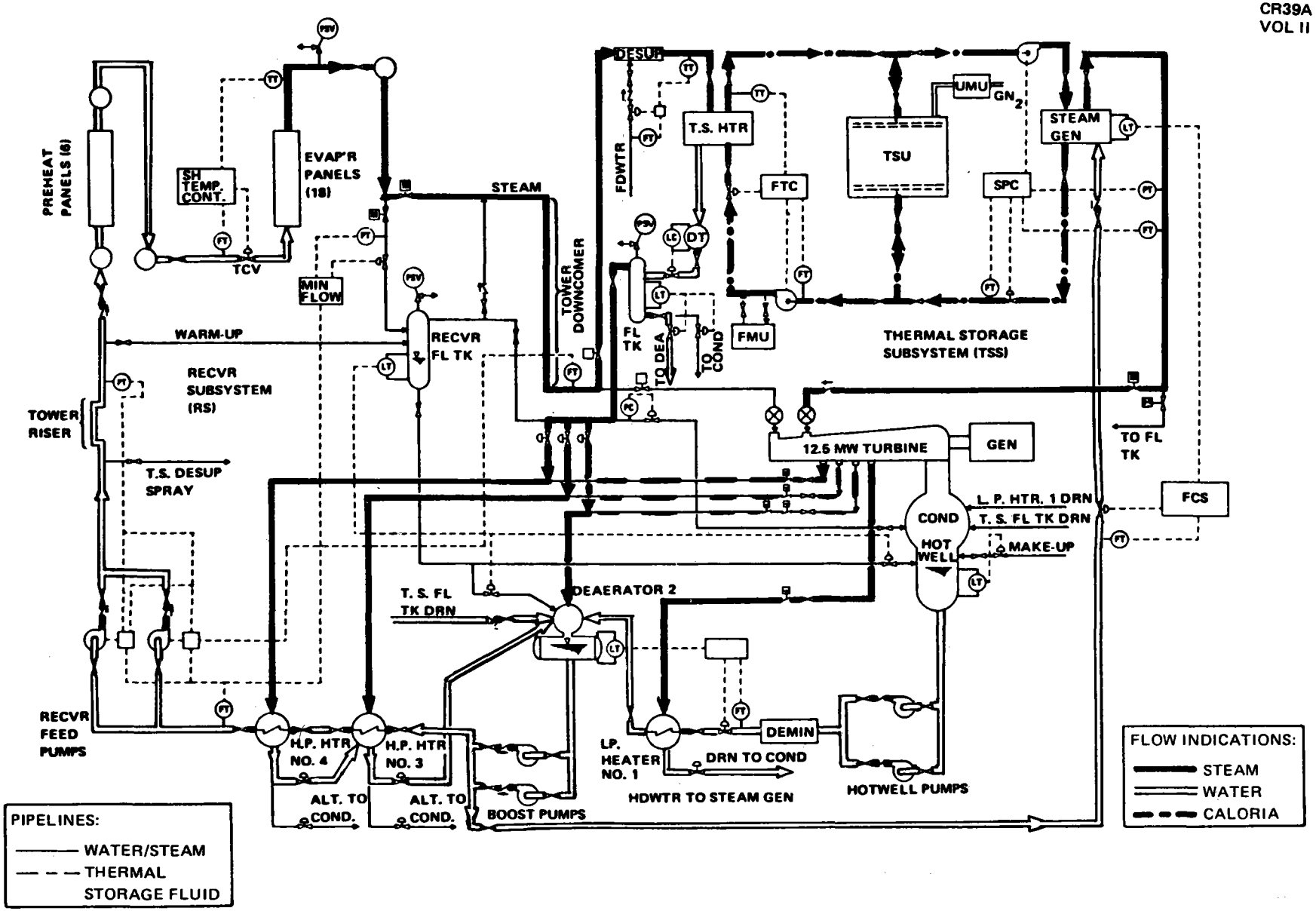

Figure 2-16. Intermittent Cloud Operation (Pilot Plant)

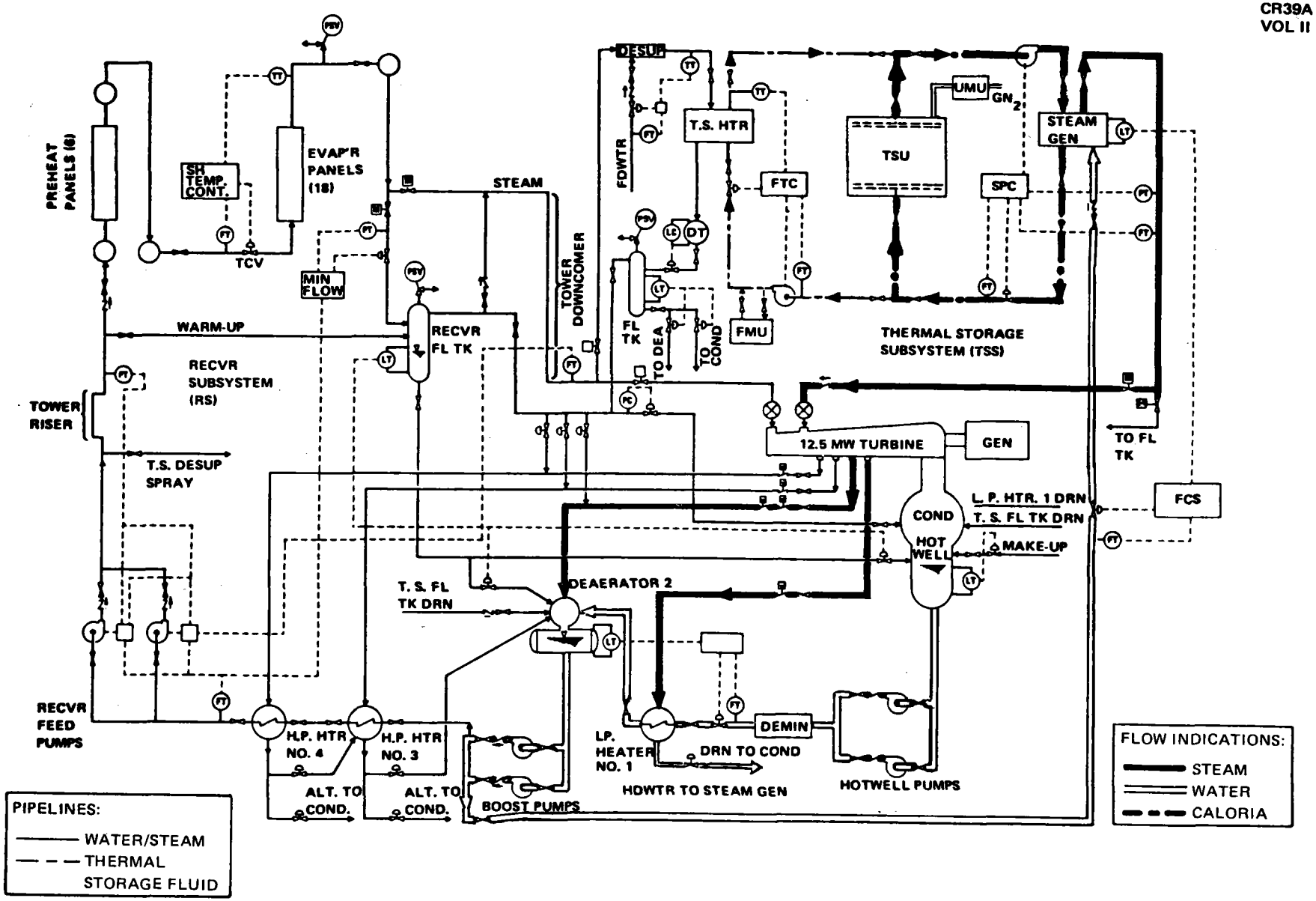

Figure 2-17. Extended Operation (Pilot Plant)

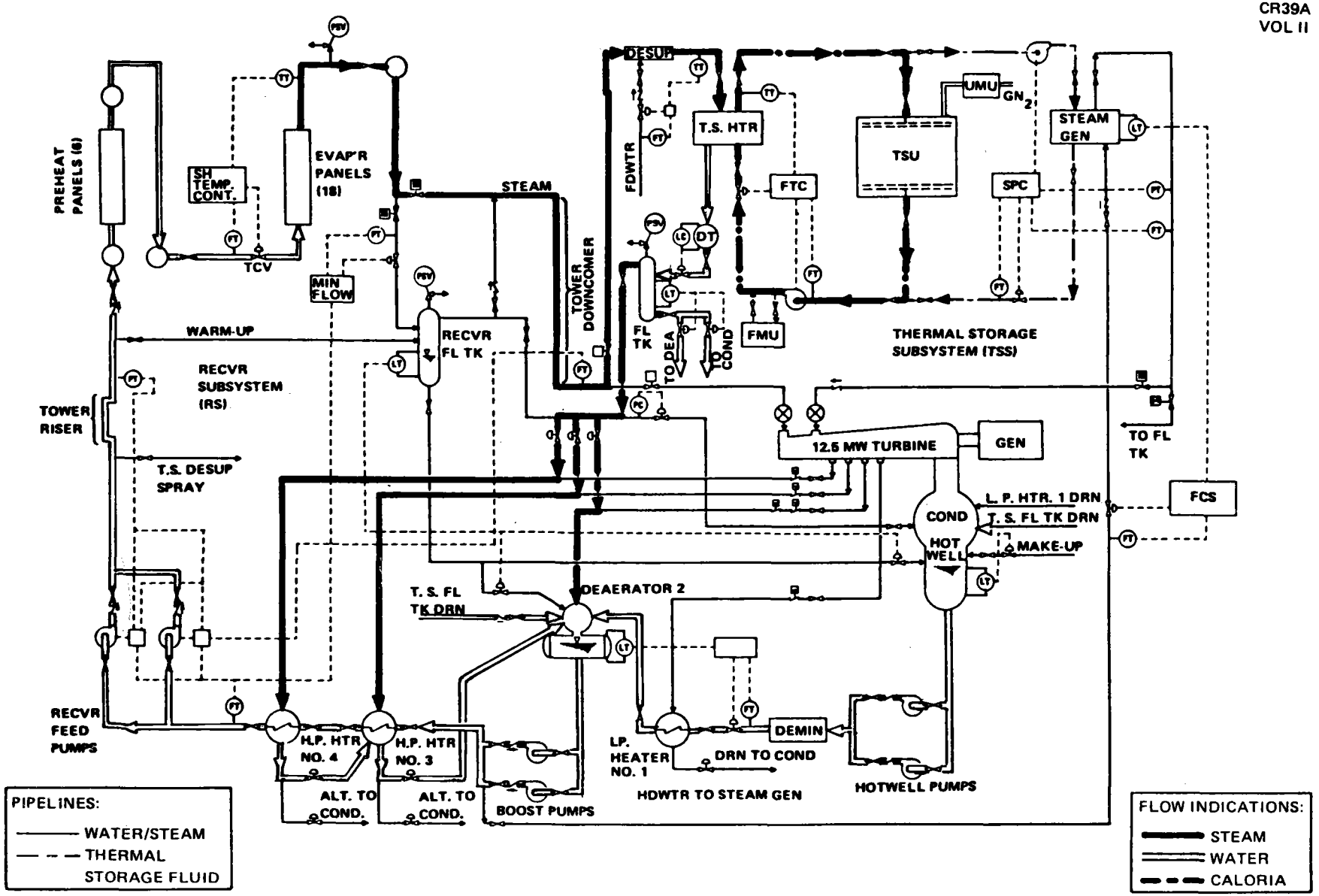

Figure 2-18. Charging of Thermal Storage Only (Pilot Plant)

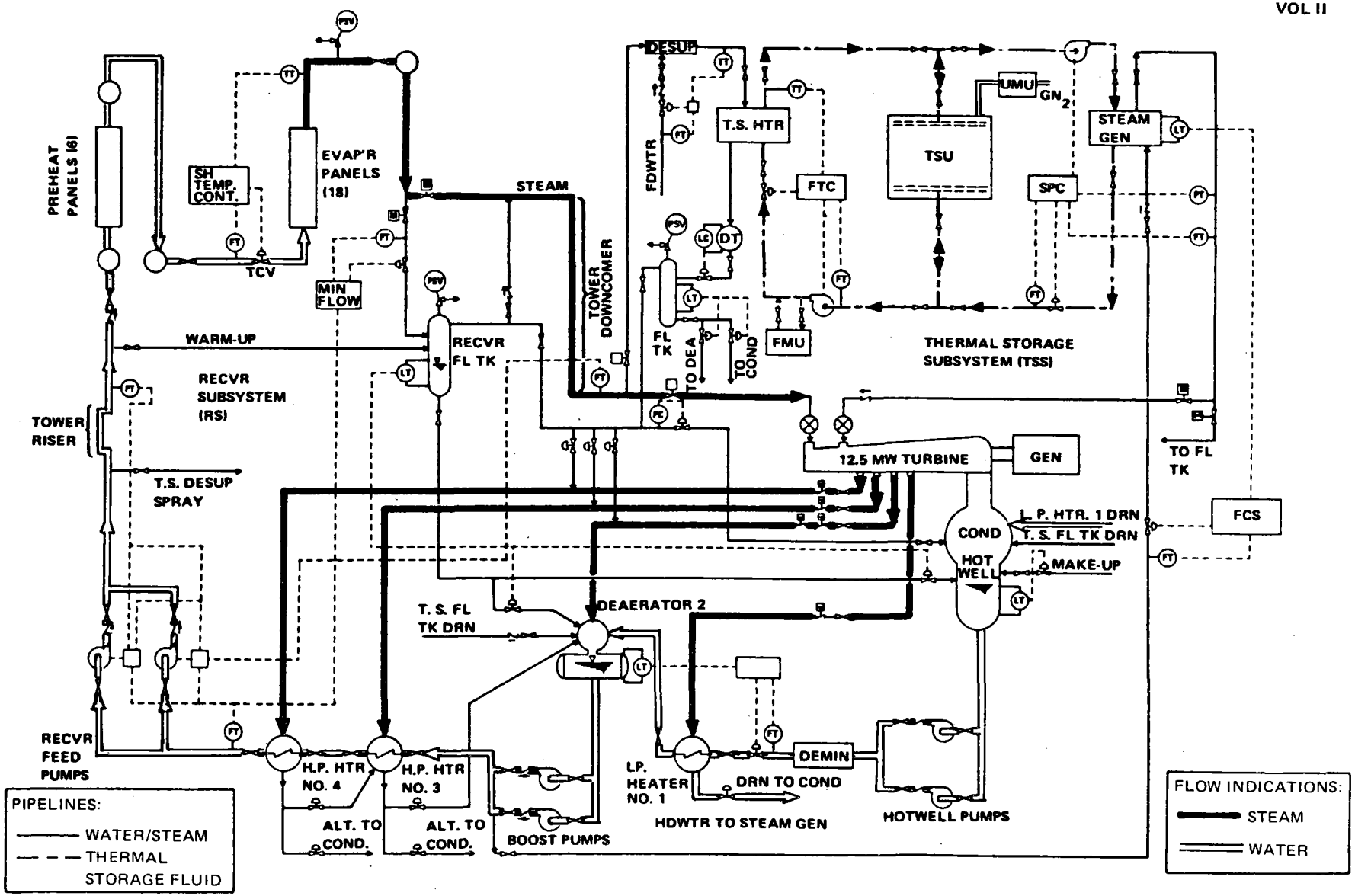

Figure 2-19. Fully Charged Thermal Storage (Pilot Plant)

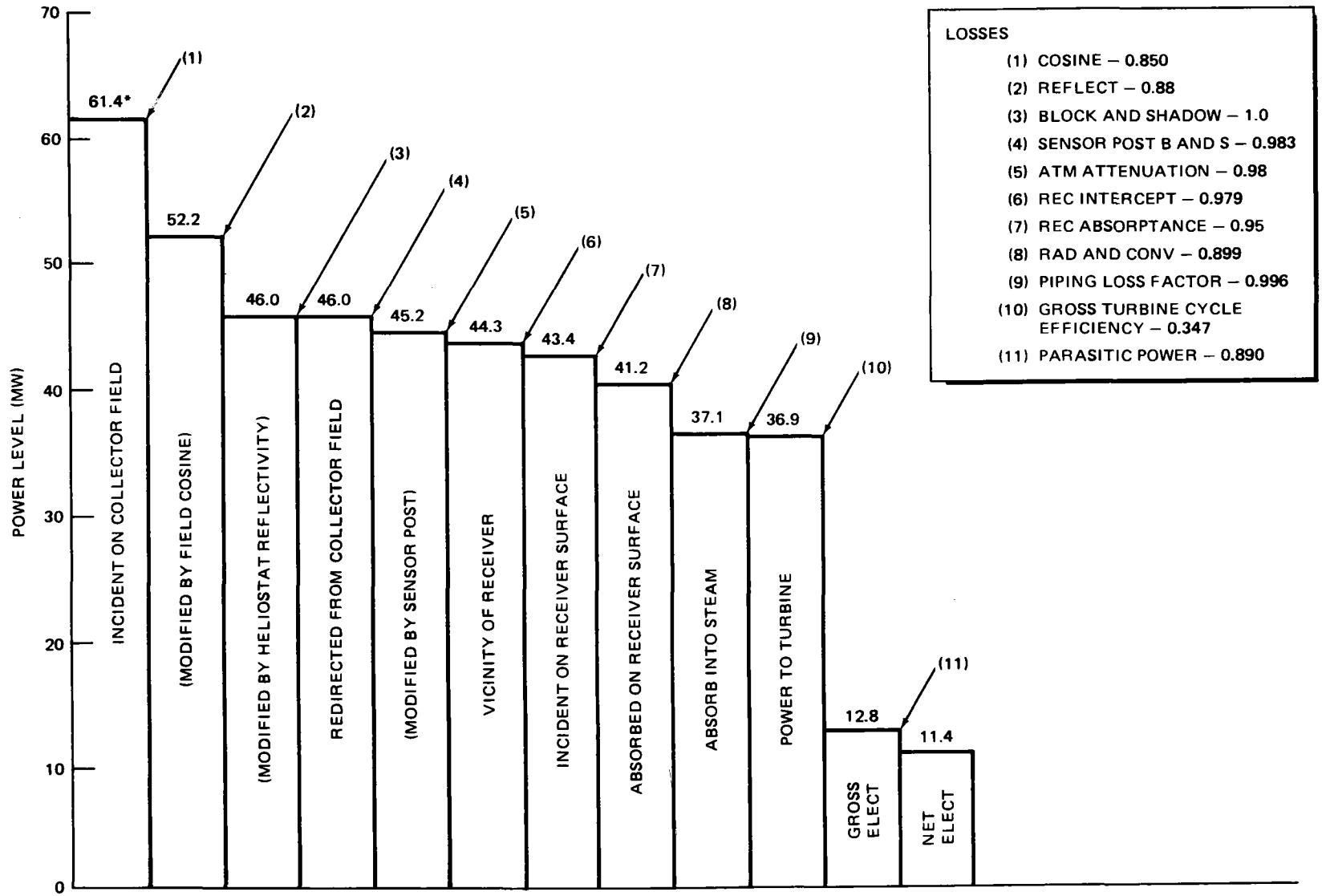

Figure 2-20. Pilot Plant System Power Flow (Equinox Noon)

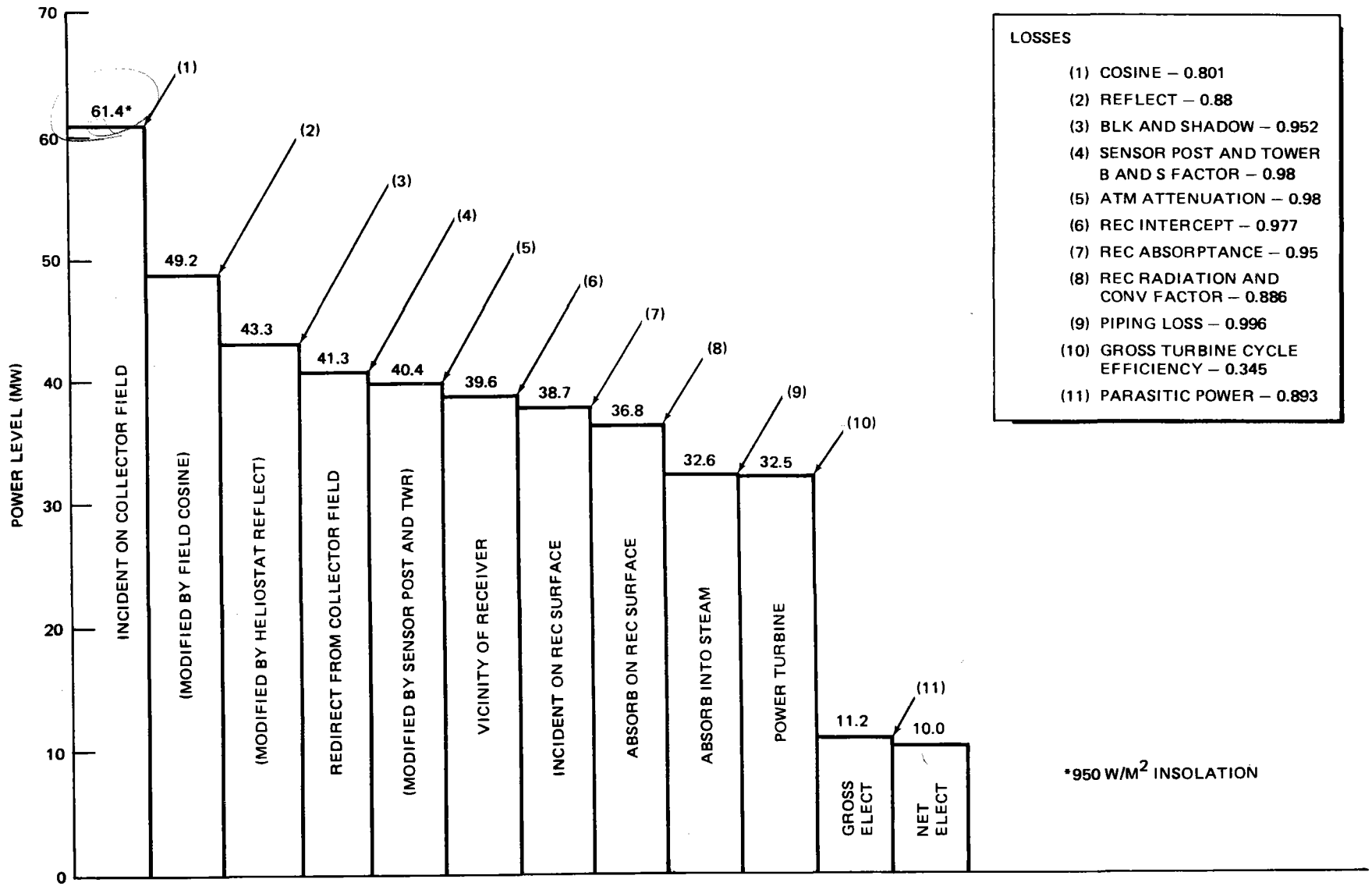

Figure 2-21. Pilot Plant System Power Flow (Winter 2 PM)

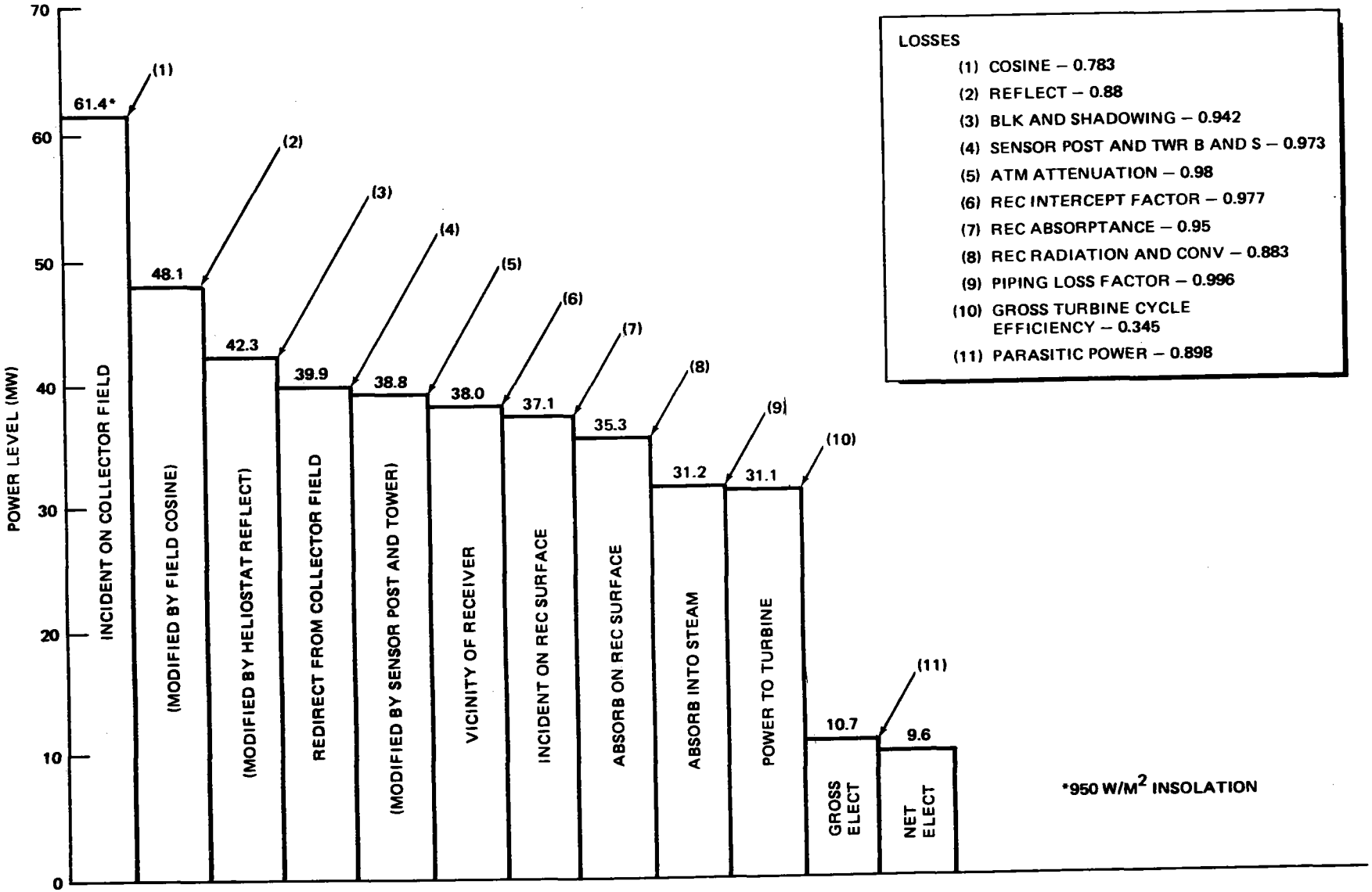

Figure 2-22. Pilot Plant System Power Flow (Annual Average)

on every other heliostat during low sun periods. This same concept of individual heliostat control allows individual heliostats to be commanded out of service or to a preferred orientation.

The receiver and thermal storage subsystems and the balance of plant equipment must be designed to satisfy a compatible set of nominal design conditions because of the close coupling that occurs through the water/steam loop. A summary of the nominal operating conditions for the receiver, thermal storage, and turbine are shown in Table 2-5. For the receiver and turbine (throttle steam operation), the nominal value corresponds to the Winter 2 PM design point. The nominal conditions for the thermal storage correspond to the maximum charge rate and the maximum discharge rate which would occur during nighttime turbine operation. Data related to the operating ranges of these subsystems are shown in Table 2-6.

2.2.1.5 Subsystem Efficiencies

The efficiency variation for the collector subsystem is shown in Figure 2-23 for various sun azimuth and elevation angles. Implicit in this data are the following assumptions:

- Heliostat reflectivity = 1.0
- Receiver interception factor = 0.977
- Sensor post blocking and shadowing = 0.98
- Atmospheric attenuation factor = 1.0

Collector subsystem efficiency at other values of heliostat reflectivity can be determined by multiplying the indicated efficiency by the actual reflectivity.

The receiver efficiency defined as the power absorbed into the steam divided by the incident power is summarized as follows:

Time	Incident Power (MWt)	Absorbed Power (MWt)	Efficiency
Equinox Noon	43.4	37.1	0.854
Winter 2 PM	38.7	32.6	0.842
Minimum Rated Steam	14.9	10.0	0.671
Annual Average	37.1	31.2	0.841

Table 2-5

PILOT PLANT NOMINAL OPERATING CONDITION

Subsystem	Temperature °C (°F)	Pressure MPa (psia)	Flow Rate Kg/sec (lb/hr)	Power Level MW (Btu/hr)
Receiver				
Rated Steam	516 (960)	10.45 (1515)	12.9 (102,440)	32.6 (111.3×10^6)
Derated Steam	349 (660)	10.45 (1515)	16.5 (130,482)	32.8 (111.9×10^6)
Thermal Storage				
Charging Steam at Heat Exchanger	343 (650)	10.1 (1465)	16.5 (130,482)	30.0 (102.4×10^6)
Discharge Steam Leaving Steam	277 (530)	2.76 (400)	13.2 (104,700)	32.1 (109.5×10^6)
Turbine				
Throttle Steam	510 (950)	10.1 (1465)	12.9 (102,440)	32.5 (110.9×10^6)
Admission Steam	274 (525)	2.65 (385)	13.2 (104,700)	32.0 (109.4×10^6)

Table 2-6

PILOT PLANT SUBSYSTEM OPERATING RANGES

Subsystem	Temperature °C (°F)	Pressure MPa (psia)	Flow Rate Kg/sec (lb/hr)	Power Range MW (Btu/hr)
Receiver				
Rated Steam	516 (960)	10.45 (1515)	3.7** - 14.8 (28,900 - 117,568)	10** - 37.1 (34.1 - 126.6 x 10^6)
Derated Steam	349 (660)	10.45 (1515)	3.7** - 16.5 (28,900 - 130,500)	7.3** - 32.8 (24.9 - 111.9 x 10^6)
Thermal Storage				
Charging Steam at Heat Exchanger	343 (650)	10.1 (1465)	0.83** - 16.5 (6,524 - 130,500)	1.5** - 30.0 (5.1 - 102.4 x 10^6)
Discharge Steam Leaving Steam Generator	277 (530)	2.76 (400)	1.27** - 13.2 (10,100 - 104,700)	3.1** - 32.1 (10.6 - 109.5 x 10^6)
Turbine				
Throttle Steam	510 (950)	10.1 (1465)	3.7** - 14.6* (28,900 - 117,568)	10.0** - 36.9* (34.1 - 125.9 x 10^6)
Admission Steam	274 (525)	2.65 (385)	1.27** - 13.2 (10,100 - 104,700)	3.1** - 32.0 (10.6 - 109.4 x 10^6)

*Requires a 2.5% turbine overflow capability (turbine is capable of 10% overflow operation)
**Approximate

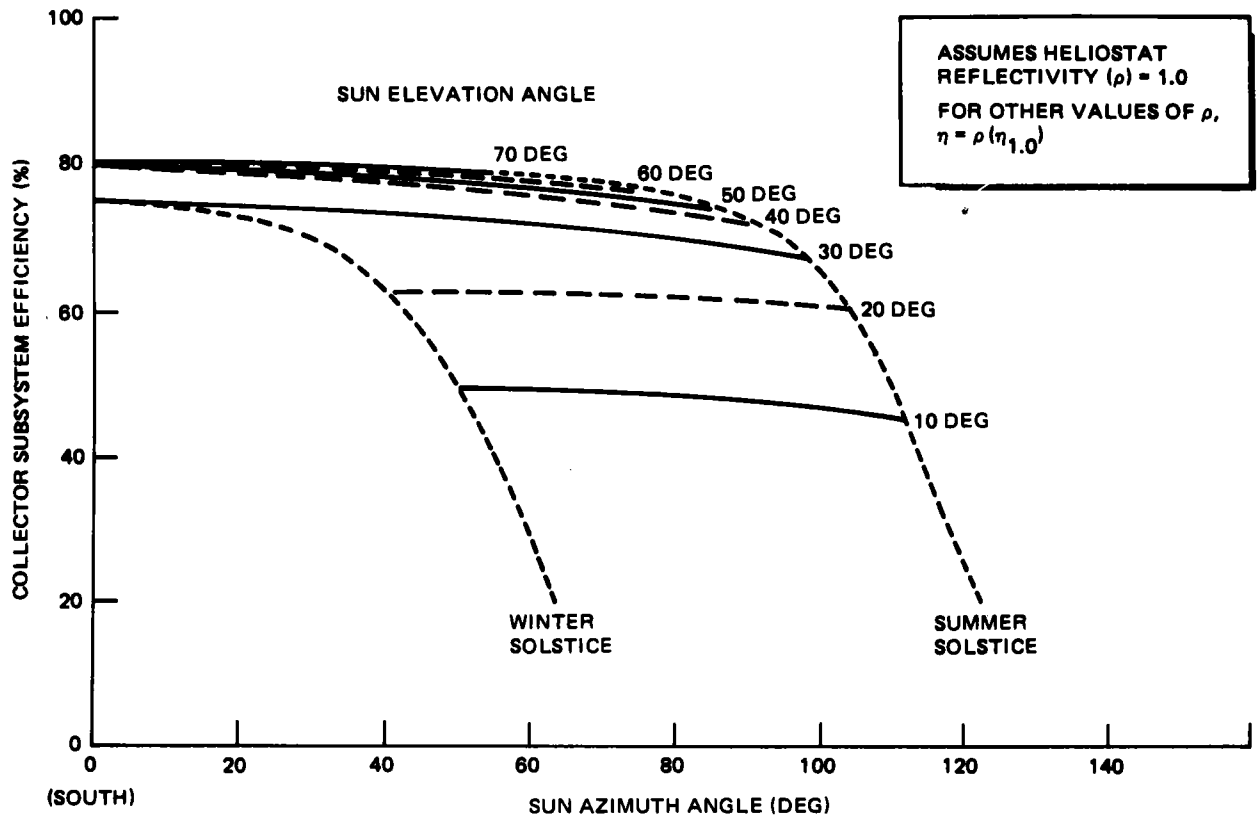

Figure 2-23. Collector Field Performance

Assumptions made in arriving at these values include an absorptivity of 0.95, an emissivity of 0.89, a wind speed of 3.5 m/s (8 mph) at 10m elevation, and an ambient temperature of 23°C (74°F). Since neither forced nor free convection dominates, a root sum squares addition of the two heat loss components was applied. Under the temperature and wind conditions defined above, ~2.3% of the incident power at equinox noon would be lost due to convection.

The thermal storage subsystem has a volumetric efficiency defined as the ratio of extractable energy to total energy in the tank of 85 to 90%. The subsystem has an energy recovery efficiency of 96 to 98%, which is defined as the ratio of extractable energy to charging energy.

The gross cycle efficiency for the turbine is shown in Figure 2-24 for operation off both receiver (throttle) steam and admission steam. These curves are based on an assumed wet cooled condenser that is capable of producing a 6.35 cm Hg (2.5 in. Hg) back pressure in the condenser. Also shown in the figure is an estimate of the turbine generator output as a function of flow rate when operating exclusively from receiver steam.

2.2.1.6 Auxiliary Power Requirements

A summary of the total Pilot Plant auxiliary power requirement is contained in the following tabulation for five different conditions. A detailed breakdown of the data is contained in Section 4.3.5.

	Auxiliary Power Requirements (kW)
• Winter 2 PM Design Point	1200
• Equinox Noon	1400
• Evening Operation from Thermal Storage	800
• Emergency Power	330 (AC) 23 (DC)
• Nighttime Standby	210

2.2.2 Design Rationale and Evolution

(See Section 4.4.)

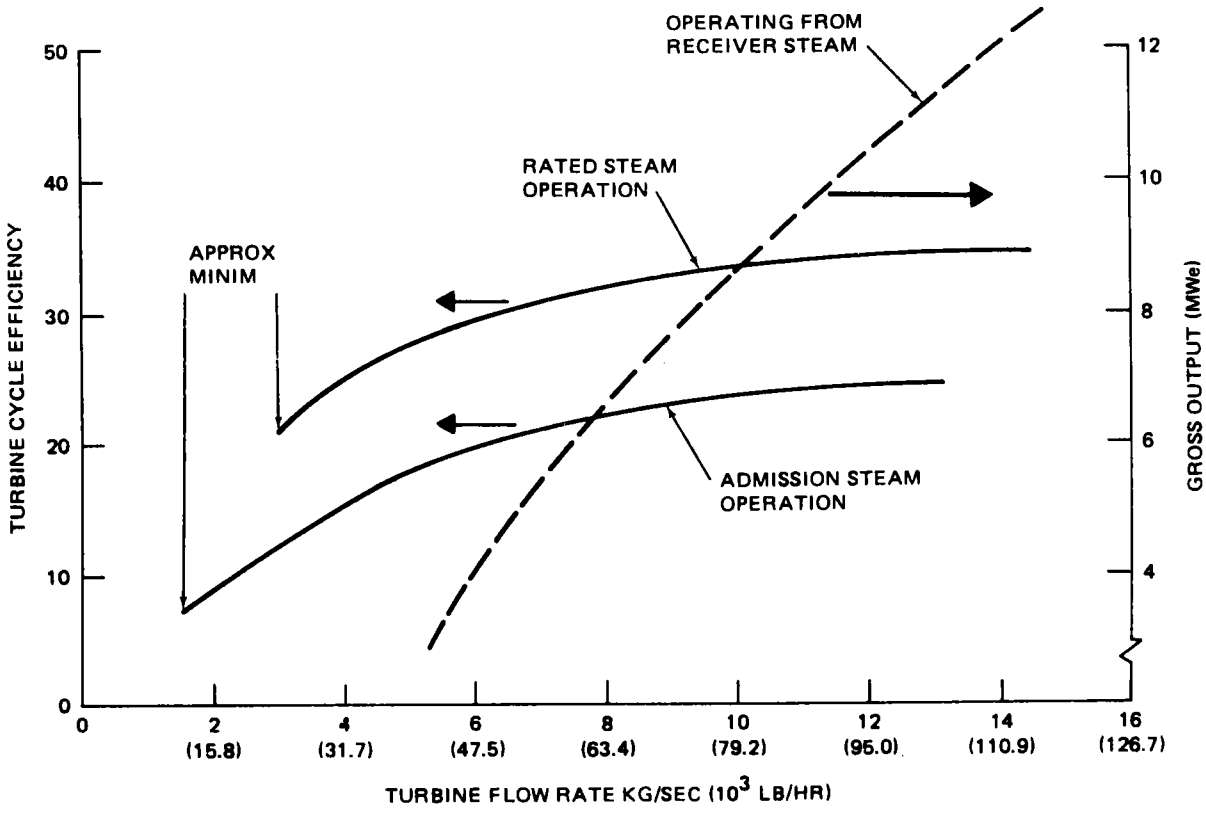

Figure 2-24. Impact of Flow Rate on Turbine Cycle (Pilot Plant)

2.2.3 Annual Energy Calculations

The Pilot Plant annual energy calculations described in detail in Section 4.5 were carried out for 1963 with Inyokern as the reference site. The environmental data including direct insolation, ambient temperature, and wind speed was taken from the Aerospace data tapes. The preferred approach to plant operation was to direct flow to the turbine whenever possible with thermal storage being charged only when the receiver is operated in a derated steam mode due to cloudy or poor insolation conditions. The predicted net energy output for the Pilot Plant operating in that environmental and mode is 27,430 MWHe.

2.2.4 Transient Plant Operations

(See Section 4.6.3).

2.2.5 Master Control

Master control consists of the control and display hardware and the associated software necessary for coordination of all subsystem processes, either automatically or manually under direction of the Pilot Plant operator.

Computer automated techniques are designed into master control to benefit the following operations:

- To continuously compute the collector subsystem synthetic track during each solar day and correct this track and subsequently the heliostat positions using algorithms influenced by current meteorology and plant performance data.
- To continuously optimize the plant heat, steam generation, and plant balance profiles at startup and during steady-state operation when immediate and temporary weather changes, coupled with varying receiver and thermal storage heat input and output demands, present a situation crucial to maintaining the plant on-line.
- To provide on-time data reduction of voluminous plant operation and performance data to the engineers during the development phase.
- To evaluate and develop the computer in a solar-power generation system as a controller for follow-on power-generation control applications of the same type.

The master control architecture is modular in design to accommodate scaling to the Commercial solar power-generation plant. The following design concepts facilitate the growth and expansion capabilities of master control:

- The computer system memory and peripheral devices are interfaced to a common bus that is expandable and can accommodate a large number and variety of peripherals.
- MDAC special-purpose devices (i.e., steering logic and collector subsystem interface) are modular and addressable by the computer making it easy to add on.
- Applications software is written in function independent modular form sharing common tables, buffers, etc. This design minimizes program rewrite and redesign to accommodate changes and expansion.
- Using the MDAC combination analog and digital automatic control design simplifies the software and provides flexibility in implementing new control functions.
- Patch panels and analog recording devices are of modular design and can be added or removed easily, as required.
- The MDAC design minimizes wiring and signal conditioning to support master control manual and automatic control using steering logic, buffered amplifiers, and patch panels. The feature permits economical add-ons and reduces maintenance.

Items in master control that require alterations to accommodate expansion are:

- The control console which will have to be enlarged and probably redesigned to accommodate the increased number of control and monitoring devices.
- The uninterruptible power source which will have to be sized to handle the increased power requirements of master control.

Additional design information pertaining to master control and its relationship to overall plant control is presented in Volume VI, Section 6.

2.2.6 Plant Safety Considerations

(See Section 4.10.3.)

Section 3
COMMERCIAL SYSTEM DEFINITION

3.1 REQUIREMENTS

Table 3-1 contains a complete listing of the Commercial system performance, environmental, and design requirements along with the corresponding values for the Pilot Plant system. Also contained in the tabulation is an indication as to the source of the requirement. Those labeled "MDAC" were developed as a result of trade studies or design conservatism introduced by MDAC, those labeled "DoE" were specified by the Department of Energy.

Reviewing first the performance requirements, the design point power levels of 100-MWe net power when operating from receiver steam and the 70-MWe net power when operating from thermal storage steam represent minimum design power levels. MDAC has chosen to design their Commercial system to these minimum levels since they represent conditions which are compatible with existing turbine equipment which would be used for a solar application and the proposed MDAC approach to low-cost thermal storage. The solar multiple of 1.7 with 6 hr of thermal storage capability (at the 70-MWe power level) resulted from an MDAC system trade study for a stand-alone solar plant. Details of the trade study are in Section 3.2.5.

The maximum thermal storage charging rate of 255 MWt corresponds to 50% of the maximum receiver power. This is consistent with the Department of Energy design guideline for charging thermal storage of using 50% of the maximum receiver output or the difference between the maximum receiver output and that required to drive the turbine at its design power level (whichever is greater). In reality, this charging limitation imposes a severe and unnecessary constraint on the design and operation of the Commercial system. The receiver, for example, is already designed for full-flow operation for rated steam; therefore, from a receiver standpoint, there is no reason to

Table 3-1 (Page 1 of 3)

SYSTEM REQUIREMENTS

Performance/Environmental	Commercial System	Pilot Plant	Requirement Source
Design Point Power Levels (950 Watts/m^2 Solar Insolation)	100 MWe Net (Rec.) (Best Sun Angle) 70 MWe Net (T.S.)	10 MWe Net (Rec.) (Worst Field Cosine) 7 MWe Net (T.S.)	DoE
Solar Multiple	1.7	1.1	MDAC
Hours of Thermal Storage	6	3	MDAC
Maximum Thermal Storage Charging Rate	255 MWt	30 MWt	DoE
System Startup Times	Hot Start - 20 Minutes* Cold Start - 6 Hours	Hot Start - 20 Minutes* Cold Start - 6 Hours	DoE
Plant Availability	0.9, Excluding Sunshine	0.9, Excluding Sunshine	DoE
Annual Energy Output	TBD	TBD	DoE
Solar Insolation	950 W/m^2	950 W/m^2	DoE
Temperature			
Operation to Performance Reqmts	TBD	TBD	DoE
Reduced Performance and Survival	-30° to +50°C (-20° to +120°F)	-30° to +50°C (-20° to +120°F)	
Design Point Operation	Wet Bulb, 23°C (74°F) Dry Bulb, 28°C (82.6°F)	Wet Bulb, 23°C (74°F) Dry Bulb, 28°C (82.6°F)	

*Minimize within practical limits

Table 3-1 (Page 2 of 3)

SYSTEM REQUIREMENTS

Environmental	Commercial System	Pilot Plant	Requirement Source
Wind Conditions (At 10M Elevation)			
Max Operational, with Gusts	16 m/sec (36 mph)	16 m/sec (36 mph)	MDAC
Max Survival			
Sustained (Tower Only)	40 m/sec (90 mph)	40 m/sec (90 mph)	MDAC
With Gusts (Other Subsystem)	40 m/sec (90 mph)	40 m/sec (90 mph)	DoE
Wind Velocity Profile	Varies Exponentially	Varies Exponentially	DoE
(Relative to 10m height)	To the 0.15 Power	To the 0.15 Power	
Seismological	Seismic Zone 3	Seismic Zone 3	DoE
	NRC Reg. Guide 1.60 Response Spectrum	NRC Reg. Guide 1.60 Response Spectrum	DoE
	OBE - 0.165 hor. "G" SSE - 0.33 hor. "G" (Revised to 0.25 hor "G")	OBE - 0.165 hor. "G" SSE - 0.33 hor. "G" (Revised to 0.25 hor "G")	MDAC
Soil Conditions	Barstow Data	Barstow Data	DoE
Lightning Protection	TBD (Cost-Risk Basis)	TBD (Cost-Risk Basis)	DoE
Precipitation			
Rain			
Average Annual	100 mm (4 in.)	100 mm (4 in.)	DoE
Max 24-hr Rate	75 mm (3 in.)	75 mm (3 in.)	
Snow (Design Snow Load)	250 pa (5 psf)	250 pa (5 psf)	DoE
Sleet (Max. Ice Buildup)	50 mm (2 in.)	50 mm (2 in.)	DoE

Table 3-1 (Page 3 of 3)

SYSTEM REQUIREMENTS

Environmental/Design	Commercial System	Pilot Plant	Requirement Source
Hail			
Any Orientation Survival	20 mm (3/4 in.) at 20 m/s (65 ft/sec) Term. Vel.	20 mm (3/4 in.) at 20 m/s (65 ft/sec) Term. Vel.	DoE
Stowed Position Survival	25 mm (1 in.) at 23 m/s (75 ft/sec) Term. Vel.	25 mm (1 in.) at 23 m/s (75 ft/sec) Term. Vel.	
System Output Voltage and Frequency	TBD	TBD (Compatible with SCE Coolwater Facility)	DoE MDAC
System Output Power Quality	Reliable and Compatible with Local Grid	Acceptable to Local Grid (No Electric Energy Dissipation)	DoE
Endurance Capability	30 Years With Maintenance	30 Years With Maintenance	DoE
System Safety	Compatible with Cal-OSHA (Cost-Risk Approach) to Sys. Definition)	Compatible With Cal-OSHA (Hazards Analysis to Establish Required Safety Criteria)	MDAC

constrain derated steam operation to something less than the receiver's maximum design flow. In addition, during system startup using receiver steam, a condition arises fairly quickly where the collected power exceeds the capability of the thermal storage subsystem and the partially loaded turbine to accept all of the flow. At that point, heliostats would have to be driven off target to limit the amount of power available to the receiver. As the turbine load (and flow rate) were increased following the normal startup procedure, the heliostats would be brought back into service.

The system startup times shown for the hot and cold start (defined by critical turbine temperature) represent Department of Energy design guidelines. When comparing these times with startup limitations imposed by existing turbine equipment, it is seen that the 20-min hot startup is optimistic by approximately a factor of 2 while the cold startup time is well within the predicted startup times using existing turbine equipment.

The environmental design data shown in Table 3-1, in general, represents a compilation of data gathered from desert locations. With the exception of the operational and survival wind and the seismic limit for continued operation, the requirements were provided by the Department of Energy as program inputs. The maximum operational wind limit which influences primarily the collector field was developed based on a trade study of heliostat strength (and cost) vs lost energy due to early heliostat stow. The indicated optimum value of 16 m/s (36 mph) including gusts resulted from the trade study to determine the wind speed at which stowage would be initiated. The design wind condition for the tower was assumed to be more severe than for the rest of the system components. The 40 m/s (90 mph) sustained value assumed represents a 100-yr wind in most areas of the desert southwest.

The requirement to design the system for a seismic Zone 3, not near a great fault, specifies the design value for horizontal acceleration at 0.33g for a safe shutdown condition. This value, along with a fixed-base soil condition, was used as the basis for the tower design work carried out for the Commercial system. An additional MDAC requirement also imposed an

"Operating Basis Earthquake" acceleration of 0.165g through which uninterrupted operation must be maintained. Superimposed on the horizontal accelerations are vertical components which are two-thirds of the indicated horizontal values.

From a design standpoint, the system will be compatible with local electrical networks while surviving in a desert environment for 30 yr with routine maintenance. In all cases, the system is to be designed to meet Cal-OSHA requirements.

In addition to these specific requirements, the Department of Energy has imposed overall design guidelines. They specify the use of conventional water/steam turbine-generator equipment and wet cooling heat rejection while ruling out the use of supplemental fossil-fired boilers for turbine steam.

3.2 SYSTEM DESIGN RATIONALE AND EVOLUTION

The evolutionary process used to arrive at the Commercial system design followed two essentially independent paths. The first focused on the optical energy part of the system which treated the collector, receiver configuration, and tower. The second part treated the fluid side of the receiver, thermal storage, and balance of plant equipment, which are all coupled together through the water/steam loop. Each of these areas contains a complex set of interactive parameters which must be treated in any optimization study. For the sake of discussion simplicity, these two areas of analysis have been broken down into discrete study areas which highlight many of the principal study results.

3.2.1 Receiver Configuration

The desired receiver configuration was an output of the overall collector field/receiver/tower optimization studies carried out early in the contract effort. The purpose of these studies was to arrive at the most cost-effective approach to energy collection. Receiver considerations treated in the analyses included weight, complexity, quantity required, absorption characteristics, radiation and convection losses, availability, thermal response, and cost. Collector field effects contained in the analyses included field size as limited

by receiver look angle, heliostat cosine, blocking and shadowing, and tracking accuracy. Additional factors included tower height and strength (which impact cost), number of towers required, and piping networks required to transport superheated steam and feedwater.

The impact of using a cavity receiver with a limited field of view on the collector field layout is shown in Figure 3-1. It is assumed in this figure that the external receiver, which is compatible with "University of Houston optimum field layout" (October 1975 version) is replaced with downward or north-tilted cavity receiver with look angles as indicated while holding tower height constant. It is seen that the limited-look angles significantly limit the useful area of the collector field. The alternatives to gain greater collector area are a higher tower or series of towers and receivers. The comparative impact on tower height and piping/tower costs as a function of module size is shown in Figure 3-2. The superiority of the external receiver configuration with its shorter tower and piping runs is apparent. The cost impact was based on work done in 1975. Current cost data indicates that a much more significant cost difference would actually occur. It should also be pointed out that tower costs associated with the cavity receiver do not reflect any consideration of the more substantial structure which would be required to support the more massive cavity receiver.

The superiority of the external receiver from a tower and look angle standpoint is partially offset by the higher heat losses experienced with the external design. A comparative analysis carried out early in the contract and summarized in Figure 3-3 shows the superiority of the cavity approach. As the module power level increases, however, the efficiency of the external receiver increases because of a higher concentration ratio, which is permitted because of higher cooling capabilities inherent in the larger receiver.

The results of the overall optimization study carried out in 1975 indicated the overall superiority of the external receiver configuration for a commercial system. This result means that the higher heat losses and poorer field cosine are more than offset by the receiver tower and piping costs. At that point, MDAC was directed by the Department of Energy to cease further comparative work and devote the full effort toward the design of a system based on the external receiver configuration.

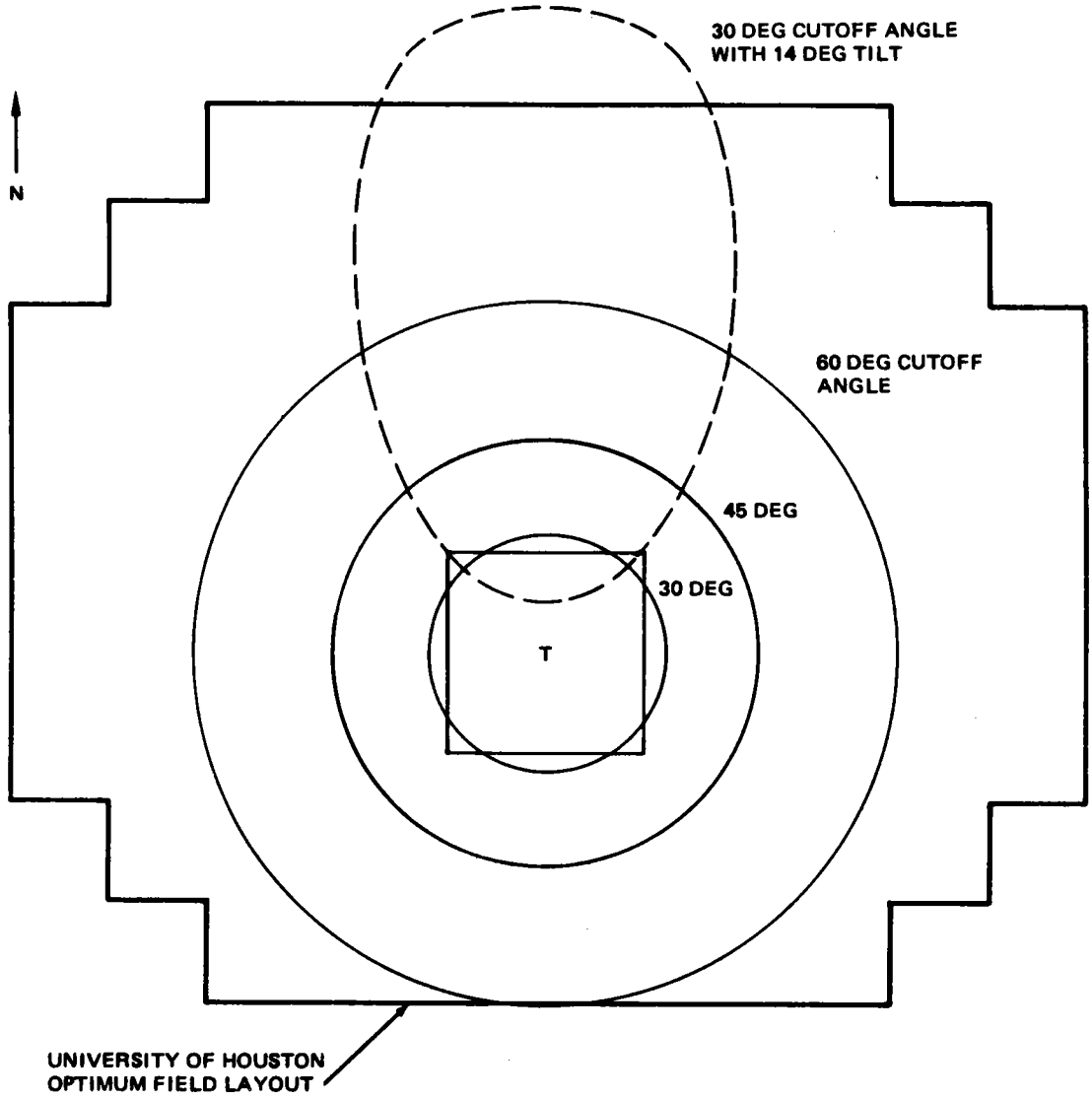

Figure 3-1. Effect of Cutoff Angle on Field Coverage

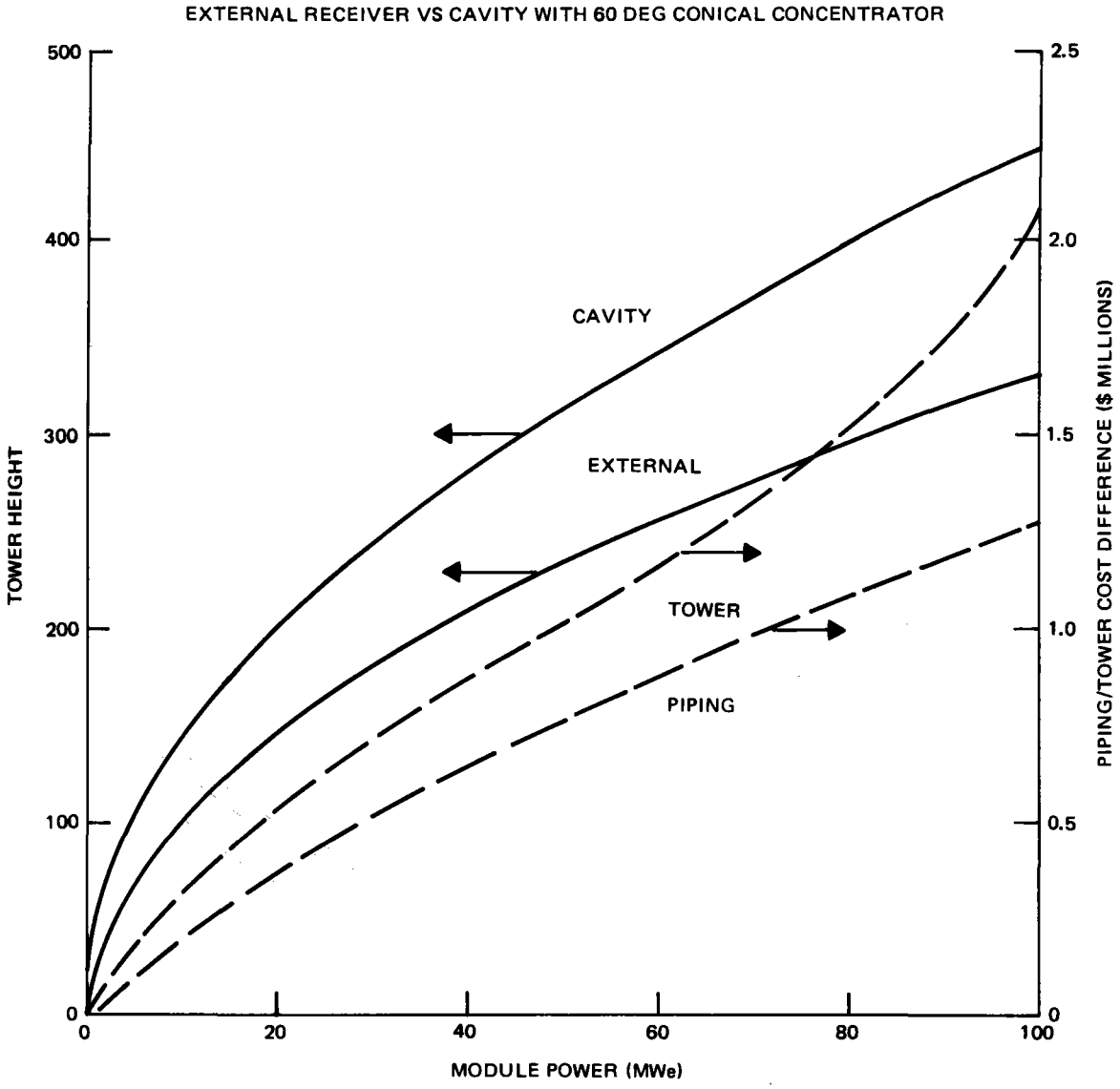

Figure 3-2. Tower Height and Cost Comparison

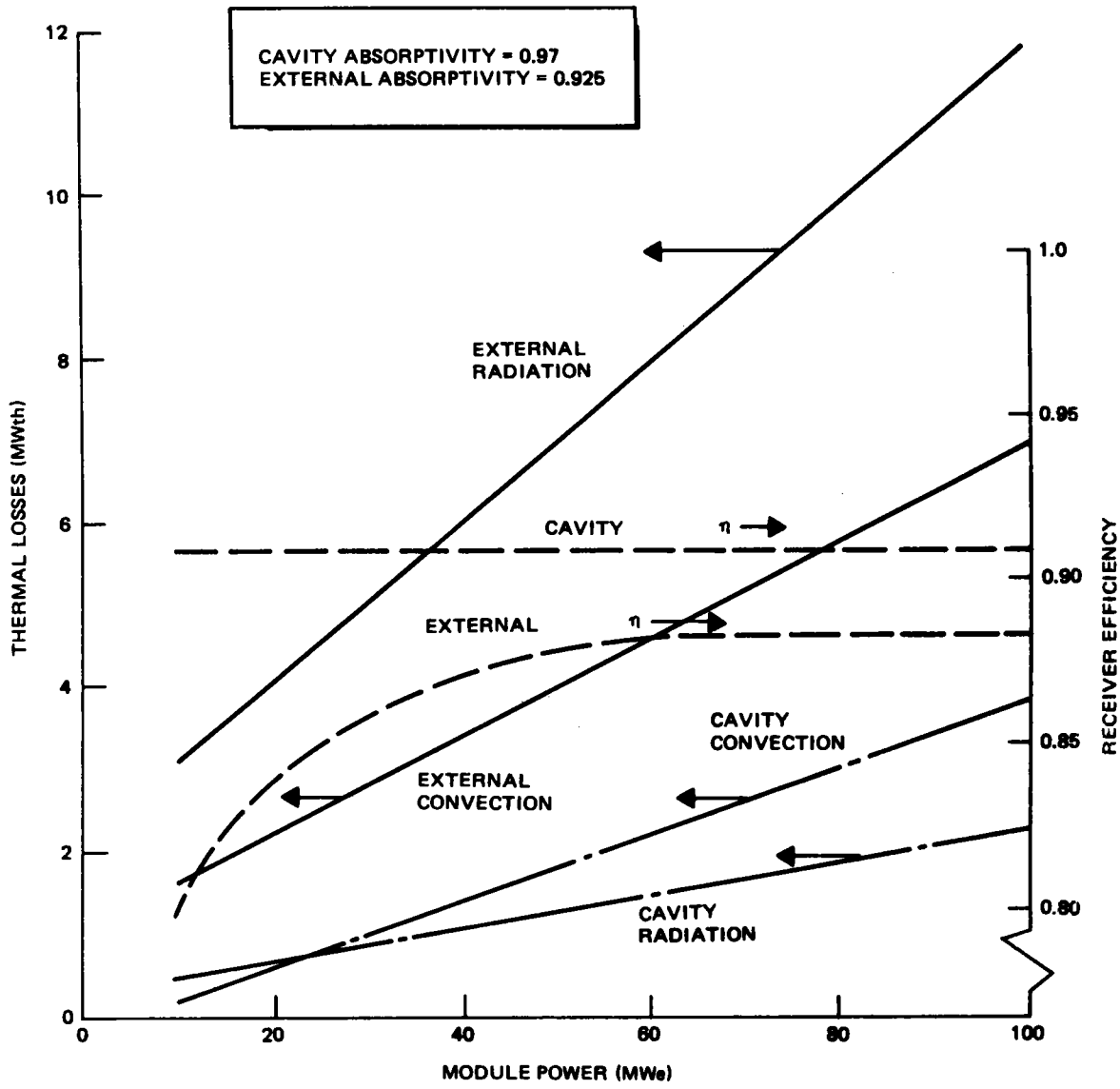

Figure 3-3. Comparison of Receiver Losses

3.2.2 Single vs Multiple Tower Module Design

With the selection of the external receiver for the baseline configuration, the next issue to investigate is the number of modules (collector fields, receivers, and towers) necessary to power an anticipated Commercial system. A comparative study was carried out which considered systems made up of 1, 3, and 10 collector field modules. In each case, the total collector field capacity was sized to produce a solar multiple of 1.7 (506 MWt power collected at equinox noon). In the study, it was assumed that the modules were all geometrically similar, i.e., a 360-deg collector field, and differed only in collection capacity.

The results of the study that were revised in March 1977 are shown on a composite basis in Figure 3-4. From an overall sense, it is clear that the single-module approach offers significant advantage over the 3- and 10-module approaches with the principal differences arising because of the excessive losses associated with the horizontal piping.

To gain a better understanding of the results, it is appropriate to treat each of the elements which contribute to the overall cost of energy. From a collector field standpoint, the starting point was the $65M Commercial system cost estimate presented in the Preliminary Design Baseline Report (PDBR) for a single-module system. The number was revised upward to $68.2M to reflect the added heliostat requirements due to atmospheric attenuation (0.953 average for the field) which was not treated initially. Because of the assumption of geometrically similar collector fields, the only collector performance difference between the approaches involves the atmospheric attenuation which favors the multiple towers. Assuming a 50-km visible range, the attenuation factors for the 3- and 10-module configuration were 0.965 and 0.98, respectively. At the same time, realistic variations in receiver efficiency were included in the analysis which also impact collector field size. The receiver designed to handle high power levels are slightly more efficient due to the higher coolant flow per unit circumference which permits slightly higher concentration ratios. As a result, receiver efficiencies of 89%, 87%, and 85%, were used, respectively, for the 1-, 3-, and 10-module configurations. When reflecting on these effects, along with the atmospheric attenuation values in collector field size required to provide the design power level, the resulting

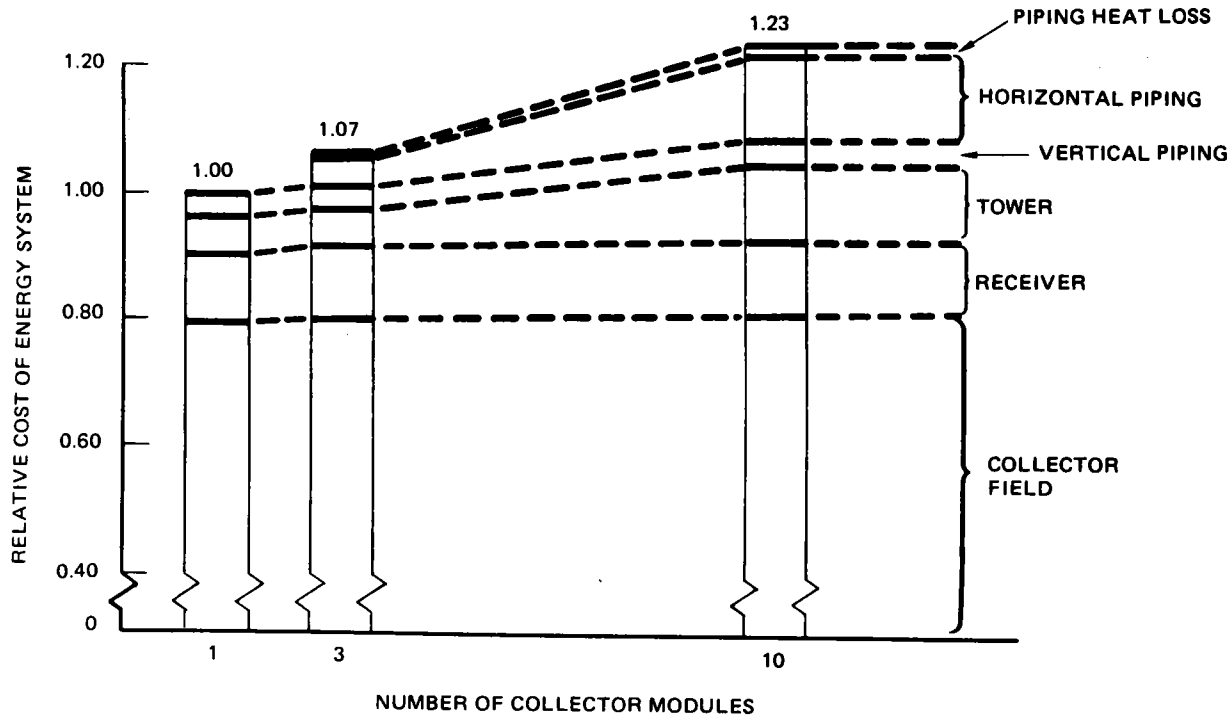

Figure 3-4. Impact of Multiple Modules on Cost (506 MW Peak Absorbed Power)

costs of $68.9M and $69.5M were developed for the 3- and 10-module configurations. As seen in Figure 3-4, these variations in cost or variations in performance assumptions which were used to arrive at these cost levels are minor in comparison to the variations introduced by the horizontal piping.

The increments of receiver cost were arrived at by scaling the estimated single-module receiver cost of $10M by existing cost-estimating relationships. The corresponding costs associated with a 1/3 and 1/10 capacity receiver are $3.37M and $1.18M, respectively. The decrease in receiver cost per unit capacity as one moves to larger units occurs because of the well-established economy of scale effect; i.e., it is less expensive to use fewer larger elements. This effect has been verified by all receiver design studies carried out to date.

The tower costs were developed by scaling the single-module tower costs by an established cost-estimating relationship which varies as tower height squared. This resulted in the incremental tower increase shown in Figure 3-4. Implicit in this analysis is the assumption of similar tower structures (concrete). As one moves to many smaller modules, steel towers become an attractive alternative of slightly lower cost. However, at the size and strength needed for the 1/10 capacity module, concrete and steel are economically competitive.

The vertical piping increment which represents a fairly small contribution to the overall cost was developed from algorithms which scale with flow rate or power level. The result is an incremental cost which is essentially constant as one moves from a single large module to 10 smaller modules.

The cost impact of the horizontal piping was based on actual cost data developed by Stearns-Roger using standard estimating techniques. Based on assumed module layouts, 2,408m (7,900 ft) of 25.4 cm (10 in.) steam distribution line and 15.2 cm (6 in.) feedwater distribution line were required for the 3-module case. The corresponding steam and feedwater line lengths for the 10-module case are 7,622m (25,000 ft) each. The same line sizes were assumed as in the 3-module case. This assumption resulted in somewhat lower costs for the 10-module case than would actually be

experienced because no penalty was assumed for the common manifolding which was used extensively in the layout of the 10-module configuration. The manifold sizes required to prevent excessive pressure drop over the extended run lengths would be significantly larger than the assumed 25.4 cm (10 in.) size. A further breakdown of the cost data associated with the piping is shown in Table 3-2. This data includes assumptions on valves, elbows, insulation, supports, labor, etc.

The final cost increment shown in Figure 3-4 involves heat loss. This effect is a 24 hr per day drain on system energy which must be added back by either increasing the size of the collector field or delaying somewhat the useful system startup point. The impact, although small, is more significant for the multiple-tower configuration due to the long piping runs. It should be noted that this study ignored pressure drop effects which would have the greatest detrimental effect on the 10-module approach again because of the long piping runs.

An attempt to improve receiver efficiency, such as through a shrouded design, was considered as a way to make the multiple-tower configurations more attractive. The required receiver efficiency necessary for a breakeven condition is shown in Figure 3-5. It is seen that a receiver efficiency greater than 100% would be necessary to arrive at a break-even situation if more than six modules were considered. For fewer modules, the curve represents a goal which must be surpassed to produce a cost-effective system design. In all cases considered, receiver design modifications were unable to make up the added efficiency necessary to shift the cost-effective design away from a single tower design.

3.2.3 Receiver/Turbine Steam Conditions and Module Size

The selection of system steam conditions and module size (generating capacity for an individual system) is governed by overall system economics subject to constraints imposed by the turbine, receiver, and thermal storage. Since the system is constrained to use conventional turbine equipment, possible limitations related to turbine size or acceptable steam conditions should be initially identified to establish design constraints for the receiver and thermal storage subsystems.

Table 3-2

HORIZONTAL PIPING COSTS

(MULTIPLE MODULES - 506 MW PEAK ABSORBED POWER)

	3 Modules ($ Millions)	10 Modules ($ Millions)
Steam Lines (Includes 10 in. Schedule 120 Pipe Plus 4 in. Insulation, Elbows, Gate Valves, Supports, Labor, and all Indirect Contractor Costs)	2.54	8.03
Feedwater Lines (Includes 6 in. Schedule 120 Pipe Plus 2 in. Insulation, Elbows, Gate Valves, Supports, Labor, and all Indirect Contractor Costs)	1.18	3.75
Total	3.72	11.78

The type of turbine required to be compatible with a solar electric system is of a nonreheat, dual-admission type, capable of daily cycling. Since the economics trend for the overall system is toward a large module size, the turbine equipment should be as large as possible subject to the above constraints. In surveying the available turbine equipment, the search rapidly narrows to a family of nonreheat, automatic admission industrial turbines manufactured by General Electric. The nominal turbine has an upper limit on generating capacity of ~100 MWe net when using 50.8 cm (20 in.) last-stage buckets in the low-pressure section. By going to a larger low-pressure section with 58.4 cm (23 in.) last-stage buckets, ~ 140 MWe could be produced. Use of the larger last-stage buckets results in a turbine design which is more susceptible to moisture erosion because of higher tip speed and poor performance under partial flow conditions. As a result, the turbine capable of producing 100 MWe of net power was selected for the baseline system. Using this turbine, some latitude exists as to the acceptable throttle steam conditions (from the receiver). General Electric has indicated that the inlet steam temperature may be specified at a level between ~482° and 538°C (~900 and 1,000°F) while the pressure may be specified somewhere in the range of

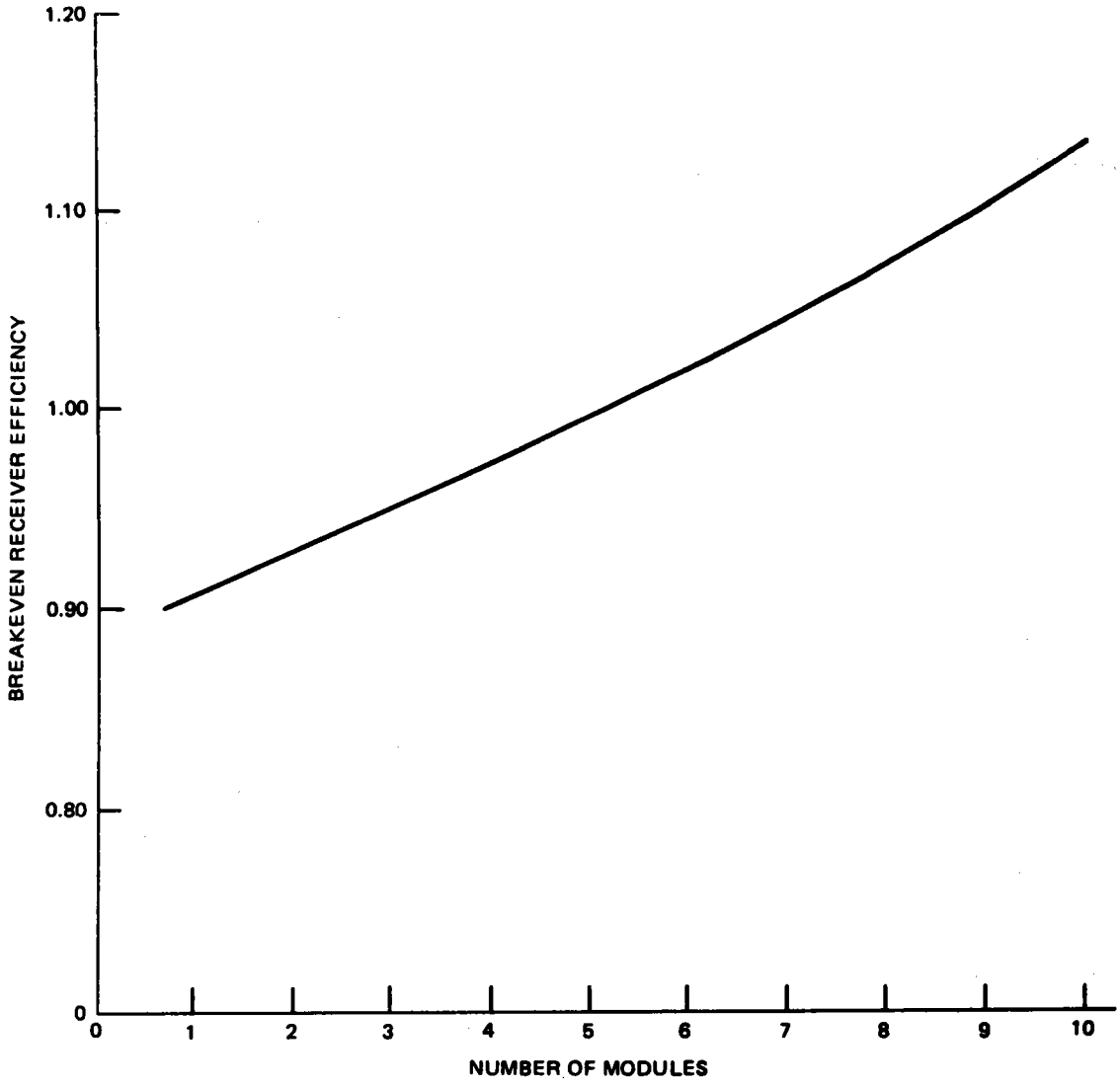

Figure 3-5. Receiver Efficiency Required for Breakeven Cost

8.72 to 10.1 MPa (1,265 to 1,465 psia). With these turbine limitations established, it is possible to introduce considerations of the other elements affecting the water/steam loop.

The final steam conditions were selected by giving consideration to all elements of the water/steam loop. Figure 3-6 indicates the nature of the interactions considered. The primary or throttle steam temperature was selected by considering limitations of the receiver and piping as well as those due to turbine. To ensure that the maximum temperature remained below 538°C (1,000°F), the receiver outlet steam temperature design point was selected at 516°C (960°F). This condition is sufficient to produce a turbine inlet steam temperature of 510°C (950°F). Thermal storage considerations were not treated in the selection of the primary steam temperature because the moderate temperature storage concept (Section 3.2.4) requires only 360°C (680°F) steam for its charging process.

The primary steam pressure condition was established by considering the thermal storage subsystem and the turbine which combine to form the major constraining factors for system pressure. To successfully charge thermal storage, it is necessary to have a sufficiently high steam pressure so that condensation occurs at a relatively high temperature. This influence of steam pressure on the charging process can be seen in Figure 3-7. It is seen that the charging flow at a pressure of 10.1 MPa (1,465 psia) stays to the right of the Caloria line which indicates that a positive temperature potential exists at all points for the heat transfer process. If steam pressure were lowered, the charging flow line would cross the Caloria line, resulting in an impossible charging condition. An increase in steam pressure would create a larger temperature potential for heat transfer, which would reduce heat exchanger requirements. The alternative of raising the charging side inlet steam temperature above the current value of 360°C (680°F) is unattractive since the Caloria is a temperature-limited fluid. By contrast, the turbine is constrained to operate at a pressure less than or equal to 10.1 MPa (1,465 psia). Thus, the only area of overlapping pressure conditions between the turbine and the thermal storage occurs at 10.1 MPa (1,465 psia), which was selected as the principal or throttle steam pressure. To allow for

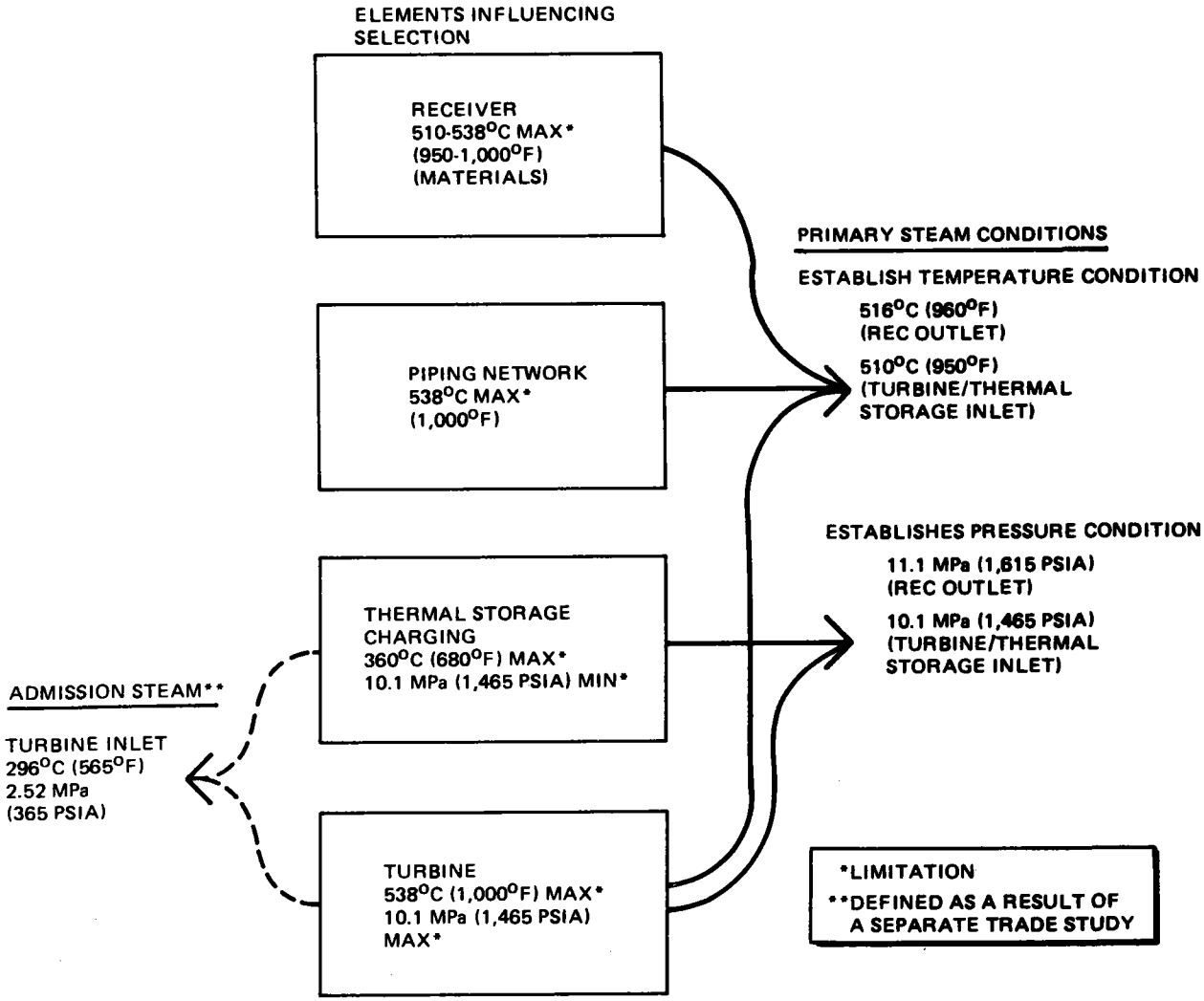

Figure 3-6. Selection of System Steam Conditions

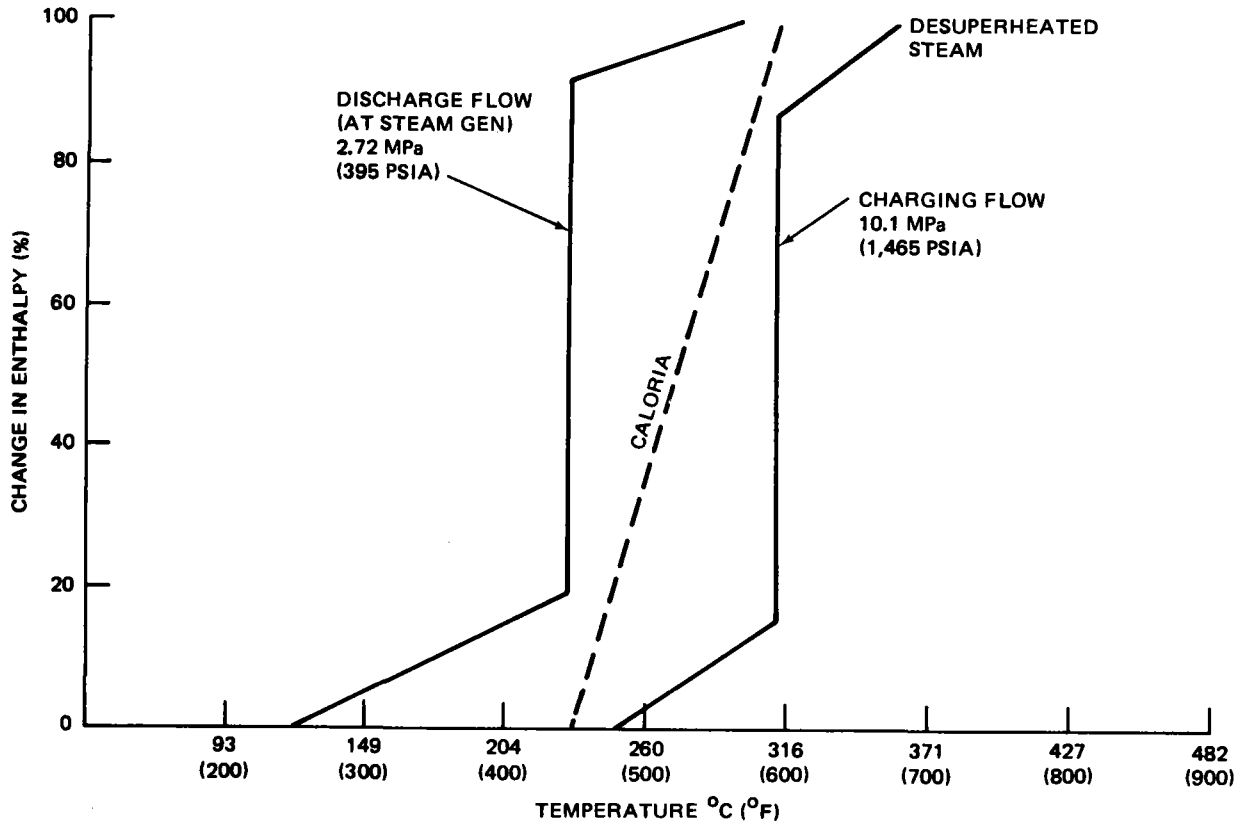

Figure 3-7. Thermal Storage Charging and Discharging Characteristics (Commercial System)

piping pressure drop between the receiver and the turbine/thermal storage, a receiver outlet design pressure of 11.1 MPa (1,615 psia) was selected.

3.2.4 Thermal Storage/Turbine Admission Steam Conditions

In selecting the preferred approach to thermal storage several key system issues were addressed. First, from an overall requirement standpoint, the thermal storage must serve as a source of steam of sufficiently high temperature and pressure to allow the turbine-generator to produce at least 70 MWe net when operating exclusively from thermal storage steam. In addition, this generation rate should occur with approximately the same turbine flow as would occur during design point operation directly from receiver steam. This eliminates the need to oversize the turbine for thermal storage operation which would result in an off-design flow condition occurring whenever the turbine operated exclusively from receiver steam. Once a thermal storage approach was determined which satisfied these minimum design and performance conditions, other options to thermal storage were considered which increased performance at an increase in cost. Before a final selection was made, issues such as simplicity and the impact on water steam loop controllability were also considered.

The baseline thermal storage approach which was originally proposed is shown schematically in Figure 3-8 along with the charging and discharging side water/steam conditions. The approach represents a minimum-cost, moderate-temperature approach to thermal storage that employs a Caloria and rock mixture as the storage media. Extensive discussions were carried out with General Electric to determine the suitability of the resulting steam conditions with the 70-MW turbine operating requirement. It was determined that these steam conditions were satisfactory for the generation of 70-MWe net power at a turbine steam flow rate which is similar to the flow rate experienced during design point operation directly from receiver steam.

A series of higher-temperature thermal storage options were considered in an effort to improve turbine cycle efficiency when operating on admission steam. A general schematic which is representative of these options is shown in Figure 3-9. These options all replaced the desuperheating function

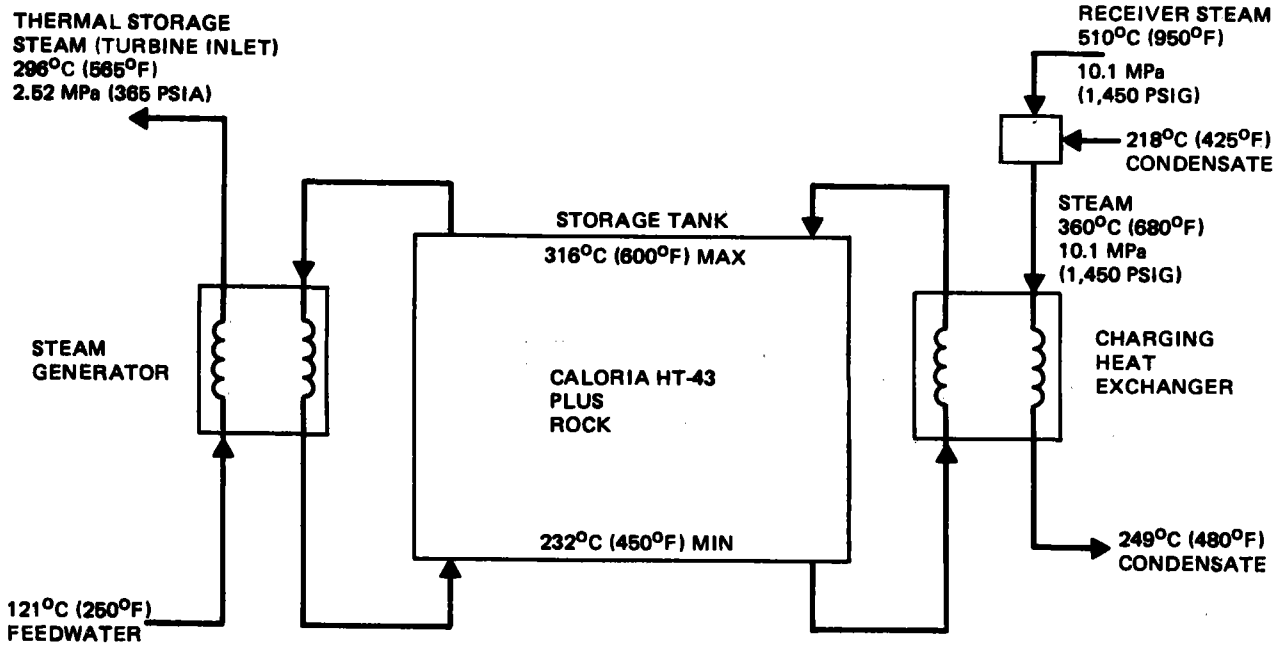

Figure 3-8. Baseline Commercial Thermal Storage Concept

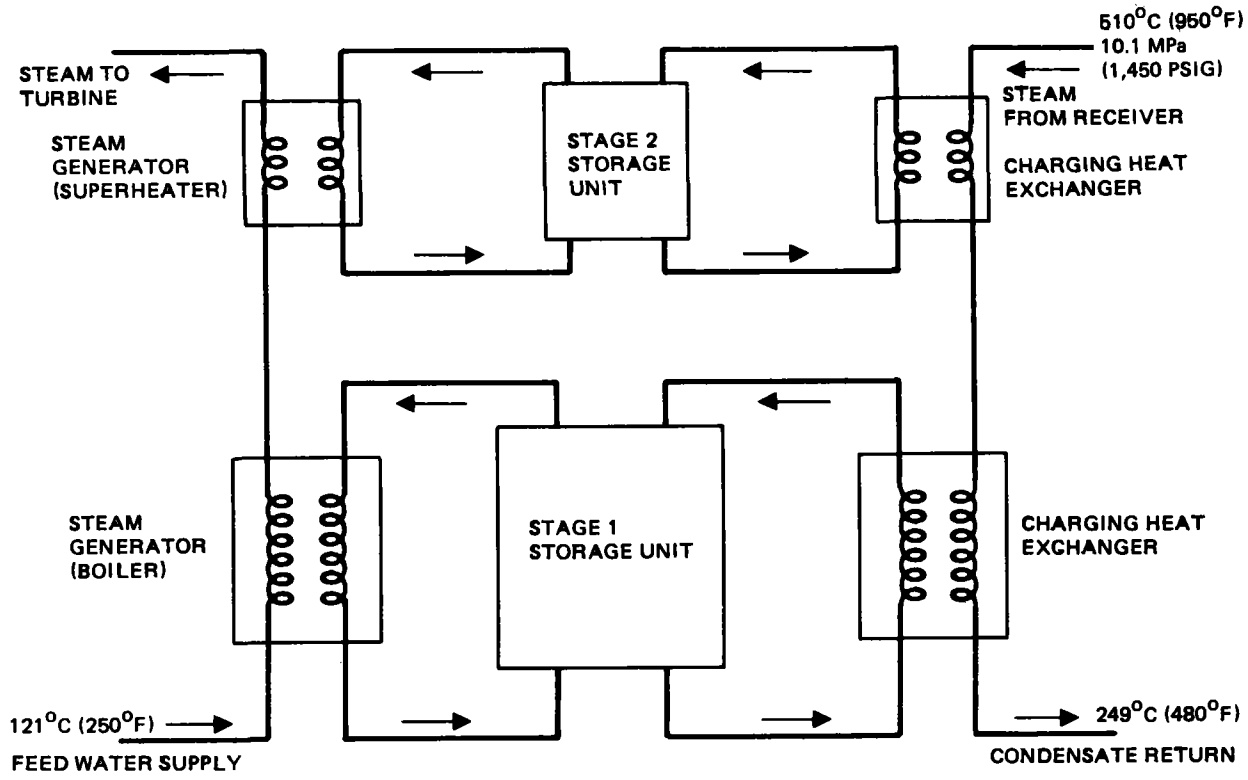

Figure 3-9. Alternate Thermal Storage Concepts

with a separate high-temperature storage loop which would be used to significantly increase the superheat level of steam produced in the steam generator.

The results of the comparative evaluation are shown in Figure 3-10. The first case represents the baseline design which is capable of producing steam at a temperature of 296°C (565°F). The rest of the cases all included a Hitec topping loop and assume a thermocline approach to energy storage. For Cases 3 and 5, a Hitec/rock mixture was assumed for the upper-storage loop. The results, expressed on a relative basis, indicate that the baseline design approach using the moderate-temperature storage approach is superior to all but the third case. This means that the storage subsystem cost associated with achieving higher steam temperatures and higher cycle efficiencies more than offset the benefit to be derived through an increase in annual energy output. The overall superiority of Case 3 is expected because it preserves the attractive Caloria/rock feature of the baseline design but also adds a cost-effective Hitec/rock topping cycle. Due to unknowns related to Hitec/rock compatibility, as well as Hitec solidification issues in a rock bed, this case was not selected as the baseline design approach. Additional subsystem development work to verify the approach appears to be attractive.

As a result of the turbine compatibility issues and economic factors just presented, the moderate temperature approach to thermal storage was selecte This approach is based on the use of a Caloria/rock mixture which employs a thermocline as the method of storage. The Caloria will be exercised over a temperature range from 232° to 316°C (450° to 600°F). The resulting steam conditions at the inlet to the turbine admission port are a temperature of 296°C (565°F) with a pressure of 2.52 MPa (365 psia). The steam-generation process which occurs in the steam generator is shown in Figure 3-7. The indicated pressure conditions correspond to that leaving the steam generator. It is seen that the pressure is limited by the lower pinch-point effect. A significantly higher pressure would cause the Caloria and discharge lines to intersect, which would be impossible from a heat-transfer standpoint.

CASE	THERMAL STORAGE STEAM TEMP (°C)	(°F)	RELATIVE COST OF ENERGY
1. CALORIA/ROCK (BASELINE)	299	(570)	1.0
2. CALORIA/ROCK PLUS HITEC	400	(750)	1.2
3. CALORIA/ROCK PLUS HITEC/ROCK	400	(750)	0.65
4. ALL LIQUID (CALORIA, HITEC)	400	(750)	2.49
5. ALL HITEC/ROCK	400	(750)	3.14

Figure 3-10. Comparison of Thermal Storage Concepts

3.2.5 System Capacity and Hours of Storage

To complete and conceptual definition of the Commercial system, it was necessary to develop a sizing relationship between the collector field, thermal storage subsystem, and turbine. The basic investigation required involved a tradeoff between energy collection capacity and the ability of the balance of the system, particularly the thermal storage subsystem and turbine-generator, to accommodate the collected energy in a cost-effective manner. The independent variables for this analysis were solar multiple, which is directly related to energy collection capacity, and hours of storage. It was assumed for this analysis that the turbine-generator equipment was sized to produce 100 MW of net electrical power at the design operating point. The results of the analysis as it impacts the relative cost of electrical energy on an annual basis are shown in Figure 3-11. The 3- and 6-hr storage levels considered represent areas of interest to the Department of Energy. As indicated, the results are based on an investigation of a single solar plant exclusive of network integration consideration. Also, when operating from thermal storage, a power output level of 70 MWe is assumed, as opposed to the 100-MWe value associated with receiver operation.

From the results in Figure 3-11, it is seen that minimum cost points occur for solar multiples of 1.4 and 1.7 for 3 and 6 hr of storage with the 3-hr optimum being ~ 2% less costly than the 6-hr optimum point. As one moves to the left of a minimum cost point, i.e., to a lower solar multiple, the increase in the cost of energy is due to the undersizing of the collector field which results in the nonuse of part or all of the thermal storage capacity that is unused capital equipment. As one moves to a solar multiple greater than the indicated optimum value, the energy collected exceeds the capability of the thermal storage subsystem and turbine-generator equipment to accommodate the energy and a condition of excessive energy spillage results. Implicit in this analysis is a solar insolation level of 950 W/m^2. The analysis was repeated for postulated varying insolation models and the results were found to be essentially identical.

Before selecting one of the two minimum-cost conditions as the baseline sizing point for the Commercial system, a more detailed investigation of system performance was carried out for these two points of interest. A comparative

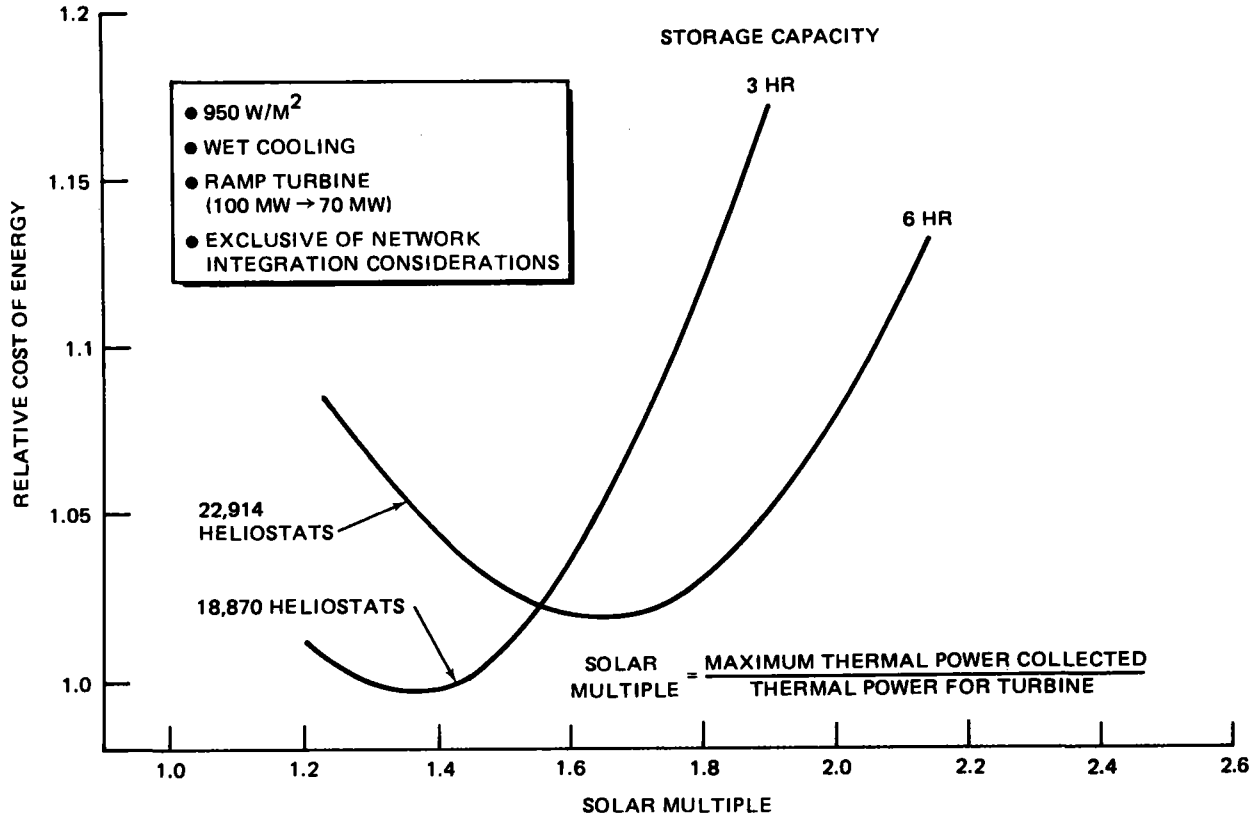

Figure 3-11. Relative Cost of Annual Energy

tabulation of the output on a daily basis for representative days of the year is shown in Tables 3-3 and 3-4 for the SM = 1.4, 3-hr storage and the SM = 1.7, 6-hr storage cases, respectively. The charts subdivide the energy collected during the day (left column) into the portion fed directly to the turbine and the excess energy which goes to charging thermal storage. In both of the tables, it is seen that the "excess energy" exceeds that necessary to fill thermal storage during summer periods of high energy collection while an underfill condition would exist during Winter periods of low energy collection. This of course is the natural result one would expect from the optimization analysis. Drawing attention to the "December 21" entries, it is seen that operation directly from the receiver could be maintained for between 6 and 6.6 hr, depending on the case considered. If operation is then shifted to thermal storage, an additional 1.62 or 2.96 hr of generation capability would exist.

Viewing these results from a network integration standpoint, it is seen that the wintertime characteristic of the SM = 1.4, 3-hr storage design, is incompatible with normal demand curves for the southwestern United States where nighttime peak demands continue until the 7 to 10 PM period. Even if daytime turbine startup is delayed to fully charge the 3-hr storage, marginal nighttime capability at best is provided. On the other hand, the SM = 1.7, 6-hr storage configuration would possess a 3-hr charge under normal conditions where excess energy is fed to storage. The capability to operate from storage could be expanded to 6-hr by delaying the startup of the turbine. This greater storage capability would be much more compatible with the typical nighttime Winter demand and thus appears to be the most attractive approach to system sizing. In addition, the cost of backup generating capacity which would be required on the network more than offsets the 2% higher system cost of energy indicated in Figure 3-11 for the SM = 1.7, 6-hr storage case. For this reason, the SM = 1.7, 6-hr storage case was selected as the baseline system capacity upon which expanded cost and performance studies could be based.

As a point of comparison to the baseline Commercial system design (solar multiple = 1.7, 6 hr of storage), upon which the detailed design and cost data was developed, an alternate Commercial system definition has been developed. The alternate configuration is sized for a solar multiple of 1.4, with 3 hr of storage, and corresponds to the minimum point on the left curve

Table 3-3

SYSTEM PERFORMANCE SUMMARY

(SOLAR MULTIPLE = 1.4, 3-HR STORAGE)

Day	Total Collection Capability (MWHt)	Direct Turbine Operation (100 MWe) Required Energy (MWHt)	Period (Hr)	(Decay)*	Excess Energy (MWHt)	Energy To Storage (MWHt)	Period of Operation From Storage 70 MWe (Hr)	Spillage MWHt	(%)
Jun 21	4,375	3,294	10.6	(0.5)	1,081	879	3	202	4.6
May 21/ Jul 21	4,228	3,234	10.4	(0.5)	994	879	3	115	2.7
Apr 21/ Aug 21	4,040	3,130	9.8	(0.4)	910	879	3	31	0.8
Equinox	3,642	2,796	9.1	(0.3)	846	846	2.89	0	0
Feb 21/ Oct 21	3,073	2,349	7.6	(0.3)	724	724	2.47	0	0
Jan 21/ Nov 21	2,572	2,037	6.6	(0.25)	535	535	1.83	0	0
Dec 21	2,333	1,859	6.0	(0.25)	474	474	1.62	0	0

*Period of transition from 100 MWe to 70 MWe net output.

Table 3-4

SYSTEM PERFORMANCE SUMMARY

(SOLAR MULTIPLE = 1.7, 6-HR STORAGE)

Day	Total Collection Capability (MWHt)	Direct Turbine Operation (100 MWe) Required Energy (MWHt)	Direct Turbine Operation (100 MWe) Period (Hr)	Excess Energy (MWHt)	Energy to Storage (MWHt)	Period of Operation From Storage 70 MWe (Hr)	Spillage MWHt	Spillage (%)
Jun 21	5,290	3,485	11.7	1,805	1,757	6.0	48	0.9
May 21/ Jul 21	5,202	3,396	11.4	1,806	1,757	6.0	49	0.9
Apr 21/ Aug 21	4,905	3,158	10.6	1,747	1,747	5.96	0	0
Equinox	4,422	2,860	9.6	1,562	1,562	5.33	0	0
Feb 21/ Oct 21	3,731	2,443	8.2	1,288	1,288	4.40	0	0
Jan 21/ Nov 21	3,122	2,115	7.1	1,007	1,007	3.44	0	0
Dec 21	2,832	1,966	6.6	866	866	2.96	0	0

of Figure 3-11. The impact of reducing the solar multiple and hours of storage not only reduces the size of the collector field and thermal storage subsystem but also reduces the tower height, receiver size, and maximum receiver flow rate. A comparative tabulation of the pertinent physical characteristics for the two commercial system configurations is shown in Table 3-5. It is seen that all parameters except the last two experienced a reduction in value when going from the baseline to alternate configuration. The thermal storage maximum charge rate was held constant since the 255-MWt level would represent a fairly good design point for the alternate design configuration whereas it is significantly undersized for the baseline configuration. The maximum discharge rate is held constant because we assume that the same admission steam requirement must be maintained in the two cases.

Table 3-5

COMMERCIAL SYSTEM CONFIGURATION COMPARISON DATA

	Baseline Design (Solar Multiple = 1.7, 6 Hours of Storage)	Alternate Design (Solar Multiple = 1.4, 3 Hours of Storage)
Number of Heliostats (37.95 m^2 per Heliostat)	22,914	18,870
Collector Field Area (x 10^6)	3.66m^2 (39.38 ft^2)	3.01m^2 (32.43 ft^2)
Tower Height	242m (794 ft)	220m (722 ft)
Receiver Centerline Elevation	268m (879 ft)	246m (807 ft)
Receiver Size		
Diameter	17m (56 ft)	15.4m (50.5 ft)
Height	25.5m (84 ft)	23.1m (75.8 ft)
Maximum Receiver Absorbed Power	506 MW	416.7 MW
Maximum Receiver Flow Rate	211.2 Kg/Sec (1.673 x 10^6 Lb/Hr)	174 Kg/Sec (1.378 x 10^6 Lb/Hr)
Thermal Storage Maximum Charge Rate	255 MWt	255 MWt
Thermal Storage Maximum Discharge Rate	284 MWt	284 MWt

3.3 COLLECTOR FIELD OPTIMIZATION

The optimization of the collector field represents a major area of concern which must be addressed in arriving at a cost-effective Commercial system design. The University of Houston has been actively investigating this problem for four years and has developed an extensive set of computer codes. The codes are designed to define the optimum collector field configuration and provide detailed receiver heat flux and panel power distribution.

The optimization process must necessarily start with a known set of cost, performance, and environmental factors. Since the cost data matures continuously as the system and subsystem design activities proceed, the optimization activity must be continuously updated. In addition, because of environmental variations which occur from one site to another, an optimized collector field is only appropriate for a specific site of interest.

The Commercial system cost estimates upon which the optimization analysis was based were developed for the PDBR and have been revised in selective areas. It is the intention of the University of Houston to reverify the Commercial system collector field subsequent to the PDR by using a complete set of PDR cost data. In addition, the latest performance and environmental data will also be used.

The present collector field optimization discussion contained in the subsequent subsections treats work carried out by the University of Houston up to May 1977. From a system design standpoint, however, a design freeze was imposed in December 1976 to which all system and subsystem design activity was to respond. As a result, the University of Houston developed and worked with some numbers which are not reflected in the Commercial system design presented in the rest of this volume. This section, however, contains an internally consistent set of information which describes the optimization problem, and the optical simulation model and computer optimization problem, and the optical simulation model and computer optimization procedure, and summarizes results of the optimization studies.

3.3.1 The Optimization Problem

This section is concerned with the optical behavior of the collector field and its interaction with the receiver. The University of Houston has a

computer model of this behavior and has considered methods which lead to an economically optimized design of the collector field. Factors treated in this section include:

A. The nature of the desired optimization and the resulting figure of merit.
B. The economic model for the Commercial system.
C. The design requirements.
D. The basic variables of the collector field geometry and various practical subsets.
E. The mathematical formulation of the optimization and its computerized solution.
F. The optimized designs and resulting system performance.

The collector field contains a large number of heliostats whose location with respect to the receiver and with respect to each other creates an intricate design problem. Heliostat location is measured with respect to the base of the tower. An optimized set of heliostat coordinates provides an optimized collector field for the present purposes.

The tower-top receiver is designed to absorb solar energy and to deliver this energy to an electric utility for electric power production. The best economic measure of performance for this composite system is a suitably adjusted busbar cost estimate for the output electric power. However, it is felt that an effort to optimize the collector field geometry via busbar cost would make the collector field design too difficult, and much too dependent on the design of the thermal storage system, the turbo-generator system, and the capacity displacement credits. It seemed desirable to consider the tower-top receiver as a source of thermal energy which can be "sold" to the utility system and therefore the cost of thermal energy at the base of the tower can be used as a suitable figure of merit for the optimization of the collector field. The specific figure of merit used for the optimization analysis was defined as the capital cost of the energy collection equipment (collector field, receiver, tower, and vertical piping) divided by the annual thermal energy delivered at the base of the tower.

A series of environmental and hardware-related factors which influence cost and performance of the energy collection equipment must be treated in the overall optimization process. The factors include:

A. Percent of possible insolation due to local weather conditions.
B. Heliostat related factors: reflectivity, dust, guidance errors, and malfunction.
C. Shading and blocking losses due to neighboring heliostats.
D. Startup and shutdown losses due to wasted insolation and heat.
E. Atmospheric transmission losses between heliostat and receiver.
F. Receiver related factors: interception, absorptivity, emissivity, convection, and conduction.
G. Parasitic energy requirements for heliostat guidance and coolant pumping.

The central receiver system concept is an optical concept and as such it can be optimized over many design variables which are not included in the collector field layout. The heliostats are optimized for mass production cost savings and performance under reasonable loads. This is basically a mechanical problem and the resulting heliostat design is an input to the collector field problem. Specifically, heliostat size is fixed. The tower design is also basically a mechanical problem; however, in this case, the tower height must be specified to satisfy the design requirement for a specified total thermal power, which in turn must satisfy the name plate power requirements for the utility power plant. Consequently, the tower height becomes a byproduct of the collector field optimization.

The receiver design also affects the optical performance of the system. However, for our purposes, it is assumed as given. Receiver size was optimized at an earlier stage when various receiver geometries were being considered. The receiver size is adequate to handle the required power and its configuration is appropriate for the anticipated variation in flux distribution with time. The resulting interception is acceptable and can be optimized by varying the aiming strategy, which is independent of the collector field layout. (See Table 3-6.)

Table 3-6

INTERCEPTION PERFORMANCE AVERAGES

System	Aiming Strategy	Interception	Flux Spillage
Commercial	3 point	95.8%	4.2%
	Hi-Lo	97.0%	3.0%
Pilot	Hi-Lo	98.0%	2.0%

The receiver design is complicated by many considerations. The basic design assumed for the optimization analysis is a cylindrical external receiver with vertical straight-through heating tubes. The two most serious design requirements (in addition to interception) are the flux density limit and the panel power minimum. Any heat-transfer device has a flux density limit, beyond which some form of damage or malfunction will occur.

The cylindrical receiver contains 24 panels subdivided into 6 preheat and 18 boiler panels with each boiler having its own sensor and flow control valve. Flow control must be positive, and because of the erratic nature of the two-phase flow, a limited range of flow control is possible. Consequently, it is necessary to maintain a minimum panel power at all times during useful operations. Furthermore, the manifolds will fail to distribute flow to all of the tubes in a given panel if the flux gradient across the panel is excessive. Hence a limitation on maximum flux gradients across a panel is also imposed.

The procedure is as follows:

A. Set scale of system by specifying the total thermal power at equinox noon.

B. Scale receiver dimensions to satisfy flux density limit assuming that adjustments will be made in the aiming strategy.

C. Optimize the collector field.

D. Adjust the aiming strategy to reduce the bright spots on the receiver.

E. Adjust the trim of the field to satisfy panel power minimum if necessary. At 35^{o} latitude, the southern field tends to be weak, and becomes weaker as latitude increases. A slight departure from

optimization may be required here, although the use of preheat panels in the southern quadrant of the receiver removes most of this problem.

F. Scale tower height and collector field to achieve exactly the desired system power level.

G. Generate final heliostat coordinates.

At this point, it is assumed that the heliostats are identical and that the centers of the heliostats are co-planar so that the collector field is flat, although it may have a slope. Allowance for contours in the collector field is a step beyond the current state of the art. The intersection of the tower center line with the plane of the heliostats determines a natural origin for coordinates of the heliostats in the collector field. The complete list of heliostat coordinates can be visualized as a set with the following additional structure. Let H be a heliostat in the set of heliostats S, so that the list of heliostat coordinates, $\hat{L}$, can be expressed as

$$\hat{L} = \{(x_H, y_H) \mid H \in S\},$$

where (x_H, y_H) gives the coordinates of heliostat H. Now let H be identified by a pair of integers (i, j) such that

$$H \leftrightarrow (i_H, j_H)$$

(i.e., H is in one to one correspondence with (i_H, j_H)). Consequently, the list of coordinates can be written as

$$\hat{L} = \{[x(ij), y(ij)] \mid (ij) \in S\}$$

and the mapping from S to the collector field is given by the functions x(ij) and y(ij) which are determined by the optimization procedure. If the coordinates are expressed in units of heliostat width, the coordinate mapping can be visualized as an actual layout process in which the heliostats are moved from a storage area where they are kept in a state of rectangular closest packing, so that their coordinates are (i_H, j_H) in heliostat units.

For the Pilot Plant, i becomes a circle label and j becomes an azimuth label. For the Commercial system, a more complicated listing will be required when the final stage is reached. A cell structure is anticipated with a list as above in each cell. In addition, some thought is required to assign heliostats to their field controllers.

Historically, the collector field design has been approached by assuming the simplest possible layout and gradually adding variables, but never allowing a chaotic solution to occur. In general, the optimization is not unique and leads to chaotic solutions similar to dislocations in a crystal. This type of result is to be expected from a straightforward rigorous minimization of the figure of merit. For example, if L is an arbitrary set of heliostat coordinates and F is the figure of merit, then the optimization implies that

$$\hat{F} = \underset{\{L\}}{\text{MIN}}\, F(L) = F(\hat{L}),$$

where $\hat{L}$ is the optimized coordinate set. The function F(L) is difficult to construct, for several reasons:

A. There are many independent variables.

B. The insolation average must be performed numerically.

C. The instantaneous reflected power from each heliostat is a function of the heliostat coordinates, which has at least eight analytic branches. (Nonanalytic behavior from every shading and blocking event is expected. Normally eight neighbors can contribute events, hence eight branches.)

However, F(L), can be defined as follows. Let

$$F(L) = C(L)/E(L)$$

where C(L) is the dollar cost of the system and E(L) is the net annual thermal power delivered at the base of the tower. C(L) is determined by the economic model and is developed explicitly in Appendix C, "A Cellwise Method for Optimization of Large Central Receiver Systems." E(L) is determined by the optical model of the system and can be written as

$$E(L) = a\, E_o(L) - b,$$

and

$$E_o(L) = \sum_{H \epsilon S} \eta_H g_H(L) A_H,$$

where

A_H is the reflective area of a heliostat,

$g_H(L)$ is the annual total thermal energy reflected by heliostat H in a field specified by L,

η_H is the receiver interception factor for heliostat H, which is assumed to be time-independent for purposes of simplicity, and

$E_o(L)$ is the annual thermal power incident on the receiver.

The coefficients a and b contain the other losses as explained in Appendix C, so that E(L) becomes the net thermal energy delivered at the base of the tower.

Currently, the University of Houston computer facility is able to generate quantities such as $E_o(L)$ for a collector field, only if the summation is limited to several hundred terms. Consequently, it is necessary to adopt a system of representative heliostats, which is called the "cell-wise approximation for large collector fields." The expression for $E_o(L)$ is replaced by

$$E_o(L) = \sum_c n_c \eta_c g_c(D_c) A_H,$$

where η_c is the number of heliostats in a cell c. Consequently,

$$\eta_c g_c(D_c) = \eta_H g_H(L),$$

where H is the representative heliostat for cell C. The variables D_c are the displacements of the appropriate neighbors with respect to the representative heliostat. Hence D_c is a function of L, but not vice-versa in general.

The cell-wise optimization procedure presented in Appendix C proceeds along lines suggested by the expression for $E_o(L)$. Unfortunately, it leads to solution for the displacements and not the coordinates themselves. Fortunately, the results for the displacements vary smoothly from cell to cell. The use of representatives implies that each heliostat in a cell has a similar neighborhood. This assumption greatly reduces the number of independent displacements. In practice, the solution is carried out for two components, a radial-x component and an azimuthal-y component, as shown in Figure 3-12. The results show that y is nearly constant throughout the

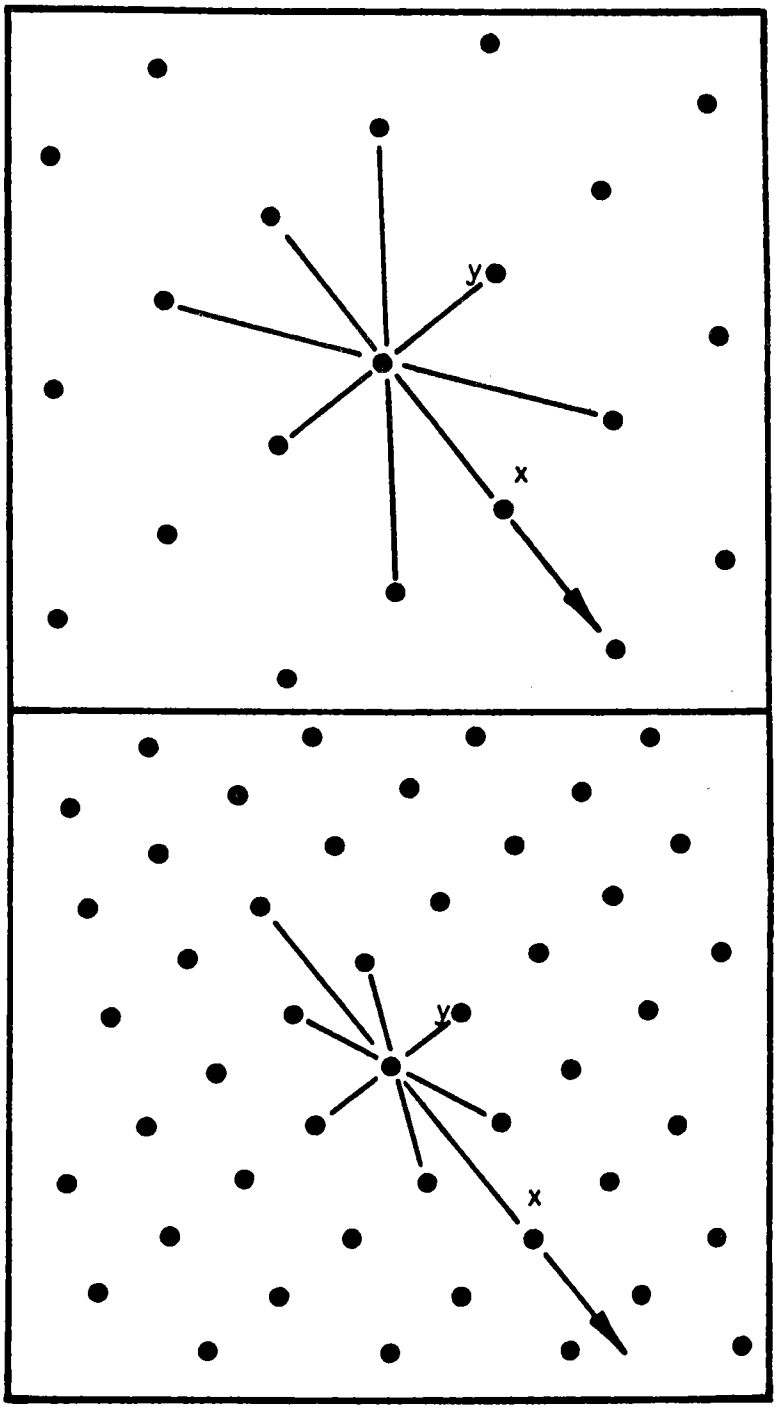

THE UPPER HALF SHOWS A CORNFIELD NEIGHBORHOOD AND THE LOWER HALF SHOWS A STAGGER NEIGHBORHOOD. THE HEAVY ARROW POINTS TO THE TOWER FOR RADIAL CASES AND IT POINTS NORTH FOR N-S CASES. THE (x, y) LABELS INDICATE THE INDEPENDENT VARIABLES OF THE GEOMETRY.

Figure 3-12. Cornfield and Stagger Neighborhoods

collector field, and that x is nearly independent of azimuth with respect to the tower. Furthermore, x can be represented as a quadratic function of the tower elevation angle.

3.3.2 Optical Simulation Model and Computer Optimization Procedure

The current view of the optical simulation model and collector field optimization problem for the large central receiver system contains the following components. (The assumptions made for the current 100-MWe study are indicated by asterisks and underlining. Relevant details will be given later.)

A. The Astronomical Model*
   1. Diurnal motion of sun.
   2. Insolation model for cloudless sky.
      a. Air mass for round earth.
      b. Water vapor, altitude, and turbidity parameters.
   3. Sample of times for daily and annual statistics.

B. The Collector Field Models
   1. Cell model with uniformly spaced representative heliostats and variable numbers of heliostats per cell. *
   2. Cell model with fixed number of heliostats per cell and suitably located representatives.
   3. Individual Heliostats each listed in computer storage.

C. The Heliostat Models
   1. Square with or without slotting and with or without canting to increase concentration. *
   2. Octagonal, and regular N-gons.
   3. Rectangular.

D. The Mounting System Models
   1. Alt-Azimuthal. *
   2. Radial-Pitch-Roll.
   3. Azimuthal-Pitch-Roll.
   4. Polar.
   5. Receiver-oriented

E. The Shading and Blocking Models*
   1. Optional inclusion of remote neighbors.
   2. Test for sun sensor.
   3. Each segment of whole heliostat.
   4. Options for greater speed and less accuracy.

F. The Guidance Error Model*
   1. Slope errors of reflectors.
   2. Aiming error of sensors (due to misaim and to mechanical flexion).
   3. Tracking errors.

G. The Image Generators (Appendix B)
   1. Analytic model.
      a. With convolution processor for guidance errors.
      b. With degraded sun to approximate guidance errors.
   2. Walzel's Hermite polynomial approximation method*

H. The Focusing Strategy and Abberation Model for Canted Heliostats

I. The Receiver Models
   1. Cylindrical external*
   2. Flat panel.
   3. Aperture for Cavity.

J. The Aiming Strategy Models
   1. Aim at belt of cylinder.
   2. Optimum two point high-low aim.
   3. Three point high-low aim*
   4. Five point high-low aim.
   5. Horizontal strategies.

K. The Cost Model
   1. Heliostats (including guidance, etc).*
   2. Tower.*
   3. Receiver.*
   4. Plumbing in tower.*
   5. Land for heliostat.*
   6. Wiring for heliostat.*
   7. Turbine generator system, etc.
   8. Thermal storage.
   9. Capacity credits.
   10. Water costs.
   11. Financial costs
   12. Operation and maintenance.

L. The Energy Loss Model
   1. Mirror reflection and receiver absorption.*
   2. Absorptivity vs angle of incidence.*

3. Reradiation and convection by receiver.*
4. Atmospheric losses between heliostat and receiver.
5. Interception losses at receiver.*
6. Thermodynamic cycle efficiency.
7. Pump power and other parasitic losses.

M. The Figure of Merit and Optimization Procedure*

1. Cost model.
2. Energy model with losses.
3. External constraints.
   a. Policy related choice of base time period.
   b. Definition of scale, i.e., power at equinox noon, etc.
   c. Mechanical clearance for heliostats and access ways.
   d. Flux limits for receiver.
   e. Flux gradient limits for receiver.
   f. Panel power minimum.

Computer programs are of four main varieties (LOSS, RCELL, YEAR, and LAYOUT).

3.3.2.1 LOSS Program

The LOSS program shows the amount of ground space required by a heliostat at each of the representative locations. This program calculates the MWH/m^2 of lost energy due to a single neighbor as a function of displacement from the representative heliostat. The LOSS program provides a good sun sample for the whole year and uses an efficient version of the shading and blocking processor which neglects overlapping events. Overlapping events are rare under optimized conditions. The LOSS prints provide a good starting point for further collector field optimization studies (see Figure 3-13). This is a small stand-alone program which can provide various comparison and/or sensitivity studies.

LOSS program outputs provide a quick estimate of the ground coverage fraction in each cell for all four optional arrangement schemes. Table 3-7 shows the percentage of advantage (i.e., higher ground coverage) for the radial stagger arrangement as compared to the next best alternative. Negatives indicate that a better alternative occurs. The radial cornfield is never best although it beats radial stagger in 3 out of 121 cells. The 24

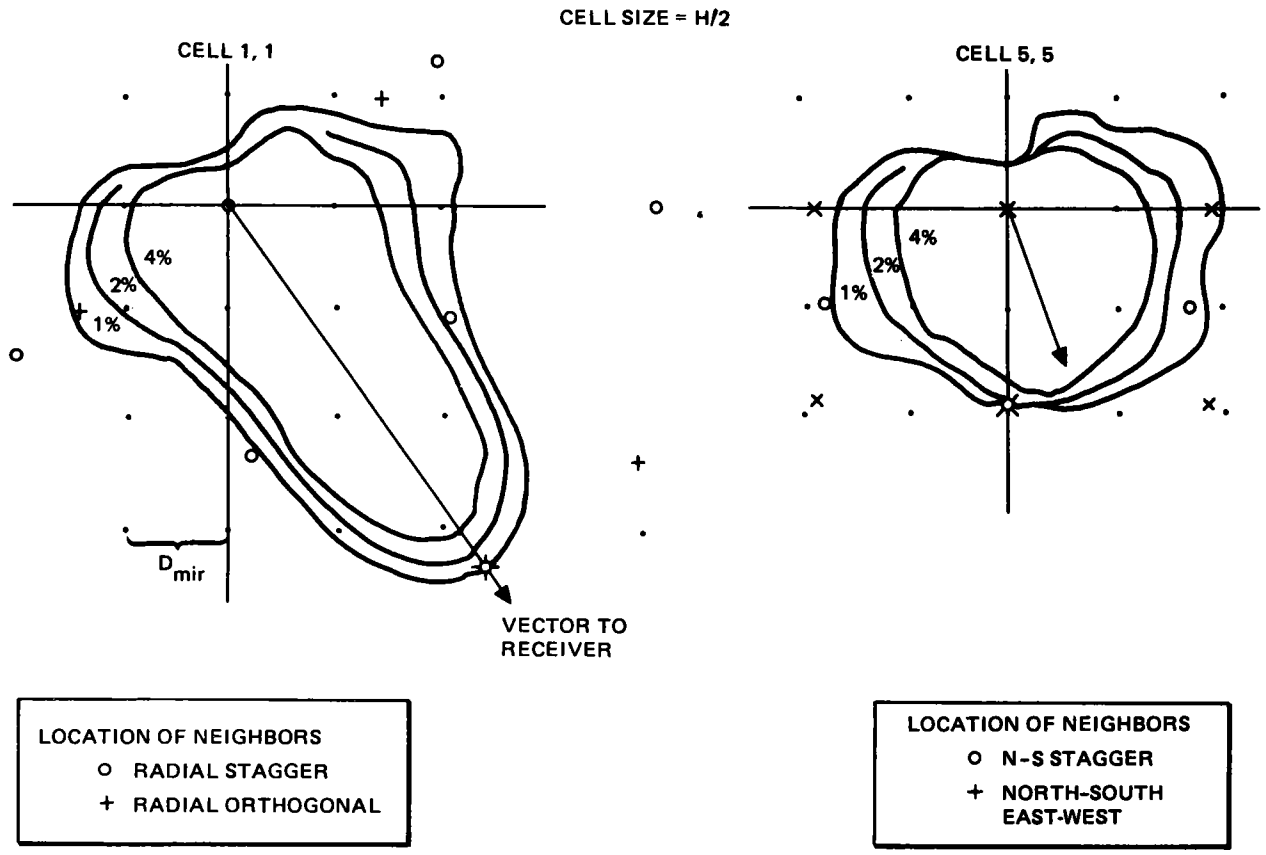

Figure 3-13. Heliostat Loss Footprints Annual Shading and Blocking Loss

Table 3-7

PERCENT OF ADVANTAGE FOR RADIAL STAGGER

(Note that J = 1 to 6 is the West Half Field)

	J =	1	2	3	4	5	6
I =	1	6.7	2.9	-3.0	-5.1	13.3	0.0
	2	6.5	12.2	1.2	2.9	13.5	0.0
	3	5.0	-0.6	-5.3	1.3	16.2	0.0
	4	-1.0	-6.8	-7.1	3.5	8.8	0.0
	5	5.9	1.0	-1.1	2.8	2.0	10.0
	6	6.8	4.3	-5.5	-7.2	-10.8	5.2
	7	11.6	12.2	7.6	6.5	-4.3	0.0
	8	12.8	3.8	3.0	-11.8	5.1	Tower
	9	-6.6	-1.5	-6.5	-12.8	4.8	0.0
	10	5.8	-18.6	-11.1	-14.3	-.006	0.0
	11	11.0	-4.9	-10.5	-11.1	7.7	0.0

negative entries represent 14 cells in which N-S cornfields are best and 10 cell in which N-S staggers are best. This picture can be modified by new results from RCELL when convergent outputs from all four options are obtained. The occurrence of large negatives in the southern field suggests that it might need special treatment, but this is not confirmed by the Pilot Plant study which assumed radial stagger throughout. The complications and unaccounted losses associated with chaotic cell boundaries and varying cell configurations were avoided by using the radial staggered array throughout our final Commercial and Pilot Plant studies.

3.3.2.2 RCELL Program

RCELL is the current collector field optimization program. It contains a complete simulation and its outputs are nearly complete. However, it requires an input data file for the panel interception factors. (These data are generated by projecting images from each representative heliostat onto the specified receiver as described in Appendix B and its references.) The RCELL program processes an input estimate of the collector field geometry and figure of merit and outputs an improved estimate. (See Figure 3-14.)

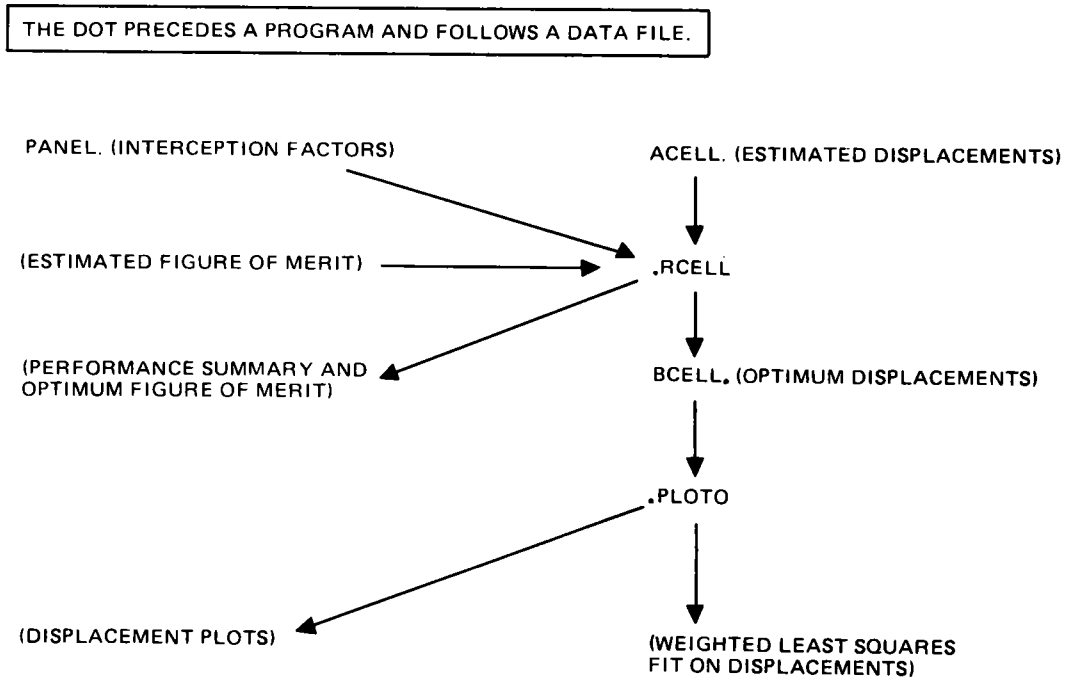

Figure 3-14. Data Flow Schematic For RCELL

It must be recycled until the step size is small enough and the output figure of merit is close to the input estimates for the figure of merit. The figure of merit converges rapidly, but the total system power is rather sensitively dependent on the input figure of merit. This program has an optional mode which allows rapid parametric studies.

Note that this program correctly accounts for the change in the total energy lost by the heliostats of a cell due to variations of geometry in the cell. Consequently, the best areas of the field (i. e., high cosine factor and good interception) will not become overcrowded, but will remain relatively "bright," meaning that they will produce more MWH/m^2 of reflected power than marginal areas.

Table 3-8 contains a sample of the inputs to RCELL.

Table 3-8 (Page 1 of 3)
RCELL INPUT DATA

JDVEQ = 2442859	Julian Day of vernal equinox for 21 March 1976
ALPHAL = .004660	Solar limb angle in radians
XLAT = 35	Latitude of site in degrees
ESUNO = 15.0	Elevation of sun at startup in degrees
NGON = 4	Number of sides for heliostat
NTOW = 1	Number of cells from center to tower
IMAX = 19	Number of sample hours = 3, 7, 11, ...
JMAX = 7	Number of sample days
NREAD = 66	Number of lines in ACELL file
ITAPE = 1	Equals 1 to write plot output: 0 not
JTAPE = 1	Equals 1 to write BCELL; 0 not
LTAPE = 1	Equals 1 to write ERGM2 :-1 to read : 0 neither
EGRND = 0	Slope of ground level in degrees
ZGRND = 180.	Azimuth of upward slope in degrees
NCEL = 11	Number of cells across collector field

Table 3-8 (Page 2 of 3)
RCELL INPUT DATA

NGEO = 4	Number of cells in displacement array
NDIV = 10	Number of divisions for interpolator
IPSAB = 0	Equals 2 for BV output; 0 not
ICNTR = 1	Equals 1 to contour: 0 not
IPDAY = 0	Equals 0 for no daily print; 1 for three days; 2 for every day
IAXIS = 1	Index of mounting system
ISUN = 1	Equals 0 for uniform WTS: 1 for Sine WTS
HT = 259.	Height of tower in meters
DA = HT*0.866025	Spacing between cell centers of collector
DMIR = 6.502	Width of heliostats in meters
HGLASS = 37.932463	Area of glass/helios in meters^2 (408.3 ft^2)
DGEO = 1./5.	Cell spacing for loss prints
DTRIM = 0.090	Trim control constant
CMW = 1.44	Centimeters of atmospheric water vapor
REARTH = 6370.	Radius of earth in kilometers
HATMOS = 8.430	Height of atmosphere in kilometers
RH = REARTH/HATMOS	Contains constants for cost model (100 MWe)
DFIXD = 7.260E6	Fixed cost in dollars
CTOWR = 8.5E6*((HT-22)/308.) **2 + 1.86E6*HT/315.	Tower cost
C1 = 66.	Heliostat cost in $/m2, first option
C2 = 83.	Heliostat cost in $/m2, second option
C3 = 100.	Heliostat cost in $/m2, third option
FM1 = 45.6	Figure of merit in $/MWH for C1 from trim
FM2 = 53.4	Figure of merit in $/MWH for C2 from trim
FM3 = 61.2	Figure of merit in $/MWH for C3 from trim
CL = 1.08	Cost of land in $/m2
CW = 5.00/.30480	Cost of wiring in $/m
CW = 3.30	Cost of wiring in $/m (alternate)
NF = 24	Number of heliostats/field controller
BOILER = 1.525	Conv and rad losses in MW per boiler panel
HEATER = 0.762	Conv and rad losses in MW per preheat panel

Table 3-8 (Page 3 of 3)
RCELL INPUT DATA

HYEARS = 3376.	Hours/year for sun above 15 deg at lat 35
PREPAN = 3	Half number of preheat panels in PANPOW
KPANL = 1	Equals first panel for FINT
ABSOR = 0.95	Absorptivity
REFLT = 0.91*1.0	Reflectivity and dust

3.3.2.3 YEAR Program

The YEAR programs occur in many configurations, depending on output requirements; however, they share a common approach to the collector field and the sun sample. Three configurations will be mentioned which yield outputs not available from RCELL.

YR/CYLN provides the receiver model. This program generates flux density and panel interception outputs. (See Figure 3-15.)

YR/PANPOW uses panel interception data to output receiver efficiencies and panel power behavior for the whole year. Some typical outputs are shown in Table 3-9.

YR/TRIM uses panel interception data. This program sorts the cells according to MWH/m^2, trims the field, and output performance for optional receiver designs with various panels deleted.

3.3.2.4 LAYOUT Program

The LAYOUT category of program is a final stage processor which generates the list of heliostat coordinates and the final output defining the associated aiming strategy. LAYOUT programs have been applied to the Pilot Plant system, but not yet to the Commercial system.

THE DOT PRECEDES A PROGRAM AND FOLLOWS A DATA FILE.

THE PANEL DATA FILE IS GENERATED BY THE SCHEME.

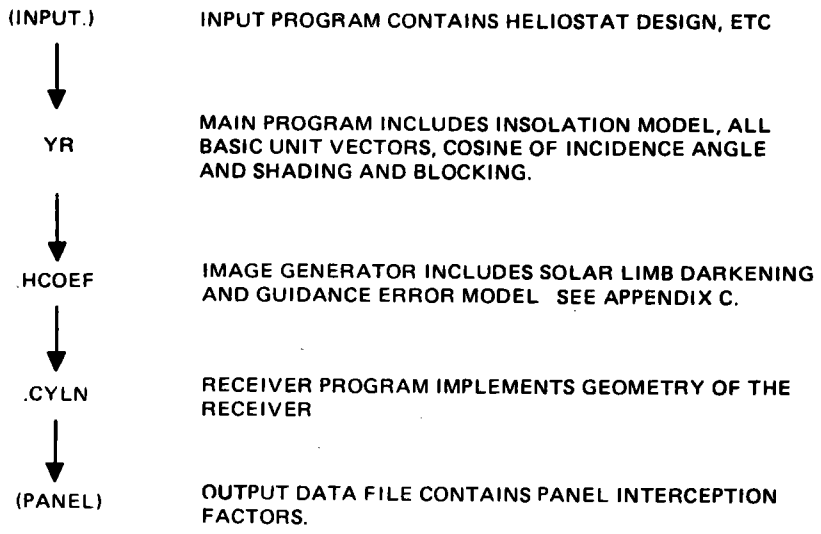

Figure 3-15. Data Flow Schematic For YR/CYLN

Table 3-9

SUMMARY OF RESULTS FOR PILOT PLANT

TOTAL ANNUAL RECEIVER POWER

(0.1724×10^6 MWH)

Diurnal Receiver Power in Megawatts

Day	Noon	1pm	2pm	3pm	4pm	5pm	6pm	Daily
92	53.79	53.17	51.54	48.89	44.75	36.98	21.74	574.80
122	53.81	53.20	51.56	48.82	44.41	35.02	19.88	565.00
152	54.02	53.44	51.70	49.67	43.26	33.19	15.02	541.80
182	53.81	53.30	51.28	47.50	39.40	25.06	2.81	491.00
212	52.85	52.16	49.62	44.16	31.27	12.08	00.00	428.20
242	50.98	49.97	46.40	39.29	24.38	1.22	00.00	376.6
272	49.83	48.53	44.33	36.56	21.55	00.00	00.00	351.3

Annual Summary of System Efficiencies (in percent)

Day	Noon	1pm	2pm	3pm	4pm	5pm	6pm
92	65.80	65.21	53.73	61.44	47.82	49.99	31.27
122	65.91	65.33	63.98	51.52	57.65	49.15	29.24
152	66.08	65.57	64.08	61.56	56.71	46.54	24.93
182	65.99	65.50	63.84	60.70	52.73	38.92	21.16
212	65.19	64.69	62.58	57.67	43.07	27.98	00.00
242	63.57	62.82	59.80	52.90	36.35	4.23	00.00
272	62.59	61.38	57.41	50.03	34.10	00.00	00.00

Annual Summary of System Efficiencies/CosI (in percent)

Day	Noon	1pm	2pm	3pm	4pm	5pm	6pm
92	77.95	77.74	77.48	77.17	76.03	69.72	46.80
122	77.88	77.71	77.51	77.18	75.79	69.61	43.91
152	77.81	77.74	77.57	77.14	74.62	65.22	31.71
182	77.97	77.84	77.49	76.35	69.75	54.93	32.28
212	77.69	77.63	76.72	73.25	57.95	21.99	00.00
242	76.93	76.33	73.94	67.94	49.01	6.07	00.00
272	79.00	75.03	71.64	64.59	46.18	00.00	00.00

Annual Summary of Cosines

92	0.8470	0.8415	0.8253	0.7990	0.7634	0.7202	0.6713
122	0.8488	0.8432	0.8267	0.7998	0.7635	0.7192	0.6692
152	0.8512	0.8454	0.8282	0.8001	0.7622	0.7159	0.6635
182	0.8486	0.8427	0.8250	0.7962	0.7573	0.7099	0.6564
212	0.8394	0.8335	0.8160	0.7875	0.7432	0.7026	0.0000
242	0.8282	0.8225	0.8056	0.7781	0.7412	0.6966	0.0000
272	0.8229	0.8173	0.8007	0.7737	0.7375	0.0000	0.0000

Annual Summary of Shading and Blocking Effects

92	0.9998	0.9991	0.9976	0.9988	0.9974	0.9619	0.8003
122	0.9997	0.9990	0.9979	0.9987	0.9969	0.9531	0.7707
152	0.9997	0.9989	0.9984	0.9984	0.9894	0.9115	0.6795
182	0.9998	0.9993	0.9989	0.9928	0.9558	0.2017	0.3917
212	0.9973	0.9974	0.9937	0.9657	0.8544	0.6452	0.0000
242	0.9834	0.9832	0.9716	0.9011	0.7506	0.5448	0.0000
272	0.9696	0.9688	0.9501	0.8625	0.7064	0.0000	0.0000

3.3.3 Results from the Optimization Studies

3.3.3.1 Conclusions

One of the conclusions developed during the optimization analysis is that the total number of heliostats in the collector field determines the approach to the optical simulation problem. For large central receiver systems, it is desirable to introduce a cell model which establishes an array of representative heliostats. An arsenal of computer programs now exists which allows the arrangement of heliostats in the collector field to be optimized subject to the approximations of the cell model. Each cell contains an arbitrary regular two-dimensional array of heliostats. For practical reasons the current study of the 100-MWe Commercial system has been limited to four categories of heliostat arrangement: (1) radial cornfields, (2) radial staggers, (3) N-S cornfields, and (4) N-S staggers. (See Figure 3-12.)

The most important results from the 100-MWe Commercial system optimization study are:

A. Staggers are better than cornfields.

B. Improved optimization techniques and heliostat arrangements, as well as increases in the estimated cost of the tower and receiver subsystems, has moved the solution to a larger cell size and a shorter tower.

C. No panels should be deleted from the south side of the cylindrical receiver; however, the four panels in the southern quadrant should be converted to preheat panels.

D. The collector field trims to a 360-deg configuration. However, the center of the collector field is north of the tower and some compromise can be made to prevent excessive panel power asymmetry.

3.3.3.2 Projections for Final Commercial System

The current Pilot Plant collector field is based on a Commercial baseline design that was frozen in December of 1976. Since then a number of events have occurred which would lead to variations in the design. A discussion of

these variations will indicate the versatility of the present University of Houston techniques and will show that the events have tended to compensate; consequently, the current commercial baseline (and hence the current Pilot Plant) represents the desired optimum configuration reasonably well.

Adoption of the radial stagger configuration along with a high-low aim strategy has led to a significant improvement in heliostat performance, particularly at lower rim angles. Consequently the "optimum" field size for a focal height of 259m has tended to increase from the baseline of about 20,000 to about 30,000 heliostats. The cell area has been increased from the original $h^2/4$ to $2h^2/4$ for the baseline study to $3h^2/4$ for subsequent studies to accommodate the larger field.

Compensating effects include the addition of atmospheric losses between the heliostats and the receiver. Application of the LoTran II computer code to this problem has revealed losses of about 0.9%/100m for a visual range of 23 km, 0.6%/100m for v_r = 50 km, and 0.3%/100m for $v_r = \infty$ (i.e., no aerosols). This factor has the same effect as an interception loss and can easily be entered into the data base. Results for the relatively high loss of 1%/100m are shown in Table 3-10.

The effect of modifications in the cost formula can be handled with equal facility. These costs were frozen prior to March 1976 and new cost models for the first and the n^{th} plants are expected on 3 May 1977. The optimized system responds to the factor (heliostat cost divided by system cost); consequently, the results are not extremely sensitive to changes in heliostat costs. Nevertheless, when these revised costs become available, additional Commercial system optimization analysis will be carried out to verify the existing design and identify potential changes which can lead to a more nearly optimum design. In all cases, design changes will represent minor perturbations on the present design.

Some concern arose late in the preliminary design effort as to the effects of changes in the cost of wiring, since this acts preferentially to exclude remote heliostats and is similar in this respect to increased atmospheric losses.

Table 3-10

EFFECT OF ATMOSPHERIC LOSSES

Iteration	0	1	2	3
Loss Factor (%/100m)	0.0	1.0	1.0	1.0
"Interception" fraction	0.944	0.895	0.883	0.884
No. of Cells	99.0	66.5	83.5	82.0
Maximum Ground Coverage	0.462	0.449	0.500	0.496
No. of Heliostats (thousands)	29.633	23.002*	28.289	27.584
Equinox Noon Power (MWth)	740.4	544.8	653.4	639.9
Input Figure of Merit	62.6	64.0	68.2	67.9
Output Figure of Merit	62.51	68.28	67.88	67.87

*Observe that a low input figure of merit reduces the number of heliostats in the output field markedly (16% and 11%) while increasing the output figure of merit for the suboptimized field only slightly, 0.6% and 0.1%; i.e., the optimization is not sensitive to marginally effective heliostats.

A comparative analysis was carried out using initial and revised estimates for wiring and trenching costs. The results are shown in Table 3-11. In comparing the left and right columns, where input and output figures of merit converge, it is seen that the more expensive wiring assumption increases the figure of merit by ~13% but the optimum number of heliostats is reduced by only 3%.

3.4 WATER/STEAM LOOP DESIGN

The water/steam loop includes all elements of the receiver, thermal storage, turbine, and balance of plant equipment necessary for the flow and transfer of energy throughout the system. The close coupling which results between these elements creates a situation where a perturbation in one element can have a significant effect on the other elements of the loop. Thus, it is necessary to view the design, operation, and control of any of the elements in terms of their overall impact on the complete loop.

A schematic which shows the major elements and flow paths of the water/steam loop is shown in Figure 3-16. This schematic can be subdivided into the receiver subsystem (upper left), thermal storage subsystem (upper right)

Table 3-11

EFFECT OF CABLE COST INCREASE

Iteration	0	1	2
Cable costs ($/m)	3.30	16.50	16.50
Loss Factor (~%/100m)	0.0	0.6	0.6
"Interception" factor	0.944	0.914	0.908
No. of Cells	99.	72.3	83.
Maximum Ground Coverage	0.462	0.490	0.510
No. of Heliostats (thousands)	29.633	25.478*	28.616
Equinox Noon Power (MWth)	740.4	614.8	680.9
Input Figure of Merit	62.6	68.2	70.6
Output Figure of Merit	62.51	70.63	70.55
Cable Costs (% of Total)	1.81%	8.25%	8.25%

*Observe that a low input figure of merit reduces the number of heliostats in the output field markedly (16% and 11%) while increasing the output figure of merit for the suboptimized field only slightly, 0.6% and 0.1%; i.e., the optimization is not sensitive to marginally effective heliostats.

and balance of plant equipment including the turbine (lower half). Reviewing the design of the various subsystems in detail brings to light the close-coupled, highly interactive nature of the various elements.

The initial operating philosophy for the water/steam loop during a typical day was to provide sufficient receiver steam flow to the turbine in order to maintain its electrical output at the design point level with the balance of the steam being diverted to thermal storage. The high-temperature condensate leaving the thermal storage charging heat exchanger was then introduced into the feedwater heaters where it was mixed with turbine condensate and sent back to the receiver. The net effect of the mixing process is to reduce the quantity of steam which must be extracted from the turbine for feedwater heating.

A problem arose in using that approach for a high solar multiple system. In that case, the quantity of high-temperature condensate being routed to the feedwater heaters contains more energy than is necessary for the feedwater

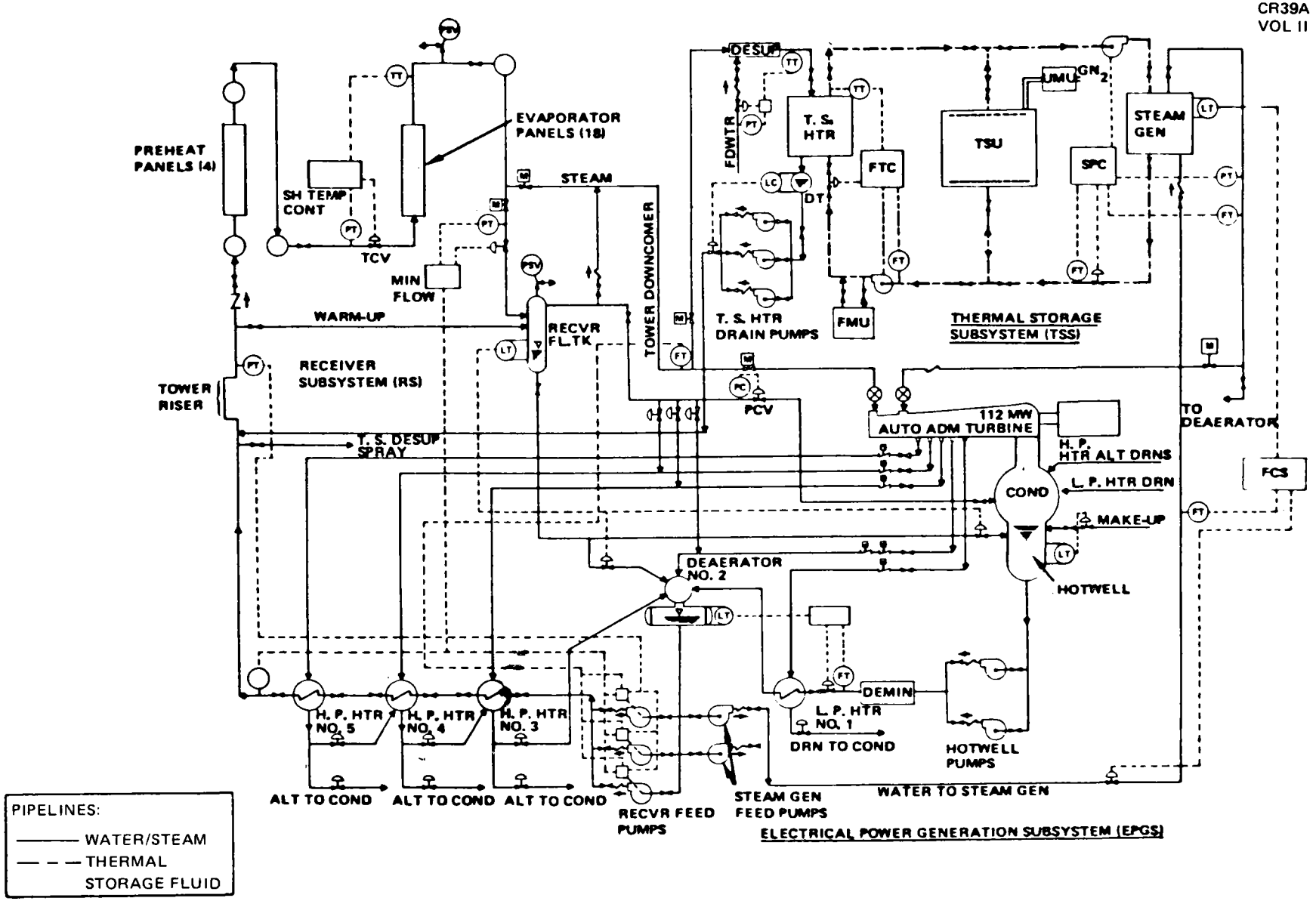

Figure 3-16. Overall Commercial System Schematic

heating operation. The effect of that flow is to shut down all turbine extraction ports with the exception of the one leading to the low-pressure heater. This resulted in an overflow situation for the turbine and an overall increase in the feedwater temperature leaving the final feedwater heater. The alternative available was to pass some of the flow through the condenser where the surplus heat could be rejected.

To alleviate this problem, a modification in the flow path was made. It is shown in Figure 3-16. In this approach, the high-temperature condensate is taken directly from the thermal storage charging heater and pumped into the riser at the base of the tower, thus bypassing the feedwater heater elements. This ensures that the turbine will operate with normal turbine extraction flows; the turbine overflow problem thus is eliminated. It does, however, require the use of additional pumps downstream of the thermal storage charging heater to inject the flow into the riser. In addition, the mixed feedwater temperature going to the receiver is now 231°C (448°F) for rated receiver steam operation and 249°C (480°F) for derated receiver steam operation. This corresponds to a value of 218°C (425°F) which occurred in the previous design approach. The net effect of the increase in receiver inlet temperature on the receiver design is to force a reduction in the number of south side preheat panels from 6 to 4.

The receiver subsystem portion of the schematic shown in Figure 3-16 depicts both the preheat and evaporator (boiler) panels that are plumbed in series. The 4 preheat panels are plumbed into two groups of 2 while the 20 evaporator panels all operate in parallel. On the outlet side of the receiver is a receiver flash tank to which the flow is diverted during startup or shutdown periods of operation when liquid or two-phase flow leaves the boiler panels. The tank provides a separation chamber where hot condensate leaves the bottom of the tank while the steam exits from the top. A small pair of downcomers which pass down the tower and into the feedwater equipment is included to provide a path for the condensate and steam leaving the receiver flash tank. If desired for preheating purposes, the steam leaving the flash tank can be diverted into the main steam downcomer and on to the turbine stop valve or thermal storage charging heat exchanger. Once

superheated steam flow is established at the receiver outlet, the line leading to the receiver flash tank is closed off, taking the flash tank out of service, while the line connecting the receiver outlet to the main steam downcomer is opened.

The warmup line shown on the schematic, which bypasses the receiver panels, provides a recirculation path for flow during nonoperating periods. This would occur during nighttime standby when it is desired to maintain the water/steam loop in a warm or "ready" condition. Also, the bypass line would be used during the circulation process required for water cleanup. No effort would be made to maintain a hot water circulation through the panels except where flow would be necessary to prevent freezing on cold nights.

The receiver feed pumps, which supply flow to the receiver, are located at the outlet side of the deaerator. The reservoir of water contained in the deaerator provides a continuous and reliable source of condensate at the pump inlets during all operating conditions, even during emergency conditions which will minimize the possibility of damage to the pump. As shown in the schematic, a separate set of pumps is used to supply feedwater to the thermal storage steam generator. These pumps will also draw from the reservoir which exists in the deaerator. Since the deaerator contains saturated water, it will be elevated approximately 21.3m (70 ft) above the pump suction inlet so that the pressure rise associated with the liquid column can be used to prevent cavitation in the pump.

3.5 SYSTEM DESIGN AND PERFORMANCE SUMMARY

This section summarizes the design and performance characteristics of the Commercial system. Subsystem-related data pertaining to operating ranges, efficiencies, and parasitic power demands are also treated.

3.5.1 Physical Characteristics

The overall characteristics of the collector field layout are shown in Figure 3-17. The sawtooth field outline reflects the trim line determined by the University of Houston's optimization analysis. The irregular nature of the line results from the cell-by-cell analysis and trim technique used by the University of Houston. In reality, this sawtooth pattern would be converted into continuous arcs such as those shown by the dashed lines with heliostats being laid out along the arcs in a radial stagger fashion. The density of glass contained in the field would vary from ~45% near the central exclusion area to ~13% along the northern edge with the average value being ~24%. The 22,914 heliostats correspond to an assumed closed-loop tracking design. A three-aim point strategy is used with successive heliostats aimed at the equator of the receiver and 6m (19.7 ft) above and below the equator. The circular exclusion area contains the tower, balance of plant equipment, and thermal storage. In addition, administrative, maintenance, and plant control areas are also contained in that exclusion area.

The tower is a slip form reinforced-concrete structure with an outer diameter of 45.7m (150 ft) at the foundation and 15.3m (50.25 ft) at the top. The concrete structure is 242m (794 ft) high. The receiver is mounted on top of the tower with the equator located 268m (879 ft) above grade. A summary tabulation of the principal characteristics for the rest of the system is shown in Table 3-12.

3.5.2 System Performance

The performance characteristics for the Commercial system at equinox noon and on an average basis are summarized in Figures 3-18 and 3-19, along with the corresponding incremental efficiency values. In each case, the power flow to thermal storage has been adjusted so that the net turbine output is 100 MWe. The extreme left side of the chart corresponds to the condition where the heliostats are oriented normal to the incident sunlight. The

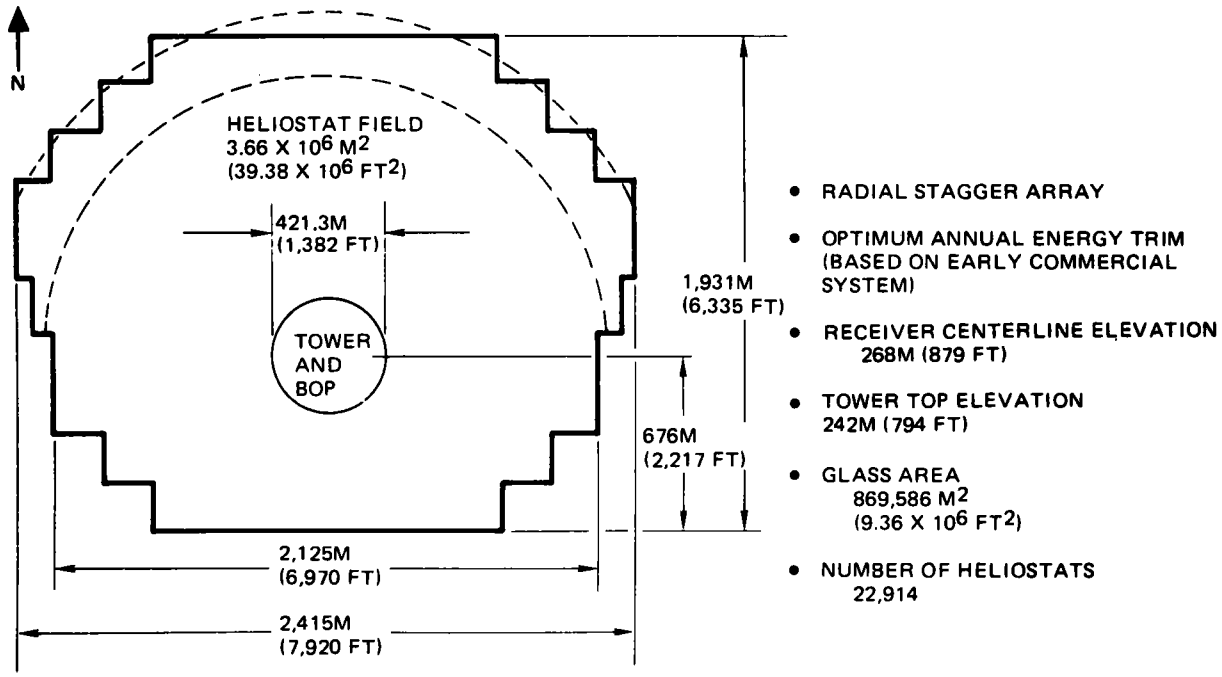

Figure 3-17. Commercial System Field Layout

Table 3-12

COMMERCIAL SYSTEM CHARACTERISTICS

Module Size		
• Capacity	100 MW	
• Solar Multiple (equinox noon)	1.7	
Receiver Configuration	External, single-pass-to-superheat	
Receiver Size		
• Diameter	17m	(56 ft)
• Height	25.5m	(84 ft)
Receiver Steam Conditions		
• Pressure	11.1 MPa	(1,615 psia)
• Temperature		
Rated Steam	516°C	(960°F)
Derated Steam	368°C	(694°F)
Thermal Storage Media	Caloria HT-43 + Rock	
Method of Storage	"Single" tank (thermocline)	
Thermal Storage Capacity	6 Hours	
Thermal Storage Temperature Range	232° to 316°C (450° to 600°F)	
Turbine Configuration	Tandem-Compound, Double-Flow, Automatic Admission, Industrial Turbine	
Turbine Steam Conditions		
• Throttle Steam	510°C (950°F)	
	10.1 MPa (1465 psia)	
• Admission Steam	296°C (565°F)	
	2.52 MPa (365 psia)	
Heat Rejection	Wet cooling towers	

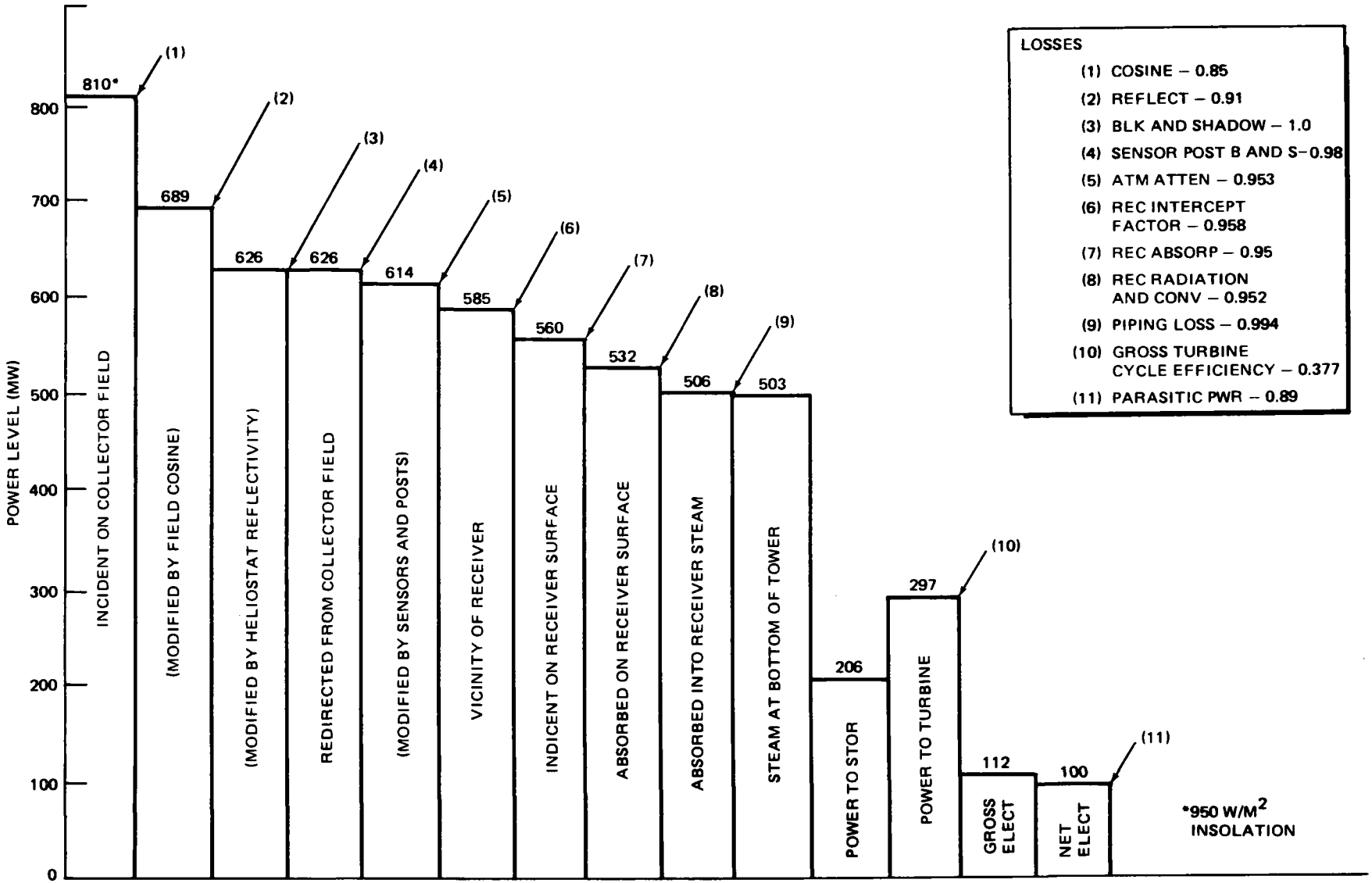

Figure 3-18. Commercial System Power Flow (Equinox Noon)

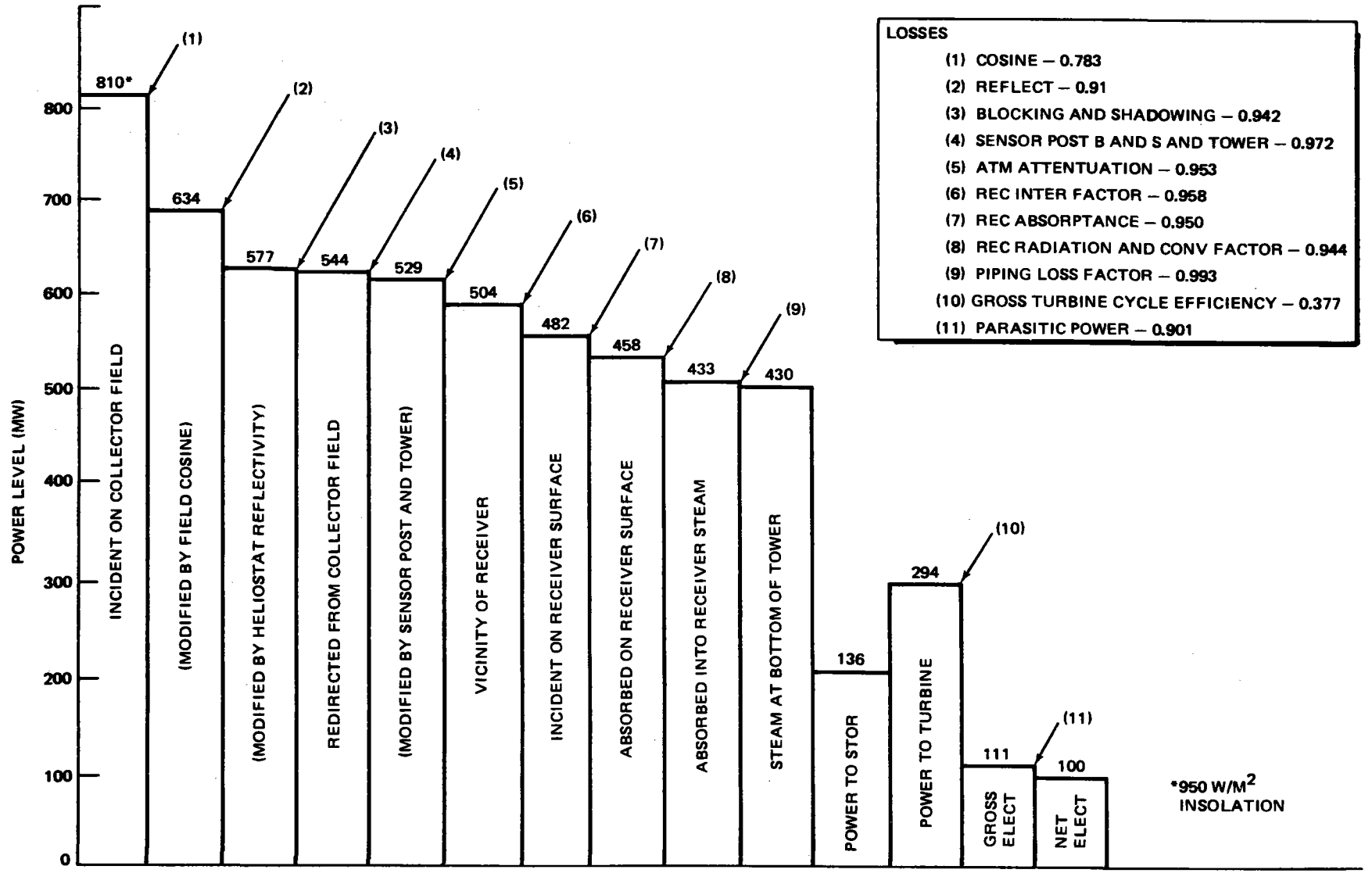

Figure 3-19. Commercial System Power Flow (Annual Average)

810-MW incident on the heliostats assumes that ~98% of the heliostats are operational or capable of adding power to the receiver; i.e., not in a control singularity. If all heliostats were to be considered, the incident power would increase to 826.1 MW. In both cases treated, an insolation level of 950 W/m^2 was assumed.

The incremental losses assumed for these two cases include estimates of atmospheric attenuation and sensor post blocking and shadowing. The 0.953 value for atmospheric attenuation is associated with a 50-km (31 mi) visible range and a subarctic winter atmosphere which is representative of a desert environment. The indicated value for sensor post blocking and shadowing corresponds to the worst case where a separate blocked and shaded region go from the center of the mirror outward. This, in general, would occur only for low sun elevation angles and on the side of the tower away from the sun where the heliostats are in a near-vertical orientation. An overall value of less than 1% loss would probably be more representative of an annual average value with something less for an equinox noon value. The gross turbine cycle efficiency of 0.377 corresponds to a turbine back pressure of 6.35 cm Hg (2.5 in. Hg). The corresponding efficiency for operation from thermal storage is 0.268. In evaluating overall system efficiency, it is important to subtract the quantity of power going to thermal storage and to adjust the receiver and collector field powers accordingly.

3.5.3 Subsystem Operating Ranges

A compatible set of operating ranges for the receiver, thermal storage, and turbine is important due to the close-coupled nature of the water steam loop. The operating ranges for these subsystems are shown in tabular form in Table 3-13. In general, these conditions define the range of power or flow rate that will be experienced while holding the pressure and temperature at a design point level.

The receiver is capable of controlled operation over a total throttling ratio of 6.3:1 which is seen from the flow range for rated steam operation. For the case of derated receiver operation, an identical minimum flow condition exists. The permitted upper flow limit for derated steam operation is a result of a DoE-imposed limit on the charging of thermal storage which would be

Table 3-13

COMMERCIAL SUBSYSTEM OPERATING RANGES

Subsystem	Temperature °C (°F)	Pressure MPa (psia)	Flow Rate Kg/sec (10^6 lb/hr)	Power Level MW (10^9 Btu/hr)
Receiver				
• Rated Steam	516 (960)	10.2 - 11.1 (1,485 - 1,615)	34.0** - 213.0 (0.269 - 1.687)	92.4** - 506.4 (0.32 - 1.73)
• Derated Steam	368 (694)	10.2 - 11.1 (1,485 - 1,615)	34.0** - 135.9* (0.269 - 1.08)	63.7** - 254.2* (0.217 - 0.868)
Thermal Storage				
• Charging Steam at Heat Exchanger	360 (680)	10.1 (1,465)	6.7** - 135.9 (0.053 - 1.08)	12.5** - 255 (0.043 - 0.870)
• Discharge Steam Leaving Steam Generator	299 (570)	2.72 (395)	12.6** - 114.3 (0.100 - 0.906)	31.4** - 284 (0.107 - 0.969)
Turbine				
• Throttle Steam	510 (950)	10.1 (1,465)	34.0** - 121.3 (0.269 - 0.960)	92.4** - 297 (0.32 - 1.01)
• Admission Steam Only	296 (565)	2.52 (365)	12.6** - 114.3 (0.100 - 0.906)	31.4** - 284 (0.107 - 0.969)

*Limited by Sandia constraint on thermal storage charging rate
**Approximate values

necessary any time the receiver were operating in a derated mode. From the receiver standpoint, there are no factors that limit the flow to anything below the maximum rated steam flow.

The range of values defined for charging thermal storage are approximately a 20:1 ratio on flow rate and thermal power. This broad range is necessary to accept anything from the maximum derated output of the receiver to a small incremental quantity of rated steam which is in excess of that required for turbine operation. In arriving at the minimum control value, it is necessary to consider more than simple energy versus economic trade studies since the thermal storage charging loop plays a major role in system pressure control. This point will be treated in greater detail in Section 3.7.

The values defined for the steam generator side of the thermal storage range from the maximum value needed to drive the turbine at a 70-MWe net output level to a minimum practical level that would be used to supplement receiver steam flow or to start the turbine using admission steam. During the early part of turbine operation from admission steam, when the flow is <10% of the maximum value, steam temperature and pressure conditions would be in a state of transition upward to the indicated design values.

The maximum values indicated for the turbine for both throttle and admission steam correspond to the flow rate or power level required to produce 100 MW or 70 MW net electrical power, respectively. The indicated flow for throttle steam corresponds to the minimum receiver flow at rated steam which is not the minimum flow condition for the turbine. The minimum condition defined for admission steam corresponds approximately to the minimum turbine flow (the actual lower limit on turbine flow has not been precisely defined by the manufacturer). Below the indicated level, the turbine would be passing through a startup or shutdown ramp. In reality, the turbine could go to zero flow and zero power, although this is not considered as part of the normal operating range.

3.5.4 Subsystem Efficiencies

The efficiency variation for the collector subsystem is shown in Figure 3-20 for various sun azimuth and elevation angles. Implicit in this data are the following assumptions:

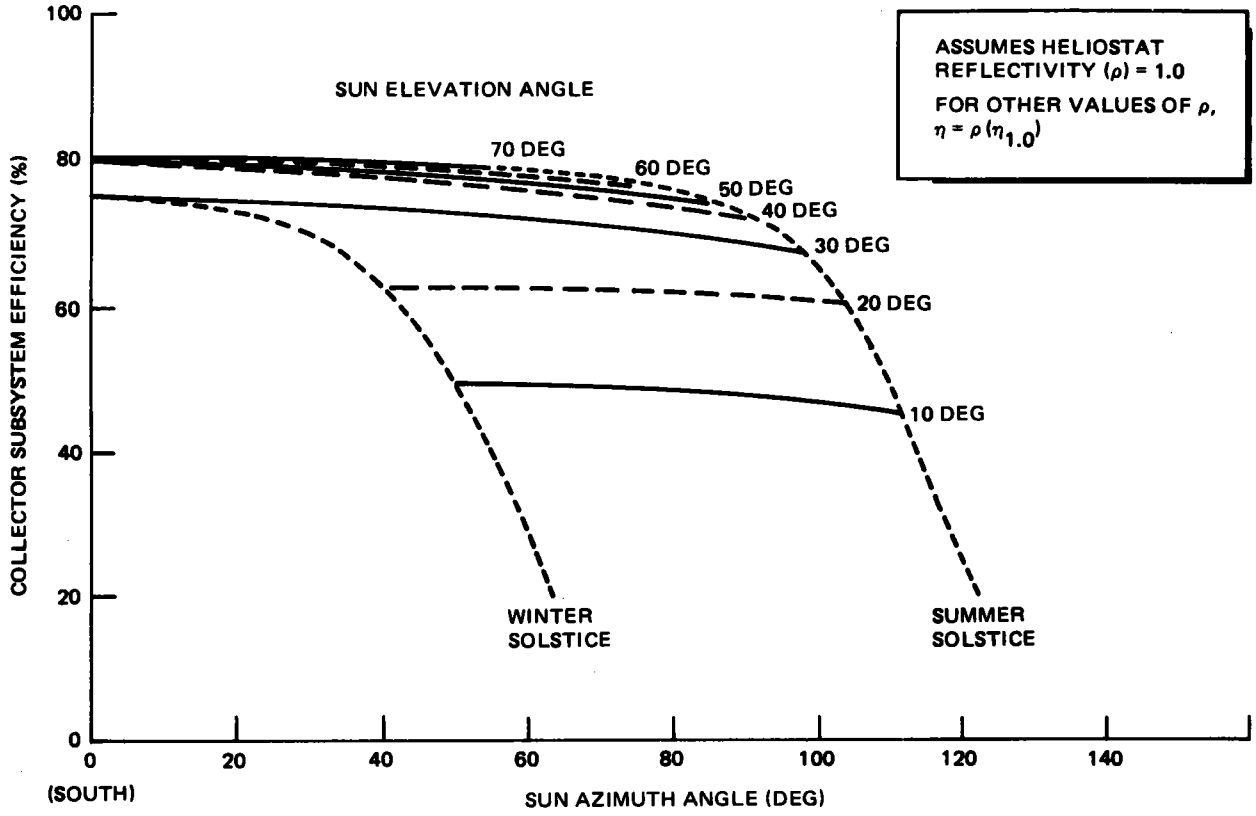

Figure 3-20. Collector Field Performance

- Heliostat reflectivity = 1.0
- Receiver interception factor = 0.958
- Sensor post blocking and shadowing factor = 0.98
- Atmospheric attenuation factor = 1.0

Collector subsystem efficiency at other values of heliostat reflectivity can be determined by multiplying the indicated efficiency by the actual reflectivity.

The receiver efficiency defined as the power absorbed divided by the incident power is summarized as follows:

Time	Incident Power (MWt)	Absorbed Power (MWt)	Efficiency
Equinox Noon	560	506.4	0.904
Minimum Rated Steam	118	92.4	0.783
Annual Average	482	433	0.898

Assumptions made in arriving at these values include an absorptivity of 0.95, an emissivity of 0.89, a wind speed of 3.5 m/s (8 mph)*, and an ambient temperature of 23°C (74°F). Since neither forced nor free convection dominates, a root sum squares addition of the two heat loss components was applied. Under the temperature and wind conditions defined above, 0.92% of the incident power would be lost due to convection.

The thermal storage subsystem has a volumetric efficiency defined as the ratio of extractable energy to total energy in the tank of 90%. The subsystem has an energy recovery efficiency of 98%, which is defined as the ratio of extractable energy to charging energy.

The gross cycle efficiency for the turbine is shown in Figure 3-21 as a function of turbine flow rate for both receiver and thermal storage steam operation. A wet cooled condenser is assumed with a turbine back pressure of 6.35 cm Hg (2.5 in. Hg).

*Wind speed at 10m elevation.

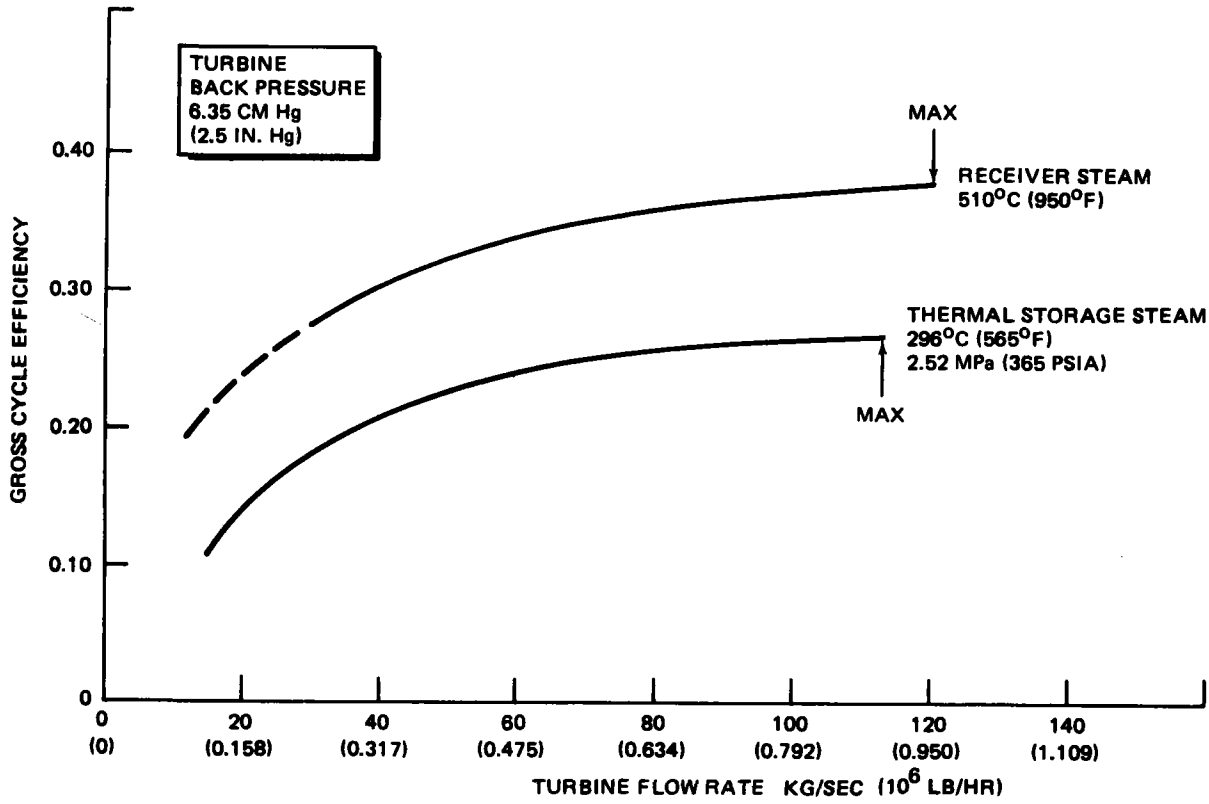

Figure 3-21. Impact of Flow Rate on Turbine Cycle Efficiency (Commercial Turbine)

3.5.5 Auxiliary Power Requirements

A detailed tabulation of the Commercial Plant auxiliary power requirements is shown in Table 3-14 for the equinox design point, the nighttime operating design point when operating from thermal storage, nighttime standby, and emergency conditions. For daytime operation, the major power consumers are the pumps and fans associated with the feedwater, heat rejection, and thermal storage charging loops. The collector field by comparison accounts for only 3% of the total parasitic load. During nighttime operation, the major power consumers are the condenser circulating water pumps, cooling tower fans, thermal storage extraction pumps, and thermal storage feed pumps. The nighttime standby power consumption is dominated by heating, ventilation, and air-conditioning requirements in addition to the balance of plant auxilaries. The emergency power demand is dominated by the heliostat emergency slew requirement. This requirement would occur when the simultaneous condition of a power failure and a rapid wind rise rate occur. During this period, the 1,308 kW of electrical power would be sufficient to slew a quarter of the total collector field at one time. The procedure would be to slew the upwind heliostats to a horizontal or feathered position first since they would afford partial protection to the unslewed heliostats on the downwind side of the field.

3.6 ANNUAL ENERGY OUTPUT

Annual energy calculations were carried out for the Commercial system for several different insolation models. The simplest analysis assumed a constant insolation level of 950 W/m^2 throughout the year. The system was assumed to have a solar multiple of 1.7 with a 6-hr storage capability. The assumption was made that the collector field was activated at a 10-deg sun elevation angle and by a 15-deg sun elevation angle, the receiver had reached a derated steam condition at which time all energy could be diverted to storage. At the time when the calculation was made, it was assumed that the threshold for rated steam operation from the receiver was 50% of maximum design flow. At this point, the turbine would be completing the starting and loading phase. An accounting of the energy collection for the various days of the year is tabulated in Table 3-15 with an indication of the quantity flowing directly to the turbine, that going to storage, and that portion lost due to over collection (rate of energy collection exceeds the capability of the turbine

Table 3-14

COMMERCIAL PLANT AUXILIARY POWER REQUIREMENTS

Component	Receiver Operation Equinox (Design) 100 Mw Net, kW	Thermal Storage Operation 70 Mw Net, kW	Night Standby kW	Emergency Power AC kW	Emergency Power DC kW
Receiver Feed Pump	3,492	-	-	-	-
TS Drain Pump	2,235	-	-	-	-
TS Feed Pump	-	500	-	-	-
Hotwell Pump	130	121	-	-	-
Condenser Vacuum Pump	41	41	41	-	-
Condensate Trans Pump	-	-	24	-	-
Service Air Compressor	60	-	-	-	-
Instrument Air Compressor	45	45	45	-	-
Cooling Tower Fans	886	886	-	-	-
Circ Water Pumps	2,313	2,313	-	-	-
Turbine AC Oil Pump	-	-	20	20	-
Turbine DC Oil Pump	-	-	-	-	20
Lube Oil Filter Pump	1	1	1	-	-
Chemical Pumps	5	5	-	-	-
Motor-Operated Valves	-	-	-	5	-
Raw Water Pump	90	70	40	-	-
Clarified Water Pump	70	60	30	-	-
Water-Treating System	25	25	10	-	-
Jockey Pump (Fire Water)	5	5	5	-	-
Auxiliary Boiler	-	-	25	-	-
Turbine Turning Gear	-	-	5	5	-
Computer	15	15	7	15	-
Miscellaneous DC	-	-	-	-	20
Controls and Computer HVAC	50	50	30	30	-
Plant HVAC	440	300	300	-	-
TS Charging Pump	750	-	-	-	-
TS Extraction Pump	-	930	-	-	-
Sewage Treatment Plant	2	2	2	-	-
Potable Water Pump	5	5	-	-	-
Receiver Tower Elevator	-	-	-	30	-
Heliostats and Controllers	350	-	-	1,308	-
Lighting and Miscellaneous AC	990	726	100	30	-
TOTAL	12,000	6,100	685	1,443	40

Table 3-15

SYSTEM PERFORMANCE SUMMARY

(SOLAR MULTIPLE = 1.7, 6-HR STORAGE)

Day	Total Collection Capability (MWHt)	Direct Turbine Operation (100 MWe) Required Energy (MWHt)	Direct Turbine Operation (100 MWe) Period (Hr)	Excess Energy (MWHt)	Energy to Storage (MWHt)	Period of Operation From Storage 70 MWe (Hr)	Spillage MWHt	Spillage (%)
Jun 21	5,290	3,485	11.7	1,805	1,757	6.0	48	0.9
May 21/ Jul 21	5,202	3,396	11.4	1,806	1,757	6.0	49	0.9
Apr 21/ Aug 21	4,905	3,158	10.6	1,747	1,747	5.96	0	0
Equinox	4,422	2,860	9.6	1,562	1,562	5.33	0	0
Feb 21/ Oct 21	3,731	2,443	8.2	1,288	1,288	4.40	0	0
Jan 21/ Nov 21	3,122	2,115	7.1	1,007	1,007	3.44	0	0
Dec 21	2,832	1,966	6.6	866	866	2.96	0	0

and thermal storage unit to accommodate the energy flow). Assuming a net cycle efficiency of 33.7%, which includes the influence of plant parasitic loads, a net annual electrical production of 423,000 MWH would be anticipated. This calculation also assumed that the system were down 35 days per year due to cloudiness or maintenance requirements.

Since the calculations were developed, changes in the receiver operating requirements and changes in receiver design will allow rated receiver steam to be maintained down to ~16% of maximum design flow. This would permit the turbine to experience a slightly longer operating day using receiver steam exclusively. The result would be a slight increase in the anticipated energy output.

3.7 PLANT OPERATION

The aspects of the Commercial system related to plant operation involve a definition of the steady-state operating modes and a description of various types of system startups depending on the thermal state of the system and the type of power used during startup.

3.7.1 Operating Modes

The system is designed to operate in six steady-state operating modes which are designed to provide complete operating flexibility. "Steady-state" is applied rather loosely with regard to the operating modes because continuously varying insolation and environmental conditions create a transient operating environment at all times. Use of the term regarding the operating modes implies that no transitions occur from one flow path or set of equipment to another although continuous variations in flow may occur along the active water/steam loop path. The operating modes are designed for system operation during sunshine, partly cloudy, or totally overcast and nighttime periods.

3.7.1.1 Normal Solar Operation

The normal solar operating mode that is shown in Figure 3-22 occurs at any time when a surplus of receiver steam exists over what can be passed through the turbine. During this condition, the excess steam is diverted to the thermal storage subsystem. As the rated steam passes through the desuperheater, its temperature is reduced to 360°C (680°F) to minimize the chances of

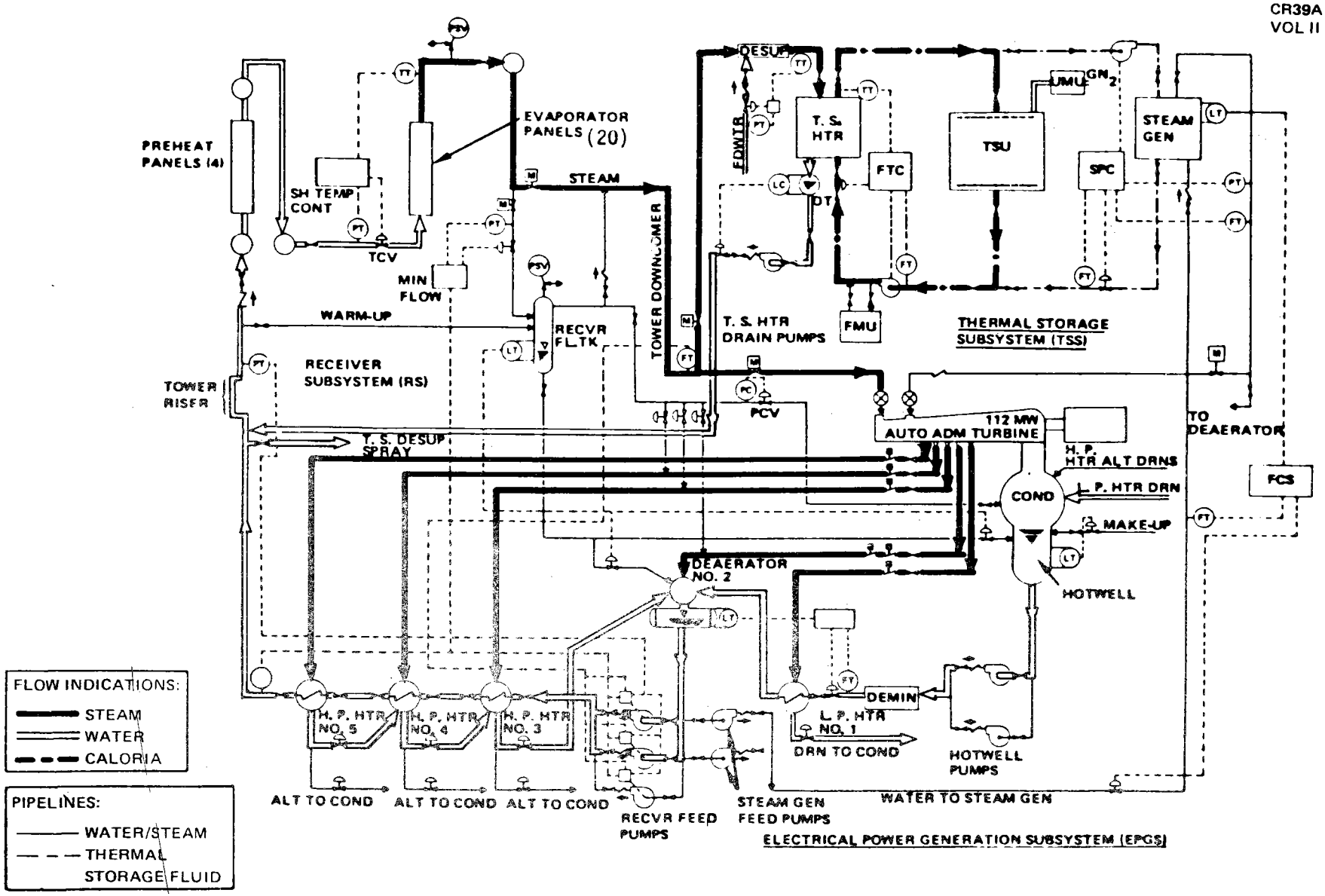

Figure 3-22. Normal Solar Operation (Commercial System)

breaking down the temperature-limited Caloria HT-43. The partially desuperheated steam then passes through the charging heat exchanger where it is condensed and slightly subcooled by the Caloria charging loop. The high-temperature Caloria leaves the charging heat exchanger and enters the top of the thermal storage tank where it is stored in a thermocline condition. The condensate leaving the charging heat exchanger passes to the injection pumps where it is reintroduced into the riser flow at the base of the tower.

The balance of the steam which was not diverted to thermal storage enters the turbine through the throttle valve. As the steam expands through the turbine, some of the flow is extracted for feedwater heating while the balance passes to the condenser. The condensate in the condenser is pumped in turn through the demineralizer, low-pressure heater, and to the deaerator where dissolved gases are expelled. The receiver feed pumps then pump the condensate through the final three stages of feedwater heating before it mixes with the thermal storage condensate. The mixed flow then moves up the tower and to the receiver inlet where the inlet pressure is maintained at a constant level.

From an operational standpoint, this mode will require simultaneous steam pressure control by the throttle valve and the thermal storage charging equipment. In general, fine tuning of the steam pressure will be accomplished with the turbine throttle valve, which will be operating in an initial pressure control mode. If the thermal storage and turbine are not capable of accepting all of the power absorbed at the receiver, the net effect on the system would be an increase in steam pressure which would continue until heliostats were taken out of service or the relief valves begin to open on the receiver.

3.7.1.2 Low Solar Power Operation

The low solar power operating mode is used when the receiver steam flow is insufficient to meet the electrical output demand. During this period, the turbine flow is supplemented with thermal storage steam introduced through the admission port. A water steam loop schematic showing the active flow elements is shown in Figure 3-23. As indicated, the entire receiver steam flow passes through the turbine throttle valve with no flow being sent to charge thermal storage. The admission steam flow that leaves the thermal storage

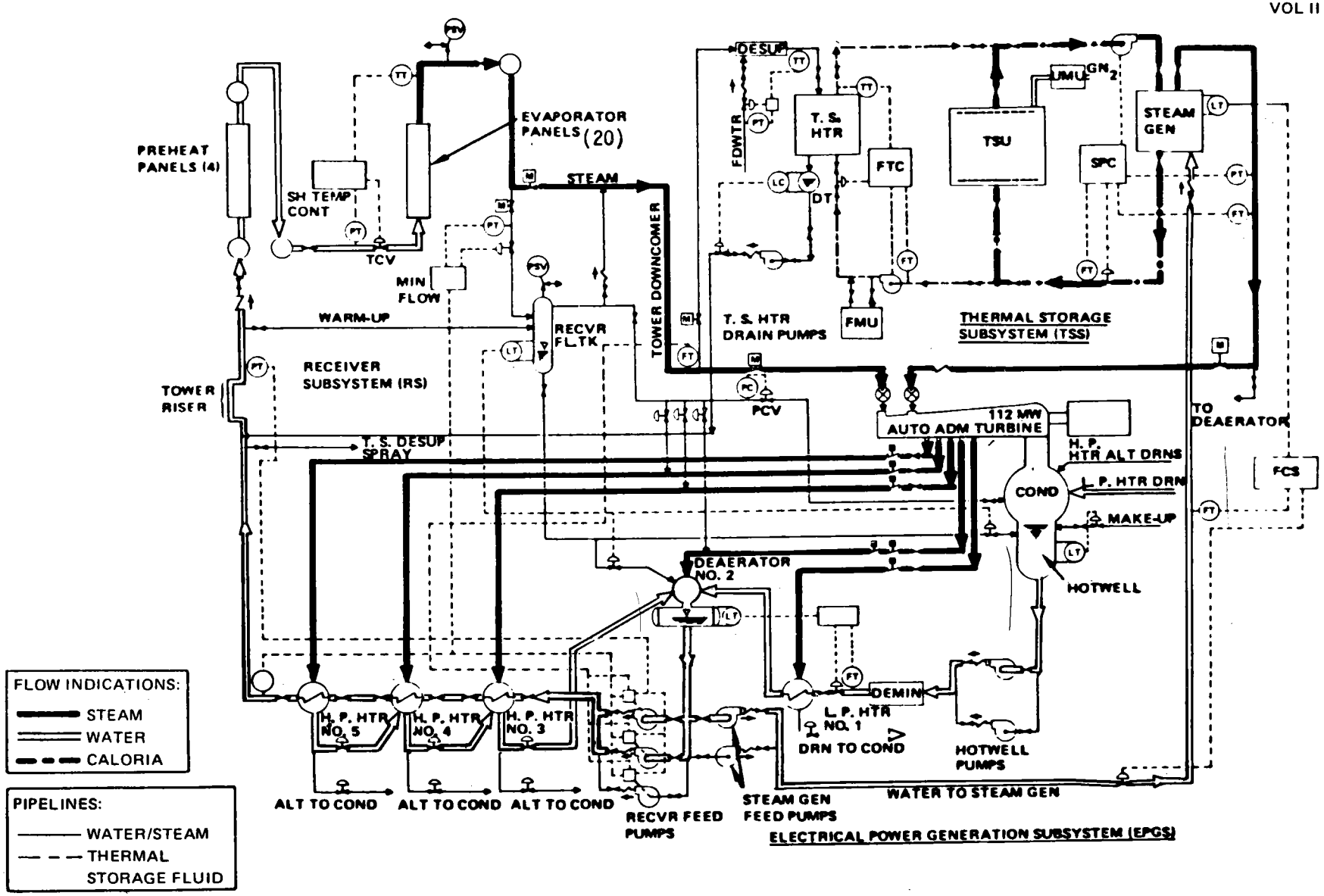

Figure 3-23. Low Solar Power Operation (Commercial System)

steam generator originates from the steam generator feed pumps which draw condensate from the deaerator. The receiver flow is provided with the receiver feed pumps in a manner similar to that described for the normal solar operating mode.

From an operating standpoint, the turbine valves exercise control over the steam pressure in both the receiver and thermal storage steam legs. This is accomplished by operating both the turbine throttle valve and the admission valve in an initial pressure control mode where upstream pressure is the controlled parameter. The admission steam flow rate is adjusted by varying the Caloria flow rate in the thermal storage extraction loop. As the Caloria flow is increased, the steam pressure in the steam generator equipment will increase, which will cause the turbine admission valve to adjust to a more open position. This will increase the total turbine flow rate and generator output. The mode introduces a great deal of flexibility into the system and serves as a natural transition between the normal solar and extended or intermittent cloud operating modes.

3.7.1.3 Intermittent Cloud Operation

During periods when excessive transients in insolation are anticipated due to the passage of opaque clouds, the system will operate in the intermittent cloud mode in which the turbine is powered completely from thermal storage steam. During this mode, shown in Figure 3-24, all receiver generated steam will be directed to the thermal storage charging heat exchanger, which is designed to accept the potential transients in inlet steam. Because the turbine is not directly powered by receiver steam, the steam conditions can be adjusted to the derated level, which is compatible with charging thermal storage without the need for desuperheating. Because of DoE limitations imposed on the thermal storage charging rate, only 50% of the maximum potential receiver power could be sent to thermal storage when operating in this mode. Thus, a close control would have to be maintained on the number of heliostats actually contributing power to the receiver. During peak insolation periods on partly cloudy days, as many as 50% of the heliostats would have to be left out of service.

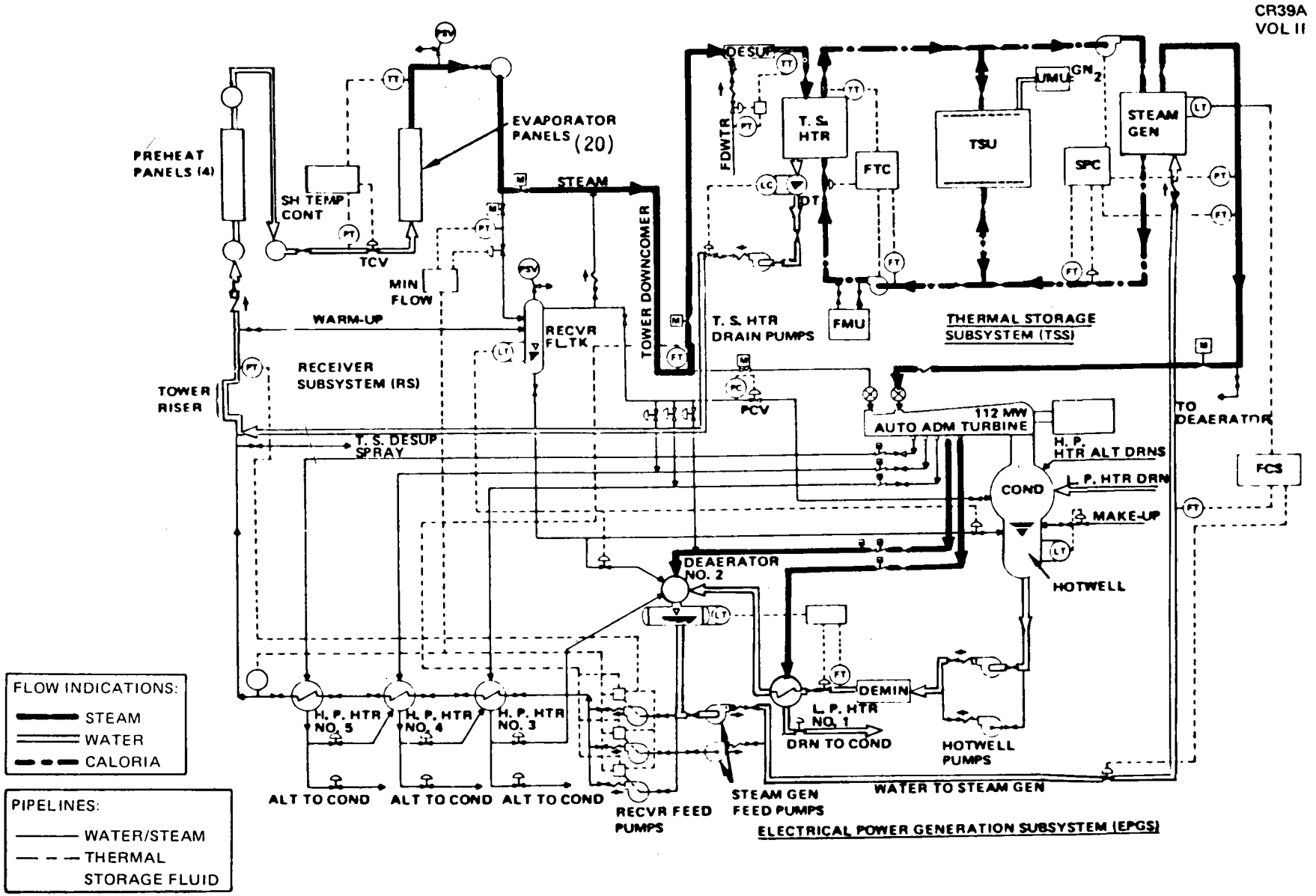

Figure 3-24. Intermittent Cloud Operation (Commercial System)

In reviewing the active flow paths shown in Figure 3-24, it is seen that high-temperature condensate which leaves the thermal storage charging heater is pumped directly back to the riser without passing through a deaeration or demineralizer stage. This approach, though somewhat unconventional, appears satisfactory since the entire receiver/thermal storage charging loop is maintained at a fairly high pressure (<9.65 MPa, or 1,400 psia) which would exclude the possibility of external air leaking into this part of the water/steam loop. If necessary, a high-pressure deaerator could be added to the layout shown in the schematic. Since the condensate also bypasses the demineralizer, a gradual accumulation of dissolved solids would be anticipated. This effect can be minimized through the use of commercially available magnetic filters downstream of the thermal storage heater drain pumps. In addition, the standard operational procedure for each day will be to completely circulate the feedwater through the demineralizer stage to ensure that high water quality exists at the beginning of each day. Since current experience on dissolved solid buildup rate in power plants is over extended periods, the Pilot Plant will provide valuable data related to variations in water quality that occur on a daily basis for various operating modes.

During the operating mode where the turbine is operated exclusively from thermal storage steam, extraction flows to the three high-pressure heaters are eliminated because they are no longer in service. Steam pressure control is maintained in the steam generator with the turbine admission valve; receiver pressure is controlled by the thermal storage charging loop. This latter case is one of the key integrated operational issues which must be demonstrated in the Pilot Plant. It is also seen that this mode involves the simultaneous charging and discharging of the thermal storage subsystem which is consistent with its design capability.

3.7.1.4 Extended Operation

The extended operation mode would be used whenever insufficient insolation is available to power the receiver while some useful charge exists in the thermal storage unit. The appropriate flow schematic for operating in this mode is shown in Figure 3-25. The indicated flow paths correspond exactly to those treated in the intermittent cloud mode which pertained to the

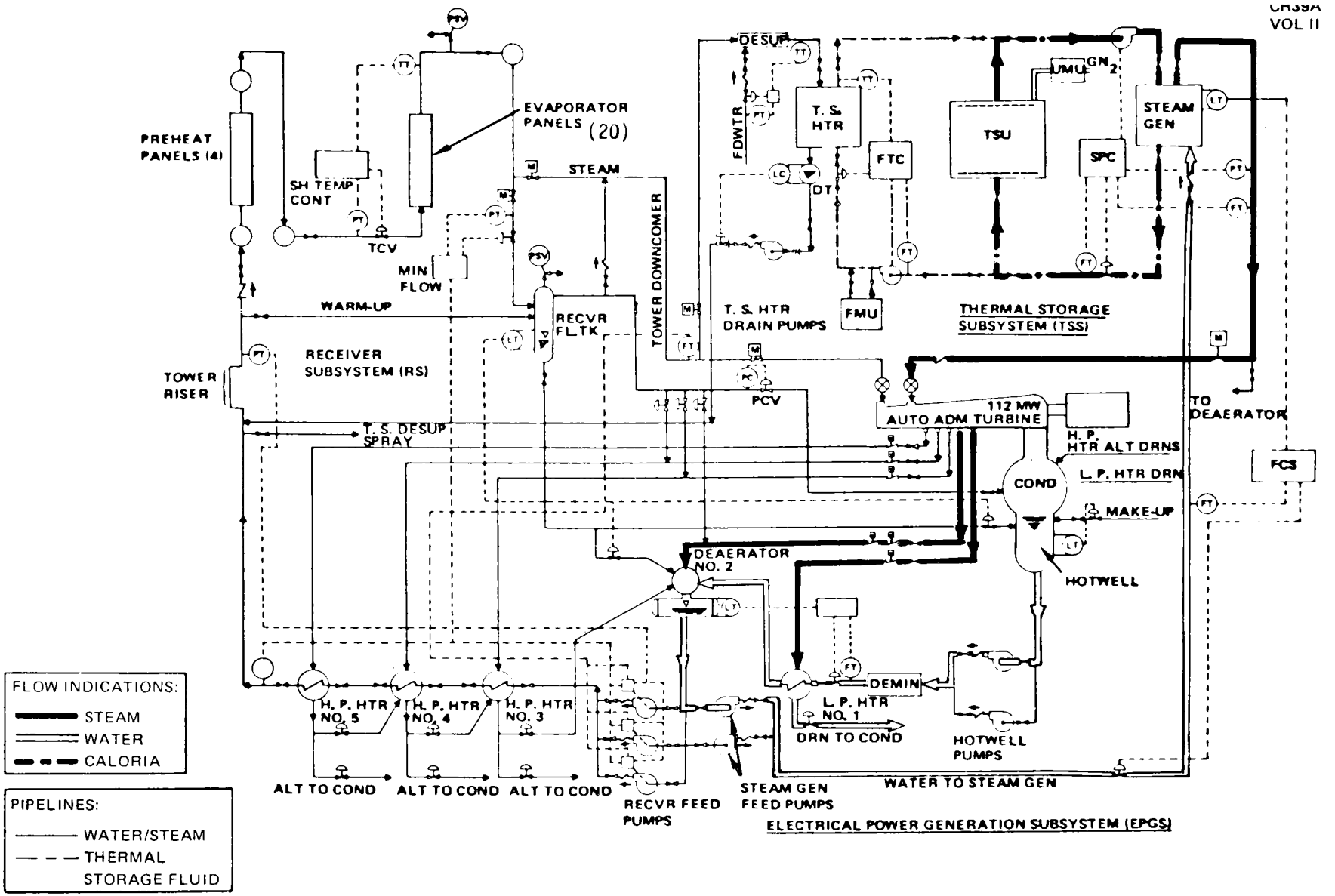

Figure 3-25. Extended Operation (Commercial System)

admission steam loop. Steam pressure control is maintained by the turbine admission valve and the Caloria circulation rate. The mode of operation could be continued until the thermocline begins to pass from the top of the tank, at which time the Caloria temperature would decay below the 3.3°C (595°F) nominal outlet design condition. An option which exists is to shut down the plant operation prior to the complete discharge of the thermal storage unit. The turbine could then be rolled and loaded the next morning in preparation for the introduction of rated receiver steam using exactly the same operating mode. It should be pointed out that any time the turbine is operated exclusively from admission steam, ~5% of the steam flow is introduced at the inlet to the high-pressure section to provide some cooling flow and thereby preventing an over-temperature condition.

3.7.1.5 Charging of Thermal Storage Only

As in the case of extended operation just discussed, the charging of thermal storage mode shown in Figure 3-26 represents a simplification of the more complicated intermittent cloud mode discussed in Section 3.7.1.3. In this mode, all of the receiver flow is diverted to the thermal storage charging heat exchangers. Because of the DoE limit on thermal storage charging capability, this mode would be practical for power levels up to ~50% of the maximum receiver/collector field output. As in the case of intermittent cloud operation, the high-temperature condensate leaving the thermal storage charging heat exchanger is passed directly to the riser without first being deaerated and demineralized. The same points presented in Section 3.7.1.3 pertaining to that condition apply equally well to this operating mode. Since the turbine is not operating during the mode, all electrical power required to operate the collector field, thermal storage heater drain pumps, and the thermal storage charging pumps must be drawn from the electrical grid.

As in the case of the intermittent cloud mode, receiver pressure is controlled by the thermal storage charging loop. This requires a close coordination between the Caloria flow in the thermal storage charging loop and the absorbed power on the receiver because variations in either can influence steam pressure.

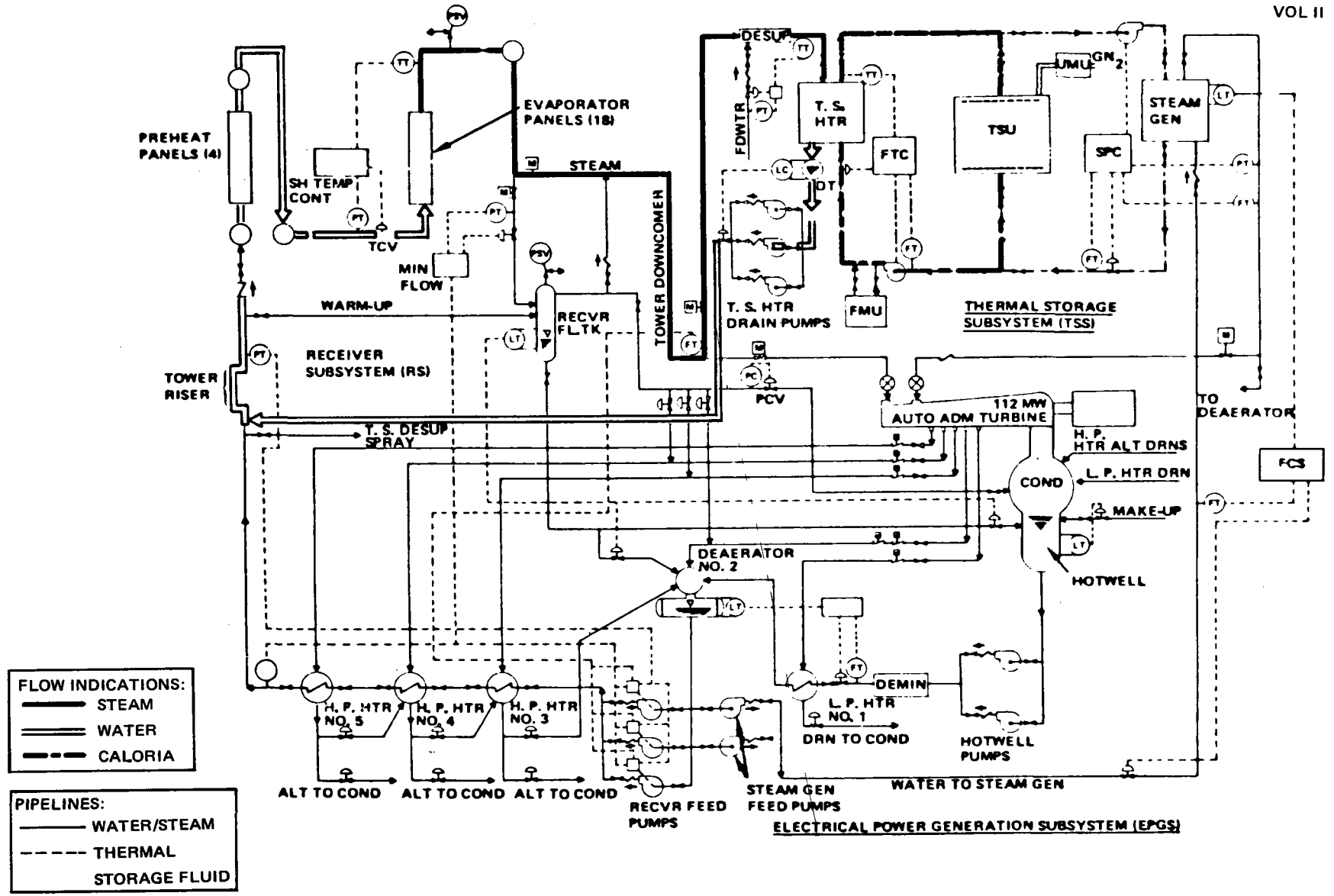

Figure 3-26. Charging of Thermal Storage Only (Commercial System)

3.7.1.6 Fully Charged Thermal Storage

The fully charged thermal storage mode would be used whenever the thermal storage unit is completely charged or when the thermal storage subsystem is unavailable for outage or maintenance reasons. The flow path, shown schematically in Figure 3-27, sends all of the receiver flow directly to the turbine with the output of the turbine-generator being dependent exclusively on the receiver flow rate.

Because the Commercial system has a high solar multiple (1.7), the potential exists for the receiver output to exceed the turbine flow rate capability. As a result, it would be necessary to carefully control the redirected power from the collector field. This requires central control over the activation and operation of individual heliostats which is within the capability of the collector subsystem design.

The turbine, in general, operates at or near its design point with normal extraction flows being routed to the feedwater heaters. The turbine throttle valve is responsible for receiver pressure control.

3.7.2 System Operating Timelines

A series of Commercial system operation timelines have been developed which depict the system startup for a variety of assumed conditions. In particular, startup sequences have been defined for cold, warm, and hot turbine conditions using steam flow from the receiver as well as warm and hot turbine conditions using steam flow from thermal storage. The definition of the turbine status and its impact on turbine acceleration and loading rate are shown in Table 3-16. For startups using receiver steam, the critical path represents the sum of the receiver and turbine startup periods. For startups employing thermal storage steam, the critical path is the rate at which the receiver can be brought on line.

3.7.2.1 Cold-System Startup From Receiver

The time-phased sequence of events necessary to start a cold system using receiver output steam is shown in Figure 3-28. Although the actual operating timeline depends on the time of day and year when the startup is carried out, along with the insolation available, the relationships illustrated in the

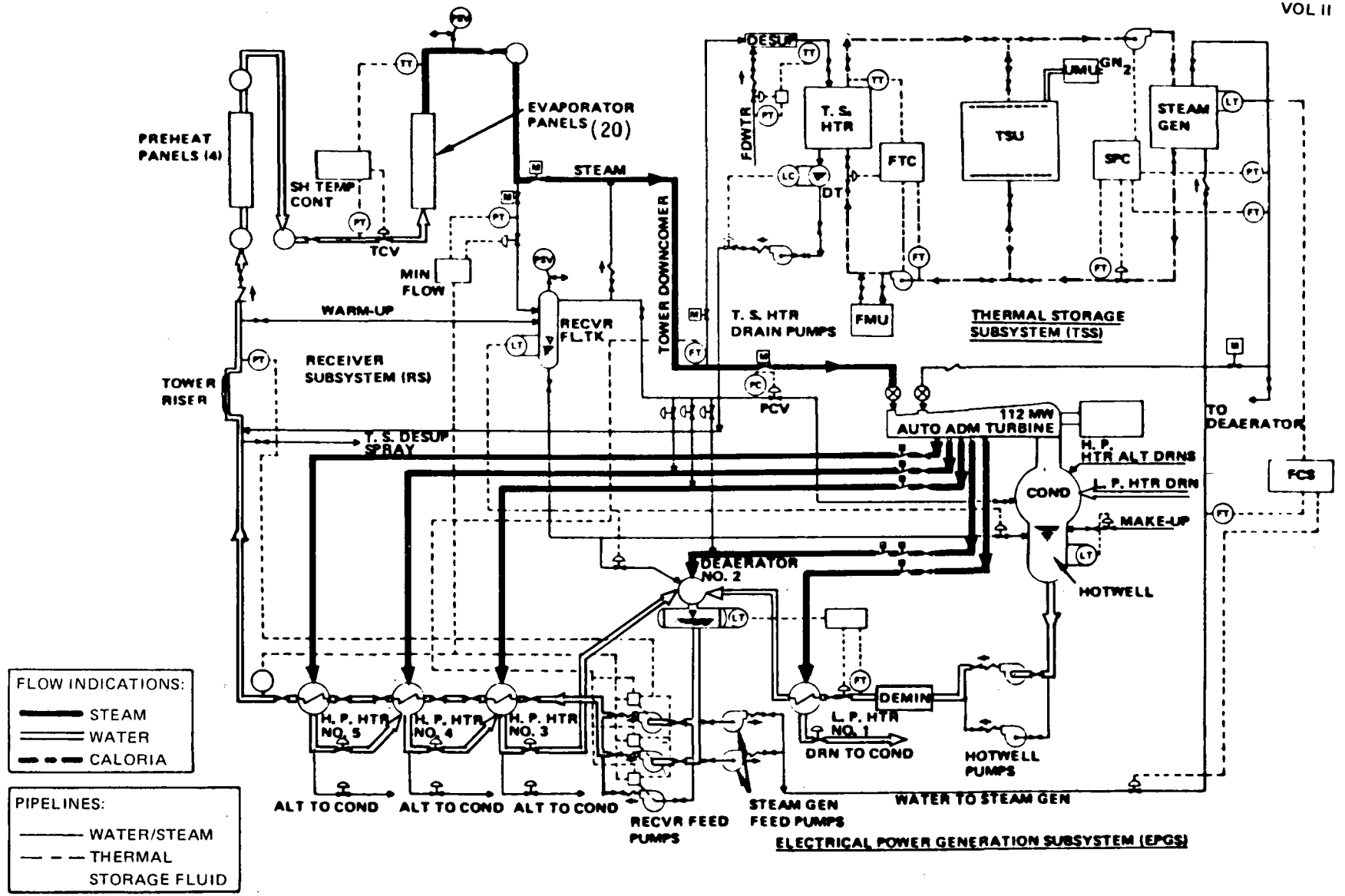

Figure 3-27. Fully Charged Thermal Storage (Commercial System)

Table 3-16

TURBINE STARTUP CHARACTERISTICS*

	Turbine Roll	Turbine/Generator Load
Cold Start -18° to 149°C (0° to 300°F)	250 RPM/min 10-min hold at 1,000 RPM	1/2% per min
Warm Start 149° to 371°C (301° to 700°F)	500 RPM/min 10-min hold at 1,000 RPM	1-1/2% per min
Hot Start 372° to 538°C (701° to 1,000°F	500 RPM/min 5-min hold at 1,000 RPM	3% per min

*Per General Electric Specification

figure are representative of a typical morning startup with a clear-sky condition. Prior to the events shown in this figure, the feedwater would be circulated through the system and in the process demineralized to ensure that a proper water quality exists at the time of receiver startup.

The actual startup sequence begins by redirecting the sun onto the receiver at time equal to 0. The receiver goes through its normal startup sequence until a derated steam condition is produced on a panel-by-panel basis. During the startup period, power collected by the receiver is diverted to the receiver flash tank in the form of hot water or a two-phase mixture. The thermal power passes down the tower through a pair of downcomer lines leaving the flash tank (one for vapor and one for condensate) and is introduced into the feedwater heater elements. At the same time, a portion of the flash tank vapor is fed to the main downcomer line where heating is initiated. Drains located at the turbine and downstream of the thermal storage charging heat exchanger are opened, allowing the preheating operation to proceed to those points. The startup continues with the receiver steam being held at a derated condition to prevent a thermal shock condition from occurring while the thermal power developed is heating the rest of the system. During the period, a significant portion of the collector field has been kept out of service to prevent overpowering of the system.

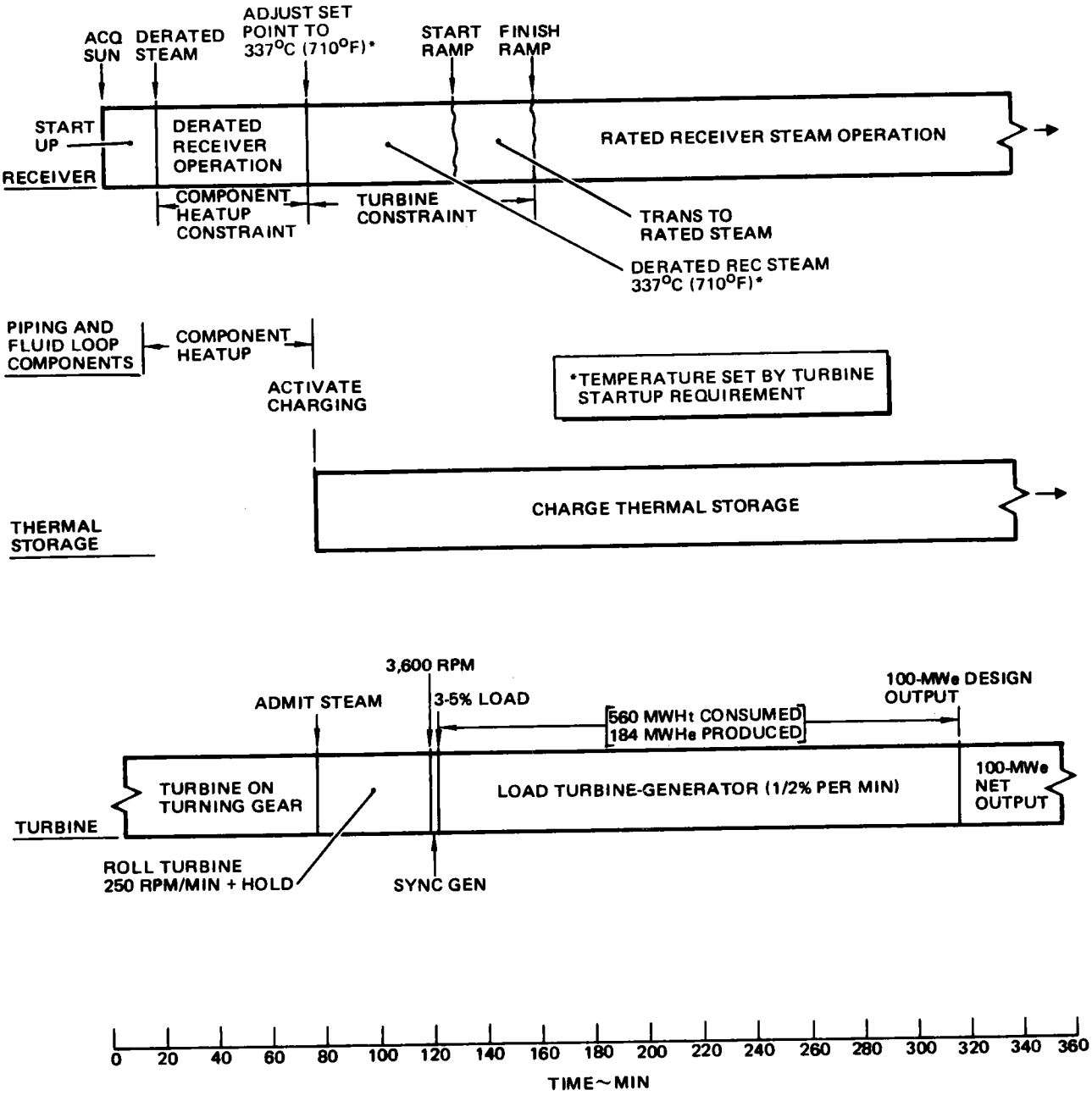

Figure 3-28. Cold System Startup From Receiver (Commercial System)

With the completion of the component heat up activity, at about 75 min into the startup cycle, the receiver outlet steam set point is ramped to ~377°C (710°F) while steam is being admitted to the turbine and the thermal storage charging loop is being activated. This steam condition has been selected so that the turbine can be supplied with steam at 40% of rated steam pressure with at least 56°C (100°F) of superheat. With the thermal storage subsystem being capable of accepting power, a greater portion of the collector field can be activated with the limiting power flow corresponding to the maximum charging rate.

The turbine roll and hold procedure meets the manufacturer's specification with full rated speed being realized at ~119 min into the startup sequence. At that point, the generator is synchronized and a 3 to 5% load is applied. The loading of the turbine-generator then proceeds at 1/2% per minute. During the period from approximately 10 to 25% load, the receiver outlet conditions are ramped to the full-rated steam conditions. With the receiver operating at a rated steam condition and the thermal storage absorbing excess power, the turbine generator load continues to increase until the full 100-MWe net power is available from the generator at 315 min after initiation of the startup sequence. During the turbine loading period ~560 MWH of thermal power was consumed while ~184 MWH of gross electrical power was produced. It should be noted that the turbine operates on a preprogrammed speed/load startup sequence during the first 50% or so of the roll/load time-line. Thus, the turbine valves are not operating in an initial pressure control mode as they would during other operational periods. As a result, the thermal storage charging loop has primary responsibility for controlling receiver pressure during the turbine roll and early loading period.

3.7.2.2 Warm-System Startup From Receiver

The sequence of events associated with a warm-system startup using receiver steam, which is depicted in Figure 3-29, are essentially identical to those just described for the cold startup condition except for an overall compression in the time scale. The startup is again initiated with the sun being directed on the receiver. During the initial phase of the receiver startup, the thermal power produced at the receiver is used for some limited component heatup, although the need should be minimal because the system is already assumed warm.

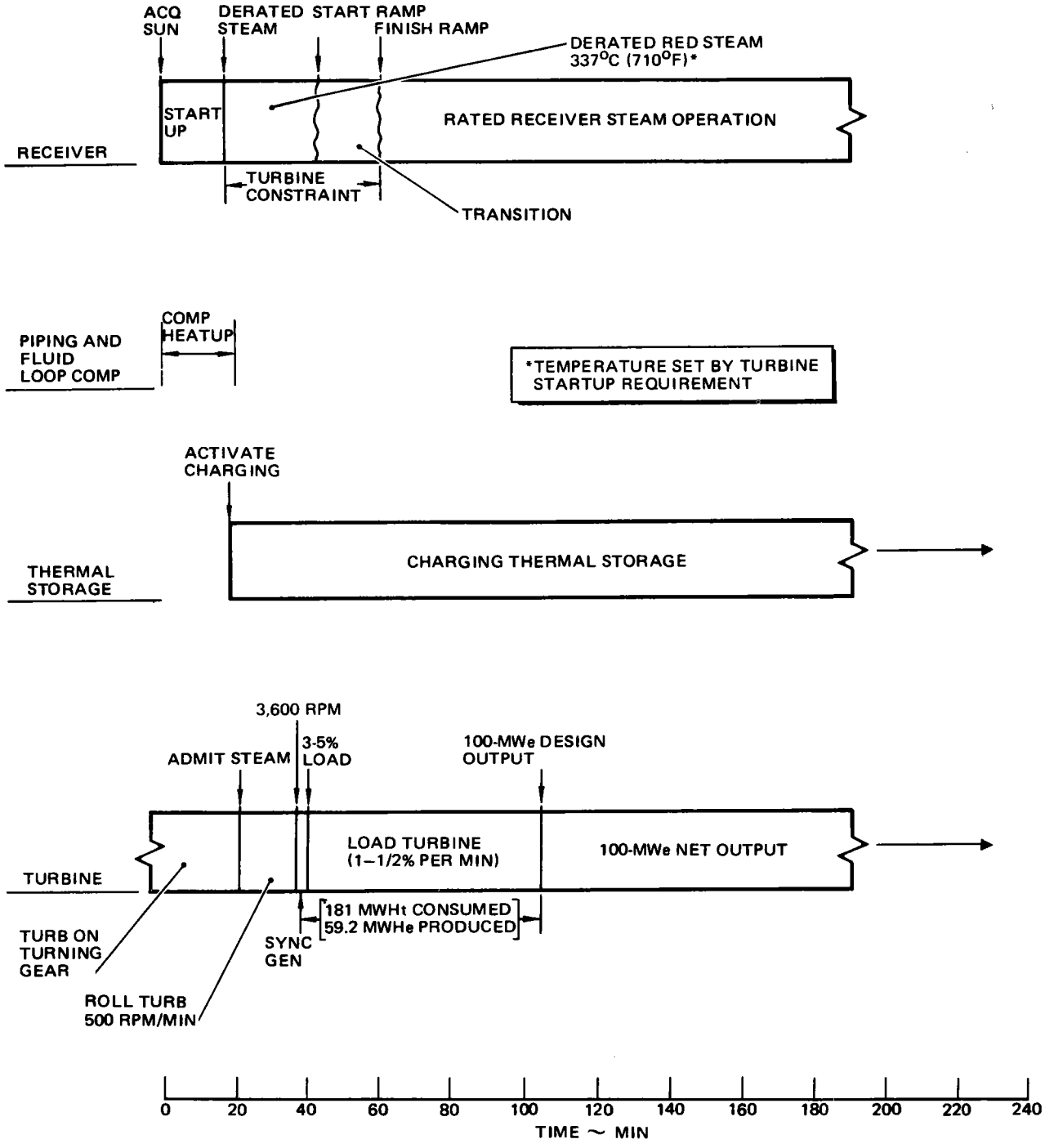

Figure 3-29. Warm System Startup From Receiver (Commercial System)

The receiver is allowed to stabilize at the indicated condition of 377°C (710°F), which is slightly above the derated steam temperature. The selection of this set point condition provides an immediate source of steam which can be introduced to the turbine while the surplus is diverted to thermal storage. The turbine roll, hold, generator synchronizing, and loading rates are carried out according to the manufacturer's specification. As in the previous case, the receiver outlet conditions are ramped to the rated steam level as the turbine loading passes between the 10 and 25% power values. During the entire loading period, the thermal storage accepts excess thermal power up to its charging limit. In addition, it is also responsible for receiver pressure control during the early turbine roll and loading phases before it is switched to initial pressure control. During the turbine loading phase, 181 MWH of thermal energy is consumed with ~59 MWH of gross electrical power being produced. The elapsed startup time required to produce 100 MWe net power is approximately 105 min.

3.7.2.3 Hot-System Startup From Receiver

The sequence of events necessary to execute a hot-system startup from receiver steam is shown in Figure 3-30. In this case, it is assumed that no component preheating is required so that the only thing limiting the initiation of turbine roll is the rate at which the receiver can be brought up to a steam condition compatible with the turbine requirement. The time period shown for receiver activation and stabilization is 17 min, which is dependent on available insolation conditions. When the stabilized receiver condition is reached, the thermal storage charging loop is activated and accepts as much power as is available or as limited by the maximum charging capability. At the same time, the turbine roll and loading cycle is initiated. Because the turbine is at full operating temperature, the roll and loading activity can occur fairly rapidly. Again, the transition in receiver outlet conditions to rated steam is timed to occur during the period when the turbine passes through the 10 to 25% load range. The duration of the complete startup requires ~65 min, with 89.5 MWH of thermal energy being consumed during the turbine-loading phase and 29.5 MWH of gross electrical energy being produced during the period. During some early morning periods, the rate of steam demand by the turbine may exceed the receiver's ability to product it because of the limited collector field power which may exist. Under such a condition, the start would be limited by the collector field.

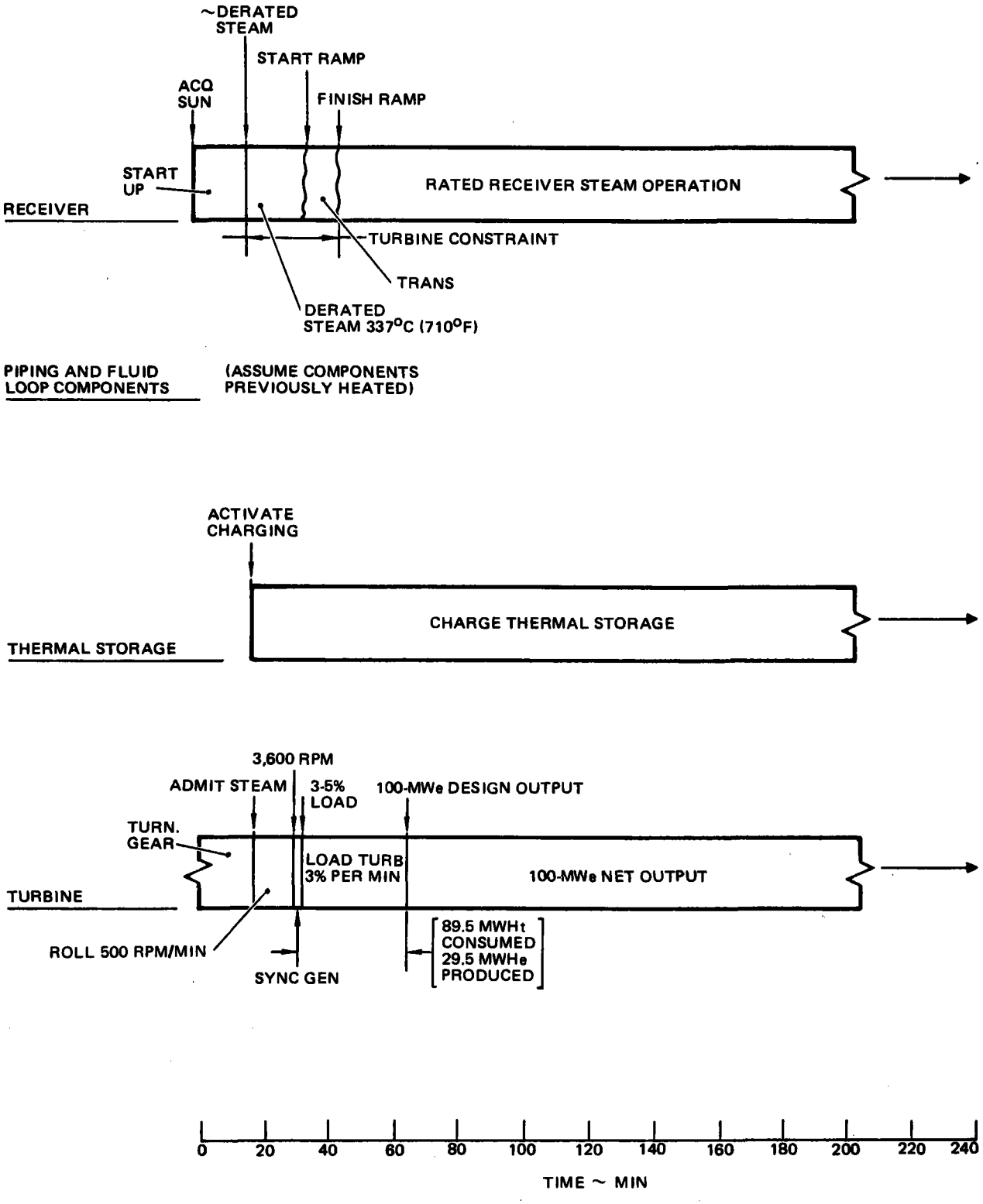

Figure 3-30. Hot System Startup From Receiver (Commercial System)

3.7.2.4 Warm-System Startup from Thermal Storage

To reduce the overall system startup time, two cases of turbine start from thermal storage steam were considered. The case treated in this section and shown in Figure 3-31 assumes a warm start condition. The critical time-phasing relationship is the point where the turbine is fully loaded (at about a 70% load point, which is the limit for operation from thermal storage steam) and the receiver is simultaneously finishing its ramp to rated steam. Working backward from that point, it is seen that the turbine roll would initiate ~25 min prior to the receiver startup. Steam would be drawn from thermal storage to power the roll and loading of the turbine.

At time equal to 0, the receiver startup would be initiated with it proceeding to a derated steam hold condition until all panels had stabilized at that level. During that period, some limited component heatup would be carried out by the receiver steam. Near the end of the derated steam hold period at the receiver, the component heatup would be complete and the charging of thermal storage is initiated. At that time, the thermal storage subsystem would be simultaneously charging and discharging the storage tank. The receiver would next be ramped to a rated outlet steam condition as rapidly as possible, arriving at the rated condition at the same time the turbine had arrived at the 70% load point. At that time, the rated receiver steam flow would be fed directly to the turbine to continue the loading cycle to 100% load while the admission steam flow from thermal storage was cut back to zero flow in a controlled manner.

This particular startup sequence represents the condition where a minimum initial thermal storage charge is required. If an earlier turbine startup is desired, a larger initial thermal storage charge would be required due to the longer discharge period that would be experienced by the thermal storage before receiver steam would be available to supplement and ultimately replace the thermal storage steam.

During the warm turbine startup, 151 MWH of thermal energy would be extracted from thermal storage although some of that would be made up by the charging flow from receiver steam once the panels had arrived at a derated steam condition. At the same time, 37.3 MWH of gross electrical

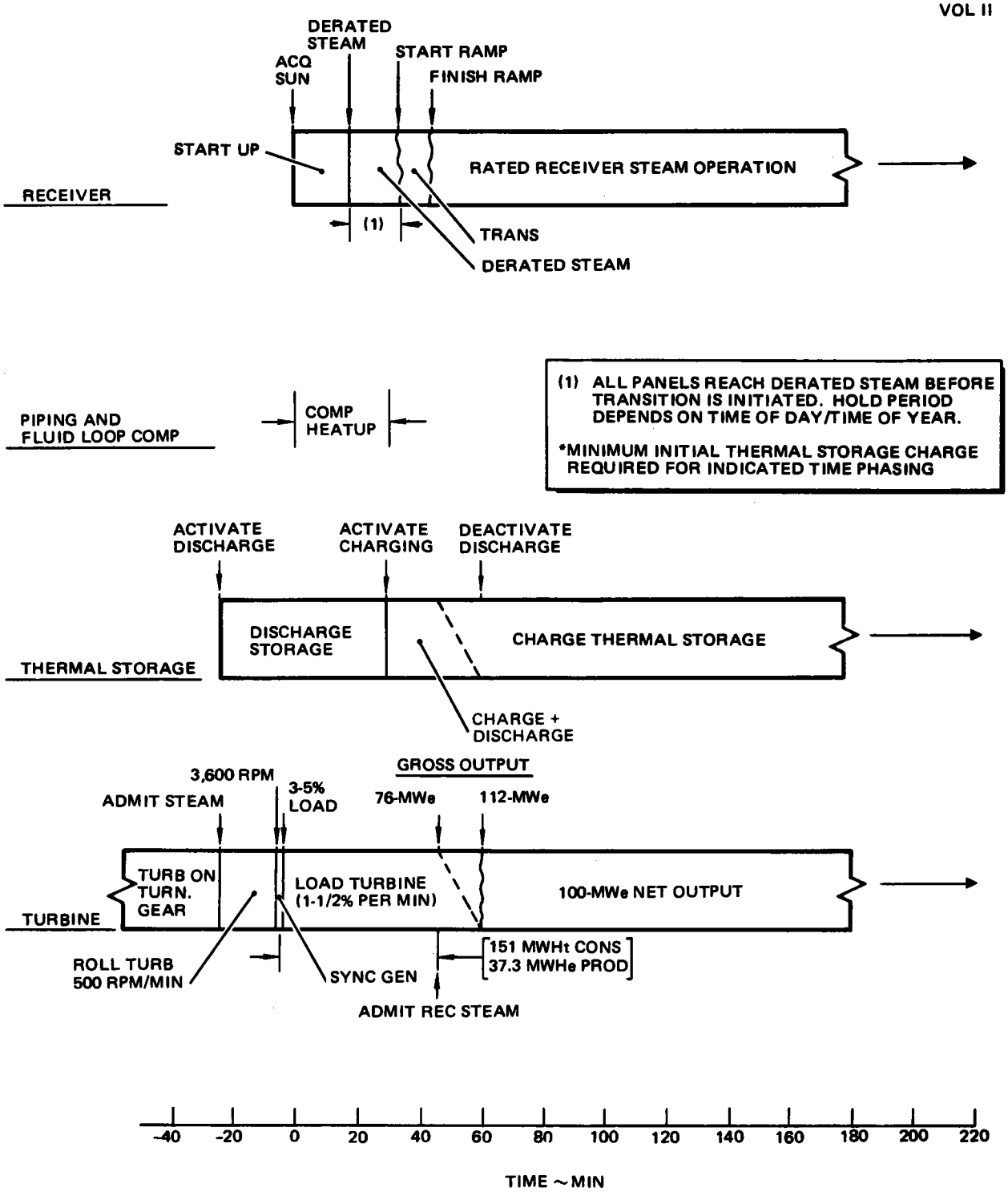

Figure 3-31. Warm System Startup From Thermal Storage* (Commercial System)

energy would be produced. The effective system startup time for this case would be 47 or 60 min, depending on the startup definition used. This compares to a startup period of 105 min for the case where the system starts exclusively from receiver steam (Section 3.7.2.2).

3.7.2.5 Hot-System Startup From Thermal Storage

The sequence of events that occur during a hot-system startup from thermal storage steam is shown in Figure 3-32. As in the previous case considered (Section 3.7.2.4), the key reference point for synchronizing the startup activities is to match, as closely as possible, the 70% load point on the turbine loading line with the availability of rated receiver steam. Again working backward from that point, the receiver startup sequence would be initiated first at time equal to 0. At the 5-min point, while the receiver startup is continuing, the turbine roll cycle is initiated using steam drawn from thermal storage. The receiver startup continues with a hold being maintained at the derated steam condition until all panels have reached that level. Just prior to the final receiver ramp to rated steam, the available derated steam is diverted to thermal storage where the charging function is initiated. As a result, during the subsequent period, the thermal storage will be operated in both the charging and discharging mode.

With a uniform derated steam condition established for all receiver panels, the final receiver ramp is carried out as rapidly as possible to rated steam. The rated steam is then fed to the turbine where it replaces thermal storage steam and continues the turbine load ramp to 100% power. A short interval has been included between the point where rated steam is produced in the receiver and when it begins to displace thermal storage steam. The interval allows for a small temperature adjustment time for the main steam downcomer and steam line to the turbine.

Using the sequence established in Figure 3-22, an effective system startup time of 47 to 54 min could be expected, depending on whether the 70 or 100% load point was assumed to constitute a complete startup. If the indicated piping temperature interval were ignored, the startup time could be reduced by 3 to 5 min. The thermal storage energy consumed during the startup was 75 MWH, while 17 MWH of gross electrical energy would be produced during the startup to the 70% power point.

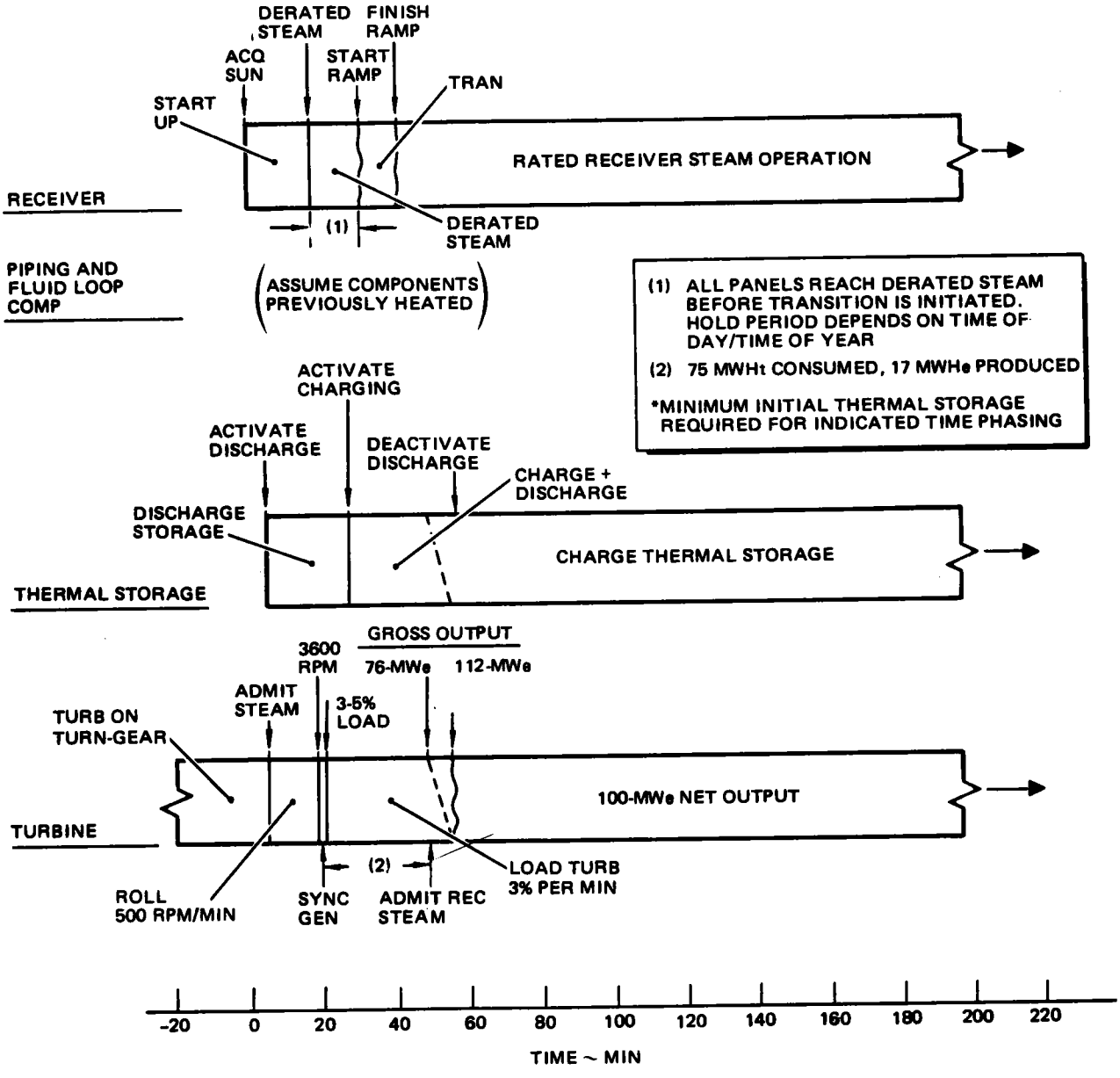

Figure 3-32. Hot System Start From Thermal Storage* (Commercial System)

It should also be pointed out that the duration of receiver hold at a derated steam condition, which directly impacts the system startup time, is influenced to a great extent by the time when the startup occurs. During typical early morning startup, some panels are inherently more sluggish than others because of locally lower incident power from the collector field. The hold period could be reduced significantly if the startup were assumed to occur at a noontime sun condition. During this period, the high level of redirected thermal power leaving the collector field would create a favorable condition for receiver startup.

3.7.3 Transient Plant Operation

One of the unique characteristics of a solar electric system over conventional electrical generating plants is that it does not have close control over its heat input. Although the selective actuation and deactivation of heliostats could be thought of as a "zeroth order" control on power input to the receiver, this approach does not provide the quality of control necessary. As a result, the system must continually operate in a reactive mode to normal diurnal variations in insolation as well as more rapid transient effects caused by cloud passage.

The key factor that influences the controllability of the system to transient power inputs is the thermal time constant of the system or, more particularly, the thermal inertia of the receiver. In general, a comparative assessment of the receiver thermal inertia can be made by considering the quantity of hot metal in the superheat section per unit flow of steam. The characteristics of the superheat section are the important factors since the turbine must be operated on steam with sufficient superheat to prevent significant condensation from occurring in the last-stage buckets. As a result, merely maintaining saturated steam conditions leaving the receiver would not be sufficient.

A useful comparison parameter which gives an indication of a superheater section's ability to operate through a transient insolation pulse (such as would be experienced during cloud passage) is the ratio of local metal cross-section for an individual tube to the cross-sectional flow area. Using the baseline receiver tubes 1.27 cm (0.5 in.) OD, 0.683 cm (0.269 in.) ID, the ratio is slightly larger than 2.4. By comparison, if a similar duty superheater (same

total flow and effective surface area) which employed more conventional tube sizes is considered, the area ratio is typically 0.6-0.7. This means that the receiver that uses small diameter, thick-walled tubes in the superheat section has four times the metal on a per-unit flow basis than the superheater constructed from large-diameter tubes. The result would be a significant improvement in the thermal stability of the small-tube design. It should be noted that this comparative effect is essentially independent of whether the receiver is of a cavity or external type since 85 to 95% of the power absorbed on the receiver surface is passed to the steam while the balance is convected and radiated away. Thus variations in the heat loss factors related to the specific receiver geometry do not significantly influence the thermal power transferred to the steam.

The receiver tube temperature response to a step decrease in insolation to zero is shown in Figure 3-33 for a series of constant flow conditions. Lines of constant flow were used to illustrate the resulting temperature decay due to lack of definition of the controllers and control valve dynamics which would influence rate of changes in panel flow. The tube wall node treated in this plot is a computational metal node located near the outlet of the superheat section of the tubes. The decay in metal temperature reflects the decay in outlet steam conditions. The "no flow" temperature decay line included a radiation loss component and a convective loss component with an assumed heat loss coefficient of 0.00227 W/cm^2-°C (4 Btu/hr-ft^2-°F).

From a turbine standpoint, an unacceptable steam condition would exist once the inlet steam fell below 343-371°C (650-700°F) as long as pressure remained constant. As seen from the figure, the steam temperature, which leads the metal temperature, could decay to that temperature level in ~2-4 min, depending on the rate of flow cutback that would be carried out without causing a turbine trip. It should be pointed out that the analysis assumed that the cloud shuts down the collector field instantaneously. In addition, no effects of downcomer thermal mass were considered. If the two effects were included, a temperature decay time at the turbine inlet of 2.5-5 min would be more representative. To accurately predict the system dynamic response to postulated cloud patterns and varying insolation models, it is necessary to have detailed design information pertaining to the system hardware and the

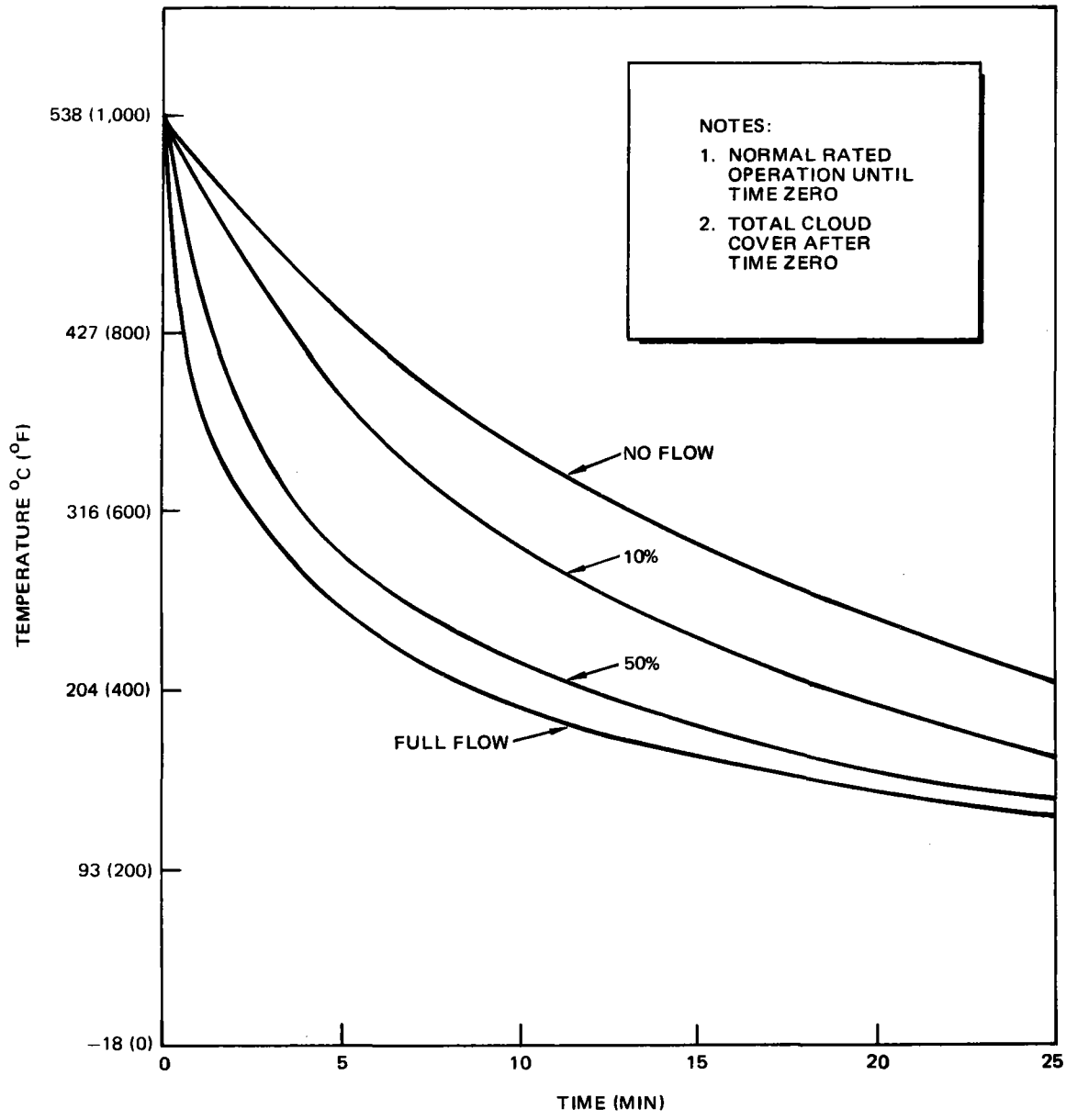

Figure 3-33. Receiver Tube Temperatures at Outlet

controller characteristics. Since this type of data is well beyond the scope of the current Commercial system design effort, the influence of these effects can be treated qualitatively at best.

Four insolation models that contain cloud-induced perturbations have been provided by Sandia and are shown in Figures 3-34 through 3-37. In discussing the impact of each of these models on system operation, it is assumed that some advance knowledge of these events is available so that maximum use of system operating options can be realized.

The insolation model shown in Figure 3-34 represents a rather typical good day from an insolation standpoint with one minor perturbation early in the morning. The timing for the perturbation corresponds to an extremely low sun angle (~10-deg elevation). As a result, the receiver startup would be in its early heatup phase when the perturbation occurred. The net effect of the perturbation would be to delay slightly the point at which derated steam would be produced and sent to the thermal storage. It should be remembered that the field cosine and blocking and shadowing factors improve rapidly as the morning sun elevation angle increases. The net effect of the improved optical characteristics of the field will be to almost completely offset the perturbation in the insolation. Once the perturbation has passed, a normal operational day would be experienced. The slight irregularities near midday would cause only minor modulations in receiver flow rate with a corresponding modulation in the power flow to thermal storage.

The second insolation model shown in Figure 3-35 contains a good morning and midday period with significant cloud-induced oscillations in the afternoon. The first dropoff in insolation would merely impact the receiver flow rate. Rated steam operation could be maintained at all times during this perturbation. The steam flow diverted to thermal storage would be adjusted to absorb this transient with turbine output being maintained at its design level. The second and more severe falloff in insolation is of a sufficient duration (20 min) to cause the receiver to lose control of the outlet temperature. This would force the activation of the thermal storage steam generators to make up for the loss of receiver steam. With the resumption of high insolation levels, the receiver could be restarted and brought back to a rated steam condition

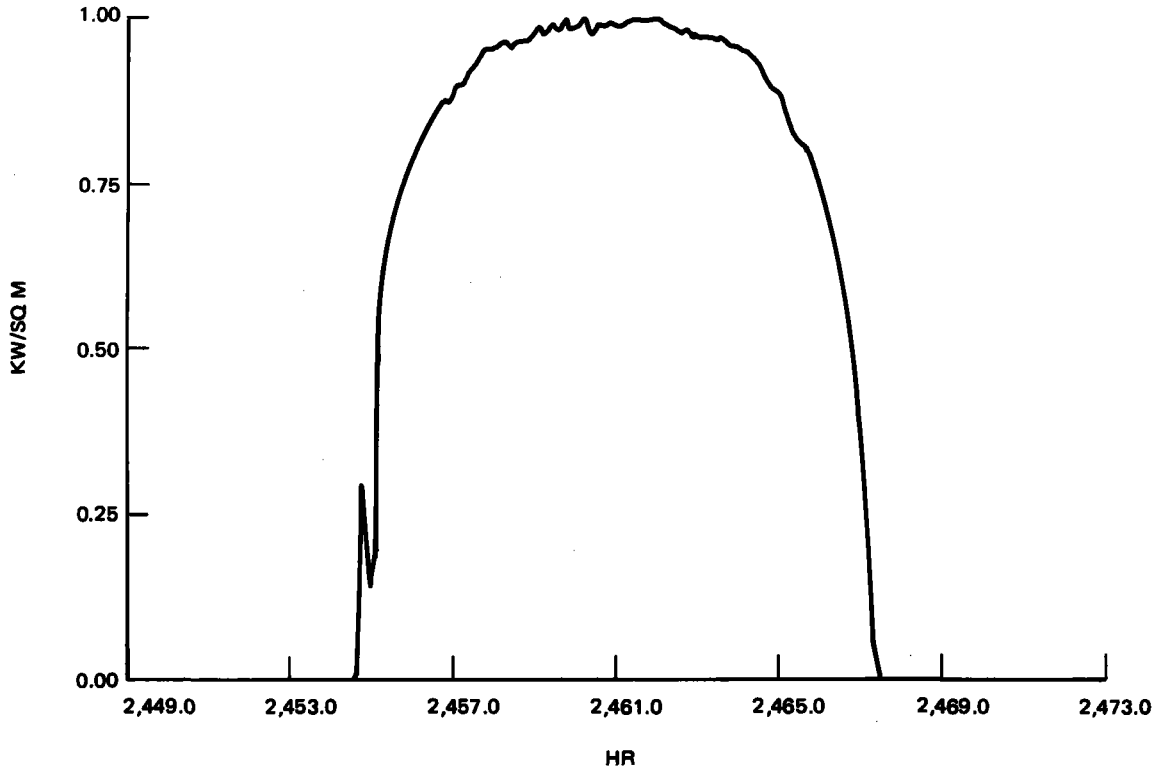

Figure 3-34. Insolation Data

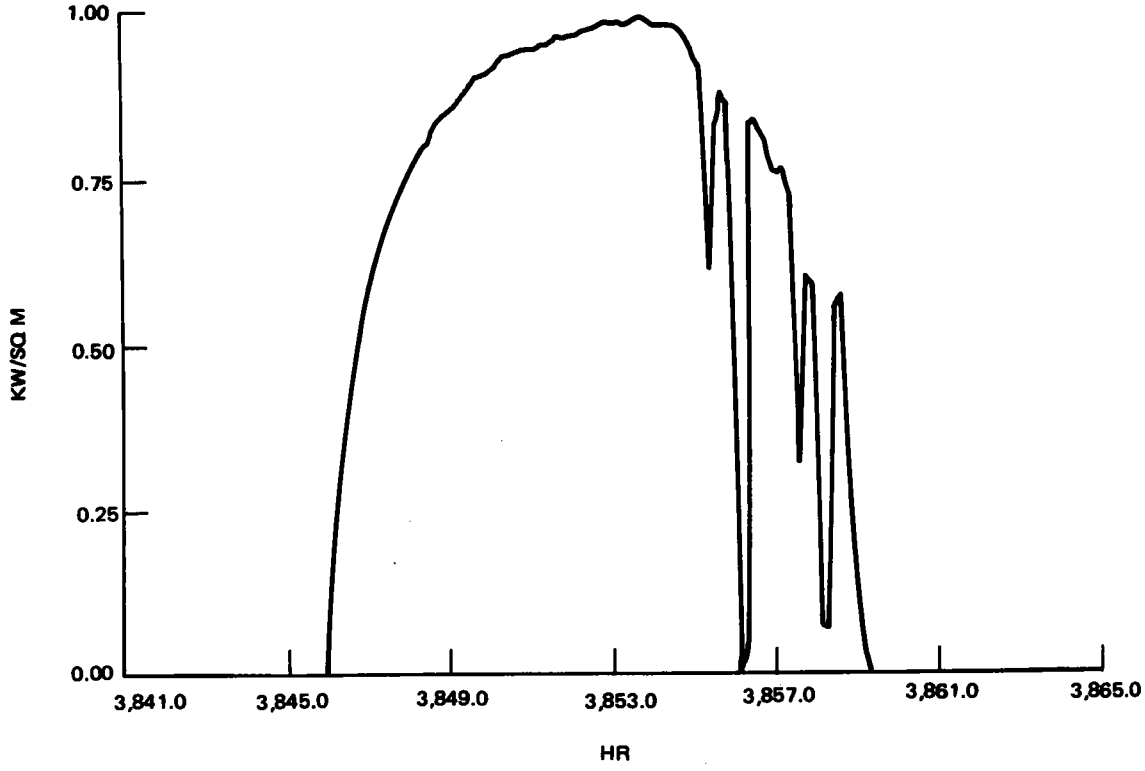

Figure 3-35. Insolation Data

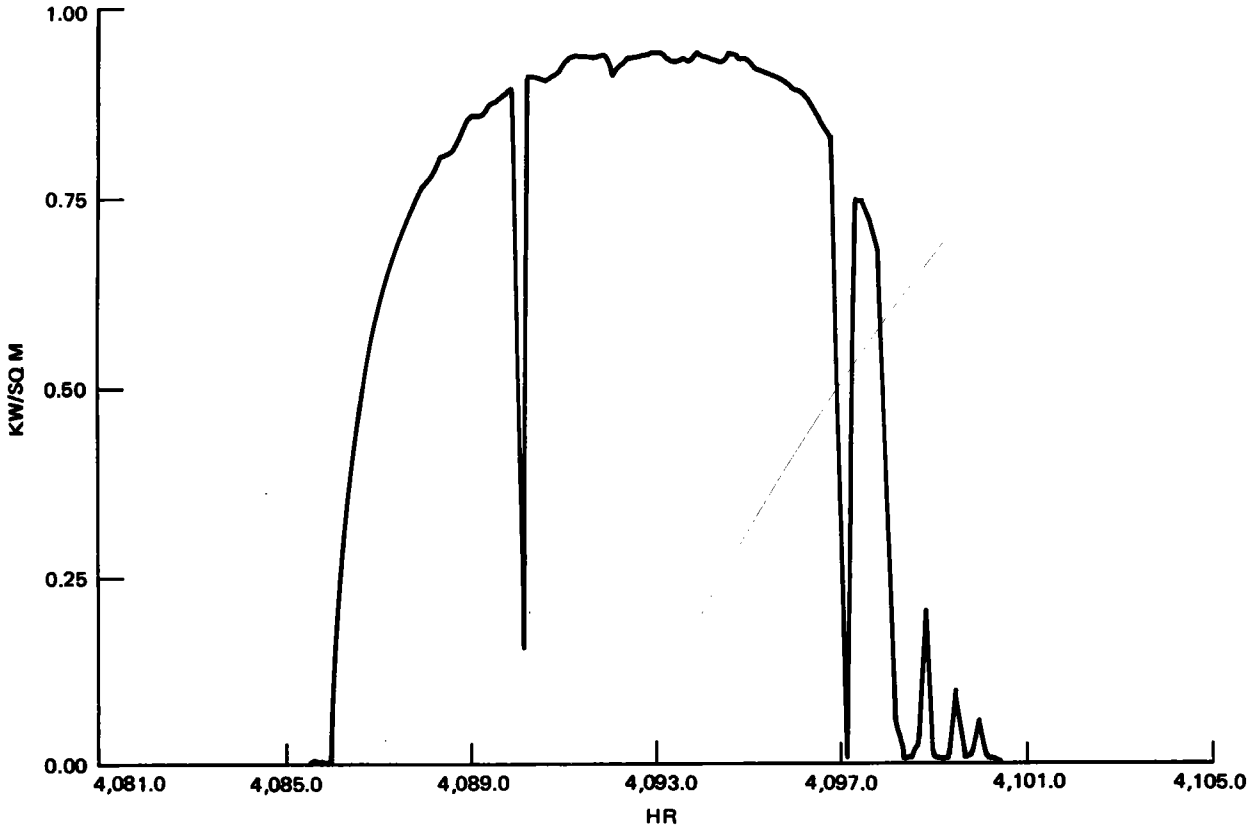

Figure 3-36. Insolation Data

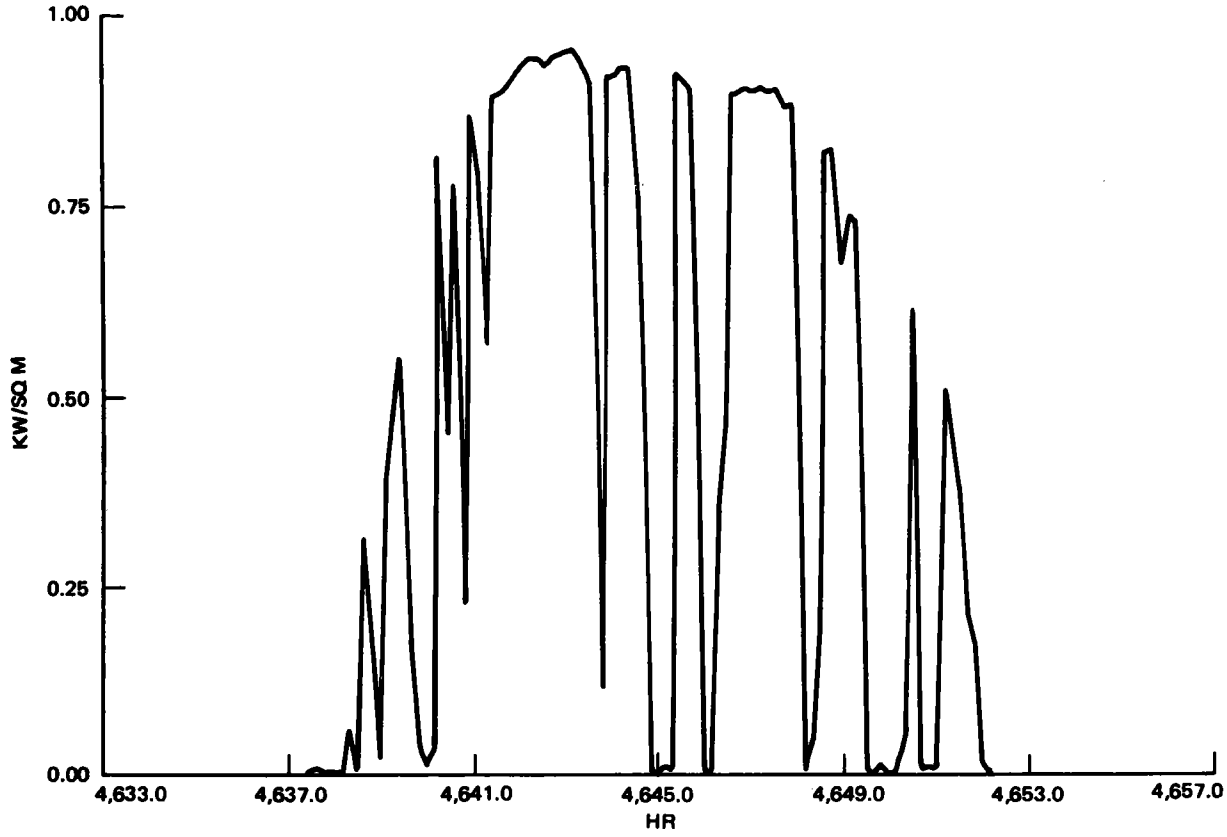

Figure 3-37. Insolation Data

in ~10 min due to its hot condition and the highly effective nature of the collector field which would exist for a high sun elevation angle. The thermal storage steam generator would be deactivated while the rated receiver steam would power the turbine and charge thermal storage. This mode of rated steam operation would continue through the third perturbation although the low solar power mode (see Section 3.7.1) may be employed to maintain the turbine output at a desired level. With the last cloud perturbation, the receiver would again lose control of the outlet temperature and the steam generator would again be activated. At that point, due to the late hour of the day, it would be impractical to start the receiver and transition to rated steam output. As a result, the receiver startup would stop at a derated steam condition for the final portion of the day's operation. All derated steam flow would be sent to the thermal storage charging heat exchanger while the thermal storage steam generator would be providing a steady-state source of steam which would carry the turbine directly into nighttime operation. (Section 3.7.1 discusses the extended operating mode.)

The insolation model shown in Figure 3-36 contains two significant cloud perturbations during the high insolation period, followed by three perturbations near sunset. The day would proceed through a normal startup and morning operational period until the first cloud perturbation occurred. At that point, the receiver flow would be cut back to accommodate the falloff in insolation. The portion of the steam flowing to thermal storage would first be cut down to zero, at which point the thermal storage steam generator would be activated and the low solar power mode would be used. The receiver flow would continue to be cut back to maintain rated or near-rated steam. Because of the limited resolution of data during the perturbation, it is difficult to determine the final receiver outlet condition at the point when the insolation recovers although it would appear that rated or near-rated steam could be maintained during this period.

The second pulse, which occurs at Hour 4097, appears to be of sufficient magnitude to cause loss of receiver outlet steam temperature control although additional data resolution is necessary to verify this fact. As the cloud begins to cover the field, the receiver flow would be reduced, first causing a cutback in the quantity of steam to thermal storage and then causing a transition to low

solar power where supplemental steam is taken from thermal storage. Assuming the receiver experienced a momentary shutdown, it would be brought back on line in ~10 min once the insolation resumed. Operation would continue until the late afternoon clouds covered the field. Due to the lateness of the day and the generally cloudy condition which exists for the rest of the afternoon, the receiver would put out rated steam as long as possible with the rest of the system being transitioned to the low solar mode followed by the extended operating mode (Section 3.7.1) as the receiver proceeded to shutdown condition. System operation in the extended mode would continue into the night. No effort would be made to start the receiver and collect power during the three short insolation pulses which occur just before sunset.

The final insolation model shown in Figure 3-37 represents a day which experiences significant cloud passage during the entire day. Assuming that knowledge of the complete day's insolation profile existed at the beginning of the day, receiver startup would be initiated at Hour 4639 as the cloud moved off the field. The receiver would produce derated steam ~15 min after startup and then could send ~15 min worth of derated steam to the thermal storage charging heat exchanger before the next cloud front shut down the receiver prior to Hour 4640. With the passage of that cloud front, a second receiver start could be made using the high insolation levels which occur after Hour 4640. The receiver would be controlled to rated steam through the oscillations in insolation which occur around Hour 4641.

This mode of operation would continue until the major cloud front hit the field at Hour 4645. At that point, the turbine would be operated from thermal storage steam while the receiver was held in a standby mode ready for a resumption in insolation. The receiver would be restarted at Hour 4646.5 and operated in a rated steam manner until the next major cloud front hit the field 1.5 hr later. The receiver then would be off line until the insolation level increased at Hour 4648.5, at which time the receiver would be restarted. Due to the increased frequency of clouds for the balance of the day, the receiver would be controlled to a derated-steam condition while the system was operated in an intermittent-cloud mode. The mode would continue until the cloud front at Hour 4649.5 covered the field. At that time, the system

would be operated in the extended operating mode while the receiver would be shut down for the day. No effort would be made to capture any power from the last two insolation pulses because of their short duration.

3.8 COMMERCIAL SYSTEM AND PILOT PLANT RELATIONSHIP

The similarities which must be preserved between the Commercial system and the Pilot Plant to satisfy that the verification objectives occur at two levels. The levels correspond to system-related and subsystem-related characteristics. In distinguishing between the two, the system-level issues are those which affect several parts or subsystems of the total system. It should be noted, however, that the system characteristics are in reality subsystem characteristics that influence other subsystems through the coupling of the water/steam loop or the optical energy transmission process.

3.8.1 System Relationships

As indicated above, the system relationships which must be preserved between the Commercial system and the Pilot Plant involve those elements which directly affect either the water/steam loop or the optical energy-transmission process. In general, the factors have a direct effect on the operation and control of the entire system. Specifically, factors which affect water/steam loop pressure and pressure dynamics must be simulated as closely as practical because pressure is the single most important control variable. Pressure modulations at one point are transmitted on a nearly instantaneous basis to all points of the water/steam loop. As discussed in the operating mode section, the turbine inlet control valves and thermal storage charging heat-exchange equipment have individual or shared responsibility for the control of receiver pressure. Since the pressure control in the receiver is a critical verification step in demonstration of the single-pass-to-superheat receiver which uses preheat panels, it will be necessary to simulate in the Pilot Plant the hardware elements which directly influence the pressure and pressure dynamics.

The second system-related area involves the optical energy transmission process, which specifically influences the collector field and receiver geometry. It is essential to preserve the collector field/receiver geometric (optical) relationships to permit the investigation of critical coupling factors, which would be of particular importance during startup, shutdown, or periods of

cloud passage. During those periods, unusual or abnormal heat flux conditions would be experienced by the receiver. Data resulting from a partial field coverage by a cloud or a startup condition where much of the field is inactive due to internal blocking and shadowing are essential in verifying the ultimate Commercial system from an overall system operation standpoint.

3.8.2 Subsystem Relationships

The subsystem relationships that must be preserved between the Pilot Plant and Commercial system involve the duplication or scaling of certain critical subsystem parameters. The relationships apply to the solar parts of the system and include the collector, receiver, and thermal storage subsystems.

The principal collector subsystem relationships involve the preservation of the close-packed Commercial system collector field and the use of full-size heliostats that are based on the current Commercial system design. The use of a close-packed collector field, which is a scaled-down version of the Commercial field, preserves the aerodynamic and optical (blocking, shadowing, and back side heating) effects that must be understood before proceeding to the Commercial system. In addition, by preserving the geometrical relationships between the two systems, heliostat tracking and control through all possible operational angles as well as operation through the singularities can be demonstrated on a large scale. From a nonoperating standpoint, preservation of the close-packed field in the Pilot Plant provides valuable data related to installation and maintenance in this type of field environment.

From an individual heliostat point of view, a replication of the Commercial heliostat design in the Pilot Plant allows for extensive manufacturing experience to be gained. In addition, extensive data pertaining to heliostat operation and life would also be available.

The critical scalability issues from a receiver standpoint involve the preserving of the characteristics of the Commercial system receiver design. Specific things to be duplicated include tube material and size as well as the 24-panel cylindrical configuration. Heat flux distribution on the surfaces

will be adjusted to produce similar tube-temperature characteristics for both Pilot Plant and Commercial system. This adjustment will force the Pilot Plant receiver to operate at a lower concentration ratio than the Commercial receiver due to the lower flow of water/steam (less cooling capacity) per unit surface area. This difference in concentration ratio results in a Pilot Plant receiver which is less efficient than its counterpart for the Commercial system.

The receiver steam conditions produced in the two systems are essentially identical with only a minor difference occurring in pressure. The Pilot Plant steam pressure condition is 10.1 MPa (1,515 psia) while the corresponding value for the Commercial receiver is 11.1 MPa (1,615 psia). In both cases, an outlet steam temperature of 516°C (960°F) will be maintained. From a scalability standpoint, this similarity will result in nearly identical heat-transfer mechanisms in the two receivers because a similarity in wall temperature will also be preserved.

From a nonoperational standpoint, the similarity in overall receiver configuration and panel design allows experience to be gained in installation, maintenance, and manufacturing areas. In addition, because of the identical nature of the panels, production facilities established for the Pilot Plant can be used directly for the Commercial receiver panels.

The critical thermal storage scalability issues include factors related to the storage tank and the changing/discharging equipment. Critical tank-related issues include the thermocline and Caloria velocities, the peak Caloria temperature and temperature range over which the fluid is exercised, and wall structural considerations. Design values for the first three of these items are shown in the following tabulation:

	Pilot Plant	Commercial System
Thermocline Velocity	2.8m/hr (9.2 ft/hr)	2.8m/hr (9.2 ft/hr)
Caloria Velocity in Tank	11m/hr (36.1 ft/hr)	11m/hr (36.1 ft/hr)
Caloria Temperature Range	302° to 219°C (575° to 425°F)	316° to 232°C (600° to 450°F)

From a tank wall standpoint, the critical issue is the long-term effect of the rock on tank wall stress. SRE test data has given no indication of stress ratcheting in the wall, although long-term effects are still a question mark. The goal for Pilot Plant is to develop sufficient structural data on the tank wall so that specifications for Commercial-size tanks can be written directly from the Pilot Plant data.

The charging and discharging equipment directly affects pressures and flow-rates in the rest of the system and therefore fall into the system relationships discussed in Section 3.7.1. The two principal factors of concern are the dynamic controllability and the throttle range for the equipment. Of the two, the dynamic control issue is the most significant because of its impact on overall plant control. The throttling range of the components ensures flow rate compatibility with the interfacing subsystems. The throttling range issue is much more significant for Pilot Plant than Commercial system because fewer components must be throttled over a wider range. Typical throttling ratios for the charging and discharging equipment are 20:1 and 10:1, respectively.

Section 4
PILOT PLANT SYSTEM DEFINITION

This section provides an in-depth discussion of the baseline Pilot Plant system. The discussion reviews the Pilot Plant requirements to which the system was designed and summarizes the pertinent design and performance characteristics of the baseline configuration. This design and performance information is broken down into two subsections: the optical portion and the water/steam loop part of the system. Some of the background studies that were carried out prior to the baseline design freeze are discussed. Additional topics such as annual energy production, plant operation, plant control simulations, and system effectiveness (including availability and safety considerations) are also treated. Finally, this section treats the Phase 2 system integration effort, the installation and test program, and the required logistics support plan.

4.1 REQUIREMENTS

The requirements which served as the foundation for the Pilot Plant design effort were presented in Table 3-1 as merely comparative points of interest to the Commercial requirements, which were the topic of discussion. An abbreviated summary of the most significant Pilot Plant requirements is in Table 4-1. The principal sizing requirement is to be capable of producing 10 MW of net electrical power at 2 PM on the worse cosine day (which is Winter solstice for the MDAC system), with an insolation level of 950 w/m^2. The system will be capable of producing at least 7 MW of net electrical power during turbine operation exclusively from thermal storage for a period of up to 3 hr. In an effort to minimize the cost of the Pilot Plant, the design approach selected to satisfy these two sizing requirements was to size the system to produce 10 MW of net electrical power at 2 PM on Winter solstice with no excess thermal power available at that time to charge thermal storage. If it is desired to meet the turbine operating requirement from thermal storage, a delay in the daily turbine startup would be necessary to ensure

Table 4-1

PILOT PLANT SYSTEM REQUIREMENTS

Design Point Power Level	
Receiver (2 PM, worst cosine day)	10 MWe net
Thermal storage	7 MWe net
Design Insolation	950 W/m^2
Solar Multiple	1.1
Thermal Storage Capacity	3 Hours
Maximum Thermal Storage Charging Rate	30 MWt
System Startup Times	
Hot	20 Minutes*
Cold	6 Hours
System Availability	90%
Electrical Output	Compatible with SCE grid

*Minimize within practical limits

that sufficient energy would be diverted to thermal storage to fully charge the unit. The resulting collector field size necessary to satisfy this requirement has a solar multiple of 1.1 when measured at equinox noon.

The thermal storage charging requirement of 30 MW corresponds to the minimum design value specified by DoE. The value was selected as a design upper limit to minimize the cost of the Pilot Plant system. Sizing the charging equipment to that value would allow the thermal storage unit to accept in excess of 85% of the maximum collector field output. Since the turbine is sized to accept 100% of the collector field output, it is felt that such a restriction in thermal storage charging rate is warranted from the standpoint of system cost-effectiveness. In addition, the options exist on the Pilot Plant to slightly overdrive the thermal storage charging pumps and allow the outlet Caloria temperature to rise slightly above the 302°C (575°F) design point.

The startup and system availability requirements specified in Table 4-1 are identical to those discussed in Section 3.1 as related to the Commercial system. Since the Pilot Plant will be part of the Southern California Edison network, the system output must be designed to be compatible with the SCE

grid. Additional Pilot Plant requirements related to environmental factors were shown in Table 3-1 and will not be treated further in this discussion. It should be pointed out that for the most part these environmental requirements represent typical locations in the desert southwest. Since Barstow has been selected for the Pilot Plant site, it is anticipated that some of those environmental factors may be modified to reflect specific characteristics of Barstow.

Additional Pilot Plant requirements imposed by MDAC call for the development of a computer-assisted control capability to aid in system startup, mode transitions, and shutdown. This was done in recognition of the unique operating nature of a solar electric system (it must react to changes in input power as opposed to controlling the input power which is done in conventional plants). In addition, the computer control capability is a necessity to command the large number of heliostats in a coordinated fashion. Also, weather factors must be continually analyzed in order to anticipate weather-induced changes in system operation and aid in making operating mode selections.

4.2 COLLECTOR FIELD LAYOUT

The collector field layout activity for the Pilot Plant involved defining a scaled version of the Commercial system collector field which is sized to produce the necessary design point power. This design effort required a significant extension of the work done for the Commercial collector field in that the final required outputs were individual heliostat coordinates. In addition, the cell-by-cell approximation used to define the Commercial collector field was inappropriate for defining the details of the Pilot Plant collector field since most Pilot Plant heliostats intersected the cell boundaries, resulting in an extremely discontinuous heliostat pattern.

4.2.1 Revised Field Layout Analysis and Design

The revised field layout analysis carried out by the University of Houston involved two major efforts. First, an appropriate layout scheme had to be defined to replace the cell-by-cell approach used for the Commercial system; second, the heliostat displacement information which was the foundation for computer calculations had to be transformed into heliostat coordinate locations.

The optimized Commercial system collector field geometry was found to be so nearly circular (see Appendix C) that it seemed appropriate to assume that the Pilot Plant could be laid out along unbroken circular rows. This assumption, which proved satisfactory, simplified the relationship between the displacement data and the ultimate objective of heliostat coordinates.

The next issue to be treated was how the radial stagger field could best be incorporated into a circular field layout on the Pilot Plant scale. The stagger arrangement required adjacent circles to have the same number of heliostats. This requirement results in a progressive compression of heliostat spacing until an unacceptable heliostat density occurs as one moves toward the center of the field. Consequently, the field was divided into a series of circular zones. The zone boundaries allowed for a decompression to occur by reducing the number of heliostats per circle in the inner zone. A total of six zones were required for the Pilot Plant layout.

The options available to define the zone boundary conditions were to separate the zones by a series of gaps or to reduce the number of heliostats in the inner zone by an exact ratio. The first approach was not pursued because it results in excessive gaps in the field with a consequential loss in valuable ground coverage area. The exact ratio reductions used in the design analysis were (3/2), (4/3), and (5/4). The following results were observed:

(3/2) provided excessive decompression, resulting in wasted space.

(4/3) provided an intermediate decompression which was ultimately adopted as the desired decompression factor.

(5/4) provided too little decompression resulting in many zones.

The (4/3) reduction leads to the situation shown in Figure 4-1.

The circles in the figure indicate heliostat locations. The vertical arrows point to bad blocking events for the D heliostats of the innermost circle of the outer zone resulting from the decompression process. The G heliostat is correctly located to maximize the "look between" capability, while the S heliostats experience some optical difficulty. The approach adopted to resolve the zone boundary problem was to delete the D heliostats and slide the S heliostats toward the newly created void locations as indicated to arrive at an optical compromise with the immediate neighbors. This combination of

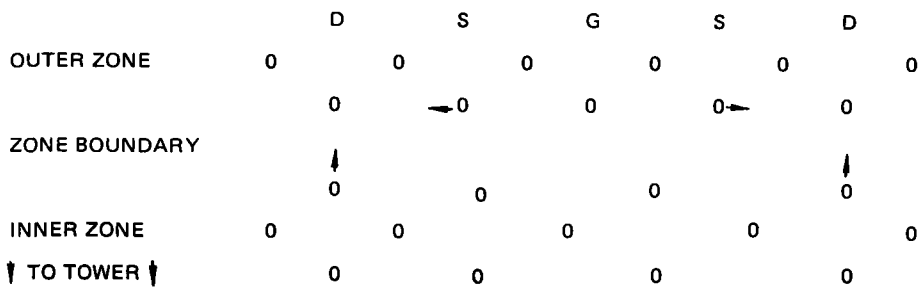

Figure 4-1. Zone Boundary

heliostat deletions and adjustments resulted in a field with a good "look between" capability, good performance, and a reasonable regular design.

The impact of these periodic deletions and location adjustments on the overall collector field performance are in general minor, particularly during the higher sun elevation angles (<20 deg). The current computer simulations ignore these atypical neighborhoods in performance calculations. They apply "typical" neighborhood performance values to the local part of the field, but reflect the deleted glass area in overall power estimates. This approach results in slightly pessimistic performance predictions. To accommodate all types of atypical neighborhoods such as road exclusions, trim boundaries, and zone boundaries, a plan is underway to develop an individual heliostat simulation for the Pilot Plant.

4.2.2 Heliostat Arrangement and Aim Strategy

The heliostat arrangement for the Pilot Plant was shown in Figure 1-6. It contains 1,760 heliostats arranged along 32 complete circles or arc segments, which result in the tower being effectively shifted to the south of center. The collector field is divided into quadrants by four access roads. The circular heliostat symbol represents the exclusion area required for the azimuthally tracking square baseline heliostat. The deleted heliostats result in the periodic voids which appear in the field. The six circular groups can be identified by noting the groups of circles, which are separated by these voids that occur along the zone boundaries. The coordinate locations of all 1,760 heliostats are contained in Appendix B of Volume III.

In aligning the heliostats on to the receiver, a prescribed vertical aim strategy is used to spread the redirected power over the surface of the receiver. The resulting distribution tends to minimize peak flux concentrations which would naturally occur if the heliostats were all aligned to point at the equator. In addition, the receiver size and flux distribution were established to produce a condition of locally similar tube-temperature characteristics for the Pilot Plant and Commercial receivers. This resulted in a lower flux intensity for the Pilot Plant receiver because of its lower flow per unit circumference, which is a direct measure of cooling ability. This resulted in the Pilot Plant receiver being designed for a lower concentration ratio

than the Commercial receiver, which is reflected in lower thermal efficiency for the Pilot Plant design. The final factor considered in the heat flux distribution process is end spillage. In distributing the flux, care must be exercised to minimize this effect consistent with reasonable receiver size and economic considerations.

The definition of the aim strategy and its impact on receiver heat flux are shown in Figures 4-2 and 4-3. A two-step process is used to arrive at the final heliostat aim strategy. The first step is to define a "simple Hi-Low" aim strategy which is then customized to remove local peak flux conditions. The "simple Hi-Low" aim strategy is illustrated in the top half of Figure 4-2; the resulting heat flux distribution on the receiver is shown as the dashed line in Figure 4-3. In the "simple Hi-Low" strategy, the heliostats which make up the collector field direct their images as high as possible or as low as possible on the receiver on an alternating-heliostat basis throughout the field. The aim point locations for beams coming from adjacent heliostats are conceptually shown in the upper right portion of Figure 4-2, as is a representation of the beam width. As indicated in the figure, the center of the beam is displaced from the top or bottom part of the receiver by an amount D, which is defined as the radius of the heliostat segment (for canted heliostats) plus a beam divergence term that is the product of the sun half-angle times the slant range. As shown by the dashed line in Figure 4-3, the effect of the aim strategy for the total field is a heat flux profile with peaks near the top and bottom of the receiver.

The final step in defining the heliostat aim strategy is to define the heliostats whose aim points must be shifted back to the equator to produce a fairly uniform heat flux profile along the receiver. After a series of computer runs, the following modifications to the "simple Hi-Low" aim strategy were selected:

A. Redirect all downward shifted heliostats in Rows 17 to 22 to an equator aim point.

B. Redirect all upward shifted heliostats in Rows 17 to 23 to an equator aim point.

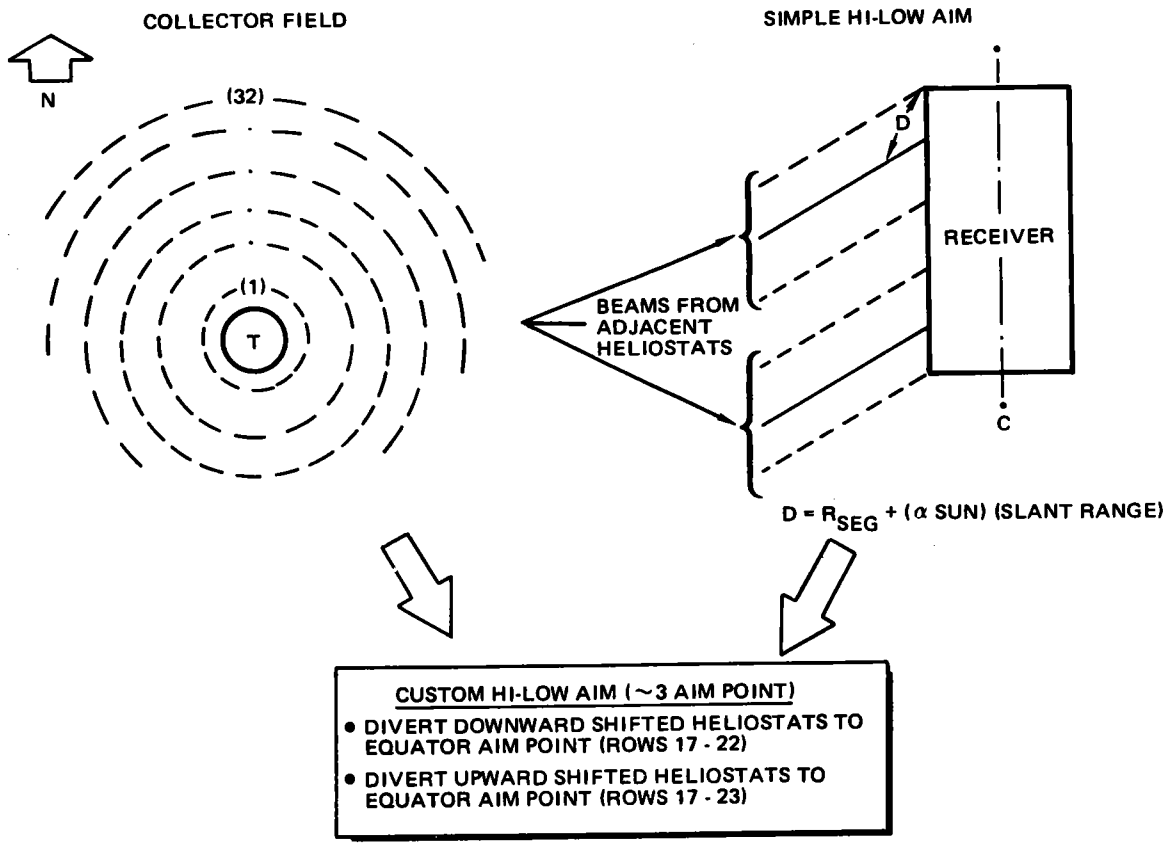

Figure 4-2. Heliostat Aim Strategy

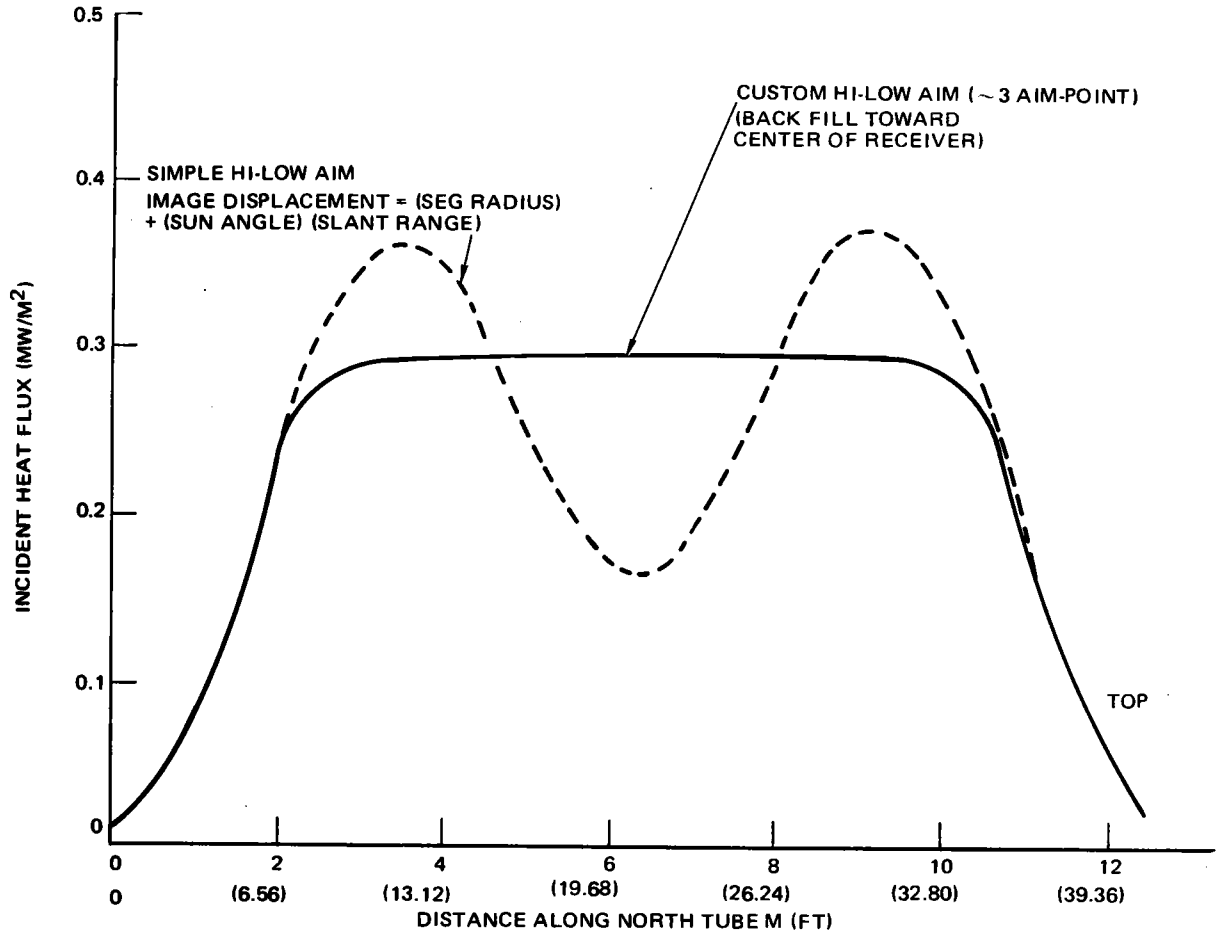

Figure 4-3. Hi-Low Aim Strategy

As shown in Figure 4-2, the row numbers start from the tower exclusion area and move outward. A summary of the aim points for the 32 circles or arcs is shown in Table 4-2. The 8 entries shown for each circle correspond to 45-deg segments for the complete circle starting at south. Since some circles are not complete, a portion of the aim point data shown for the southern part of the field is not applicable. These aim points are based on an equinox noon sun elevation and heliostat orientation. The result of this "customized Hi-Low" aim strategy is a heat flux distribution which approximates the flat idealized profile shown in Figure 4-3 by ±5%. On the east and west side of the receiver, where the peak heat flux is 0.18 to 0.25 MW/m^2, the idealized flat profile is approximated to within ±10%. On the south-facing panels, where an idealized heat flux intensity of 0.07 to 0.12 MW/m^2 would be experienced, the customized aim strategy would be within ±18%. These fairly significant variations in heat flux on not facing north panels are not significant because the most severe design condition occurs on the northern panels which experience the highest heat flux. The variations on the other panels are minor in an absolute sense in comparison to the intensity experienced by the northern panels and have little, if any, effect on the boiling or preheating processes.

4.2.3 Field Performance and Correlation to Commercial System

Performance predictions have been developed for the idealized version of the actual Pilot Plant layout. As discussed in Section 4.2.1, this version ignores the atypical neighborhoods associated with the slip plane deletions and local heliostat readjustments. Field performance predictions developed for the idealized model tend to be slightly pessimistic because they do not recognize the performance improvements realized as a result of the heliostat deletion and local readjustment. It should be noted however, that these effects are significant, on a local basis, only for low sun elevation angles. Even during those periods, the impact on total field performance is diluted by the weighting given to the "regular" parts of the field. During periods of high sun elevation angle, the performance change due to the atypical neighborhoods is 0 since no blocking and shadowing occur.

Table 4-2 (Page 1 of 2)

HELIOSTAT AIM STRATEGY BY ROW

SHIFT UP ON RECEIVER IN METERS

	(Row)	(South)				(North)			(South)
Outer Circle	32	1.305	1.848	2.107	2.236	2.258	2.117	1.839	1.280
	31	1.528	2.065	2.318	2.438	2.460	2.327	2.055	1.504
	30	1.734	2.264	2.489	2.624	2.645	2.483	2.255	1.709
	29	1.939	2.316	2.502	2.750	2.732	2.496	2.319	1.914
	28	2.128	2.349	2.513	2.740	2.722	2.507	2.353	2.103
	27	2.316	2.381	2.523	2.728	2.710	2.517	2.385	2.292
	26	2.490	2.411	2.531	2.716	2.698	2.526	2.415	2.465
	25	2.664	2.440	2.539	2.703	2.684	2.533	2.443	2.639
	24	2.825	2.466	2.545	2.688	2.670	2.539	2.469	2.800
	23								
	22								
	21								
	20				EQUATOR AIM POINT				
	19								
	18								
	17								
	16	3.007	2.612	2.460	2.448	2.470	2.469	2.615	3.016
	15	3.003	2.620	2.397	2.397	2.419	2.407	2.610	3.013
	14	2.999	2.550	2.333	2.344	2.365	2.342	2.540	2.008
	13	2.992	2.471	2.260	2.284	2.305	2.270	2.461	2.981
	12	2.921	2.389	2.184	2.220	2.242	2.194	2.379	2.896
	11	2.826	2.297	2.099	2.148	2.170	2.108	2.287	2.800
	10	2.725	2.199	2.007	2.071	2.092	2.017	2.189	2.699
	9	2.614	2.093	1.907	1.985	2.007	1.916	2.082	2.588
	8	2.489	1.971	1.792	1.887	1.909	1.802	1.961	2.463
	7	2.350	1.837	1.664	1.777	1.799	1.674	1.827	2.324
	6	2.199	1.691	1.523	1.656	1.678	1.533	1.681	2.174
	5	2.028	1.523	1.361	1.515	1.537	1.371	1.513	2.002
	4	1.840	1.337	1.179	1.357	1.379	1.183	1.327	1.814
	3	1.626	1.121	0.966	1.170	1.192	0.976	1.111	1.600
	2	1.393	0.978	0.723	0.356	0.978	0.733	0.868	1.368
Inner Circle	1	1.137	0.592	0.434	0.700	0.722	0.444	0.582	1.112
Arc Angle		(0-45°)	(45-90°)	(90-135°)	(135-180°)	(180-225°)	(225-270°)	(270-315°)	(315-360°)

Table 4-2 (Page 2 of 2)

HELIOSTAT AIM STRATEGY BY ROW

SHIFT DOWN ON RECEIVER IN METERS

	(Row)	(South)				(North)			(South)
Outer Circle	32		1.305	1.848	2.107	2.236	2.258	2.117	1.839	1.280
	31		1.528	2.065	2.318	2.438	2.460	2.327	2.055	1.504
	30		1.734	2.264	2.489	2.624	2.645	2.483	2.255	1.709
	29		1.939	2.316	2.502	2.750	2.732	2.496	2.319	1.914
	28		2.128	2.349	2.513	2.740	2.722	2.507	2.353	2.103
	27		2.316	2.381	2.523	2.728	2.710	2.517	2.385	2.292
	26		2.490	2.411	2.531	2.716	2.698	2.526	2.415	2.465
	25		2.664	2.440	2.539	2.703	2.684	2.533	2.443	2.639
	24		2.825	2.466	2.545	2.688	2.670	2.539	2.469	2.800
	23		2.966	2.491	2.549	2.572	2.654	2.543	2.484	2.953
	22									
	21									
	20				EQUATOR AIM POINT					
	19									
	18									
	17		3							
	16		3.007	2.612	2.460	2.448	2.470	2.469	2.615	3.016
	15		3.003	2.620	2.397	2.397	2.419	2.407	2.610	3.013
	14		2.999	2.550	2.333	2.344	2.365	2.342	2.540	2.008
	13		2.992	2.471	2.260	2.284	2.305	2.270	2.461	2.981
	12		2.921	2.389	2.184	2.220	2.242	2.194	2.379	2.896
	11		2.826	2.297	2.099	2.148	2.170	2.108	2.287	2.800
	10		2.725	2.199	2.007	2.071	2.092	2.017	2.189	2.699
	9		2.614	2.093	1.907	1.985	2.007	1.916	2.082	2.588
	8		2.489	1.971	1.792	1.887	1.909	1.802	1.961	2.463
	7		2.350	1.837	1.664	1.777	1.799	1.674	1.827	2.324
	6		2.199	1.691	1.523	1.656	1.678	1.533	1.681	2.174
	5		2.028	1.523	1.361	1.515	1.537	1.371	1.513	2.002
	4		1.840	1.337	1.179	1.357	1.379	1.183	1.327	1.814
	3		1.626	1.121	0.966	1.170	1.192	0.976	1.111	1.600
	2		1.393	0.978	0.723	0.356	0.978	0.733	0.868	1.368
Inner Circle	1		1.137	0.592	0.434	0.700	0.722	0.444	0.582	1.112
Arc Angle			(0-45°)	(45-90°)	(90-135°)	(135-180°)	(180-225°)	(225-270°)	(270-315°)	(315-360°)

Table 4-3 summarizes overall field cosine and the blocking/shadowing effects. Each section of the table is divided into 7 days and a series of hours for each day. For reference, Day 92 corresponds to Summer solstice, Day 182 corresponds to equinox (both vernal and autumnal), and Day 272 corresponds to Winter solstice. The other days represent approximately 1-mo intervals between the reference days. Due to the symmetry which exists between Winter and Summer solstice, the 7 days shown actually represent a reference day in each of the 12 mo. The hour values shown correspond to afternoon conditions. Due to symmetry in the collector field and in the sun's apparent motion, a mirror image of the data would hold for morning operational periods. The principal feature to note in the data is the minimal blocking and shadowing which occurs during most of the good sunshine hours. This is evidence of the soundness of the collector field layout, which minimizes blocking and shadowing and maximizes ground coverage consistent with overall system cost and performance consideration.

The extent to which the baseline collector field is a representative scaled version of the Commercial collector field is of interest because of the basic goal of attempting to simulate the Commercial system. Two ways in which performance comparisons can be made are through a comparison of ground coverage density and annual energy per unit area for various test locations in the collector field (equivalent collector field locations for the Commercial system and Pilot Plant are identified by identical angular locations as measured from north and identical elevation angles to the receiver).

Figure 4-4 presents a comparison in ground coverage for the two systems. The dashed lines labelled 1, 2, 3, and 4 represent Commercial system coverage factors for four different 45-deg sectors on the east side of the field (the west side would be identical due to symmetry). Superimposed on these lines are the coverage factors for the Pilot Plant field layout (solid lines). These lines cut diagonally across the Commercial system lines. This trend is caused by the compression in heliostat layout which occurs as one moves toward the tower. The six heliostat groups, as well as the successive compression and relaxation that occur on either side of the slip plane, are apparent from the six discrete lines which represent the Pilot Plant. The agreement between the two systems is fairly good except near the

Table 4-3

AVERAGE COLLECTOR FIELD COSINE AND BLOCKING/SHADOWING EFFECTS

	Day	Noon	1 PM	2 PM	3 PM	4 PM	5 PM	6 PM	7 PM	8 PM	9 PM	10 PM
Annual Summary of Cosines												
(Summer Solstice)	92	0.8442	0.8388	0.8225	0.7961	0.7605	0.7171	0.6681	0.6167	0.0000	0.0000	0.0000
	122	0.8463	0.8407	0.8241	0.7971	0.7607	0.7163	0.6660	0.0000	0.0000	0.0000	0.0000
	152	0.8492	0.8434	0.8252	0.7980	0.7600	0.7136	0.6610	0.0000	0.0000	0.0000	0.0000
(Equinox)	182	0.8475	0.8415	0.8238	0.7950	0.7560	0.7086	0.6555	0.0000	0.0000	0.0000	0.0000
	212	0.8391	0.8332	0.8158	0.7873	0.7488	0.7021	0.0000	0.0000	0.0000	0.0000	0.0000
	242	0.8287	0.8230	0.8061	0.7786	0.7416	0.6966	0.0000	0.0000	0.0000	0.0000	0.0000
(Winter Solstice)	272	0.8236	0.8180	0.8015	0.7746	0.7384	0.0000	0.0000	0.0000	0.0000	0.0000	0.0000
Annual Summary of Blocking and Shadowing												
(Summer Solstice)	92	0.9974	0.9958	0.9952	0.9966	0.9923	0.9423	0.7411	0.5258	0.0000	0.0000	0.0000
	122	0.9964	0.9952	0.9955	0.9969	0.9905	0.9328	0.7174	0.0000	0.0000	0.0000	0.0000
	152	0.9950	0.9951	0.9961	0.9967	0.9799	0.9014	0.6715	0.0000	0.0000	0.0000	0.0000
(Equinox)	182	0.9960	0.9967	0.9961	0.9899	0.9322	0.7940	0.7455	0.0000	0.0000	0.0000	0.0000
	212	0.9957	0.9962	0.9902	0.9615	0.8128	0.5557	0.0000	0.0000	0.0000	0.0000	0.0000
	242	0.9891	0.9846	0.9633	0.9097	0.7272	0.2963	0.0000	0.0000	0.0000	0.0000	0.0000
(Winter Solstice)	272	0.9813	0.9716	0.9396	0.8745	0.7071	0.0000	0.0000	0.0000	0.0000	0.0000	0.0000

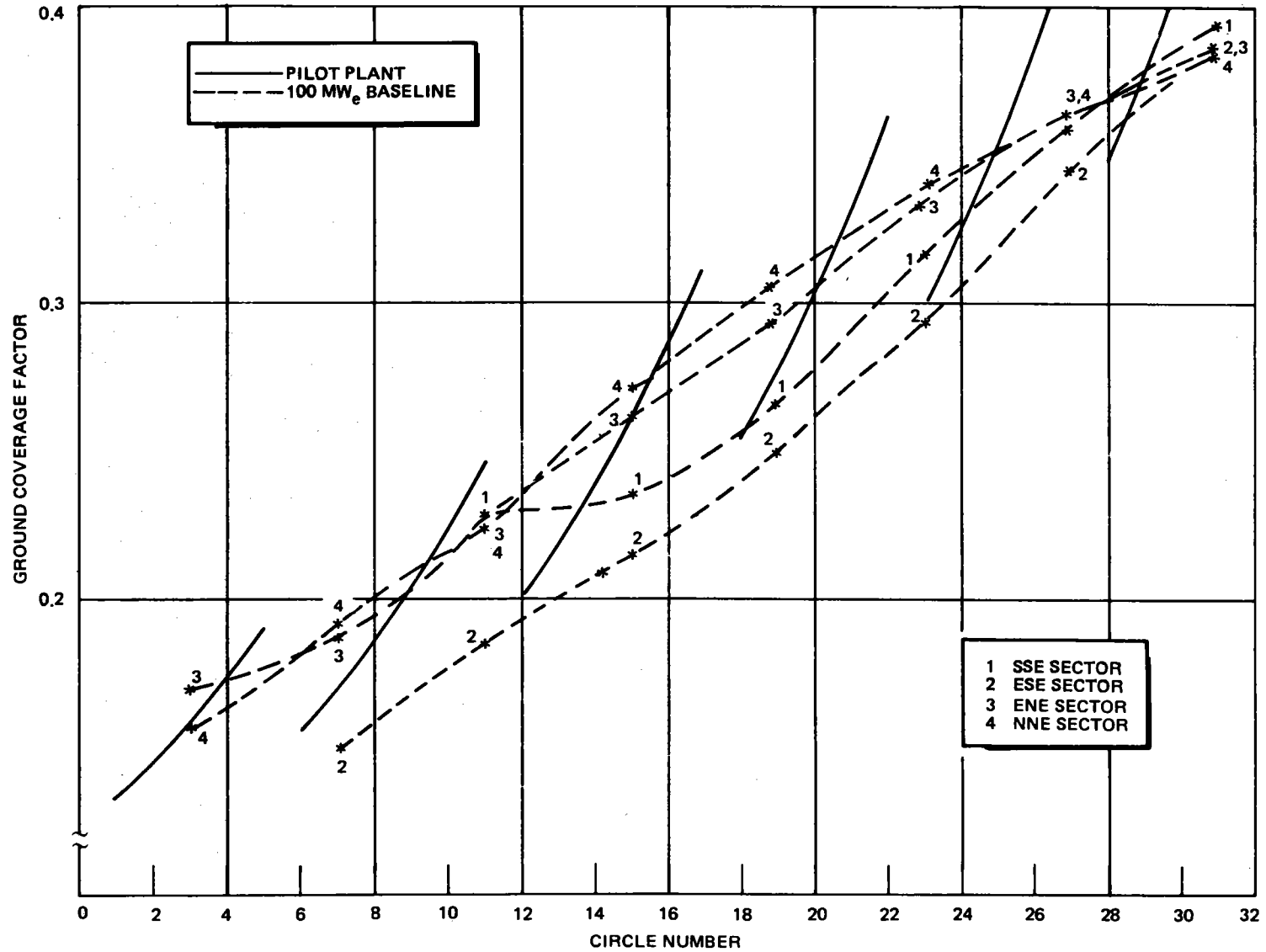

Figure 4-4. Ground Coverage Factor Comparison

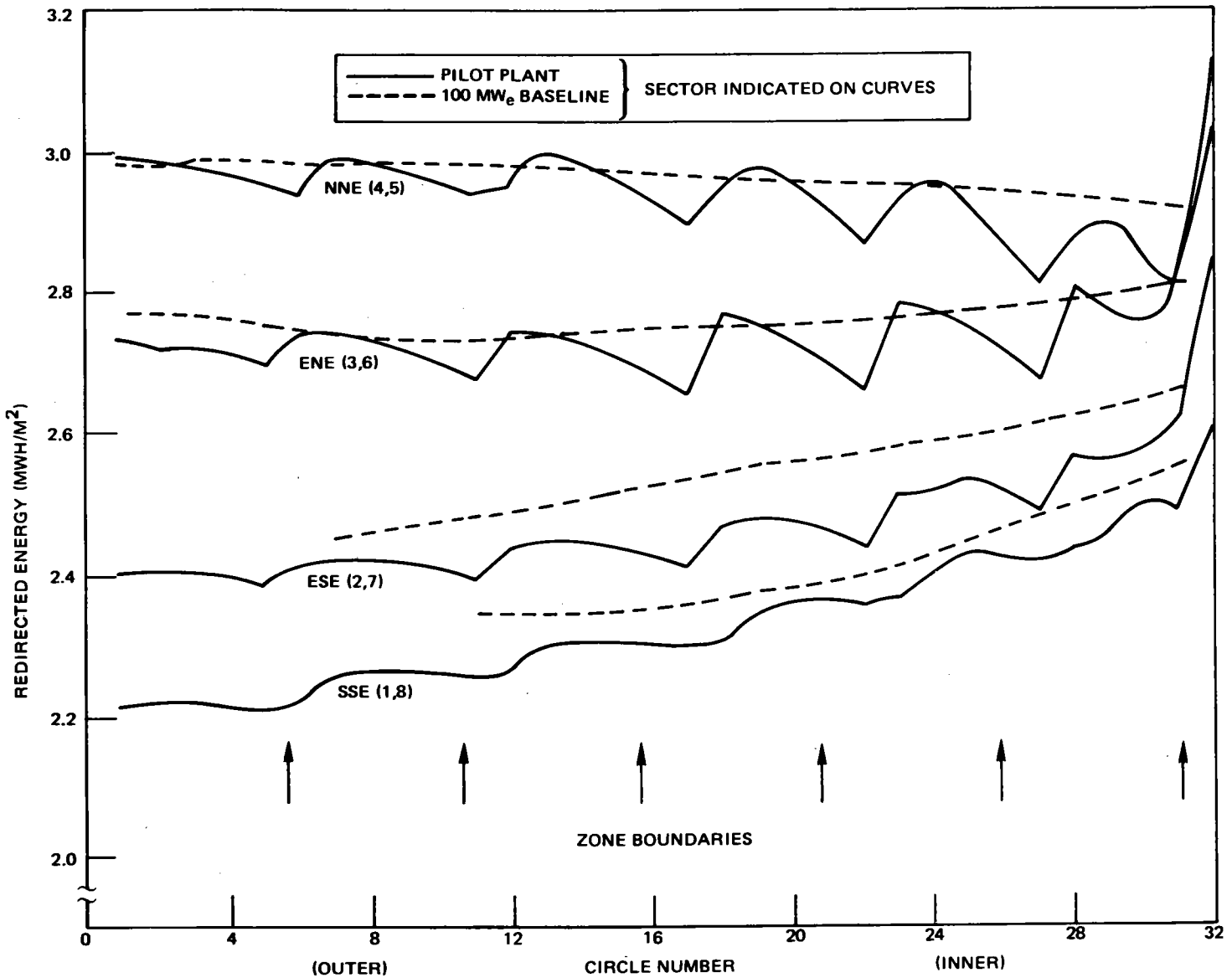

Figure 4-5. Annual Field Performance Comparison

tower, where the Pilot Plant coverage is significantly higher than that for the Commercial system (note that the circle numbering scheme on Figures 4-4 and 4-5 have been reversed from the convention of "Circle 1" designating the inner circle). This discrepancy is partially explainable by the fact that the Pilot Plant has a much higher resolution in ground coverage density because it is specified on a circle-by-circle basis whereas the Commercial system has resolution only to a much coarser cell-by-cell level. In addition, some minor expansions were carried out on the inner six circles of the Pilot Plant which are not represented in this figure. The net effect was to drop the ground coverage factor for the inner six rows by ~10%.

The results of the second comparison, which treats annual redirected energy per unit heliostat or relative "brightness," is shown in Figure 4-5. This figure treats the same four field sectors as were treated in Figure 4-4. Again the sawtooth pattern occurs for the Pilot Plant, which is indicative of the six circular zones and slip planes. It is seen that the comparison is good, particularly when noting the expanded vertical scale. Problems which seem to exist in the ESE and SSE sectors are partially attributable to changes in local heliostat field arrangements in the southern portion of the field which have not been included in this comparison. However, on a whole, the local "brightness" over a complete year cycle compares favorably between the two systems.

4.3 SYSTEM DESIGN CHARACTERISTICS

This section summarizes the design and performance characteristics of the Pilot Plant system. Subsystem related data pertaining to operating ranges, efficiencies, and parasitic power demands are also treated.

4.3.1 Physical Characteristics

The top-level characteristics of the collector field that were shown in Figure 1-6 are summarized in Table 4-4. As previously indicated, the field contains 1,760 heliostats of the square, invertible design laid out in a radial stagger array along circular arcs. The overall collector field area which actually contains heliostats is ~ 3×10^5 m^2 (75 acres). The glass packing density ranges from a maximum value of ~ 45% near the central tower exclusion circle to ~ 13% at the northern perimeter with a field average

Table 4-4

COLLECTOR FIELD PHYSICAL CHARACTERISTICS

Field Arrangement	Radial Stagger/Circular Arcs
Number of Heliostats	1,760
Collector Field Area	$3.04 \times 10^5 m^2$ (75 acres)
Glass Packing Density	
Maximum	45%
Minimum	13%
Average	23%
Central Exclusion Area	$10,387 m^2$ (2.6 acres)
Tower Height	65m (213 ft)
Receiver Centerline Elevation	80m (262 ft)

density of 23%. The density values consider only the outer envelope of the heliostat, ignoring the fact that each heliostat contains a slot for inverting purposes. This assumption was made to give a clearer indication of heliostat-to-heliostat packing which is of interest when comparing with nonslotted, noninverting designs. If the slots were included in the glass density numbers, appropriate reductions in the above numbers would be required. Each heliostat in the collector field requires a 4.54m (179 in.) radius exclusion circle to accommodate the azimuthal motion of the square heliostat for both the face-up and face-down orientation. The exclusion circles in turn are allowed to approach within ~38.1 cm (15 in.) of one another.

The tower corresponding to this collector field layout is a free-standing steel structure 65m (213 ft) high. The receiver that is placed on top of the steel tower is designed so that the equator of the absorbing panels is at an elevation of 80m (262 ft). The central exclusion area, which contains the powerhouse, thermal storage subsystem, control center, and miscellaneous auxiliaries in addition to the tower, is a circular area 115m (377 ft) in diameter or $10,387 m^2$ (2.6 acres) in area. Considering equipment positioned outside the perimeter of the collector field, a total field area of $3.24 \times 10^6 m^2$ (80 acres) is required for the Pilot Plant.

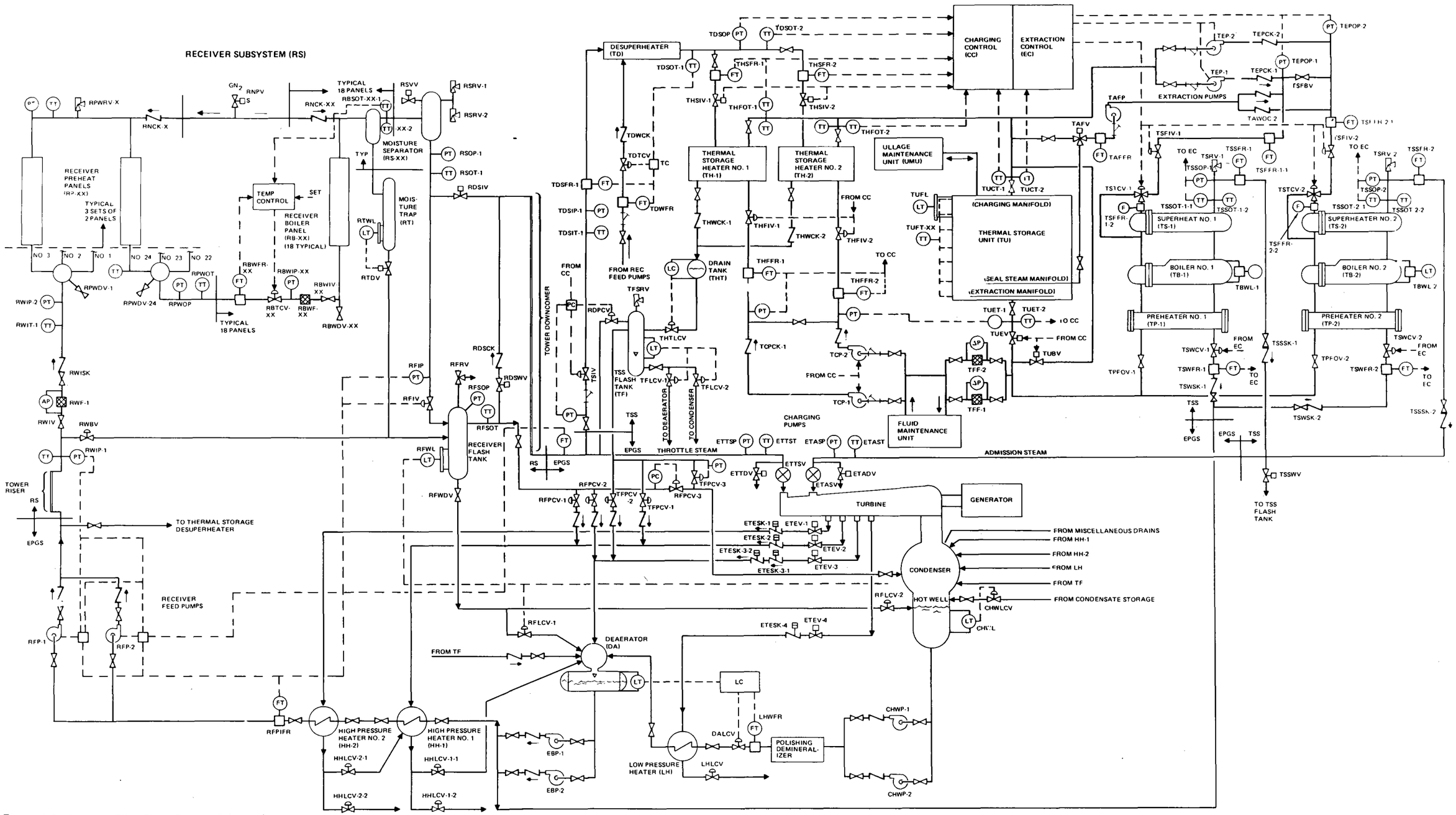

Figure 4-6. Detailed Pilot Plant System Schematic

The principal elements of the water/steam loop, which include the receiver and thermal storage subsystems and the balance of plant equipment, are shown in Figure 4-6. The nomenclature used to specify each element can be interpreted from the code explanation in Table 4-5. Included in the schematic are not only the operational hardware items but the principal control sensors and sensor/control signal paths. A summary of some of the principal hardware and operating characteristics of the water/steam loop is in Table 4-6.

4.3.2 System Performance

The performance characteristics of the Pilot Plant at equinox noon, Winter 2 PM, and on an annual average basis are summarized in Figures 4-7 through 4-9. In all cases, the performance estimates start with the amount of power incident on the heliostats, assuming they are all oriented normal to the incident sunlight. The power degrades on an incremental basis according to the tabulated efficiencies until the last bar is reached which represents net electrical output. For the equinox noon case, which represents the point of maximum output power, a net output of 11.4 MWe would be expected. The corresponding 12.8 MWe gross power produced exceeds the turbine nameplate rating but is well within the 10% continuous overflow capability. The Winter 2 PM condition, which represents the system design point, produces the required 10 MW of net electrical power with a corresponding gross power production of 11.2 MWe. The annual average performance chart shown in Figure 4-9 was developed by averaging the performance factors over the useful collection hours of the year. The results indicate a slightly lower electrical output than would occur at the Winter 2 PM design point. The difference is principally due to the lower cosine and blocking/shadowing factors.

For all of the performance cases treated in this section, a collector field outage factor based on the loss of one field controller (loss of 24 heliostats) and five individual heliostats was assumed. By comparison, collector field availability studies indicated that three field controller failures per year and one heliostat failure per day would be anticipated. As a result, the performance data shown for each of the cases includes a significant degree of conservatism regarding collector field outage effects. If all heliostats were available, the performance estimates would increase by ~1.6%.

Table 4-5 (Page 1 of 2)

SCHEMATIC NOMENCLATURE

HARDWARE IDENTIFICATION CODE: RPWRV-22-2

RP = Location (i.e., Receiver Preheater Panel)

W = Media (i.e., Water)

R = Function (i.e., Relief)

V = Component type or instrumentation parameter (i.e., Valve).

22 = Assembly number if multiple major assemblies (i.e., Receiver Panel 22).

2 = Component number if multiple components on each major assembly.

Location	Media	Function	Component or Parameter
Condenser = C	Heat-Transfer Fluid = F	Bypass = B	Boost Pump = BP
Condenser Hot Well = CHW	Nitrogen = N	Charging = C	Controller = C
Deaerator = DA	Oil = O	Drain = D	Check Valve = CK
High-Pressure Heater = HPH	Steam = S	Extraction = E	Charging Pump = CP
Low-Pressure Heater = LPH	Water = W	Inlet = I	Extraction Pump = EP
Receiver = R		Level Control = LC	Filter = F
Receiver Boiler Panel = RB		Main = M	Feed Pump = FP
Receiver Downcomer = RD		Outlet = 0	Flow Rate = FR
Receiver Flash Tank = RF		Pressure Control = PC	Flow Transmitter = FT
Receiver Preheater Panel = RP		Relief = R	Level Transmitter = LT

Table 4-5 (Page 2 of 2)

SCHEMATIC NOMENCLATURE

Location	Media	Function	Component or Parameter
Receiver Moisture Separator = RS		Stop = S	Inlet Pressure = IP
Receiver Moisture Trap = RT		Temperature Control = TC	Outlet Pressure = OP
Thermal Storage = T		Throttle Stop Valve = TSV	Pressure = P
Thermal Storage Desuper-heater = TD		Vent = V	Pressure Switch = PS
Thermal Storage Heater = TH		Warmup = W	Solenoid = S
Thermal Storage Unit = TU			Stop/Check Valve = SK
			Temperature = T
			Temperature Switch = TS
			Temperature Trans-mitter = TT
			Valve = V

Table 4-6

WATER/STEAM LOOP CHARACTERISTICS

Receiver Size	
• Diameter	7m (23 ft)
• Height	12.5m (41 ft)
Receiver Steam Conditions	
• Pressure	10.45 MPa (1,515 psia)
• Temperature	
Rated Steam	516°C (960°F)
Derated Steam	349°C (660°F)
Receiver Panels	
• Preheat	6 (3 sets of 2)
• Boiler	18 (Parallel)
Thermal Storage Temperature Range	219° to 302°C (425° to 575°F)
Thermal Storage Heat Exchangers	
• Charging Heat Exchanger	2 Parallel Units
• Steam Generator	2 Parallel Trains
Turbine Steam Conditions	
• Throttle Steam	510°C (950°F)
	10.1 MPa (1465 psia)
• Admission Steam	274°C (525°F)
	2.65 MPa (385 psia)
Receiver Feed Pumps	2-Full Capacity, Variable Speed
Boost Pumps	2-Full Capacity, Constant Speed

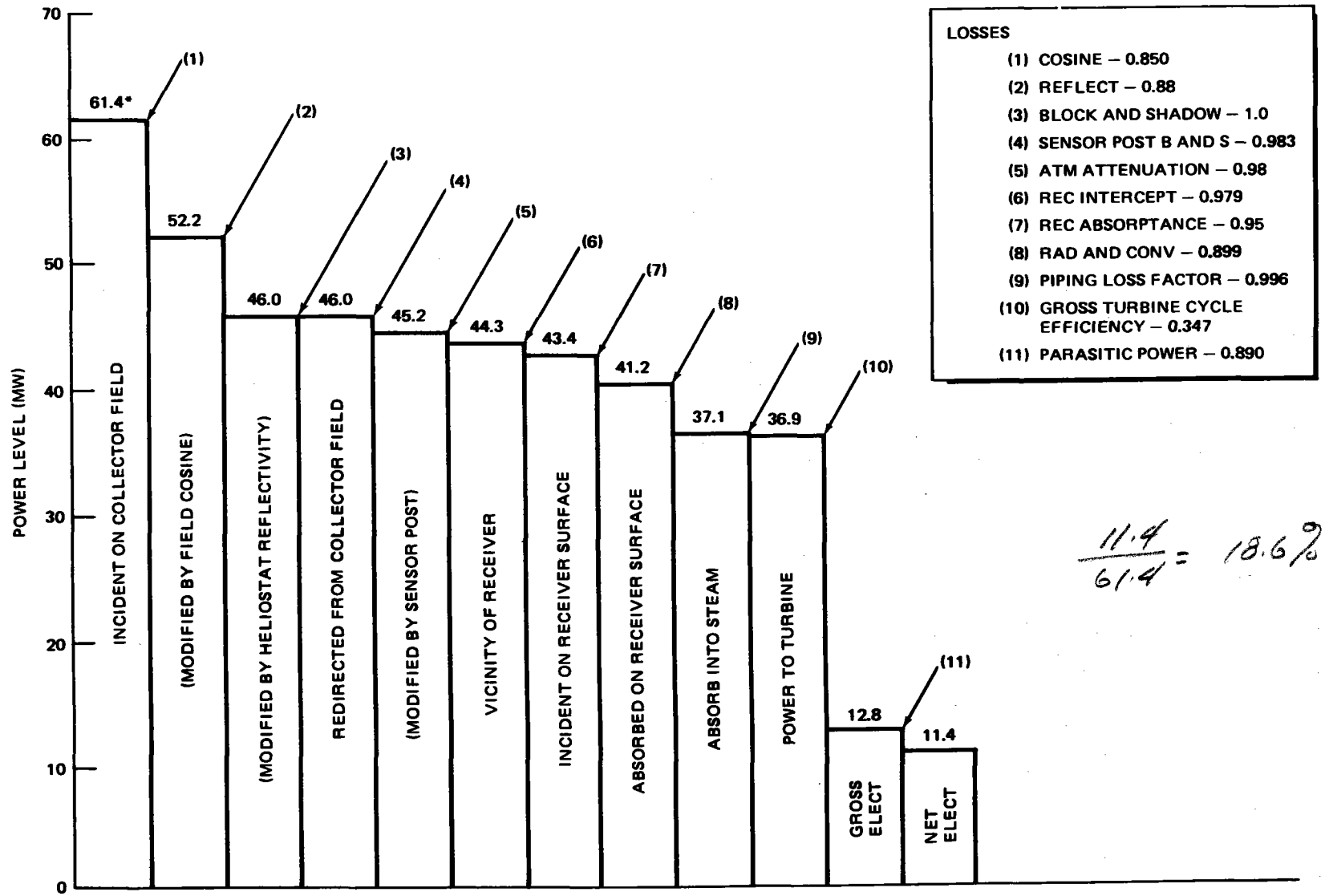

$\frac{11.4}{61.4} = 18.6\%$

Figure 4-7. Pilot Plant System Power Flow (Equinox Noon)

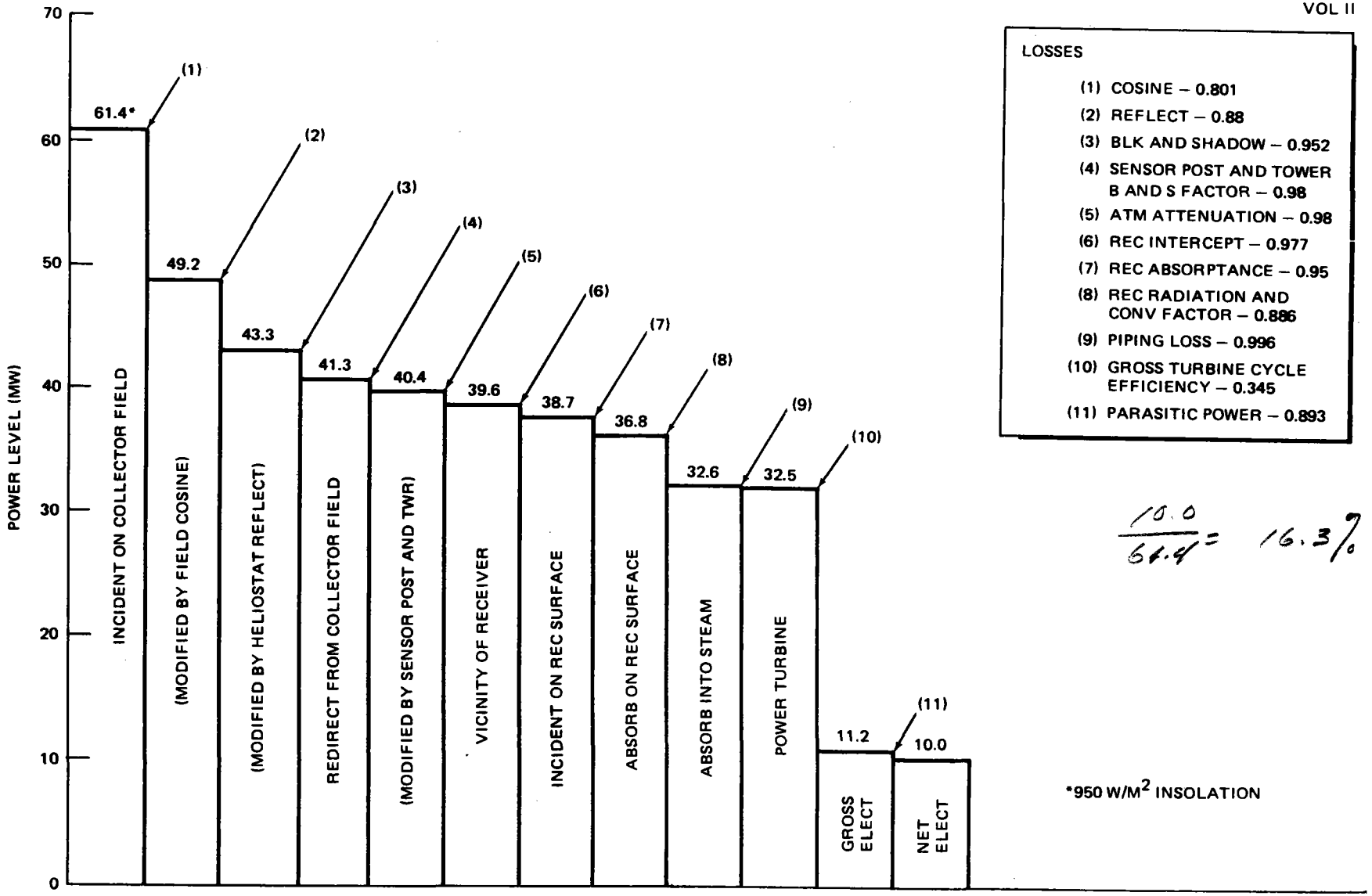

$\frac{10.0}{61.4} = 16.3\%$

Figure 4-8. Pilot Plant System Power Flow (Winter 2 PM)

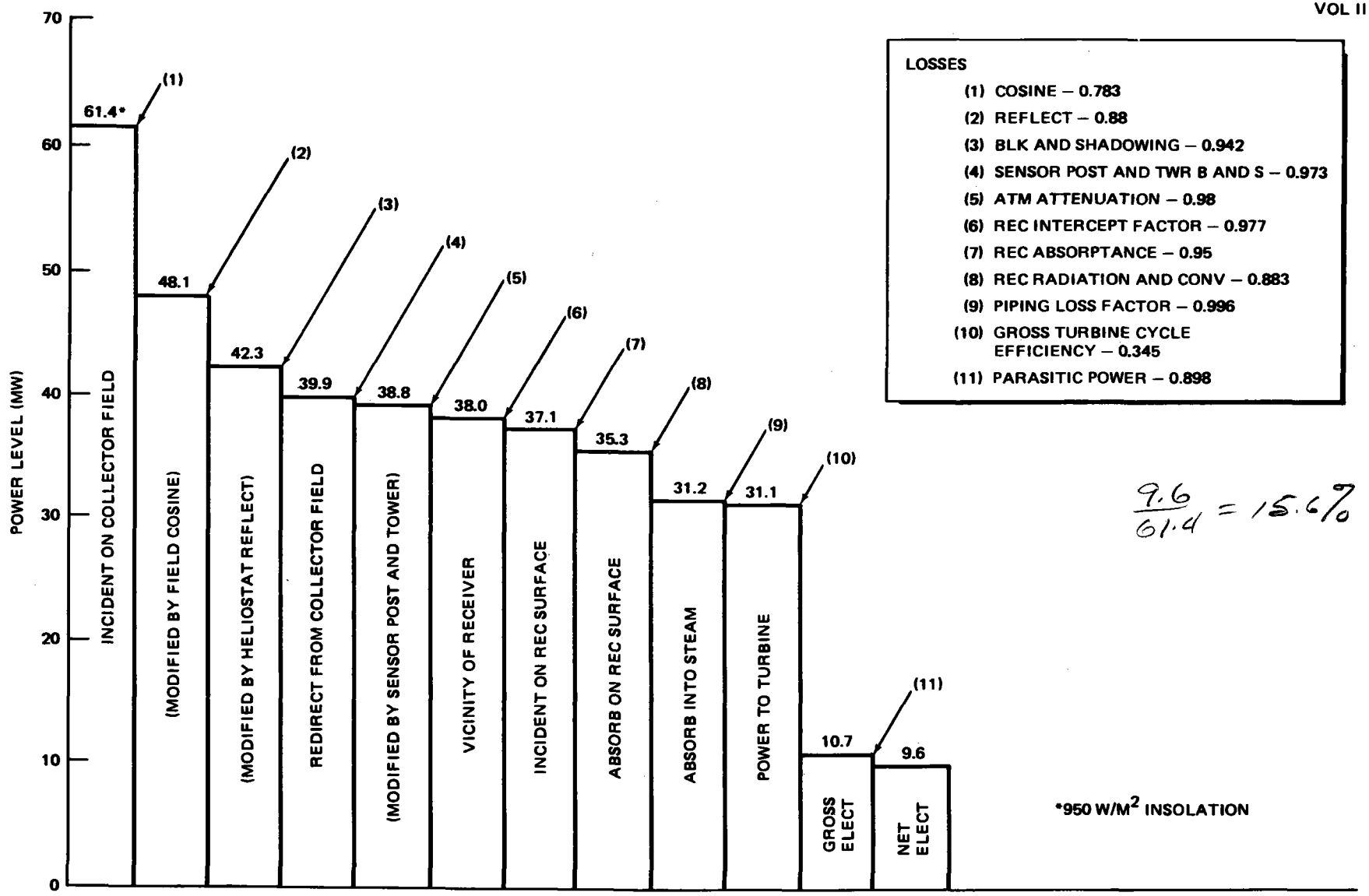

$\frac{9.6}{61.4} = 15.6\%$

Figure 4-9. Pilot Plant System Power Flow (Annual Average)

4.3.3 Subsystem Operating Ranges

A compatible set of operating ranges for the receiver, thermal storage, and turbine is important due to the close-coupled nature of the water/steam loop. The operating ranges for the subsystems are shown in Table 4-7. In general, the conditions define the range of power or flow that will be experienced while holding the pressure and temperature at a design point level. The indicated minimum values represent design requirements which were established through an overall system analysis effort. Actual values which may be significantly lower than these levels will be established once the final design is complete and the equipment is installed and operated.

The maximum flow range for the receiver occurs during derated steam operation where total flow can vary over a 4.5:1 throttling ratio. The somewhat lower maximum flow range for rated steam operation occurs because of (1) collector field limitations that limit the amount of power to the receiver, and (2) higher enthalpy change experienced by the water/steam. From the receiver point of view, maximum-rated steam flow could be increased to the indicated upper limit for derated steam if sufficient collector field capability existed with no impact on the receiver design or hardware selection. The maximum power collection capability for derated steam is limited by the thermal storage charging capability (30 MWt into the tank with the balance being passed to the feedwater heater circuit) and the top flow limit for the receiver. On the other hand, the maximum power collection capability for rated receiver steam operation is limited exclusively by collector field considerations.

The operating range for the thermal storage charging heat exchanger is bracketed by the 30-MWt charging rate (into the tank) on the top end and the desire to maintain operation at fairly low flow rates. Such rates may occur periodically with the Pilot Plant, which is a low solar multiple system. The operating range for the steam-generation equipment was determined by the turbine admission steam flow range, with the upper limit corresponding to the requirement to produce 7-MWe net power from thermal storage steam.

The indicated ranges for the turbine correspond to the approximate minimum flow threshold on the low end to slightly in excess of the nameplate rating

Table 4-7

PILOT PLANT SUBSYSTEM OPERATING RANGES

Subsystem	Temp °C (°F)	Pressure MPa (psia)	Flow Rate Kg/Sec (Lb/Hr)	Power Range MW (Btu/Hr)
Receiver				
Rated Steam	516 (960)	10.45 (1515)	3.7**-14.8 (28,900-117,568)	10**-37.1 (34.1-126.6 x 10^6)
Derated Steam	349 (660)	10.45 (1515)	3.7**-16.5 (28,900-130,500)	7.3**-32.8 (24.9-111.9 x 10^6)
Thermal Storage				
Charging Steam at Heat Exchanger	343 (650)	10.1 (1,465)	0.83**-16.5 (4,350-130,500)	1.5**-30 (5.1-102.4 x 10^6)
Discharge Steam Leaving Steam Generator	277 (530)	2.76 (400)	1.27**-13.2 (10,100-104,700)	3.1**-32.1 (10.6-109.5 x 10^6)
Turbine				
Throttle Steam	510 (950)	10.1 (1,465)	3.7**-14.6* (28,900-117,568)	10.0**-36.9* (34.1-125.9 x 10^6)
Admission Steam	274 (525)	2.65 (385)	1.27**-13.2 (10,100-104,700)	3.1**-32.0 (10.6-109.4 x 10^6)

*Requires a 2.5% turbine overflow capability (turbine is capable of 10% overflow operation)

**Approximate

on the high end for rated steam and at the nameplate rating for derated steam. The 10% continuous overflow capability is available for anomolous conditions that may result because of increased collector field and receiver or thermal storage power outputs.

4.3.4 Subsystem Efficiencies

The efficiency variation for the collector subsystem is shown in Figure 4-10 for various sun azimuth and elevation angles. When comparing this data with that presented in Section 3.5.4 for the Commercial system, it is seen that the Pilot Plant collector field efficiency is ~2% higher. The difference can be attributed primarily to differences in the receiver interception factor between the two systems. Implicit in the data shown in Figure 4-10 are the following assumptions:

A. Heliostat reflectivity = 1.0
B. Receiver interception factor = 0.977
C. Sensor post blocking and shadowing factor = 0.98
D. Atmospheric attenuation factor = 1.0

Collector subsystem efficiency at other values of heliostat reflectivity can be determined by multiplying the indicated efficiency by the appropriate reflectivity. In addition, atmospheric attenuation effects can be included by multiplying the efficiency value by the appropriate field-weighted atmospheric transmittance factor. For the Pilot Plant, a transmittance of 0.98 is appropriate for a 50-km (31 mi) visible range which would be representative for the Barstow site.

The receiver efficiency defined as the net power absorbed divided by the incident power is summarized as follows:

Time	Incident Power (MWt)	Absorbed Power (MWt)	Efficiency
Equinox Noon	43.4	37.1	0.854
Winter 2 PM	38.7	32.6	0.842
Minimum Rated Steam	14.9	10.0	0.671
Annual Average	37.1	31.2	0.841

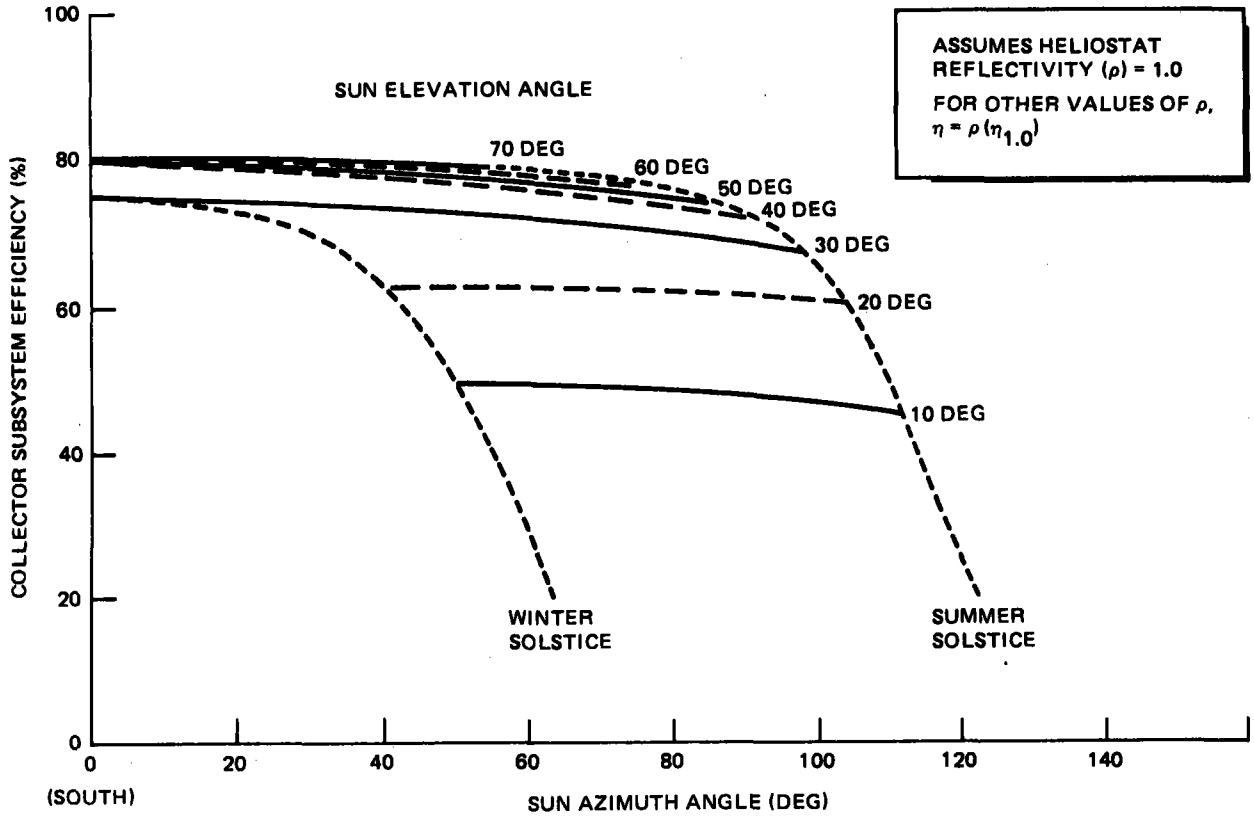

Figure 4-10. Collector Field Performance

Assumptions made in arriving at these values include an absorptivity of 0.95, an emissivity of 0.89, a wind speed of 3.5 m/s (8 mph) at 10m elevation, and an ambient temperature of 23°C (74°F). Since neither forced nor free convection dominates, a root sum squares addition of the two heat loss components was applied. Under the temperature and wind conditions defined above, ~2.3% of the incident power at equinox noon would be lost due to convection.

The thermal storage subsystem has a volumetric efficiency defined as the ratio of extractable energy to total energy in the tank of 85 to 90%. The subsystem has an energy recovery efficiency of 96 to 98%, which is defined as the ratio of extractable energy to charging energy.

The gross cycle efficiency for the turbine is shown in Figure 4-11 for operation off both receiver (throttle) steam and admission steam. These curves are based on an assumed wet cooled condenser that is capable of producing a 6.35-cm Hg (2.5-in. Hg) back pressure in the condenser. Also shown in the figure is an estimate of the turbine generator output as a function of flow rate when operating exclusively from receiver steam.

4.3.5 Auxiliary Power Requirements

A detailed tabulation of the Pilot Plant auxiliary power requirements is shown in Table 4-8 for representative daytime, nighttime operational and standby periods, and emergency conditions. For the operational periods, the major power consumers are the feedwater and condenser pumps and cooling tower fans. The collector field by contrast accounts for ~2.5% of the total parasitic load. During standby periods, the parasitic loads are principally associated with balance of plant power requirements. The emergency AC power requirement is dominated by collector field requirements. During emergency periods when the wind is rising rapidly and a power failure has occurred (double failure condition), the indicated collector field power would be sufficient to slew half of the collector field at a time to a safe orientation. The emergency power drawn for the collector field is higher than the operating power requirement because the motors operate on a continuous basis during slew as opposed to the intermittent mode of

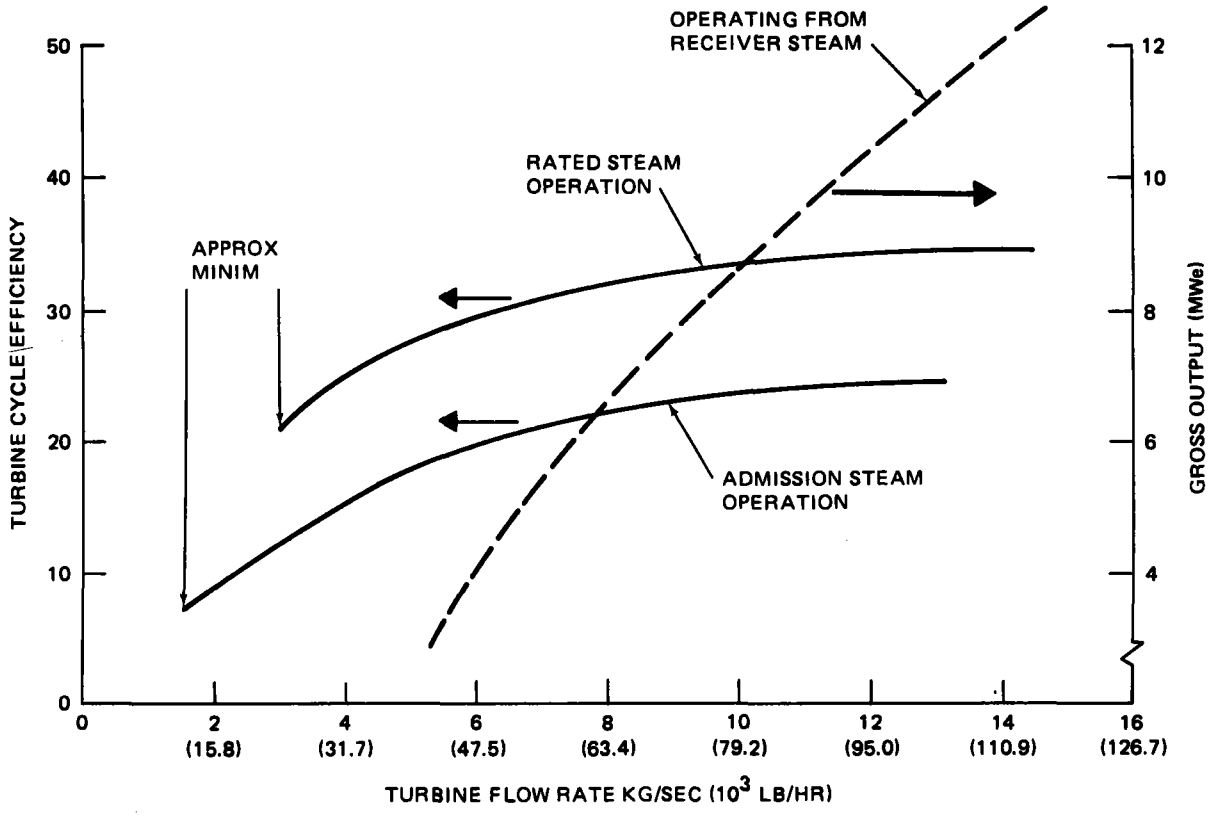

Figure 4-11. Impact of Flow Rate on Turbine Cycle (Pilot Plant)

Table 4-8 (Page 1 of 2)

PILOT PLANT AUXILIARY POWER REQUIREMENTS

Component	Receiver Operation Equinox 11.4 MW Net kW	Receiver Operation Winter (Design) 10.0 MW Net kW	Evening Thermal Storage 7.0 MW Net kW	Night Standby kW	Emergency Power AC kW	Emergency Power DC kW
Receiver Feed Pump	325	282	-	-	-	-
Booster Pump	90	77	77	-	-	-
Hotwell Pump	20	18	18	-	-	-
Condenser Vacuum Pump	22	22	22	22	-	-
Condensate Trans Pump	-	-	-	7	-	-
Service Air Compressor	50	50	-	-	-	-
Instrument Air Compressor	28	28	28	28	28	-
Cooling Tower Fans	150	150	150	-	-	-
Circulation Water Pumps	203	203	203	-	-	-
Gland Seal Vacuum Pumps	2	2	2	2	-	-
Bearing Cool Water Pump	15	15	5	5	15	-
Turbine AC Oil Pump	-	-	-	13	13	-
Turbine DC Oil Pump	-	-	-	-	-	13
Lube Oil Filter Pump	1	1	1	1	-	-
Chemical Pumps	3	3	3	-	-	-
Motor-Operated Valves	-	-	-	-	3	-
Raw Water Pump	20	18	18	12	-	-
Clarified Water Pump	12	10	10	5	-	-

Table 4-8 (Page 2 of 2)

PILOT PLANT AUXILIARY POWER REQUIREMENTS

Component	Receiver Operation		Evening Thermal Storage 7.0 MW Net kW	Night Standby kW	Emergency Power	
	Equinox 11.4 MW Net kW	Winter (Design) 10.0 MW Net kW			AC kW	DC kW
Water-Treating System	16	14	14	8	-	-
Jockey Pump (Fire Water)	5	5	5	5	-	-
Auxiliary Boiler	-	-	-	10	-	-
Turbine Turning Gear	-	-	-	3	3	-
Computer	10	10	10	5	10	-
Miscellaneous DC	-	-	-	-	-	10
Controls and Computer HVAC	41	41	33	33	33	-
Plant HVAC	150	138	22	-	-	-
Thermal Storage Charging Pump	-	-	-	-	-	-
Thermal Storage Extraction Pump	-	-	104	-	-	-
Sewage Treat Plant	1	1	1	1	-	-
Potable Water Pump	4	4	4	-	-	-
Receiver Tower Elevator	-	-	-	-	15	-
Collector Subsystem	30	30	-	-	200	-
Lighting and Misc AC	202	78	70	50	10	-
TOTAL	1,400	1,200	800	210	330	23

operation that occurs during normal track. Due to the requirement for computer control of the collector field during emergency conditions, the computer will be powered with an uninterruptable power source at all times.

4.4 DESIGN EVOLUTION

A major portion of the system engineering effort during this contract dealt with transforming the Pilot Plant requirements into the final Pilot Plant design. Since some latitude existed as to the exact nature of the Pilot Plant and the degree of Commercial system verification required, a series of design alternatives were considered at both the system and subsystem level. The principal issue in deciding among any of the alternatives was a tradeoff between degree or extent of the similarity to the Commercial system and the cost or performance penalty involved. In addition, because of changes in design guidelines such as the switch from dry cooling to wet cooling or the refinement in the receiver design point wind speed and ambient temperature, a continual design evolution or refinement activity was carried out.

4.4.1 Alternate System Designs

In order to define the optimum commercial system, several cost and performance trade studies were done. The cost data contained many assumptions concerning such things as mass production, local or regional manufacturing sites, cost reductions due to well-established learning curve effects, etc. As a result, the studies assumed relatively inexpensive heliostats which, when included in the optimization analysis, produced a 360-deg collector field that completely surrounded the tower. This meant that it was economically desirable to place some of the heliostats into the southern field even though they will experience relatively poorer performance than the balance of the system. This would imply that, for a truly scaled version of the Commercial system, a southern field should also be included in the Pilot Plant design.

By contrast, however, if the optimization analysis were carried out exclusively for a 10-MW Pilot Plant, a different set of component and subsystem cost assumptions would be appropriate. In particular, the biggest difference would be the loss of many of the mass production and learning curve

assumptions that were made for the Commercial system. The most significant effect of the change would occur in the heliostat costs. Since they would be a much more expensive part of the system on a percentage basis than for the Commercial system, the optimization would dictate that they be placed in only the highest efficiency areas of the field relative to the tower, i.e., the north field. Thus, a paradox exists in the design of the Pilot Plant. If economy is the overriding goal, a Pilot Plant with a north-only collector field is appropriate, but if the overriding goal is to simulate the ultimate Commercial system, a full 360-deg collector field is dictated.

In addition to the 360-deg collector field that was ultimately selected for the Pilot Plant, two alternative north field designs were also considered along with appropriate receiver configurations. To give design visibility, one of the alternate fields was designed to minimize investment cost by sizing exclusively to the Winter 2 PM design point. The second field was defined to minimize the cost of energy on an annual basis.

The first of these fields, labelled "Winter Optimum Field Layout," is shown in Figure 4-12, along with the approximate field dimensions, tower height, and receiver centerline elevation. In contrast to the baseline design discussed in Section 4.2, the tower in this case is well to the south of the collector field. Since the system was designed exclusively for a Winter 2 PM sun condition, the resulting collector field is fairly narrow though the receiver is located on top of a reasonably tall tower. The receiver configuration defined for this collector field was cylindrical with the 13 northernmost panels remaining as single pass-to-superheat panels while the balance of the 24 (on the southern side) were replaced with sheet metal. This assumption was made to preserve aerodynamic symmetry.

The second alternate field configuration, which was designed to optimize annual energy, is shown in Figure 4-13. Since it was designed for an annual average sun condition which has a moderately high elevation angle and moves between the east and west sky, the resulting collector field is wider with less depth in comparison to the Winter Optimum design. In addition, the higher average sun angle permits the use of a shorter tower. As in the previous

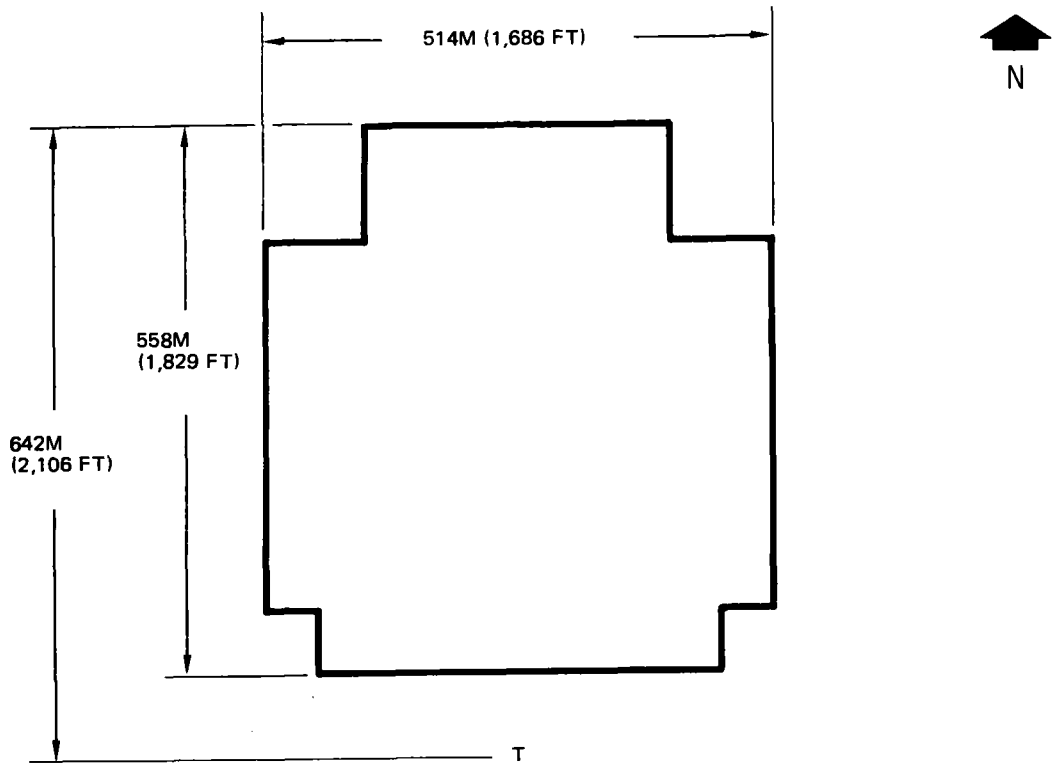

TYPICAL FIELD

ASSUMED HELIOSTAT COSTS – $300/M^2

TOWER HEIGHT
132M

RECEIVER MID-POINT
147M

Figure 4-12. Winter Optimum Field Layout

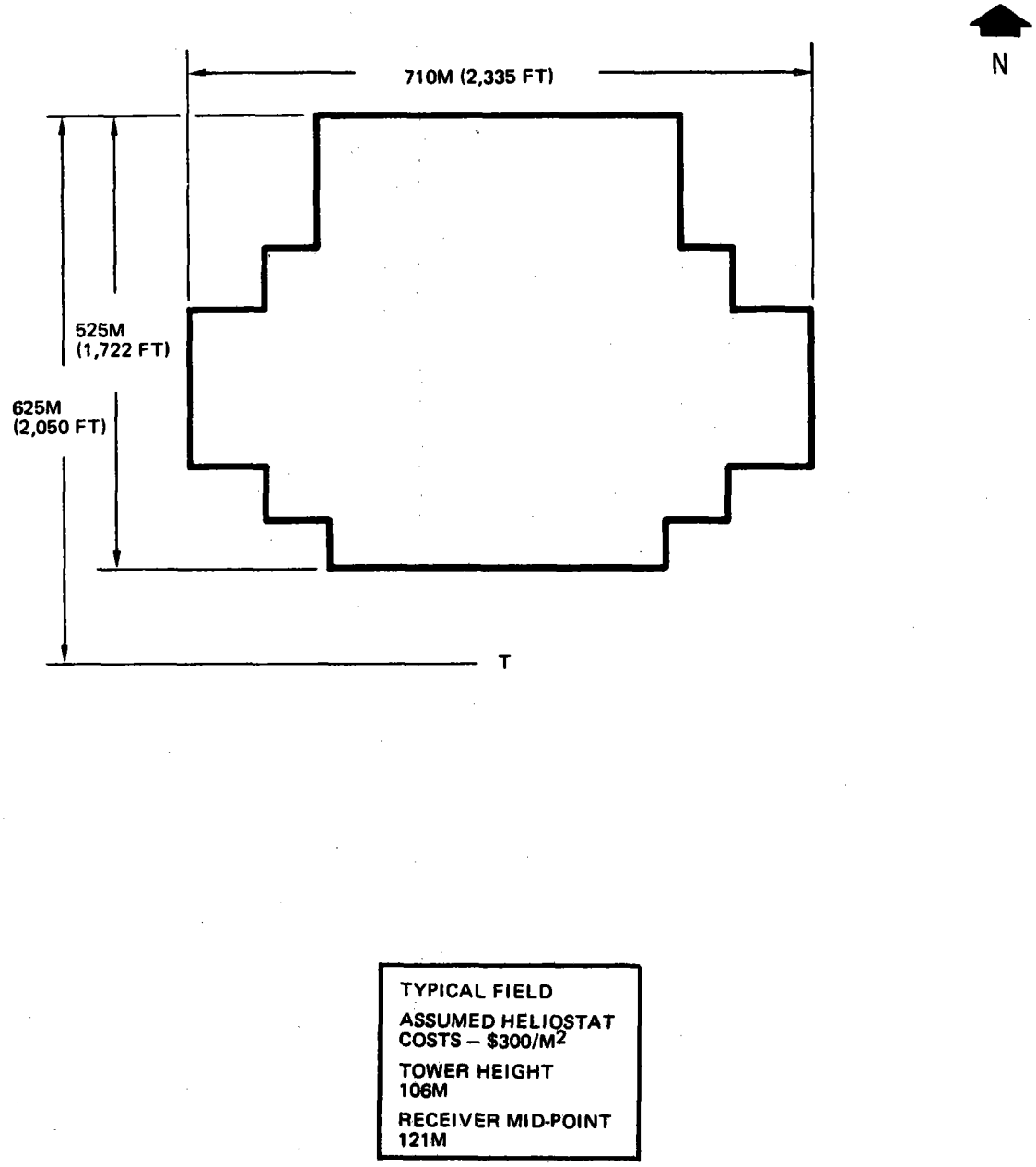

Figure 4-13. Optimum Annual Energy Field Layout

case, a cylindrical receiver with 13 active northern panels was assumed. In both of the cases considered, a heliostat cost of $\$300/m^3$ was assumed, which is representative of early heliostat costs prior to the implementation of large mass-production facilities.

Before considering the potential cost savings of the optional collector fields in detail, it is useful to investigate their performance on an annual basis. The annual energy characteristics of the two options are given in Figures 4-14 and 4-15 for the Optimum Annual Energy and Winter Optimum fields, respectively. In comparing the two, both from a total annual energy and a detailed daily and hourly variation standpoint, it is noted that only minor differences exist. From an annual energy standpoint, the Winter field is capable of producing approximately 5% less electrical energy than the annual optimum field. On a daily and hourly basis, the principal difference occurs in the vicinity of noon, where the Winter Optimum field produces superior performance over the equinox to Winter solstice time period (Figure 4-15). The summer noon performance, on the other hand, is degraded from that indicated for the Annual Optimum case (Figure 4-14).

A cost and performance comparison between the two alternate designs and two scaled Commercial system configurations with complete 360-deg collector fields is given in Table 4-9. Since these cost estimates were developed in April 1976, they may not be completely consistent with current estimates; however, the trends are still valid. Since the nonenergy collection equipment is identical in all cases, only those elements which vary from design to design are listed. It is seen that the more expensive configurations are associated with the full 360-deg fields, which would be near optimum if Commercial cost assumptions were used. By contrast, it is seen that the Winter Optimum configuration would produce savings in excess of $7M, if it were adopted as for the Pilot Plant. Note that the lowest-cost system has the tallest tower, which would experience the greatest difficulty in scaling to a 100-MWe Commercial System.

In spite of the potential cost savings to be realized, the final Pilot Plant collector field layout and receiver configuration were selected on the basis of scalability to the Commercial system while cost factors were given secondary attention.

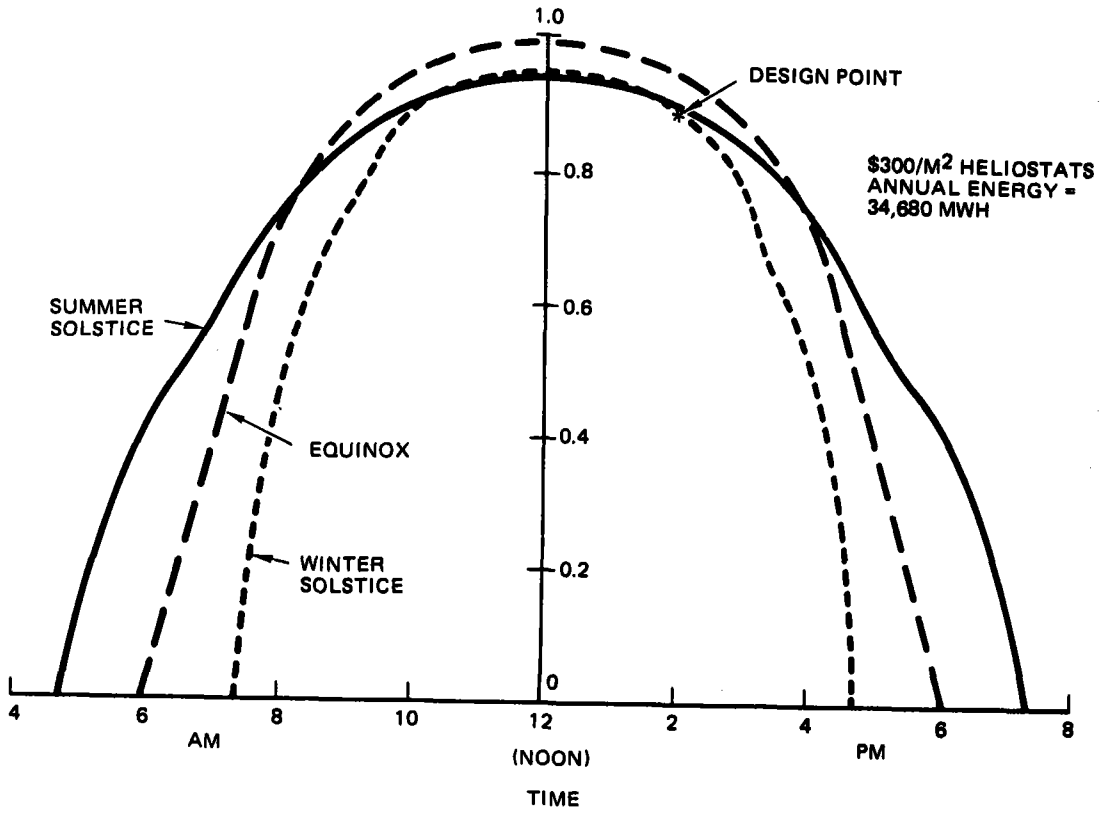

Figure 4-14. Relative Incident Receiver Power (Annual Optimum)

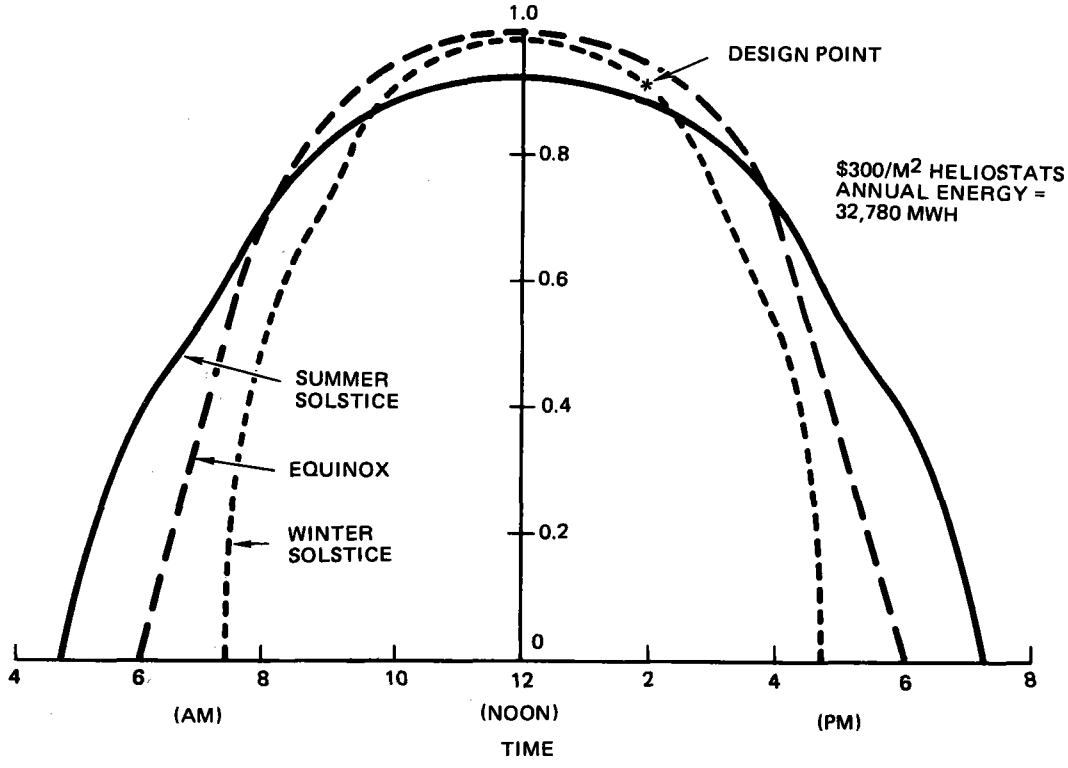

Figure 4-15. Relative Incident Receiver Power (Winter Optimum Layout)

Table 4-9

PILOT PLANT CONCEPTS COMPARISON

Solar Collection Equipment	Configuration			
	Modified Commercial (Baseline)	Minimum Cost (Annual Energy Option)	Minimum Cost (Winter Option)	Scaled Commercial System
Hardware Investment Cost				
Collector	$28.4M	$25.2M	$22.6M	$26.8M
Receiver	6.3M	4.0M	4.0M	5.8M
Tower	1.0M	1.3M	1.9M	1.0M
Total	$35.7M	$30.5M	$28.5M	$33.6M
Annual Energy (MWH)	36,670	34,680	32,780	35,600
Comment	Most Expensive Complete Simulation	Lowest Cost of Energy	Lowest Investment Cost Tallest Tower	Complete Simulation (Preheat Panels)

*Cost estimates were developed in April 1976 and therefore do not necessarily reflect the PDR cost numbers. The indicated trend is still valid.

4.4.2 Receiver Configurations

During the course of this contract, a series of receiver design alternatives were considered with some being implemented in an effort to improve receiver performance. Gross changes in concentration ratio, however, were not permitted because they would negate some of the receiver scalability issues. Since modifications in the receiver necessarily influence the collector field, the study was treated as part of the total system analysis.

At the time of the Preliminary Baseline Design Review (PBDR), the receiver was sized to absorb ~50 MW of thermal power at the maximum noontime power collection point. A significant percentage of the power requirement resulted from the use of dry cooling, which produced a double penalty in that it reduced gross cycle efficiency while increasing the parasitic load. In addition, although the panels were designed to withstand in excess of 0.3 MW/m^2 incident flux, the performance analyses at that time predicted that the peak heat flux would not exceed ~0.26 MW/m^2. Thus, substantial design conservatism was included. The baseline receiver size at that time was 17m (56 ft) high and 7m (23 ft) in diameter.

To minimize the thermal losses off the receiver surface, shrouded configurations of the type shown in cross section in Figure 4-16 were considered. The purpose of the shroud was to protect the upper high-temperature portion of the receiver from excessive convection and radiation losses. The shrouds would not be subjected to direct reflected energy from the collector field on a steady-state basis and therefore would not require active cooling. Clearly, as the length of the shroud increases or the shroud angle decreases, the anticipated receiver heat losses would be reduced. However, a negative effect related to the interaction with the collector field occurs. This effect involves the limit on collector field size or receiver look angle. To overcome the restriction, a taller tower would be necessary to permit the heliostats to redirect their power up under the shroud without a direct impingement.

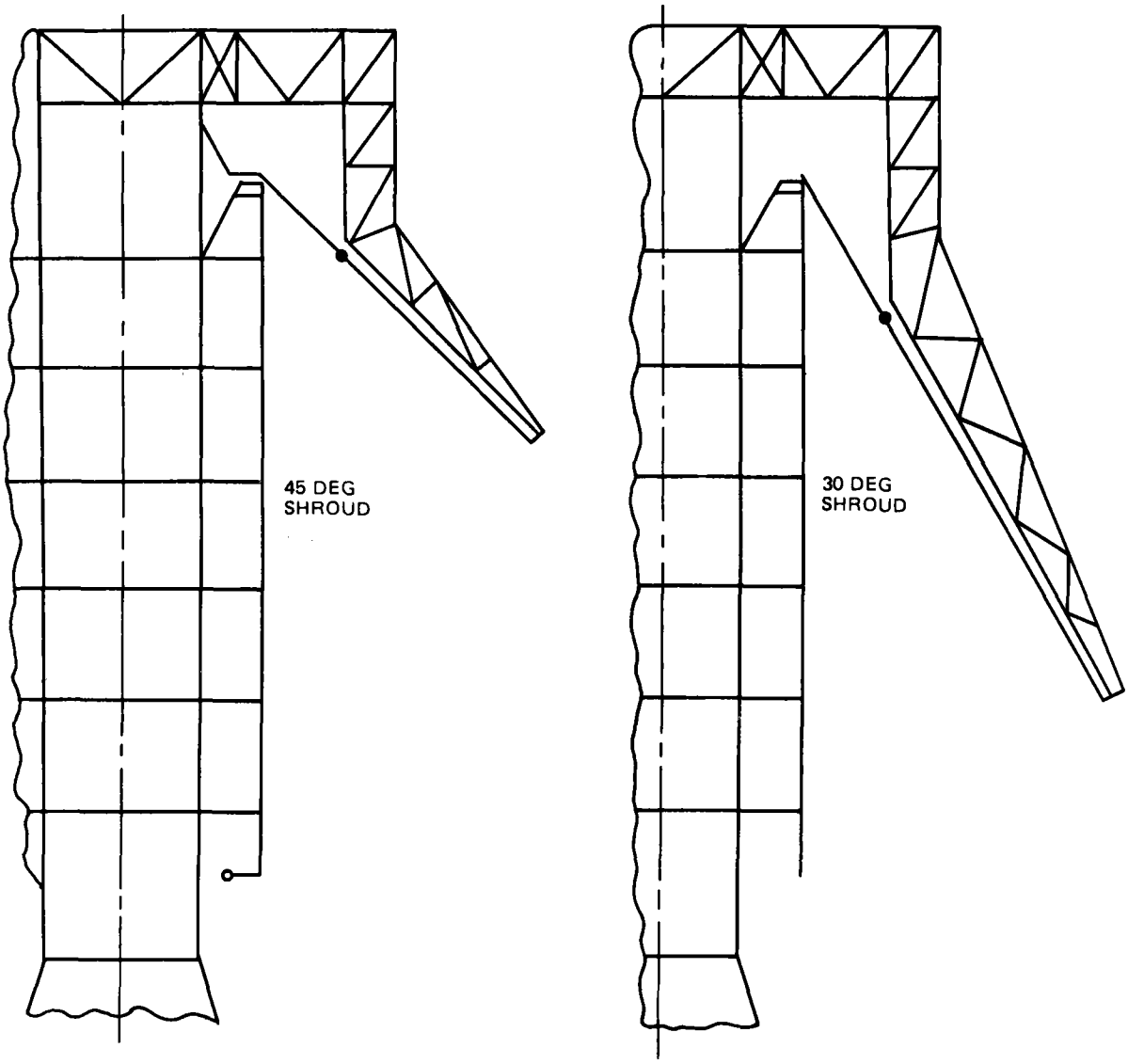

Figure 4-16. Shrouded Receiver Concepts

Trade studies carried out for the Pilot Plant indicated that the losses could be reduced by as much as 15 to 20% depending on the time of year and ambient conditions. When the cost penalties associated with the shroud and increased tower structure required to support the added hardware were considered, a net saving of less than $0.5M was predicted for the Pilot Plant while the effects washed out for the Commercial design.

With the change to wet cooling, the improved cycle efficiency and reduction in parasitic loads that resulted allowed a significant reduction in the collector field size and receiver power rating. In addition, continued work on the Commercial collector field had reduced some of its asymmetric power characteristics from the receiver standpoint. Finally, the upgrading of the steam conditions further increased plant efficiency, thus adding to the reduction in collector field/receiver thermal requirement. The net effect of these changes from a receiver standpoint was a situation where the receiver was grossly over-designed to meet the current thermal power requirement. For example, the maximum incident flux to be delivered on the north panel had reduced to 0.2 MW/m^2 from the original design level of 0.3 MW/m^2.

Two receiver design modifications were considered at that point. The first involved adding a shroud to minimize heat losses while the heliostat aim points were adjusted so that no thermal power was directly incident on the shroud. The resulting heat profiles for several different shroud configurations are shown in Figure 4-17. The net effect is to have a high heat flux concentrated near the bottom of the tubes while the shroud severely restricted the amount of power reaching the upper part of the tubes. The results directly suggest the possibility of shortening the receiver, eliminating the shroud, and operating with an elevated heat flux that approaches the original design level. This approach represents the second design modification considered.

In reducing the length of the receiver, the peak heat flux varies inversely with length, ignoring end effects. This effect is shown in Figure 4-18, which treats three receiver sizes. It is seen that by shrinking the length from 17m to 12.5m, the peak heat flux intensity is increased from 0.2 MW/m^2 to

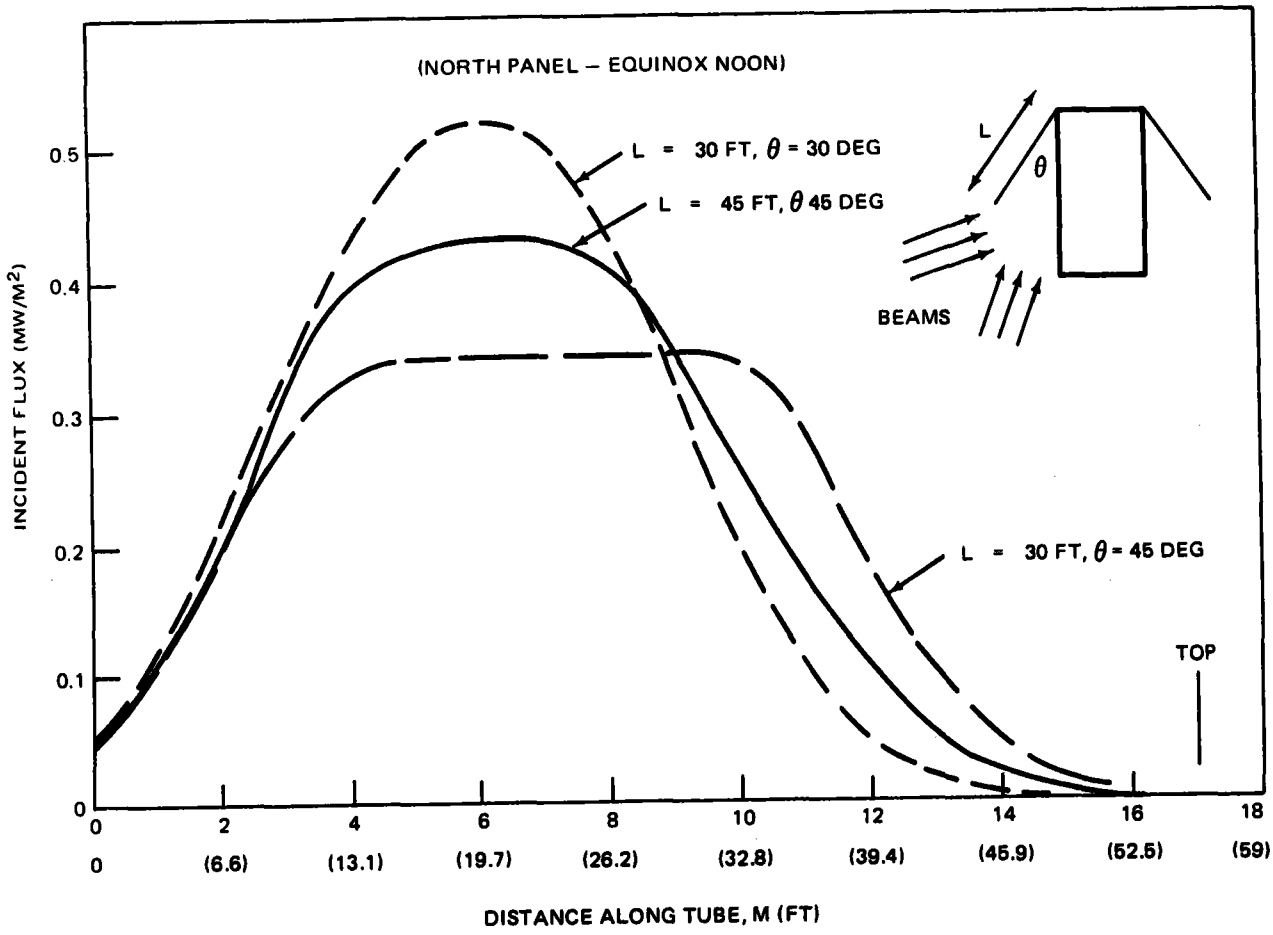

Figure 4-17. Impact of Shroud on Heat Flux Profile

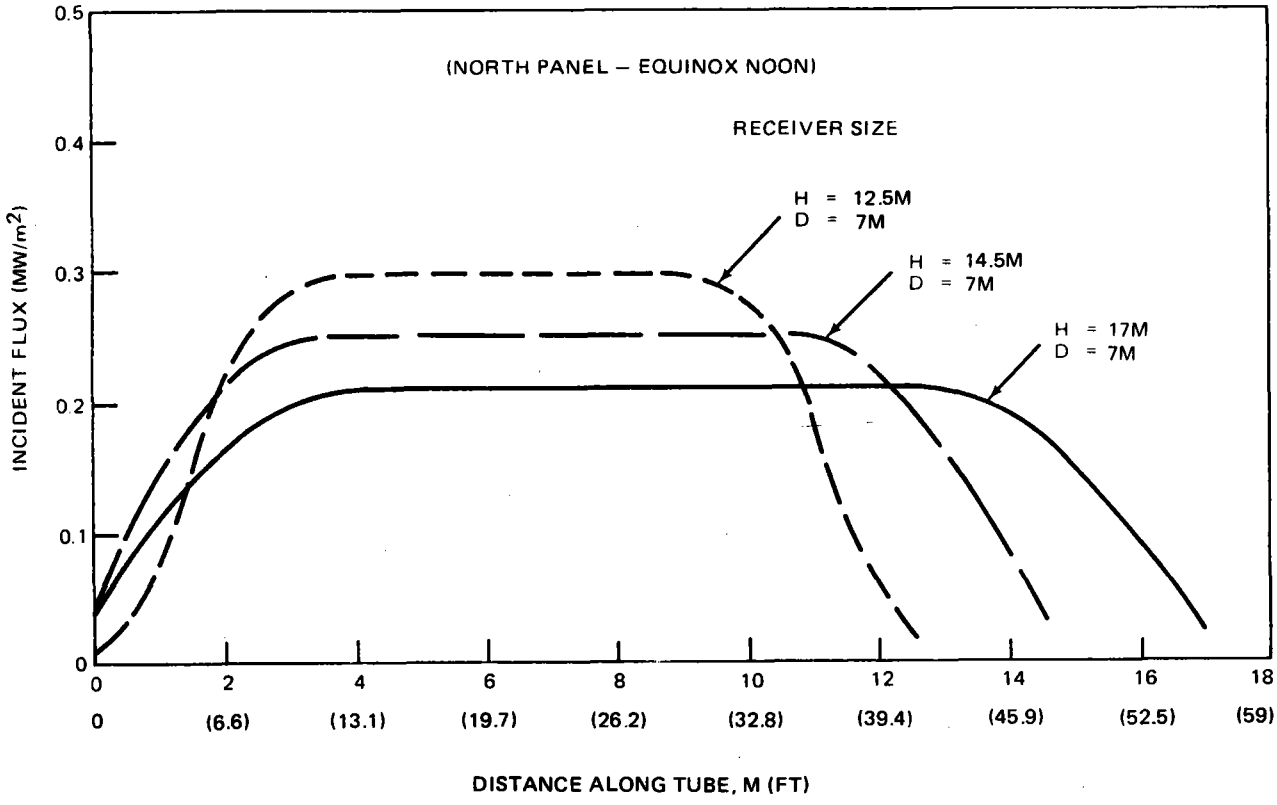

Figure 4-18. Pilot Plant Heat Flux Alternatives

0.3 MW/m^2, which was the original design value. As a result, the baseline receiver length was decreased to 12.5m (41 ft). It should be noted that the heat loss from the receiver decreases in almost direct proportion to the decrease in surface area. Thus the decrease in receiver length accomplished the same effect on receiver heat loss percentage without adding the shroud.

4.4.4 Operating Steam Conditions

As in the case of the Commercial system discussed in Section 3, the operating steam conditions for the Pilot Plant are determined by turbine and thermal storage-related requirements. The baseline turbine selected for the Pilot Plant is an automatic admission industrial machine with throttle steam conditions of 510°C (950°F), 10.1 MPa (1,450 psig).

In addition to providing good cycle efficiency (34.7% at 2.50 in. Hg), it also corresponds to the throttle steam conditions selected for the 100-MWe Commercial turbine. Since nearly identical steam conditions would be required for both the Pilot Plant and Commercial receivers, selection of these steam conditions provides an additional verification of the Commercial system.

The operational aspects of thermal storage for the Pilot Plant are shown in Figure 4-19. In comparing these conditions with corresponding Commercial system conditions, two important changes are noted. First, the Caloria HT-43 temperature is reduced by 14°C (25°F) over its entire operating range in the Pilot Plant for reasons of design conservatism. The effect of the change is to relax the pinch point (the minimum horizontal distance between the charging steam line and the thermal storage fluid line) on the charging side, while tightening the pinch point on the discharge side. Secondly, the maximum discharge steam temperature for the Pilot Plant thermal storage configuration is 277°C (530°F). Again, based on turbine design considerations, the maximum admission steam pressure acceptable for this temperature is 2.65 MPa (370 psig) at the admission port or 2.76 MPa (385 psig) at the steam generator. It should be noted that the admission steam at the turbine inlet port for the Pilot Plant has 17°C (30°F) less

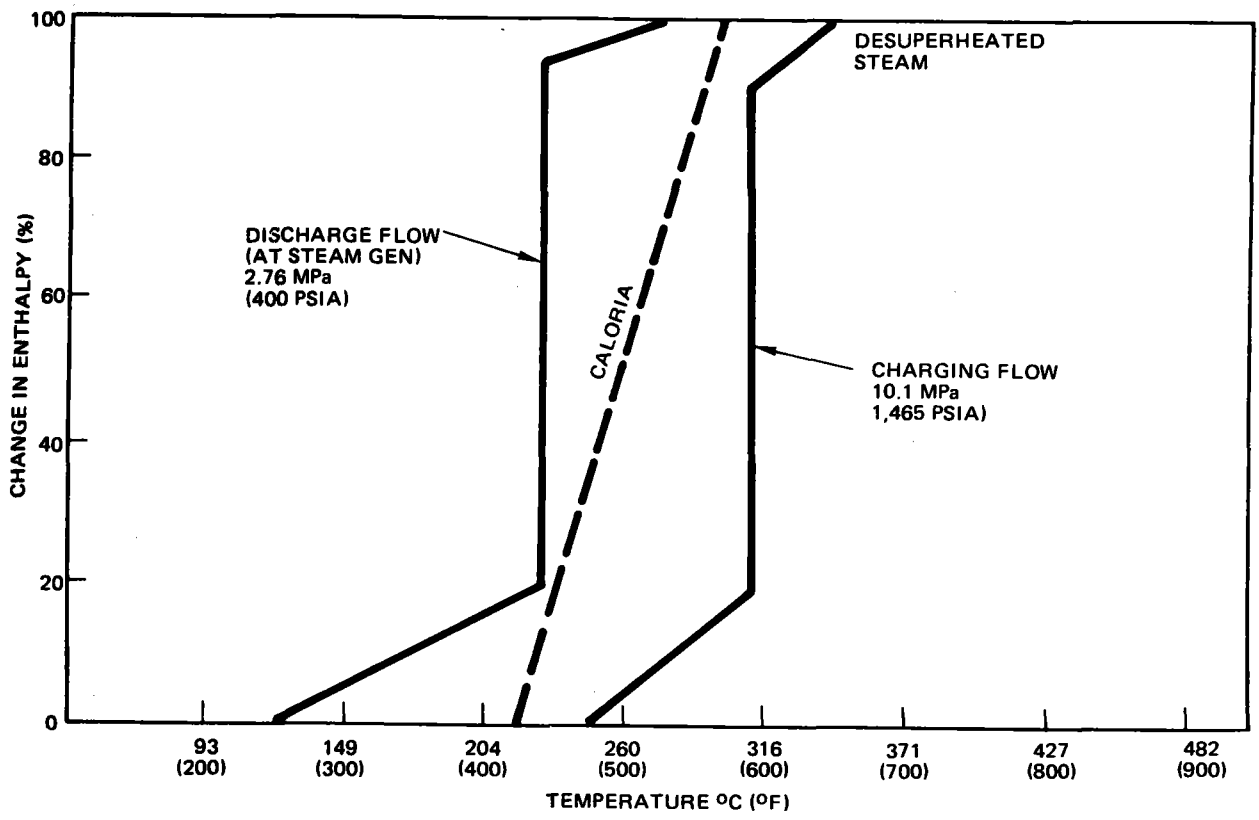

Figure 4-19. Thermal Storage Charging and Discharging Characteristics (Pilot Plant)

superheat than the admission steam for the Commercial system. The result is a greater moisture level at the last-stage buckets for the Pilot Plant turbine. The condition is acceptable because of the smaller bucket wheel diameter and corresponding lower bucket tip speed in the Pilot Plant turbine, which results in a reduced tendency for moisture erosion.

4.5 ANNUAL ENERGY CALCULATIONS

As estimate of the net annual energy output of the Pilot Plant was made based on the Aerospace data tape for Inyokern, California (1963). To carry out this calculation, as well as to develop the capability of analyzing the Pilot Plant performance for a variety of other sites, a computer code was prepared which is capable of working with the Aerospace tapes on other input data. The code uses direct insolation data as well as ambient temperature and wind speed to make its performance calculation.

The program begins by surveying an entire day to determine the desired operating mode or whether a plant startup is warranted. Once a system startup is initiated, the program moves through a series of calculations shown in Figure 4-20 to arrive at the instantaneous level of power production and the incremental energy output. In addition to calculating electrical output, the analysis treats collector field performance for the appropriate time of day and year; receiver performance, including heat losses, piping flows, and pressure drops; thermal storage factors; and a detailed accounting of parasitic loads. In addition to predicting the gross and net electrical plant output on an instantaneous or incremental basis, the program outputs pertinent performance data on the various subsystems and tabulates energy purchased from the grid during nongenerating periods such as startup and charging thermal storage.

In making the calculations over a simulated one-year period, certain plant operating assumptions were required. For example, a daily startup was made only on days which experienced at least 2 consecutive hours with insolation levels in excess of 500 W/m^2. The receiver steam conditions were correlated to insolation level with rated receiver steam being produced when insolation levels exceeded 500 W/m^2; derated steam was assumed for insolation values between 250 and 500 W/m^2. Below 250 W/m^2,

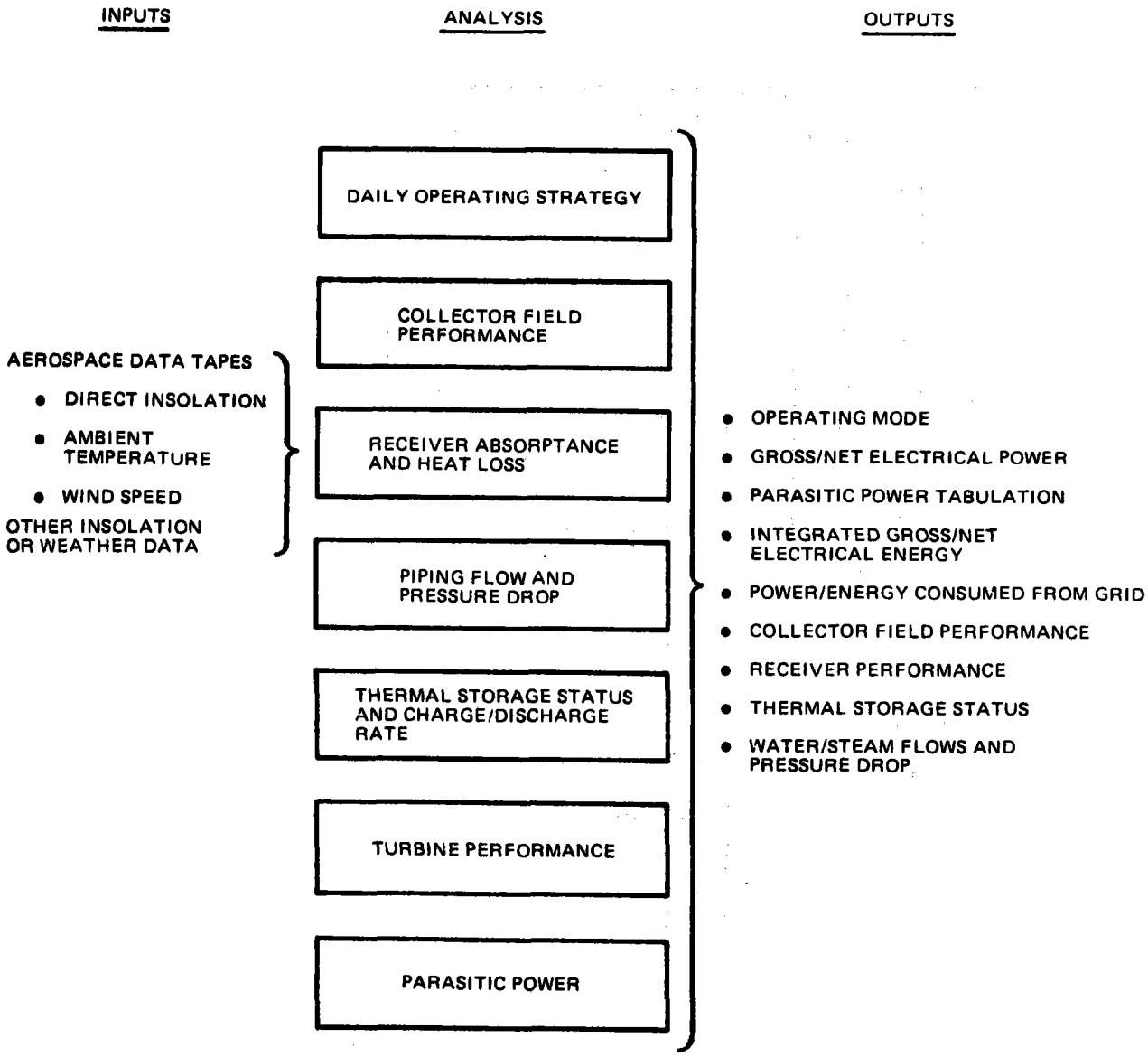

Figure 4-20. Annual Energy Calculation (Computer Model)

the receiver would be shut down. The mode switch conditions are somewhat arbitrary in that they attempt to reflect the incidence of cloud cover. Receiver switch points could be correlated to cloud cover numbers that appear on the data tape although the correlation is in general more difficult and therefore was not selected for the analysis.

From an overall system operating standpoint, the desired steam flow path was directly to the turbine whenever possible and thermal storage was charged only when the receiver was operated in a derated steam condition. This maximized the annual energy output of the system and was consistent with Sandia guidelines for carrying out annual energy calculations. During evening periods, the turbine was operated until storage had been depleted to the predetermined minimum level required to start the turbine the next morning. During morning startup, the first 15 minutes of thermal power collection was assumed to go into component heatup, turbine roll, etc with no useful power being produced. The next half-hour collection interval was primarily diverted to thermal storage for later extraction and power generation. At the same time, the turbine roll and loading phases were completed. During the balance of the day, power was generated from either receiver steam or thermal storage steam, or a turbine shutdown occurred, depending on the insolation and availability of thermal power from the receiver and thermal storage.

The calculations were made at 15-min intervals for the entire year as defined by the Inyokern 1963 Aerospace data tape. Typical results are shown in Figures 4-21 and 4-22 for a representative day and on a monthly basis for the entire year. The hourly data contained in Figure 4-21 shows how the turbine output responds directly to variations in insolation. The monthly energy production data shown in Figure 4-22 reflects directly gross weather and insolation variations which occurred on the Inyokern data tapes. As indicated, the net annual output of electricity for a Pilot Plant at Inyokern was estimated to be 27,430 MWHe.

4.6 PLANT OPERATIONS

The aspects of the Pilot Plant related to plant operation involve the steady-state operating modes, system startup timelines, and transient operational considerations.

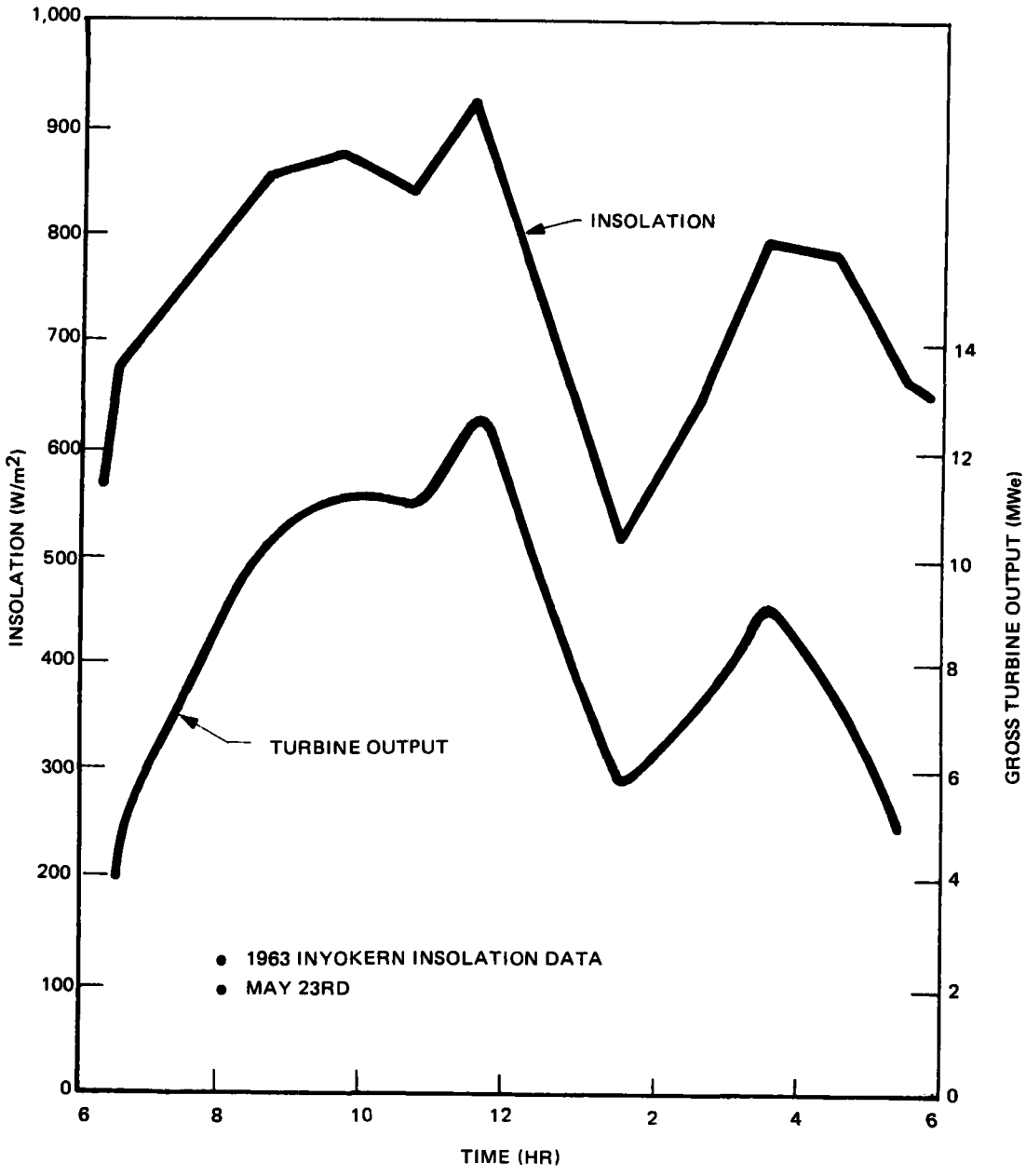

Figure 4-21. Typical Daily Performance

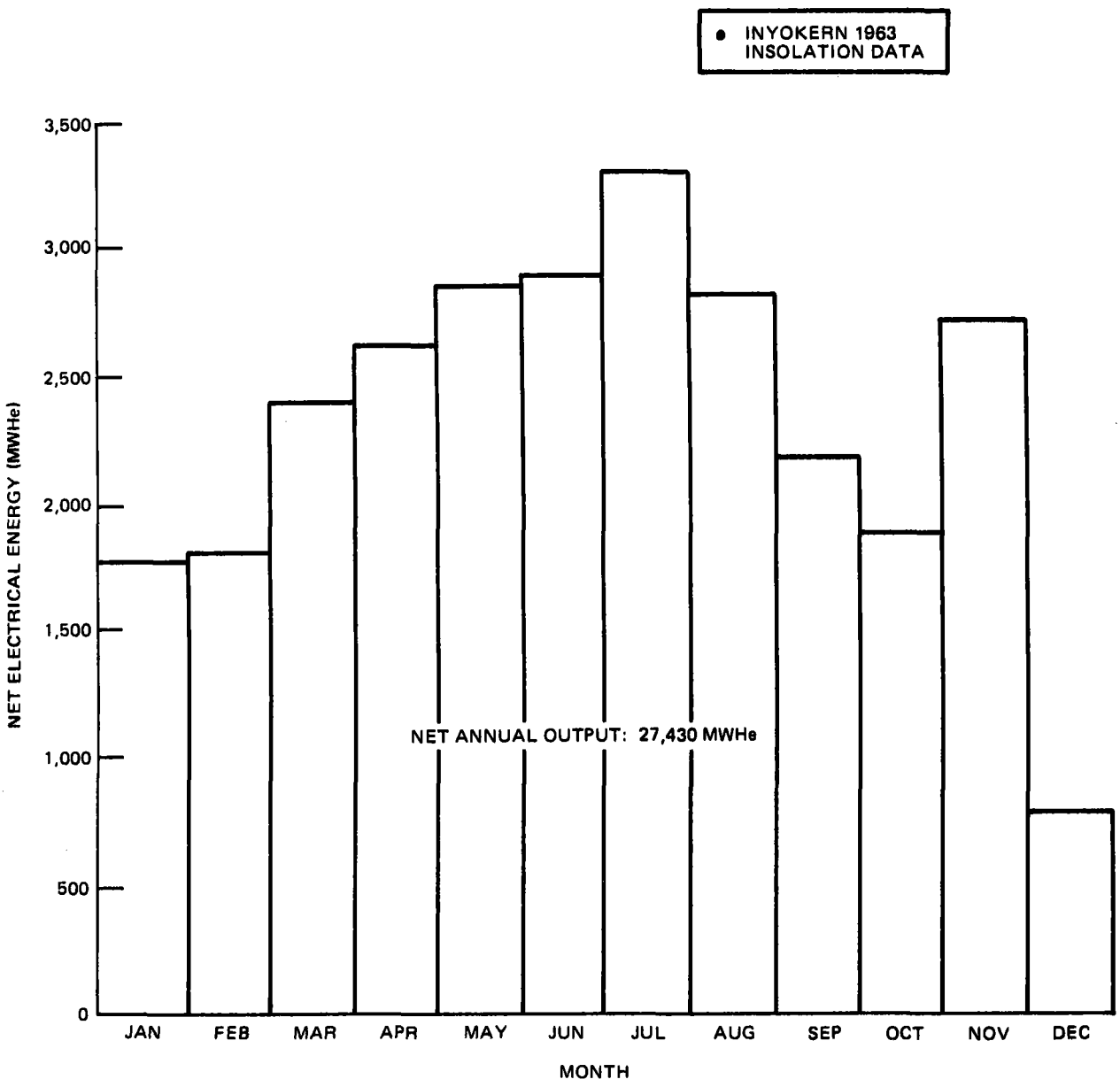

Figure 4-22. Predicted Annual Energy (Pilot Plant)

4.6.1 Operating Modes

The Pilot Plant is designed to operate in one of the six steady-state operating modes which were defined in Section 3.7.1 for the Commercial system. The mode descriptions presented here for the Pilot Plant represent the Pilot Plant version of these modes. Since they are conceptually the same as those defined for the Commercial system, discussions in this section focus on the unique aspects of the modes at the Pilot Plant level.

4.6.1.1 Normal Solar Operation

The Pilot Plant version of the normal solar mode which was described in Section 3.7.1.1 for the Commercial system is shown in Figure 4-23. As in the case of the commercial system, this mode is used whenever the receiver produces an excess amount of steam over that which is required for turbine operation. The excess flow of rated steam is shunt fed to the desuperheater prior to entering the thermal storage charging heat exchanger. At the desuperheater, the steam temperature is reduced to 343°C (650°F), which is 16°C (30°F) lower than the corresponding Commercial system level. The lower steam temperature is permitted due to the lower Caloria temperature used in the Pilot Plant. As the steam enters the thermal storage charging heat exchanger, it is condensed and passes to the drain tank, which empties into the thermal storage flash tank. The resulting condensate/steam mixture is introduced into the feedwater heaters where it displaces a portion of the turbine extraction flows. This method differs somewhat from the Commercial system in that the latter pumps the condensate from the drain tank directly into the riser, thereby bypassing the feedwater heater elements. This is necessary to prevent the closing down of all turbine bleed ports, which would result in an overflow situation in the turbine. Such is not a problem for the Pilot Plant because of the low solar multiple of the system and the slightly oversized turbine that is available to pass larger steam flows. From a design standpoint, the Pilot Plant approach eliminates the high-pressure pumping station at the outlet of the thermal storage. Thus, operating complexity is reduced. With the exception of the differences described above, the balance of the Pilot Plant operation is conceptually identical to that defined for the Commercial system.

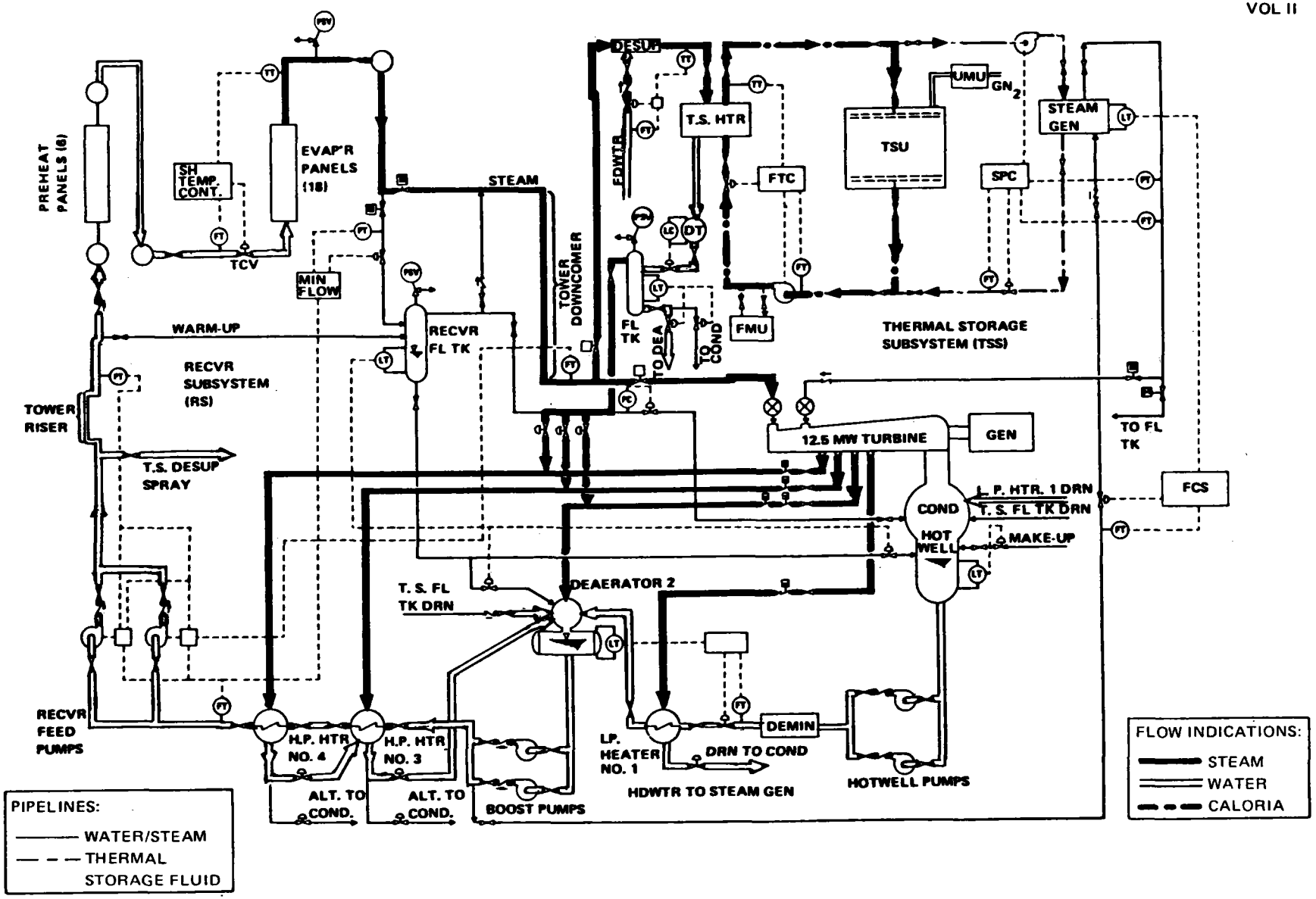

Figure 4-23. Normal Solar Operation (Pilot Plant)

4.6.1.2 Low Solar Power Operation

The low solar power mode is used whenever insufficient solar power is available to operate the turbine generator at the desired output level. In this mode, shown in Figure 4-24, the receiver flow to the turbine is supplemented by thermal storage steam which enters the admission port. Since the Pilot Plant operation during this mode is conceptually identical to the Commercial version presented in Section 3.7.1.2, that section should be referred to for a detailed description of the plant operation.

4.6.1.3 Intermittent Cloud Operation

The intermittent cloud mode of operation shown in Figure 4-25 is used whenever a potentially transient insolation condition exists due to the passage of clouds. To protect the turbine from suddenly varying steam conditions, as well as provide a reasonably steady-state source of steam flow, the turbine is decoupled from the receiver with all receiver flow going to thermal storage. On a simultaneous basis, the thermal storage discharge equipment is operated to produce a steady-state source of steam in the steam generator which enters the turbine through the admission port. Since no receiver flow enters the high-pressure turbine port, ~ 5% of the admission steam must be introduced into the port to remove excess heat that is produced by blade windage, thus maintaining temperature control in the high-pressure section. With the exception of the interface between the thermal storage heater drain and the balance of the system, the operation of the Pilot Plant is identical to the Commercial system. Additional information pertaining to this operating mode can be found in Section 3.7.1.3.

4.6.1.4 Extended Operation

The extended-operation mode is used whenever insufficient insolation is available to power the receiver while some useful charge exists in the thermal storage unit. The flow paths, which are schematically shown in Figure 4-26, are identical to the admission steam loop flow used in the intermittent-cloud mode described previously. As in the case of the Commercial system, steam pressure control is maintained by the turbine admission valve and the Caloria circulation rate. This mode of operation could be continued until the thermocline begins to pass from the top of

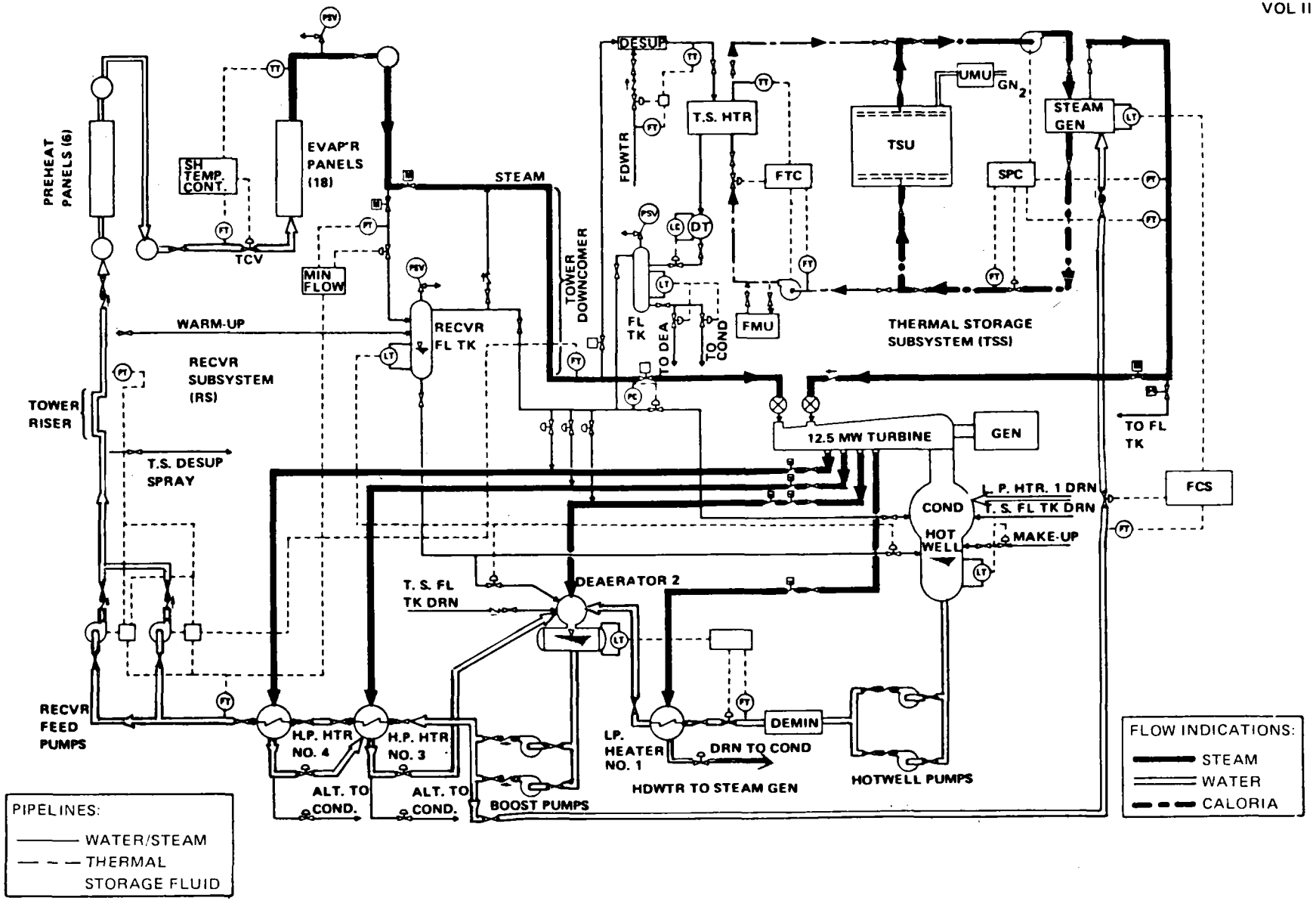

Figure 4-24. Low Solar Power Operation (Pilot Plant)

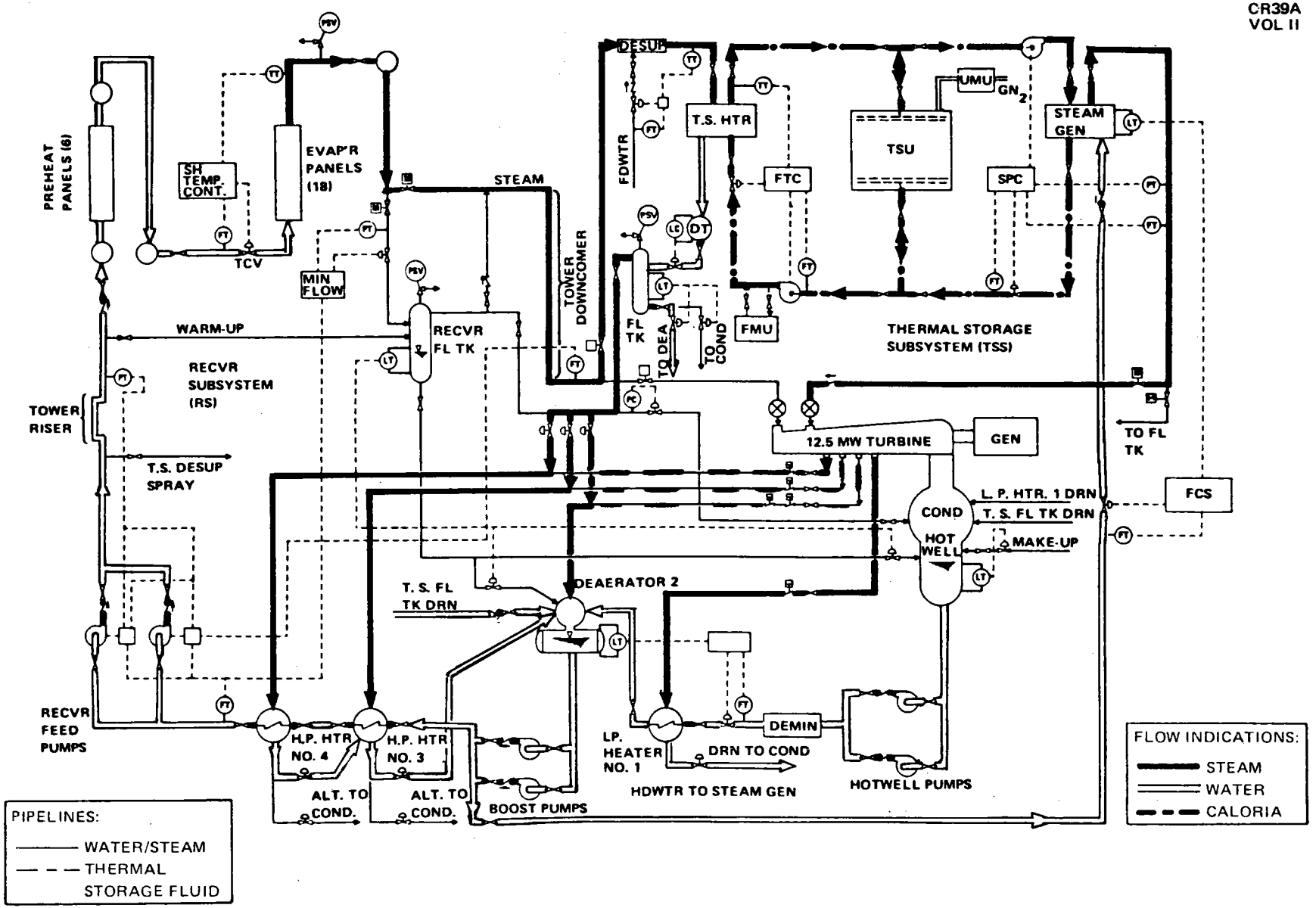

Figure 4-25. Intermittent Cloud Operation (Pilot Plant)

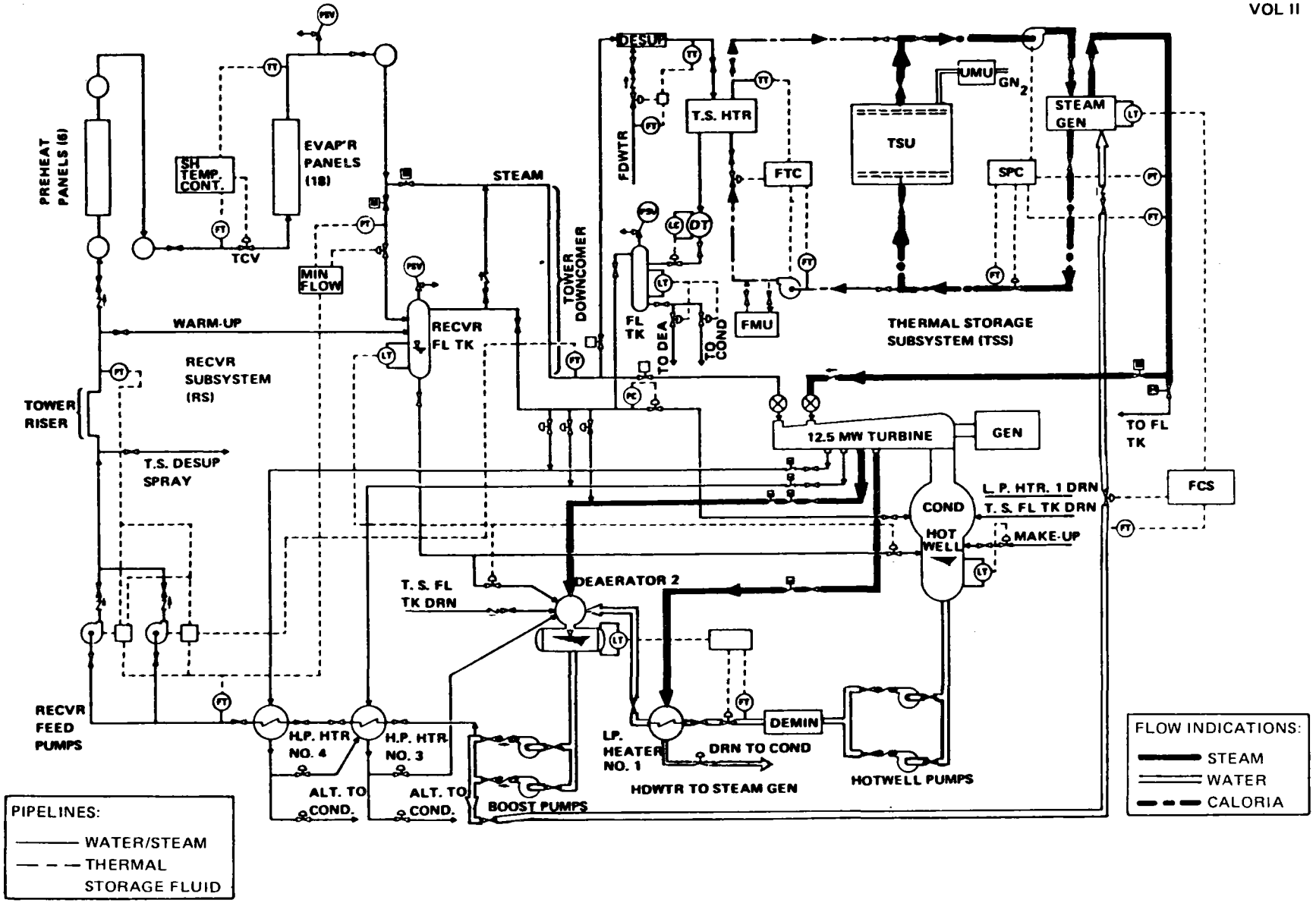

Figure 4-26. Extended Operation (Pilot Plant)

the storage tank, at which time the Caloria temperature would decrease rapidly. The thermal storage steam generator is designed to maintain controlled steam conditions with Caloria inlet temperatures as low as 293°C (560°F). Thus, the Caloria temperature can degrade by 8°C (15°F) before thermal storage extraction must be terminated. An option exists to shut down the turbine prior to the complete discharge of the thermal storage unit. The turbine can then be rolled and loaded the next morning using thermal storage steam prior to the availability of rated receiver steam using exactly the same operating mode. As in the case of the intermittent cloud, ~5% of the admission steam must be bypassed through the high-pressure port to maintain temperature control in the high-pressure section.

4.6.1.5 Charging of Thermal Storage Only

As in the case of the extended-operation mode just discussed, the charging of thermal storage only mode, which is shown in Figure 4-27, represents a simplification of the more complicated intermittent-cloud mode. In this mode, a maximum of 32.8 MWt of power in the form of derated steam is diverted to the thermal storage charging heat exchanger. Of this flow, 30 MWt is absorbed and transferred to the storage tank; the remaining 2.8 MWt passes to the feedwater heaters in the form of high-temperature condensate. The charging rate was established based on the Sandia minimum charge rate specification. About 86% of the maximum collector field output can be accommodated with this mode with the power levels defined above. For higher power levels, a portion of the collector field would have to be defocused or the Caloria temperature could be allowed to rise above the 302°C (575°F) maximum temperature design condition. As in the case of the intermittent-cloud mode, all condensate leaving thermal storage would enter the feedwater heater loop where it would be recirculated to the receiver. Because the turbine is not operated in this mode, all electrical power required to operate the system must be drawn from the electrical grid.

4.6.1.6 Fully Charged Thermal Storage

The fully charged thermal storage mode would be used whenever the thermal storage unit is completely charged or when the thermal storage subsystem is unavailable for outage or maintenance reasons. The flow path, which is shown schematically in Figure 4-28, sends all of the receiver flow directly

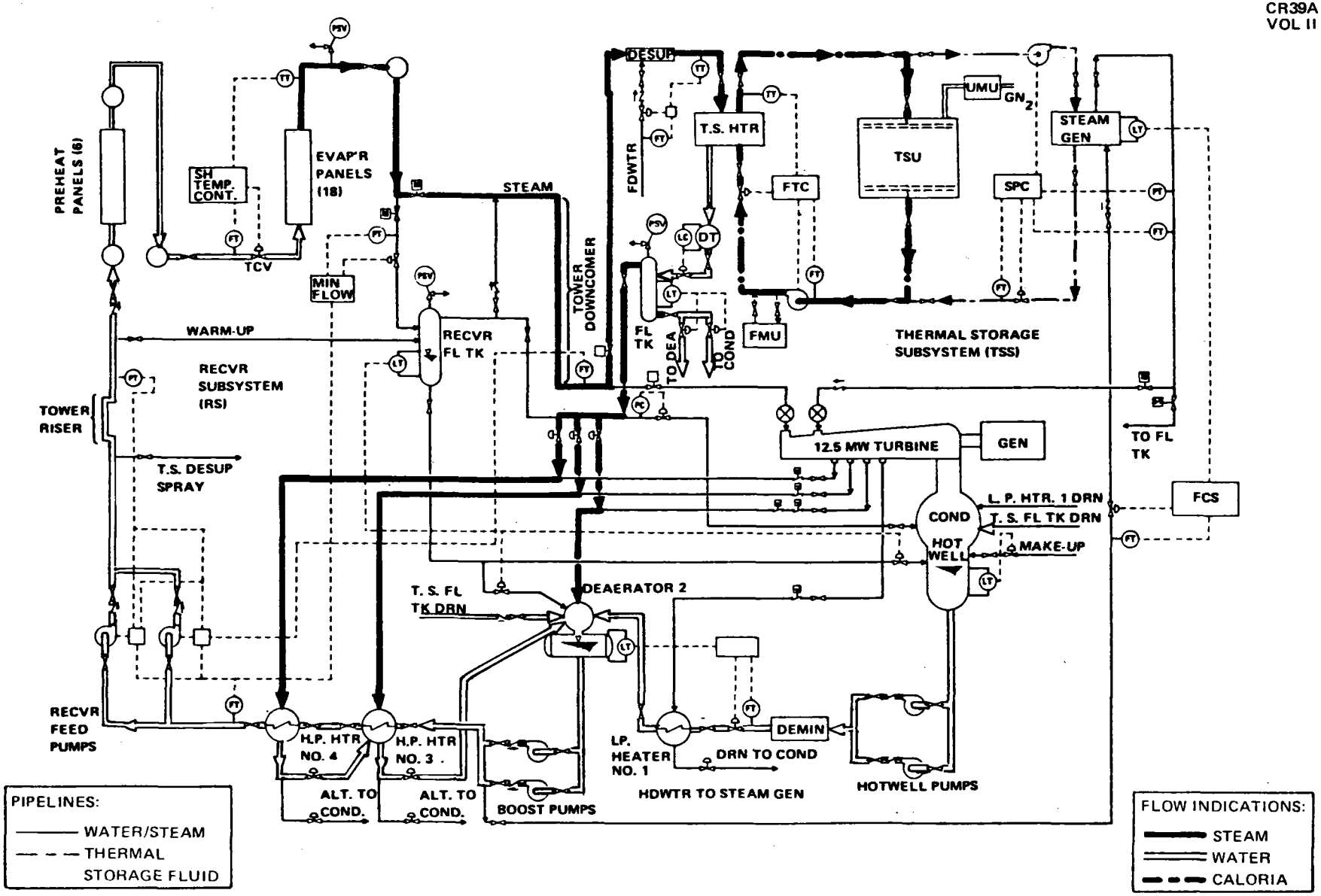

Figure 4-27. Charging of Thermal Storage Only (Pilot Plant)

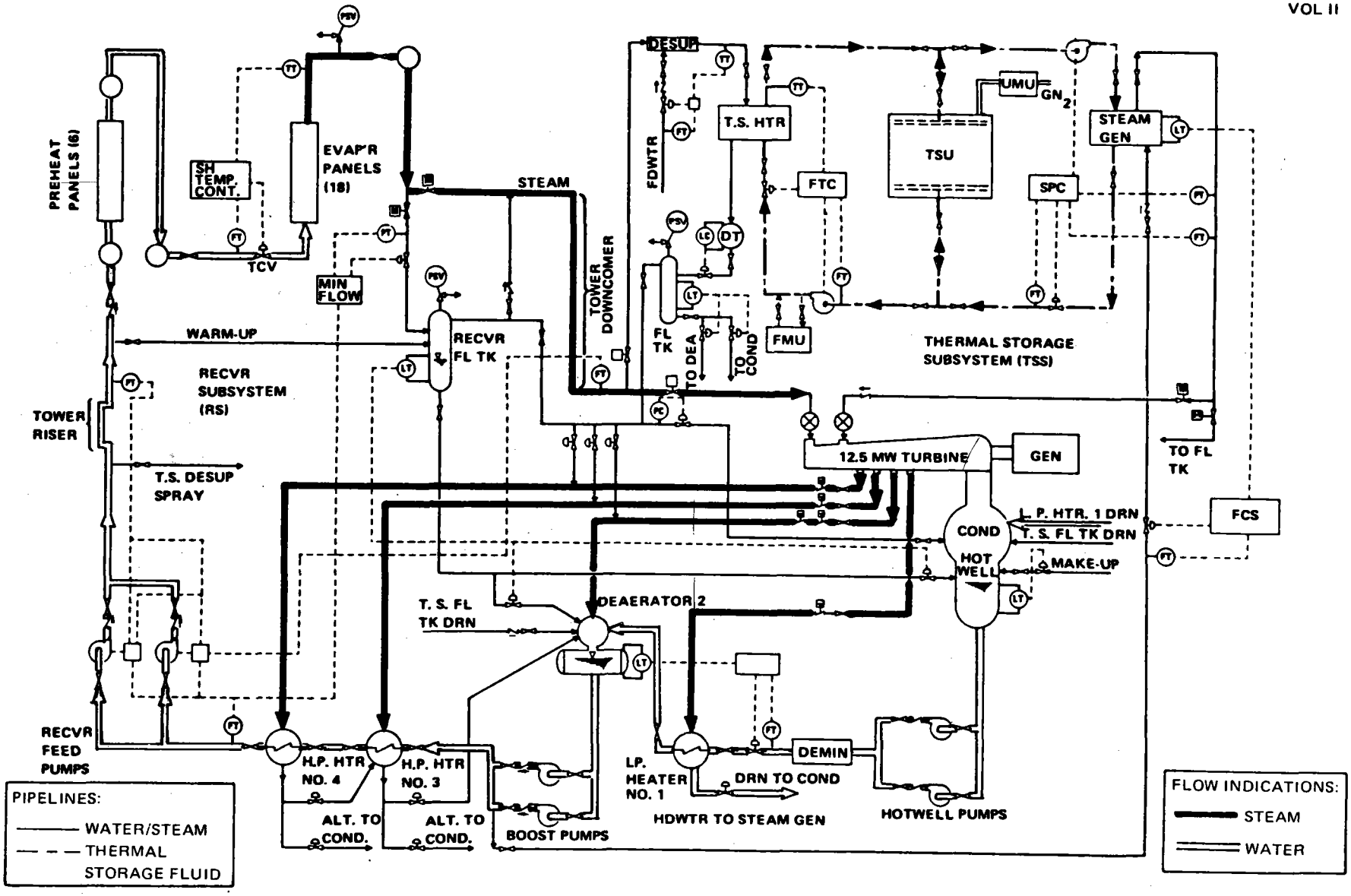

Figure 4-28. Fully Charged Thermal Storage (Pilot Plant)

to the turbine with the output of the turbine-generator being dependent exclusively on the receiver flow rate.

Due to the low solar multiple for the Pilot Plant, along with the slightly oversized turbine, the maximum receiver flow can be accommodated by the turbine directly. This action removes the need to defocus a portion of the collector field and allows the turbine to have complete responsibility for receiver pressure control.

4.6.2 System Operating Timelines

A series of operating timelines have been developed for the Pilot Plant which depict the system startup for a variety of assumed conditions. In particular, startup sequences have been defined for cold, warm, and hot turbine conditions using steam flow from the receiver as well as warm and hot turbine conditions using steam flow from thermal storage. The definition of the turbine status, along with its impact on turbine acceleration and loading rate, are identical to those shown in Section 3.7.2 for the Commercial system. For startups using receiver steam, the critical path represents the sum of the receiver and turbine startup periods. For startups employing thermal storage steam, the critical path is the rate at which the receiver can be brought online.

4.6.2.1 Cold-System Startup from Receiver

The time-phased sequence of events necessary to start a cold system using receiver output steam is shown in Figure 4-29. Although the actual operating timeline depends on the time of day and year when the startup is carried out, and the insolation available, the relationships illustrated in the figure are representative of a typical morning startup with a clear-sky condition. Prior to the events shown in this figure, the feedwater would be circulated through the system and in the process demineralized to ensure that a proper water quality exists at the time of receiver startup.

The actual startup sequence begins by redirecting the sun onto the receiver at time equal to 0. The receiver goes through its normal startup sequence until a derated steam condition is produced on a panel-by-panel basis. During the startup period, power collected by the receiver is diverted to the receiver

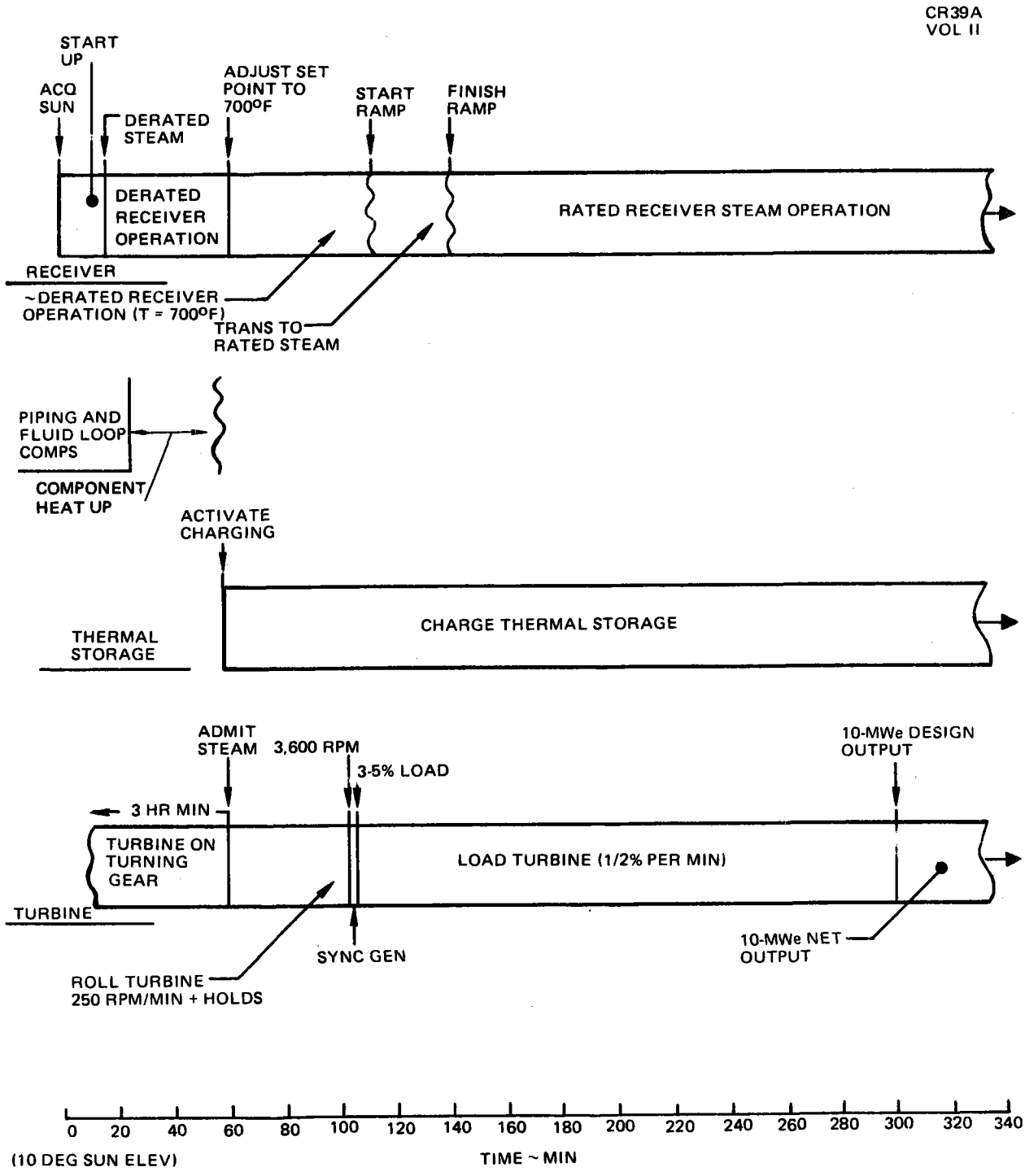

Figure 4-29. Cold System Startup From Receiver (Pilot Plant)

flash tank in the form of hot water or a two-phase mixture. The thermal power passes down the tower through two downcomer lines leaving the flash tank (one for vapor and one for condensate) and is introduced into the feedwater heater elements. At the same time, some flash tank vapor is fed to the main downcomer line where heating is initiated. Drains at the turbine and downstream of the thermal storage charging heat exchanger are opened, allowing preheating to proceed to those points. Startup continues with the receiver steam being held at a derated condition to prevent a thermal shock condition from occurring while the thermal power developed is heating the rest of the system. During this period, a significant portion of the collector field is kept out of service to prevent the system from being overpowered.

With the completion of the component heatup activity, at about 65 min into the startup cycle, the receiver outlet steam set point is ramped to ~ 371°C (700°F) while steam is being admitted to the turbine and the thermal storage charging loop is being activated. This steam condition has been selected so that the turbine can be supplied with steam at 40% of rated steam pressure with at least 56°C (100°F) of superheat. With the thermal storage subsystem being capable of accepting power, a greater portion of the collector field can be activated with the limiting power flow corresponding to the maximum charging rate.

The turbine roll and hold procedure is per the manufacturer's specification with full-rated speed being realized at ~ 104 min into the startup sequence. At that point, the generator is synchronized and a 3 to 5% load is applied. The loading of the turbine-generator then proceeds at 1/2% per minute. During the period from approximately 10 to 25% load, the receiver outlet conditions are ramped to the full-rated steam conditions. With the receiver operating at a rated steam condition and the thermal storage absorbing excess power, the turbine generator load continues to increase until the full 10-MWe net power is available from the generator at a point in time 300 min after initiation of the startup sequence. During the turbine loading period ~ 65 MWH of thermal power was consumed and ~ 20 MWH of gross electrical power was produced. It should be noted that the turbine operates on a preprogrammed speed/load startup sequence during the first 50% or so of the roll/load timeline. Thus, the turbine valves are not operating in an initial pressure

control mode as they would during other operational periods. As a result, the thermal storage charging loop has primary responsibility for controlling receiver pressure during this turbine roll and early loading period.

4.6.2.2 Warm-System Startup from Receiver

The sequence of events associated with a warm-system startup using receiver steam, which is depicted in Figure 4-30, are essentially identical to those just described for the cold startup condition except for an overall compression in the time scale. The startup is again initiated with the sun being directed on the receiver. During the initial phase of the receiver startup, the thermal power produced at the receiver is used for some limited component heatup although, since the system is already assumed warm, the need should be minimal.

The receiver is allowed to stabilize at the indicated condition (371°C, or 700°F), which is slightly above the derated steam temperature. The selection of this set point condition provides an immediate source of steam which can be introduced to the turbine while the surplus is diverted to thermal storage. The turbine roll, hold, generator synchronizing, and loading rates are carried out according to the manufacturer's specification. As in the previous case, the receiver outlet conditions are ramped to the rated-steam level as the turbine loading passes between the 10 and 25% power value. During the entire loading period, the thermal storage accepts excess thermal power up to its charging limit. In addition, it is also responsible for receiver pressure control during the early turbine roll and loading phases before it is switched to initial pressure control. During the turbine loading phase, 21 MWH of thermal energy is consumed with ~6.7 MWH of gross electrical power being produced. The elapsed startup time required to produce 10-MWe net power is approximately 105 min.

4.6.2.3 Hot-System Startup From Receiver

The sequence of events necessary to execute a hot-system startup from receiver steam is shown in Figure 4-31. It is assumed that no component preheating is required so that the only thing limiting the initiation of turbine roll is the rate at which the receiver can be brought up to a steam condition compatible with the turbine requirement. The time period shown for receiver

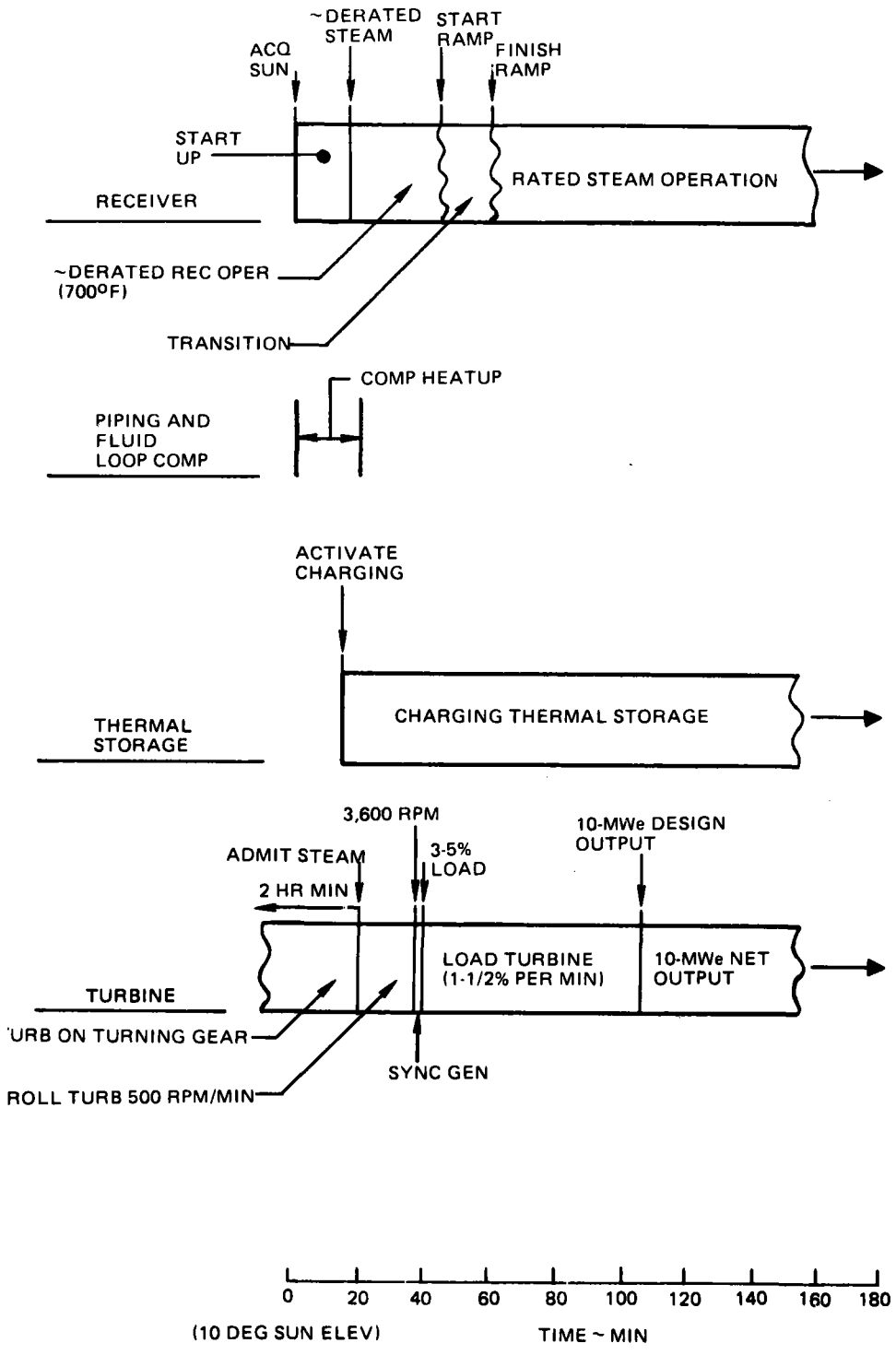

Figure 4-30. Warm System Startup From Receiver (Pilot Plant)

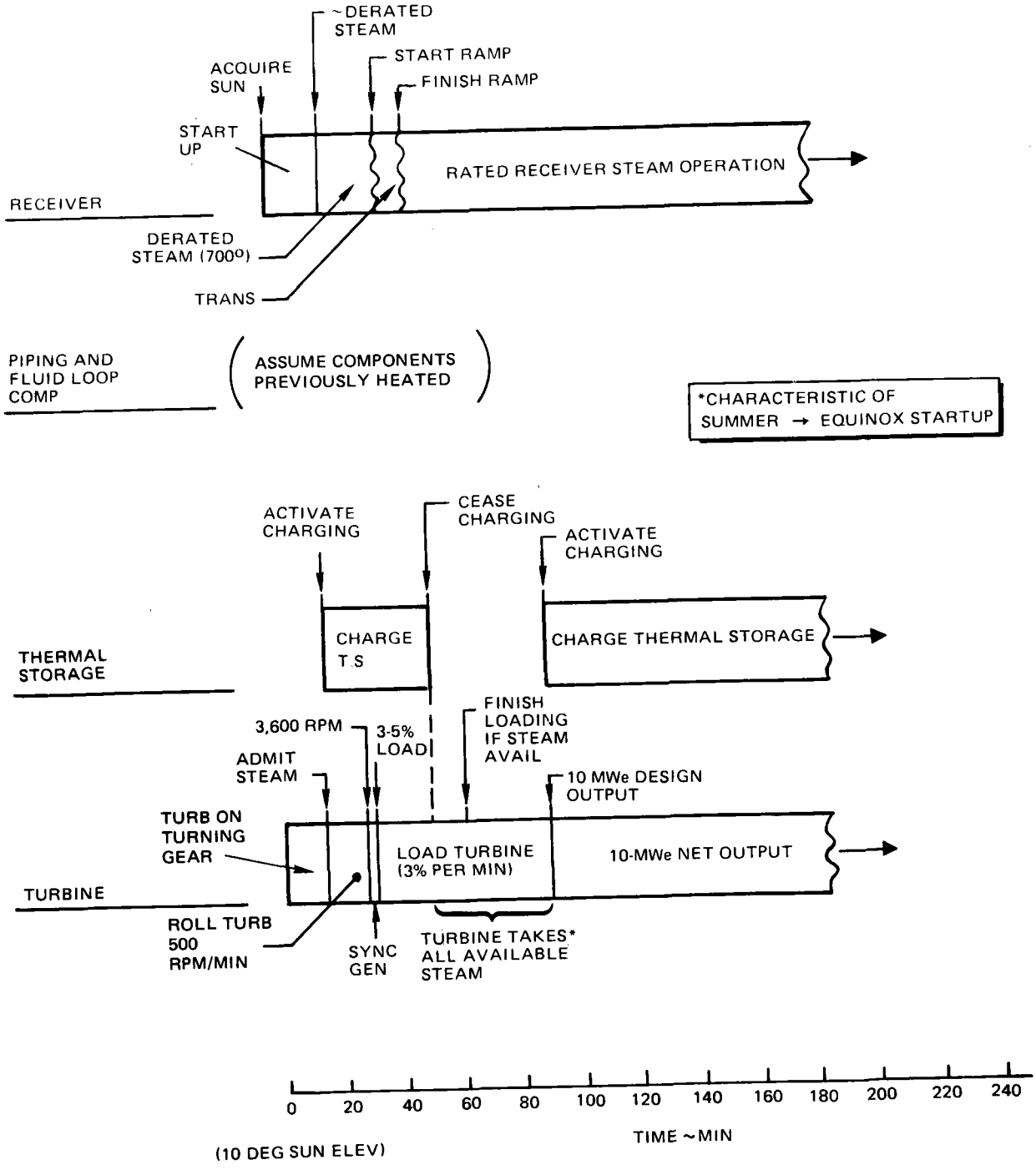

Figure 4-31. Hot System Startup From Receiver (Pilot Plant)

activation and stabilization is 15 min, which is dependent on available insolation conditions. When the stabilized receiver condition is reached, the thermal storage charging loop is activated and accepts as much power as is available or as limited by the maximum charging capability. At the same time, the turbine roll and loading cycle is initiated. Because the turbine is at full operating temperature, the roll and loading activity can occur fairly rapidly.

Again, the transition in receiver outlet conditions to rated steam is timed to occur during the period when the turbine passes through the 10 to 25% load range. If sufficient thermal power is available at the receiver, the loading cycle would be completed approximately 62 min after sun acquisition. During that period, ~ 10 MWHt would be consumed and ~ 3.3 MWHe would be produced.

During some early morning startups, the increase in turbine steam demand exceeds the rate of buildup of receiver steam due to insolation limitations. In that case, shown in Figure 4-31, the turbine loading operation is limited by the rate of increase in receiver steam output. For the case shown, the turbine would be fully loaded 90 min after sun acquisition. It should be noted that this condition of turbine and receiver steam flow matching is most sensitive for the Pilot Plant, which is a low solar multiple system. By contrast, in the case of the Commercial system, which has a high solar multiple, the receiver power rapidly exceeds the turbine steam demand during a startup sequence. Thus, collector field induced limitations on turbine startup are most critical to the Pilot Plant system.

4.6.2.4 Warm-System Startup from Thermal Storage

In an effort to reduce the overall system startup time, two cases where the turbine was started from thermal storage steam were considered. The case treated in this section and shown in Figure 4-32 assumes a warm start condition. In the startup sequence, the critical time-phasing relationship is the point where the turbine is fully loaded (at about a 70% load point, which is the limit for operation from thermal storage steam) and the receiver is simultaneously finishing its ramp to rated steam. Working backward from that point, it is seen that the turbine roll initiates about 25 min prior to the

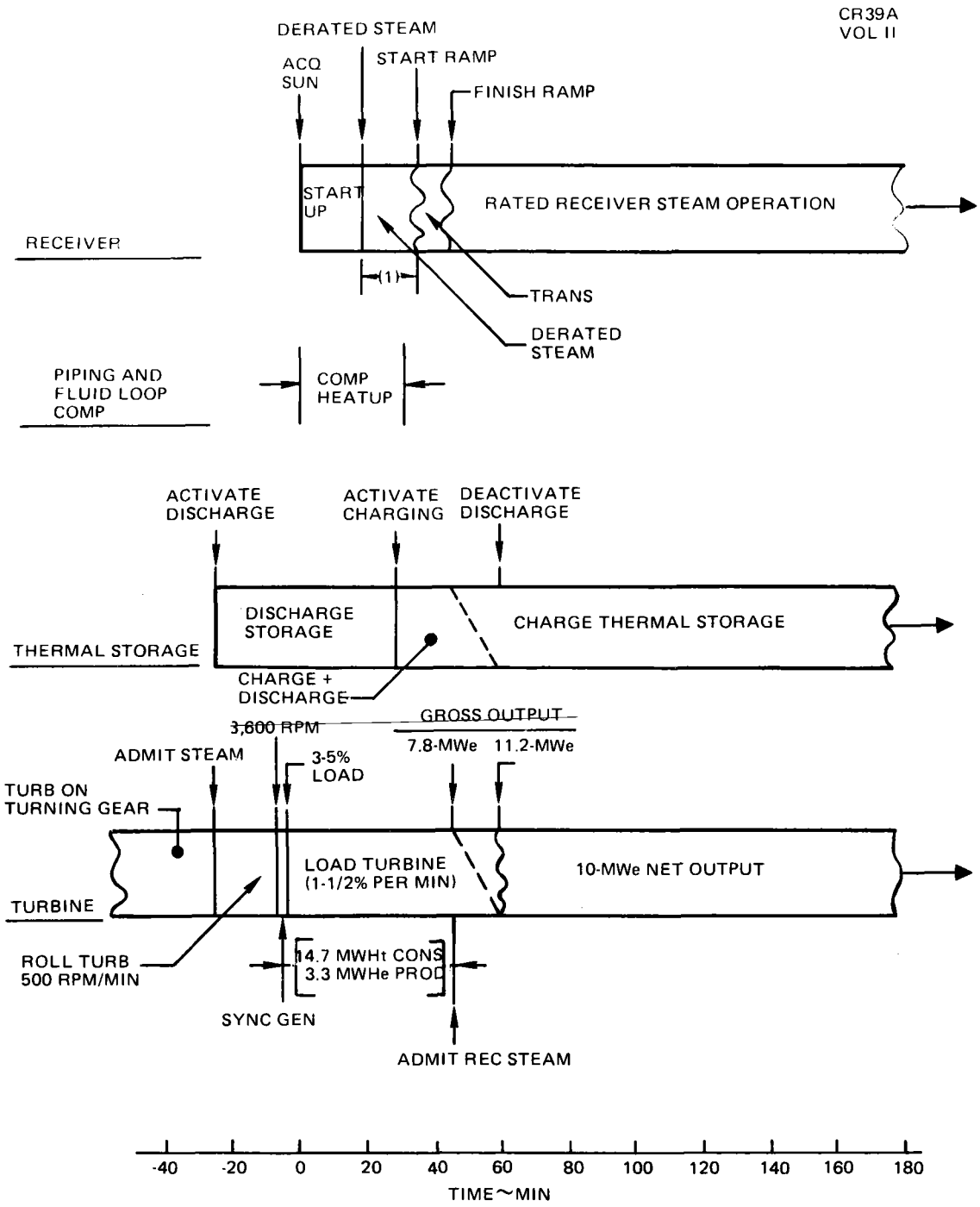

(1) ALL PANELS REACH DERATED STEAM BEFORE TRANSITION IS INITIATED. HOLD PERIOD DEPENDS ON TIME OF DAY/TIME OF YEAR.

*MINIMUM INITIAL THERMAL STORAGE CHARGE REQUIRED FOR INDICATED TIME PHASING

Figure 4-32. Warm System Startup From Thermal Storage* (Pilot Plant)

receiver startup. Steam is drawn from thermal storage to power the roll and loading of the turbine.

At time equal to 0, the receiver startup is initiated, proceeding to a derated steam hold condition until all panels are stabilized at that level. During that period, some limited component heatup is carried out by the receiver steam. Near the end of the derated steam hold period at the receiver, the component heatup is complete and the charging of thermal storage is initiated. At that time, the thermal storage subsystem is simultaneously charging and discharging the storage tank. The receiver is next ramped to a rated outlet steam condition as rapidly as possible, arriving at the rated condition at the same time the turbine arrived at the 70% load point. The rated receiver steam is then fed directly to the turbine to continue the loading cycle to 100% load while the admission steam flow from thermal storage is cut back to zero flow in a controlled manner.

This particular startup sequence represents the condition where a minimum initial thermal storage charge is required. If an earlier turbine startup is desired, a larger initial thermal storage charge would be required because of the longer discharge period that would be experienced by the thermal storage before receiver steam could supplement and ultimately replace the thermal storage steam.

During the warm turbine startup, 15 MWH of thermal energy is extracted from thermal storage although some of that is made up by the charging flow from receiver steam once the panels arrive at a derated-steam condition. At the same time, 3.3 MWH of gross electrical energy is produced. The effective system startup time for this case is 47 or 60 min depending on the startup definition used. This compares to a startup period of 105 min for the case where the system starts exclusively from receiver steam (Section 4.6).

4.6.2.5 Hot-System Startup From Thermal Storage

The sequence of events that occur during a hot-system startup from thermal storage steam is shown in Figure 4-33. As in the previous case considered (Section 4.6.2.4), the key reference point for synchronizing the startup activities is to match, as closely as possible, the 70% load point on the

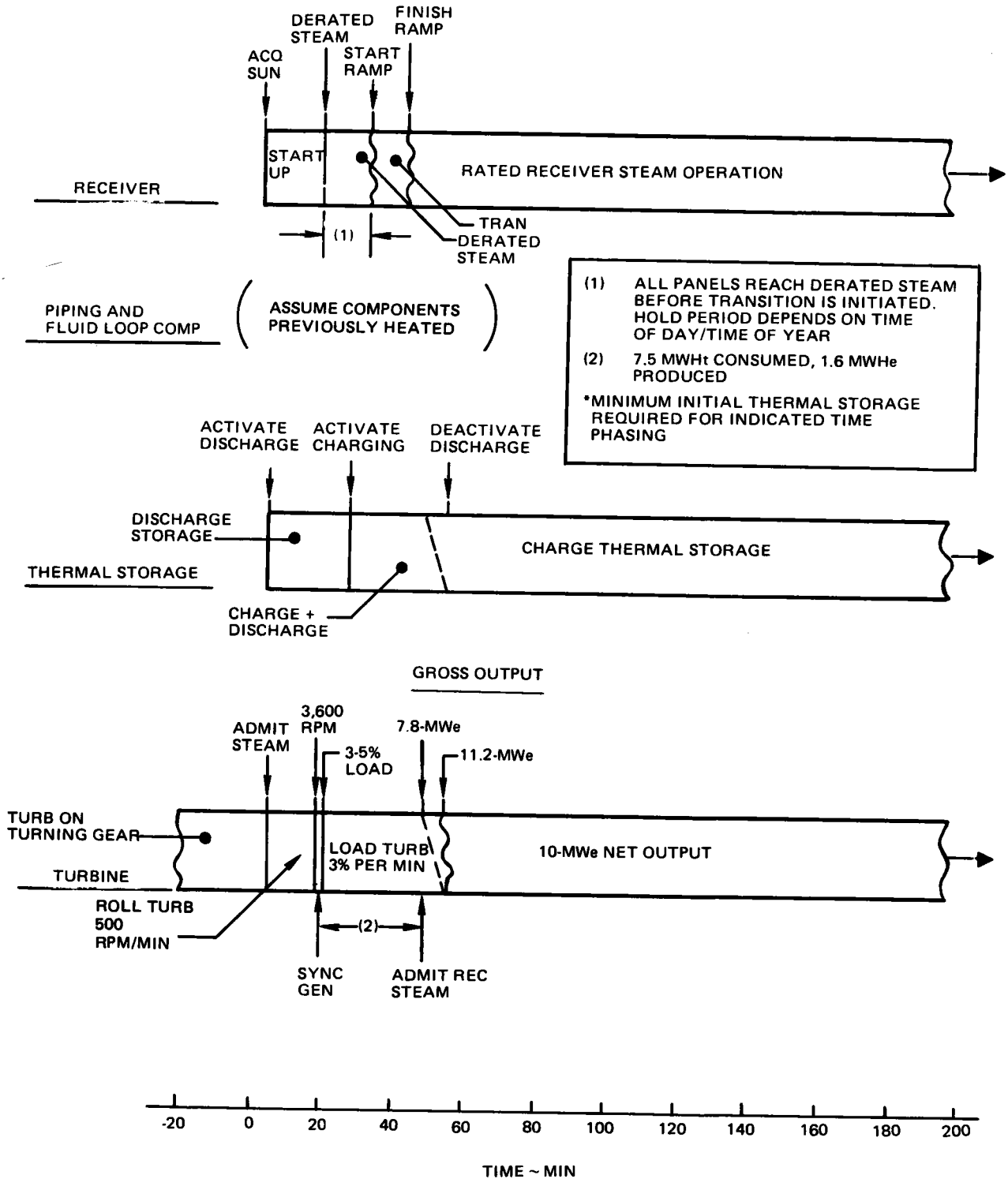

Figure 4-33. Hot System Start From Thermal Storage* (Pilot Plant)

turbine loading line with the availability of rated receiver steam. Again working backward, first the receiver startup sequence is initiated at time equal to 0. At the 5-min point, while the receiver startup is continuing, the turbine roll cycle is initiated with steam drawn from thermal storage. The receiver startup continues with a hold maintained at the derated steam condition until all panels reach that level. Just prior to the final receiver ramp to rated steam, the available derated steam is diverted to thermal storage where the charging function is initiated. As a result, during the subsequent period, the thermal storage is operated in both the charging and discharging mode.

With a uniform derated steam condition established for all receiver panels, the final receiver ramp is carried out as rapidly as possible to rated steam. The rated steam is then fed to the turbine where it replaces thermal storage steam and continues the turbine load ramp to 100% power. A short time interval has been included between the point where rated steam is produced in the receiver and when it begins to displace thermal storage steam. This interval allows for a small temperature adjustment time for the main steam downcomer and steam line to the turbine.

Using the sequence established in this figure, an effective system startup time of 47 to 54 min could be expected depending on whether the 70 or 100% load point is assumed to constitute a completed startup. If the indicated piping temperature interval is ignored, the above startup times can be reduced by 3 to 5 min. The thermal storage energy consumed during the startup was 7.2 MWH, and 1.6 MWH of gross electrical energy was produced during the startup to the 70% power point.

It should also be pointed out that the duration of receiver hold at a derated steam condition, which directly impacts the system startup time, is influenced to a great extent by the time when the startup occurs. During typical early morning startup, some panels are more sluggish than others because of locally lower incident power from the collector field. This hold period could be reduced significantly if the startup were assumed to occur at a noontime sun condition. The high level of redirected thermal power leaving the collector field would create a favorable condition for receiver startup.

4.6.3 Transient Plant Operation

As in the case of the Commercial system that was discussed in Section 3.8.3, the Pilot Plant must be capable of operating with a continually varying input power level. In addition, because the system has only a marginal capability to control input power (through heliostat defocusing), it must be capable of operating in a reactive mode to variations in input power to the receiver or use a predictive capability to anticipate variations in input power. As a result, significant attention must be given to the proper design of the overall control system. Details related to the master control definition effort are in Volume VI. Since that effort was undertaken late in the contract period, a complete understanding of the transient system characteristics is impossible at present. As a result, system operating characteristics can be described at best in a qualitative manner or with the aid of quasi steady-state assumptions.

A series of insolation models which contain various transient characteristics are shown in Figures 4-34 through 4-37. The insolation model shown in Figure 4-34 represents a relatively satisfactory insolation profile that has no significant transient characteristics. The early morning pulse occurs during a low sun elevation angle and at a sufficiently low power level that the receiver would be in its early warmup period. The net effect would be to delay slightly the point at which derated steam would be produced and sent to the thermal storage.

A quasi steady-state analysis was carried out for this insolation model, using the computer code described in Section 4.5 to determine anticipated daily performance. In addition to using the insolation model as an input, an ambient temperature of 28°C (83°F) and a wind of 3.5 m/s (8 mph) at 10m (32.8 ft) elevation were assumed. The predicted net energy produced by the Pilot Plant for that day was 102.57 MWHe. The corresponding gross energy production was predicted to be 115.13 MWHe.

The second insolation model, shown in Figure 4-35, contains a satisfactory morning and midday period with significant cloud-induced oscillations in the afternoon. The first dropoff in insolation would merely impact the receiver flow rate. Rated steam operation could be maintained at all times during

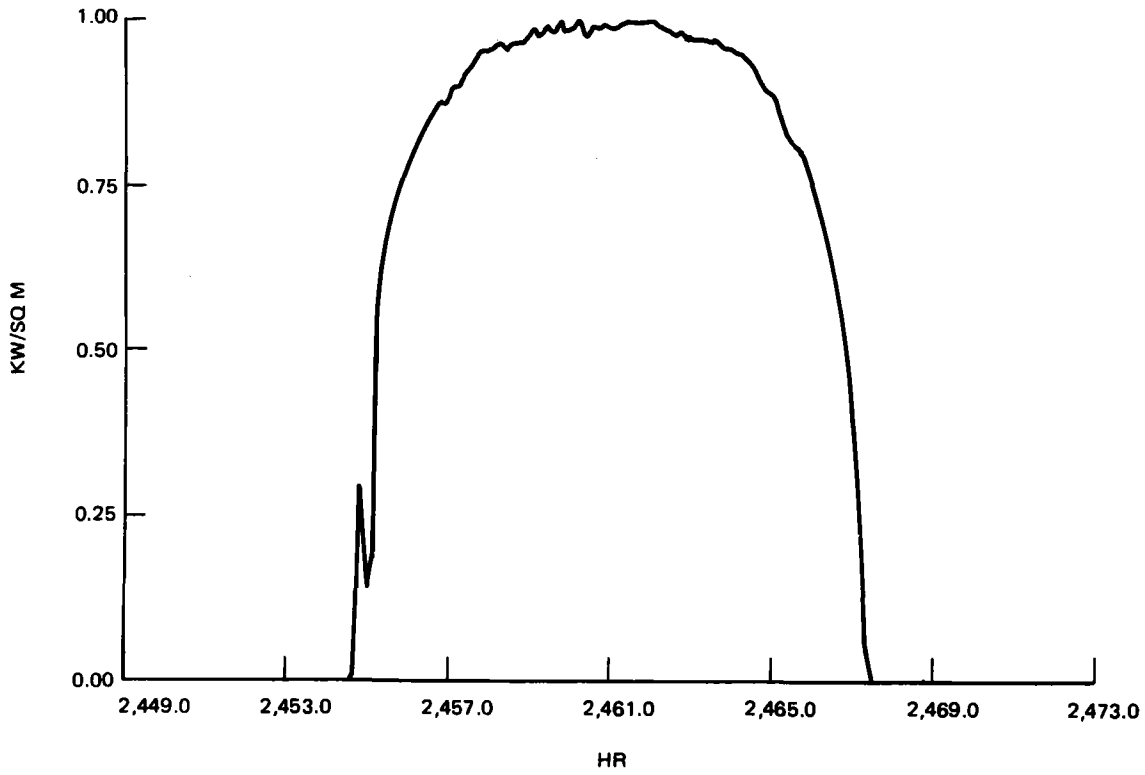

Figure 4-34. Insolation Data

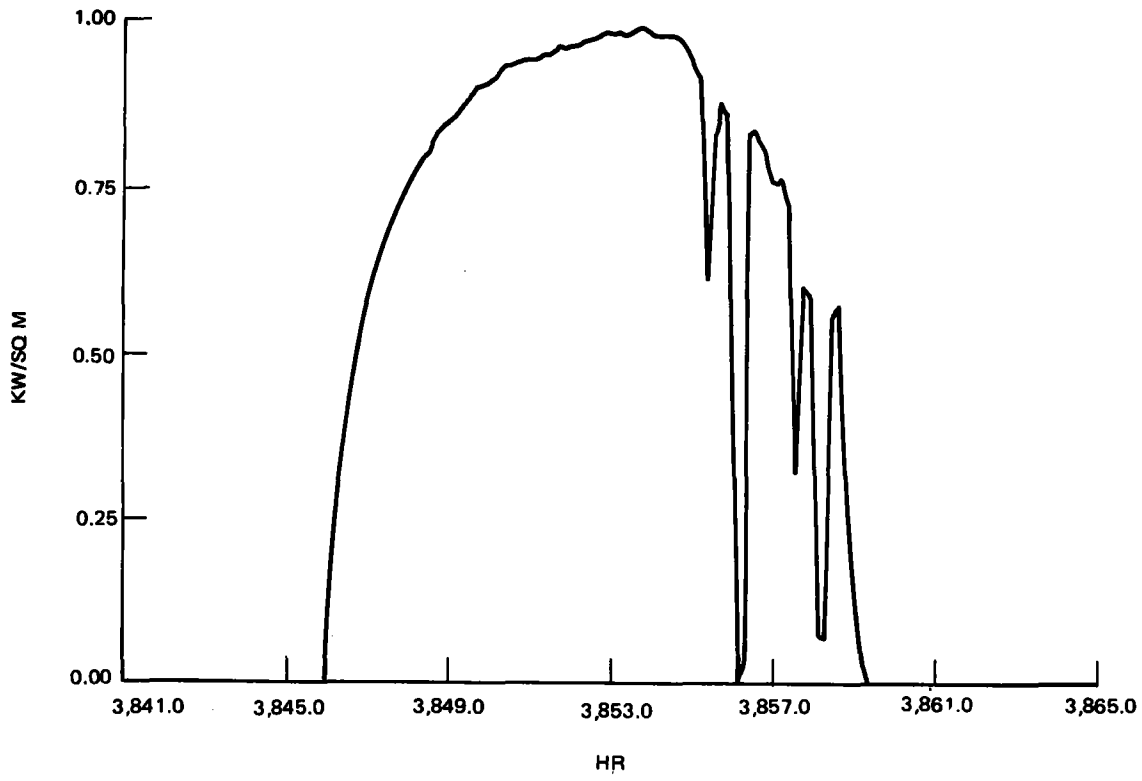

Figure 4-35. Insolation Data

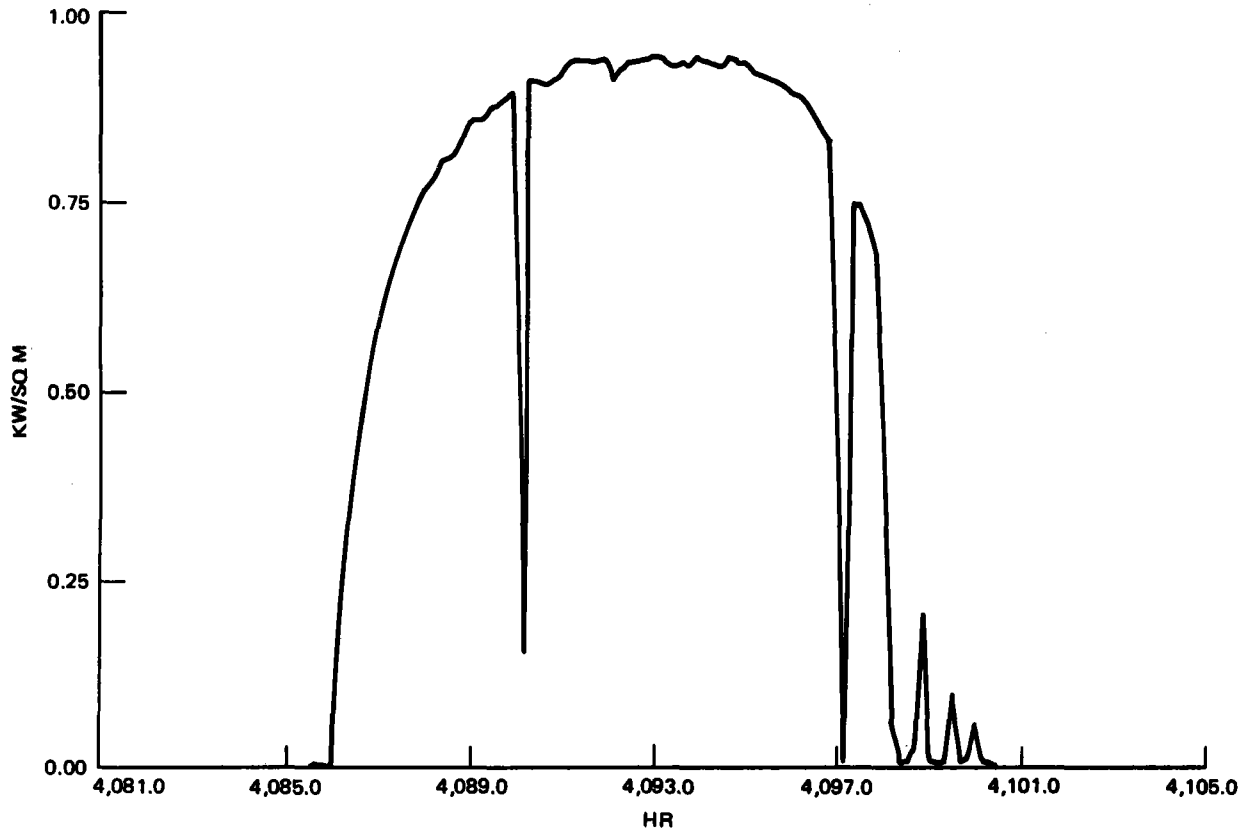

Figure 4-36. Insolation Data

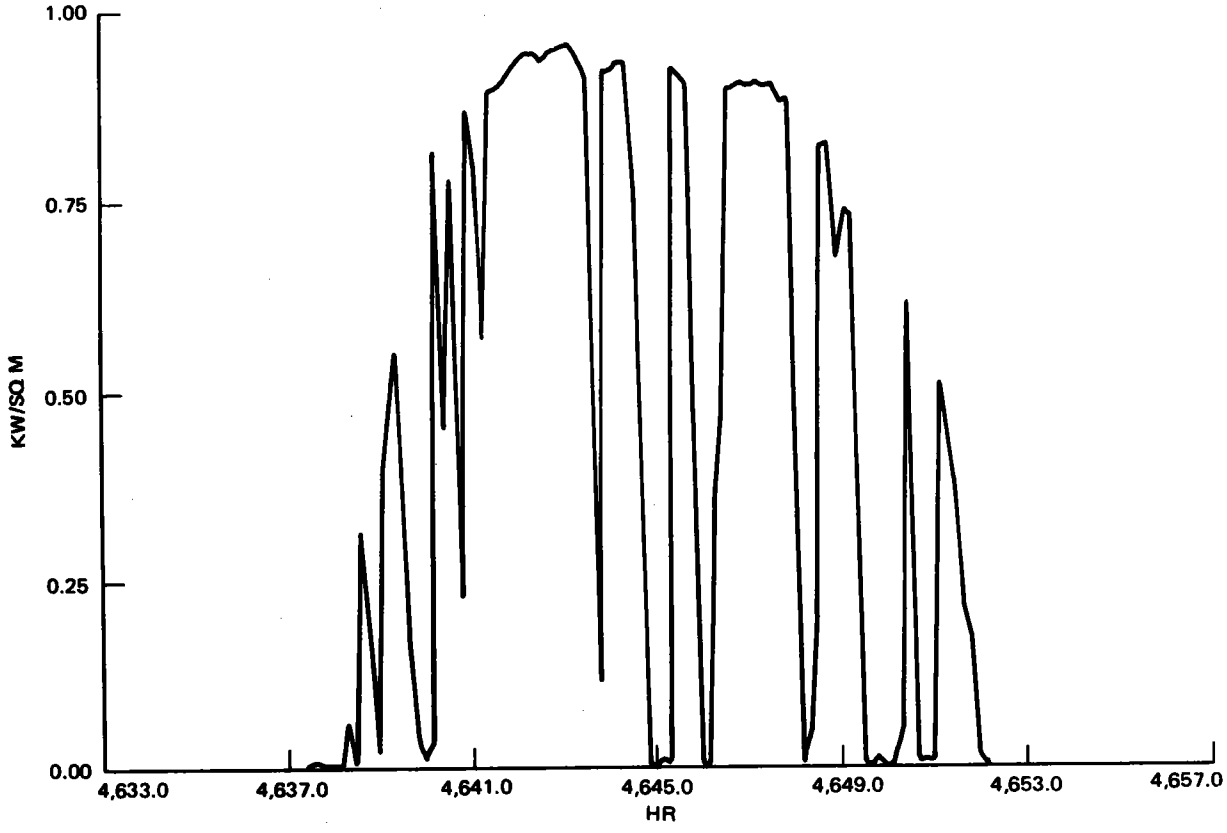

Figure 4-37. Insolation Data

this perturbation. The steam flow diverted to thermal storage would be adjusted to absorb this transient with turbine output being maintained at its design level. The second and more severe falloff in insolation is of a sufficient duration (~20 min) to cause the receiver to lose control of the outlet temperature. This would force the activation of the thermal storage steam generators to make up for the loss of receiver steam. With the resumption of high insolation levels, the receiver could be restarted and brought back to a rated steam condition in ~ 10 min due to its hot condition and the highly effective nature of the collector field which would exist for a high sun elevation angle. The thermal storage steam generator would be deactivated while the rated receiver steam would power the turbine and charge thermal storage. This mode of rated steam operation continues through the third perturbation although the low solar power mode may be employed to maintain the turbine output at a desired level. With the last cloud perturbation, the receiver again loses control of the outlet temperature and the steam generator is again activated. At that point, due to the late hour of the day, it is impractical to start the receiver and transition to rated steam output. As a result, the receiver startup stops at a derated steam condition for the final portion of the days operation. All derated-steam flow is sent to the thermal storage charging heat exchanger while the thermal storage steam generator is providing a steady-state source of steam which carries the turbine directly into nighttime operation.

A quasi steady-state analysis carried out using the insolation model shown in Figure 4-35 resulted in a predicted net electrical output of 98.6 MWHe. The corresponding gross electrical output was predicted to be 110.6 MWHe.

The insolation model shown in Figure 4-36 contains two significant cloud perturbations during the high insolation period followed by three perturbations near sunset. The day proceeds through a normal startup and morning operational period until the first perturbation occurs. At that point, the receiver flow is cut back to accommodate the fallout in insolation. The portion of the steam flowing to thermal storage is first cut down to zero, at which point the thermal storage steam generator is activated and the low solar power mode used. The receiver flow continues to be cut back to maintain rated or

near-rated steam. Due to the limited resolution of data during this perturbation, it is difficult to determine the final receiver outlet condition at the point when the insolation recovers although it does appear that rated or near-rated steam can be maintained during this period.

The second pulse, which occurs at Hour 4097, appears to be of a sufficient magnitude to cause loss of receiver outlet steam temperature control although additional data resolution is necessary to verify the fact. As the cloud begins to cover the field, the receiver flow is reduced, first causing a cutback in the quantity of steam to thermal storage and then causing a transition to low solar power where supplemental steam is taken from thermal storage. Assuming the receiver experienced a momentary shutdown, it would be brought back on line in about 10 min once the insolation resumed. Operation would continue until the late afternoon clouds hit the field. Due to the lateness of the day and the generally cloudy condition which exists for the rest of the afternoon, the receiver would put out rated steam as long as possible, with the rest of the system being transitioned to the low solar mode followed by the extended operating mode as the receiver proceeded to a shutdown condition. System operation in the extended mode would continue into the night. No effort would be made to start the receiver and collect power during the three short insolation pulses that occur just before sunset.

Applying the quasi steady-state computer code to this day resulted in a predicted net electrical output of 97.8 MWHe. The corresponding gross energy output was predicted to be 109.4 MWHe.

The final insolation model shown in Figure 4-37 represents a day which experiences significant cloud passage during the entire day. Assuming that knowledge of the complete day's insolation profile existed at the beginning of the day, receiver startup would be initiated at Hour 4639 as the cloud moved off the field. The receiver would produce derated steam ~ 15 min after startup and then could send ~ 15 min worth of derated steam to the thermal storage charging heat exchanger before the next cloud front shutdown the receiver prior to Hour 4640. With the passage of that cloud front, a second

receiver start could be made using the high insolation levels that occur after Hour 4640. The receiver would be controlled to rated steam through the oscillations in insolation that occur around Hour 4641.

This mode of operation would continue until the major cloud front covered the field at Hour 4645. Then, the turbine would be operated from thermal storage steam while the receiver was held in a standby mode ready for a resumption in insolation. The receiver would be restarted at Hour 4646.5 and operated in a rated steam manner until the next major cloud front hit the field 1-1/2 hr later. The receiver would be off line until the insolation level increased at Hour 4648.5, at which time the receiver would be restarted. Due to the increased frequency of clouds for the balance of the day, the receiver would be controlled to a derated steam condition while the system was operated in an intermittent-cloud mode. This mode would continue until the cloud front at Hour 4649.5 covered the field. At that time, the system would be operated in the extended operating mode while the receiver would be shut down for the day. No effort would be made to capture any power from the last two insolation pulses because of their short duration.

A quasi steady-state analysis carried out for this model indicated that 66.4 MWHe of net energy would be produced on that day with a corresponding gross output of 74.5 MWHe.

4.7 PLANT CONTROL SIMULATION

A simulation of the dynamic characteristics of the plant control is required in order to investigate and evaluate the stability and the transient performance characteristics of the total power plant system. The power plant simulation also serves as an effective design and analysis tool to aid in the development, mechanization, verification, and performance evaluation of the major system control systems. By means of this simulation, both the dynamic per-performance of each subsystem and the performance sensitivities to major design parameters are defined and evaluated with respect to meeting both performance and system design requirements. A real-time simulation of the dynamics of the power plant and subsystem interfaces is also used to design, evaluate, and verify the performance of the master control system

algorithms. After the master control system algorithms are defined and implemented into the master control computer, the simulation checks out and verifies the integrity and compatibility of the master control subsystem hardware with the simulated power plant prior to integration into the actual power plant.

In the following paragraphs, the purpose and simulation philosophy are presented, in addition to a complete description of the total power plant simulation (POPS). Some typical transient responses of the power plant generated from the presently operational POPS simulation are presented, in addition to the present simulation status.

4.7.1 Simulation Purpose and Guidelines

The purpose of the power plant simulation is to provide a design and analysis tool for definition and performance evaluation of the dynamic characteristics of both the major subsystems and the total coupled steam power-generation system. As a design tool, the simulation is used to evaluate the stability, the controllability, the transient response characteristics, and the steady-state accuracy of the major subsystems. As a performance evaluation tool, the simulation is used to evaluate the nonlinear transient performance of the system relative to both design and performance requirements, as well as to define performance sensitivities to plant disturbances and major subsystem parameter variations. For example, the stability of the receiver temperature-flow control system can be evaluated throughout the full range of expected temperature-flow conditions to assure that adequate stability margins exist within the control system throughout the full range of expected operating and environmental conditions. The temperature and flow transient responses of the receiver to variations in input flux or disturbances in system pressure can then also be evaluated relative to performance or design requirements. This performance evaluation is used to substantiate the adequacy of the design or to assess the effect of a design change within the receiver subsystem.

The general philosophy used in the development of the simulation is to generate and substantiate mathematical models of both representative hardware (valves, turbine, sensors, etc.) and physical processes (convection heat transfer,

change of phase system, fluid thermodynamics), which are accurate representations of the actual system within the frequency range of interest. The method used to generate a large system simulation like POPS is to develop and verify each subsystem model in a progressive building-block manner. In the case of POPS, the receiver subsystem simulation is developed, checked out, and verified; then the simulation is expanded, one subsystem at a time, to include the turbine-generator, thermal storage subsystem, balance of plant, and master control subsystem. This assures that by a systematic development of each subsystem model, we will have a high level of confidence that the resultant total system simulation is a valid, accurate representation of the actual power plant.

4.7.2 Simulation Description

The POPS simulation is composed of a set of mathematical models which describe the dynamic performance of the receiver, turbine/generator, thermal storage subsystem, and pertinent ancillary devices within the balance of the plant and the master control subsystems. A functional schematic of the major power plant system elements, as shown in Figure 4-38, presents some of the key features of the simulation as well as the major functional flow between major subsystems. A detailed simulation block diagram of the total power plant system is shown in Figure 4-39 in which each of the major subsystems is expanded into its major elements. The following paragraphs discuss in detail each of the subsystem models, model verification, primary simulation input and output parameters, and the simulation mechanization.

4.7.2.1 Receiver Subsystem Simulation Model

The receiver model consists of a preheater section and water-steam transition section. The 24-panel receiver is modeled as a lumped system consisting of one preheater panel, two boiler panels, and a downcomer section, as shown in Figure 4-40. The mathematical model that describes the dynamic characteristics of the system is derived from equations based on an energy balance on the receiver walls and on the working fluid inside the receiver tubes, a conservation of mass within the system, and the thermodynamics and fluid dynamics of nonsteady fluid flow. System losses due to frictional flow, radiation and convection, and nonideal fluid flow are included.

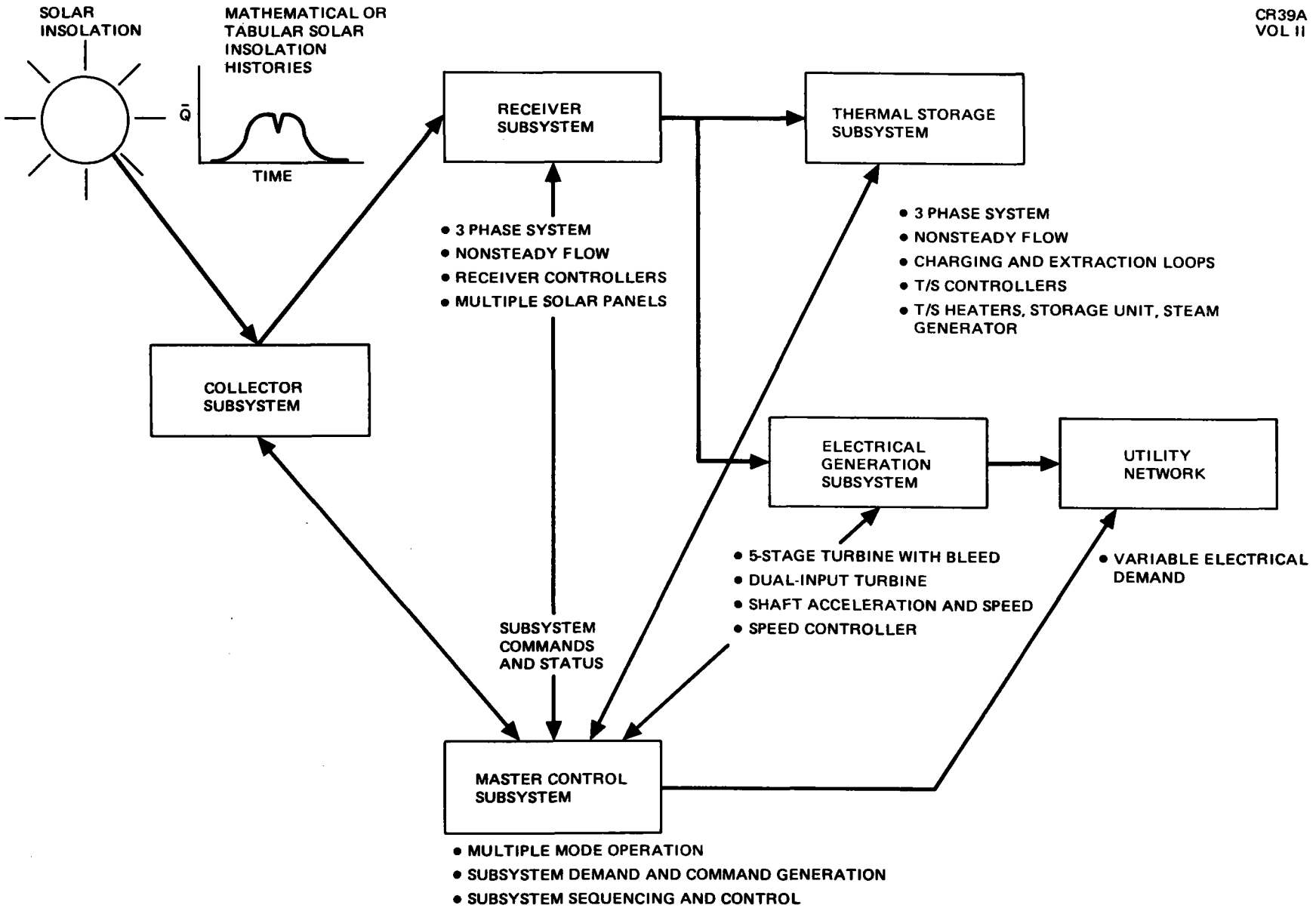

Figure 4-38. Power Plant System Simulation Functional Schematic

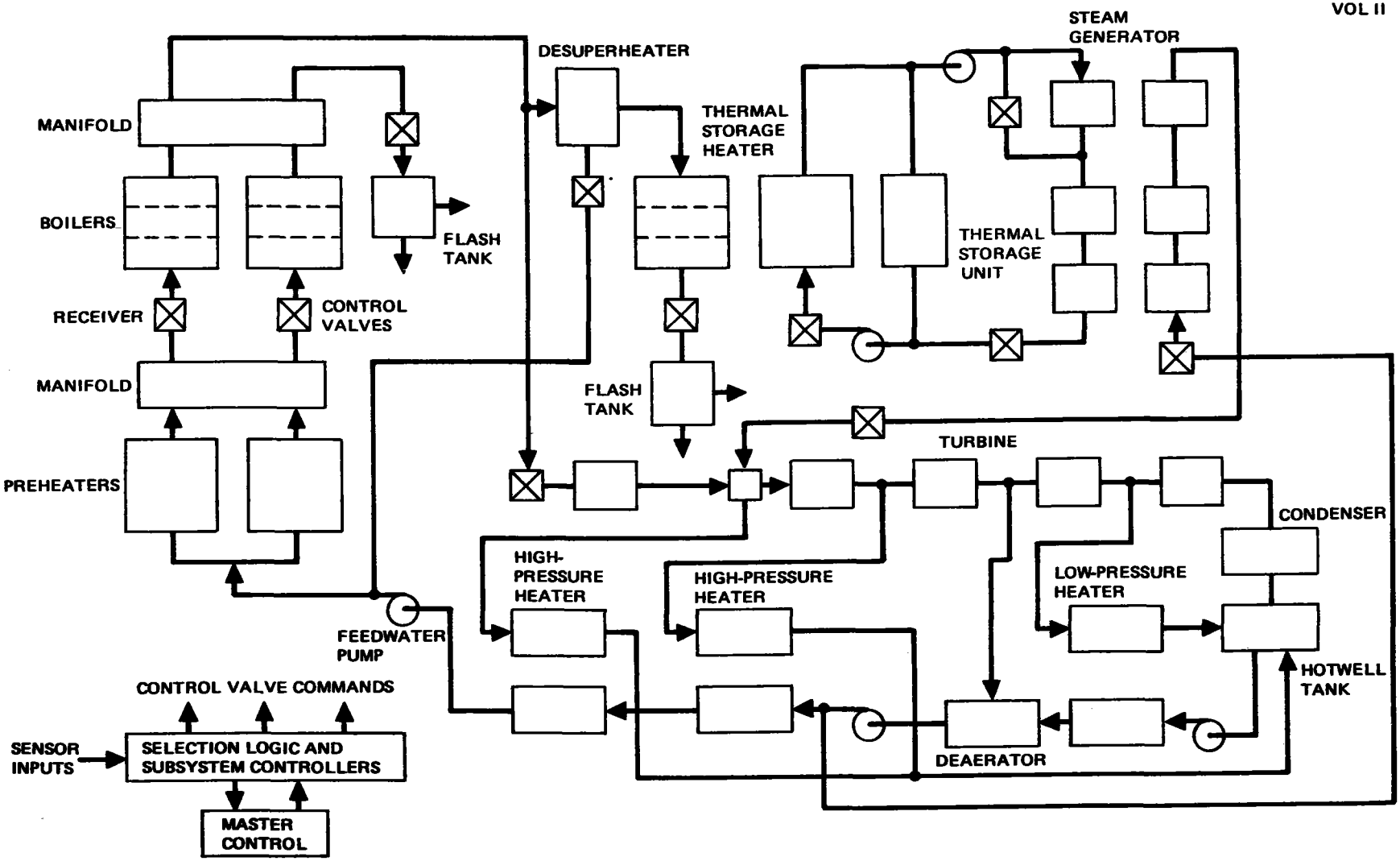

Figure 4-39. Solar System Simulation Block Diagram

RECEIVER SIMULATION MODEL

KEY FEATURES

- EQUATIONS OF STATE
  - CONSERVATION OF ENERGY ON WALL AND FLUID
  - MASS BALANCE FOR NONSTEADY FLUID FLOW
  - THERMODYNAMIC MIXING OF GASES AND IDEAL GAS LAW
  - ORIFICE FLOW EQUATIONS
  - RADIATION AND CONVECTION HEAT TRANSFER
- LUMPED PARAMETER SYSTEM

  3 SECTION RECEIVER
  - SUPERHEATED STEAM
  - SATURATED STEAM
  - SUBCOOLED LIQUID

  } STEAM TABLES
- STATE VARIABLES
  - WALL TEMPERATURES (T_1, T_2, T_3, T_5, T_6, T_7, T_{PH})
  - FLUID TEMPERATURES (θ_1, θ_2, θ_3, θ_5, θ_6, θ_7, θ_{PH})
  - FLUID MASSES
- FLUID STATES
  - SYSTEM PRESSURES (P_0, P_1, P_2, P_3, P_5, P_6, P_7)
  - SYSTEM FLOWRATES ($\dot{\omega}_p$, $\dot{\omega}_1$, $\dot{\omega}_2$, $\dot{\omega}_3$, $\dot{\omega}_5$ $\dot{\omega}_6$ $\dot{\omega}_7$)
- INPUTS
  - SOLAR INSOLATION Q
  - INLET WATER FLOW AND PRESSURE

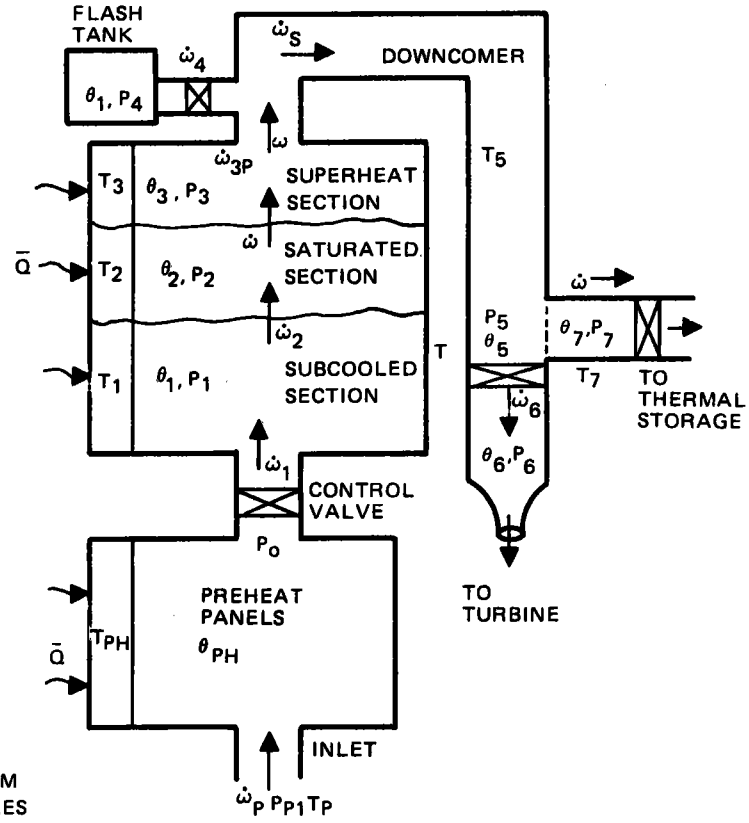

SOLAR RECEIVER MODEL

Figure 4-40. Receiver Simulation Model

The boiler panels, which convert the subcooled liquid into superheated steam, are lumped into the three distinct fluid phases of subcooled liquid, saturated steam, and superheated steam. The dynamics of the receiver subsystem are described by a set of 16 nonlinear differential equations and additional algebraic relationships which describe the dynamic response characteristics of the receiver in the frequency range from zero to approximately 2 Hz. In general, the state variables in each section are described by the wall temperatures, fluid temperatures, and fluid masses with additional algebraic equations defining the pressure and flow rates within each section. As a typical example, the equations for the preheater and the superheat section of the receiver are described in detail in Figure 4-41.

The feedback control systems which control the receiver consist of temperature and pressure-controlled valves on the inlet water flow, in addition to the outlet superheated steam flow into the turbine. A typical control system simulation model, shown in Figure 4-42, includes dynamic models of the sensor, valve actuation system dynamics, and control system compensation. The control system mechanized within the simulation is flexible and allows for rapid evaluation of such effects as blended temperature/pressure control, alternative control system compensations, and either analog or digital mechanization of the controller. The primary simulation driver is the solar heat flux incident on the receiver panels. The net incident heat flux can be either described mathematically (i.e., sinusoid, ramp, etc) or is input as a tabular function of time (refer to Figure 4-38).

4.7.2.2 Turbine Generator Subsystem Simulation Model

The turbine generator simulation model of a multistage combination impulse-reaction stage steam turbine and a two-pole 3,600-rpm electrical power generator. The simulation model transforms the available energy from a form of steam through an impulse-momentum exchange in the turbine blades into mechanical energy and then into electrical energy in the generator. The model consists primarily of a dynamic torque balance on the turbine generator shaft between the applied torque (impulse-momentum exchange in the turbine blades), the electrical load torque due to the generator, various damping and loss torques due to mechanical, electrical, friction, and flow losses, and

ENERGY BALANCE

WALL

$M_{\omega 3} C_{\omega 3} \dot{T}_3 = \bar{Q} A_{\omega 3} - \bar{h}_3 A_3 (T_3 - \theta_{3_{av}})$ (BTU/HR)

ENTHALPY

$h_3 = f(\theta_3, P_3)$ (STEAM TABLES)

FLUID

$m_{F3} C_{p3} \dot{\theta}_3 = \bar{h}_3 A_{\omega 3} (T_3 - \theta_{3_{av}}) + \dot{\omega}_3 h_2 - \dot{\omega}_4 h_3$ (BTU/HR)

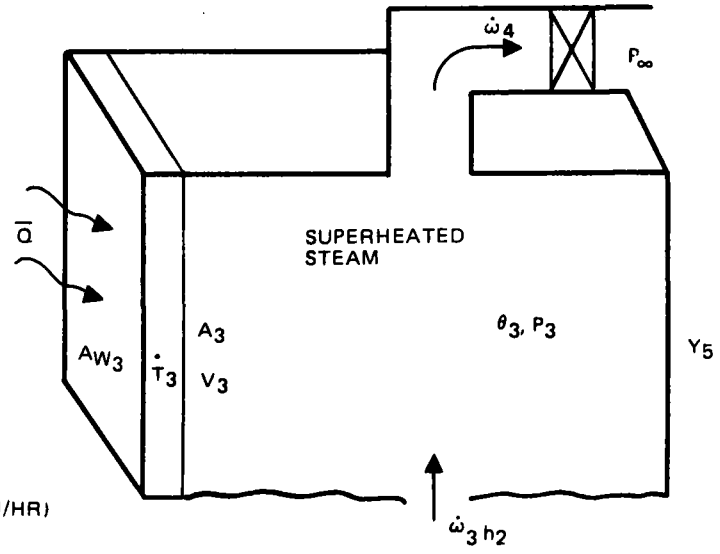

MASS BALANCE

$$\dot{M}_{F_3} = \frac{\dot{\omega}_3 - \dot{\omega}_4}{3600} \text{ LB/SEC}$$

PRESSURE

$$P_3 = \frac{M_{F3} R \theta_{3r}}{V_3}$$

FLOW

$$\dot{\omega}_4 = KA \frac{P}{\sqrt{\theta_R}} f(P_\infty / P)$$

GENERAL ISENTROPIC GAS FLOW THROUGH A NOZZLE

SYMBOLS	
M	MASS
C	SPECIFIC HEAT
θ	FLUID TEMP
T	WALL TEMP
P	PRESSURE
h	ENTHALPY
$\bar{h}$	HEAT TRANSFER COEFFICIENT
A	AREA
$\bar{Q}$	SOLAR INSOLATION

WALL

$M_{\omega PH} C_\omega \dot{T}_{PH} = \bar{Q} A_{PH} - \bar{h} A (T_{PH} - \theta_{PH})$ (BTU/HR)

FLUID

$M_{f_{PH}} C_f \theta_{PH} = \bar{H} A (T_{PH} - \theta_{PH}) + \dot{\omega}_1 C_p (\theta_p - \theta_{pH})$

(BTU/HR)

STEADY FLOW $\dot{\omega}_p = \dot{\omega}_1$

$\dot{\omega}_1 = \sqrt{(P_1 - P_p)/R}$ NO./HR, R – FLOW RESISTANCE

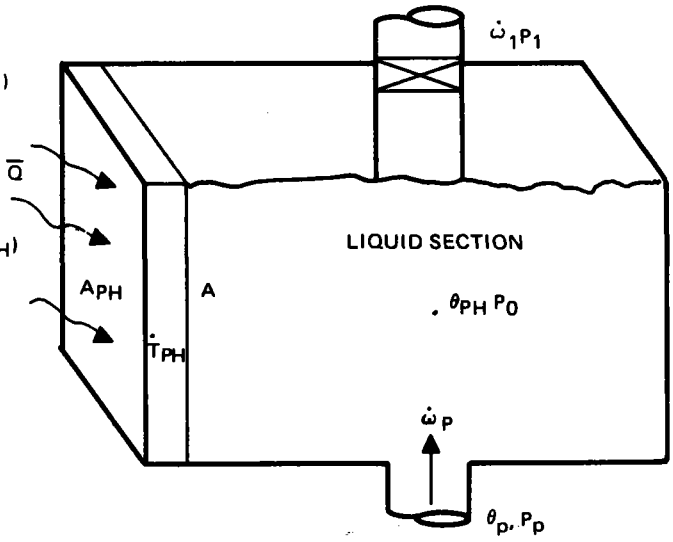

Figure 4-41. Typical Receiver Model Equations

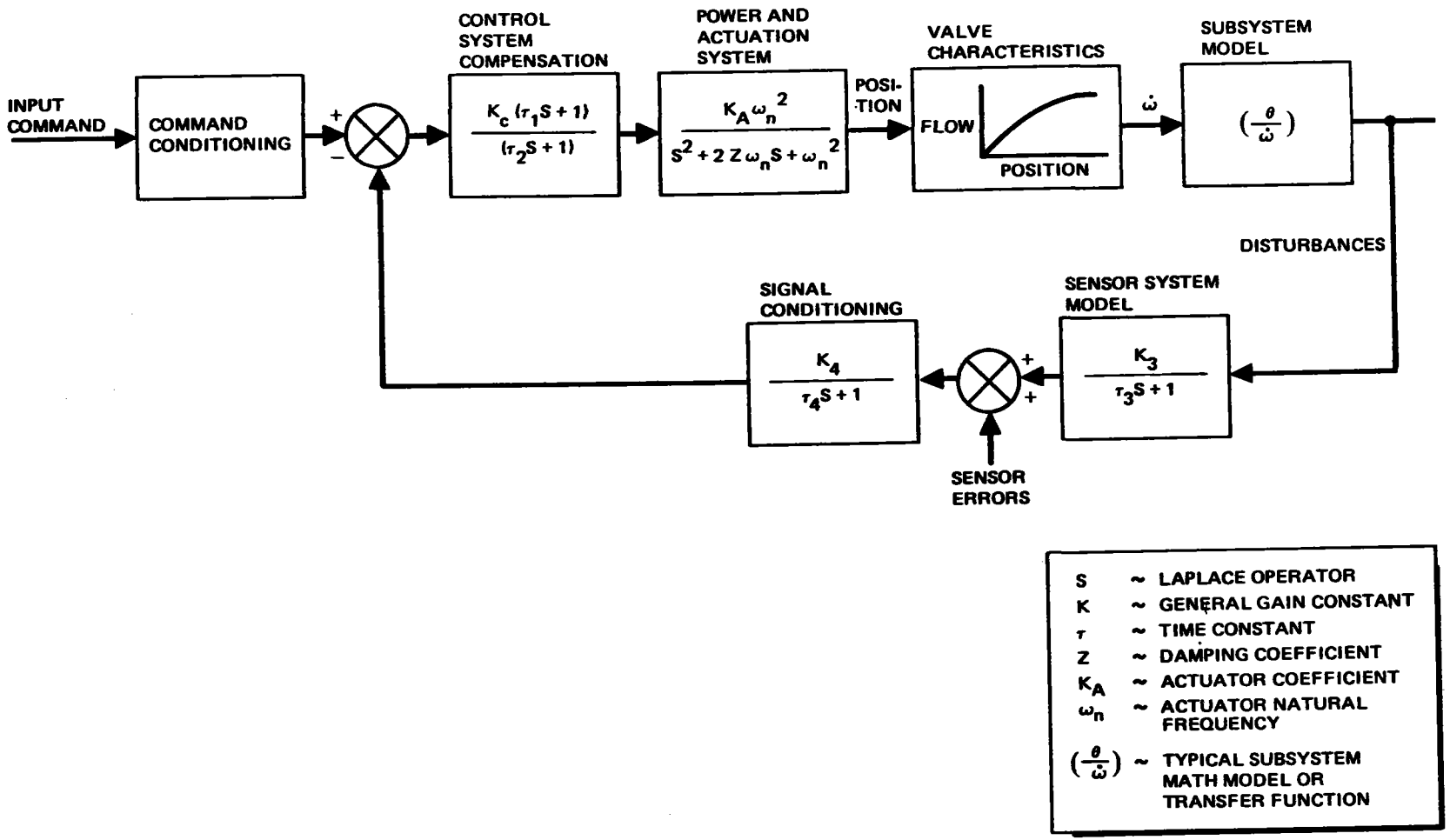

Figure 4-42. Typical Model of Subsystem Control System

the associated time constants with the turbine due to flow of gases within a constrained volume.

A simplified functional schematic of the turbine-generator simulation model and a functional block diagram are shown in Figure 4-43. The most complex modeling in the subsystem is within the description of the applied torque on the turbine blades due to the impulse-momentum exchange between the flowing steam and impulse/reaction turbine blading. In general, the torque is a function of the type of stage (impulse or reaction or combination of both), compounded staging, turbine blade geometry and blade efficiencies, and the relative velocity between the fluid and the turbine blades. These relationships are generally complex for a simple-impulse stage and even more complex for a reaction stage. The general mathematical relationship for the torque is similar for all stages and is described in Figure 4-44 for a simple compounded impulse stage. For a reaction type of stage, the velocity-enthalpy exchange is more distributed throughout the stage, but the general form of the model still applies as a good approximation for the torque contributed by each set of moving blades. Frictional torques and damping torques on the turbine shaft are proportional either to shaft speed, relative speed, or steam flow rate as shown in Figure 4-43.

The load torque on the turbine shaft when a synchronous load is applied is proportional to the load output current and the sine of the torque power angle. The input to the turbine is the inlet steam flow at specific enthalpy conditions and the output is the current and voltage generated by the electrical generator. The steam is assumed to undergo a nonideal, nearly isentropic expansion through each turbine state, finally exhausting into a constant-pressure condenser controlled to 2.5 in. Hg. A typical turbine steam expansion line is shown in Figure 4-45 for the various allowable operating conditions for both throttle steam and admission steam conditions. These expansion conditions and the blade geometries, efficiencies, and physical constants and parameters used in both the turbine and generator models are representative of a typical 12.5-MW turbine-generator and will be continually re-evaluated and updated as more data are made available on the actual turbine-generator unit.

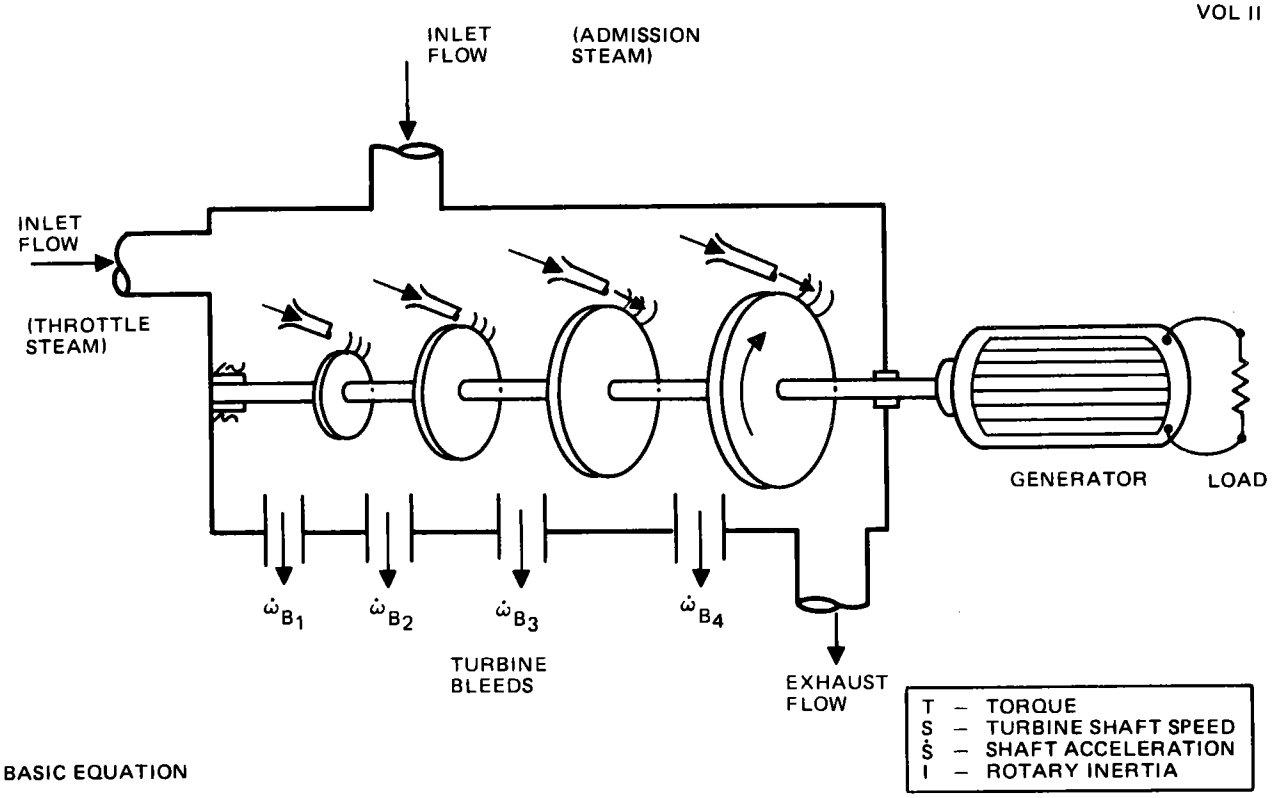

BASIC EQUATION

$$\Sigma_{TORQUE} = I\dot{S}$$

$$\Sigma'_{TORQUE} = T_{MOMENTUM\ EXCHANGE} - T_{ELECTRICAL\ AND\ MECHANICAL\ DAMPING} - T_{FLOW\ LOSSES} - T_{ELECTRICAL\ LOAD}$$

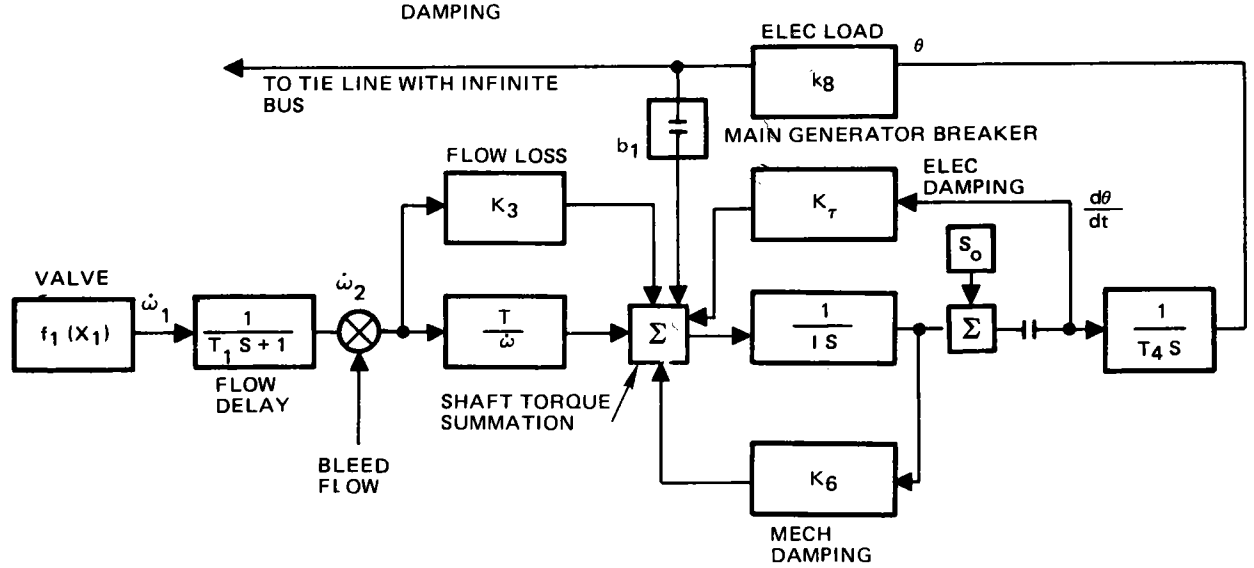

TURBINE-GENERATOR BLOCK DIAGRAM

Figure 4-43. Turbine-Generator Simulation Model

DEFINITION OF SYMBOLS

$\dot{\omega}_1$	– INLET STEAM FLOWRATE
V_1	– INLET FLOW VELOCITY
V_2	– OUTLET FLOW VELOCITY
V_b	– LINEAR VELOCITY OF TURBINE BLADE
θ_1	– INLET ANGLE OF STEAM
V_r	– VELOCITY RELATIVE TO BLADE
ϕ,γ	– ANGLES TO INLET AND OUTLET RELATIVE VELOCITIES
r_1	– BLADE RADIUS
η	– BLADE EFFICIENCY

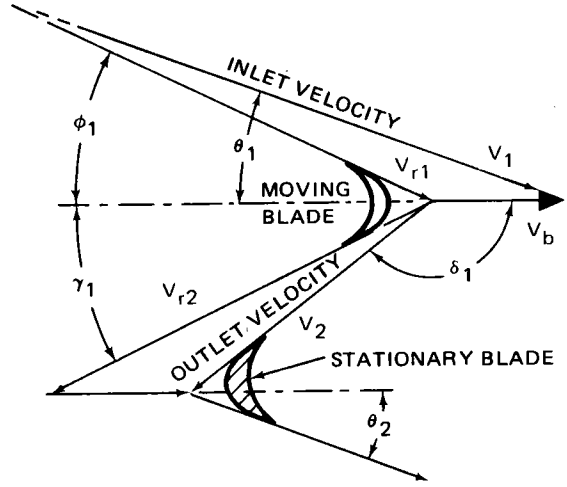

TYPICAL VELOCITY DIAGRAM ON TURBINE BLADES

$$\text{TORQUE} = K_1\dot{\omega}_1[K_2V_1 - V_b]$$

(SINGLE STAGE)

$$\text{WHERE } K_1 = \frac{r_1}{g}\left(1 + n_f\,\frac{\cos\gamma_1}{\cos\phi_1}\right)$$

$$K_2 = \cos\theta_1$$

GENERAL TORQUE EQUATION (MULTIPLE STAGES)

$$T = \sum_{i=1}^{\eta \text{ STAGES}} K_{1_i}\omega_i\,[K_{2_i}V_i - V_{b_i}] \text{ FOR } i^{TH} \text{ STAGE}$$

NOTE: FOR COMPOUNDED AND REACTION STAGES, THE INLET VELOCITY IS A FUNCTION OF OUTLET VELOCITY V_2 (PREVIOUS STAGE) AND PRESSURE DROP THROUGH STATIONARY BLADES.

Figure 4-44. Simplified Turbine Torque Model

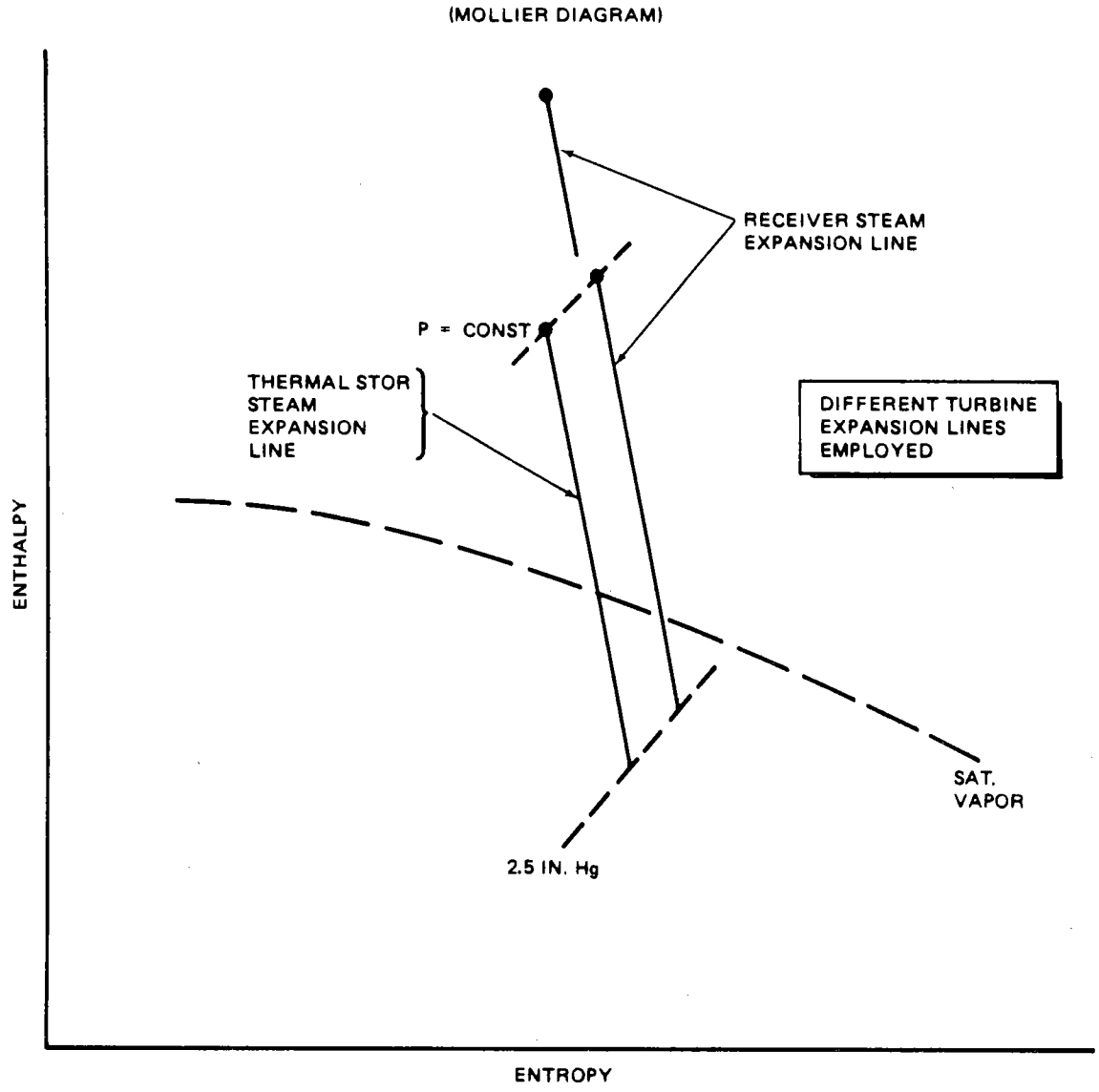

Figure 4-45. Steam Turbine Expansion Lines

4.7.2.3 Thermal Storage Subsystem Simulation Model

The thermal storage simulation model consists of a desuperheater model, a thermal storage heater, heater pump, thermal storage unit and charging phase control systems for the charging cycle; and a steam generator, steam generator pumps, discharge control systems, and thermal storage unit for the discharge-steam generation cycle. The simulation of the thermal storage unit is formulated to describe the system dynamic characteristics throughout the full operating range in both the charging and extraction modes of operation. The mathematical model which describes the dynamic characteristics of the system are based upon energy balance on the heat exchangers and the working fluids. Mathematical models of the dynamics of the physical hardware (pumps, valves, sensors, etc) are included, in addition to system losses due to friction and heat losses. A functional schematic of the thermal storage unit simulation is presented in Figure 4-46 in addition to some of the key features of the simulation.

The actual system consists of two sets of pumps, thermal storage heaters, and steam generators connected in parallel; for simplicity, only one set is implemented in the simulation with little impact on overall simulation fidelity. The equations which describe the models for the thermal storage heater and steam generator are analagous to those equations for the receiver. A set of representative equations, in addition to a function schematic for the thermal storage heater and charging loop feedback control systems, is shown in Figure 4-47.

4.7.2.4 Balance of Plant Subsystem Simulation

The simulation of the balance of the plant describes the steady-state operation of the condenser, feedwater heaters, feedwater pumps, deaerator, and the appropriate flash tanks within the system. At present, it is felt that the dynamics related to these elements play a less significant role in the overall system dynamics than the elements just discussed, thus justifying the current steady-state assumptions. As the overall simulation matures, selective expansions of these steady-state models will be considered to enhance the accuracy and validity of the model. A functional schematic of the current balance of plant simulation is shown in Figure 4-48.

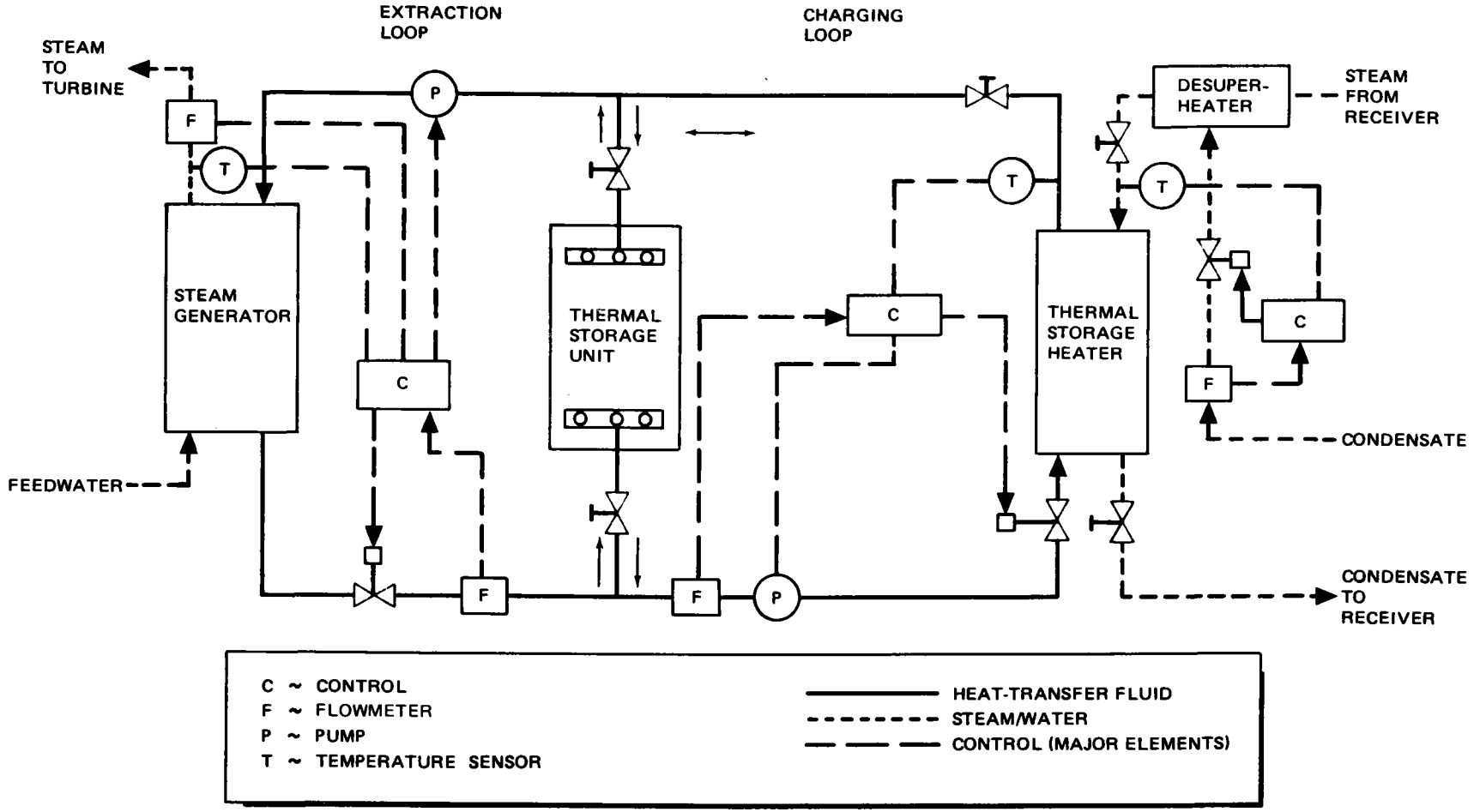

Figure 4-46. Thermal Storage Simulation Model Functional Block Diagram

ENERGY EQUATIONS

STEAM SIDE

$\dot{U}_A = \dot{\omega}_A(H_{S2}-H_A) - \bar{h}_A A_A [T_{SA}-T_{W1}]$

$\dot{U}_B = \dot{\omega}_A(H_A-H_B) - \bar{h}_A A_B [T_{SB} - T_{W3}]$

$\dot{U}_C = \dot{\omega}_A(H_B-H_C) - \bar{h}_A A_C [T_{SC}-T_{W5}]$

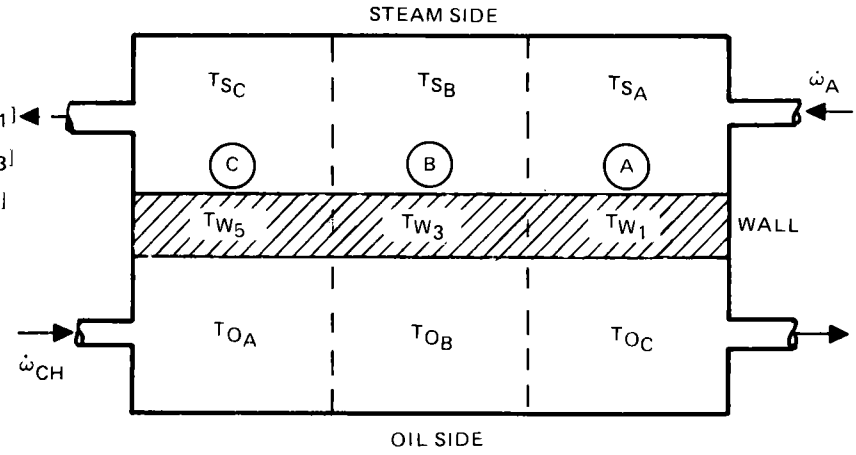

OIL SIDE

$\dot{T}_{OA} = 1/C_{P_0} W_A \; [\dot{W}_{CH} C_{P0}(T_{0B} - T_{0A}) - \bar{h}_c A_A (T_{0A} - T_{W5})]$

$\dot{T}_{0B} = 1/C_{P_0} W_B \; [\dot{W}_{CH} C_{P_0} (T_{0A} - T_{0B}) - \bar{h}_c A_B (T_{0B} - T_{W5})]$

$\dot{T}_{0C} = 1/C_{P_0} W_c \; [\dot{W}_{CH}\, C_{PO} (T_{0B} - T_{0C}) - \bar{h}_C A_C (T_{0C} - T_{W1})]$

WALL

$\dot{T}_{W1} = 1/C_{P_M} W_{W1} \; [\bar{h}_A A_A (T_{SA} - T_{W1}) + h_c A_A (T_{0C} - T_{W1})]$

$\dot{T}_{W3} = 1/C_{P_M} W_{W3} \; [\bar{h} A A_B (T_{SB} - T_{W3}) + \bar{h}c\, A_B (T_{0B} - T_{W3})]$

$\dot{T}_{W5} = 1/C_{P_M} W_{W6} \; [\bar{h} A A_C (T_{SC} - T_{W3}) + h_C\, A_C (T_{0C} - T_{W5})]$

THERMAL HEATER

$\bar{h}_A = \bar{h}_{A_0} (\dot{\omega}_A)^{0.8}$

$\bar{h}_c = \bar{h}_{C_0} (\dot{\omega}_{CH})^{0.8}$

(TYPICAL SUBSYSTEM EQUATIONS)

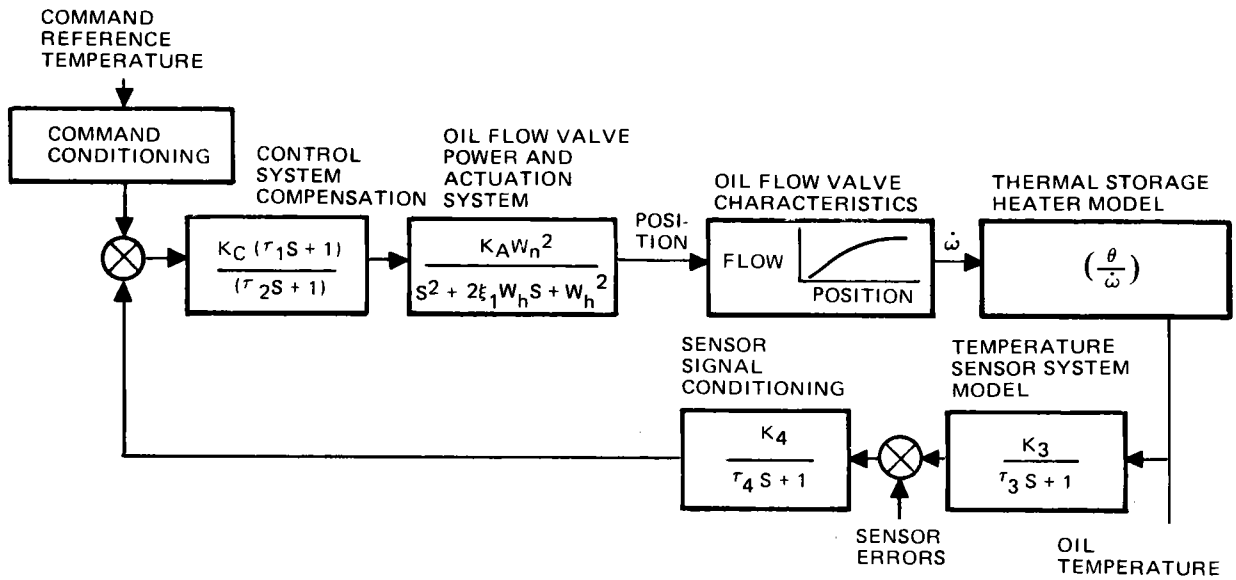

TYPICAL MODEL OF THERMAL STORAGE HEATER CONTROL SYSTEM (CHARGING LOOP)

Figure 4-47. Thermal Storage Subsystem Simulation Models

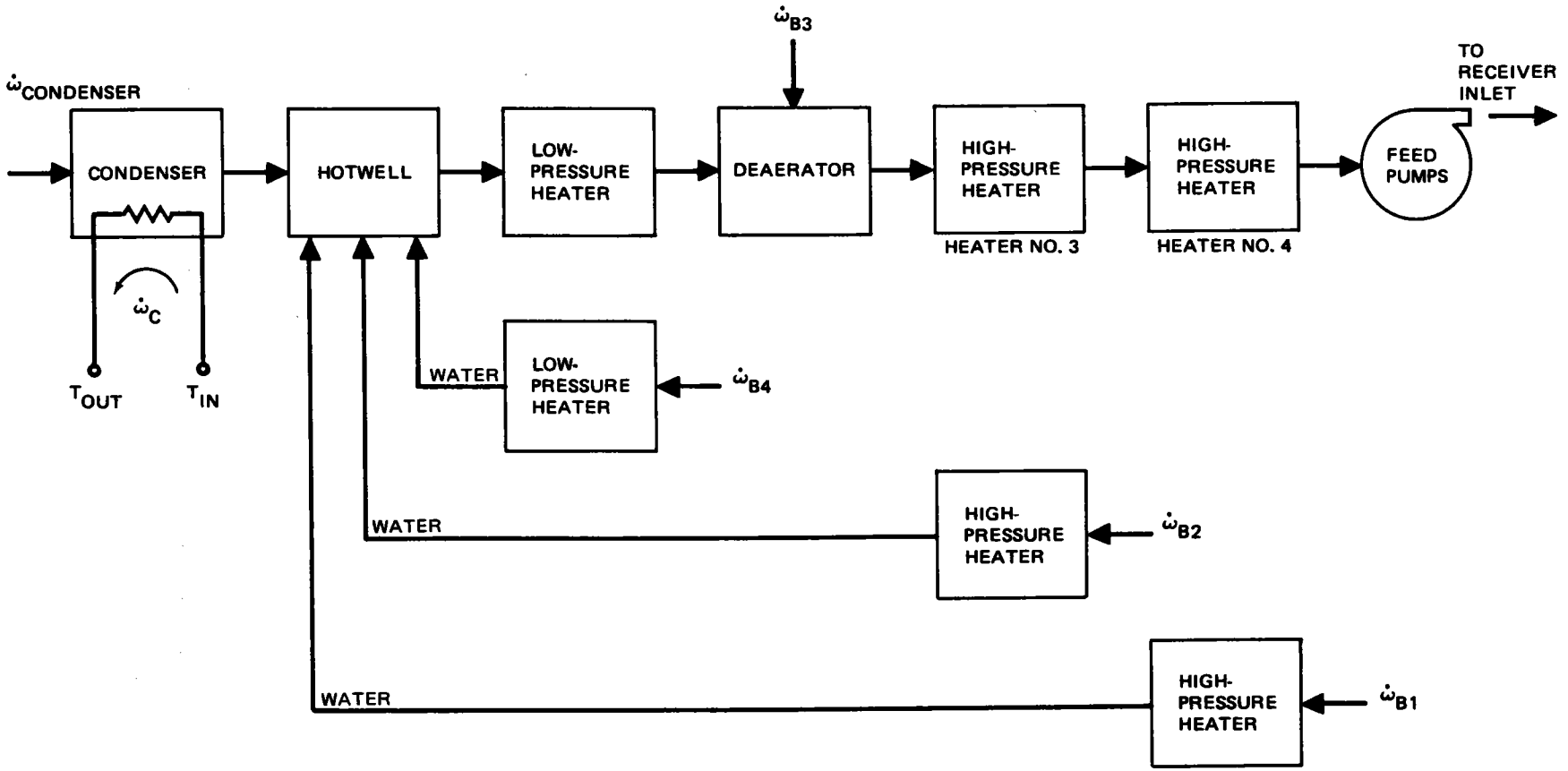

Figure 4-48. Balance of Plant Simulation Functional Block Diagram

4.7.2.5 Simulation Model Verification

To verify the integrity of the overall POPS simulation, the fidelity of each of the subsystem models is established by comparing the simulation performance characteristics to either reference models of higher fidelity or to available subsystem test results. The validity of the subsystem models is also established by comparison of simulation results to both analytical results, as well as a comparison to steady-state operating conditions. Comparison of simulation results to vendor-supplied data on hardware components such as sensors, valves, pumps, etc, substantiates the validity of component elements within the simulation.

As a typical example, the method of simulation model verification used to substantiate the receiver subsystem simulation was to initially verify that the equations for the model were exact and complete. The simulation is then compared to previously computed steady operating conditions. The receiver simulation was then compared to predicted results, based on a small signal linear model of the receiver. The transient performance was then verified for large signal inputs by a comparison to a reference simulation of higher fidelity (Thermodynamics Program G-189 - 240 node model).

When test data are available, for example from SRE tests on the receiver, the simulation is modified to represent the test conditions and a comparison between test results and simulation results is made and the fidelity of the simulation is established. If discrepancy exists, then the model equations are re-evaluated and system constants and parameters re-examined and updated until the simulation and test results agree with the accuracy of the test conditions and available data.

4.7.2.6 Simulation Input-Output and Implementation

The POPS simulation is designed to be basically a design and analysis tool; therefore, the input and output are geared for analysis and subsystem design considerations. The inputs are representative of typical system inputs of system pressure, solar flux history, commanded set point operating conditions, and the selected operation mode of the power plant. The simulation outputs are typical of power plant monitored variables such as receiver

temperature and pressure, flowrates, water and steam temperatures, turbine speed and inlet conditions, turbine steam pressure, and generator load. The simulation is designed such that system parameters such as valve position and flow characteristics, ambient conditions, flow rates, heat-transfer coefficients, and subsystem time constants can be easily varied and the impact on system performance rapidly evaluated. A tabulation of some of the key input-output and design parameters within the simulation is shown in Table 4-10.

The goal of the simulation is that it be an efficient, effective, and accurate representation of the dynamics of the power plant system. As a design tool, it must be efficient and accurate to supply the designer with the necessary data to design the plant controls and master control subsystem. Because of the large number of simulation conditions and modes to be evaluated, the simulation must be efficient to operate and must also have rapid access and turnaround time for evaluation of the effects of master control subsystem designs and their impact on system performance. For ease in checkout of the master control subsystem and verification of the real hardware prior to system integration, it is desirable to be able to integrate real hardware with a simulated power plant and plant interfaces to completely check out the master control subsystem prior to installation. For these reasons, the POPS simulation is implemented on a hybrid (combined analog-digital) computer using the MDAC on line system facility (OLSF). By implementing the POPS simulation on the hybrid computer, it is possible to operate the simulation in a mode that executes the simulation faster than real time. In general, the differential equations are solved on the analog portion of the hybrid facility and complex algebraic functions and tabular functions such as steam tables, master control algorithms, and mode control and logic are performed in the digital portion of the hybrid computer. The hybrid facility also affords the capability of real-time and hands-on operation of the simulation with high-quality strip charts, X-Y plotters, and digital data processing available for recording simulation results. The computing capability of the hybrid computer facility is presented in Figure 4-49, with a physical picture of the hybrid computer shown in Figure 4-50.

As an alternate tool to provide a backup capability to the POPS hybrid simulation, as well as to provide an alternate check on the hybrid simulation

Table 4-10 (Page 1 of 2)

KEY SIMULATION PARAMETERS

Parameter	Symbol	Description
Solar Insolation	$\bar{Q}$	Input solar insolation incident on the receiver.
Inlet Water Flow	$\dot{\omega}_1$	Controlled inlet flow to receiver used to regulate outlet steam temperature.
Inlet Valve Area	A_V	Area of inlet valve to receiver; its linearity and response impact on the receiver controller design.
Inlet Water Enthalpy	h_o	Enthalpy of inlet water into receiver; effects amount of subcooled liquid in receiver.
Superheated Steam Pressure	P_3	Sets the pressure within the receiver system; impacts both inlet and outlet receiver flow.
Superheated Steam Temperature	θ_3	Controlled system temperature of the receiver.
Turbine Inlet Flow	$\dot{\omega}_6$	Determines delivered torque and power to the electrical subsystem.
Turbine Inlet Enthalpy	h_6	A measure of the specific energy of the turbine inlet steam.
Turbine Inlet Pressure	P_6	Establishes flow rate through turbine.
Thermal Storage Inlet Flow and Enthalpy	$\dot{\omega}_7, h_7$	A measure of the energy delivered to the thermal storage system.
Oil Charging and Extraction Flow Rates	$\dot{\omega}_{CH}$ $\dot{\omega}_{EX}$	Regulated oil flow in thermal storage heaters and steam generators.
Steam Generator Output Flow	$\dot{\omega}_{SG}$	Delivered output flow from the steam generator; admission steam to turbine.

Table 4-10 (Page 2 of 2)
KEY SIMULATION PARAMETERS

Parameter	Symbol	Description
Turbine Speed and Acceleration	$S, \dot{S}$	Turbine rotation velocity and acceleration; critical to turbine design and operation.
Generator Electrical Torque Angle	$\theta-\theta_o$	Relative angle between generator shaft angle and synchronous (reference) angle.
Control System Gains and Compensation, Time Constants	K, τ	Required control system gain and compensation characteristics required for stability and good transient performance of the subsystem controllers.

results, a digital version of POPS is generated and exists. This digital simulation is written in Fortran language and is a nearly one-to-one mapping of the identical equations used in the hybrid simulation. This digital version is less efficient to operate than the hybrid simulation, but for rapid evaluation of major trade studies and for verification of the hybrid simulation, it is a valuable alternate design tool.

4.7.3 Plant Control System Simulation Results

In the following section, some typical results from the POPS simulation are discussed to describe the dynamic behavior of the coupled receiver-turbine system when subjected to typical input and operating conditions. The results presented are based on the best estimates of the hardware and physical system constants to date and a representative of typical expected system performance.

4.7.3.1 Sinusoidal Response

The receiver and the turbine responses to a 10% sinusoidal variation in solar flux are shown in Figures 4-51 through 4-54. Figures 4-51 and 4-52 represent a condition of near-normal operation, but without temperature or pressure controls on the receiver. This response is in effect an open-loop frequency

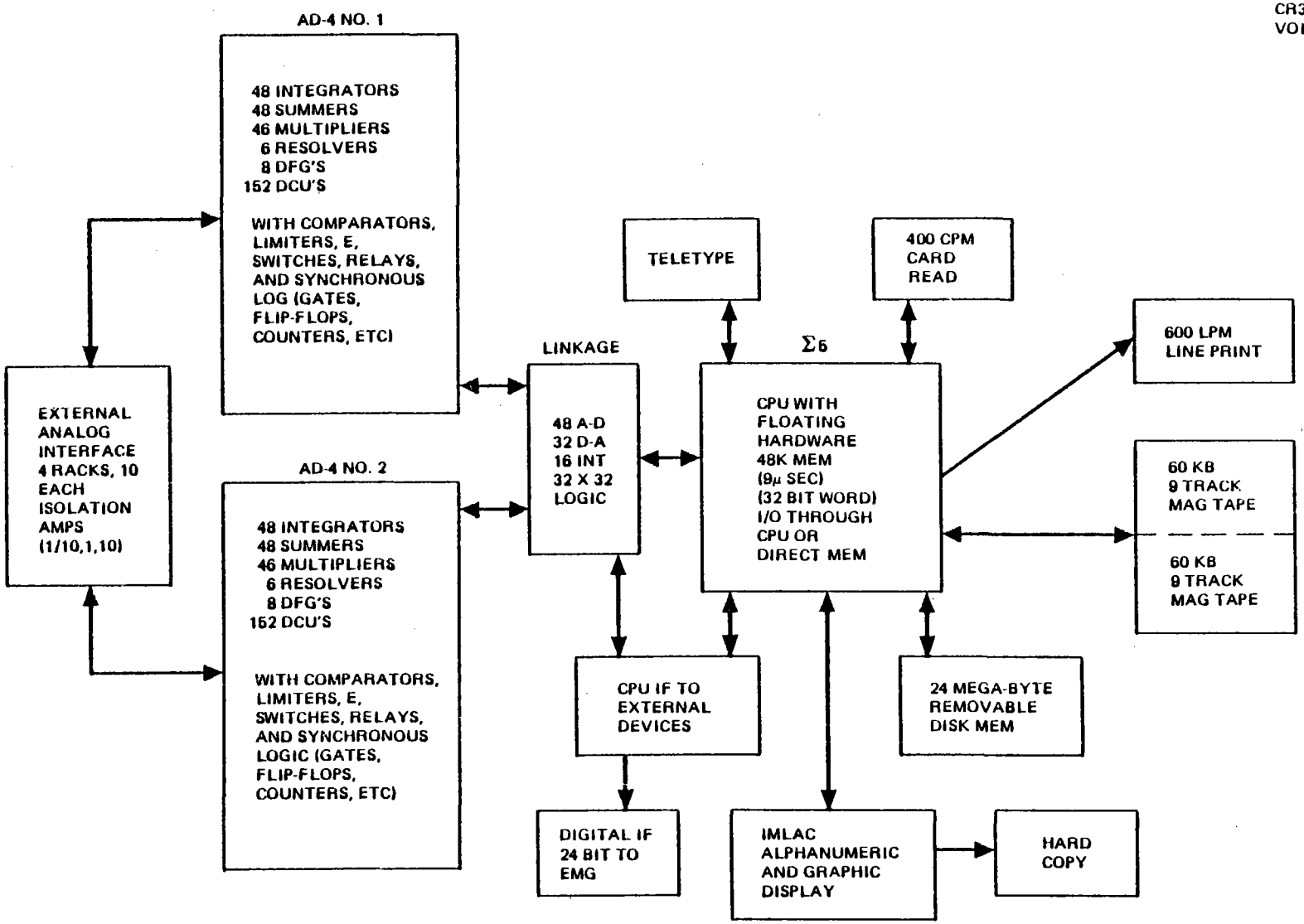

Figure 4-49. OLSF Data Processing Capability

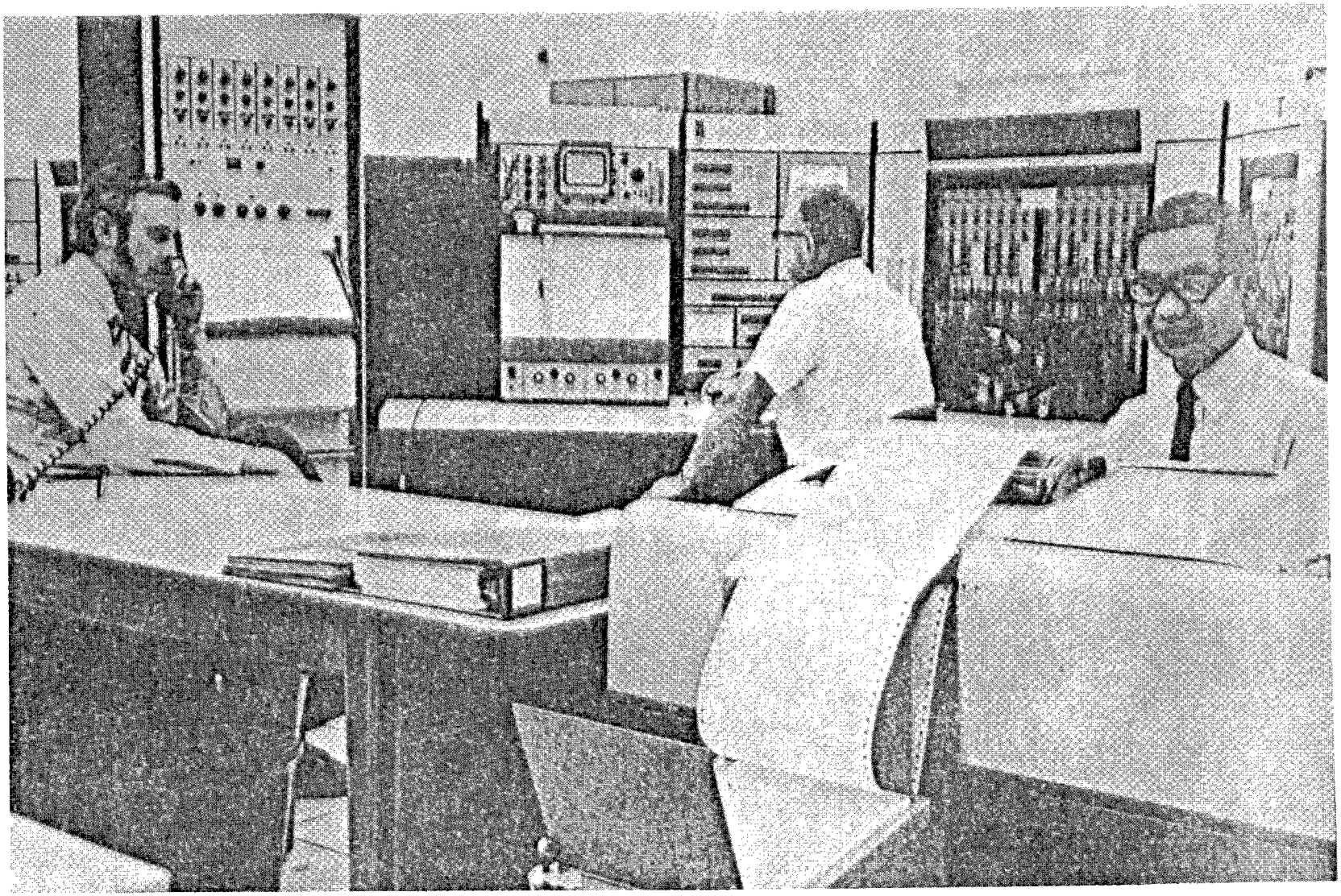

Figure-4-50. On-Line Subsystem Facility Hybrid Computer

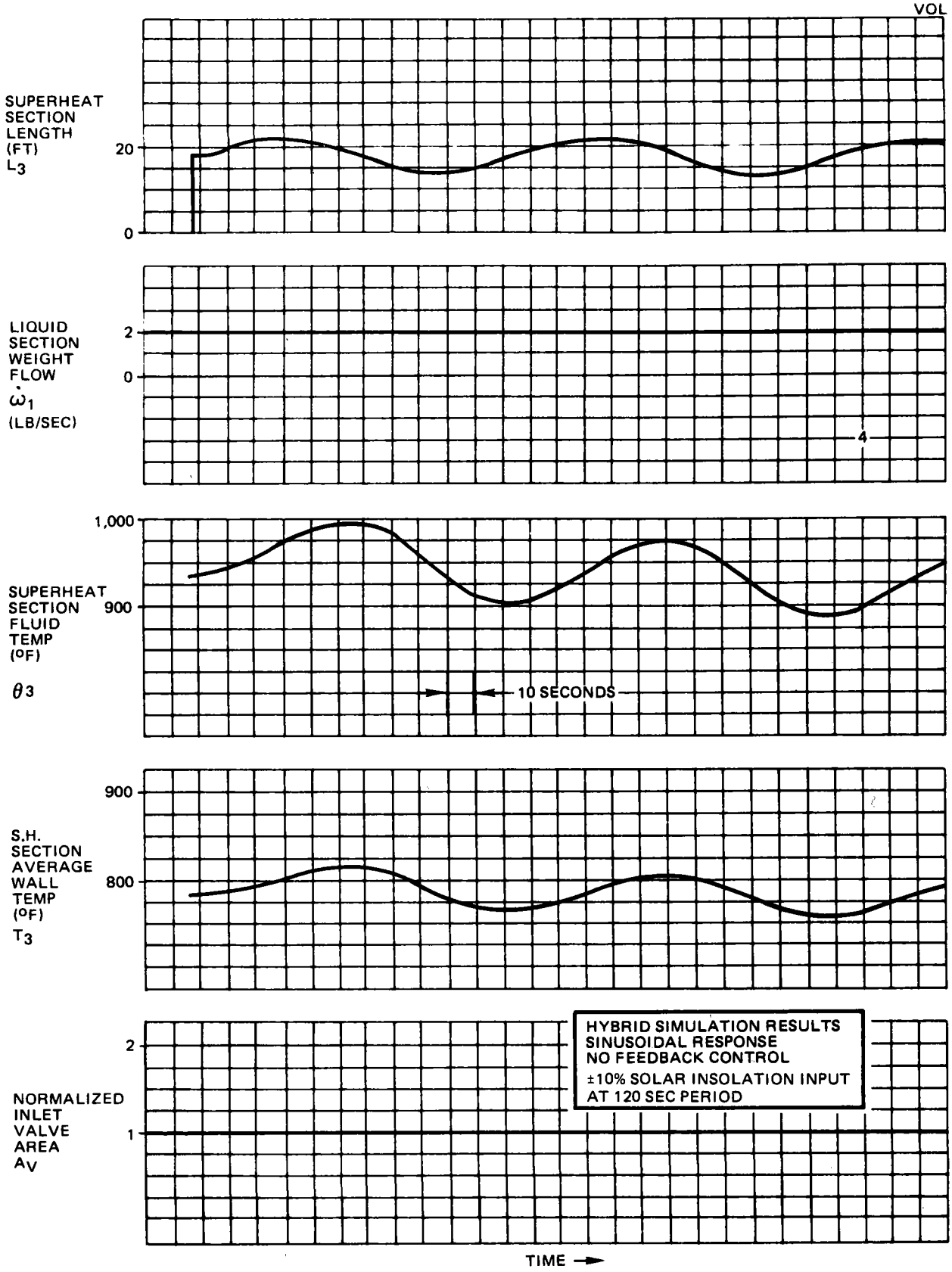

Figure 4-51. Hybrid Simulation Results – Sinusoidal Response – Without Feedback Control

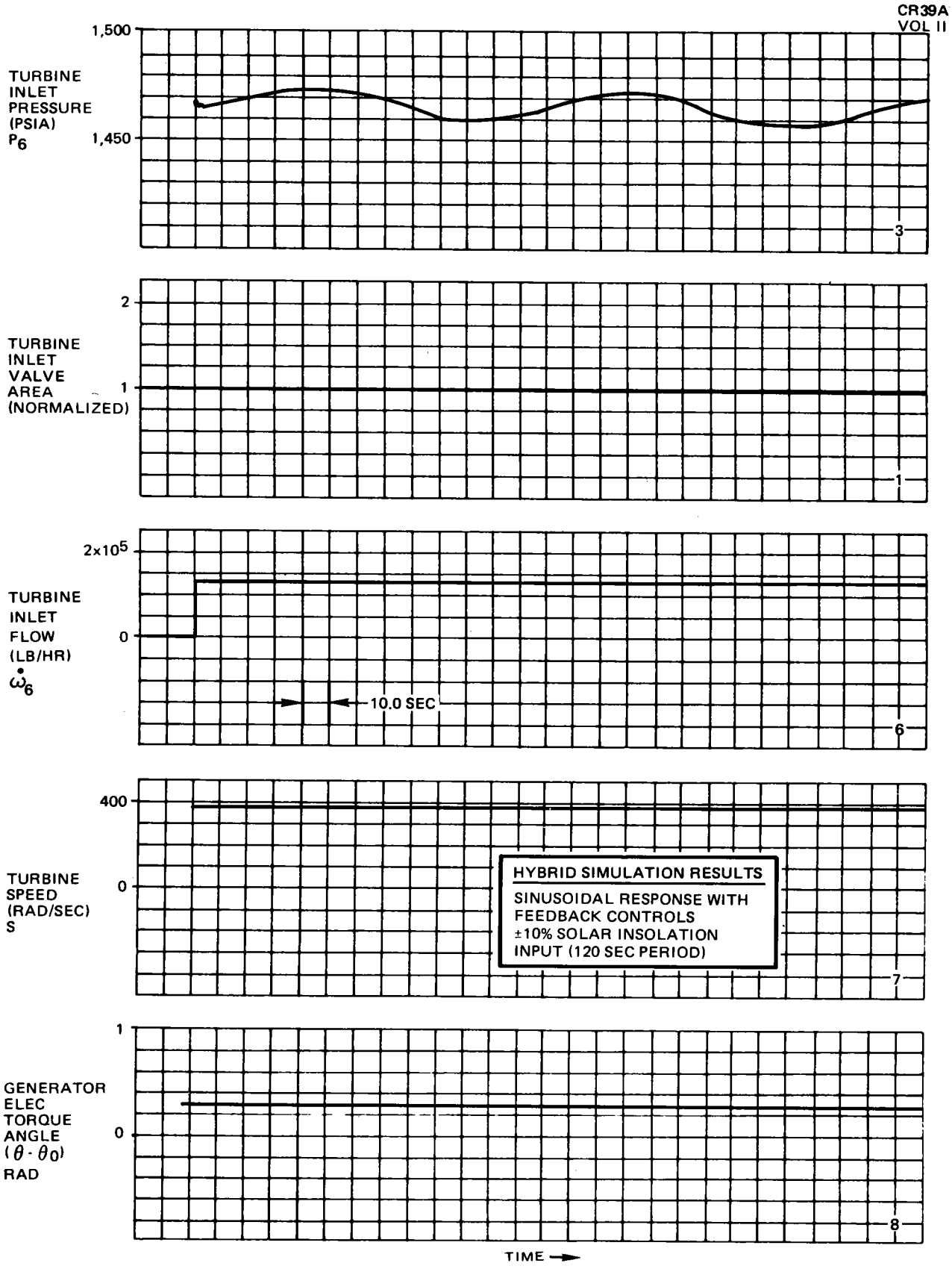

Figure 4-52. Hybrid Simulation Results – Sinusoidal Response – Without Feedback Control

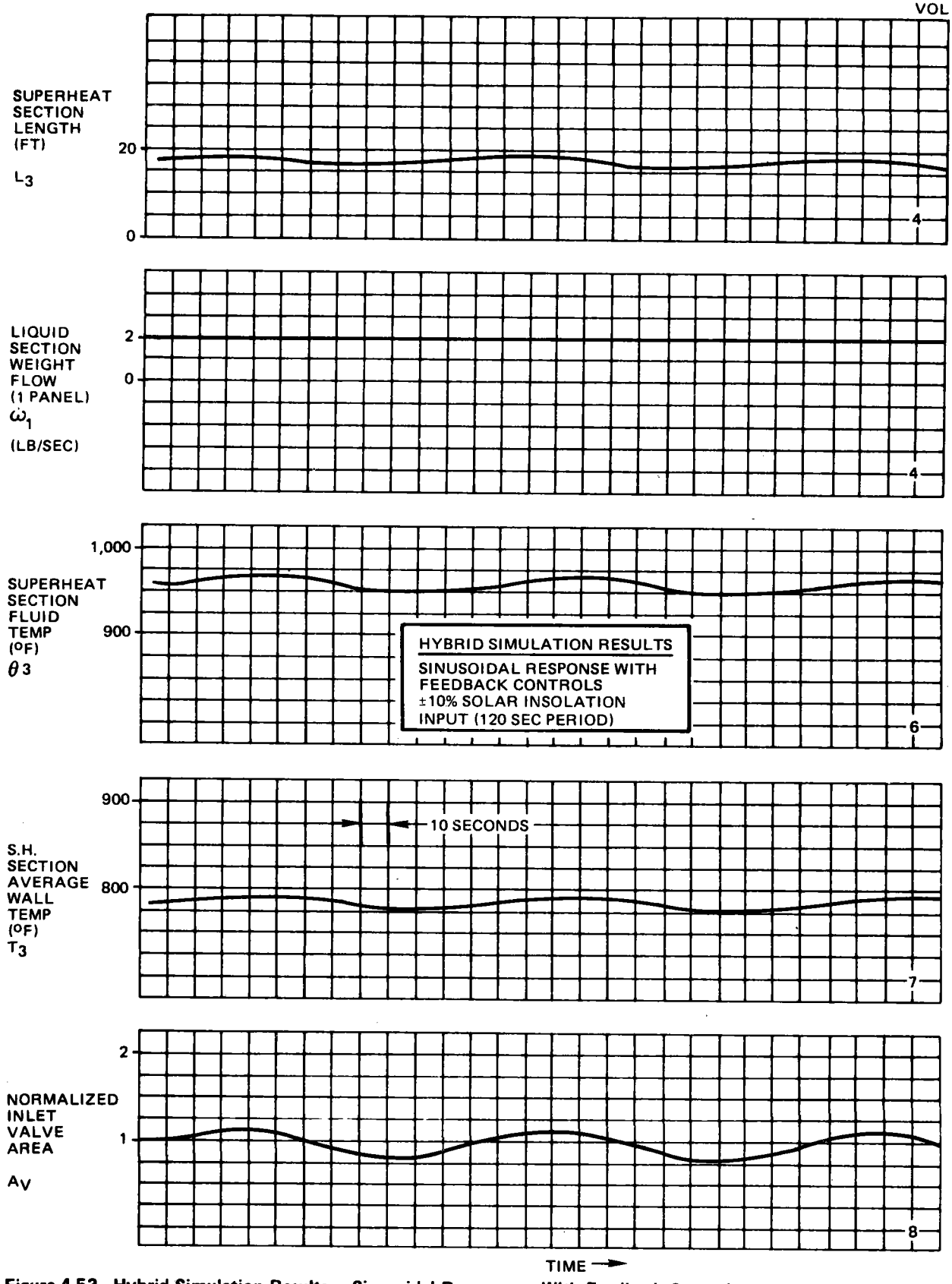

Figure 4-53. Hybrid Simulation Results – Sinusoidal Response – With Feedback Control

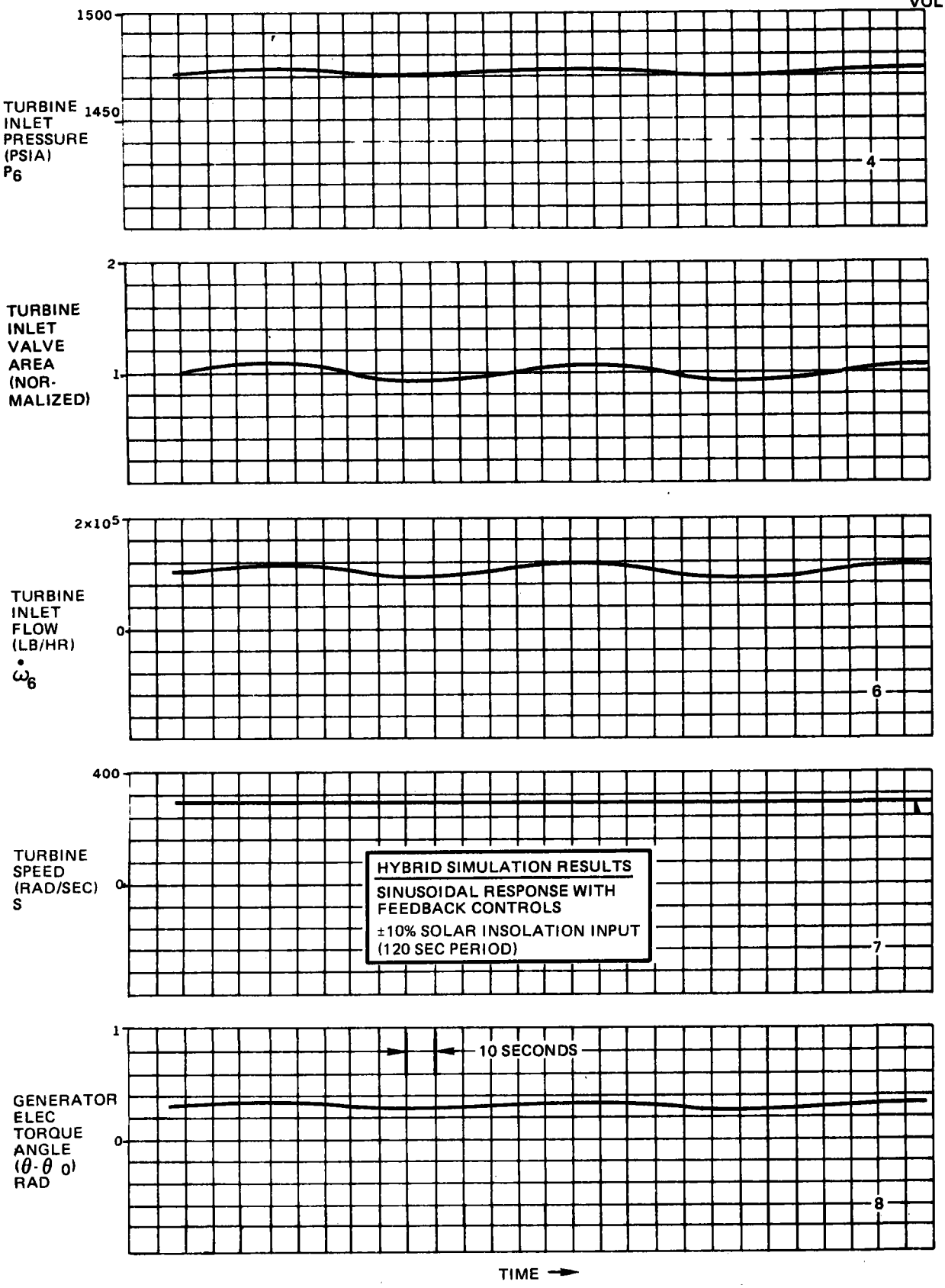

Figure 4-54. Hybrid Simulation Results – Sinusoidal Response – With Feedback Control

response of the system to sinusoidal solar flux input with a period of 60 sec. Similar transients are presented in Figures 4-53 and 4-54 with the exception that the control loops on outlet steam temperature and downcomer pressure are closed. For the open-loop system, temperature variations of + 50° and pressure excursion of + 8.0 psia, are observed for only small variation in flow. For the closed-loop system response of Figures 4-53 and 4-54, the temperature variations are reduced to + 10° and pressure excursions reduced to + 2.0 psia by maintaining a controlled flow variation in each panel of + 0.2 lb/sec.

4.7.3.2 Simulated Cloud Transient

In Figures 4-55 and 4-56, the response of the controlled receiver-turbine system is shown when subjected to a simulated variation in solar heat flux imputs due to a transient cloud condition. The equivalent solar flux transient is assumed to vary linearly from 100 to 50% in 60 sec and then return to normal 60 sec later. This set of simulation results demonstrates the capability of the receiver to meet design conditions when subjected to simulated realistic solar flux transients. These results are presented as typical of the power plant system and demonstrates the types of capability that exist within the POPS simulation.

4.7.3.3 Turbine Startup Transient

A simulated condition of a turbine startup sequence is shown in Figures 4-57 and 4-58 for a condition of varying solar heat flux inputs. The turbine speed is commanded to follow a commanded ramp-hold profile while the receiver is subjected to a variation in input solar flux. The inlet steam flow to the turbine is throttled to control the turbine speed while the excess flow out of the receiver is diverted to thermal storage. This set of results is typical of the solar power plant turbine startup mode and demonstrates the capability to simulate a turbine start sequence under realistic solar transient conditions.

4.7.3.4 Thermal Storage Heater Response

A typical response of the thermal storage heater is presented in Figure 4-59 for a system configuration without feedback controls. The system is allowed to reach steady-state conditions, and a step change in the inlet oil flow of

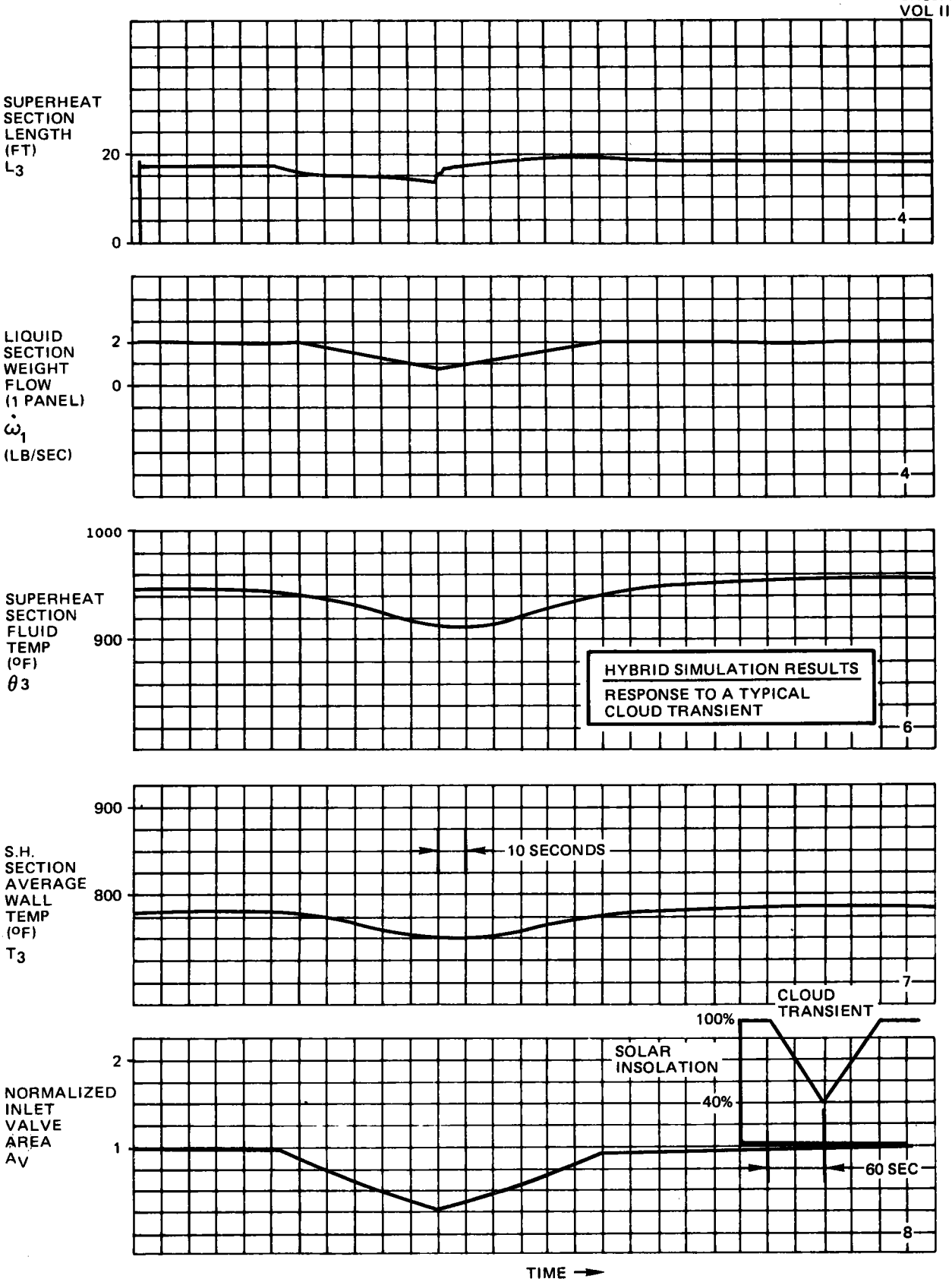

Figure 4-55. Hybrid Simulation Results – System Response to Cloud Transient

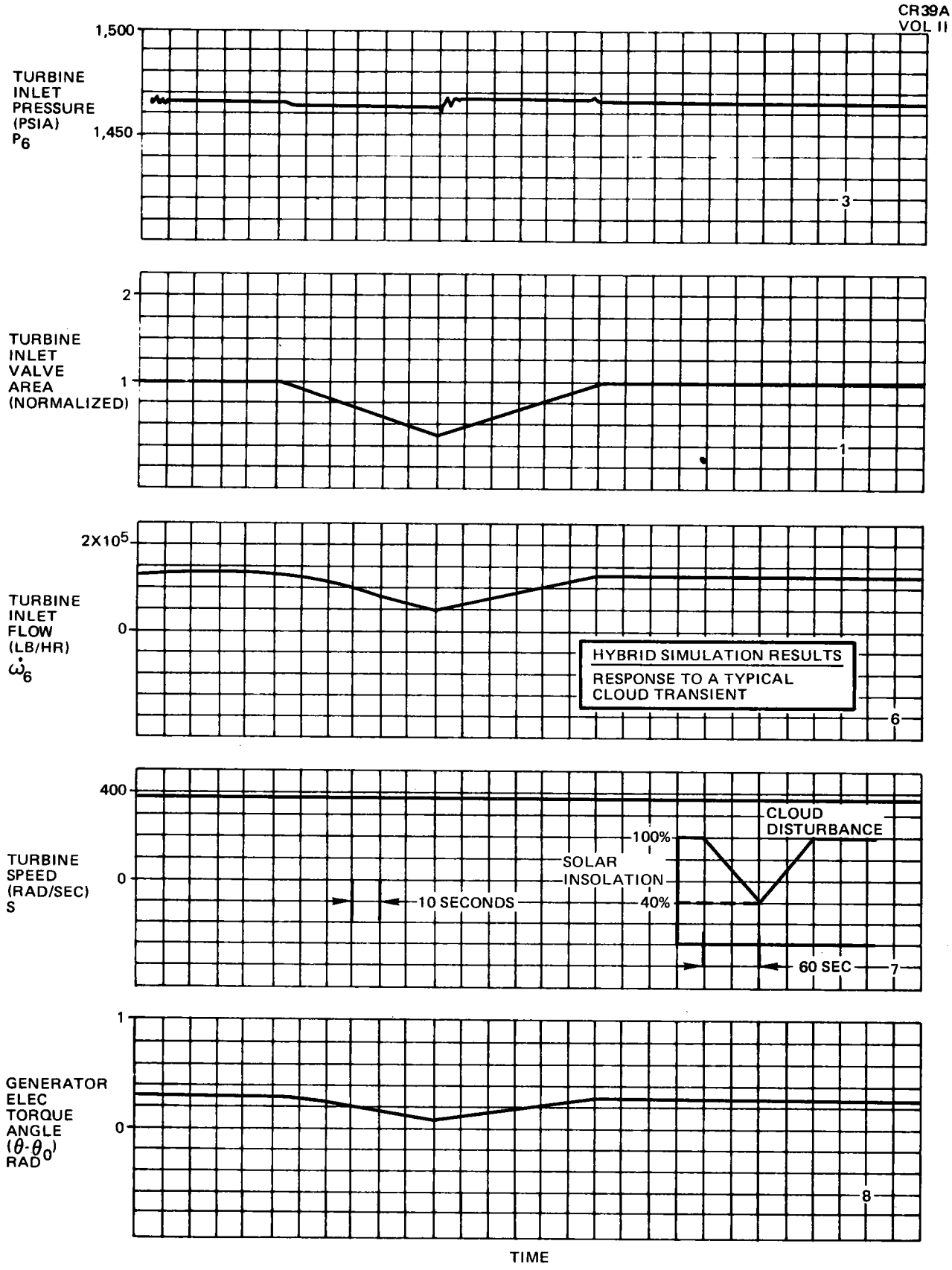

Figure 4-56. Hybrid Simulation Results – System Response to Cloud Transient

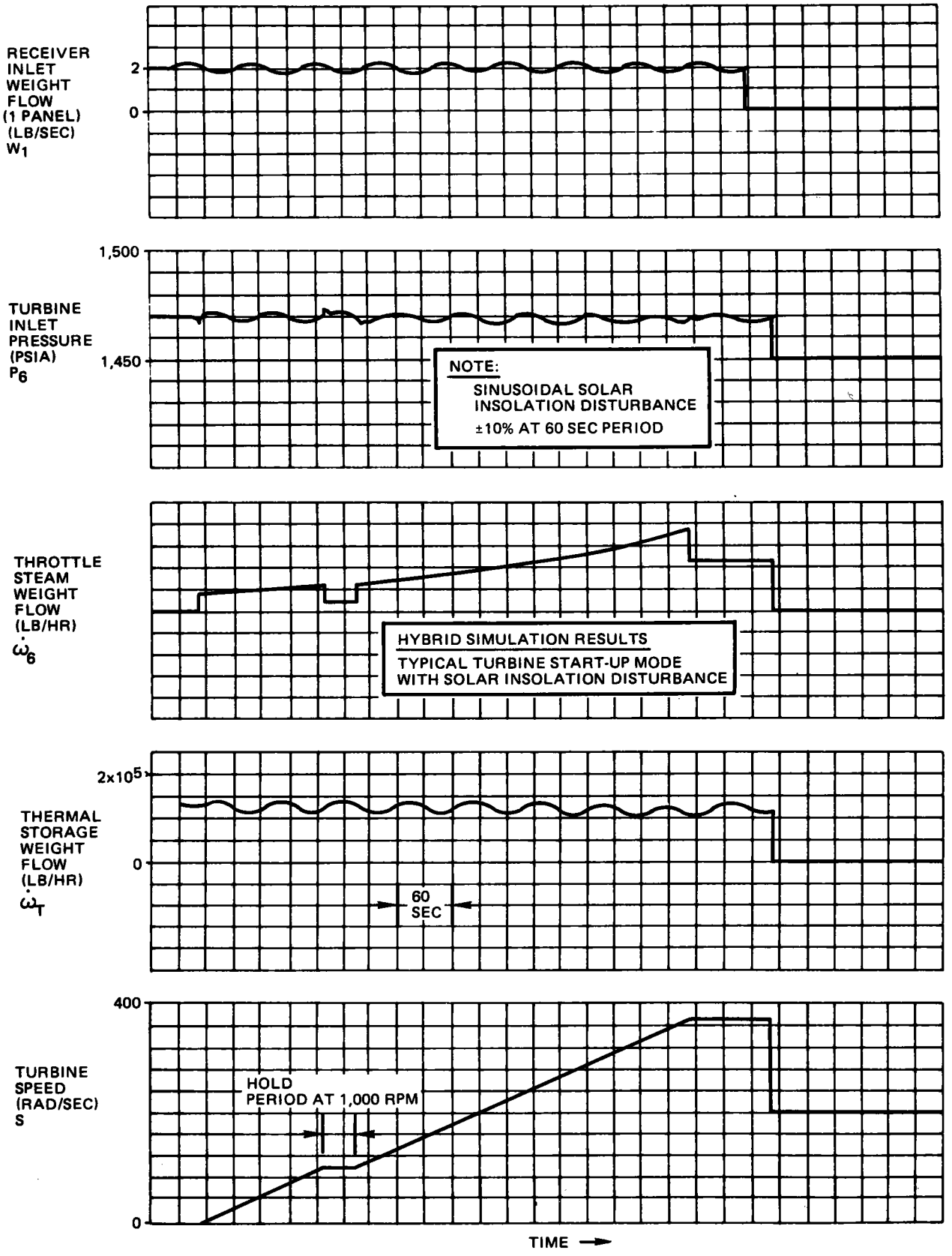

Figure 4-57. Hybrid Simulation Results – Turbine Start-Up Mode

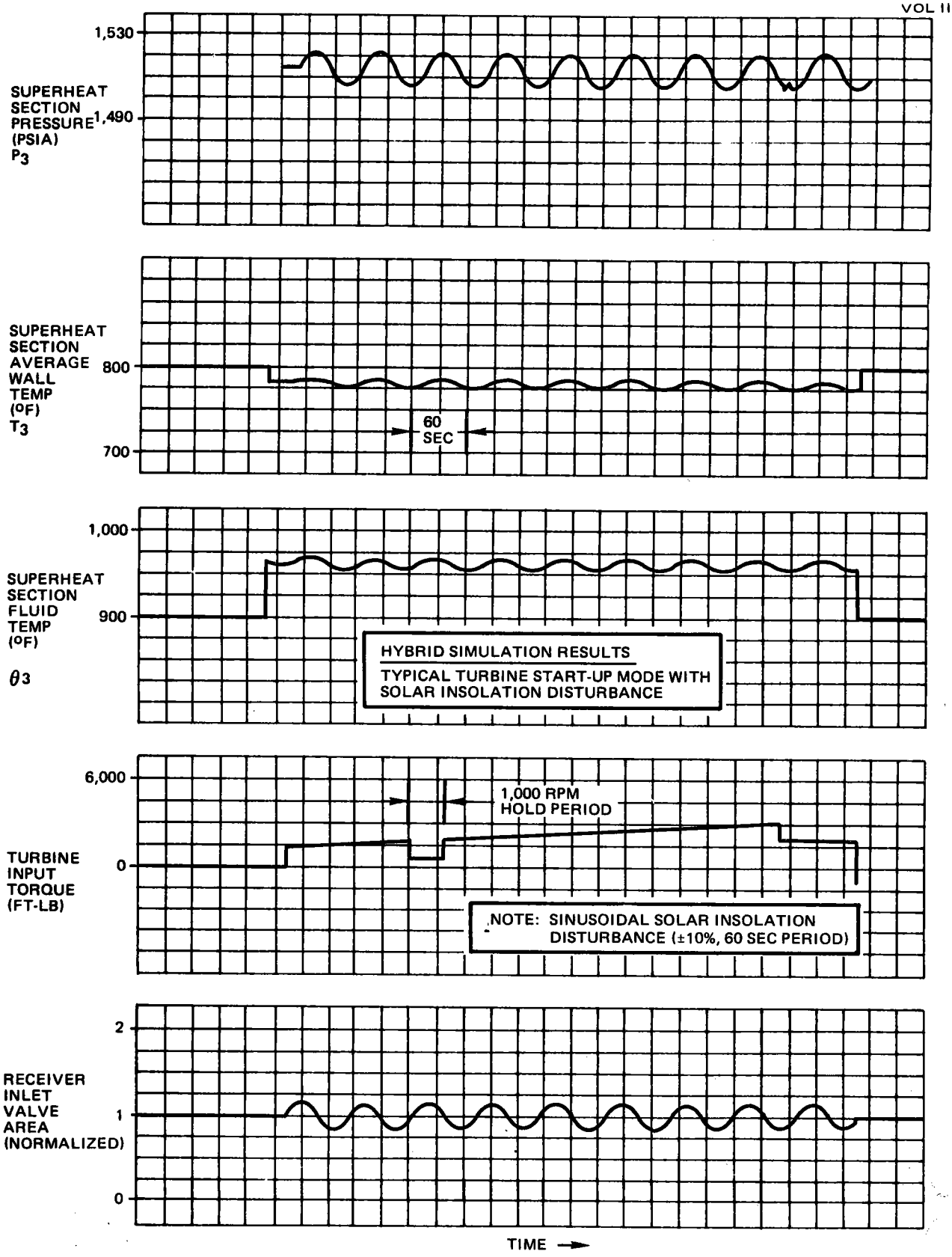

Figure 4-58. Hybrid Simulation Results – Turbine Start-Up Mode

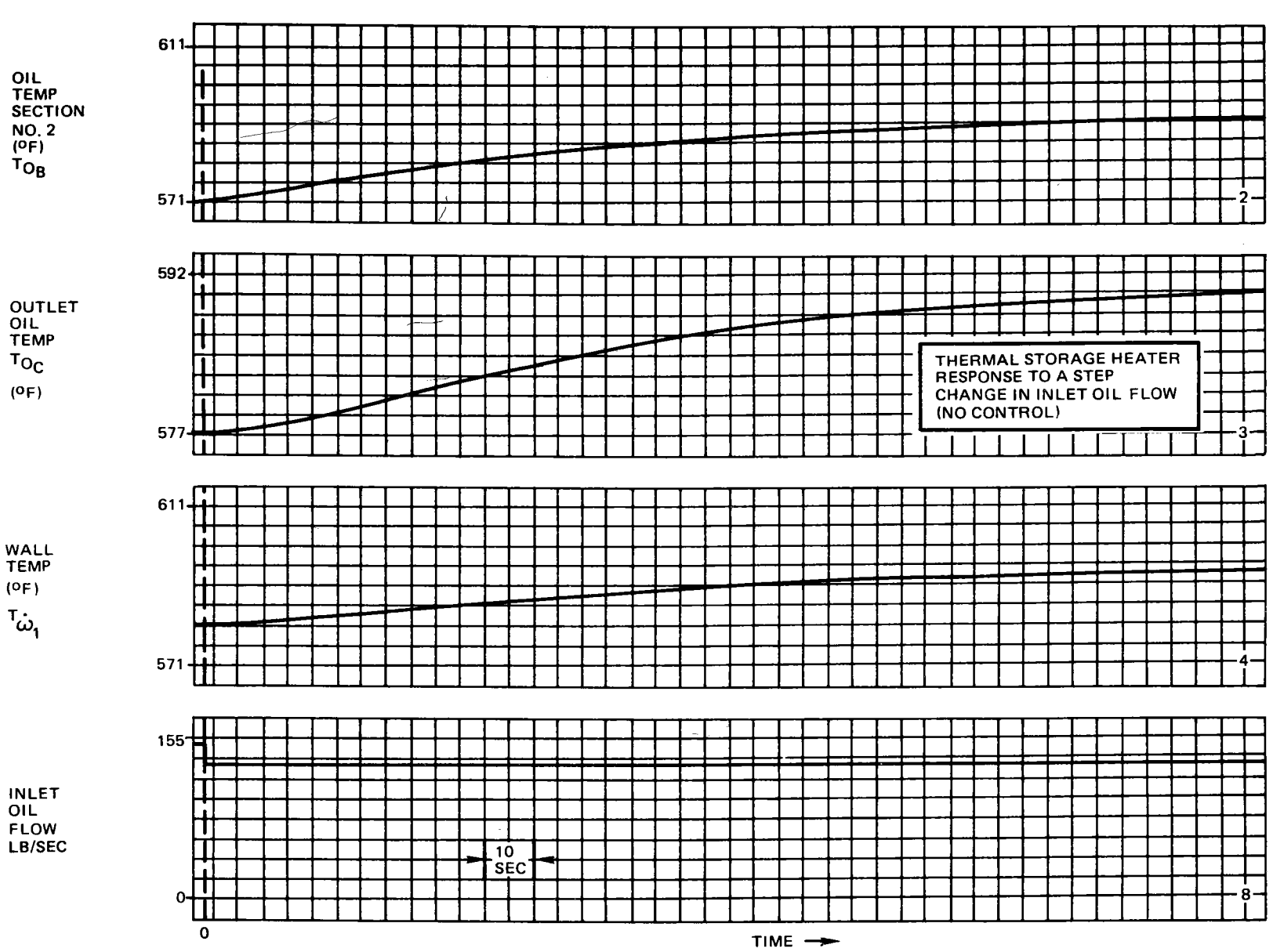

Figure 4-59. Hybrid Simulation Results – Thermal Storage Heater Response

-20 lb/sec is applied to the system at t = 0 sec. The steady-state outlet oil temperature increases approximately 20°F and the open-loop system response has an equivalent first-order time constant of approximately 100 sec.

4.7.4 POPS Simulation Status

At present, the POPS simulation is in an operational mode. The receiver subsystem and the turbine-generator subsystem simulations are implemented and checked out and are in an operational mode. The results presented in Section 4.7.3 are taken directly from that simulation. The balance of plant subsystem equations have been defined and are to be implemented in the future. The mathematical models for the thermal storage charging and extraction loops have been defined and are to be implemented into POPS as the next logical step in the development of the total system simulation. Each major subsystem is implemented and checked out in module form on both the digital and hybrid versions of POPS. After the thermal storage subsystem is implemented, the master control subsystem algorithms will be defined, designed, and integrated into the total power plant simulation.

It is the goal of the simulation effort to have a representative operational simulation of the total power plant with preliminary plant control systems and a preliminary master control subsystem algorithm by late fall 1977.

The development of the POPS simulation is an ever-evolving process. As more sophisticated models become available and better defined, the simulation is continually updated to reflect the most recent estimate of system configuration, constants, parameters, and hardware characteristics. The simulation is continually evaluated with respect to its function and purpose and the simulation effort is directed toward addressing the critical design issues and meeting the goals of the total solar program.

The POPS simulation is designed to be flexible enough to adjust to new program requirements with an end goal of providing a system integration capability for the checkout and verification of the integrity of the total power plant system master control concept.

4.8 PHASE 2 SYSTEM INTEGRATION EFFORT

System integration has been identified by MDAC as a significant task during the Phase 2 Pilot Plant program, and MDAC views on the subject are summarized in the following paragraphs. A top-level schedule of the major activities is included.

4.8.1 System Integration Assumptions

The specific tasks and responsibilities that the system integration contractor will have in Phase 2 are not clearly defined now because the total role of the Department of Energy and any of its contractors, e.g., Sandia or Aerospace, have not been announced for Phase 2. Therefore, the approach we took was to outline the efforts we assume that the integration contractor will have, and to schedule and man-load the tasks as a means of arriving at a justifiable estimate of system integration costs.

As the CBS Item 8100.3 title, "Solar Subsystem Integration Contractor," implies, we have assumed that a fundamental task will be that of managing the functional and physical interfaces between the collector, receiver, thermal storage, and master control subsystems. The task would involve the definition and control of all interface documentation, performance and design criteria, and program control, such as schedule monitoring, to ensure that Phase 2 milestones are met on time.

Additionally, since the steam/feedwater loop knows no clean solar plant/balance of plant boundaries, but pervades the entire system, there is a need for the coordination of the functional and physical interfaces between each of the subsystems, including collector, receiver, thermal storage, electrical power generator subsystem (EPGS), and master control. The physical dimensions, as well as the temperatures, pressures, flow rates, operating mode constraints, and other characteristics, should be coordinated and controlled from a single point to minimize the probabilities of incompatible interfaces between subsystems during installation and checkout of the Pilot Plant program.

It has been assumed that the system integration contractor will also have responsibility for conducting the six-month integrated system tests during

the last half of calendar year 1980. (The tests are described in Section 4.9.) Corollary assumptions are that MDAC, as the system integration contractor, will be assisted by Stearns-Roger in the conventional plant startup activities, and that this will be a period during which Southern California Edison (SCE) operating personnel will be familiarized with the operations and maintenance aspects of the Pilot Plant.

Another assumption is that SCE will have overall responsibility for operation of the Pilot Plant during the 2-year test program, with support from MDAC. A corollary assumption is that MDAC will be responsible for preparing the test plan, subject to review and approval by SCE and the Department of Energy. More specifics of the first and second year of the test program are treated in Section 4.9. Another corollary assumption is that MDAC will have primary responsibility for analysis and evaluation of the test data acquired during the program.

A final assumption to provide the overall framework for the delineation of all the system integration tasks is that the system integration contractor will be responsible for semiannual program reviews and documentation in Phase 2.

4.8.2 System Integration Tasks

A list of tasks defined for the system integration contractor, consistent with the assumptions stated in Section 4.8.1, is shown in Table 4-11. It should be recognized that this list is not necessarily all-inclusive, and would change, depending upon specific program requirements, but it is presented here as representative of how MDAC views the overall job of system integration.

4.8.3 System Integration Schedule

The tasks listed in Table 4-11 have been distilled into fewer, more general, efforts, and are shown against a calendar year time frame in Figure 4-60. The top bar for solar subsystem integration is intended to show the anticipated effort for coordination and management of the collector, receiver, thermal storage, and master control interfaces, as well as performing analyses, e.g., dynamic simulations of the total system operation. It has been assumed that the effort will be completed during the first 3 years of the program.

Table 4-11

PILOT PLANT SYSTEM INTEGRATION FUNCTIONS

System and Subsystems Performance Analysis (Including Sizing and I/F Definition)
System and Subsystems Operations Analysis (Including Dynamic Anal and IF Definition)
Preparation of System Test Plan (Including Subsystem Checkout and Integrated System Tests)
Preparation of System Safety Plan (If Required)
Preparation of Training Programs and Documentation (for Contractor and SCE Personnel)
Preparation of Final System and Subsystems Specifications
Preparation and Maintenance of Interface Control Documentation
Preparation and Maintenance of Integrated Solar Subsystem Program Schedule
Participation in Finalization of Environmental Impact Report
Perform Safety and Hazards Analyses
Participati ı in Risk Vs Cost System and Subsystem Design/Operation Trades
Monitoring of Compliance with OSHA Regulations and Other Safety Codes
Two-Year Test Program Operations and Support (Including On-Site and Off-Site)
Preparation and Publication of Program Documentation
Coordination and Monitoring of Solar Subsystem Contractor Activities
Coordination of Interfaces Between Balance of Plant and Solar Subsystem Contractors and A&E Contractors
Coordination with SCE
Coordination with Construction Manager
Coordination with Department of Energy/Sandia/Aerospace, as Appropriate
Preparation for, and Participation in, Program Reviews with Department of Energy and Others
Perform Specialized Field Performance Analyses (University of Houston)
Perform Integrated System Tests (Phase 2 of Test Program)

The system interface effort is shown for the entire 5-year period, as required, and it denotes the total system interface effort that is relative to the steam/feedwater loop, as described previously. Milestones are indicated for preliminary and final versions of interface documentation during the initial detailed system design effort. The documentation will be updated regularly, and will form the basis for configuration management.

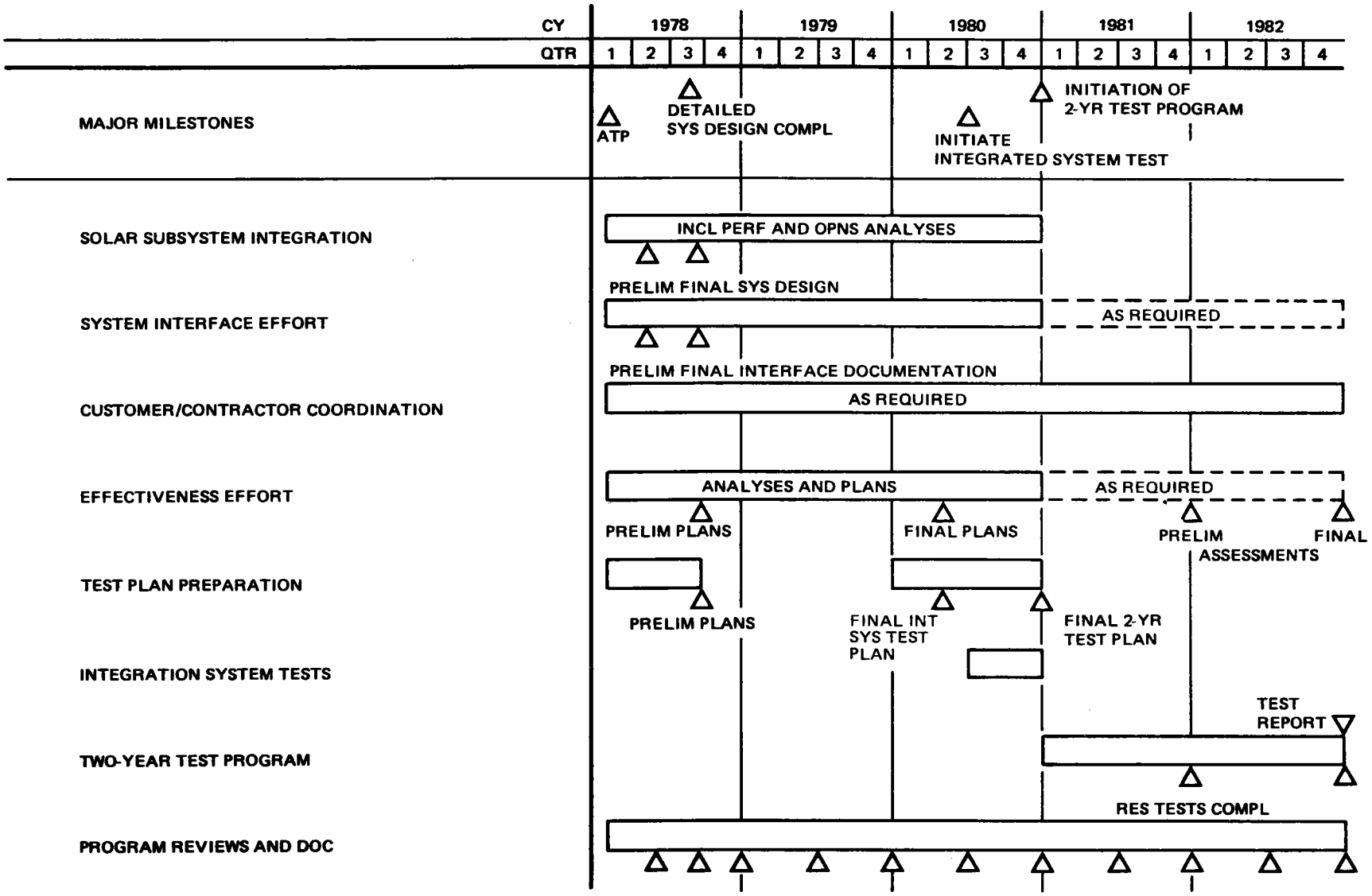

Figure 4-60. Pilot Plant System Integration Schedule

Lastly, the customer/contractor coordination effort, which is shown for the entire 5-year program, is meant to show activity that would involve interactions between the system integration contractor and any party not providing hardware to the program, e.g., Department of Energy/Sandia/Aerospace/Construction Manager.

4.9 FIELD INSTALLATION AND TEST OPERATIONS

Verification of requirements for the Pilot Plant system--by inspection, analysis, similarity, test and/or demonstration--as specified in the System Requirements Specification for the Central Receiver Solar Thermal Power System Pilot Plant, will take place during the course of a planned 42-mo field installation and test operations program. The assumed Pilot Plant program ATP date is January 1978. The field installation and test operations program is scheduled to begin in July 1979 with field site installation of the Pilot Plant subsystems and end in December of 1982 after the Pilot Plant has been operating for 2 years in both the system research and power production modes.

As shown in Figure 4-61, the planned 42-mo program has been divided into the following three major phases:

- Phase A. A 12-mo period devoted to subsystem installations and checkouts.
- Phase B. A 6-mo period of integrated system tests.
- Phase C. A 24-mo period during which the Pilot Plant is operated in the system research mode for one year and in the power production mode for a year.

Phase A activities will consist of installation of the master control and collector, receiver, thermal storage, and EPGS, followed by the functional checkouts of each of the subsystems to verify subsystem performance up to, but not including, subsystem-to-subsystem interface performances. During the checkouts, hot water/steam from special test equipment (STE) will be used to leak check and functionally evaluate the individual performances of the receiver and thermal storage subsystems. Phase A will be concluded when subsystem performances have been verified--within the limitations of subsystem internal controls (master control will not be on-line during Phase

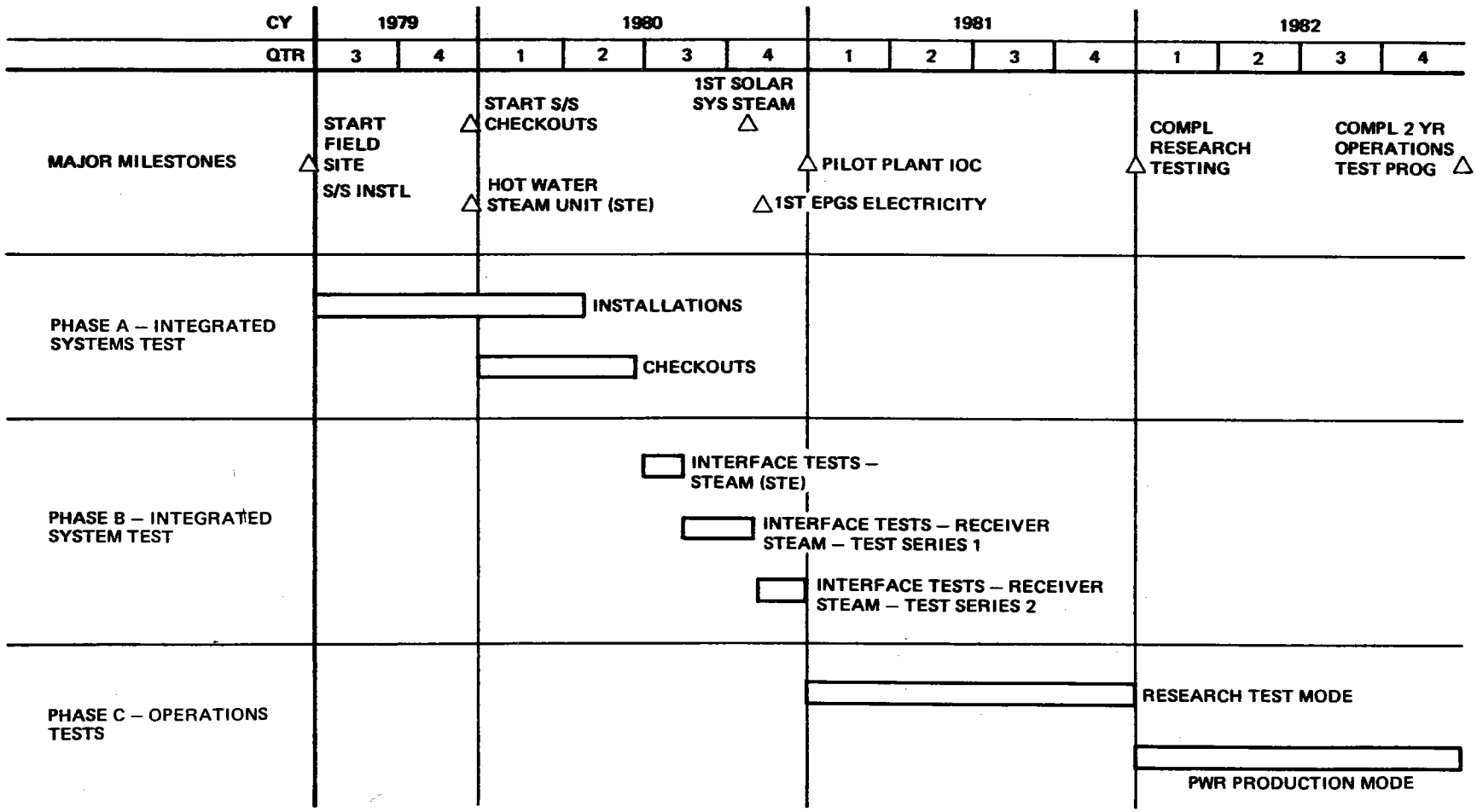

Figure 4-61. Pilot Plant Field Installation and Test Operations

A) and special test equipment – and all subsystem-to-subsystem electrical and mechanical installations have been completed.

Phase B activities will be initiated with the verification of electrical interfaces between the master control and the subsystem controllers of the collector, receiver, thermal storage, and EPGS. These interface verifications will establish the proper transmittal and receipt of data between master control and the Pilot Plant subsystems in the three operational modes--fully manual, fully automatic, and the combination mode using manual control supported by computer monitoring and alarm. Subsequent to these verifications, hot water/steam from the STE will be reintroduced into the receiver and thermal storage subsystems to demonstrate the monitoring and control capability of master control. At the conclusion of the demonstrations, and the successful checkout of the 1,760 heliostats under the direction of master control, the following two important events will take place:

- First generation of steam from solar energy.
- First generation of electricity from receiver-generated steam.

Phase B will be concluded when all subsystem-to-subsystem interfaces have been operationally verified and adequate Pilot Plant test data have been collected and analyzed to verify performances of each of the subsystem when integrated into the Pilot Plant system.

During Phase C of the three-phase field installation and test operations program, all required Pilot Plant operational modes – normal startup, normal solar operation, low solar power operation, intermittent cloudiness operation, thermal storage charging, extended operation (stored energy), fully charged thermal storage, normal shutdown, emergency shutdown, and subsystem conditioning – will be activated for adequate periods of time to permit the collection and analysis of test data concerning Pilot Plant performance. For the first year of the 2-year Phase C, the Pilot Plant will be operated in the research testing mode to demonstrate stable controlled operation of the Pilot Plant in all operational modes. In addition, data pertaining to the technical feasibility of a commercial-size solar thermal electric system will be obtained. In the second year of Phase C, the Pilot Plant will be operated in the

power production mode. This mode of operation will demonstrate the technical feasibility of a commercial-size solar thermal electric system in addition to providing an indication of solar thermal electric system economics. Phase C will be concluded when the Pilot Plant Program objectives have been achieved.

All Phase A through Phase C field installations and test operations will be performed in accordance with master program phasing schedule (MPPS) requirements to ensure that program milestones and critical events have been met. From the MPPS, detailed working schedules for each individual field installation and test operation will be prepared. At frequent intervals, schedule reviews will be conducted to review progress, discuss actual or potential soft spots within the activity schedules, and to decide what, if any, corrective action is required.

Installation and checkout activities of the Pilot Plant (Phase A) will be performed and/or supervised by contractor personnel. Utility personnel will be trained and phased into plant operations beginning with Phase B until the second year of Phase C, by which time they will be completely responsible for plant operations. Contractor personnel will continue to provide technical support during the switchover period, as shown in Figure 4-61.

Each installation and test operation will be conducted in accordance with written procedures derived from the applicable installation or test requirements drawing. Test operations procedures will be both manual and automated (for master control implementation), and automated procedures will be verified in the laboratory prior to field site implementation.

Data requirements for each test operation, including nominal read-out values, will be an important part of each test requirement drawing and test procedure. Data required for the safe and proper operation of each subsystem during a test operation will be displayed for real-time analysis and recorded, as well as other data required for overall subsystem evaluation, off-line data analysis and evaluation. Progression of the overall field installation and test operations program within a given phase as well as from one phase to the next will be based on the results of these data analyses and evaluations.

4.9.1 Subsystem Installation and Checkout, Phase A

Phase A of the three-phase, 42-mo field installation and test operations program will be a 12-mo effort devoted to the installation and checkout of the Pilot Plant master control and the collector, thermal storage, receiver, and electrical power generation subsystems. As shown in Figure 4-62, Phase A is initiated in July 1979 and is scheduled for completion in June 1980 (Pilot Plant program ATP of January 1978 assumed). A brief summary of Phase A activities follows with additional information pertaining to the various subsystem installations and checkouts presented in the individual subsystem report volumes.

4.9.1.1 Master Control

Master control hardware and software will be developed, integrated, and tested at MDAC prior to delivery to the field site. Installation of the equipment in the control room at the field site, including interface equipment such as steering logic, patch panels, relay junction boxes, and analog recorders, will be done in conjunction with the installation of control and instrumentation cables between the control room and Pilot Plant subsystems.

Following equipment installations, computer self-check routines will be conducted to verify the operational readiness for Phase B where the three master control modes of operation – fully manual, fully automatic, and combination using manual control supported by computer monitoring and alarm – will be exercised. In addition, integrity checks of all cable and instrumentation installations (including that instrumentation required for air weather monitoring and forecasting) will be performed.

4.9.1.2 Collector Subsystem

The 1,760 heliostats of the collector subsystem will be assembled in the field site assembly building and then transported to the field. There, they will be lowered and secured onto the previously installed and leveled foundations. Power, control, and instrumentation cables will be connected to the field/heliostat controllers, after which electrical and instrumentation checks of the heliostats using STE in lieu of master control will be performed.

Installation of the sensor poles and sensors, for the closed-loop subsystem, will be followed by electrical checks performed to verify heliostat/sensor

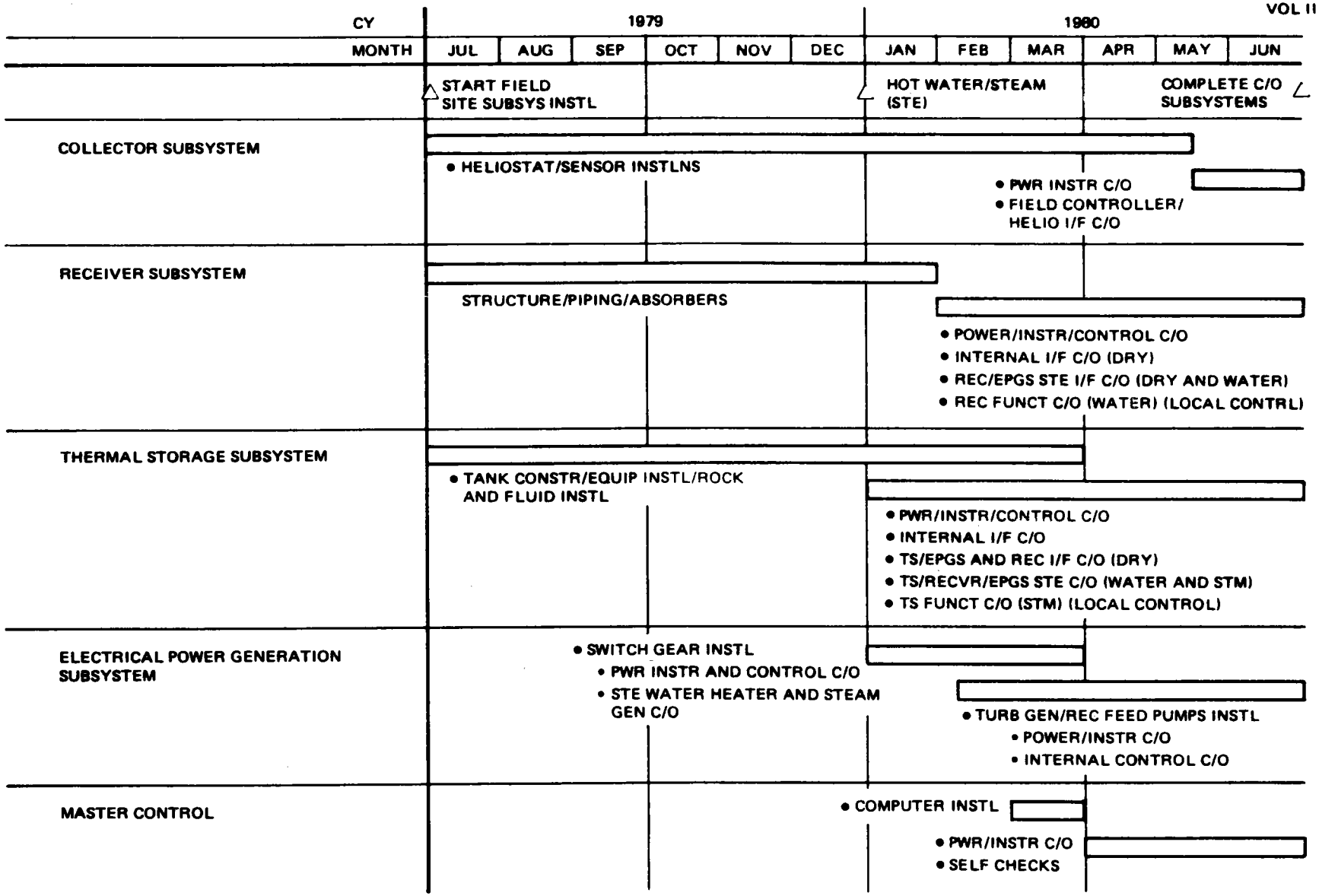

Figure 4-62. Pilot Plant Subsystem Installation and Test Schedule

interfaces. Subsequent to these verifications, individual heliostat and sensor combinations will be aligned through a series of heliostat tracking exercises using the STE and receiver panels mounted on the receiver tower.

Phase A activities for the collector subsystem will be concluded with a series of tests performed to verify the performance of each field controller and its associated cell of 24 heliostats. For the tests, a wet receiver will be required. The STE will be connected to each field controller, and each cell of heliostats will be commanded to acquire the sun, normal track, synthetic track, slew off receiver unit, wash position, inverted position, and stow position. While in normal tracking, at least one heliostat out of 24 will be evaluated for pointing error and beam quality, using the digital image radiometer in the STE. Procedures for using the digital image radiometer are described in Section 6.4 of Volume III.

4.9.1.3 Thermal Storage Subsystem

The thermal storage unit of the thermal storage subsystem will be erected in the field subsequent to field shop fabrication and preparation of site foundations. The installation will be followed by other equipment and piping installations such as the ullage maintenance unit, field maintenance unit, heat exchangers, etc, and the hookup of all power, control, and instrumentation cables.

Subsystem checkout performed after installation completion will be divided into preoperational checkout and operational checkout. Preoperational checkout will verify all electrical and pneumatic circuit connections after which power will be selectively applied to all circuits with verification that the appropriate activation occurs. All pumps, valves, etc, will be activated during the verification. During the checkouts, including the operational checkout discussed below, STE in lieu of master control will be interfaced with the subsystems controllers and be used to provide initiation signals as required for operating control components.

Operational checkout will involve operation and verification of the heat-transfer fluid and the hot water/steam networks of the thermal storage subsystem. Filling of the lines with heat-transfer fluid from the filled thermal storage unit will be followed by leak checks of all joints and flanges.

Subsequent to these checks, the charging and heat-extraction loops will be leak-checked and functionally evaluated by the introduction of hot water/steam into the subsystem from the STE. During the evaluations, all instrumentation will be monitored and readings checked against pretest estimates with any anomalies resolved as required.

4.9.1.4 Receiver Subsystem

Receiver subsystem installations will be initiated with the erection of the tower required to elevate and support the receiver unit and the riser/downcomer assembly. Assembly of the receiver unit will take place on top of the tower. Subsequent to this assembly, the installation of piping and controls and the hookup of all power, command, and instrumentation cables will take place, followed by inspections of all installations.

Receiver subsystem checkout, facilitated by STE interfacing with the subsystem controllers in lieu of master control, will first verify all electrical and pneumatic circuit connections followed by the selective applications of power to all circuits to verify proper activation of all pumps, valves, etc. Subsequent to these verifications, hot water from STE will be introduced into the subsystem for purposes of: (1) leak-checking pipes, joints, and flanges, (2) functionally evaluating performance of the subsystem under a loaded and dynamic condition, and (3) supporting the collector subsystem performance verification tests. Monitoring and analysis of all instrumentation readings to verify pretest performance predictions will be made during these operations. At the completion of Phase A checkouts, the subsystem will be made ready for the Phase B integrated system tests.

4.9.1.5 Electrical Power Generation Subsystem (EPGS)

Early installation and checkout of the EPGS equipment necessary to support the other subsystem installations and checkouts will be required. The equipment will include the power and power cables to each of the subsystems, water-treatment equipment, and the STE hot water/steam equipment. Prior to the installations and the required leak-functional checkouts, the turbine-generator equipment will be installed and checked out.

Checkout of the turbine-generator equipment will follow the conventional checkout sequences established for the initial startup of all new generating

units. These sequences are in terms of weeks before initial turbine roll and include such functions as instrumentation checks, pressure checks, hydro tests, alarm tests, and no-load turbine checks. At the completion of these Phase A checkouts, the EPGS equipment will be made ready for the Phase B integrated system tests, including initial turbine roll under receiver steam scheduled for October 1980 (Pilot Plant program ATP of January 1978 assumed).

4.9.2 Integrated System Tests, Phase B

Subsequent to the Phase A completion of the installation and checkout of the Pilot Plant subsystems, including master control, integrated Pilot Plant system tests will commence. This second phase of the 3-phase, 42-mo installation and test operations program has a planned duration of 6 mo and, as shown in Figure 4-63, runs from July through December 1980 (Pilot Plant program ATP of January 1978 assumed).

Phase B activities are designed to gradually and safely expand upon the Pilot Plant test data obtained in Phase A; therefore, they have been grouped and sequenced as follows:

- Integrated system tests using the Phase A STE for generating hot water and steam.
- Integrated system tests using receiver generated steam with all steam routed to the thermal storage subsystem and from there to the EPGS.
- Integrated system tests using receiver generated steam with steam routed directly to the EPGS.

4.9.2.1 Integrated System Tests, STE Hot Water and Steam

In Phase A, Pilot Plant subsystem checkouts were limited to functional tests of the individual subsystems under the control of each subsystem's controller. STE was required to (1) provide appropriate commands and readouts, in lieu of master control which itself was undergoing checkout, to the individual subsystem controllers, and (2) provide hot water and steam to the receiver and thermal storage subsystems, respectively. Building upon these tests,

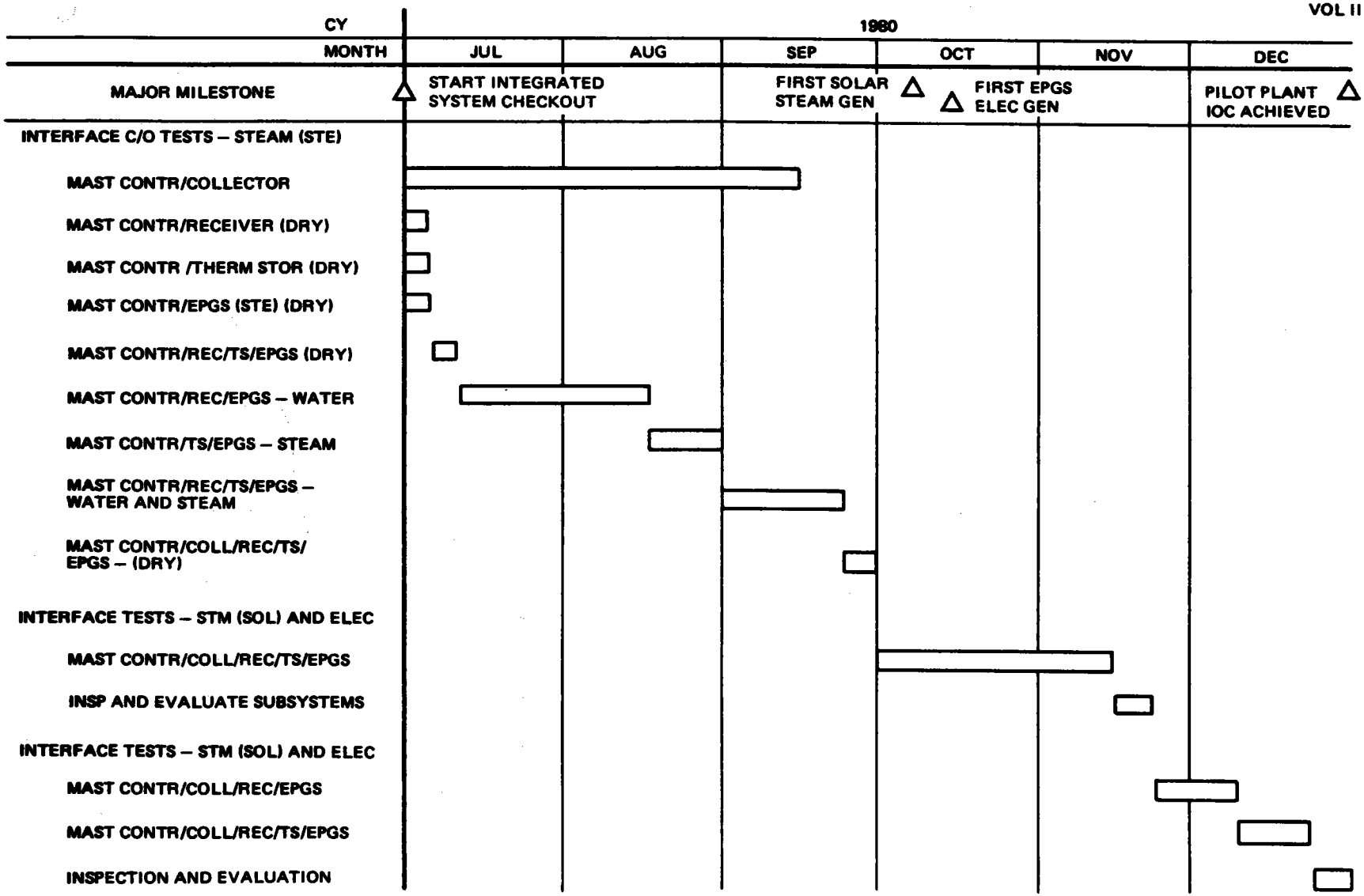

Figure 4-63. Pilot Plant Integrated System Test Schedule

Phase B will be initiated with a series of tests to verify the following electrical interfaces:

- Master control to collector field controllers.
- Master control to receiver controller.
- Master control to thermal storage controller.
- Master control to electric power generation controller.

This test series, using automated test procedures developed and verified by MDAC-Huntington Beach, will establish proper data flow between the master control and each of the Pilot Plant subsystem controllers and will ready the Pilot Plant for the functional tests that follow.

Subsequent to the establishment of proper electrical interfaces between master control and each of the Pilot Plant subsystem controllers, an integrated master control/receiver/thermal storage/electrical power generation interface (electrical) test will be performed, followed by the introduction of hot water and steam into the system by the STE. Like Phase A, STE-provided hot water and steam are used to ensure available and controlled working fluids throughout test periods. The introduction of hot water and steam into the system at this stage of Phase B provides additional receiver and thermal storage subsystem performance and integrity data. Also, and more important, the action verifies the capability of the master control to work in conjunction with the receiver and thermal storage subsystem controllers in regulating and controlling the flow of working fluids in and between these two subsystems.

At the completion of the functional flow tests involving master control and the receiver and thermal storage subsystems, a final integrated system interface (electrical) test, including the collector subsystem, is performed prior to the introduction of receiver-generated steam into the system.

4.9.2.2 Integrated System Tests, Receiver Steam, Test Series 1

Throughout Phase A and the initial tests of Phase B, subsystem and integrated system tests have been performed to verify the readiness of the system to accept receiver-generated steam. As can be seen from Figure 4-63, this milestone for the Pilot Plant program has been scheduled to occur, if weather

conditions permit, in October 1980 (Pilot Plant program ATP of January 1978 assumed) or midway through the integrated system tests of Phase B.

The initial test series in the second half of Phase B will be devoted to (1) the final aiming and alignment of the field heliostat array with the receiver, and (2) demonstrating the capability of the heliostats to be off-targeted in a controlled manner upon command from the master control. As described below, a wet receiver will be required for these operations; therefore, master control and all subsystems of the Pilot Plant will be brought on-line as required.

The planned sequence of operations for the first series of tests involving receiver-generated steam will be as follows:

- From approximately 2 AM to 4 AM, using power from the auxiliary source of the EPGS, heliostats will be oriented to their predicted sun acquisition positions by commands from master control.
- When the sun is 10 deg above the horizon, the system will be started by the initiation of heated water flow through the receiver unit. Startup will be by command of the master control.
- Heliostats will acquire the sun sequentially to control the system powerup. As heliostats acquire the sun and reflect the direct incident solar insolation onto the receiver unit, aiming and alignment of all heliostats will be verified and adjustments made as necessary to obtain the required vertical aiming strategy.
- Hot water and low-quality steam developed in the receiver during this operation will be cycled through the thermal storage subsystem, bypassing the turbine, until the thermal storage unit is sufficiently charged at which time the heliostat field will be shut down (both normally and under simulated emergency conditions) and the steam from the thermal storage subsystem will be directed to the turbine-generator for generation of electricity.
- Shutdown of the EPGS will be automatically initiated when the outlet temperature of the thermal storage heat-transfer fluid falls below a given value.

Subsequent to the completion of final heliostat field alignment and slew checks, system operation in the extended-operation mode will be continued to gather

and analyze data pertaining to (1) system startup, (2) thermal storage charging, (3) extended operation (stored energy), (4) fully charged thermal storage, (5) normal shutdown, and (6) heliostat shutdown, both normal and emergency modes. (Operation of the power plant in the above sequence is, of course, dependent upon actual weather conditions at the time of test. During initial trial runs of the system, unfavorable weather conditions will be just cause for either not attempting system startup or for instigating an early system shutdown.)

4.9.2.3 Integrated System Tests, Receiver Steam, Test Series 2

With the accomplishment of heliostat field final alignment and the gathering and analysis of data on the operation of the Pilot Plant in selected operational modes, the last series of tests in Phase B will be dedicated to the operation of the Pilot Plant in the normal solar operation mode. The planned sequence of operations for this test series is similar to that of the preceding series except that receiver-generated steam will be routed directly to the electric power generation subsystem rather than to the thermal storage subsystem. Pilot Plant operation will continue in this mode for the remainder of Phase II to verify that high-quality steam can be provided to the EPGS within specification requirements. (Once again, the actual operation of the Pilot Plant for the scheduled period of time will depend upon weather conditions at the time of test. Unfavorable conditions will cause a variation in the planned series of test operations and therefore could cause a variation in the proposed test schedules.)

At the conclusion of Phase B, the Pilot Plant will be shut down for a week to allow a thorough evaluation of test data collected as well as visual inspection of all elements of the various subsystems. Subsequent to these analyses and inspections, the plant will be made ready for the scheduled 2-yr Phase C program.

4.9.3 Operations Tests, Phase C

The third and last phase of the 42-mo field installation and test operations program will be devoted to operating the Pilot Plant in the research testing and power production modes, in accordance with Pilot Plant System Requirements Specification requirements. As presented in Figure 4-64, the first

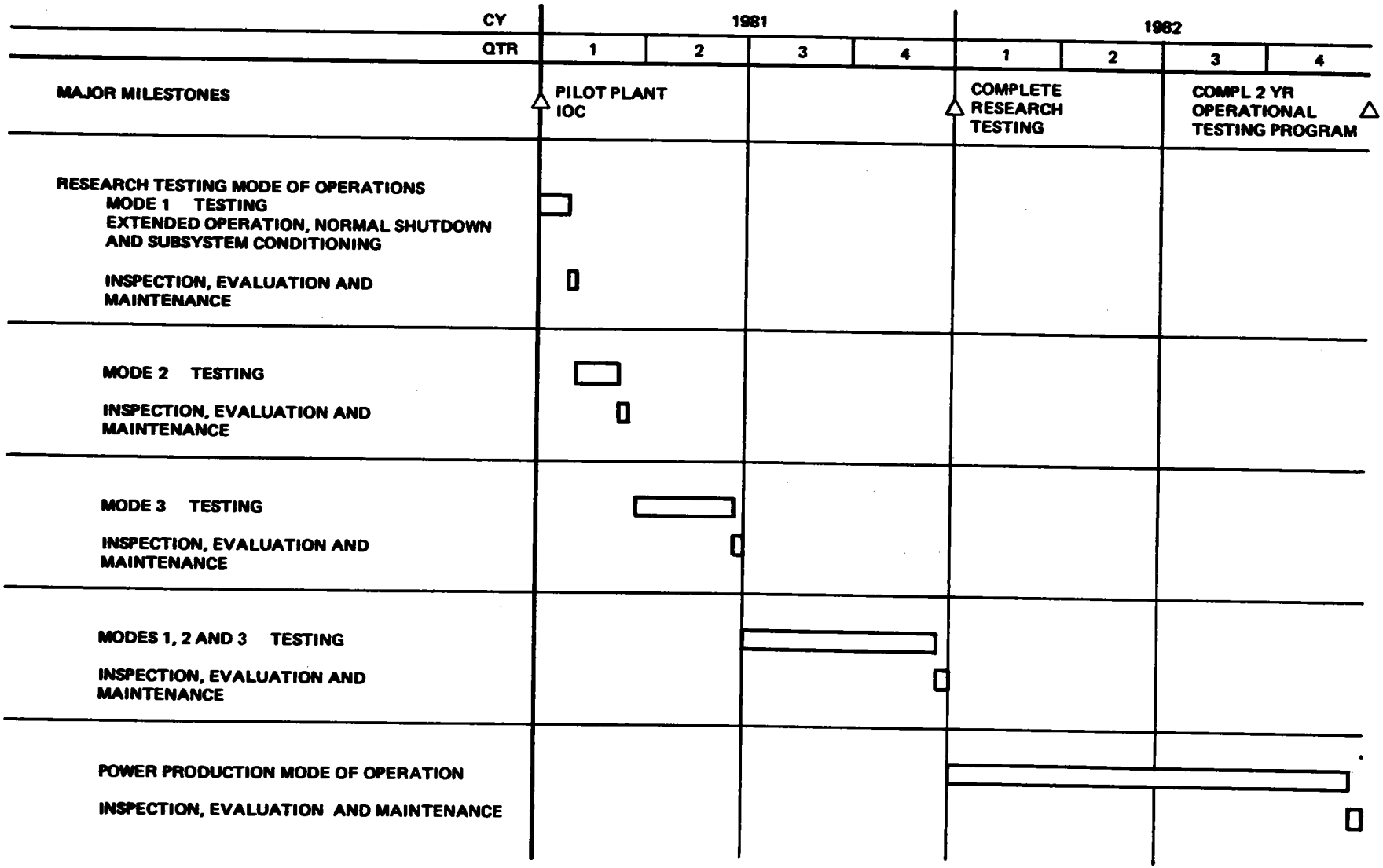
CY
1981
1982
QTR
1
2
3
4
1
2
3
4
MAJOR MILESTONES
PILOT PLANT IOC
COMPLETE RESEARCH TESTING
COMPL 2 YR OPERATIONAL TESTING PROGRAM
RESEARCH TESTING MODE OF OPERATIONS
MODE 1 TESTING
EXTENDED OPERATION, NORMAL SHUTDOWN AND SUBSYSTEM CONDITIONING
INSPECTION, EVALUATION AND MAINTENANCE
MODE 2 TESTING
INSPECTION, EVALUATION AND MAINTENANCE
MODE 3 TESTING
INSPECTION, EVALUATION AND MAINTENANCE
MODES 1, 2 AND 3 TESTING
INSPECTION, EVALUATION AND MAINTENANCE
POWER PRODUCTION MODE OF OPERATION
INSPECTION, EVALUATION AND MAINTENANCE

year of Phase C will be dedicated to plant operation in the research testing mode and the second year to plant operation in the power production mode. The sequence of operations will result in extensive operator training plus plant debugging prior to operation of the plant in the power production mode to formally demonstrate the technical feasibility of a commercial-size thermal electric system, and to provide an indication of system economics.

4.9.3.1 Research Testing Mode of Operation

The objective of the 1-yr operational period, during which time the Pilot Plant will be operated in the research testing mode, will be to demonstrate stable controlled operation of the Pilot Plant system in the following operational modes:

- Normal startup.
- Normal solar operation.
- Low solar power operation.
- Intermittent cloudiness operation.
- Thermal storage charging.
- Extended operation (stored energy).
- Fully charged thermal storage.
- Normal shutdown.
- Emergency shutdown.
- Subsystem conditioning.

To achieve the objective, it will be necessary to operate the plant in each of the required modes for a period of time sufficiently long that a meaningful demonstration can be obtained. This can be accomplished, assuming a sufficient number of clear days are available, in two ways:

1. By taking maximum advantage of actual weather conditions during the test period.
2. By simulating conditions such as low solar power operation and intermittent cloudiness operation as required by shutting down the required number of heliostats in the field for the required periods of time.

To take maximum advantage of actual weather conditions during the test period, accurate weather data (both actual and predicted) for the immediate and surrounding Pilot Plant locations will be continuously provided to the

Power Plant control station. These data will include wind speed and direction; cloud coverage, type, and movement; visibility; precipitation; etc. Based on these data and an overall Phase C operational plan, Pilot Plant operational schedules will be prepared (for 1 wk, for example) including requirements for simulated conditions. These schedules, of course, will be sufficiently flexible to incorporate revisions due to unexpected changes to forecasted environmental conditions.

In Figure 4-64, an overall operational plan representative of possible Pilot Plant operational modes and time periods for the entire 1-yr research testing mode is presented. Note that during this 1-yr period, 5 wk of plant down time have been scheduled for inspection, evaluation, and maintenance; between down times, operation periods are continually increased.

During the first 3 wk of plant operation, the plan calls for the following modes of operation (environmental conditions permitting):

- Normal startup, including thermal storage charging.
- Normal solar operation with receiver steam in excess of that required for turbine design point operation delivered to the thermal storage subsystem.
- Extended operation (stored energy).
- Normal shutdown.
- Subsystem conditioning.

During this period, emergency shutdowns, including heliostats off target upon master control command, will be demonstrated.

Following a 1-wk down period for Pilot Plant inspection, evaluation, and maintenance, the plant is brought back on-line for 6 wk of operation in the following operational mode (environmental conditions permitting):

- Test period 1 modes.

  plus

- Normal startup.
- Thermal storage charging (maximum).
- Fully charged thermal storage.
- Extended operation.

- Normal shutdown.
- Subsystem conditioning.

Again during this period, emergency shutdown, including heliostats off target upon master control command, will be demonstrated.

Subsequent to a 1-wk down period for Pilot Plant inspection, evaluation, and maintenance, the Plant is brought back on-line for 12 wk of operation in the following operational modes (environmental conditions permitting):

- Test period 1 and 2 modes.

plus

- Normal startup.
- Intermittent cloudiness (simulated as required).
- Low solar power (simulated as required).
- Normal shutdown.
- Subsystem conditioning.

Following a 1-wk down period for Pilot Plant inspection, evaluation, and maintenance, the plant is again brought back on-line for 22 wk of operation in the operational modes (environmental conditions permitting) of test periods 1, 2, and 3.

Subsequent to this 22-wk period of operation, the plant will be taken off line for 2 wk to review the results of the test data obtained and to prepare the plant for the 1-yr period of operation in the power production mode.

4.9.3.2 Power Production Mode of Operation

The last year of the 42-mo Pilot Plant installation and test operations program will be devoted to Pilot Plant operation in the power production mode. The Plant will demonstrate the operational capability of supplying electrical busbar power using thermal energy from the storage system, or thermal energy directly from the receiver subsystem. The power supplied by the Pilot Plant will be used by the utility to partially meet the electrical demand.

To provide an indication of Pilot Plant system economics, the plant will be operated as a Commercial power plant by utility personnel, as opposed to

contractor personnel who will be responsible for the conduct of operations during previous phases. Plant operational and maintenance procedures previously developed and verified such as system startup, normal shutdown, emergency shutdown, subsystem conditioning, etc will be exclusively used throughout this 1-yr program. Training of utility personnel in the use of the procedures will be accomplished primarily in Phase C during the 1-yr research testing mode.

In addition to providing an indication of system economics, operation of the Pilot Plant in the power production mode will formally demonstrate that the Plant is capable of (1) delivering 10-MWe net busbar power to the electrical transmission network at 2 PM on a clear day at Winter solstice when operating on energy directly from the receiver subsystem, (2) storing thermal energy in the thermal storage subsystem for concurrent or deferred conversion to electrical power, (3) when absorbed thermal power exceeds 32.6 MWth, storing energy while simultaneously generating 10 MWe net, (4) delivering at least 7 MW net electrical power for 3 hr and lesser power levels for longer periods of time to the electrical transmission network when operating solely on energy drawn from the fully charged thermal storage subsystem, and (5) delivering at least 7 MWe net power to the electrical transmission network when operating on energy from the thermal storage subsystem while it is being charged by the receiver subsystem.

During the power production mode, master control will be operating mostly in the automatic mode with the other modes available as required. Plant operational modes (normal solar, low solar, intermittent cloudiness, etc) will be dependent upon environmental conditions and network demand. In the automatic mode, the Pilot Plant will be under the control of application programs resident in the computer. The programs provide control and monitoring of the subsystems, fault detection and isolation, and generation of status and error data to hardcopy or recording devices and operator display.

Since the Pilot Plant is still in a research and development status in Phase C, test data concerning the operation and performance of the overall plant, as well as the individual subsystems, will continue to be recorded and analyzed

and changes to operational procedures incorporated as required. Of particular importance to the Central Receiver Solar Thermal Power System will be the data collected and analyzed pertaining to Pilot Plant availability, maintainability, and reliability because these factors directly influence the economic aspects of the solar thermal power system concept.

4.10 SYSTEM EFFECTIVENESS

4.10.1 Introduction

An important characteristic of any Commercial power plant is a high level of systems effectiveness that includes a minimum of failures, downtime, and maintenance, and a maximum amount of safety. It is even more important for a solar power plant to have a high degree of systems effectiveness because the fuel for the plant is free; the only costs are capital cost and maintenance. The higher the degree of systems effectiveness, the lower the cost of electricity. Also, the solar plant presents hazards that are not present in a conventional fossil fuel plant.

Systems effectiveness includes reliability, maintainability, and safety. However, in a power system the term availability is used, which effectively combines reliability (failures) and maintainability.

Reliability is usually defined as the probability that a system or component will perform its intended function for a specified period of time. However, the question that is, or should be, asked when referring to a power plant is: what is the fraction of time that a system will be operating, or ready for operation, out of the total desired operating time. This availability includes reliability and maintenance. It is basically a calculation of the number of failures in a given period times the amount of time required to recover from the failures. The time is termed the outage time, the time the system is down and not available for operation.

The requirement or the justification for a high level of systems effectiveness is economic and to some extent contractual. A high amount of availability is important in any power plant, but it is even more important in a plant where the fuel cost is zero and the entire cost of the final product, electricity, is caused by capital cost and operating cost.

4.10.2 Availability

Availability is the fraction of the total desired operating time that a system or component is operating or available for operation. The electrical power industry (Reference 1)* divides the time when a system is not available (unavailability) into three classes: forced outage, maintenance outage, and planned outage. Forced outage is an occurrence of a component failure or other condition which requires that the unit be removed from service immediately or up to and including the next weekend. A maintenance outage is defined as the removal of a unit from service to permit work on specific components which would have been postponed past the next weekend and is work done to prevent a potential forced outage and which could not be postponed from season to season. A planned outage is the removal of a unit from service for inspection or general overhaul of one or more major equipment groups. This is work that is usually scheduled well in advance (e.g., annual boiler overhaul, 5-year turbine overhaul). The Edison Electric Institute also defines a forced partial outage as the occurrence of a component failure or other condition which requires that the load be reduced 2% or more immediately or up to and including the next weekend.

The forced partial outages are considered in the equivalent total forced outage by calculating an equivalent full-load outage duration. This is done by considering the outage time and the percentage reduction from full load.

As discussed above, availability is the product of reliability (component failures) and maintenance (the time to recover from a failure) and thus is calculated by determining the number of failures and the average time to fix the failures.

4.10.2.1 Conventional Plant Statistics

The historical data on availability of conventional power plants is found in several references (References 2, 3, 4, and 5). Table 4-12 (from Reference 3) gives the relationship between the size of a unit and the percentages of forced, planned, and maintenance outages. The relationship between size and forced outage rate is further emphasized by Figure 4-65

*References are listed at the end of Section 4.10.

Table 4-12

TIME UNIT AVAILABILITY FOR 1964-1973 PERIOD

Type of Unit	No. of Units	Average Percentage of Time Unavailable: Forced Outage	Planned Outage	Maintenance Outage	Total Percent
Fossil					
200-389 MW	234	4.4	6.5	3.1	14.0
390-599 MW	99	7.7	8.7	3.8	21.2
600 MW and above	59	14.0	8.5	4.5	27.0
Nuclear	20	6.9	9.3	4.9	21.1

(which is from Reference 5); Figure 4-66, taken from Reference 1, also shows this relationship. The relationship between drum-type boilers (used in the MDAC design) is shown in Figures 4-67 and 4-68. All of these figures show that if historical data is to be used to determine either availability goals or as estimates of expected results, the data of the appropriate facility size must be used.

Table 4-13, from Reference 1, gives the data on the outage for a 90-129 MW plant.

4.10.2.2 Solar Power Plant Allocations

The historical data given above, gives us a basis upon which to develop availability allocations for the Central Receiver Solar Thermal Power Plants. The allocations developed below are for a 100-MW plant. However, when data for a 10-MW plant is not available, it would be expected that the availability would be higher (Figures 4-65 and 4-66) but, because the 10-MW plant will be a Pilot Plant and thus experimental, it would also be expected that the experienced availability would be lower. Thus, the data given is for a 100-MW Commercial Plant or a 10-MW Pilot Plant.

The established availability goal for the 10-MW Pilot Plant is 90% or an unavailability of 10%. This goal was subdivided into outage categories and subsystems availability allocations at the beginning of the design period.

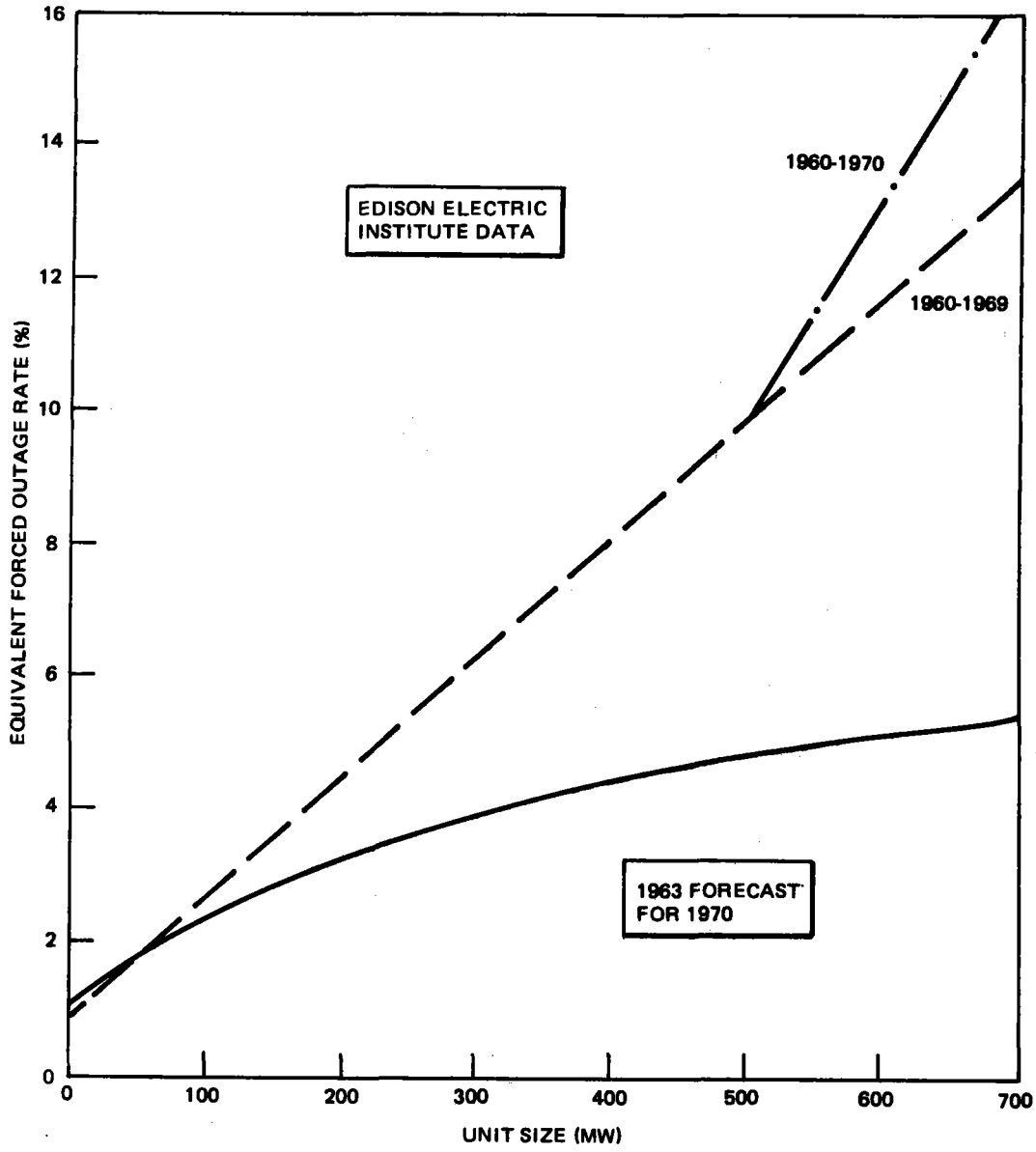

Figure 4-65. Forced Outage Rate as Function of Unit Size

10-YEAR PERIOD 1964-1973

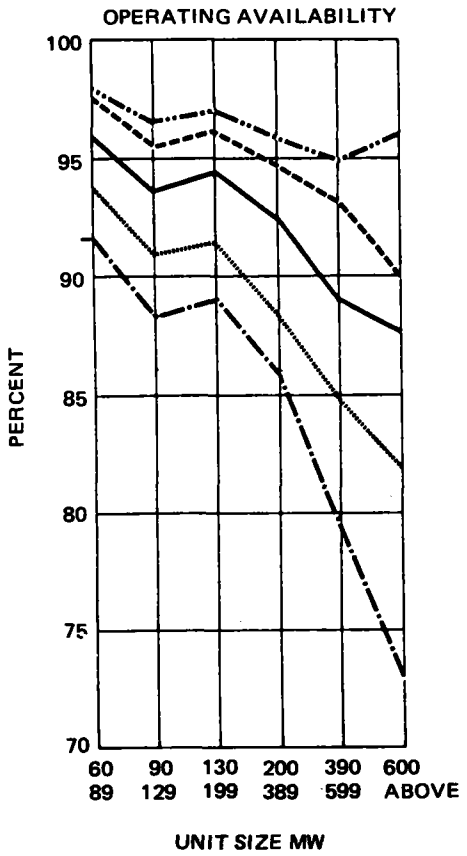

SAMPLE TABLE

MW SIZE	NO. OF UNITS	NO. OF UNIT YRS
60-89	83	368
90-129	191	1043
130-199	259	1693
200-389	234	1486
390-599	99	454
600-ABOVE	59	203

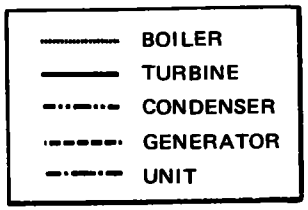

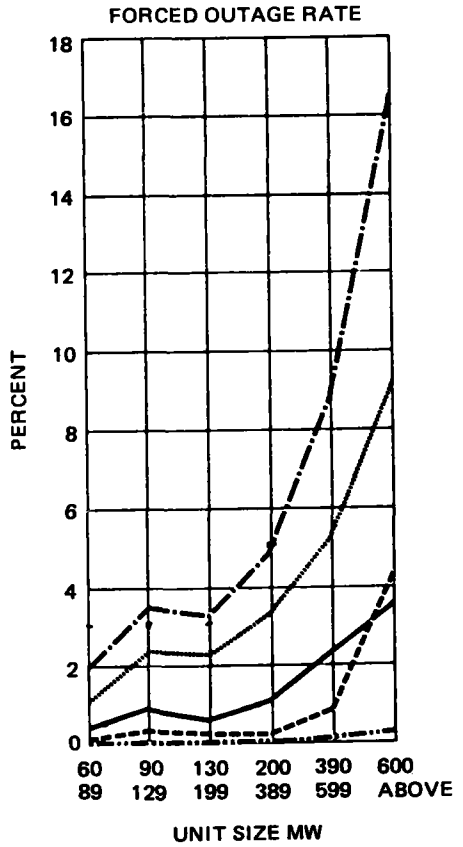

Figure 4-66. Fossil Unit and Major Equipment Outage Rate vs Unit Size

DRUM TYPE, ONCE-THRU (SUB-CRITICAL) AND ONCE-THRU (SUPER-CRITICAL) BOILERS
UNIT YEAR AVERAGES
1964-1973

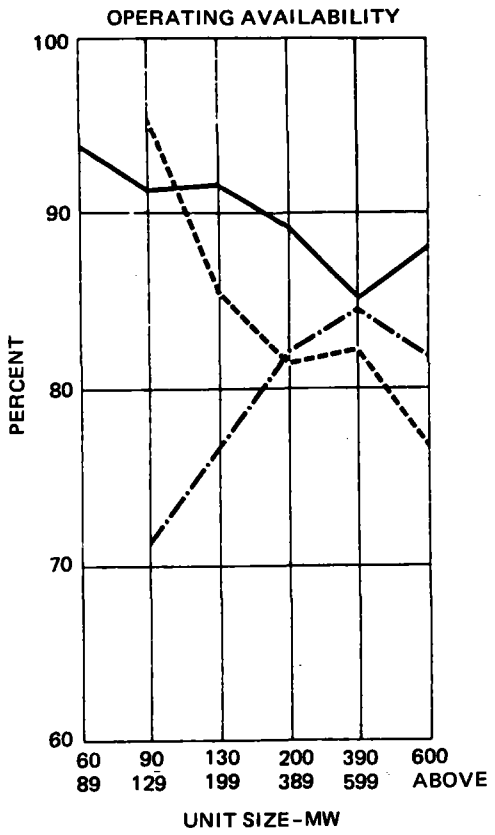

SAMPLE TABLE

DRUM-TYPE		
MW SIZE	NO. OF UNITS	NO. OF UNIT YRS
60-89	81	366
90-129	181	989
130-199	248	1623
200-389	205	1298
390-599	47	226
600-ABOVE	10	32
ONCE-THROUGH SUB-CRITICAL		
MW SIZE	NO. OF UNITS	NO. OF UNIT YRS
90-129	1	6
130-199	4	37
200-389	10	72
390-599	5	20
600-ABOVE	6	35
ONCE-THROUGH SUPER-CRITICAL		
MW SIZE	NO. OF UNITS	NO. OF UNIT YRS
90-129	1	8
200-389	13	89
390-599	45	206
600-ABOVE	40	126

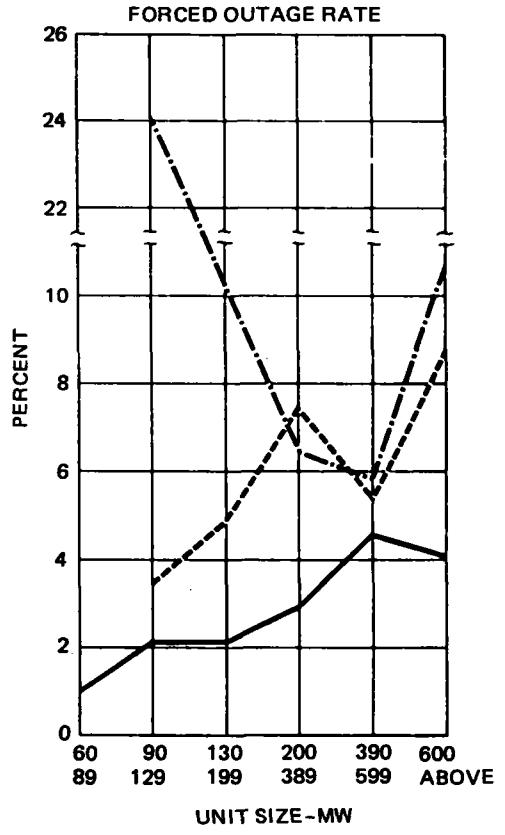

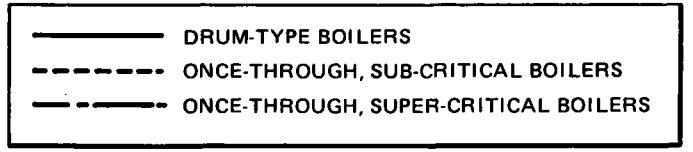

Figure 4-67. Boiler Outage Rate vs Unit Size

DRUM TYPE, ONCE-THRU (SUB-CRITICAL) AND ONCE-THRU (SUPER-CRITICAL) BOILERS
UNIT YEAR AVERAGES
1964–1973

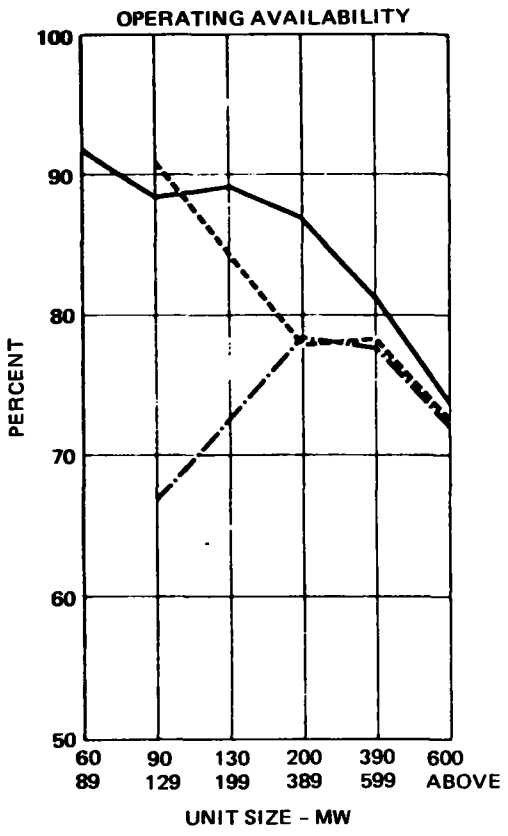

SAMPLE TABLE

DRUM-TYPE		
MW SIZE	NO. OF UNITS	NO. OF UNIT YRS
60-89	81	366
90-129	181	989
130-199	248	1623
200-389	205	1298
390-599	47	226
600-ABOVE	10	32
ONCE-THROUGH SUB-CRITICAL		
MW SIZE	NO. OF UNITS	NO. OF UNIT YRS
90-129	1	6
130-199	4	37
200-389	10	72
390-599	5	20
600-ABOVE	6	35
ONCE-THROUGH SUPER-CRITICAL		
MW SIZE	NO. OF UNITS	NO. OF UNIT YRS
90-129	1	8
200-389	13	89
390-599	45	206
600-ABOVE	40	126

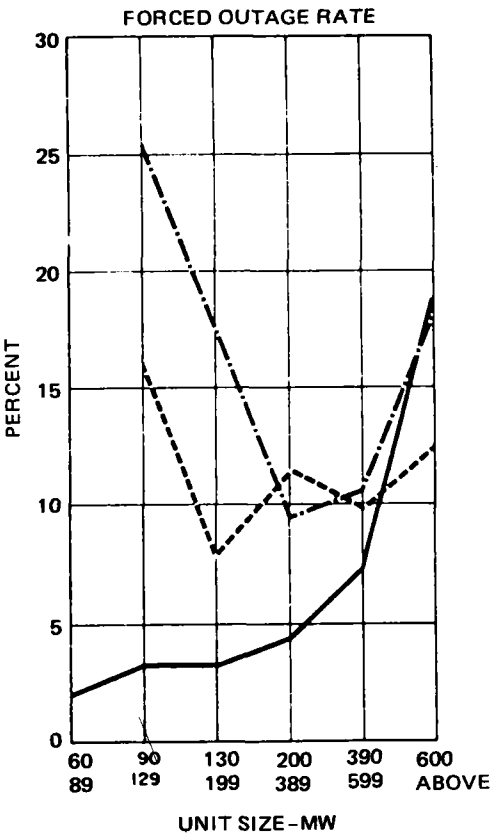

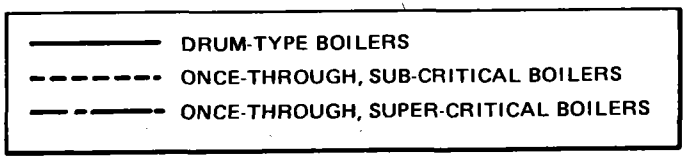

Figure 4-68. Unit Outage Rate vs Unit Size

Table 4-13

FOSSIL UNIT SUMMARY REPORT, 1964-1973
(FOSSIL UNITS 90-129 MW, 191 UNITS, 1043 UNIT YEARS)

Cause	Forced Outages	Maintenance Outages	Planned Outages
Boiler	167 Hr/Yr/Unit	149 Hr/Yr/Unit	465 Hr/Yr/Unit
Turbine	59	93	401
Condenser	4	57	242
Generator	23	58	299
Others	5	46	150
Unit	256	198	566

This allocation was based on historical data, some of which is discussed above, and preliminary reliability and maintainability calculations. The results are shown in Table 4-14.

Table 4-14

ORIGINAL AVAILABILITY ALLOCATIONS

Subsystem	Forced Outage (%)	Planned Outage (%)
Collector	0.51	0.25
Receiver	1.36	0.25
Thermal Storage	2.24	
Master Control	0.34	3.3
Electric Power Generation	1.75	
Total	6.20	3.80

Total Unavailability = 10.0%
Total Availability = 90.0%

The subsequent analysis and more comprehensive historical data showed this to be optimistic in some cases and pessimistic in others. The actual forced outage rates came out somewhat lower and the planned outage rates were higher, as discussed below. The collector has a much smaller unavailability due to the incorporation of the assumption, as used in the Commercial Power Plant field, that a reduction of less than 2% in power is not counted as a forced outage. The thermal storage is also much lower because of the incorporation of partial forced outage calculations and an assumption that the control system can be performed manually.

The receiver forced outage is somewhat higher due to a revised design and the electric power-generation subsystem (EPGS) is higher due to better historical data. The planned outage is also higher for the same reason.

The availability allocations should be updated as more and better information is obtained. Therefore, a new availability allocation of the 90% goal is shown in Table 4-15.

Table 4-15
REVISED AVAILABILITY ALLOCATIONS

Subsystem	Forced Outage (%)	Planned Outage (%)
Collector	0.01	0
Receiver	1.60	1.40
Thermal Storage	0.55	1.40
Master Control	0.05	0
Electric Power Generation	2.45	4.50
Total	4.66	5.34*

Total Unavailability = 10%
Total Availability = 90%

*Total assumes some preventive maintenance performed simulataneously

4.10.2.3 Availability Analysis

The availability analysis includes failure analysis, estimating the failure rate or mean time between failures (MTBF), and a maintenance analysis, estimating the mean time to repair (MTTR). The MTBF is then used to calculate the expected number of failures per year for the specific component. The value is then multiplied by the MTTR to determine the expected component unavailable hours per year. The subsystem, and then system, unavailable hours become the sum of the component unavailable hours with system considerations taken into account.

The failure analysis was initiated by performing failure mode effects analyses (FMEA) as shown in Table 4-16 to determine the applicable failure modes and their effects on the subsystem, system, personnel, and the environment. The first two effects are used to determine if a component failure and its attendant unavailability are to be charged against the system unavailability. For example, it was assumed that, in general, a failure of a temperature or pressure sensor would not affect system unavailability due to the fact that manual control of most functions is available and feasible.

A failure analysis is then conducted to determine the failure rate, the MTBF and, considering the number of the specific components and the required operating time, the number of failures per year. The basic failure rate data and the environmental adjustment factor (K) are obtained, in general, from historical data on similar components. The historical source on individual components are References 6 through 9, historical data on power plants and major subsystems are given in Reference 1.

Much of the data was from Reference 6, which was a study to determine the accident probabilities in commercial nuclear power plants. Data were obtained from reference handbooks, reports, and commercial power plant experience (both fossil and nuclear) and were considered for the applicable environment of standard operational power plant conditions. The compilation is particularly useful because it performs the analysis required to incorporate data from different reporting sources and different operational and environmental conditions and reports a median value and a 90% likelihood range for each component. It is also particularly useful for a solar power plant because it was performed for a commercial power plant.

Table 4-16 (Page 1 of 3)

FAILURE MODE EFFECTS ANALYSIS

PHASES

A - STARTUP
B - NORMAL SOLAR
C - LOW SOLAR
D - INTERMITTENT CLOUDS
E - FULLY CHARGED THERMAL STORAGE
F - NIGHTTIME
G - NORMAL SHUTDOWN
H - EMERGENCY SHUTDOWN
J - STANDBY

System THERMAL STORAGE
Analyst C. Boehmer
Date October 21, 1975

ITEM	FUNCTION	FAILURE MODE	CAUSE OF FAILURE	PHASE	EFFECT ON				DESIGN ALTERNATIVE	RECOVERY ACTION	COMMENTS
					SUBSYSTEM	SYSTEM	PERSONNEL	ENVIRONMENT			
TDWCV Desuperheater control valve	Control flow of water to Desuperheater (TD)	Failure to open, failure to remain onen	Random failure, loss of power, incorrect command signal	B	Actual loss - Desuperheater (TD) cannot desuperheat receiver steam, Thermal Storage Unit (TSU) cannot receive thermal energy, possible excessive thermal fluid temperature.	Actual loss - system cannot operate or continue to operate in phase B	Possible hazard from steam released from relief valve (RSRV)	Release of steam to atmosphere		Detect, isolate thermal storage heater, replace/ renair	Add relief valve (RSRV)
				C D E F J	None Flow in item not required	None	None	None		Same as above	Thermal storage unit must be charged with low temperature (650°F) steam
				A G H	Partial loss - Desuperheater (TD) cannot be used to reduce receiver steam temperature	Partial loss - system must startup and shutdown without Desuperheater (TD)	Possible hazard from steam released from relief valve (RSRV)	Release of steam to atmosphere		Same as above	
		Failure to control	Pandom failure, incorrect command	B	Actual loss - steam temperature to Thermal Storage Heater (TH) cannot be controlled	Actual loss - system cannot operate in phase B	Same as above	Same as above		Same as above	
				C D E F J	None Flow in item not required	None	None	None		Same as above	

PHASES

A - STARTUP
B - NORMAL SOLAR
C - LOW SOLAR
D - INTERMITTENT CLOUDS
E - FULLY CHARGED THERMAL STORAGE
F - NIGHTTIME
G - NORMAL SHUTDOWN
H - EMERGENCY SHUTDOWN
J - STANDBY

System THERMAL STORAGE
Analyst C. Boehmer
Date October 21, 1975

ITEM	FUNCTION	FAILURE MODE	CAUSE OF FAILURE	PHASE	EFFECT ON				DESIGN ALTERNATIVE	RECOVERY ACTION	COMMENTS
					SUBSYSTEM	SYSTEM	PERSONNEL	ENVIRONMENT			
TDWCV Desuperheater control valve (cont.)	Control flow of water to Desuperheater (TD)	Failure to control	Random failure, incorrect command	A G H	Partial loss - Desuperheater (TD) cannot be used to reduce receiver steam temperature	Partial loss - system must start-up and shutdown without Desuperheater (TD)	Possible hazards from steam released from Relief Valve (RSRV)	Release of steam to atmosphere		Same as above	
		Internal leak	Seal failure, structural failure	B	Possible loss - of fluid temperature control	Possible loss - possible loss of Thermal Storage Heater (TH)	None	None		Same as above	Output of Desuperheater will be at reduced temperature
				D	Partial loss- leakage of cold water into Desuperheater (TD) will reduce receiver steam temperature	Partial loss - thermal input to Thermal Storage Unit (TU) reduced	None	None		Same as above	Isolation values required
				A G H	Possible loss - possible loss of fluid temperature control	Possible loss - possible loss of Desuperheater (TD) system may be required to startup and shutdown without Thermal Storage Heater (TH)	None	None		Same as above	
				C E F J	None No fluid in unit	None	None	None		Same as above	
		External leak	Seal failure, structural failure	B D	Possible loss - loss of steam or water to atmosphere	Possible loss - Thermal input to Thermal Storage Unit (TU) reduced	Possible hazard from released steam or hot water	Release of steam or hot water to atmosphere		Same as above	

Table 4-16 (Page 3 of 3)

FAILURE MODE EFFECTS ANALYSIS

PHASES

A - STARTUP
B - NORMAL SOLAR
C - LOW SOLAR
D - INTERMITTENT CLOUDS
E - FULLY CHARGED THERMAL STORAGE
F - NIGHTTIME
G - NORMAL SHUTDOWN
H - EMERGENCY SHUTDOWN
J - STANDBY

System THERMAL STORAGE
Analyst C. Boehmer
Date October 21, 1975

ITEM	FUNCTION	FAILURE MODE	CAUSE OF FAILURE	PHASE	EFFECT ON				DESIGN ALTERNATIVE	RECOVERY ACTION	COMMENTS
					SUBSYSTEM	SYSTEM	PERSONNEL	ENVIRONMENT			
TDWCV Desuperheater Control Valve (cont.)	Control flow of water to Desuperheater (TD)	External leak	Seal failure, structural failure	C E F J	None No fluids in valve	None	None	None		Same as above	
				A G H	Possible loss - loss of steam or water to atmosphere	Possible loss - system may be required to startup and shutdown without Thermal Storage Heater (TH)	Possible hazard from released steam or hot water	Release of steam or hot water to atmosphere		Same as above	

The results of the availability analysis of the collector subsystem are shown in Table 4-17.

The component with the largest failure rate (smallest MTBF) is the Compudrive actuator, and a search of historical data on this component was negative. Therefore, data on similar components (linear actuators, variable-speed drives, constant-speed drives, gear boxes, etc) were used to make an estimate. A failure rate value of 10.4 per 10^6 hours was assigned to the primary mechanism, and a value of 7.6 per 10^6 hours to the larger secondary drive. The larger failure rate was applied for the primary drive because of the smaller sizes of bearings and expected higher contact stress on the lobe interface rollers.

The next largest failure item is the heliostat electronics where the failure rate was established by a part count and failure rates from Reference 8. The failure rates for the drive motors were obtained from Reference 6.

The results show that the predicted overall heliostat failure rate is 59 per 10^6 hours or an MTBF of 17,000 hr. The estimated yearly operating time is 3,300 hr based on a calculated average of 10 hr per day and a 330-day year. The figure assumes that the system will be unavailable for 35 days per year because of inclement weather. The results for a collector field of 1,760 heliostats show that we can expect to have 342 heliostat failures per year or 1.035 failures per day.

The failure rate for the field controllers was estimated at 8.6 per 10^6 hours by a parts count. This value, plus the estimated failure rate of the cables gives an MTBF of 83,056 hours and three failures per year or one failure per 110 days for the 74 field controllers in the Pilot Plant field.

There are eight transformers to provide power for the collector subsystem with an estimated failure rate of 0.8 per 10^6 hours. This value, plus the failure rate for the cables, and the distribution panel gives an expected failure rate of 0.11 per year.

Table 4-17 (Page 1 of 2)

COLLECTOR AVAILABILITY ANALYSIS

Item	Component	MTBF (Hr)	MTTR (Hr)	Pilot Plant		Commercial	
				Failures Per Yr	Unavailable Hr/Yr	Failures Per Yr	Unavailable Hr/Yr
1	Transformer	$1.2(10^6)$	7.96	0.02	0.16	0.27	2.15
2	Power Cables to Transformers	$9.3(10^6)$	3.11	0.003	0.009	0.04	0.23
3	Distribution Panels	$2.9(10^5)$	1.51	0.09	0.14	1.2	1.8
4	Field Controllers	$1.2(10^5)$	1.29	2.10	2.7	27.1	35
5	Cables to Field Controllers	$9.3(10^6)$	3.11	0.03	0.09	0.33	1.03
6	Field Controller Junction Box	$2.9(10^5)$	1.84	0.81	1.49	10.8	20
7	Heliostat Controller	$2.1(10^5)$	1.04	27.5	28.6	359	373
8	Cables to Heliostat	$9.3(10^6)$	1.50	1.22	1.80	16.0	24
9	Heliostat Circuit Breaker	$5.7(10^5)$	1.66	10	16.6	129	214
10	Azimuth Drive Motor	$5(10^5)$	2.15	11.6	25.0	151	325
11	Elevation Drive Motor	$5(10^5)$	1.54	11.6	17.9	151	233
12	Azimuth Position Sensor	$8.3(10^5)$	1.62	7.0	11.4	91	147
13	Elevation Position Sensor	$8.3(10^5)$	1.10	7.0	7.7	91	100
14	Azimuth RPM Counter	$7.4(10^5)$	1.33	7.8	10.4	102	136
15	Elevation RPM Counter	$7.4(10^5)$	1.05	7.8	8.2	102	107

Table 4-17 (Page 2 of 2)

COLLECTOR AVAILABILITY ANALYSIS

Item	Component	MTBF (Hr)	MTTR (Hr)	Pilot Plant		Commercial	
				Failures Per Yr	Unavailable Hr/Yr	Failures Per Yr	Unavailable Hr/Yr
16	Azimuth Primary Compudrive	$9.6(10^4)$	2.15	60	129	786	1690
17	Azimuth Secondary Compudrive	$1.3(10^5)$	2.68	44	118	575	1540
18	Elevation Primary Compudrive	$9.6(10^4)$	1.54	60	92	786	1211
19	Elevation Secondary Compudrive	$1.3(10^5)$	2.43	44	107	575	1396
20	Sun Sensor	$2(10^6)$	1.12	3	3.36	38	42
21	Mirror Panels	$1(10^6)$	1.12	35	39.2	454	508
22	Pedestal	$10(10^6)$	1.49	0.58	0.86	7.56	11.3
23	Reflector Structure	$2(10^6)$	2.96	2.9	8.58	38	112
24	Sun Sensor Pedestal	$10(10^6)$	1.01	0.58	0.59	7.6	7.6
	Total Failures Per Year			344.63		4498.90	
	Total Failures Per Day			1.04		13.63	
	Total Heliostat Outages Per Day			1.32		17.30	

A loss of a field controller will cause a loss of 24 heliostats and a loss of a power transformer will cause a loss of 220 heliostats. Therefore, as shown in Table 4-17, while the expected failure rate for heliostats is 1.035 per day the expected heliostat outage due to failures of all components (heliostats, field controller, and transformers) is 1.32 per day or 437 per year.

Any reliability improvement effort on the heliostats would logically be accomplished by installing components with a higher reliability; for example, Hi-Rel electronics components. It would be impractical to provide redundancy because a great deal of redundancy is already provided (1,760 heliostats) and the loss of one (or ten) heliostats does not materially affect system performance. In fact, the loss of a field controller, with the attended loss of 24 heliostats, only causes an average reduction of 1.36% in system power level. However, the loss of a transformer will cause a reduction of 12.5% in system power.

The results for the Commercial system collector field are also shown in Table 4-17. It was assumed that the MTBF and MTTR values for the individual components would be the same for the Commercial field and the Pilot Plant. However, the number of components change. The Pilot Plant collector field has 1,760 heliostats, and the Commercial field has 22,914 heliostas. The Pilot Plant field has 74 field controllers and eight power transformers, the Commercial field 955 field controllers and 104 power transformers. Therefore, the failures per year and the unavailable hours per year are scaled up by the ratio of components. The results show that we can expect to have 4,460 heliostat failures, 38 field controllers and 1.5 transformer failures per year, or a total of 13.6 failures per day for the entire field.

The determination of the repair times (MTTR) for the specific collector field components was aided by the experience gained on the SRE heliostat test program (discussed in Volume III, Section 6). The actual analysis used to generate the MTTR values given in Table 4-17 is discussed in Volume III, Section 5.2.3.

As discussed above, the accepted definitions of availability and forced outages do not count as a forced outage a failure that causes a reduction of system power of less than 2%. Therefore, the loss of three to four heliostats on a field controller will not affect system availability. A loss of a transformer will affect system availability as shown in Table 4-17.

The results of the availability analysis for the receiver are shown in Table Table 4-18. The receiver components are listed in the table, along with estimated MTBFs. The receiver configuration is depicted in Figure 4-6. The analysis assumes an operating time of 3,300 hr per year based on an average 10-hr day and 330 days of favorable weather. The failure rates were obtained as discussed above. The repair time (MTTR) estimates were obtained by considering the time to locate the failed component, any waiting time (time to obtain parts, time for the receiver to cool down, etc.), the time to repair or replace the component and the time to adjust and check out the repaired component.

The major failure items in the receiver are the 20 control valves with an estimated MTBF of 27,000 hr and predicted failure rate of about 3 per year. The 18 electronic temperature controllers are next with an estimated MTBF of 27,400 hr and an estimated failure rate of two per year. The preheater and boiler panels are next with a predicted one failure per year.

The calculations of system unavailability assume that if we have a failure of one of the control valves, a remote shutoff valve, one of the relief valves, a check valve, a filter on one of the preheater or boiler panels, the receiver must shut down for repair – a forced outage. However, a failure of one of the temperature or pressure sensors or one of the temperature controllers will not require a receiver shutdown. This is consistent with fossil power plant experience and assumes that manual control of the control valves is available and feasible. It is also assumed that the only applicable failure mode of the manual valves is failure to close(or open) when required and thus will not affect system availability. The external (and internal) leak failure mode is neglected.

The preventive maintenance assumes a 1-wk shutdown for tube cleaning every 18 mo.

Table 4-18 (Page 1 of 2)

AVAILABILITY ANALYSIS OF PILOT PLANT RECEIVER

Operation (Hr/Yr)	Item No.	Component	Mean Time Between Failure MTBF (Hr)	Failures/Yr	Mean Time to Repair MTTR (Hr)	Component Failure Outage FO Unavail (Hr/Yr)	Component Planned Outage PO (Hr/Yr)	System Unavail (Hr/Yr)	Comments
3300	RPWDV-1	Manual Valve	250,000	0.01	8.5	0.09	0	0	*
	RPWDV-24	Manual Valve	250,000	0.01	8.5	0.09	0	0	*
	RP	Preheater Panels	62,500	0.32	14	4.5	47	4.5	
	RPWRV-1 -2 -3	Relief Valves	100,000	0.09	9	0.81	0	0.81	
	RWIP-1	Pressure Sensor	1,000,000	0.003	6	0.018	0	0	**
	RWIT-1	Temperature Sensor	1,000,000	0.003	6	0.018	0	0	**
	RPWOP	Pressure Sensor	1,000,000	0.003	6	0.018	0	0	**
	RPWOT	Temperature Sensor	1,000,000	0.003	6	0.018	0	0	**
	RBTC-XX	Temperature Controller	27,400	2.17	6	13.0	0	0	**
	RBSOT-XX-1 -2	Temperature Sensor	1,000,000	0.12	6	0.72	0	0	**
	RBWFR-XX	Flowmeter	83,000	0.71	9	6.39	0	0	**
	RBTCV-XX	Control Valve	24,000	2.5	9	22.5	0	22.5	
	RBWF-XX	Filter	125,000	0.48	9	4.32	0	4.32	

*Not used during operations.
**Control component — non-critical.

Table 4-18 (Page 2 of 2)

AVAILABILITY ANALYSIS OF PILOT PLANT RECEIVER

Operation (Hr/Yr)	Item No.	Component	Mean Time Between Failure MTBF (Hr)	Failures/Hr	Mean Time to Repair MTTR (Hr)	Component Failure Outage FO Unavail (Hr/Yr)	Component Planned Outage PO (Hr/Yr)	System Unavail (Hr/Yr)	Comments
3300	RBWIV-XX	Manual Valve	250,000	0.24	8.5	2.04	0	0	*
	RBWDV-XX	Manual Valve	250,000	0.24	8.5	2.04	0	0	*
	RB	Boiler Panel	62,500	0.96	14	13.44	47	13.44	
	RNPV	Manual Valve	250,000	0.24	8.5	2.04	0	0	*
	RNCK-XX	Check Valve	250,000	0.01	8.5	0.09	0	0	*
	RSRV-1, 2	Relief Valve	100,000	0.07	9	0.63	0	0.63	
	RSVV	Manual Valve	250,000	0.01	8.5	0.09	0	0	*
	RFIV	Control Valve	24,000	0.14	9	1.26	0	1.26	
	RDSIV	Shutoff Valve	24,000	0.14	8.5	1.26	0	1.26	
	RFWDV	Shutoff Valve	24,000	0.14	8.5	1.26	0	1.26	
	RDSCK	Check Valve	250,000	0.01	8.5	0.09	0	0.09	
	RDSWV	Shutoff Valve	24,000	0.14	8.5	1.26	0	1.26	
	RFRV	Relief Valve	100,000	0.03	9	0.27	0	0.27	
	RFWL	Level Sensors	1,000,000	0.003	6	0.018	0	0	**
	RTWL	Level Sensors	1,000,000	0.003	6	0.018	0	0	**
	RFSOP	Pressure Sensors	1,000,000	0.003	6	0.018	0	0	**
	RFSOT	Temperature Sensors	1,000,000	0.003	6	0.018	0	0	**
	RSOP-1	Pressure Sensors	1,000,000	0.003	6	0.018	0	0	**
	RSOT-1	Temperature Sensors	1,000,000	0.003	6	0.018	0	0	
	RWBV	Control Valve	24,000	0.14	9	1.26	0	1.26	
	RWIV	Manual Valve	250,000	0.01	8.5	0.09	0	0	*
	RWISK	Stop Check Valve	250,000	0.01	8.5	0.09	0	0.09	
	RWF-1	Filter	125,000	0.02	6	0.12	0	0.12	
	RWIP-2	Pressure Sensor	1,000,000	0.003	6	0.018	0	0	**

*Not used during operations.
**Control component — non-critical.

The availability analysis of the thermal storage system is shown in Table 4-19. The configuration of the system is shown in Figure 4-6. The failure rates and repair times are determined as discussed above.

It was assumed that the required operating time of the thermal storage charging (input) circuit is 8 hr per day and 330 days per year or 2,640 hr. The duty cycle for the discharge (outlet) side is 3 hr per day or 990 hr per year. The thermal storage unit and its associated components must operate during both of these operations and during the time that steam is being provided for feedwater blankets and for the turbine seals. Therefore, it is assumed that these components have a 24-hr per day duty cycle or 7,920 hr per year.

The major failure item in the thermal storage subsystem is the pumps, where about one failure per year is expected. The heat exchangers (TH, TS, TB, and TP) require periodic tube cleaning; it is estimated this will require one week every 18 mo or about 112 hr/year. However, this will be performed simultaneously and at the same time that the tubes of the receiver and the feedwater heaters are cleaned and the preventive maintenance is performed on the turbine and the generator.

It is assumed that failures of the sensors and controllers will not affect system unavailability in accordance with current commercial power plant experience. The thermal storage unit has dual input and dual output paths. Therefore, a failure in one path will not cause a system shutdown but will only cause a reduction in charging or discharging to 50% of the rated value. The effect on system unavailability is treated as discussed in Section 4.10.2 and is chargable as one-half of the single component unavailability.

The master control subsystem availability was calculated by observing that the central computer and its perpherical equipment are not required for operations except for use in the synthetic track mode of the collector field. All other operations can be handled by the manual operators. It was calculated that the synthetic track mode would be required 25% of the time, assuming the closed-loop heliostat control configuration. It was also estimated that the MTBF of the central computer, and its associated equipment, is 500 hr and the MTTR is 1 hr. Using these three factors and a

Table 4-19 (Page 1 of 3)

AVAILABILITY ANALYSIS-PILOT PLANT THERMAL STORAGE

Item No.	Component	Operating Hr/Yr	Mean Time Before Failures (hr)	Failures (Yr)	Mean Time To Repair (Hr)	Component Forced Outage (Hr/Yr)	Component Planned Outage (Hr/Yr)	System Unavailability (Hr/Yr)	Comments
TD	Desuperheater	2,640	31,250	0.17	14.0	2.4	37	2.4	
TDTC	Controller	2,640	27,400	0.10	2.0	0.20	0	0	*
TDSFR	Flow Meter	2,640	83,000	0.03	4.5	0.14	0	0	*
TDTCV	Control Valve	2,640	23,800	0.11	4.0	0.44	0	0.44	
TDWFR	Flow Meter	2,640	83,000	0.03	4.5	0.14	0	0	*
TDWCK	Check Valve	2,640	250,000	0.01	4.0	0.04	0	0.04	
TDSIT	Temp Sensor	2,640	1,000,000	0.003	2.5	0.01	0	0	*
TDSIP	Pressure Sensor	2,640	1,000,000	0.003	2.5	0.01	0	0	*
TH-1,2	Thermal Storage Heaters	2,640	31,000	0.17	14.0	2.4	112	0.6	**
CC	Controller	2,640	27,400	0.1	1.5	0.15	0	0	*
THFFR-1,2	Flow Meters	2,640	83,000	0.06	4.5	0.27	0	0	*
TCP-1,2	Pumps	2,640	14,000	0.38	4.5	1.71	0	0.43	**
THWCK-1,2	Check Valves	2,640	250,000	0.02	4.0	0.08	0	0.02	**
THSIV-1,2	Control Valves	2,640	23,800	0.22	4.5	1.0	0	0.25	**
THFIV-1,2	Control Valves	2,640	23,800	0.22	4.5	1.0	0	0.25	**
THSFR-1,2	Flow Meter	2,640	83,000	0.06	4.5	0.27	0	0.065	*
TDSOT-1	Temp Sensor	2,640	1,000,000	0.003	2.5	0.01	0	0	*

*Control Component – Not Critical
**Redundant Components

Table 4-19 (Page 2 of 3)

AVAILABILITY ANALYSIS-PILOT PLANT THERMAL STORAGE

Item No.	Component	Operating Hr/Yr	Mean Time Before Failures (Hr)	Failures (Yr)	Mean Time To Repair (Hr)	Component Forced Outage (Hr/Yr)	Component Planned Outage (Hr/Yr)	System Unavailability (Hr/Yr)	Comments
THFOT-1,2	Temp Sensors	2,640	1,000,000	0.006	2.5	0.02	0	0	*
TDSOP	Press. Sensors	2,640	1,000,000	0.006	2.5	0.01	0	0	*
TDSOT-2	Temp Sensors	2,640	1,000,000	0.003	2.5	0.01	0	0	*
TFF-1,2	Filter	2,640	125,000	0.04	4.0	0.08	0	0.02	
TFFDP-1,2	Delta P Sensor	2,640	1,000,000	0.006	2.5	0.02	0	0	*
UMU	Ullage Monitor	7,920	27,400	0.29	2.0	0.58	0	0	*
TUFL-1,2	Level Sensors	7,920	1,000,000	0.02	2.5	0.05	0	0	*
TUFT-1,9	Temp Sensors	7,920	1,000,000	0.07	2.5	0.17	0	0	*
TUET-1	Temp Sensor	7,920	1,000,000	0.01	2.5	0.03	0	0	*
TUEV	Control Valve	7,920	23,800	0.33	4.5	1.5	0	0	*
TAFV	3-Way Valve	7,290	23,800	0.01	4.0	0.04	0	0.04	
TAFFR	Flow Meter	7,290	83,000	0.10	4.5	0.45	0	0	*
TAFP	Pump	7,920	14,000	0.57	4.5	2.6	0	2.6	
TSTCV	3-Way Valve	7,920	23,800	0.01	4.0	0.04	0	0.04	
TAWOC-1,2	Check Valve	7,920	250,000	0.06	4.0	0.24	0	0.24	**
TEP-1,2	Pump Valve	990	14,000	0.14	4.5	0.63	0	0.16	**
EC	Outlet Controller	7,920	27,000	0.29	2.0	0.58	0	0	*

*Control Component – Not Critical

**Redundant Components

Table 4-19 (Page 3 of 3)

AVAILABILITY ANALYSIS-PILOT PLANT THERMAL STORAGE

Item No.	Component	Operating Hr/Yr	Mean Time Before Failures (Hr)	Failures (Yr)	Mean Time To Repair (Hr)	Component Forced Outage (Hr/Yr)	Component Planned Outage (Hr/Yr)	System Unavailability (Hr/Yr)	Comments
TUBV	Bypass Valve	7,920	23,800	0.33	4.5	1.5	0	1.5	
TEPCK-1,2	Check Valves	990	250,000	0.01	4.0	0.04	0	0.01	**
TSFBV	Shutoff Valve	990	23,800	0.04	4.0	0.17	0	0.17	
TSFIV-1,2	Control Valves	990	23,800	0.08	4.5	0.36	0	0.09	**
TSTCV-1,2	3-Way Valves	990	23,800	0.08	4.0	0.32	0	0.08	**
TSSFR	Flow Meters	990	83,000	0.02	4.5	0.09	0	0	*
TSWCV-1,2	Control Valves	7,920	23,800	0.67	4.5	3.02	0	0.76	**
TS-1,2	Superheaters	7,920	91,000	0.17	82.0	14.3	112	3.58	**
TB-1,2	Boilers	7,920	91,000	0.17	82.0	14.3	112	3.58	**
TP-1,2	Preheaters	7,920	91,000	0.17	82.0	14.3	112	3.58	**
TBWL-1,2	Level Monitors	7,920	1,000,000	0.02	2.0	0.05	0	0	*
TSFFR-1,2	Flow Meters	990	83,000	0.02	4.5	0.09	0	0	*
TSWFR-1,2	Flow Meters	7,920	83,000	0.19	4.5	0.86	0	0	*
TSSOT-1,2	Temp Sensors	7,920	1,000,000	0.02	2.5	0.05	0	0	*
TSSOP-1,2	Pressure Sensors	7,920	1,000,000	0.02	2.5	0.05	0	0	*
TEPOP-1,2	Pressure Sensors	990	1,000,000	0.002	2.5	0.005	0	0	*
TU	Thermal Storage Unit	7,920	1,000,000	0.01	82.0	0.82	112	0.82	

*Control Component – Not Critical
**Redundant Components

coliector field operating time of 3,300 hr per year, the system unavailability for the master control is calculated at 0.05%. It was assumed that the software failure rate was negligible.

The unavailability for the electric power generation subsystem was not analyzed on an individual basis. The data of Reference 6 on the failure characteristics and availability of 191 commercial power plants in the 90-129 MW range over a 10-yr period (1,043 unit-years of operation) was used to determine the expected unavailability.

The data of Reference 6 show that the overall forced outage rate for this size plant is about 2.92%, the maintenance outage is 2.26%, and the planned outage is 6.47%, for a total unavailability of 11.65% and availability of 88.3%. If we eliminate the unavailability of the boiler, consider only the turbine, generator, condenser and other equipment, and assume that the same amount of common downtime exists (more than one component is repaired or maintained while the system is down), the values reduce to 1.031%, 1.428%, and 4.498%.

The availability analysis was based on the so called random failures which are described by the exponential failure distribution. Early failures ("infant mortality") and wearout failures were not considered. It is assumed that any components which historically have substantial infant mortality failures will have a "burn-in" prior to installation in the system. The only components that are considered to be in this category are the electronic components. It is also assumed that all components will have the required 30-yr operational life. A receiving inspection will be conducted to assure correct assembly of the components.

4.10.2.4 Availability Results

The results of the availability calculations are shown in Table 4-20.

The only collector subsystem components where a failure would cause even a partial system shutdown are the eight field transformers, their distribution panels, and the cables leading to the panels. The total unavailable hours

Table 4-20
SYSTEM AVAILABILITY RESULTS

Subsystem	Forced Outage	Planned Outage
Collector	0.01%	0%
Receiver	1.61	1.42
Thermal Storage	0.55	1.41
Master Control	0.05	0
Electric Power	2.46	4.50
Total	4.68	7.34
Adjust Planned Outage	4.68	5.52
Total Unavailability	10.20%	
Total Availability	89.80%	

from the three items amount to 0.309 hr per year. According to the rules of partial forced outage (Section 4.10.2), only one-eighth is counted against the system unavailability, giving a result of 0.00117%.

The results of the receiver availability calculations show 53.07 hr per year of forced outages. It is assumed that if any of the 24 panels have a failure, all panels must shut down. With an operating time of 3,300 hr/year the result is a forced outage of 1.608%. The planned outages are 47 hr/yr or 1.424%.

The results of the thermal storage analysis give 5.16 unavailable hours in the portion of the system with 2,640 operating hours, 16.80 unavailable hours in the 7,920 operating hour portion, and 1.40 unavailable hours in the 990-hr portion. This gives system unavailable percentages of 0.195%, 0.212%, and 0.141%, or a total of 0.549%. The planned outage is 112 hr in the 7,920-hr portion or 1.414%.

The master control unavailability is 0.050% with no planned outage.

The component analysis for the collector, receiver, thermal storage and master control did not distinguish between forced outages and maintenance

outages (see Section 4.10.2). Therefore, these factors for the EPGS will be combined into the forced outage classification, giving a total of 2.46%. The planned outage is 4.50%.

Table 4-20 shows a total of 4.68% for the forced outages and 7.34% for the planned outages. It can be assumed that some of the planned outages for the five subsystems will be conducted simultaneously. Using data from Reference 6, it was estimated that the planned outages would actually be composed of the 4.50% of the electric power generation subsystem plus 36% of the 2.83 of the remainder, or 5.52%. The total unavailability is then 10.19% and estimated availability 89.81%, compared with a goal of 90%.

4.10.3 Safety

The safety precautions for a solar thermal power plant consist of the conventional industrial or occupational safety laws in state and federal statutes and hazards controls unique to a solar plant.

4.10.3.1 System Safety Analysis

The system safety analysis included a brief analysis of preliminary hazards to obtain a preliminary picture of the hazard characteristics of the plant. It was initiated as part of the FMEA (Table 4-16) and then expanded into a safety analysis (Table 4-21). The analysis was designed to list conventional occupational hazards and the appropriate regulations and also to delineate any special problems.

The hazards include:

A. Platform, railing, stairway, ladder and elevator hazards on the receiver tower and elements of the thermal storage and EPGS.
B. Occupational noise exposure in the electrical power subsystem.
C. Flammable and combustible liquids in the thermal storage subsystem.
D. Venting and relief valve locations in the receiver, thermal storage, and EPGS.
E. Electrical equipment in all subsystems.
F. Ventilation in thermal storage and the EPGS.

Table 4-21

SAFETY ANALYSIS

SYSTEM THERMAL STORAGE

ANALYST C. Boehmer

DATE October 21, 1975

ITEM	FUNCTION	NORMAL HAZARDS	FAILURE HAZARDS	PREVENTATIVE/CORRECTIVE ACTION	STANDARD	COMMENTS
TDWCV Desuperheater Control Valve	Control flow of water to Desuperheater (TD)	Surface of item will be at high temperature (475°F)	Release of steam or hot water to atmosphere	Thermal Insulation, guard structure	Cal. OSHA Title 8 Subchapter 7	
				Identification of piping	Cal. Title 8 Subchapter 7	
				Provide relief valve(s) Location of relief valve(s)	ASME Section VIII Part UG-125	
				Structural Pequirements	ASME Section VIII	

The hazards specific to a solar power plant include the concentrated solar energy and the heating of the air by the receiver. Other hazards include the fire potential of the thermal storage fluid and the unexpected movement of heliostats. The heliostat hazard arises from the fact that the heliostat is normally under closed-loop control or under control from a remote location (master control). Thus, there is a possibility that unexpected heliostat movement could cause injury to personnel or equipment, even considering the slow movement of the mirror. A local control with a positive remote control lockout should be provided for use when maintenance is to be performed.

The fire potential from leaks or structural failure of the thermal storage subsystem arises because of the characteristics of the fluid. The fluid is a petroleum fraction similar to light lube oil. The flash point is 216 °C (420 °F) and the auto ignition point is 404 °C (759 °F). The operating point, 302 °C (575 °F), is between these values; therefore, a leak with a subsequent mixture with air would require an ignition source before a fire would be initiated. The presence of an ignition source can be assumed. Therefore, the potential of a fire as a result of a leak must be assumed. Control of such a hazard would include suitable leak control, ignition source control, and fire protection.

4.10.3.2 Occupational Safety

The conventional occupational safety is controlled by the appropriate Occupational Safety and Health Administration (OSHA) standards. In general, the Federal OSHA standards will apply but in some states (e.g., California) the state OSHA regulations will control. From a practical matter, the more restrictive of any two regulations should apply.

The 10-MW Pilot Plant will be constructed in San Bernardino County, California, therefore, the California Administrative Code, Title 8, Chapter 4 with revisions, will apply. The two subchapters of the code that are specifically applicable are subchapters 5 and 7. The applicable Federal OSHA rules are included in Parts 1910 and 1926 of Title 29 of the Code of Federal Regulations, with revisions.

The specific subchapters or safety orders of the California Administrative Code, Title 8, Chapter 4 that are applicable are:

- Subchapter 1 - Unfired Pressure Vessel
- Subchapter 2 - Boiler and Fired Pressure Vessel
- Subchapter 3 - Compressed Air
- Subchapter 4 - Construction
- Subchapter 5 - Electrical
  - Group 1 - Low-voltage Electrical Safety Orders (below 600V)
  - Group 2 - High-voltage Electrical Safety Orders (above 600V)
- Subchapter 6 - Elevator
- Subchapter 7 - General Industry
  - Group 1 - General Physical Conditions and Structures
  - Group 2 - Safe Practices and Personal Protection
  - Group 4 - General Mobile Equipment and Auxiliaries
  - Group 6 - Power Transmission Equipment, Prime Movers, Machine Parts
  - Group 9 - Compressed Gas and Air Equipment
  - Group 10 - Gas Systems for Welding and Cutting
  - Group 11 - Electric Resistance Welding
  - Group 13 - Cranes and other Hoisting Equipment
  - Group 15 - Noise Control Safety Order
  - Group 16 - Control of Hazardous Substances
  - Group 18 - Explosives and Fireworks
  - Group 20 - Flammable Liquids, Gases, and Vapors
  - Group 25 - Federal Regulations (Federal rules which have been adopted by California)
  - Group 27 - Fire Protection-Articles
- Subchapter 15 - Petroleum - Refining, Transportation, and Handling
- Subchapter 21 - Telecommunications Safety - Article 1

The applicable Federal regulations from Title 29 of the Code of Federal Regulations are Part 1926, Safety and Health Regulations for Construction, and Part 1910, Occupational Health and Health Standards. The applicable subparts of Part 1926 are as follows:

- Subpart A - General - All Sections
- Subpart B - General Interpretations
- Subpart C - General Safety and Health Provisions

Subpart D - Occupational Health and Environmental Controls
Subpart E - Personal Protective and Life Saving Equipment
Subpart F - Fire Protection and Prevention
Subpart G - Signs, Signals, and Barricades
Subpart H - Materials Handling, Storage, Use, and Disposal
Subpart I - Tools (hand and power)
Subpart J - Welding and Cutting
Subpart K - Electrical
Subpart L - Ladders and Scaffolding
Subpart M - Floors and Wall Openings, and Stairways
Subpart N - Cranes, Derricks, Hoists, Elevators, and Conveyors
Subpart O - Motor Vehicle, Mechanized Equipment, and Marine Operations
Subpart P - Excavations, Trenching and Shoring
Subpart Q - Concrete, Concrete Forms, and Shoring
Subpart R - Steel Erection
Subpart S - Tunnels and Shafts, Caissons, Cofferdams, and Compressed Air
Subpart T - Demolition
Subpart U - Blasting and Use of Explosives
Subpart V - Power Transmission and Distribution
Subpart X - Effective Dates

The applicable subparts of Part 1910 are as follows:

Subpart A - General - All Sections
Subpart B - Adoption and Extension of Established Federal Standards
Subpart D - Walking - Working Surface
Subpart E - Means of Egress
Subpart F - Powered Platforms, Manlifts, and Vehicle-Mounted Work Platforms
Subpart G - Occupational Health and Environmental Control
Subpart H - Hazardous Materials
Subpart I - Personal Protective Equipment
Subpart J - General Environmental Controls
Subpart K - Medical and First Aid
Subpart L - Fire Protection

Subpart M - Compressed Gas and Compressed Air Equipment
Subpart N - Materials Handling and Storage
Subpart O - Machinery and Machine Guarding
Subpart S - Electrical
Subpart Z - Toxic and Hazardous Substances

Additional safety regulations that will be imposed on the project will include:

A. National Fire Protection Association (NFPA) codes.
B. American National Standards Institute (ANSI) standards.

4.10.3.3 Operational Safety

Reflected Light Energy

There is a potential personnel and equipment hazard from the reflected sunlight from the heliostats and a potential personnel hazard from the radiated and reflected energy from the receiver. To understand these potential hazards, a brief study was conducted on the sensitivity of the human eye and skin to sunlight.

A drawing of the human eye is given in Figure 4-69. The light enters the eye through the cornea and is transmitted through the anterior chamber to the lens where the light is focused on the retina through the vitreous body. The iris of the eye acts as a control of the amount of light that enters the eye. The iris or pupil will automatically close down to about 2-mm diameter in bright light and will open to about 8 mm in a dark room. This gives a variation factor of 16 in the light that enters the eye.

The transmission of the several parts of the eye vary with the wavelength of the energy. The lens of the eye is a strong absorber of (and thus does not transmit) energies less than 400 nano meters (nm), which is known as ultraviolet radiation. The cornea is a strong absorber of infrared energy (wavelengths greater than 1,400 nm). Therefore, the damage from ultraviolet light occurs in the lens. The damage from infrared energy occurs in the cornea. Visible light (400 to 1,400 nm), however, is transmitted by the other parts of the eye to the retina. Therefore, if damage is to occur from visible light, or sunlight, it will occur in the retina.

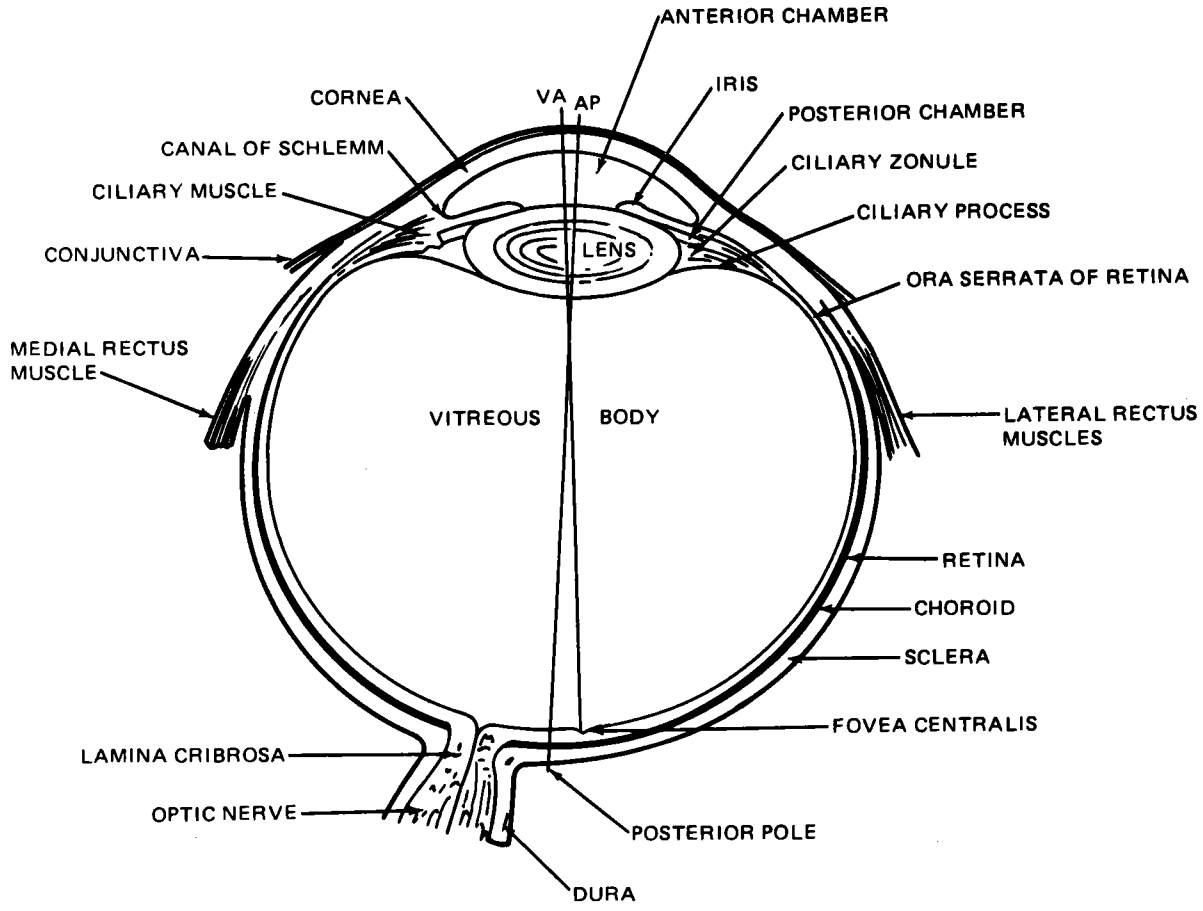

VA – VISUAL AXIS AP – ANTERIOR POLE

Figure 4-69. Horizontal Section of the Eyeball

The damage mechanism for the retina is primarily a temperature phenomenon. A temperature rise of 10° to 20°C will cause damage to the retina. However, the local temperature rise is a function of the irradiance (or power level) of the image on the retina, the size of that image, and the length of time the image is imposed on the retina. Therefore, we must investigate these three factors to determine the potential of retina damage from the operation of our heliostats and the receiver.

The retinal irradiance (power density on the retina) can be calculated by using equation 1 from Reference 10

$$E_R = 0.27\ L\ T\ D_p^{\ 2}\ V \qquad (1)$$

where

E_R = retinal irradiance (w/cm^2)
L = source radiance (w/cm^2-sr)
T = ocular media transmittance
D_p = pupil diameter (cm)
V = fraction of L between 400 and 1,400 nm

using direct sunlight as an example where $L = 1,600\ w/cm^2$-sr, $D_p = 2mm$, $T = 0.74$, and $V = 0.62$, the retinal irradiance is $7.93\ w/cm^2$.

The retinal image size can be calculated using the basic geometry and optics displayed in Figure 4-70, where D_H is the size of the source, f_H is the distance of the source and f_e is the focal length of the eye (17 mm). The retinal image (D_R) can then be calculated by

$$D_R = \frac{f_e D_H}{f_H} = f_e \tan\theta \qquad (2)$$

or for small angles

$$D_R = fe\ \theta \qquad (3)$$

If we use the sun again as an example where the subtended angle (θ) is about 9.3 mr the retina image is 158 μm.

$$D_R = \frac{f_e D_H}{f_H}$$

OR

$$D_R = f_e \text{ TAN } \theta = f_e \theta$$

FOR HUMAN EYE f_e = 17 MM

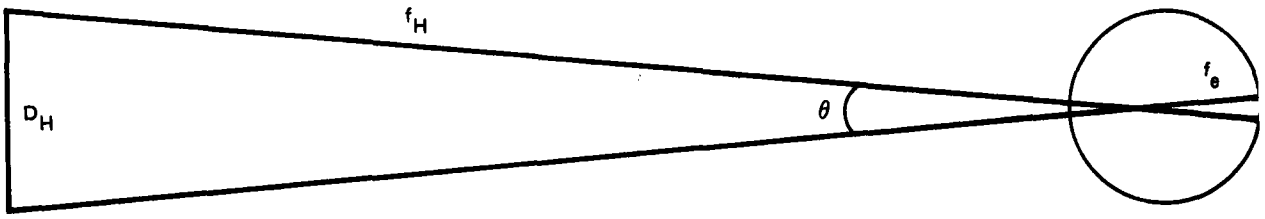

Figure 4-70. Relationship Between Source Size and Retinal Image

Using the above data for the sun (retinal irradiance of 12.8 W/cm^2 an image size of 158 μm) and the data on retinal injury thresholds in the monkey shown in Figure 4-71 from Reference 11, it can be seen that a exposure of about 300 sec is required to cause retinal damage.

Fortunately, since we live in a one-sun environment, it is difficult for person to experience a retinal burn by looking at the sun. If one attem to look directly at the sun the eye will automatically blink (close) and protect the eye. This blink reaction is rapid (~0.15 sec). Also, the p of the eye will contract to its minimum size. A further attempt to loo the sun becomes painful and one normally looks away. There are case where people have been under the influence of drugs, which removed th normal reflex actions, and eye damage was reported. In addition, the observation of a solar eclipse, where the pupil is dilated (larger than 2 to 3 mm), can cause retinal damage. Usually, however, cases of so retinitis are not irreparable and the patients recover (Reference 12). viewing the sun through an optical instrument such as binoculars will ir the size of the retinal image, which will decrease the heat transfer and increase the temperature and cause retinal damage in a shorter period time. (Observe the upper curve of Figure 4-72, which is also from Reference 2.) A comparison of absorbed retinal irradiance (which is a 50% of the incident retinal irradiance) vs retinal image size for various light sources is given in Figure 4-73 from Reference 10.

The retinal irradiance and retinal size received as a result of looking a the MDAC receiver (height = 17m) is shown in Table 4-22. As can be s the retinal image is larger than the sun image (up to 3,060 μm as oppos 158 μm), but the retinal irradiance is smaller by a factor of 1,500. Th receiver radiance was calculated by using the power radiated from the p which receives the greatest amount of incident radiation (10% of 0.3 MW or 0.03 MW/m^2. The radiance is then calculated by using Lambert's cosine law (Reference 13) by multiplying by π, which gives a radiance of 0.00955 MW/m^2-sr or 0.955 W/cm^2-sr. The retinal irradiance is then calculated using equation 1. As shown in Figure 4-72, the effect of imag size on temperature rise is slightly greater than linear (about 1.45),

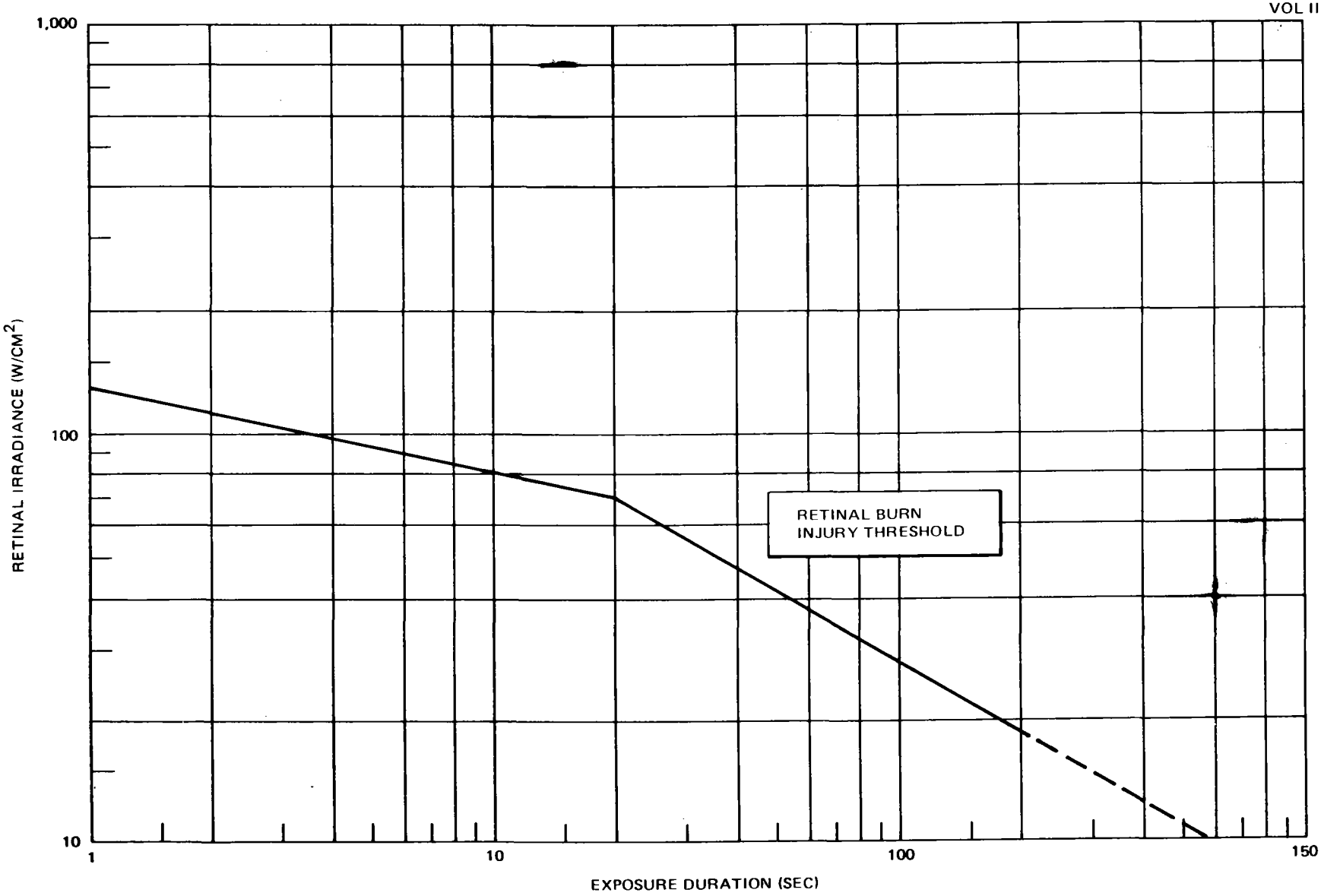

Figure 4-71. Retinal Injury Thresholds in Monkeys – 158 μM Solar Disk

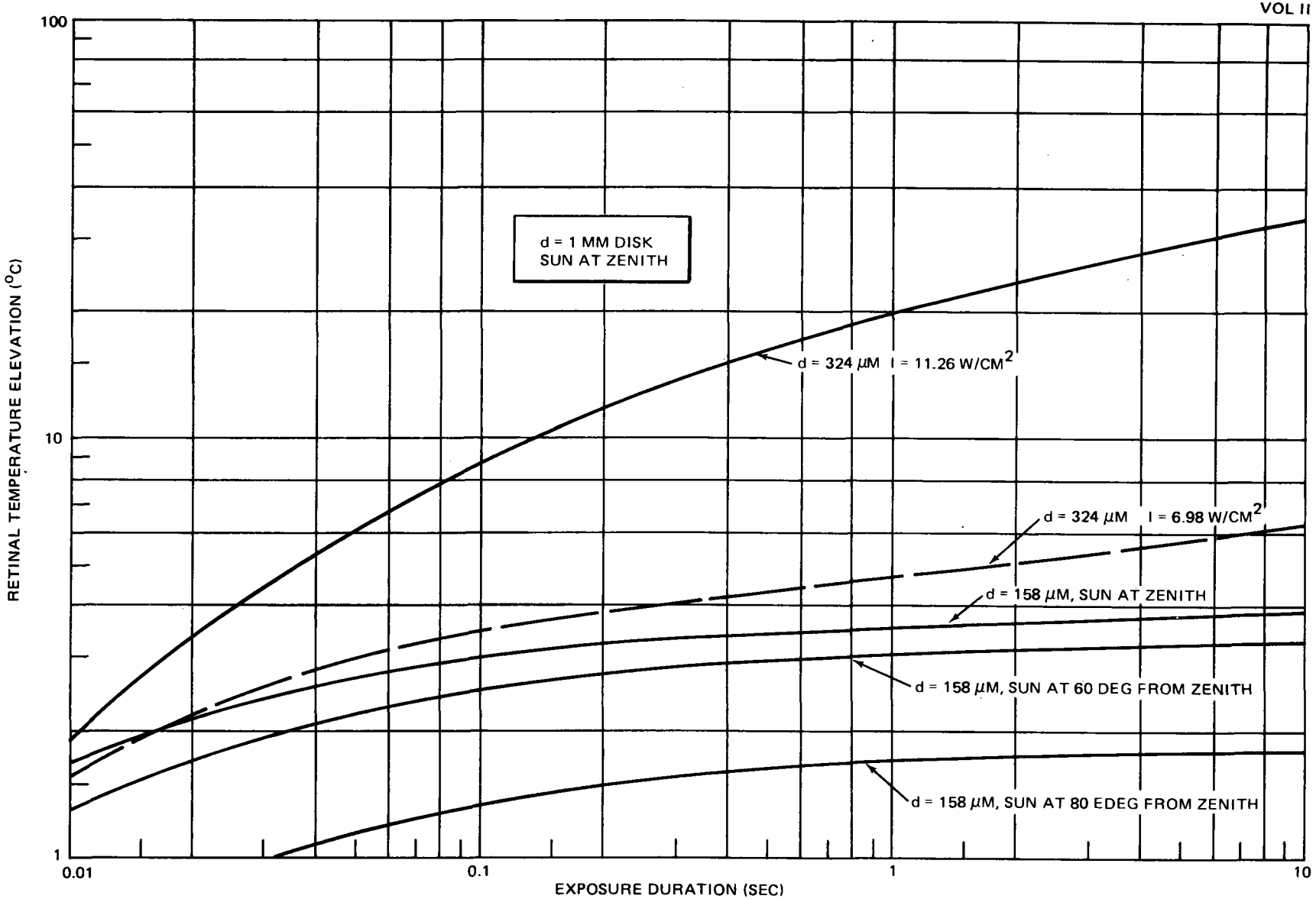

Figure 4-72. Temperature Elevation at Retinal Pigment (3 MM Pupil)

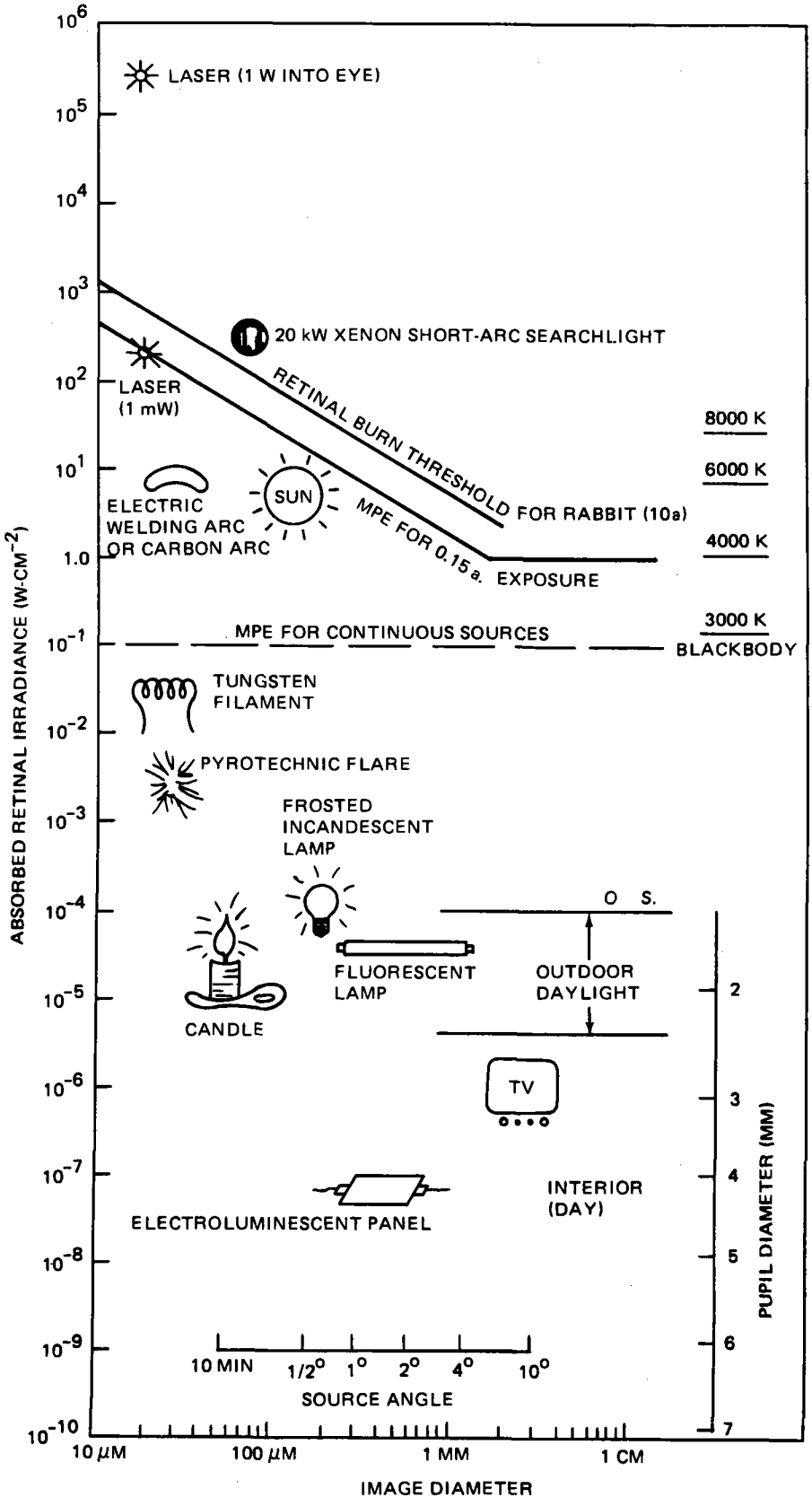

Figure 4-73. Absorbed Retinal Irradiance

Table 4-22

MDAC RECEIVER IRRADIANCE AND RETINAL SIZE

Distance From Base (m)	Radiance	Retinal Size	Retinal Irradiance
50	0.955 (W/cm^2-SR)	3,060 μm	0.0047 W/cm^2
100	↓	2,210	↓
200		1,340	
500		580	
1000		290	

therefore, the very small retina irradiance will assure a very small temperature rise and thus will assure that no retina damage will occur even for long periods of observation.

The retinal irradiance produced by personnel looking at the MDAC Pilot Plant heliostat will have a value produced by looking at the sun (7.93 W/cm^2) multiplied by the reflectance of the heliostat (0.88) or 6.98 W/cm^2.

The retinal irradiance produced by the MDAC Commercial heliostat is somewhat higher due to the higher reflectance (0.91) at 7.22 W/cm^2.

The retinal image size produced by personnel looking at the MDAC Pilot Plant heliostat, which is focused by the slight canting of the six segments, is obtained by using equation 2 and the dimensions of the heliostat (660 cm by 651 cm), the heliostat focal length of 350m (assumes that a person is standing at the focal point -- a worst case situation) and by calculating an equivalent circle that has the area of the image of the sun on the mirror. This gives a retinal image diameter of 323.5 μm. The temperature rise of this image size and irradiance should appear as shown in Figure 4-72.

The MDAC Commercial heliostat, which has a flat mirror configuration, will produce a retinal image with a diameter equal to or less than that produced by the sun (158 μm).

The possibility of retinal damage from viewing the Pilot Plant heliostat is higher than that from viewing the sun as shown in Figure 4-74. The effect of standing in the beam of the Commercial heliostat and looking at the mirror will be less than looking directly at the sun. At the present time, there is no nationally accepted criteria or standard for the maximum amount of sun light or white light to which personnel can be exposed. Such limits, called maximum permissible exposure (MPE) limits, have been established for narrow-wavelength coherent laser beams by the American National Standards Institute and have been universally accepted (Reference 14). A standard has, however, been proposed by the US Army Environmental Hygiene Agency in Reference 10 and is shown in Figure 4-73. This criteria, reproduced in Figure 7-74, is set a factor of 4 below the 10-sec retinal burn threshold for rabbits but specified for a 0.15-sec exposure, the length of time for the eye blink reaction.

The retinal injury threshold for 0.15 sec is about a factor of 3 above that for 10 sec((Figure 4-74). Also, the threshold injury threshold for rabbits is known to be lower than the thresholds for humans by a factor of 5 to 20 (Reference 10). Therefore, the safety factor in the criteria of Figure 4-74 is at least 12. The relationship of the absorbed retinal irradiance and image size for the two MDAC heliostats is plotted on Figure 4-74. The data show that the MDAC pilot plant heliostat hazard potential is marginal but safe, considering the margin of safety in the criteria. The Commercial heliostat is safer than viewing the sun.

A second potential hazard from the reflected sunlight exists in the possibility of skin burns. A worst-case situation, a person standing at the focal point of the Pilot Plant heliostat, can be calculated by determining the size of the image at the focal point (3.26m), and thus the irradiance at this focal point (0.37 W/cm^2). It can be pointed out that this irradiance from the heliostat (0.37 W/cm^2) is approximately 3.3 times the maximum solar irradiance (0.11 W/cm^2). To determine if this is a potential hazard and the magnitude of that hazard, we can refer to Figure 4-75 from Reference 11, which gives the threshold for injury to pig skin as a function of time. As shown in Figure 4-75, the threshold time for injury from the Pilot Plant heliostat, at an irradiance of 0.37 W/cm^2, is over 80 sec. The threshold time for the

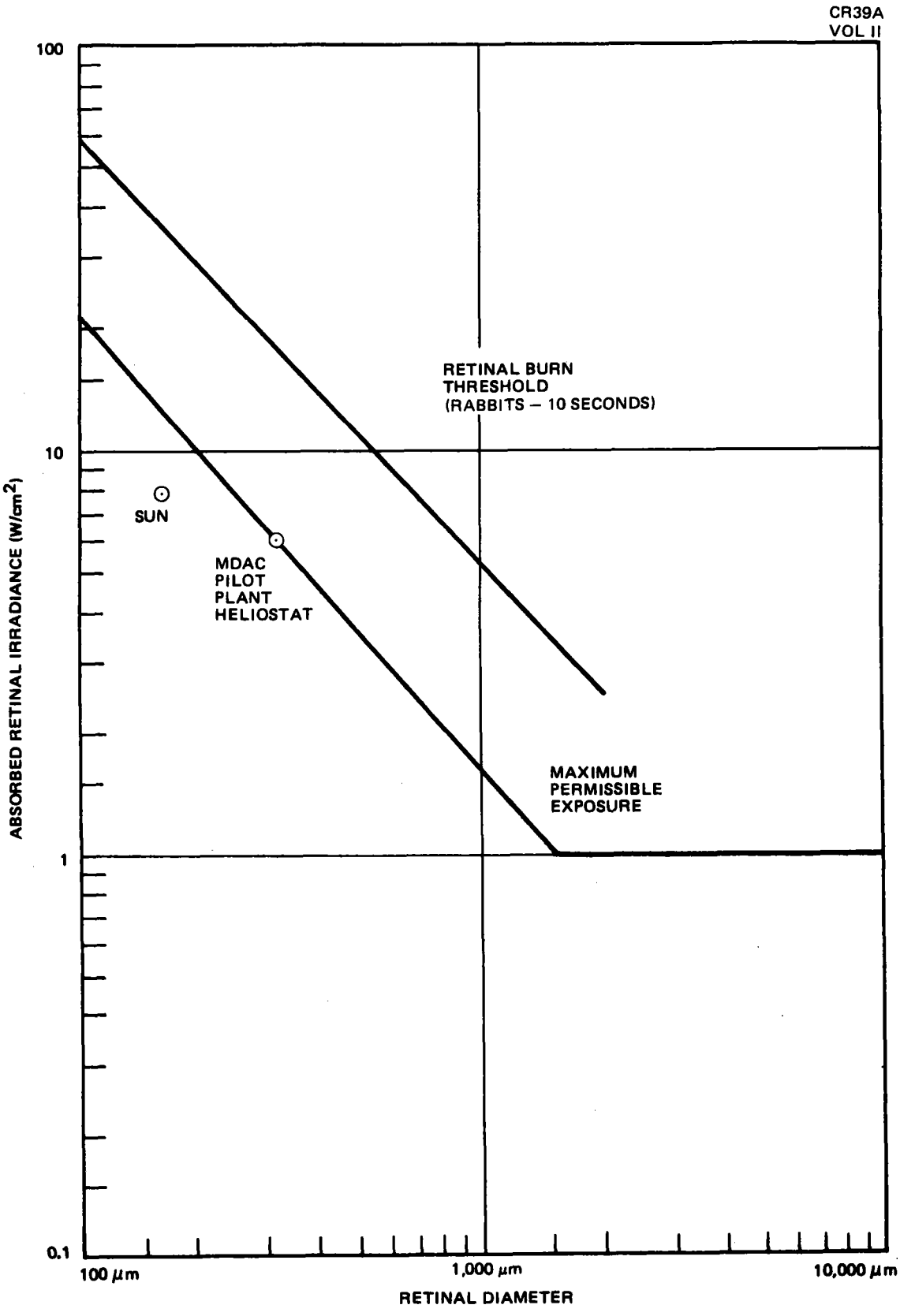

Figure 4-74. Retinal Burn Threshold Safety Exposure

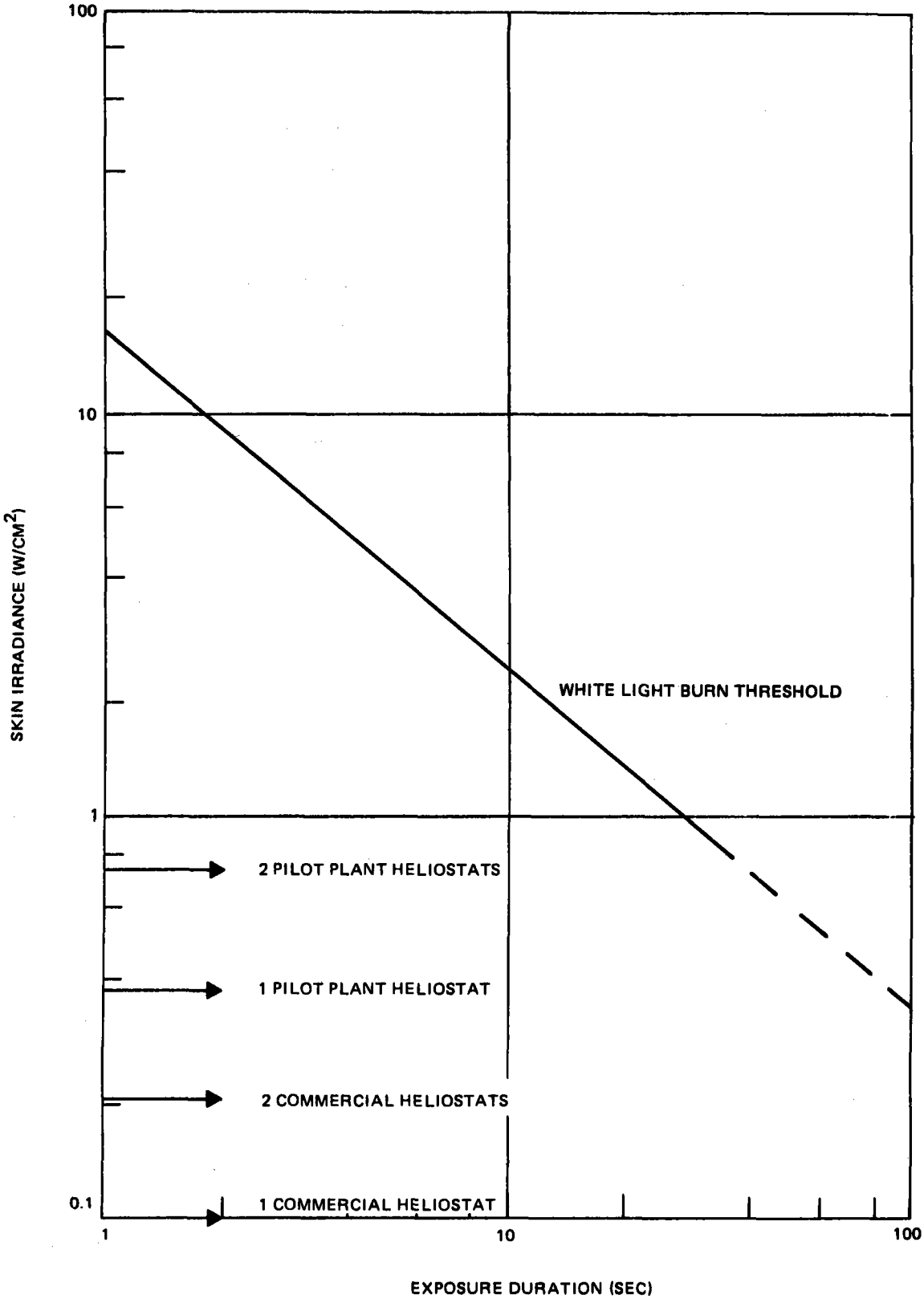

Figure 4-75. Pig Skin Injury Data

Commercial heliostat is many minutes. This means that a person would have to stand at the focal point of the Pilot Plant heliostat for over 80 sec (longer for the Commercial heliostat) before an injury could occur. In fact, the person would have to move with the moving image of the sun because, with a fixed mirror, the sun will move off the specific spot in about 20 sec. Also, the person would have to ignore the heat generated by the beam.

The above discussion can lead to a conclusion that there are no hazards to personnel from a single MDAC Pilot Plant or Commercial heliostat.

It has been estimated that an irradiance of over 5 suns (0.55 W/cm^2) is required to initiate combustion in a brush. The irradiance from the MDAC Pilot Plant heliostat is only about 3.3 suns (0.37 W/cm^2); therefore, a single MDAC heliostat should not present a brush fire hazard.

The hazards from multiple heliostats are potentially more severe, but operational procedures and suitable personnel exclusion areas will eliminate the hazards or reduce them to acceptable levels.

Potential problems include:

A. Personnel or equipment situated at a point on the ground where multiple beams intercept.
B. The possibility that an aircraft (or glider or balloon) will appear at a point above the collector field and intercept the solar beam from a number of heliostats.

Either or both of these can occur during normal operations as the heliostat field is activated or deactivated, or during heliostat storage operations, or as a result of heliostat failures.

When the collector field is activated in the morning (or after a cloud passage) and deactivated in the evening, the heliostats will be controlled by the master control in such a way that the focal point of the several heliostats

will move in a controlled and safe manner. For example, the focal point can be designated as a point on the ground (in a personnel exclusion area) and then moved to the receiver on a path which does not intercept any equipment. This should preclude any hazards to personnel, equipment, or brush on the ground. However, there will be a volume of airspace where a potentia hazard will exist.

To determine the dimensions of this airspace, a brief analytical study was conducted. An observer above the receiver and looking down toward the heliostat field will see sunlight reflected from a small number of heliostats. The actual number is beyond the scope of this analysis. However, an observer at an altitude of twice the tower height (160m) would be exposed to a power level of less than one sun because of the fact that a one-to-one image is located at that point. Above that level, less than one heliostat is seen at any location. An approximate value of the average irradiance may be obtained from

$$E_c = \frac{\dot{q} f_{gc} \overline{C}}{(h/H - 1)^2} \tag{4}$$

where

E_c = irradiance outside eye
$\dot{q}$ = solar power level
f_{gc} = ground cover fraction
$\overline{C}$ = average incidence angle cosine
h = observer altitude
H = tower height

However, the peak irradiance will occur when looking down at the closest-in heliostats where the angle is 52.2 deg. The irradiance from this heliostat can be calculated from

$$E = \frac{A_p}{(h/\sin \phi)^2 \pi (\theta/2)}$$

where

A_p = area of heliostat (37.58 m^2)

ϕ = angle of heliostat

θ = sun angle (9.3 mr)

from this equation we can calculate that the irradiance from these mirrors are 3.3 suns at 160m, 2.14 suns at 200m, 0.94 suns at 300m, and 0.54 suns at 400m altitude.

Another aspect of the airspace problem is during heliostat stowage. If the heliostats are stowed face down, there is no possibility of a reflection of the sun. The only possibility of a potential problem when the heliostats are stowed in a vertical position is when the sun is at a zero degrees elevation and at that time the irradiance is very low. A computer study of stowage in a face-up position showed that the maximum solar irradiance, under any condition, at 305m (1,000 ft) from one heliostat is 0.231 W/cm^2 or about 2.1 suns. With accurately controlled stowage position, the laws of optics will preclude the observer seeing the sun in more than one mirror at any instant of time at this altitude. To ensure that the heliostat beams do not intersect, a divergent stowage orientation with the divergence between adjacent heliostats greater than the stowage orientation error will be used if face-up stowage is used. Hence, the only crossing beams will be from widely separated heliostats. The effect of one heliostat with this solar magnification was shown to be safe in the discussion above for both skin burn and retinal burn. At higher altitudes, one can see the sun in more than one heliostat, but the irradiance will drop due to (1) divergence of the light past the focal point of a central focus heliostat and (2) open spaces between heliostats. Either of these effects is sufficient to ensure continued safety with increased altititude.

The probability of two simultaneous random independent failures (within the repair time) is about 7 (10^{-5}). This must be multiplied by the probability that that both heliostats would fail in such a way that both beams are pointed at the same spot (1×10^{-5}) and the probability that someone would be in this spot at that time. It can be seen that this probability is less than 7×10^{-2} and thus extremely low.

This analysis has shown that there are no hazards to ground-based personnel which cannot be controlled by proper procedures and that there are no hazards above about 300m altitude. Both of these conclusions are subject to further analysis and the acceptance of an MPE for visible light.

Since it has been shown that heliostat failures are most unlikely to produce an unsafe condition, it is concluded that multiple, redundant power cables to individual heliostats are not required. Redundant cables to components which control multiple heliostats (transformer, field controllers) may be necessary. Redundant heliostat cables would only prevent 0.36% of the heliostat failures (1.25 failures per year out of 345). Nor is automatic stowage of a failed heliostat, communication link, or power supply required. It is much more cost-effective to stow a failed heliostat using the mobile test set. The mobile test set is capable of stowing or repairing a failed heliostat within 3 hr, regardless of the nature of the failure. If the heliostat is completely inoperable, an opacifying solution, can be applied to prevent specular reflection from the heliostat. Other procedures available include commanding stowage through the field controller or heliostat controller, providing manual stowage through an auxiliary power supply direct to the drive motors, and direct drive of the drive unit through an auxiliary motor (1/2-in. drill applied to the input shaft).

With the procedures indicated above, MDAC believes that the operation of the Pilot Plant, or the Commercial Plant, will present no undue hazards.

The overall conclusion of the safety analysis completed to date is that with proper compliance with applicable Federal and state OSHA requirements, and other applicable standards, and with proper safety procedures (personnel exclusion area, operating constraints, etc.) the Pilot Plant and the Commercial Plant can be operated in a safe manner.

Thermal Connection Plumes

The receiver operates at high temperature atop a high tower, and the neighboring air is heated by a combination of radiation and conduction from the receiver, and by absorption of approaching solar radiation. The question at issue is whether or not, by virtue of the intense local heating of the air,

thermal convection generates a plume of sufficient energy to present a significant hazard (for example, to overflying aircraft). Rough estimates were made of the magnitude of such plumes. The estimates show that there is no significant hazard associated with this thermal plume.

For the sake of discussion we will consider solar thermal power system designed to deliver 100 MW of electrical power. At 20% efficiency, the cylindrical receiver intercepts 500 MW of solar radiation. It is assumed to have a diameter of 17m, a height of 25m, and a surface temperature of 800°K. The results do not depend critically on these parameters.

As a basis for comparison, a Boeing 747, which leaves a hazardous turbulent column of air behind it, can generate 150 MW of thrust power (four engines of 50,000-lb thrust at perhaps 600 fps exhaust velocity). Air-cooled fission power systems have been built which generate roughly 200 MW of electrical power and these systems must dispose of perhaps 300-400 MW of waste heat by means of huge natural convection cooling towers (Reference 15). The local air-heating power near the receiver of a solar thermal power system is inevitably one or two orders of magnitude smaller than either the 747 thrust power or the cooling tower heat-rejection system power.

The receiver radiates approximately as a blackbody the thermal emission then being partially absorbed by the local atmosphere. The approximate thermal emission from the cylindrical surface is in MKS units:

$$W_E' = \sigma T^4 \pi DL$$

$$= (5.67 \times 10^{-8}) (800)^4 \pi (17) (25) \text{ Watt}$$

$$= 31 \text{ MW}$$

The fraction of this energy absorbed locally was estimated by four different approximate methods, which agreed sufficiently well to generate some confidence in the order of magnitude of the result. Just one method will be presented here. As a worst case, a hot day was chosen, on which the air

might hold about 20 gm/m^3 of water vapor. The standard subarctic summer model atmosphere is appropriate. An 800°K blackbody spectrum dE/d (lnλ), plotted against the logarithm of the wavelength, peaks at 4.6 μm and has roughly 70% of its energy in the band of 2.5 to 7.4 μm. Roughly 20% of the total radiation lies in the band 5.43 to 7.35 μm, which is strongly absorbed by water vapor. For our purposes, it is sufficient to ignore absorption outside this band. In order to estimate absorption inside this band, line absorption data calculated by McClatchey (Reference 16) were used. Sea-level absorption coefficients of 44 lines of CO laser radiation were assumed to be representative of the band. The results of the approach are plotted in Figure 4-76, which indicates for example that 1 MW is absorbed within 10m of the receiver surface, and 3 MW within 40m.

The absorption of approaching solar radiation, in a worst-case estimation, is attributed primarily to aerosol absorption. On a hazy day (visibility 5 km) the sea-level aerosol absorption coefficient exceeds its clear day (visibility 23 km) value by a factor 4.5 in McClatchey's model (Reference 17). Over a broadband of wavelengths (0.5 8 μm) the clear-day absorption coefficient does not exceed 0.01 km^{-1}, and it has approximately this value over much of the solar spectrum (Reference 17). Thus, $\alpha = 0.045\ km^{-1}$ is a reasonable estimate of the absorption coefficient for haze absorption of solar radiation near the receiver. The power absorbed is approximately $W_A = P_R \alpha R$, where P_R = 500 MW is the approaching solar radiation, and this line is also plotted in Figure 4-76.

To calculate heating by convection from the receiver, a no-wind, natural convection condition was assumed. No expression for the heat transfer at sufficiently high Grashof numbers is immediately available, and we must depend upon an extrapolation of the expression (Reference 18).

$$Nu = 0.13\ (GrPr)^{1/3},\ 10^9 < GrPr < 10^{12},$$

beyond the upper limit. Here

$$Nu = \frac{gL}{k\theta} \qquad Gr = \frac{g\theta L^3}{V2_T} \qquad Pr = \frac{V_p C_p}{k}$$

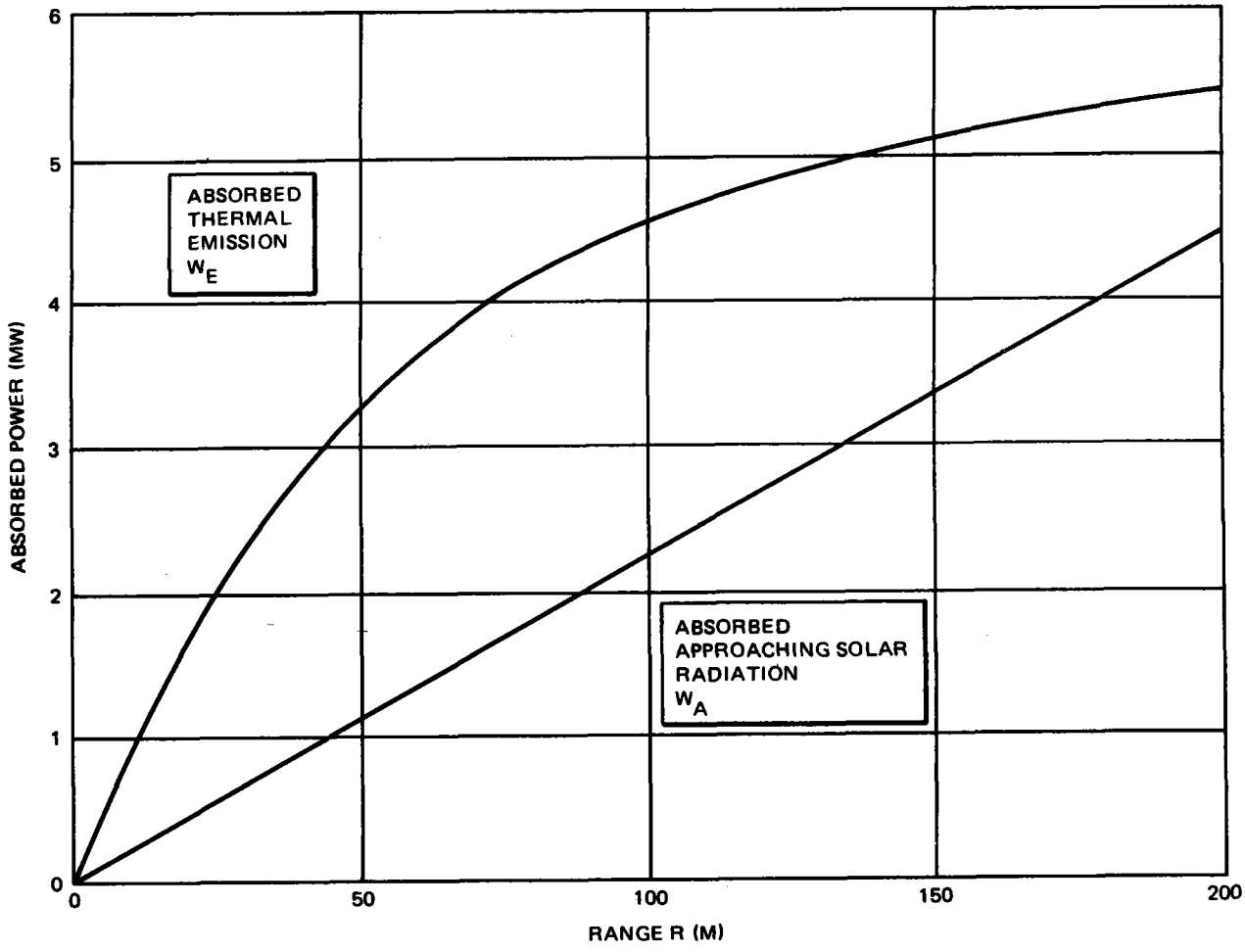

Figure 4-76. Radiation Absorbed Within a Distance R from the Receiver Surface

are the Nusselt, Grashof, and Prandtl numbers, and q is the heat transfer per unit area. For air the Prandtl number is Pr = 0.72, and the total convective heating from the receiver is

$$W_C = q \pi DL = 0.12\ Gr^{1/3} \frac{k\theta}{L} \pi DL,$$

where the heat transfer per unit area is dependent of distance from the leading edge in the turbulent regime. We adopt the following values:

g = Acceleration of gravity = 10 m/s,

θ = Temperature difference = (800-300)°K = 500°K,

L = Cylinder height = 25m,

υ = Kinematic viscosity = $\frac{\mu}{\rho}$

$$= \frac{1.72 \times 10^{-4} \text{ poise}}{1.29 \times 10^{-3} \text{ g/cm}^3} = 1.33 \times 10^{-5} \text{ m}^2/\text{s},$$

T = Mean Temperature = $\sqrt{(800)\ (300)°K}$ = 500°K,

k = Thermal conductivity = 5.6×10^{-5} cal/s cm-°K

= 0.0234 Watt/m-°K

Then the Grashof number is

$$Gr = 9 \times 10^{14},$$

the heat flux per unit area is

$$q = 5.4 \text{ KW/m}^2,$$

and the total convection heating is

$$W_C = 7.2 \text{ MW}.$$

We surmise that this heat is deposited in a boundary layer which grows to a thickness of 1 to 5m at the top of the receiver. Closer estimates of the boundary layer thickness are difficult to make. Nevertheless, a conservation of energy argument allows us to estimate the product $U\delta$ of the mean flow velocity and the boundary layer thickness. The energy goes mostly into

increasing the enthalpy of the air, the changes in potential and kinetic energies being relatively small. The boundary layer mass flow is

$$\dot{M} = \rho U \delta \pi D = \frac{W_C}{1/2\ C_p \theta} = 30 \text{ kg/s},$$

where we use

$$\rho = 1 \text{ kg/m}^3,$$

and

$$C_p = 1,005 \text{ Joule/kg-°K}.$$

If δ is in the range of 1 to 5m, then the flow velocity is in the range of 0.1 to 0.5 m/s.

The possible hazards are due to the fact that the heated air is hot, and it will mix turbulently with colder air and rise in the manner of ordinary smoke-stack plumes to moderate altitudes, depending on the weather (particularly on the temperature lapse rate). The mass flow has been calculated to be of the order of 30 kg/s, and the flow velocity is estimated to be less than 0.5 m/s. These values obviously present no hazard when they are compared with ordinary wind and turbulence levels.

The radiation heated air beyond the natural convection boundary layer is also expected to rise due to buoyant convection. Following Smith (Reference 19, page 606), we argue as follows:

The power $W_R = W_E + W_A$ is absorbed in an annular cylindrical volume

$$V = \pi (D+R) RL,$$

in which the air is heated according to

$$\rho C_p U_c \frac{T}{L} = \frac{W_R}{L}$$

as it rises with mean velocity U_c. The vertical component of the momentum conservation equation suggests

$$\frac{1}{2} \rho U_c^2 = g L(-\Delta\rho) = \frac{gL\rho}{T} \Delta T,$$

as the buoyancy force accelerates the air to velocity U_c. These two equations then lead to

$$U_c = \left[\frac{2(\gamma-1)}{\pi \gamma} \frac{W_R g L}{(D+R) RP} \right]^{1/3}$$

We adopt (see Figure 4-76)

γ = ratio of specific heats = 1.4,
W_R = radiation absorbed within 20m = 2 Mw,
L = receiver height = 25m,
D = receiver diameter = 17m,
R = representative distance from receiver = 20m,
P = atmospheric pressure = 10^5 Newton/m^2,

and obtain the representative convection velocity

$$U_c = 0.5 \text{ m/s}$$

The mass flow in this case is

$$\dot{M} = \rho U_c \pi (D+R) R$$

$$= (1.3 \text{ kg/m}^3) (0.5 \text{ m/s}) \pi (37\text{m}) (20\text{m})$$

$$= 1,500 \text{ kg/s},$$

some 3,000 times that generated in the natural convection boundary layer. The temperature rise may be expected to be correspondingly smaller, and it turns out to be

$$\Delta T = \frac{U_c^2 T}{2gL} = \frac{(0.5)^2 (300)}{2(10)(25)} °K = 0.15°K.$$

All the foregoing analysis is valid for a neutrally stable atmosphere with an adiabatic lapse rate. The adiabatic lapse rate is about 10°K/km, which leads to a natural temperature difference of 0.25°K between the top and bottom of the receiver. Thus, in a stable atmosphere with a smaller lapse rate, the buoyant convection plume generated by the absorbed radiation is likely to be stabilized and rise only tens of meters. We conclude that the buoyant convection plume associated with radiative heating of the air near the receiver leads to no significant hazard.

4.10.4 References

1. Report on Equipment Availability for the Ten-Year Period, 1964-1973. Edison Electric Institute, EEI-74-57.
2. A Report on Improving the Productivity of Electric Power Plants. Federal Energy Administration, March 1975.
3. Electrical Generating Plant Availability. Federal Power Commission, May 1975.
4. Evaluation of Nuclear Power Plant Availability. US Atomic Energy Commission, January 1974.
5. R. Bellenton. Practical Application of Reliability and Maintainability Concept to Generating Station Design.
6. An Assessment of Accident Risks in US Commercial Nuclear Power Plants. US Atomic Energy Commission. WASH-1400, Reactor Safety Study.
7. Summaries of Failure Rate Data and Summaries of Replacement Rate Data. Government-Industry Data Exchange Program (GIDEP).
8. Failure Rate Data Handbook (FARADA). Naval Weapons Station, Corona, California.
9. Reliability Stress and Failure Rate Data for Electronic Equipment. MIL-HDBK-217B.
10. D. Sliney and B. Freasier. Evaluation of Optical Radiation Hazards. Applied Optics, January 1973, Vol 12, No. 1.

11. W. Ham and D. Sliney. A Study of Optical Radiation Hazards Associated with a Solar Power Facility Proposal.

12. R. Penner and J. McNair. Eclipse Blindness. Ames J. Ophthalmology, 1966.

13. E. Eckert. Heat and Mass Transfer. McGraw Hill, 1959.

14. American National Standard for the Safe Uses of Lasers. American National Standards Institute, Inc. ANSI Z136.1, 1973.

15. Sir Christopher Hinton. Atomic Power in Britain. Scientific American 198, March 1958.

16. R. A. McClatchey. Atmospheric Attenuation of CO Laser Radiation. AFCRL-71-0370, 1 July 1971.

17. R. A. McClatchey and John E. A. Selby. Atmospheric Attenuation of Laser Radiation from 0.76 to 31.25 um. AFCRL-TR-74-0003, 3 January 1974.

18. J. Thewlis (editor). Encyclopaedic Dictionary of Physics, Pergamon Press, 1962.

19. David C. Smith. Thermal Defocusing of CO_2 Laser Radiation in Gases. IEEE J. Quant. Elect. QE-5, 600-607, December 1969.

4.11 LOGISTICS SUPPORT PLAN

This section presents preliminary planning that covers the support requirements for a 10-MWe Solar Thermal Pilot Plant. The plan is to the extent feasible, compatible with those concepts developed for a Commercial Plant. During Pilot Plant construction and test operations, application of this plan, which will be revised and expanded as field operations progress, will prove its validity and reveal its inadequacies. The concepts that may prove to be inadequate will be improved and tested to the extent feasible during the Pilot Plant program, and necessary changes will be incorporated into the Commercial Plant support concepts. The following Pilot Plant support plan is of a preliminary nature and subject to modifications caused by design changes, program direction, and other influencing factors.

4.11.1 Installation and Checkout (I&C)

During Pilot Plant equipment installation and test, the Commercial Plant support concepts will be applied except where there are significant differences between the two programs. These differences are identified as follows:

A. The quantity of material to be delivered to site is much smaller for the Pilot Plant than for the Commerical Plant.

B. The size and weight of the receiver absorber panels, the turbine, and the thermal storage unit components are considerably smaller for the Pilot Plant than for the Commercial Plant.

C. The materials, mirrors, steel members, and adhesives for heliostat reflector production for the Pilot Plant will be delivered to the MDAC production facility instead of to the site as done for the Commercial Plant. This, of course, imposes an additional transportation requirement on the Pilot Plant program, i.e., delivery of completed heliostat reflector panels to the site.

4.11.1.1 Transportation, Handling, and Packaging (THP)

This section of the Logistics Support plan is presented by subsystem, i.e., collector, thermal storage, receiver, and EPGS. The master control subsystem is not included as no analysis of its THP requirements has been made.

Collector Subsystem

The basic components of the collector subsystem to be shipped to the final assembly facility are the pedestal, sensor pole, torque tube, cross beam, drive unit, reflector panel assemblies, tracking mirror, controllers, and sensor components. All are readily transportable by commercial carriers. Packaging designs provide protection and handling provisions to assure safe delivery to site.

Procedures and schedules to control movement of material will minimize multiple handling and assure conformance to schedule. Purchased items will be shipped direct to the assembly location. Waste management will be implemented for disposal of excess packaging materials. Reusable designs will be used where cost-effective. Packs exceeding 75 lb can be handled with forklifts.

The pedestal and sensor pole will be shipped on open-flatbed trucks with lumber spacers between layers. Units will be alternated to provide flange-nesting for obtaining a tight load. Pairs of pedestals will be strapped in steel to reduce handling and provide safety from rolling during transportation and storage. Sensor poles will be strapped in groups of four.

Torque tubes have the drive unit mounting supports and inboard beam mounting flanges attached, creating an irregular item to handle and stack. Three assemblies will be handled together by placing them across and strapping to 4-in. x 4-in. lumber spacers. Alternate units can be offset to achieve a tight pack for handling and storage.

The flanged cross beams will be reverse-nested and bundled in fours with filament tape. Three bundles are then strapped together for shipping and storage. Lumber dunnage between layers of bundles provides spacing for fork entry during handling.

Drive units will be strapped to a skidded base. The drive is dense (700 lb) so that a single-tier truck load achieves shipping weights of near capacity. Film wrap will be used for moisture protection.

Edge strength of reflector panel assemblies is capitalized on by shipping and storing the reflective panels vertically. Tracking mirrors will be packed in standard reusable crates. The large mirrors will be handled on a shipping and storage fixture designed for maximum truck loading. Pairs of assemblies will be unitized face to face separated with adhesive-backed cushioning patches and secured with filament tape. Because of the cushion characteristics of the foam sandwich construction, the mounting disks will be allowed to contact one another directly. The slightly sloped back provides stability in loading the fixture and during removal of the panels. Strapping is used to maintain a snug pack for handling, shipment, and storage.

Sensors, calibration equipment, controllers, and other electrical equipment will be packed in fiberboard or wooden containers, depending on weight, to protect the items from shock and vibration.

Highway transportation is the most cost-effective mode for the relatively short distance required for the Pilot Plant. Shipments will be in truckload quantities when practical for transportation economy. Reflective panels loaded face to face will have a tarpaulin cover to protect the load from casual road hazards and blowing sand, and to assure no hazardous reflections

are produced from exposed reflectors. Loaded trailers of reflector panels can be dropped at site and the return load of empty fixtures picked up for a quick turnaround. Average usage is two trucks per week for reflector panels and only two or three trucks per month for the other major items.

Components can be handled and stored in their shipping configuration until ready for further assembly. To minimize handling, items will be moved directly to the using area without going to storage, an application of the last-in, first-out inventory principal. Special handling instructions will be provided for each critical item. These instructions will include trailer loading, tiedown and off-loading procedures.

Biodegradable and recyclable materials (e. g., wood, fiberboard) have been selected as primary packaging materials. Containers, skids, fixtures, and other packagings that are not salvaged or reused will be removed to a community refuse disposal area. No packagings will be left as trash or rubbish at the assembly area or installation site.

Thermal Storage Subsystem

The thermal storage unit will be erected at the construction site with inspection and acceptance based upon the completed unit. Prefabricated work will be delivered as needed by the erecting foreman. Special site storage will not be needed.

The heat exchangers will be off-loaded onto foundations by the mechanical contractor.

Equipment items and raw stock will be warehoused at the construction site by the mechanical contractor. Off-loading of carrier vehicles will be performed by the mechanical contractor.

The construction contractor will employ a receiving inspector and a warehouse clerk to control quality of all received equipment and stock and to process receiving and stock reports.

Special transportation is not required. Off-loading at the construction site will be performed by the mechanical contractor.

Packaging will be specified by the procurement specifications when special packaging is needed to retain essential characteristics.

Lowest rates compatible with delivery requirements will be used. Government bills of lading will be used for major items, if such a service is available.

Shipping clearances to the site will determine the largest shop fabrication subassemblies. Shop fabrication will be preferred and used to the full economic advantage over field fabrication, wherever possible.

Equipment and stock will be received at the construction site, off-loaded by the mechanical contractor, and inspected and warehoused by the mechanical contractor. The receiving inspection function and the warehousing operation will be monitored. The receiving inspector will retain records showing that received material conforms to the procurement specifications and all certifications of physical and chemical properties have been filled with the receiving records. Acceptance of equipment and stock by the receiving inspector will be the basis for payment of the supplier. The warehouse function will maintain the inventory status, as well as to provide physical protection for the material. The warehouse function will also maintain records showing equipment and stock removed from the warehouse for contractor installation.

Receiver Subsystem

Transportation of all hardware items to the Pilot Plant site will be by common carrier. During Subsystem Research Experiements (SRE), a complete Pilot Plant panel was fabricated in-house and delivered by common carrier on a flatbed truck to the test facility some 40 mi from Rocketdyne. The delivery was made during mid-day. No special provisions for transportation are considered necessary. The absorber, which is the largest single item, will be placed on a flatbed truck two at a time and delivered to the Pilot Plant site.

All structural steel valves, etc, that will be delivered directly to the site will be similarly carried by common carrier. It is anticipated that none of the hardware items required in the Pilot Plant will exceed the size of the absorber panel. It has been found during the SRE that no special provisions for handling are necessary for the absorber and that procurement of the transportation services will simply be done by using standard commercial practice.

Electrical Power Generation Subsystem

The major elements of the EPGS, including the turbine, generator, deaerator, etc, will be transported from the manufacturer to the Southern California Edison (SCE) Coolwater facility by rail. Packaging, protective covers, tie-down techniques, and off-loading provisions will be in accordance with established procedures and techniques. Movement of the equipment from the Coolwater rail spur to the installation site will be accomplished with flatbed trucks. Smaller elements will be shipped directly from the manufacturer to the site by truck. Packaging of the elements will be in accordance with normal shipping practices for each hardware item and will depend on the quantity of each item shipped.

4.11.1.2 Facilities

To adequately support site assembly, installation, and test operations, the permanent site facilities will have to be augmented during the I&C period with additional temporary facilities. At the moment, facilities requirements can be conceptualized although facilities criteria have not been developed.

This section is also presented by subsystem with the master control omitted.

Collector Subsystem

A rigid-frame, fabric-membrane structure of 15,750 ft^2 will be used as the heliostat assembly building and installation and checkout operations office. Heliostat assembly use of the building is described in the Production Plan, Volume III. The building contains two doors, one of which is 25 ft wide by 15 ft high, and will allow for removal of a completely assembled heliostat to the adjacent collector subsystem installation site.

Outside area of the building will be paved with asphalt for parking and storage. Foundation pads will be installed outside to serve as temporary storage positions for as many as 10 completely assembled heliostats.

Installation and checkout operations office space provided inside the building will be sufficient for 6 desks, 1 drawing board, and 13 file cabinets.

Thermal Storage Subsystem

No dedicated facilities are anticipated for the thermal storage subsystem to support site assembly, installation, and test operations. All equipment and materials delivered to site will be erected in place. Equipment required for erection will be for the most part portable. The equipment includes cranes, welding machine, X-ray equipment, hydrostatic test equipment, and miscellaneous checkout hardware. Assembly activities requiring shop facilities will be carried out in the permanent assembly facility to be built on site, which is discussed in Volume VI.

Receiver Subsystem

No dedicated facilities to support the site assembly, installation, and test operations are anticipated for the receiver. Structural steel and piping components will be off-loaded near the base of the tower, where they will be raised to the top of the tower and installed. Receiver panels, which are inspected and pressure-checked prior to leaving the manufacturing facility, are off-loaded in the panel laydown area. With the completion of the receiver structure, the panels will be raised to the top of the tower and installed in place. Specialized assembly activities requiring shop facilities will be carried out in the permanent assembly facility.

Electrical Power Generation Subsystem

Facilities required to support the assembly and installation of the EPGS equipment will be included in the permanent on-site warehouse and assembly buildings, which will be shared with the receiver and thermal storage related activities. Since all elements of the EPGS will arrive at the site as manufactured components or assemblies, the principal site work involves the field erection and installation of these elements. During this activity, portable assembly and checkout equipment will be used wherever possible.

4.11.1.3 Support Equipment

Collector Subsystem

Types and quantities of equipment for installation and checkout operations shown in Table 4-23 have been selected for economical and dependable program accomplishments. All equipment is portable. Upon completion of collector subsystem installation and checkout operations, the major portion of equipment will be used for maintenance operations. MDAC will deliver necessary items of equipment to the customer for maintenance purposes prior to Pilot Plant system testing or as dictated by the customer's operational plans.

Of the support equipment selected for the collector subsystem installation phase of the program, two items require brief descriptions: the heliostat handling fixture, which is mated with a forklift, and the collector field test support station, which is mounted in a van. The balance of the support equipment is considered to be standard handling and test hardware.

Because the heliostat is to be completely assembled before being transported to its foundation, a special handling fixture is required. The fixture is shown in Figures 4-77 and 4-78. It is a steel weldment consisting of two 6-in. x 10-ft channels joined by intermediate tie plates with a cantilevered support at one end and a wood saddle at the other. A tube is mounted near the upper end contains adjustable feet to restrain the heliostat from rotating. Hooks are welded to the channels that will adapt to the vertical travel plate of a standard forklift. A safety hook is secured to the cantilevered support, and a sling and strap are provided as loose items.

During the I&C phase, the master control will not be available for use in heliostat operational checkout. In lieu, a collector field test support station will be used. The unit will be designed so as to provide power and command inputs to either a field controller or a heliostat controller so as to power and command either a cell of 24 heliostats or a single heliostat. For mobility and equipment environmental control, field units will be installed in an air-conditioned van. The van will be equipped with an auxiliary power generator size to provide van power and power sufficient to drive a minimum of

Table 4-23

INSTALLATION AND CHECKOUT EQUIPMENT

Nomenclature	Qty
Heliostat Handling Fixture	2
Handling Sling, Heliostat Mirrors	2
Mobile Workstand (Cherry Picker)	2
Pedestal-Leveling Fixture	2
Power Torque Wrench	2
Forklift	1
Multimeter-Volt Ohmmeter	6
Digital Voltmeter	6
Pickup Truck - Modified to Incorporate Workstand in Truckbed	2
Mobile Crane	1
Walkie-Talkie Communications Sets	4
Inclinometer	2
Theodolite	2
Collector Field Test Support Station	2
Reflector Washing Equipment	TBD

24 heliostats. The unit will be used during I&C to test and check out heliostats under the control of both heliostat controller and field controllers. Following the completion of I&C, the van-mounted test sets will be used for collector field maintenance and for emergency positioning of heliostats. The basic equipment making up the test set is shown in Figure 4-79.

A typical field application of the test set is shown in Figure 4-80.

4.11.1.4 Maintenance

Maintenance activities during I&C will be initiated in response to (1) protecting installed equipment from the environment, (2) damage caused by installation activities, and (3) discovery of discrepant items during checkout and test.

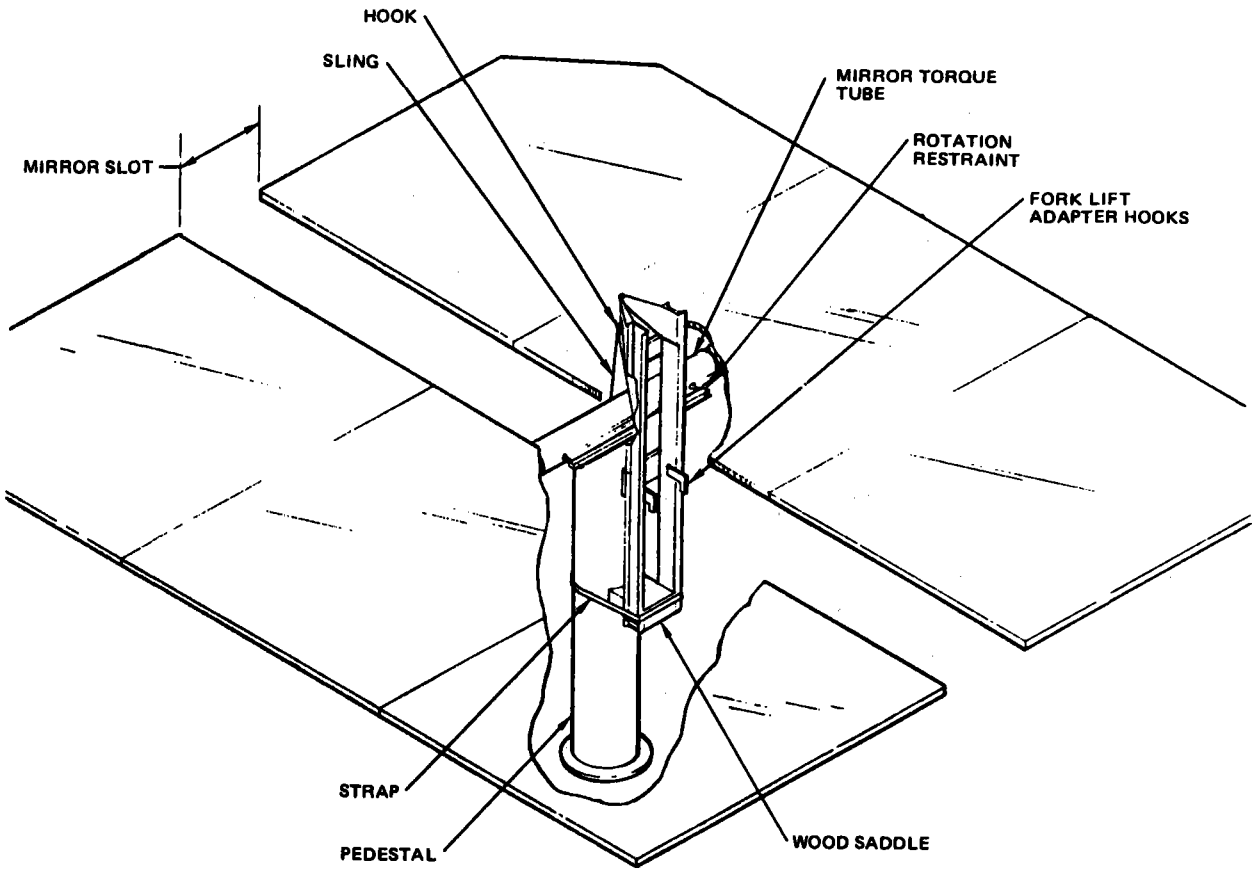

Figure 4-77. Handling Fixture Mated to Heliostat

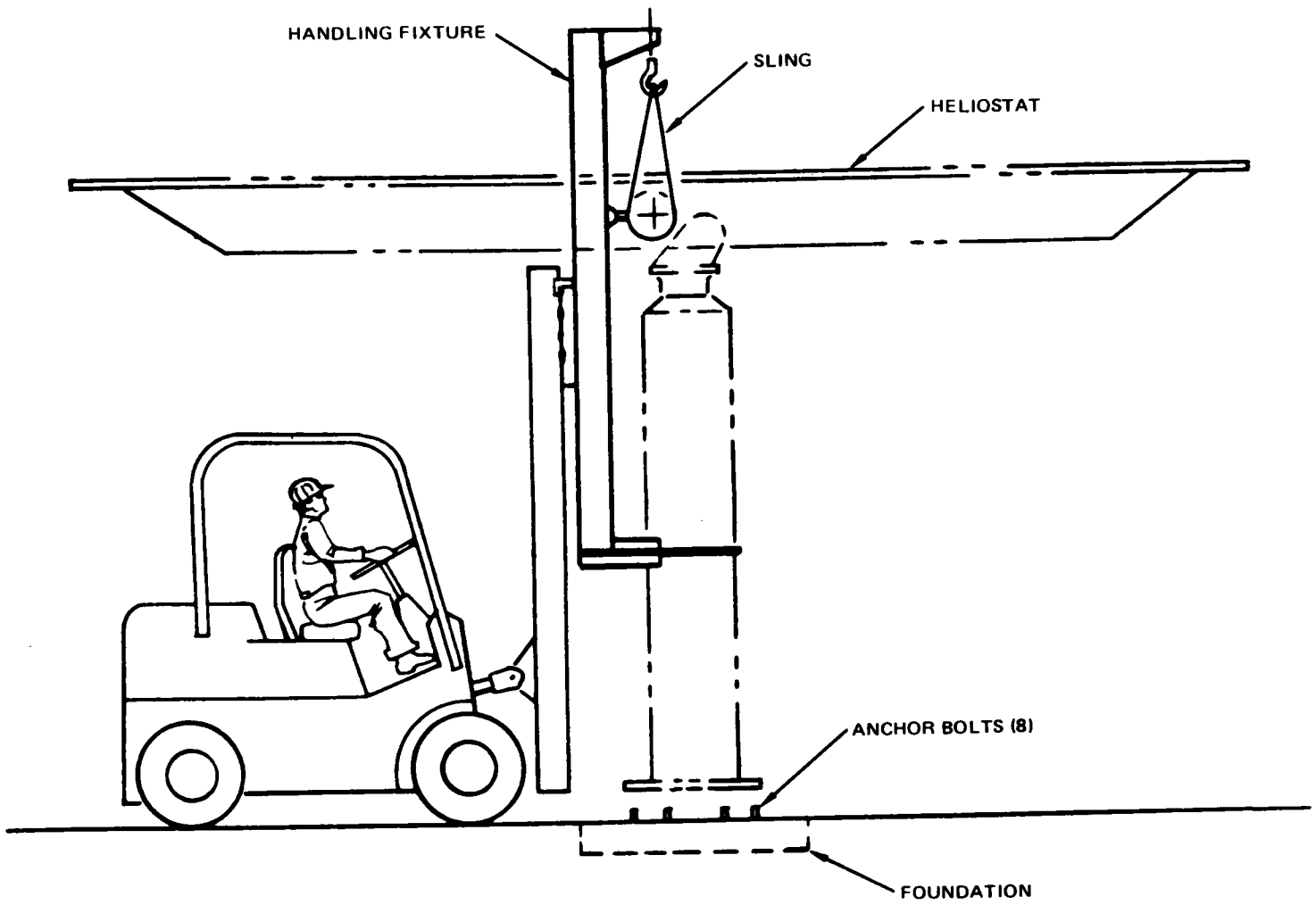

Figure 4-78. Heliostat Installation on Foundation

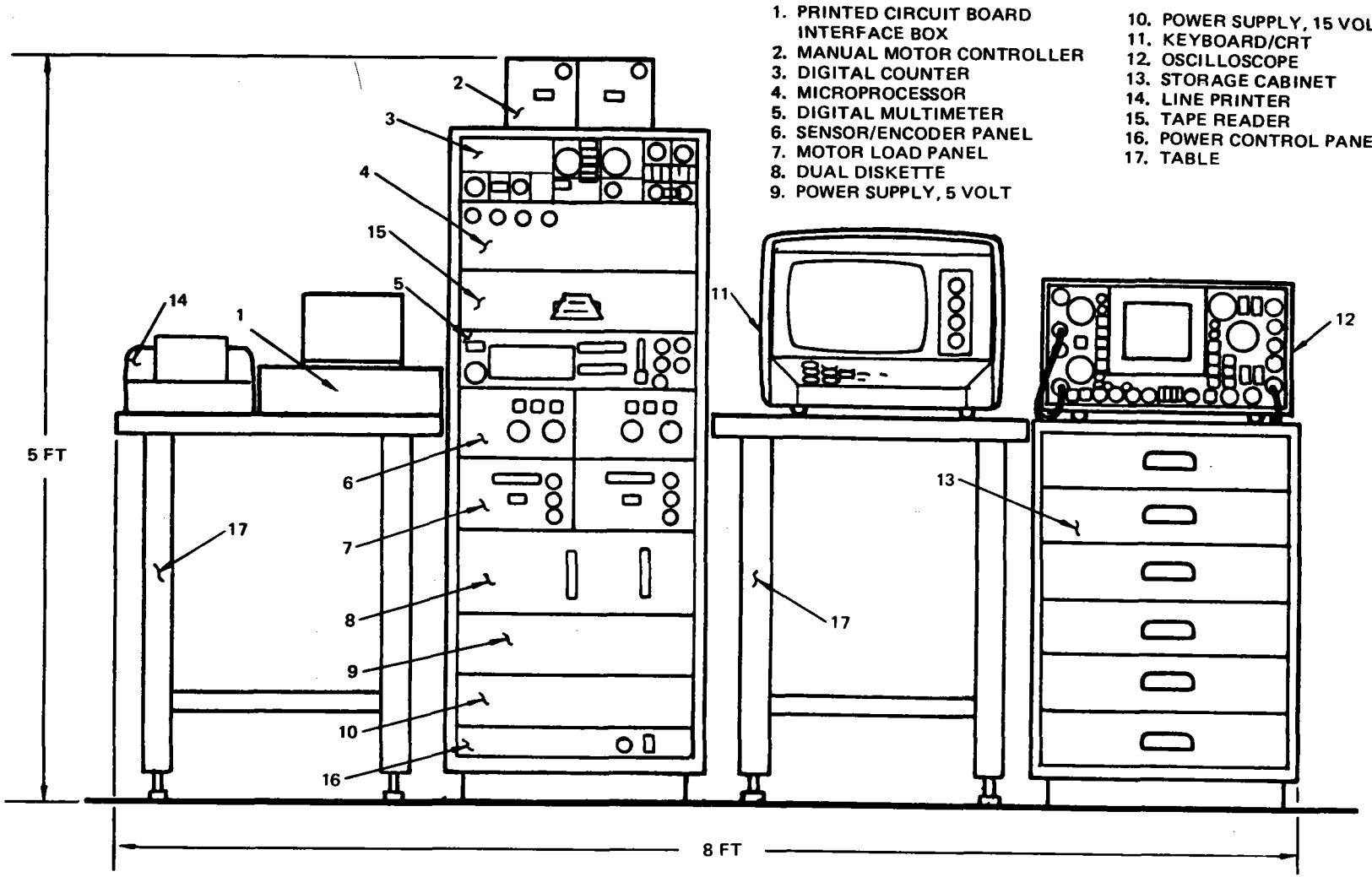

Figure 4-79. Collector Field Test Support Station

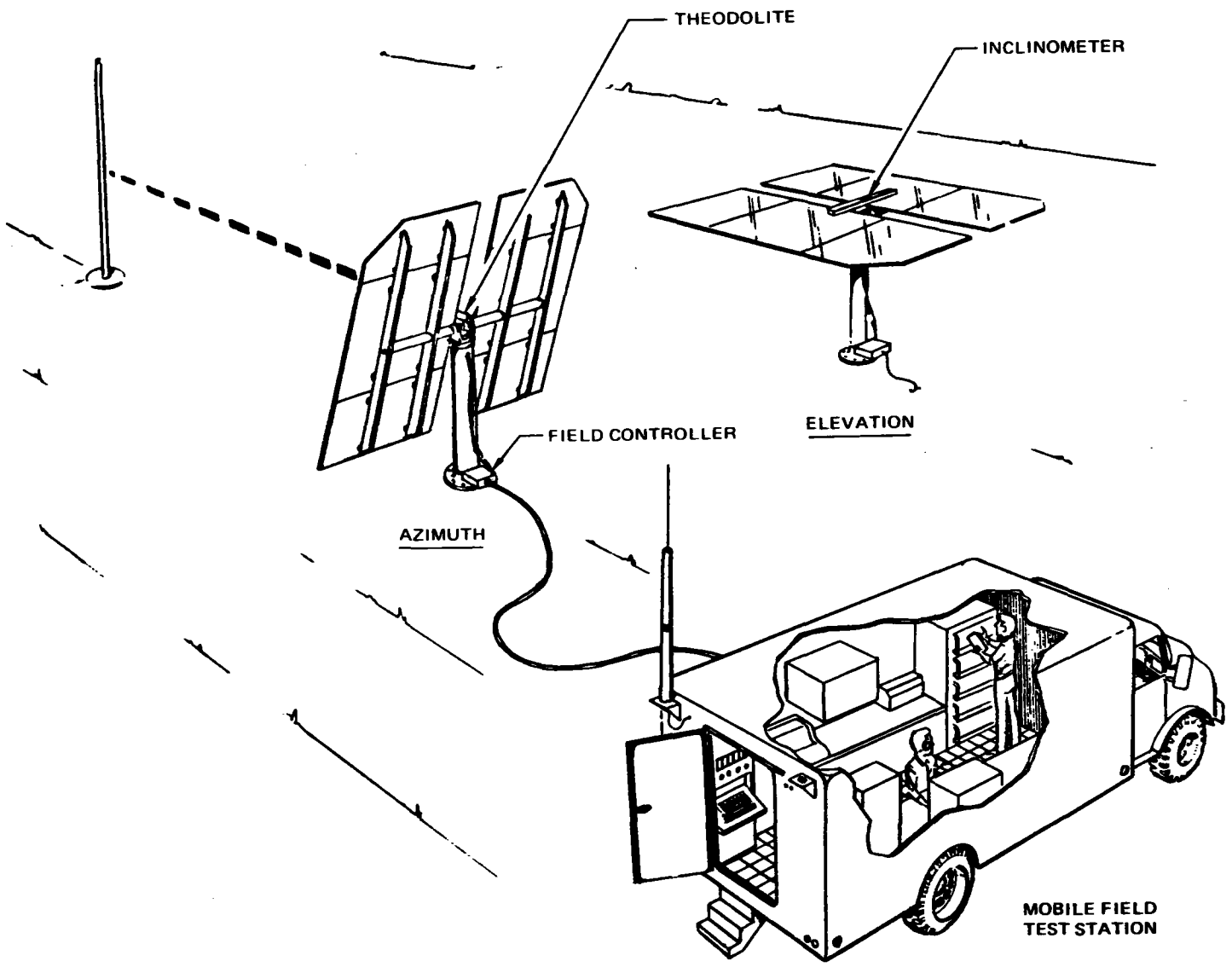

Figure 4-80. Heliostat Referencing

Preventive maintenance will be scheduled for periodic inspection of installed equipment as necessary to detect environmental damage. Equipment found to be deteriorating will be serviced, repaired, or replaced as its condition warrants.

Corrective maintenance will be accomplished by removal and replacement of damaged or discrepant items. Damaged and discrepant items removed at site will be recycled through the appropriate manufacturer's facility for repair and recertification.

The thermal storage subsystem and receiver subsystem are treated essentially the same as the collector subsystem.

4.11.1.5 Supply Support

Approved quantities of consumables and low-cost spares and repair parts, as defined by maintenance data analyses, will be acquired and delivered to support installation and checkout operations and maintenance tasks.

High-cost spares such as reflector panels and field controllers will not be acquired. If the need arises for this type of spare, the item will be diverted from the production line. Following this action, a spare will be ordered and then turned over to the production line as a replacement. This concept reduces investment in high-cost spares, while ensuring installation and checkout scheduled completions.

4.11.1.6 Installation Procedures

The procedures to be prepared and validated for use during the installation phase are listed in Table 4-24.

4.11.1.7 Training

Maintenance training courses will be developed during the production phase of the program and will be conducted for maintenance personnel during the installation and checkout phase. The training material will be delivered to the customer to train new personnel and provide refresher courses. Training assistance is provided by field service representatives assigned to the site.

Table 4-24

COLLECTOR SUBSYSTEM INSTALLATION PROCEDURES

Number	Title/Description
MDAC-CSIP-01	Foundation Leveling. Provide procedure for adjusting pedestal leveling nuts using special leveling tool.
MDAC-CSIP-02	Heliostat Installation. Provide procedures for installing heliostat handling fixture, transporting heliostat, and installing heliostat on foundation.
MDAC-CSIP-03	Power and Control Cables Connection. Provide procedures for connecting power cable to field and heliostat controllers, control cables to field and heliostat controllers.
MDAC-CSIP-04	Heliostat Referencing and Checkout. Provide procedures for aligning heliostat to known reference point. Provide procedures for operational checkout of a heliostat using field controller test set. Provide procedures for adjusting elevation and azimuth encoders.
MDAC-CSIP-05	Sensor Pole Installation. Provide procedures for installing and leveling pole on foundation (if required).
MDAC-CSIP-06	Sensor Installation. Provide procedures for installing sensor mount and sensor on pole, and connecting electrical cable.
MDAC-CSIP-07	Sensor Alignment. Provide procedures for aligning and locking sensor.
MDAC-CSIP-08	Test and Checkout. Provide procedures for test and checkout of a cell of heliostats using the field controller test set. Refer to available engineering drawings for cabling, wiring, logic, and functional diagrams.

4.11.2 Operations

4.11.2.1 Transportation

Two modes of transportation are required to support Pilot Plant operation. The first in intrasite movement of maintenance personnel and operating equipment. These needs will be satisfied through use of installation and

checkout vehicles that are to be transferred to operations at the completion of installation and checkout activities. The second mode is the transportation of replenishment supplies to the site and the movement of reparable components to and from the manufacturer's facility for repair. The needs will be served best through the use of commercial carriers.

Packaging of reparable components should comply with commercial packaging practices, except for items having reusable containers transferred from installation and checkout.

4.11.2.2 Maintenance Equipment

Much of the equipment needed to support the Pilot Plant maintenance activities consists of standard items such as are used at any electric generating station. However, there are some items required which are unique to the solar power generating system. They include the following:

COLLECTOR SUBSYSTEM

1.	Mobile Workstand (Cherry Picker)	Beam Sensor Alignment
2.	Mobile Crane	Heliostat Hoisting
3.	Forklift	Miscellaneous Heavy Equipment Handling
4.	Hoisting Slings, General Purpose	Heliostats and Miscellaneous Equipment Hoisting
5.	Pickup Truck	General Purpose
6.	Inclinometer	Pedestal Leveling
7.	Mobile Communications Set	Field Communications
8.	Theodolite	Heliostat Alignment
9.	Hoisting Sling, Heliostat Mirror	Mirror Panel Replacement
10.	Pedestal-Leveling Fixture	Pedestal Leveling
11.	Reflector Washing Equipment	Heliostat Reflector Cleaning
12.	Collector Field Test Support Station	Subsystem and Component Level Fault Isolation and Test

RECEIVER SUBSYSTEM

1. Absorber Flushing Equipment
2. Standard Hard Tools
3. Grinder, Welder, Portable X-ray Unit
4. Sand blasting and Spray Paint Equipment
5. Power Hacksaw or Pipe Cutter
6. Panel Handling Sling
7. Standard Electronics Checkout Equipment (Digital Voltmeter, Counter, Oscilloscope, Ohmmeter, etc)
8. Pressure Gage Calibration Bench
9. Ultrasonic Filter Cleaner

4.11.2.3 Maintenance

Pilot Plant maintenance, as determined to date, is identified in the following subsection. For a more detailed description of maintenance actions, the reader is referred to Volume III for the collector subsystem, Volume IV for the receiver subsystem, and Volume V for the thermal storage subsystem.

Collector Subsystem

The level of detail and confidence in the requirement estimates at this time are constrained by the current hardware design definition. Also, collector subsystem requirements must be integrated with the overall Pilot Plant support requirements to assure a cost-effective support operation. The basic corrective and scheduled maintenance tasks for the collector subsystem have been determined by a hardware analysis to identify maintenance significant components. Maintenance significant components are defined as hardware items for which a discrete maintenance action is required based on the maintenance concept. These maintenance actions result from equipment failures or may be scheduled actions such as cleaning or lubrication to prevent equipment deterioration or to sustain performance characteristics. Table 4-25 lists the maintenance significant components and provides a brief description of the required maintenance actions.

Receiver Subsystem

No firm maintenance schedule exists now. A schedule of frequency and type of maintenance will be developed during the checkout, integration, and 2-yr

Table 4-25 (Page 1 of 2)

MAINTENANCE SIGNIFICANT ITEM LIST

Component	Corrective Maintenance	Scheduled Maintenance
Field Controller	Remove and replace on failure. Minor repair on-site. Major repair and overhaul at MDAC.	None
Heliostat Controller	Remove and replace on failure. Minor repair on-site. Major repair and overhaul at MDAC.	None
Elevation and Azimuth Drive Assemblies	Remove and replace on failure. Repair and overhaul at MDAC.	Lubrication
Elevation and Azimuth Drive Motor and Reducer	Remove and replace on failure. Repair at manufacturer.	None
Elevation and Azimuth Shaft Encoder	Remove and replace on failure. Repair at manufacturer.	None
Elevation and Azimuth Shaft Turn Pickoff	Remove and replace on failure. Repair at MDAC.	None
Pedestal J-Box	Remove and replace detail parts on failure. Remove and replace box for major damage.	None
Pedestal	Structural repair. Remove and replace for major damage.	None
Reflector Panel	Remove and replace. Discord. Clean (in addition to scheduled requirements due to severe weather conditions).	Clean
Reflection Structure	Structural repair. Remove and replace for major damage.	None
Beam Sensor	Remove and replace on failure. Repair at MDAC	None
Sensor Pole	Structural repair. Remove and replace for major damage	None

Table 4-25 (Page 2 of 2)

MAINTENANCE SIGNIFICANT ITEM LIST

Component	Corrective Maintenance	Scheduled Maintenance
Field Cables	Electrical Repair. Remove and replace for major damage	None
Power Distribution Panel	Remove and replace detail parts. Replace panel for major damage	None
Power Transmission	Remove and replace on failure.	None
Test Support Station	Remove and repair components on failure. Repair components at MDAC.	Calibrate test equipment; inspect, clean, adjust and lubricate CRT/keyboard, tape reader, and recorder

operational test program. The SRE program has demonstrated that the Pyromark paint on the receiver surface will last in excess of a year and industrial experience with the paint indicates many years of maintenance-free service. Acid flushing of the receiver will probably be necessary once a year; however, this can routinely be done at night or during cloudy days without impact. Maintenance of electronic equipment is standard procedure and these services are normally purchased at the time the equipment is bought.

Two types of maintenance, preventive and corrective, will naturally be required. The plan is to develop during the operational test phase the type and frequency of preventive maintenance and the type of corrective maintenance required. The types of preventive maintenance expected are painting, cleaning, continuity checks, functional checks, visual inspection, routine or periodic parts replacement, and periodic flushing. The types of corrective maintenance expected are part replacement, part servicing or overhaul in place, flushing, and part servicing, repair, and overhaul in shop. All of these types of activities are standard for fluid systems, especially steam-generation equipment operated by utility firms.

There are only two preventive maintenance items planned for the absorber assembly. The first involves repainting of the external face of the absorber to ensure the high performance discussed herein. This will be accomplished with scaffolding and spraying, identical to the means used during the fabrication procedure. The sand blasting and painting activity would be carried out at TBD intervals based on periodic visual inspection of the receiver surface. This activity would be carried out during planned maintenance periods, thus minimizing the impact on plant availability.

The other preventive maintenance item will be periodic acid flushing of the boiler and preheater panels. It is anticipated that this operation will be done at 18-mo intervals. The activity will also be done as part of the planned maintenance cycle to maximize plant availability.

Corrective maintenance insofar as the absorber is concerned will be simply to remove an affected panel and replace it. It is anticipated that a panel can be replaced overnight with no effect on the solar plant mission other than downtime immediately subsequent to the failure. The panel will be removed with the crane located on top of the receiver. The technique used is described in Section 5.3, Volume IV. Panels will be replaced to repair or replace damaged tubes or leaks. In general, the panel can be returned to the factory for corrective action; however, some damage may be slight enough that it can be repaired on-site. Tube replacement and/or repair procedures and techniques will be developed during the detailed design and fabrication of the Pilot Plant panels.

Controls maintenance is concerned with two areas, mechanical parts and the electronic parts. Most electronic equipment will be maintained on a routine basis normally by the equipment supplier. These types of activities are normally done on a monthly basis, but in certain instances biweekly maintenance is necessary. This activity will be done at night with no impact to the Pilot Plant mission. It would normally include replacement of transistors, continuity checks, and checks of computer logic. Mechanical parts that will be maintained on a regular basis are the filters upstream of the absorber panels. The preventive procedure will involve cleaning these.

Corrective maintenance for the controls hardware also refers to the electronic and mechanical parts and in both cases involves replacement of faulty hardware. Electronics activity normally requires extensive troubleshooting using, where possible, troubleshooting routines designed into master control. Maintenance of the mechanical parts for the most part requires removal of valve components and replacement and/or repair for reinstallation into the valve.

Proper maintenance is essential to sustain the thermal storage subsystem (TSS) in a continued state of operation, high efficiency, and safety over its 30-year life. Maintenance will include all actions taken to retain an item in a specified condition by providing systematic inspecting, detecting, and servicing for the prevention of incipient failure and the action taken to restore

an item to a specified operational condition. This includes fault isolation, item replacement, and repair. To accomplish this two types of maintenance are considered. They are scheduled maintenance and corrective maintenance, and are defined as follows:

- Scheduled Maintenance. Actions performed to retain an item in an operable condition by systematic inspection, detection, prevention of incipient failures, replacement of life/cycle limited components, adjustment, calibration, cleaning, and lubrication. Scheduled preventive actions will be minimized during operating periods and emphasized during nonoperating periods of portions of the thermal storage subsystem to sustain equipment/system availability. Servicing activities will be minimized and conducted on a noninterference basis.

  In addition to these scheduled procedures, plant operation will be continuously monitored for out-of-spec performance. When component and subsystem deviates from established norms operations will notify maintenance and corrective procedures will be established that will provide rapid return to establish performance levels with a minimum of outage time.

- Corrective Maintenance. Actions performed to restore an item to a satisfactory condition by correction of known or suspected malfunctions or defects that have caused degradation of the item below the specified performance level.

  Corrective maintenance consists of repair, replacement, checkout, and verification of repaired equipment. It is performed as a result of condition monitoring, or unexpected or unpredicted failure or malfunction.

Table 4-26 is the summary schedule for periodic maintenance and inspections required for unscheduled maintenance. It shows the suggested frequency with a reference code for the work to be performed on the listed items of the TSS. It is expected that this schedule will be modified and updated with experience gained during operation of the Pilot Plant. Maintenance experience with the Pilot Plant will be directly applicable to the Commercial Plant.

Table 4-26 (Page 1 of 2)

TSS MAINTENANCE SUMMARY SCHEDULE

	Item	Maintenance Period and Maintenance Action					
		Daily	Weekly	Monthly	SemiAnnual	Annual	Other
1	Thermal Storage Unit (TSU)	A		G		B, C, D	
2	Ullage Maintenance Unit (UMU)	A	E, F	G		B, C, D	
3	Fluid Maintenance Unit (FMU)	A	E	G			
4	Pump Units (Including Motors)	A		G			
5	Heat Exchangers (TSH and SG)	A		A			H
6	Desuperheater	A		A			H
7	FMU Filters	A		J			
8	Valves						
	• Manual	A	K				K
	• Control	A					L
	• Relief	A					L
9	Instrumentation and Transducers						
	• Flowmeters			A			L
	• Pressure and Delta-p Transducers			A	L		
	• Temperature Transducers						
	Thermocouple			A			
	Resistance Bulbs			A	L		

Table 4-26 (Page 2 of 2)

TSS MAINTENANCE SUMMARY SCHEDULE

	Item	Maintenance Period and Maintenance Action					
		Daily	Weekly	Monthly	SemiAnnual	Annual	Other
10	Control Subsystem				M		
11	General Maintenance - Descaling, Cleaning, Painting, Etc						Every TBD years required

A. Walkaround visual and audible check for leaks, mechanical, and electrical abnormalities.

B. Check bolt torque.

C. Check tank settling or distortions.

D. Check for weathering and insulation spauling.

E. Draw off waste fluids and submit a sample for analysis.

F. Check oil levels for pumps, motors, compressor, etc. Replenish as required.

G. Lubricate bearings, shafts, etc that require periodic lubrication.

H. Check for scaling and corrosion, primarily steam and/or water systems.

J. Inspect and clean FMU filters as required. (Requirement for cleaning will be as indicated by differential pressure readouts.)

K. Check manual valves for verification of open/close operation.

L. Service, calibration, and proof test changeouts. (Applies to valves and transducers.)

M. Check for dust, sand, corrosion, connector integrity.

4.11.2.4 Facility Requirements

No facilities dedicated to collector subsystem maintenance are required. Indoor storage space is limited to that required for spare parts and minor maintenance support equipment items. Temperature or environmental conditioning is not a significant factor. Packaging and crating area requirements are minimal because no large items are sent off-site for repair. Outside parking is adequate for all vehicles, including the van that houses the collector field test station. Office space requirements for maintenance records and documentation can be integrated with similar requirements for other subsystems.

During the first year of test operations, a determination will be made, in conjunction with the operator of the plant, regarding the most effective approach to component repair. Startup and test operations will be supported by a factory repair service for discrepant components, but expectations are that a trade study of factory versus at-site component repair will favor at-site repair when facility and tooling costs are amortized over a 28-yr period. If this conclusion is reached, facility criteria for an at-site repair capability will be prepared. This facility would most likely serve component repair needs for all subsystems.

4.11.2.5 Spares

Collector

Spares and repair parts to support collector subsystem will be determined by analysis concurrent with hardware design release. The selection and quantity of items to be procured is based on the maintenance concept, the predicted component failure rates, operational availability requirements, and the repair cycle turnaround time. Spares and repair parts lists including quantities, unit cost, and procurement leadtime will be submitted for review and approval in sufficient time for procurement and on-site beginning 30 days prior to need dates. Ordering of system peculiar spares (non-commercial items) will be made prior to completion of production runs to reduce acquisition costs.

Inventory control, warehousing, receipt, and issuing of on-site spares and repair parts will be the responsibility of the site operator. MDAC-Huntington Beach will be responsible for these functions for off-site repair parts. Accountability and consumption reporting will be in accordance with customer requirements. In addition, MDAC will be responsible for accountability, tracking, control, and status reporting for all reparable items in the repair pipeline.

A preliminary spares analysis has been conducted based on the current hardware design definition. Results of this analysis are presented in Table 4-27. Reparable items, upon failure, are removed from the system, placed in the repair cycle, and returned to spare stock inventory when repair is complete.

Thermal Storage

The required initial spares provisioning plan is summarized in Table 4-28. Stocking of these spares will allow rapid and economical repair with a minimum of outage time. Since all large valves will be welded in place, repair will be done by replacement of major subassemblies (such as complete bonnet assemblies). Major control valve downtime will be minimized by tools that facilitate rapid removal and repair in place.

Rocketdyne's experience has been that the most cost-effective method of providing a minimum amount of downtime is to provide a high percentage of transducer/sensor spares and to schedule periodic replacement and recalibration.

Spares for the main pumps and electric motor drives will consist of replacement bearings, seals, gaskets, and the necessary electrical hardware. During the 30-yr lifetime it is expected that the large pumps and electric motors can be repaired in place. It is usually more economical to replace small motors and auxiliary equipment.

The large charge and extraction heat exchangers will be disassembled in place for cleanout and/or repair. The appropriate gaskets will be stocked and replaced as needed.

Table 4-27 (Page 1 of 2)
SPARES REQUIREMENTS

Component	System Quantity	Failures Per Year	Repair Location	Repair Cycle (Days)	Pipeline Quantity	30-Day Cont	Spares Quantity
Field Controller (F/C)	74	2.1	MDAC	30	1	1	2
Heliostat Controller (H/C)	1,686	27.5	MDAC	30	3	3	6
Drive Motor, Azimuth and Elevation	3,520	23.2	Mfr	90	6	2	8
Input Reducer	3,520	120	MDAC	30	10	10	20
Drive Unit, Azimuth	1,760	44	MDAC	30	4	4	8
Drive Unit, Elevation	1,760	44	MDAC	30	4	4	8
Shaft Encoder	3,520	14	Mfr	90	4	1	5
Shaft Turn Pickoff	3,520	15.6	MDAC	30	2	2	4
Pedestal J-Box (F/C)	74	0.41	Site	1	-	-	1
Pedestal J-Box (H/C)	1,686	10	Site	1	-	-	1
Beam Sensor Unit	1,760	3	MDAC	30	1	1	2
Power Transformer	8	0.02	-	-	-	-	1
Power Distribution Panel	8	0.09	Site	1	-	-	1
Reflector Panel	10,560	35	-	-	-	-	*70
Tracking Mirror	1,760	6	-	-	-	-	*12
Reflector Structure	1,760	2.9	Site	1	-	-	1
Pedestal	1,760	0.58	Site	1	-	-	1

*2-yr Quantity

Table 4-27 (Page 2 of 2)

SPARES REQUIREMENTS

Component	System Quantity	Failures Per Year	Repair Location	Repair Cycle (Days)	Pipeline Quantity	30-Day Cont	Spares Quantity
Sensor Tower	1,760	0.58	Site	1	-	-	1
Electric Cable Set, Pedestal	1,760	1.22	Site	1	-	-	1
Electric Cable Set, Field	1	0.033	Site	1	-	-	0
Collector Field Test Station	2	TBD	Site	1	-	-	0

Table 4-28 (Page 1 of 2)

PILOT PLANT THERMAL STORAGE SUBSYSTEM

INITIAL SPARES PROVISIONING

Item	Scheduled Maintenance Cycle	Probable Condition Requiring Servicing	Servicing	Required Spares*
Transducers/Sensors				
Pressure	6 Mo	Out of calibration	Lab repair/calibration	50%**
Thermocouple	6 Mo	Out of calibration	Lab repair/calibration	10%
Temperature Bulbs	12 Mo	Out of calibration	Lab repair/calibration	50%
Electronic Controllers	12 Mo	Dirt, bad connection	Clean and check in place	
Flowmeters	12 Mo	Sticking, leaking ball worn	Lab repair/calibration	1 each type and size.
Sight Gages	12 Mo	Sticking, leaking bearings worn	Lab repair/calibration	1 each type and size.
Heat Exchangers (change and extract)	5 Yr or 10 to 15 Yr	Cleaning	Remove U-tube bundle and clean	Gaskets.
		Tube replacement	Replace tubes	Tubes. Order when ready.
Valves				
Control (large)	12 Mo	Out of calibration, sticking, leaking or worn stem	Shop repair/ calibration	1 bonnet assembly each type plus 10% trim, seats, seals, actuators and EP converters.

*Integrated with other major subsystems

**Percent of thermal storage subsystem

Table 4-28 (Page 2 of 2)

PILOT PLANT THERMAL STORAGE SUBSYSTEM

INITIAL SPARES PROVISIONING

Item	Scheduled Maintenance Cycle	Probable Condition Requiring Servicing	Servicing	Required Spares*
Manual (large)	As Req	Sticking, leaking	Shop repair bonnet assembly	1 bonnet assembly each type and size.
Small (≤ 2 in.)	As Req	Sticking, leaking worn	Shop repair valve assembly	1 valve each type and size.
Pumps/Motors	As Req	Worn bearings, seals, belts, gaskets	On-line or shop repair	1 each set plus bulk gasket material.
Piping	As Req	Leakage	Replace gasket and remount component if excessive thermal movement is causing leakage	1 gasket each flanged joint.

*Integrated with other major subsystems

Piping gaskets and sealing compounds will be adequately stocked in all sizes to allow leaks and/or repair and replacement of line sections.

The spares provisioning list in Table 4-28 provides for the thermal storage subsystem independently. When detailed designs are completed during Phase 2, a master spares provisioning list encompassing all subsystems will be prepared. Where commonality exists, spares will not be duplicated. This will provide cost saving, particularly in the areas of transducers, steam/water line gaskets, and small pumps and motors.

Receiver

Philosophy will be the same as for thermal storage, and common spares will not be duplicated.

4.11.2.6 Maintenance Documentation

Documentation requirements for maintenance of subsystem components and support equipment will be satisfied by providing low-cost procedural instructions.

Procedures will be prepared in consonance with the development of maintenance data analyses for subsystem logistics requirements. Maintenance data analyses will define subsystem requirements for scheduled and corrective maintenance, fault detection, inspection, alignment, adjustment, lubrication, repair, and spare parts. Simple, commercially acceptable methods will allow quick-reaction preparation and reproduction of drawings.

Procedures will be validated to the maximum possible extent during the installation and checkout phase at site. Technical data in maintenance procedures, such as diagrams, certain repair and fault-isolation instructions, and preventive maintenance schedules, which cannot be validated, will be verified at meetings of MDAC and customer personnel. Final maintenance procedures will be updated to reflect equipment modifications and procedural improvements.

4.11.2.7 Training Requirements

The subsystem support planning data developed for establishing an efficient maintenance program capability will be the basis for the development of the training program. The planning data includes manpower, crew size, task, maintenance procedures, and personnel skills required to maintain the Pilot Plant system.

When evaluated and compared with the existing capability of personnel as assigned to the Pilot Plant system, the data will determine the type and depth of training provided.

The training program will be time-phased to operational requirements to within 3 mo of actual personnel assignment to maintenance activities. Although constrained by current hardware configuration definition, the following preliminary identification of training courses have been completed for the collector subsystem:

A. Reflector repair and handling.
B. Heliostat removal and replacement.
C. Heliostat alignment.
D. Heliostat handling and transportation.
E. Sensor removal and replacement.
F. Field controller repair.

The primary method of presentation will be on-the-job/on-equipment training and will consist of approximately 25% classroom lecture and discussion and 75% on equipment using the actual operational procedures for training. The latter will be directly supervised by a knowledgeable training engineer to prevent possible damage to operational equipment.

APPENDIX A

PILOT PLANT SYSTEM REQUIREMENTS SPECIFICATION

1.0 SCOPE

This document defines performance, design, and test requirements for the Central Receiver Pilot Plant System. The Central Receiver Pilot Plant is hereinafter referred to as the Pilot Plant or the system.

2.0 APPLICABLE DOCUMENTS

The equipment, materials, design, and construction of the Pilot Plant shall comply with all Federal, state, local, and user standards, regulations, codes, laws, and ordinances which are currently applicable for the selected site and the using utility. These shall include but not be limited to the government and nongovernment documents itemized below. If there is an overlap in or conflict between the requirements of these documents and the applicable Federal, state, county or municipal codes, laws, or ordinances, that applicable requirement which is the most stringent shall take precedence.

The following documents of the issue in effect on the date of request for proposal form a part of this specification to the extent specified herein. In the event of conflict between the documents referenced herein and the contents of this specification, the contents of this specification shall be considered a superseding requirement.

2.1 Government Documents

2.1.1 Specifications

Regulations of the Occupational Safety and Health Administration (OSHA)

Regulations of the California Occupational Safety and Health Administration (Cal/OSHA) - if required

The International System of Units, 2nd Revision, NASA SP-7012

Regulations of the Federal Aviation Administration

Regulations of the Civil Aeronautics Board

2.1.2 Standards

MIL-STD-1472, Human Engineering Design Criteria

2.1.3 Other Publications

U. S. Weather Bureau Maximum Wind Velocities, 50-year Mean Recurrence, Fastest Mile (1 Minute)

Design Handbook on Electromagnetic Compatibility (AFSC DH1-4)

Checklist of General Design Criteria (AFSC DH1-X)

Instrumentation Grounding and Noise Minimization Handbook (AFRPL-(AFRPL-TR-65-1)

National Motor Freight Classification 100B - Classes and Rules Apply on Motor Freight Traffic

Uniform Freight Classification 11 - Railroad Traffic Rates Rules and Regulations

CAB Tariff 96 - Official Air Transport Rules Tariff

CAB Tariff 169 - Official Air Transport Local Commodity Tariff

R. H. Graziano's Tariff 29 - Hazardous Materials Regulations of the Department of Transportation

CAB Tariff 82 - Official Air Transport Restricted Articles Tariff

2.2 Non-Government Documents

2.2.1 Specifications

Collector Subsystem Requirements Specification

Receiver Subsystem Requirements Specification

Thermal Storage Subsystem Requirements Specification

Electrical Power Generation Subsystem Requirements Specification

Master Control Requirements Specification

Pilot Plant Environmental Conditions

Pilot Plant/Site Interface Specification (TBP)*

Pilot Plant/Electrical Power Transmission Network Interface Specification (TBP)

Collector Subsystem/Receiver Subsystem Interface Specification (TBP)*

Collector Subsystem/Electrical Power Generation Subsystem Interface Specification (TBP)

Collector Subsystem/Master Control Subsystem Interface Specification (TBP)

Receiver Subsystem/Thermal Storage Subsystem Interface Specification (TBP)

*(TBP) - To be prepared

Receiver Subsystem/Electrical Power Generation Subsystem Interface Specification (TBP)

Receiver Subsystem/Master Control Subsystem Interface Specification (TBP)

Thermal Storage SubsystemElectrical Power Generation Subsystem Interface Specification (TBP)

Thermal Storage Subsystem/Master Control Subsystem Interface Specification (TBP)

Electrical Power Generation Subsystem/Master Control Subsystem Interface Specification (TBP)

Additional interface specifications will be prepared as required for individual subsystems being provided by more than one contractor (for example, a receiver assembly/tower interface specification will be prepared as part of the receiver specification).

2.2.2 Standards

American National Standards Institute, B31.1, Power Piping Code Manual of Steel Construction, 7th Edition, 1974, American Institute of Steel Construction

American National Standards Institute (Y10.19-1969 and C1.1-1971)

Building Code Requirements For Reinforced Concrete (ACI 318-71), American Concrete Institute

National Electrical Code, NFPA 70-1975 (ANSI C1-1975)

NFPA Bulletin No. 78 (ANSI C5.1)

National Electrical Manufacturers Association Standards

National Tubular Exchanger Manufacturers Association Standards

Seismology Committee Structural Engineers Association of California

American Society of Mechanical Engineers, Boiler and Pressure Vessel Code:

Section I, Rules for Construction and Power Boilers

Section II, Material Specifications

Section V, Nondestructive Examination

Section VIII, Unfired Pressure Vessels

Section IX, Welding and Brazing Qualifications

Uniform Building Code - 1973 Edition, Vol 1 by International Conference of Building Officials

American Society for Testing Manuals Standards

*(TBP) - To be prepared

3.0 REQUIREMENTS

The Pilot Plant system shall comply with all requirements specified herein and in the specifications listed in Section 2.2.1.

3.1 Pilot Plant System Definition

3.1.1 General Description. The Pilot Plant shall be described in the International System of Units in accordance with NASA SP-7012 and ANSI Y10.10-1060, but all reporting shall be in both systems of units, i.e., 0 °C (32°F). The Pilot Plant is comprised of the following:

(a) The collector subsystem shall consist of a series of individual tracking heliostats that continuously reflect the direct incident solar insolation onto a central tower mounted receiver at sufficient power levels to operate a steam Rankine turbine-generator set capable of providing a 2 PM on Winter solstice 10-MW net electrical power to a grid and/or recharge the thermal storage subsystem. The subsystem shall include all hardware and software identified in the Collector Subsystem Requirements Specification.

(b) The receiver (central receiver) shall provide a means of transferring the incident radiant flux energy from the collector subsystem into superheated steam which serves as the fluid (1) for generating electrical power by the electrical power generation subsystem, (2) for conversion to stored thermal energy by the thermal storage subsystem, and (3) for generating electrical power by the electrical power generation subsystem while also charging the thermal storage subsystem.

The receiver subsystem shall consist of an elevated receiver unit to intercept the radiant flux from the collector subsystem, the tower structure to support the receiver unit, the riser to transport feedwater to the receiver unit, and the downcomer to transport steam from the receiver unit to the ground. The receiver unit shall include the absorber (boiler/superheater); the receiver support structure; water and steam headers; valves and receiver control necessary to regulate the fluid flow, temperature and pressure; and the required thermal control necessary for safe and efficient operation, startup, shutdown, and standby of the receiver subsystem.

(c) The thermal storage subsystem shall consist of a desuperheater, heat exchanger, one or more thermal storage media, storage structure,

pumps, steam generator, valves, piping, and subsystem control as necessary to accept thermal energy from the receiver subsystem and store the energy for later reconversion to steam for use by the electrical power generation subsystem or for use in the receiver and/or the electrical power generation subsystem for thermal management.

(d) The electrical power generation subsystem shall consist of a steam Rankine turbine-generator set, power conditioning equipment, heat rejection unit, feedwater circulation pumps, feedwater heating equipment, and water treatment facilities. The turbine-generator set shall transform the thermal energy of the steam into 60 Hz electrical power at 13,200 volts. The turbine-generator set shall produce 10,000 kilowatts net of power when operating from receiver steam and 7,000 kilowatts net when operating from thermal storage steam. Intermediate power output levels shall be produced when operating the turbine-generator set off both receiver and thermal storage steam simultaneously. The subsystem shall, in addition, satisfy the sytem parasitic power requirements and shall provide an independent emergency source of power. The power conditioning equipment shall transform, switch, regulate, and control the electrical output of the turbine-generator set to ensure compatible integration into an existing electrical power transmission network. The heat-rejection unit shall reject waste heat from the turbine-generator set in a manner consistent with all site restrictions and limitations and minimize deleterious effects on the collector subsystem. The feedwater circulation pumps shall provide a flow of feedwater at the required pressure and flow rate conditions to the receiver and/or thermal storage subsystems. The feedwater heating equipment shall heat the feedwater to the desired temperature prior to being pumped to the receiver and/or thermal storage subsystem. The water treatment facility shall condition local water to the purity and chemical composition required by the receiver subsystem as stipulated in the Receiver Subsystem Requirements Specification.

(e) The master control consists of the control and display hardware and the associated software necessary for coordination of all subsystem processes, either automatically or manually under direction of the plant operator. The master control shall be capable of continuously computing the collector subsystem synthetic track commands and transmitting the encoded data to the collector subsystem. It shall control the system start-up, shut-down, and mode changes in a coordinated fashion while adjusting power flow splits between the turbine and thermal storage. It shall continuously monitor the

system and identify out of spec conditions. The master control shall be capable of recording and reducing plant operating data as well as making plant performance predictions based on available environmental data and options in operating modes.

3.1.2 Pilot Plant Application. Central receiver solar thermal power plants are expected to provide electrical power to the electrical transmission/distribution network. These solar thermal plants, initially sited in the Southwestern United States, would produce power to meet grid demands. The objective of the Pilot Plant is to establish the technical feasibility and indicate the potential economic feasibility of supplying power with a central receiver thermal power system. It is intended that the Pilot Plant design concepts be used by scaling or, in the case of the heliostats, as modular building blocks for construction of a 100- to 300-MWe commercial size central receiver power plant to demonstrate the economic feasibility of the central receiver concept on a commercial scale.

3.1.3 System Diagrams

3.1.3.1 Central Receiver Solar Thermal Power System Diagram. The central receiver solar thermal power system and the relationships of the various subsystems are shown in block form in Figure 1 and pictorially in Figure 2.

3.1.3.2 Functional Block Diagram. The Pilot Plant function block diagrams depicting normal solar, low solar power, intermittent cloudiness, extended operational, thermal storage charging, and fully charged thermal storage modes are shown in Figure 3.

3.1.3.3 Central Receiver Pilot Plant Layout. The plant layout for the Pilot Plant is shown in Figure 4.

3.1.4 Interface Definition. The Pilot Plant shall be physically and functionally compatible with the electrical power interface per the Pilot Plant/Electrical Power Transmission Network Specification and physically and functionally compatible with the site per the Pilot Plant/Site Interface

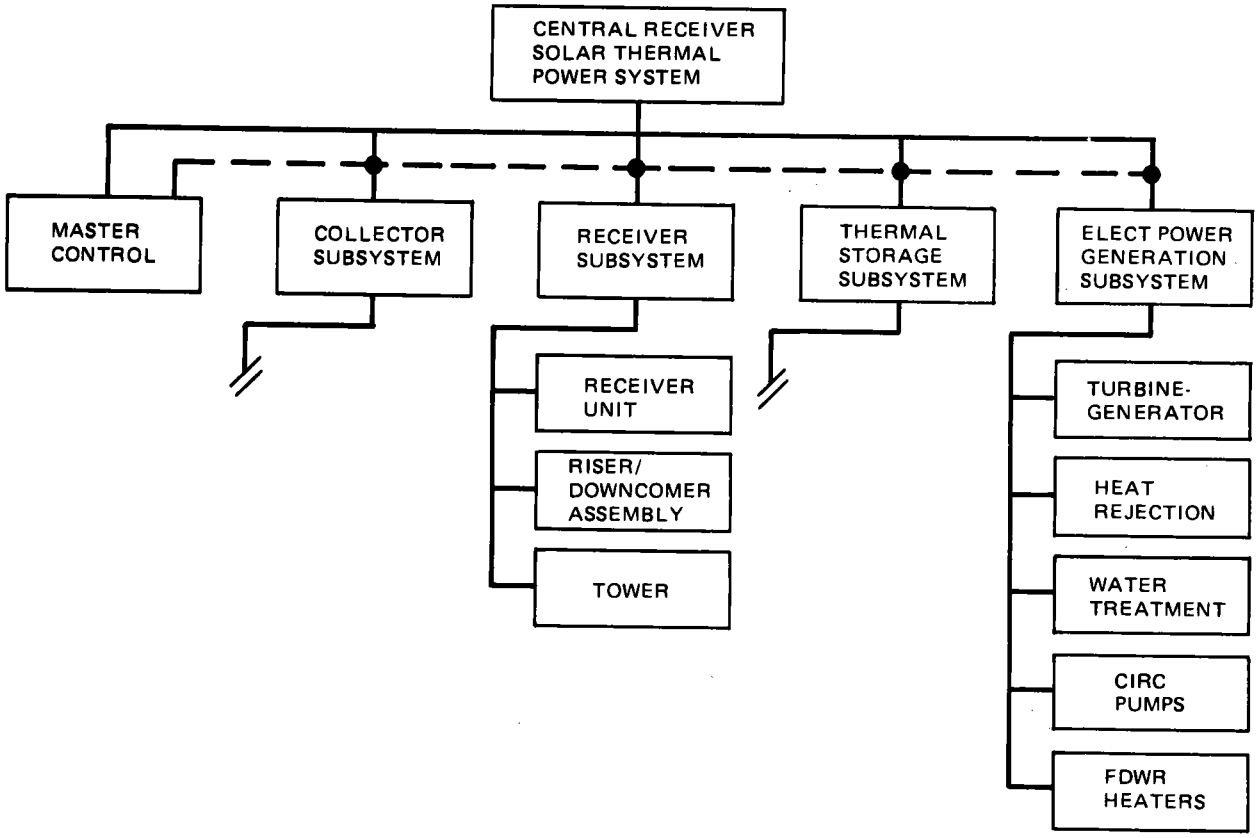

Figure 1. Central Receiver Solar Thermal Power System

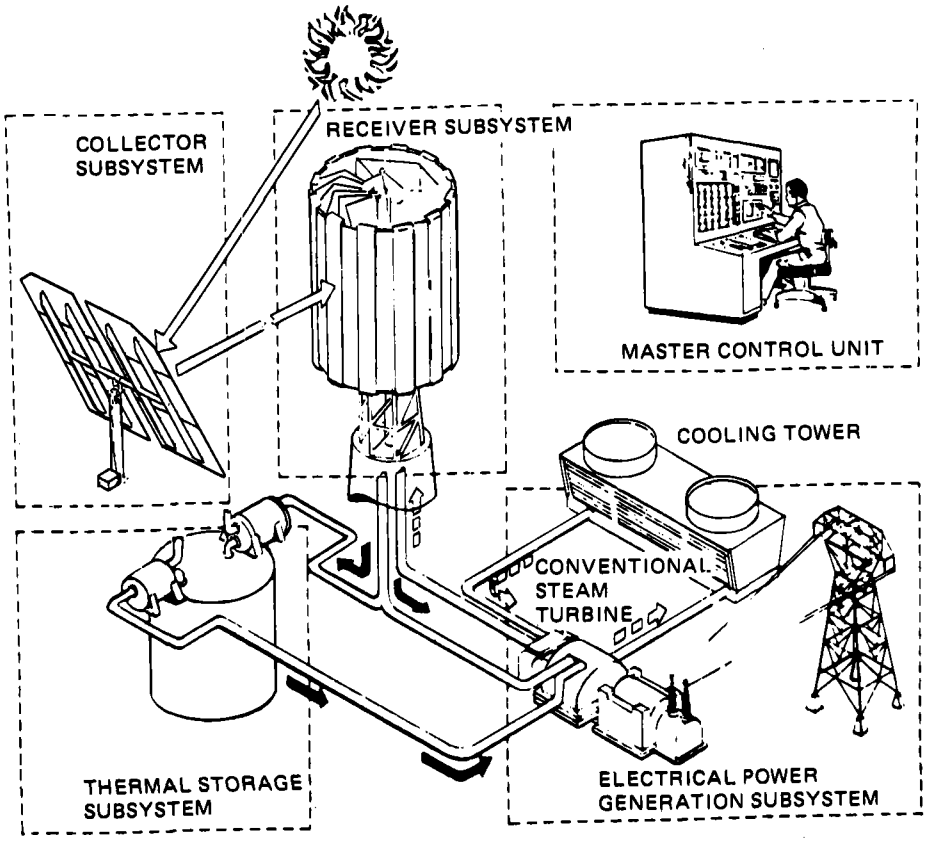

Figure 2. Central Receiver Baseline Concept

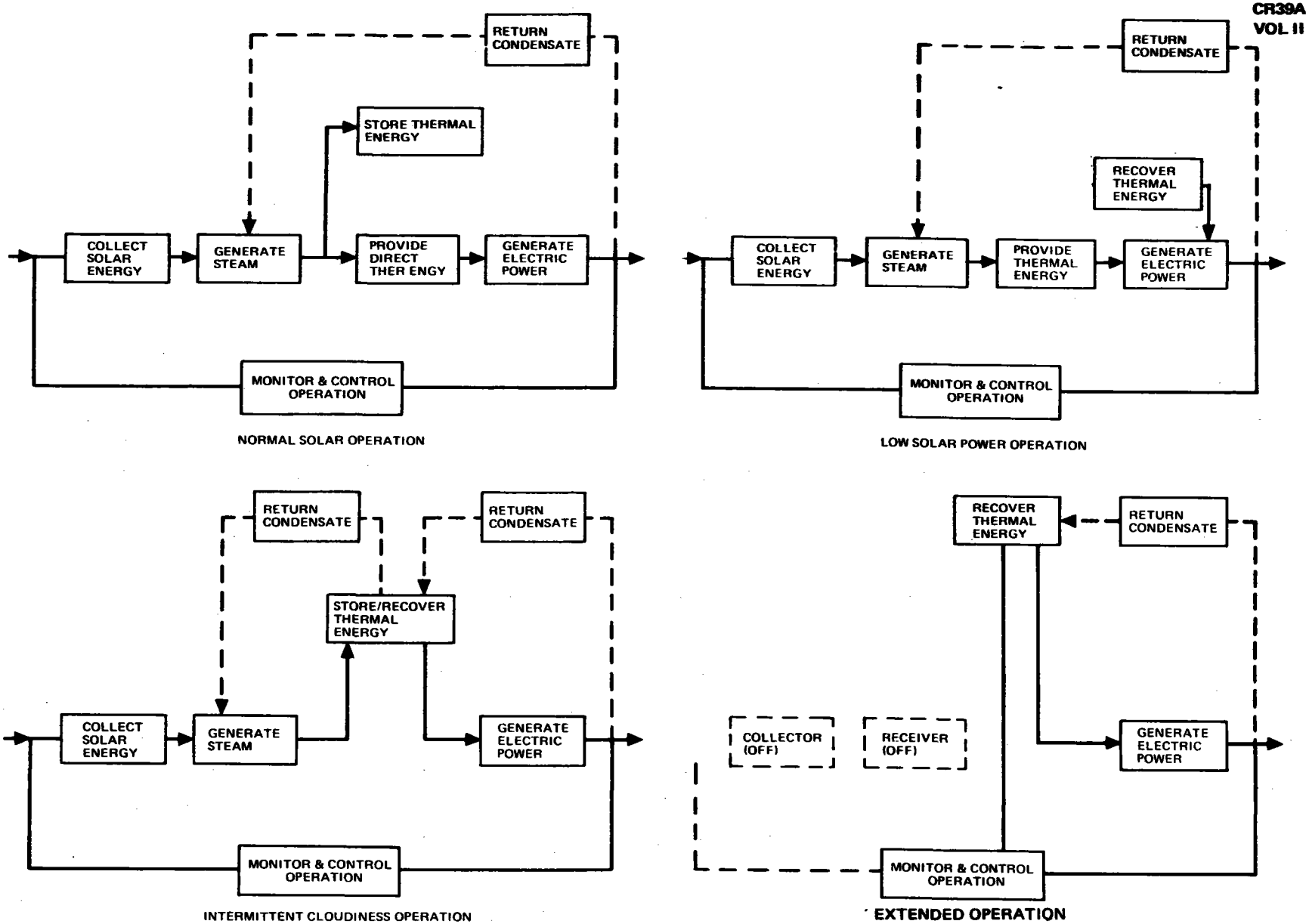

Figure 3. Central Receiver—Functional Block Diagram

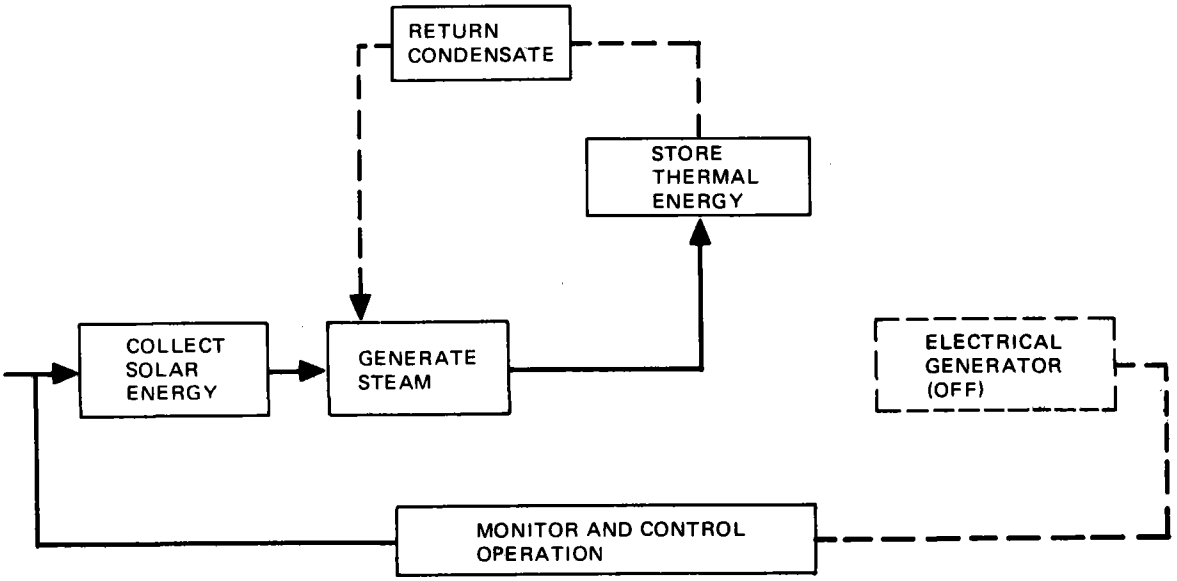

THERMAL STORAGE CHARGING

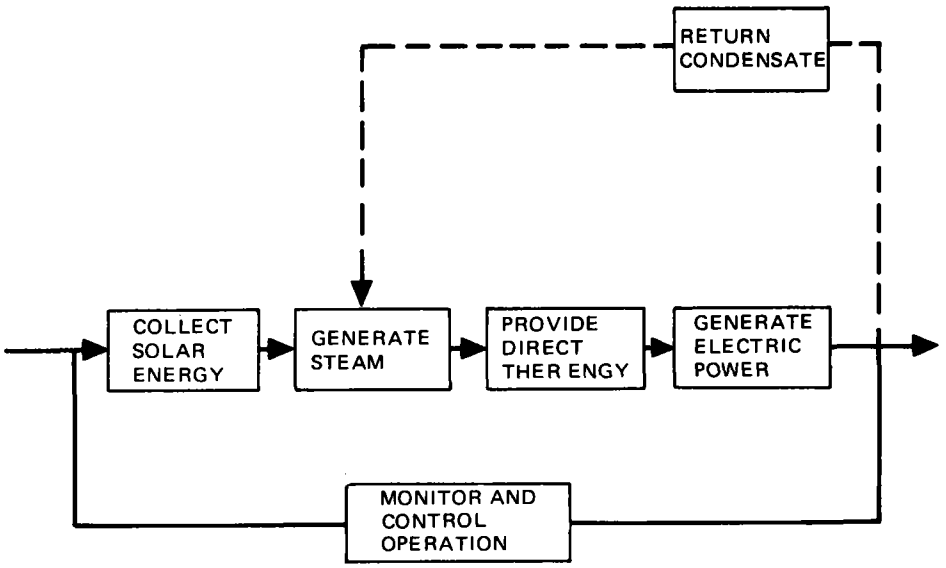

FULLY CHARGED THERMAL STORAGE

Figure 3. Central Receiver – Functional Block Diagram (Continued)

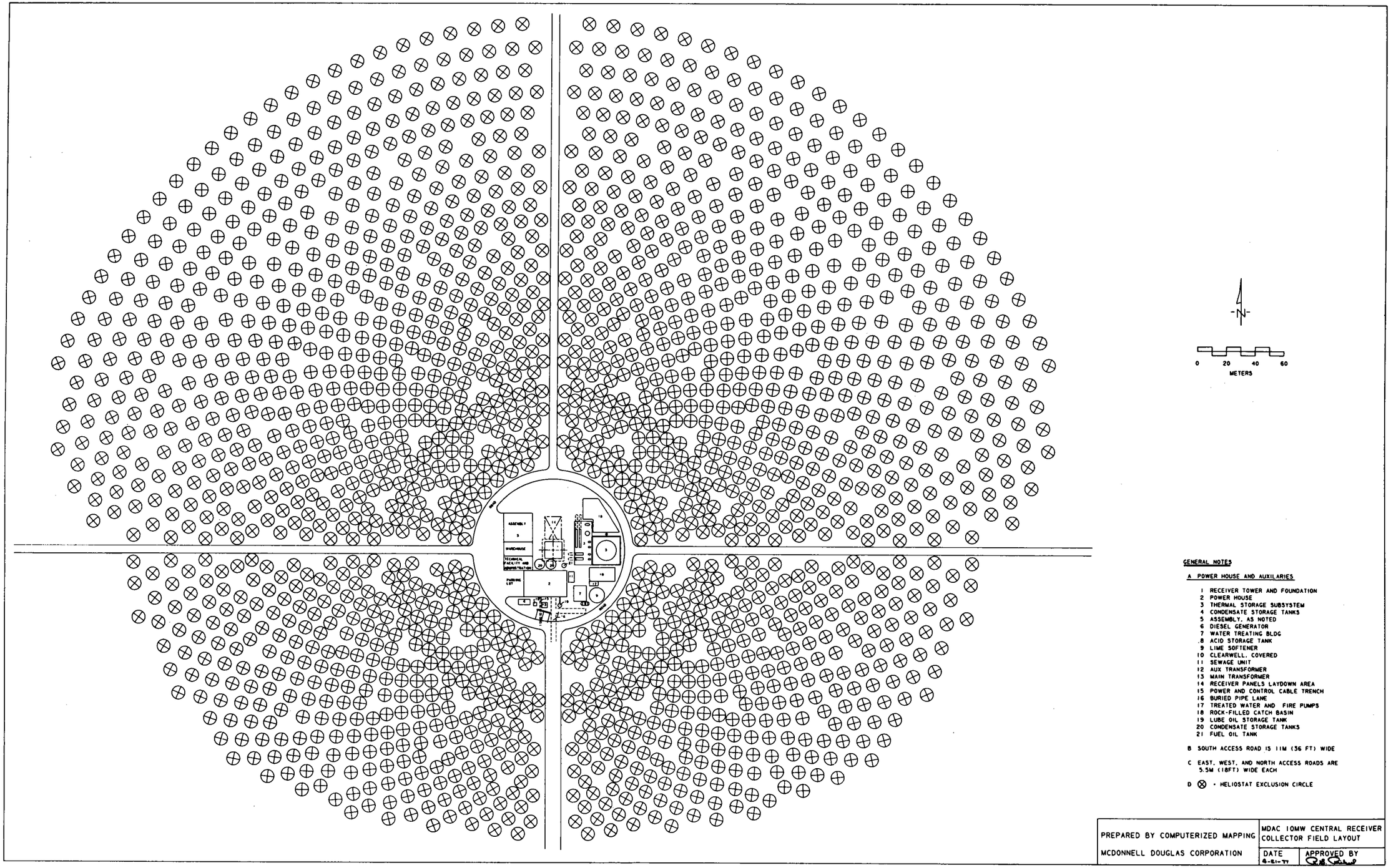

Figure 4. MDAC 10-MW Central Receiver Collector Field Layout

Specification. The Pilot Plant subsystems shall be physically and functionally compatible. The subsystem interface requirements shall be as specified in:

Collector Subsystem/Receiver Subsystem Interface Specification

Collector Subsystem/Electrical Power Generation Subsystem Interface Specification

Collector Subsystem/Master Control Subsystem Interface Specification

Receiver Subsystem/Thermal Storage Subsystem Interface Specification

Receiver Subsystem/Electrical Power Generation Subsystem Interface Specification

Receiver Subsystem/Master Control Subsystem Interface Specification

Thermal Storage Subsystem/Electrical Power Generation Subsystem Interface Specification

Thermal Storage Subsystem/Master Control Subsystem Interface Specification

Electrical Power Generation Subsystem/Master Control Subsystem Interface Specification

3.1.4.1 Electrical Power Transmission Network/Pilot Plant Interface. Electric power shall be provided to the electrical power transmission network at a power level of 7 to 10 MWe at a voltage of 13.2 kV. The frequency shall be 60 Hz. Physical connections shall be through standard high-tension cables per the standard of the National Electrical Manufacturers Association. Parasitic power shall be drawn from the network during nonoperational periods of the turbine-generator set.

3.1.4.2 Pilot Plant/Site Interface. The Pilot Plant shall be compatible in design with the environmental and soil conditions of the Barstow, CA. site in accordance with the Pilot Plant/Site Interface Specification. Source of water shall be provided for cooling tower and feedwater makeup which can supply 568 liters/min (150 gal/min) on a continuous basis.

3.1.5 Operational and Deployment Concepts. The Pilot Plant shall be designed for use in a power production mode and a system research mode.

3.1.5.1 Power Production Mode. In the power production mode, power from the Pilot Plant will be used by the utility to partially meet the electrical demand. The Pilot Plant will establish the operational capability of supplying electrical busbar power using thermal energy from the storage subsystem,

or thermal energy directly from the receiver subsystem. The power producing mode shall be capable of automatic operation within and between the operational modes described in paragraph 3.1.5.2.

3.1.5.2 Research Testing Mode. In the research testing mode, stable controlled operation of the Pilot Plant system shall be demonstrated in the following operational modes.

3.1.5.2.1 Normal Startup. An integrated system startup shall be coordinated through the master control. The heliostats shall be oriented to their predicted sun acquisition positions during the period from approximately 2 to 4 AM using power from the network or the auxiliary source. The startup shall begin when the sun is <10 deg above the horizon. Water flow shall be initiated through the receiver unit. The heliostats shall acquire the sun sequentially in order to control the full system powerup. Hot water/low quality steam developed in the receiver shall be cycled through the thermal storage subsystem, bypassing the turbine until high-quality dry steam is available (thermal storage charging mode). Steam shall be introduced into the turbine at a controlled rate for turbine heatup and roll. The turbine shall be loaded and the electrical power shall be synchronized with the interconnecting power network.

3.1.5.2.2 Normal Solar Operation. Normal solar power operation is defined as any period when receiver absorbed thermal energy exceeds 32.6 MWth and transient fluctuations are sufficiently small so that the turbine-generator can operate at its design point within the equipment guarantee specifications provided by the manufacturer. This condition corresponds to a receiver unit outlet steam condition of 516°C (960°F) at a pressure of 10.45 MPa (1,515 psia) with a minimum (winter solstice) steam rate entering the turbine of 12.9 kg/s (102,440 lb/hr) and a maximum (equinox noon) rate of 14.8 kg/s (117,570 lb/hr). In this mode, receiver steam in excess of that required for turbine design point operation is delivered to the thermal storage subsystem.

3.1.5.2.3 Low Solar Power Operation. A low solar power operation mode exists when the available thermal power from the receiver is between 10.0 and 32.6 MWth due to a reduction in insolation (either normal diurnal or

haze-induced). In this mode, all available receiver steam is sent through the high-pressure throttle port of the turbine and supplemental steam produced by the thermal storage being introduced into the admission port. The quantity of supplemental steam required is governed by the electrical power demand and the availability of receiver steam.

3.1.5.2.4 Intermittent Cloudiness Operation. During periods when excessive transients in solar insolation are anticipation due to intermittent cloud cover, all of the collected thermal energy shall be directed to the thermal storage subsystem. The turbine-generator shall be simultaneously operated from steam produced by the thermal storage subsystem and be capable of producing a minimum of 7 MW net electrical power to the busbar.

3.1.5.2.5 Thermal Storage Charging. The charging operation mode is defined as delivery of all collected thermal energy to the thermal storage subsystem without concurrent operation of the turbine-generator. This mode shall be employed during normal startup until high-quality steam is available. It may be a required daytime mode during the winter in order to fully charge the thermal storage subsystem so that peak nighttime grid demands can be satisfied.

3.1.5.2.6 Extended Operation (Stored Energy). During periods when the receiver is incapable of producing useful steam (either at rated conditions for direct use by the turbine or at derated conditions for use in charging thermal storage), the turbine may continue to operate by deriving all of its steam flow from energy contained in the thermal storage subsystem. The steam rate and state to the turbine shall be maintained at such a level that the net electrical output to the busbar is a minimum of 7 MWe.

3.1.5.2.7 Fully Charged Thermal Storage. During periods of system operation when the thermal storage subsystem is incapable of accepting thermal energy, either as a result of being fully charged or due to a malfunction in the charging equipment, the system energy collection rate is adjusted if necessary, through partial heliostat field shutdown, to be compatible with the maximum turbine capacity. This mode represents the

threshold between normal solar and low solar power operation in that rated receiver steam is used completely while neither the thermal storage charging nor discharging function is required.

3.1.5.2.8 Normal Shutdown. An integrated system shutdown shall be coordinated through the master control. The system shall be capable of initiating shutdown from any of the above operation modes. When operating with steam developed by the thermal storage subsystem, the shutdown of the electrical power generation subsystem shall be automatically initiated when the outlet temperature of the thermal storage heat-transfer fluid falls below 292° C (560°F). At this point, the generator shall be taken off line and the steam flow to the turbine shall be reduced in a manner consistent with the turbine specifications. Once the turbine rotation stops, a turning gear shall be activated to provide for slow turbine rotation in order to prevent differential cooling.

3.1.5.2.9 Emergency Shutdown. The master control shall monitor the status of all subsystems and shall be capable of diagnosing subsystem malfunctions. In the event a malfunction is deemed "serious" (leading to potential equipment damage or safety hazard) and no redundancy is available, an emergency shutdown procedure shall be automatically initiated with manual backup. The procedure shall depend on the nature of the failure but in all cases shall be designed to maximize safety while minimizing equipment damage.

In the event of approaching adverse environmental conditions (wind, sandstorm, rain, hail, etc), a system shutdown and heliostat reorientation shall be executed after issuance of command by the master control. The heliostats shall be off targeted in a controlled manner to ensure a controlled receiver shutdown. They shall then be directed to a minimum damage orientation in a manner compatible with reflected beam safety considerations. The system shutdown may be limited to the collector and receiver portions (i. e., extended operation mode) if sufficient energy exists in the thermal storage subsystem to maintain power plant operation.

3.1.5.2.10 Subsystem Conditioning. During nonoperational periods, subsystems shall be protected from damage due to environmental or cooling

effects. This shall include the prevention of freezing of components containing water and the use of turning gear to prevent permanent set in the turbine rotor.

3.2 CHARACTERISTICS

3.2.1 Performance. The system shall be capable of (1) delivering 10 MWe net busbar power to the electrical transmission network at 2 PM on a clear day at winter solstice when operating on energy directly from the receiver subsystem, (2) storing thermal energy in the thermal storage subsystem for concurrent or deferred conversion to electrical power, (3) when absorbed thermal power exceeds 32.6 MWth, storing energy while simultaneously generating 10 MWe net, (4) delivering at least 7 MW net electrical power for a period of 3 hr and lesser power levels for longer periods of time to the electrical transmission network when operating solely on energy drawn from the fully charged thermal storage subsystem (see Figure 5), and (5) delivering at least 7 MWe net power to the electrical transmission network when operating on energy from the thermal storage subsystem while it is being charged by the receiver subsystem (Intermittent Cloudiness Mode).

The receiver unit shall be capable of producing rated steam at 10.45 MPa (1,515 psia), 516°C (960°F) from inlet feedwater at temperatures from 157 to 218°C (315 to 425°F) at receiver unit output power levels greater than the threshold value of 10.0 MWth and less than the 37.1 MWth output associated with equinox noon. The receiver unit shall also be capable of producing derated steam at 10.45 MPa (1,515 psia) and 349°C (660°F) from inlet feedwater at 190 to 218°C (375 to 425°F) at output power levels between 7.3 MWth and 32.8 MWth. The receiver unit shall be designed to produce rated outlet steam at an absorbed thermal power level of 37.1 MWth. The corresponding flowrate shall be 14.8 kg/s (117,570 lb/hr). The receiver unit shall also be designed to produce derated outlet steam at an absorbed thermal power level of 32.8 MWth. The corresponding flowrate shall be 16.5 kg/s (130,500 lb/hr). All flow control components shall be sized to accommodate a 10% overflow condition above that specified above. The nominal inlet feedwater temperature for both cases shall be 210°C (412°F).

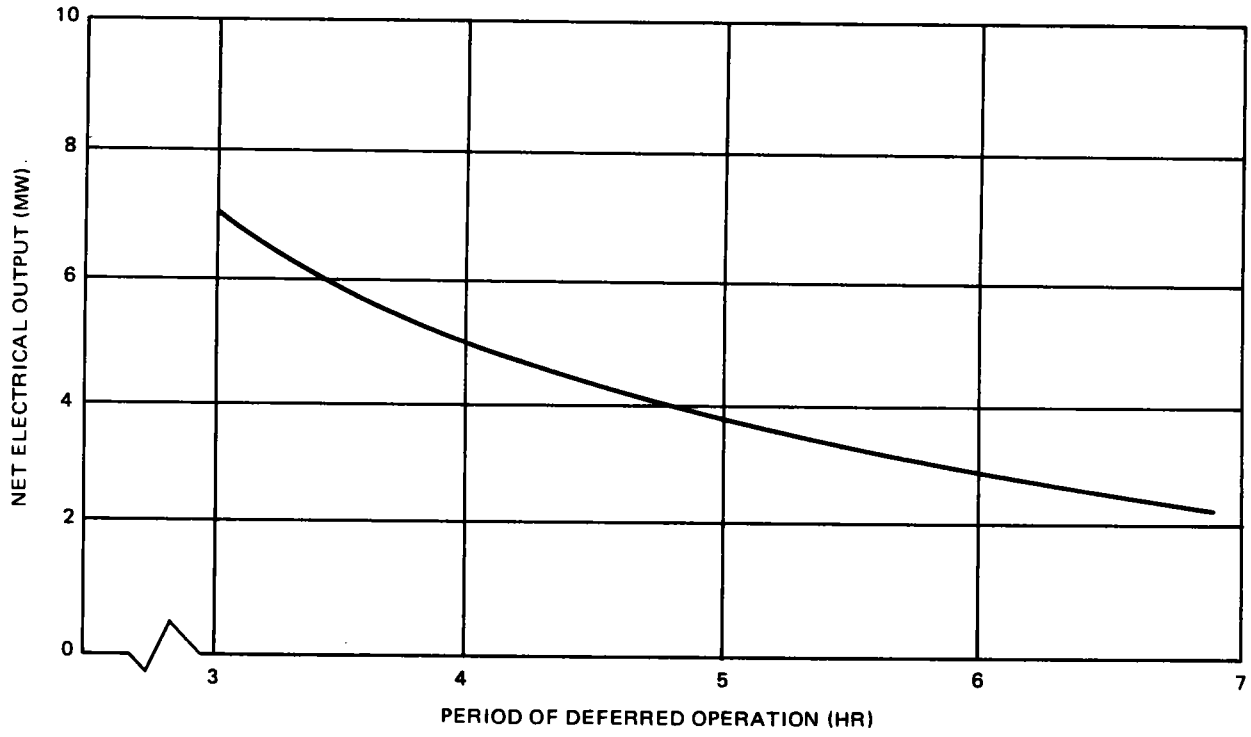

Figure 5. Net Electrical Output Characteristics at Reduced Power Level

The thermal storage shall be designed to the worst case condition which corresponds to a 343°C (650°F) desuperheater inlet temperature at the 32.8 MWth power level. The corresponding flowrate and pressure shall be 16.5 kg/s (130, 500 lb/hr) and 10.1 MPa (1, 465 psia), respectively. The thermal storage charging equipment shall be capable of absorbing 30.0 MWth while passing the remaining thermal power in the form of high temperature condensate to the thermal storage flash tank.

The electrical power generation subsystem shall be designed to efficiently convert the available thermal energy into 60 Hz electrical power at 13, 200 volts and to provide feedwater heating at a rate compatible with the steam available for extraction. The power conditioning equipment shall be designed to condition all output power to be compatible with the existing power grid. The heat rejection unit shall be capable of rejecting a maximum of 27.8 MW (95.0×10^6 Btu/hr) of thermal power. The water treatment facility shall be capable of treating and purifying water to a dissolved solids content of 20-50 PPB and a pH of 9.5 to satisfy the receiver water chemistry requirement (per the Receiver Subsystem Requirements Specification).

3.2.1.1 Dynamic Performance.

3.2.1.1.1 Startup. The system shall be capable of developing full power within 5 hr from a cold startup condition. The system shall be capable of developing full power within 62 min after a 10-hr shutdown. The system shall be designed for an anticipated 300 hot startup and 5 cold startups annually.

3.2.1.1.2 Emergency Shutdown. The system shall be capable of a coordinated emergency shutdown. The time for such shutdown shall be determined to minimize equipment damage and provide maximum safety. The minimum shutdown times shall occur as a result of a water circulation failure in the receiver. During such an occurrence, the radiation incident on the receiver surface shall be reduced to 3% of its initial value in 120 sec.

3.2.1.1.3 System Dynamic Variation. The system shall be capable of stable controlled operations during all normal operating modes. The frequency of the electrical network varies about a nominal 60 Hz in a manner

which reflects grid load. Once synchronized, the system shall provide power to the network at the network frequency.

3.2.1.2 Endurance Capability. The hardware shall be designed to have a 30-year operational lifetime with normal maintenance while exposed to the environments specified in the Pilot Plant Environmental Conditions.

3.2.1.3 Other Performance Requirements

3.2.1.3.1 Annual Power Output. The expected net annual power output of the pilot plant shall be 27,430 MWHe based on insolation and environmental data contained on the Aerospace data tape for Inyokern 1963 and ignoring downtime for maintenance. The annual energy number assumes all thermal power passes through the turbine whenever rated receiver steam is available.

3.2.1.3.2 Collector Operations. The collector subsystem shall not inflict damage on any system element or present a safety hazard due to a misdirection of the reflected solar energy.

3.2.2 Physical Characteristics

3.2.2.1 System Characteristics. The Pilot Plant shall possess the physical characteristics identified in Table 1. Vehicular traffic shall have access to all major parts of the system. Sufficient ingress, egress, and access shall be provided to all areas of the system of the system for maintenance purposes. Major roadways shall be paved to minimize traffic-induced dust. Field protection shall be provided by suitable fencing. Ground foilage shall be permitted to grow in all areas unless it impacts the operation and/or maintenance of the system.

3.2.2.2 Collector Subsystem Characteristics. The collector subsystem shape limitations shall be determined only by the collector field layout, shadowing restraints and servicing functions together with the resulting receiver tower height. The collector field layout shall be developed to optimize collector performance on an annual basis. Spacing between heliostats in the field must permit access by service vehicles, utility lines, and ground maintenance

personnel. Heliostat weight and size shall be limited only by manufacturing, transportation, operation, maintenance and servicing constraints, pointing accuracy requirements, and structural requirements. Heliostats shall have a stowed or safe position for use at night, during periodic maintenance, and during periods when the Pilot Plant is subjected to environmental conditions exceeding those specified in the Pilot Plant Environmental Conditions.

Table 1

PILOT PLANT SYSTEM CHARACTERISTICS

CHARACTERISTICS		
Tower Height: 65m (213 ft)		
Receiver Centerline Elevation 80m (262 ft)		
No. Heliostats: 1760		
Heliostat Configuration: 6.5m Square, Slotted		
Receiver Unit Configuration: cylindrical with longitudinal axis vertical		
Peak Incident Thermal Power: 43.4 MW (Equinox Noon)		
Design Incident Thermal Power: 38.7 MW (2 PM Winter Solstice)		
Peak Absorbed Thermal Power: 37.1 MW (Equinox Noon - Rated Steam)		
32.8 MW (Equinox Noon - Derated Steam)		
Design Absorbed Thermal Power: 32.6 MW (2 PM Winter Solstice)		
Thermal Storage Capacity: 103.8 MWh		
Design Net Electrical Power Output: 10 MWe (2 PM Winter Solstice)		
7 MWe (Thermal Storage)		
Parasitic Power Load: 1.2 MW (Daytime), 0.80 MW (Nighttime)		
Plant Efficiencies:	Daytime Gross = 34.5%	2 PM Winter Solstice
	Daytime Net = 30.8%	
	Nighttime Gross = 24.3%	
	Nighttime Net = 21.8%	

3.2.2.3 Receiver Subsystem Characteristics. The receiver subsystem shall be composed of the receiver unit (absorber, headers, manifolds, valves, controls, instrumentation, and support structure), the riser/downcomer assembly, and the tower.

The absorber shape shall be cylindrical, oriented such that it is illuminated by the collector subsystem on all external curved surfaces. Physical characteristics of the receiver unit shall be such that it will accommodate a peak incident solar flux of 0.3 MW/m^2. The receiver unit shall be designed such that it can be erected and removed from the top of the tower in a limited number of pieces. The receiver unit shall be designed for easy repair and maintainability. The contractor shall provide access to the receiver unit by means of permanent or temporary platforms. The riser and downcomer shall be rigidly attached to the top of the tower and shall be designed to accommodate the thermal expansion and contraction over their lengths.

The tower shall be designed to provide ingress, egress, and access for maintenance and inspection of tower structure, receiver steam lines, utilities, and other subsystem elements. Adequate provisions shall be made to ensure crew safety at all times for required operation, inspection, maintenance, and repair.

3.2.2.4 Thermal Storage Subsystem Characteristics. The thermal storage subsystem shall be designed to maximize the economic and safe recovery of useful thermal energy from storage and to minimize thermal energy losses. Specific size, shape, and configuration constraints will be governed only by the Pilot Plant layout and design to facilitate efficient and safe operation and maintenance. The thermal storage subsystem shall be designed to provide safe and reasonable ingress, egress, and access for proper inspection, maintenance and repair of the structure, storage media, steam lines, utilities, instrumentation and controls. The thermal storage subsystem shall be so configured and located within or adjacent to the Pilot Plant to minimize adverse interfaces with or impact on operations of the other subsystems.

3.2.2.5 Electrical Power Generation Subsystem (EPGS) Characteristics. The specific size, shape, and configuration constraints imposed on the individual EPGS components shall be governed only by the Pilot Plant layout and design to facilitate efficient and safe operation and maintenance, to minimize the effects of thermal shock on the turbine power loop, and to provide for rapid response to variations in the inlet steam conditions. The electrical power generation subsystem shall be designed to provide safe and reasonable

ingress, egress, and access for proper inspection, maintenance and repair of the structure, fluid flow lines, utilities, heat-rejection unit, instrumentation and controls for each element or component. The elements and components of this subsystem shall be so configured and located within or relative to other portions of the Pilot Plant as to minimize adverse interfaces with or operations of the other subsystems.

3.2.2.6 Master Control. The master control shall be designed to ensure the stable integrated operation of the system. The master control shall be operated in either an automatic (computer control) or manual mode. Computer peripheral equipment shall include redundant disk files, line printer, typewriter, and magnetic tape unit. Control and display consoles shall be available for overall system control as well as individual units dedicated to each subsystem. The characteristics of these individual pieces of equipment are presented in the Master Control Requirements Specification.

3.2.3 Reliability. High reliability shall be achieved in the system design by providing adequate operating margins, maximizing the use of proven standard parts, and using conservative design practices such that the reliability performance shall not degrade the capability to achieve the availability specified in paragraph 3.2.5 when operated in the environments specified in the Pilot Plant Environmental Conditions.

Single-point failures that disable the automatic mode of system operation shall be eliminated wherever practical. In cases where it is impractical to eliminate such failure modes, suitable devices shall be used to detect and signal the occurrence of a failure.

The Pilot Plant design shall employ the following reliability design criteria:

(a) Design for maximum "fail-safe" characteristics for subsystems and equipment performing the most critical functions. Components in fluid or pneumatic subsystem loops shall be applied so that failure in their most likely mode results in a safe-condition. The ability of the component to revert to a "safe" condition after sustaining a failure shall be enhanced through sound design practices; such as, low working stress in springs, high margin

of spring force versus known resistive forces such as friction, high wear-out margin in elements essential to the "safe-return" position, and adequate allowances for travel, adjustment, and degradation from handling, storage, maintenance, or lack of maintenance.

(b) Redundant functional paths, including equipment, fluid lines, electrical wiring, and electrical connectors, shall be located to ensure that an unexpected event which damages one path is not likely to damage the other path.

(c) Redundant components shall operate from separate and independent power supplies.

(d) The design of the subsystem incorporating redundancies shall include a means of verifying satisfactory operation of each redundant path at any time the subsystem is determined to require testing.

(e) Electrical circuit relays, switches, circuit breakers, etc shall be designed to fail open when continuous power creates a hazard and fail to a closed position where a power interruption would be hazardous.

(f) Power system surges outside nominal limits resulting from equipment turn-on, turn-off, and momentary power interruptions shall be provided for in the design of electrical equipment.

(g) Electrical connectors and wiring junctions of connectors shall be sealed from moisture to prevent open and short circuits.

(h) Connectors shall be limited only to those applications requiring disconnection.

(i) Wires attached to normally moving parts shall be routed to twist with rather than bend across adjacent moving parts.

(j) Supports shall be provided to prevent abrasion or chafing of wires.

(k) Cable installation shall consider rodent damage.

(l) Pressure vessels shall be protected from exceeding structural limitations by relief devices.

(m) Primary relief devices shall not be obstructed.

(n) Relief valves shall relieve pressure at no higher than 110% of maximum operating pressure.

(o) Pressure drop in plumbing between any relief valve and vent outlet shall be minimized by valve location and/or dump design.

(p) Flow restrictions shall be provided such that no failure of lines or components will allow flow into a tank at a rate exceeding the pressure relief capacity of the tank.

(q) Relief/vent valves shall be sized to exceed the maximum flow capacity of the pressure source. If relief is not provided, safety factors shall be sufficient to safely contain the source pressure.

(r) Plumbing downstream of any regulator shall be designed to meet the requirements of full upstream pressure, or shall be protected by relief valves sized to handle the flow rate resulting from stuck-open regulators.

(s) Mechanisms shall be protected against damage or jamming by debris through use of debris-proof covers, containers, or equivalent features.

(t) Filters shall be installed in the receiver circuits to prevent clogging of tubes with contaminants.

(u) The design of the system shall consider thermal expansion and contraction of all components.

3.2.4 Maintainability. Maintainability shall be considered in all elements of the Pilot Plant design to ensure minimum cost for maintenance and servicing throughout the 30-year system life, and a downtime consistent with the availability requirement of paragraph 3.2.5. A Pilot Plant maximum allowable downtime shall be determined based on trade studies which consider system reliability and cost. This requirement shall be allocated to the various subsystems and major components of the system. Maintainability predictions prepared in support of subsystem design shall provide median and maximum (90 percentile) values, assuming an overall log normal distribution.

In order to achieve the required system maintainability, the system shall be designed such that:

(a) Items that are critical to availability (because of high failure risk, high downtime, or major effect on system performance) shall be provided with automatic failure detection and fault isolation.

(b) Potential maintenance points can be easily reached and replaceable components such as electronic units, sensors, motors, drives, etc can be readily replaced.

(c) Elements subject to wear or damage such as supporting wheels, gears, etc are easily serviced or replaced.

(d) Test points and calibration adjustments are accessible and repairs can be accomplished by module replacement.

(e) The Pilot Plant can be serviced by personnel of normal skills requiring a minimum of specialized equipment or tools.

(f) On-line maintenance may be conducted without reducing subsystem performance.

(g) The equipment shall be designed to contain the minimum number of test points required to ascertain satisfactory performance of all primary and redundant circuits.

(h) Electrical and fluid or gas handling systems shall include test points which will permit normal planned subsystem checkout to be made without disconnecting tubing or electrical connectors which are normally connected in service. Equipment expected to require servicing or maintenance shall be designed to be accessible without the removal of other equipment, wire bundles, and fluid lines.

(i) All electrical connectors and cable installations shall be designed with sufficient flexibility, length, and protection to permit disconnection and reconnection without damage to wiring or connectors.

(j) Electrical systems shall be designed so that all necessary mating and demating of connectors are accomplished without producing electrical arcs which will damage connector pins or ignite surrounding materials.

(k) Sufficient space shall be allowed around connectors for engaging and disengaging, particularly where wrenches are required.

(l) Components shall be designed so that they cannot be installed improperly.

(m) Mechanical systems involving linkages or other devices requiring accurate alignment by adjustment shall include built-in provisions for alignment and accessible rigging points for verification of alignment without equipment removal.

(n) Lines shall be identified by contents, pressure, and direction of flow.

(o) All tanks shall have inspection capability.

(p) Automatic valves shall be designed to have manual bypass or shutoff capabilities.

(q) Hand valves and adjustment shall be readily accessible and identified to indicate function and sequence of operation.

(r) Reservoirs and storage vessels shall be provided with shutoff valves for maintenance.

(s) Drain valves shall be located in the low point of the system.

(t) The electrical signatures of all remote valves shall be recorded to facilitate preventive maintenance.

(u) Manually operated shutoff valves shall not be placed so that they are rendered unreachable by a downstream line rupture.

3.2.5 Availability. The system shall operate in accordance with paragraph 3.2.1 performance requirements 90% of its scheduled operating time, based on reliability and maintainability exclusive of isolation conditions, using a period of 1 yr as a time reference, and assuming 30 days annual downtime for scheduled maintenance. Availability is defined as the percent of the total scheduled time that the system is able to operate in accordance with the specified system performance requirements.

The system availability is calculated according to the formula

$$A_s = 1 - \sum_{J=1}^{N} (1 - A_{(J)})$$

where

$A_{(J)}$ = Availability of the Jth subsystem for one year of scheduled operation.

The availability of each subsystem ($A_{(J)}$) shall be calculated according to the formula

$$A_{(J)} = \frac{T_U - T_D}{T_U}$$

where

T_U = Total scheduled operating time in 1 yr for the Jth subsystem.

T_D = Expected (or realized) downtime during the scheduled operating time for subsystem maintenance to return the subsystem to full

performance as required by paragraph 3.2.1 of the applicable subsystem specification.

T_D is defined as the median of the probability distribution of downtime for maintenance of the Jth subsystem.

3.2.6 Environmental Conditions. The subsystems shall be designed to withstand the site, transportation, and operating conditions defined in the Pilot Plant Environmental Conditions. Those conditions shall be considered to represent the minimum environment design requirements. The system elements shall withstand the maximum earthquake environment described in the Pilot Plant Environmental Conditions without structural damage or yielding.

3.2.7 Transportability. System elements shall be designed for transportability within applicable Federal and state regulations by highway and railroad carriers using standard transport vehicles and materials handling equipment. Whenever feasible, components shall be segmented and packaged to sizes that are transportable under normal commercial transportation limitations (see (a) below). Subsystem components that exceed normal transportation limits (see (b) below) shall be transportable with the use of special routes, clearances, and permits.

(a) Transportability Limits for normal Conditions (Permits Not Required)

	Truck	Rail
Height	13 ft 6 in. above road	16 ft 0 in.
Width	8 ft 0 in.	10 ft 6 in.
Length	55 ft 0 in. - Eastern States 60 ft 0 in. - Western States	60 ft 6 in.
Gross Wt	73,280 lb, 18,000 lb/axle	200,000 lb

(b) Transportability Limits for Special Conditions

	Truck	Rail
Height	14 ft 6 in. above road	16 ft 0 in. above rail
Width	12 ft 0 in.	12 ft 0 in.
Length	7 ft 0 in.	80 ft 6 in.
Gross Wt	100,000 lb, 18,000 lb/axle	400,000 lb

The design requirements for component packaging and tiedown techniques shall be compatible with the following limit load factors.

Vibration

Transportation Mode	Amplitude (G_{op})	Frequency Range (Hz)
Highway	±0.6	1 - 85
	±0.9	85 - 300
Air	±0.05 in D.A.	3 - 38
	±2.0	38 - 1,000
Rail	±1.0	1 - 100
	±1.6	100 - 1,000

Shock Load Factors

	Acceleration (G)		
Transportation Mode	Longitudinal	Lateral	Vertical
Air	±3.0	±2.5	±2.0
Highway	±3.5	±2.0	±3.0
Rail			
Rolling	±3.0	±0.75	±3.0
Humping (Hydro cushion car)	±3.0	±2.0	±3.0

All critical components shall be designed or packaged such that the conditions described above do not induce a dynamic environmental condition which exceeds the structural capability of the component. These conditions reflect careful handling and firmly constrained (tied down) transporting via common carrier. All components shall be designed to withstand handling/hoisting inertial loads up to 2 g's considering the number, location and type of hoisting points.

Handling shock will result from normal handling drops of large packaged equipment. Corresponding acceleration peak may be of the order of 7 g's vertical and 4 g's horizontal with a sinusoidal profile and a duration of 10 to 50 milliseconds.

Smaller components shall be properly packaged to prevent structural damage during normal handling and inadvertent drops to a maximum specified height. The handling shocks for these components are a function of the weight and dimensions of the packaged item. Structural analyses shall be performed for critical items to establish the structural integrity of the packaged component for the shock levels experienced in the shipping package. The drop height noted below shall be used as design guidelines for the packaged item.

Gross Weight Not Exceeding (lb)	Dimensions of Any Edge, Height, Diameter (In.)	Free Fall Height of Drop on Corners, Edges, or Flat Faces (In.)
50	36	22
100	48	16
150	60	14
No Limit	No Limit	12

3.3 Design and Construction

Design and construction standards compatible with the end use shall be employed.

3.3.1 Materials, Processes, and Parts. To the maximum extent possible, standard materials and processes shall be employed. Highly stressed components and unusual materials shall be avoided. As far as practical, off-the-shelf components used in industry shall be employed. Materials and components, susceptible to environmental deterioration shall be protected with a suitable coating or protective layer.

3.3.2 Electrical Transients. Pilot Plant operation shall not be adversely affected by external or internal power line transients caused by normal switching or fault clearing. Switching transients and fault clearing functions shall require less than six cycles of the fundamental frequency (100 milliseconds)

and shall be limited to 1.7 P. U. voltage (1.7 per unit or 170%). The receiver and tower shall be protected against damage due to lightning termination.

The design shall include an air terminal(s) on the top of the receiver unit. The air terminal design and installation shall be in accordance with NFPA Bulletin No. 78 (ANSI C5. 1). Design level used shall be for the important case as described in NFPA No. 78. The rest of the system shall avail itself of the umbrella of protection afforded by the receiver and tower. No additional lightning protection shall be provided outside this umbrella.

3. 3. 3 Electromagnetic Radiation. The system shall be designed to minimize susceptibility to electromagnetic interference and to minimize the generation of conducted or radiated interference. The design criteria contained in the following Air Force design handbooks shall be used to assure electromagnetic compatibility: Design Handbook on Electromagnetic Compatibility (AFSC DH1-4), Checklist of General Design Criteria (AFSC DH1-X), and Instrumentation Grounding and Noise Minimization Handbook (AFRPL-TR-65-1).

3. 3. 4 Nameplate and Product Marking. All deliverable end items shall be labeled with a permanent nameplate listing, as a minimum, manufacturer, part number, change letter, serial number, and date of manufacture.

All access doors to maintainable items shall be labeled to show equipment installed in that area, and any safety precautions or special considerations to be observed during servicing.

3. 3. 5 Workmanship. The level of workmanship shall conform to practices defined in the codes, standards, and specifications applicable to the selected site and the using utility. Where specific skill levels or certifications are required, current certification status shall be maintained with evidences available for examination. Where skill levels or details of workmanship are not specified, the work shall be accomplished in accordance with the level of quality currently in use in the construction, fabrication, and assembly of commercial power plants. All work shall be finished in a manner such that it presents no unintended hazard to operating and maintenance personnel, is neat and clean, and presents a generally uniform appearance.

3.3.6 Interchangeability. Major components and circuit cards and other items with a common function shall be produced with standard tolerances and connector locations to permit interchange for servicing. Components with similar appearances but different functions shall incorporate protection against inadvertent erroneous installation through the use of such devices as keying, connector size, or attachment geometry.

3.3.7 Safety. The Pilot Plant shall be designed to eliminate or acceptably control safety hazards to operating and servicing personnel, the public, and to equipment. Sufficient analyses shall be conducted to assure that system designs and operational procedures consider the following:

(a) Controlling and minimizing the potential damage to personnel, equipment, and material of hazards which cannot be avoided or eliminated.

(b) Isolating hazardous substances, components, and operations from other activities, areas, personnel, and incompatible materials.

(c) Incorporating "fail-safe" principles where a failure would disable the system to prevent a catastrophe either through injury to personnel or damage to equipment.

(d) Locating equipment components so that access to them by personnel during operation, maintenance, repair, or adjustment shall not require exposure to hazards such as burns, electrical shock, cutting edges, sharp points, insecure footing, or toxic atmospheres.

(e) Avoiding undue exposure of personnel to physiological and psychological stresses which might cause errors leading to mishaps.

(f) Providing suitable warning and caution notes in operations, assembly, maintenance, and repair instructions; and distinctive markings on hazardous components, equipment, or facilities for personnel protection.

(g) Grounding and insulating electrical supplies and components and insulating parts or components with elevated temperatures or shock potential to prevent contact with or exposure to personnel.

(h) Shielding moving elements to avoid entanglements and providing safety override controls and/or interlocks for servicing.

(i) Providing emergency shutoff valves and switches, fire extinguishers and fire escape paths for areas that have hazardous material or ignition sources.

(j) Establishing criteria and recommendations for restricted operations or personnel access.

(k) Providing appropriate circuit and line safeguard devices (such as current limiters, voltage regulators, relief valves and interlocks) for power source, personnel, and equipment protection.

3.3.8 Human Engineering. The system shall be designed to facilitate manual operation, adjustment, and maintenance as needed, and to provide the optimum allocation of functions for personnel or automatic control. Particular design attention shall be given in the receiver subsystem to location of equipment in relation to elevators, walkways, and ladders, provision of adequate lighting for night maintenance, and placarding of hazardous work areas. MIL-STD-1472, Human Engineering Design Criteria, shall be used as a guide in designing control stations and equipment, with consideration given to personnel operations and interfaces - e.g., displays, controls, labels and placards, equipment handling, and providing a desirable working environment.

3.4 Documentation

Documentation of subsystem design, performance, operating, and test characteristics; instructions; construction drawings, procedures and parts lists and related information shall be prepared in accordance with the requirements of the Subsystem Requirements Specification listed in Section 2.2.1.

3.5 Logistics

Elements required to support the Pilot Plant are:

(a) Maintenance including support and test equipment, technical publications, field services, and data file.

(b) Supply including spares, repair parts, and consumables; and transportation, handling, and packaging.

(c) Facilities.

3.5.1 Maintenance. Maintenance activities shall be categorized as follows:

Level 1, On-line maintenance

Level 2, Off-line on-site maintenance

Level 3, Off-line off-site maintenance

Maintenance actions for each level are identified in the Subsystem Requirements specification listed in Section 2.2.1.

3.5.2 Supply. The following criteria shall be used for selecting and positioning spares, repair parts, and consumables:

Protection Level - Items shall be packaged in accordance with the requirements of Section 5.0.

Demand Rate - The mean-time-between-maintenance-actions shall be the initial basis for spares determinations. The quantities and mix for each subsystem shall be such that there is a 98% probability of a part being available on demand.

Pipeline - Pipeline quantities shall be determined on the basis of system location, demand rate, and repair cycle times. Resupply methods, distribution and location of system stocks shall be determined after site selection.

Procurement and Release for Production - Long lead time supply items shall be procured or drawings released early enough to be on site 30 days prior to initial operation. Other items shall be procured or released lead time away so as to minimize obsolescence due to design changes, except for those items for which significant cost savings can be achieved through acquisition concurrent with production.

Minimum/Maximum Levels - Minimum and maximum quantities of spares and repair parts to be stocked shall initially be determined by using predicted failure rates. These levels are to be adjusted as actual usage rates are established.

3.6 Personnel and Training

3.6.1 Personnel. The Pilot Plant is to be installed, checked out, and tested by contractor personnel; then taken over and operated as a commercial power plant by utility personnel. Operation and maintenance personnel requirements shall be satisfied by recruitment from the established utility labor pool. Specific skills and numbers of personnel required for Pilot Plant operation are shown in the Subsystem Requirements Specification listed in Section 2.2.1.

3.6.2 Training. The system interface and uniqueness dictate a need for training existing utility people but do not establish a need for new skills or

trades. The types and numbers of utility personnel requiring training, along with the unique tasks, are listed in the Subsystem Requirements Specification listed in Section 2.2.1.

3.7 Pilot Plant System Functional Characteristics

3.7.1 Collector Subsystem

3.7.1.1 Functional Modes. The collector subsystem shall comply with the collector subsystem requirements specification during normal tracking, synthetic tracking, and emergency operation modes, and while slewing to nonoperational heliostat positions.

3.7.1.1.1 Normal Solar Operation. The heliostats shall begin to acquire the sun in a controlled manner when it is visible and < 10 deg above the horizon. The sun's image shall be reflected onto the receiver unit with a maximum beam pointing error of 2.5 mrad standard deviation whenever the insolation exceeds 300 w/m^2, with a wind speed of 8 m/sec at 10m elevation and an ambient temperature of 28°C (83°F).

The reflected sunlight shall be applied to the receiver target at predetermined aim points to prevent the peak receiver heat flux from exceeding 0.3 MW/m^2. Reflected beam position updates shall maintain each heliostat image within 0.5 m of the nominal aim point. Normal operation shall be maintained until the direct solar insolation falls to 30% of the maximum summer noon insolation. A portion of the collector subsystem shall be disabled upon command of the master control to prevent overcharging of the thermal storage subsystem.

3.7.1.1.2 Synthetic Tracking Operation. Heliostat tracking shall be maintained by the master control during periods of obscured sunlight in a manner that permits the resumption of normal operation within 180 sec after passage of the shadow. At no time during the synthetic tracking operation shall reflected sunlight from the affected heliostats pose a safety hazard or damage any system component.

3.7.1.1.3 Emergency Shutdown. The solar radiation incident on the receiver shall be reduced to less than 3% of initial value within 120 sec after the issuance of an "off target" command as prescribed in the Collector Subsystem Requirements Specification.

3.7.1.1.4 Nonoperational Modes. Automatic nonoperational heliostat slewing provisions shall be incorporated so that the entire array of heliostat reflectors can be (1) aligned horizontally within 15 min to accommodate high winds and sand or dust storm conditions, and (2) aligned in any preferred orientation within 15 min to facilitate cleaning or maintenance. The elevation and azimuth gimbals shall remain in their last commanded positions for all operating and non-operating conditions when electrical power is removed.

3.7.1.2 Functional Interfaces. The collector subsystem shall interface directly with the receiver unit, the EPGS, the master control, and the physical site.

3.7.1.2.1 Collector Subsystem/Receiver Unit Interface. The collector subsystem shall be operated in a manner such that at least 97.7% of the redirected energy is intercepted by the absorber.

3.7.1.2.2 Collector Subsystem/Electrical Power Generation Subsystem Interface. The collector subsystem and the EPGS shall be interconnected by the AC power distribution cabling.

3.7.1.2.3 Collector Subsystem/Master Control Interface. The collector subsystem shall respond to all control commands issued by the master control. The master control shall receive, store, and/or process all information originating from the collector subsystem. All interface connections shall be physically and electrically compatible.

3.7.2 Receiver Subsystem

3.7.2.1 Functional Modes. The receiver subsystem shall exhibit stable, controlled operation during normal, startup, shutdown, emergency, and transient operations.

3.7.2.1.1 Normal Solar Operation. The receiver unit shall accept preheated feedwater from the riser exit, convert it to superheated steam, and deliver it to the entrance to the downcomer during all periods when normal collector subsystem conditions exist (per paragraph 3.7.1.1.1) excluding the startup and shutdown phases. The water temperature entering the receiver unit shall be 157 to 218°C (315 to 425°F) at a nominal pressure of 13.8 MPa (2,000 psia). The outlet steam shall be maintained at a temperature of 516°C (960°F) and pressure of 10.45 MPa (1515 psia) at a peak power level of 37.1 MWth. The steam from the downcomer shall be regulated so that a predetermined amount of available steam is admitted into the turbine. The remaining flow shall be bypassed to charge the TSS. An option shall exist to divert all of the steam to the TSS.

The riser shall accept water from the EPGS at a flowrate comparable to that entering the EPGS and at a temperature of 157-218°C (315-425°F).

3.7.2.1.2 Receiver Startup. The receiver unit shall be started in a controlled manner to ensure local flow stability in the absorber panels. An initial water flowrate of 3.2 kg/sec (25,000 lb/hr) shall be used prior to the acquisition of the sun by the collector subsystem.

The water temperature shall be allowed to rise until the average thermal power on the receiver is 14 MW. At this point, the boiling process will initiate and the panel flow controllers will regulate the flow to produce 10.45 MPa (1515 psia), 516°C (960°F) steam at the outlet of the receiver unit.

3.7.2.1.3 Receiver Shutdown. When the average absorbed thermal power into the receiver steam falls below (7.3 MW), the inlet flow controllers shall be adjusted to increase the water flowrate to a sufficient level to prevent boiling. Flow shall be continued until the heliostats are off-targeted.

3.7.2.1.4 Emergency Shutdown. In the event an overheating condition is observed locally in the receiver unit, the master control shall command the receiver control to institute maximum flow into the affected panel while off targeting the appropriate heliostats affecting the panel.

3.7.2.1.5 Transient Operation. The inlet water flow to the absorber panels of the receiver unit shall be controlled automatically to maintain a constant outlet

steam condition of 10.45 MPa (1515 psia) and 516°C (960°F). During the passage of clouds, the receiver unit control point may be changed to 349°C (660°F) to minimize chances of damage. At this control point all steam shall be diverted to the TSS. When the average power absorbed by the receiver steam falls below (7.3 MW), the receiver shutdown procedure shall be initiated. With the increase of incident thermal power to a value greater than the above, the receiver startup procedure shall be reinitiated.

3.7.2.2 Functional Interfaces. The receiver subsystem shall interface directly with the collector, thermal storage, and electrical power generation subsystems as well as the master control.

3.7.2.2.1 Receiver Subsystem/Thermal Storage Subsystem Interface. The downcomer shall be physically compatible with the TSU desuperheater inlet.

The steam rate from the downcomer shall be automatically controlled between 3.7 and 16.5 kg/s (28,900 - 130,500 lb/hr) at a pressure in excess of 10.1 MPa (1,465 psia) and temperature >343°C (650°F).

3.7.2.2.2 Receiver Subsystem/Electrical Power Generation Subsystem Interface. The receiver downcomer shall terminate at the turbine throttle station where physical compatibility is required. The steam shall enter the EPGS at a pressure in excess of 10.1 MPa (1,465 psia) and at 510°C (950°F). The return water flow from the condensate loop of the EPGS shall enter the riser inlet, upstream of the receiver feed pump at nominal temperature of 210°C (412°F) and a pressure of 3.45 MPa (500 psia. A physically compatible interface is required.

3.7.2.2.3 Receiver Subsystem/Master Control Interface. The receiver subsystem shall respond to all control commands issued by the master control. All interface connections shall be physically and electrically compatible.

3.7.3 Thermal Storage Subsystem

3.7.3.1 Functional Modes. The TSS shall exhibit stable, controlled operations during charging and steam generation operations and during the required transitions between these operational modes.

3.7.3.1.1 Charging Operation. The TSS shall be capable of circulating a heat-transfer fluid through a heat exchanger at a flowrate required to increase the

fluid temperature from 218°C (425°F) to 302°C (575°F) while transferring 30.0 MW of a possible 32.8 MW of thermal power which enters the charging heat exchanger. The heated heat-transfer fluid shall be stored and subsequently used for steam generation and feedwater heating options.

3.7.3.1.2 Steam Generation Operation. The high-temperature heat-transfer fluid shall be supplied to the steam generator in sufficient quantities to produce 274°C, 2.66 MPa (525°F, 385 psia) steam at a flowrate of 13.2 kg/s (104,700 lb/hr) while reducing the temperature of the fluid to 218°C (425°F).

3.7.3.2 Functional Interfaces. The TSS shall interface directly with the receiver, EPGS and master control.

3.7.3.2.1 Thermal Storage Subsystem/Electrical Power Generation Subsystem Interface. The piping, connections, and mounting fixture shall be physically compatible with those of the EPGS. The steam entering the EPGS shall be at a temperature of 274°C (525°F), a pressure of 2.66 MPa (385 psia), and a flowrate of 13.2 kg/s (104,700 lb/hr). The water shall return to the TSS from the condensate loop at a temperature 121°C (250°F) and pressure of 2.90 MPa (420 psia) at the inlet to the steam generator.

3.7.3.2.2 Thermal Storage Subsystem/Master Control Interface. The TSS shall respond to all control commands issued by the master control. The master control shall receive, store, and/or process all information originating from the TSS. All interface connections shall be physically and electrically compatible.

3.7.4 Electrical Power Generation Subsystem (EPGS)

3.7.4.1 Functional Modes. The EPGS shall exhibit stable, controlled operation during normal and extended operation modes as well as during the transition between modes.

3.7.4.1.1 Normal Solar Operation. During normal operating periods, the EPGS shall draw steam directly from the receiver subsystem at the conditions specified in paragraph 3.7.2.2.2. Steam extraction from the turbine for feedwater heating shall be controlled to maintain the receiver feedwater temperature between 157-218°C (315-425°F) throughout the range of flowrates that will be experienced during this operating mode.

3.7.4.1.2 Intermittent Cloudiness Operation and Extended Operation. In these modes, the EPGS shall operate on steam produced in the thermal storage steam generator at the steam conditions defined in paragraph 3.7.3.2.1. The condensate shall be preheated to 121°C (250°F) with extracted steam before it is returned to the steam generator. At all times during these operational modes, the net electrical power delivered to the busbar shall be maintained in excess of 7 MWe.

3.7.4.2 Functional Interfaces. The EPGS shall interface directly with the receiver and TSS as well as the master control.

3.7.4.2.1 Electrical Power Generation Subsystem/Master Control Interface. The EPGS shall respond to all control commands issued by the master control. The master control shall receive, store and/or process all information originating from the EPGS. All interface connections shall be physically and electrically compatible.

3.7.5 Master Control

3.7.5.1 Functional Modes. Master control shall monitor and control all plant subsystems in an integrated fashion in order to ensure stable, controlled system operation and proper procedures during emergency periods to maximize safety and minimize potential equipment damage.

3.7.5.1.1 System Mode Determination. The master control shall be capable of identifying the proper mode of system operation and generating the required commands to the appropriate control elements to properly execute the required functions. The master control shall be capable of anticipating required changes in operational modes in response to insolation or environment factors and initiating the appropriate transition. Operational modes shall include system startup, normal solar, low solar power, intermittent cloudiness, thermal storage charging, extended operation, fully charged thermal storage, normal shutdown, emergency shutdown, and subsystem conditioning. A self-check procedure, in which all subsystems are interrogated concerning their operational status, shall be performed after final shutdown.

3.7.5.1.2 Emergency Detection and Operation. At all times during the system operation, all subsystems shall be continuously monitored to verify operation in accordance with Pilot Plant system and subsystem requirements. In the event of a malfunction, the activation of redundant elements shall be initiated where possible or the operator notified of the action required. Where no redundancy exists, the impact of the malfunction shall be assessed. In the event the situation can lead to a safety problem or result in additional equipment damage, a system shutdown shall be initiated. The nature of the shutdown procedure shall depend on the nature of the malfunction.

3.7.5.1.3 Operational Information. The master control shall be capable of displaying pertinent data required to completely determine the status of the Pilot Plant system. System performance projections shall be available based on current and past subsystem performance and on future system supply capabilities, including availability of stored thermal energy and solar isolation.

3.7.5.2 Functional Interfaces. The master control shall interface with the collector, receiver, thermal storage, and electrical power generation subsystems.

3.8 Environmental Impact

The Pilot Plant system shall be designed so that the environmental impact associated with construction, installation, maintenance, and operation of the system conforms to that authorized for the selected site in accordance with applicable environmental control regulations. Environmental impact data required by the contract shall be developed for the specified site and submitted to ERDA.

3.9 Precedence

Specific characteristics and requirement precedence shall be established based on system cost-effectiveness sensitivity analyses. This specification has precedence over documents referenced herein. The contractor shall notify the procuring activity of each instance of conflicting, or apparently conflicting, requirements within this specification or between the specification and a referenced document.

4.0 QUALITY ASSURANCE PROVISIONS

4.1 General

4.1.1 Responsibility for Tests. All tests shall be performed by the contractor. These tests may be witnessed by ERDA or its representatives or the witnessing may be waived. In either case, substantive evidence of hardware compliance with all test requirements is required.

4.1.2 General Test Requirements. Tests required for the subsystems and the master control shall be as defined in the detail requirements specifications. The test of a subsystem in conjunction with another subsystem or the master control (e.g., an integration test) is regarded as a system test and shall be as required by this specification. The contractor shall prepare a test plan for ERDA approval. Tests shall be classified in the test plan as follows:

(a) Compatibility tests - Must be performed on site to establish that Pilot Plant hardware is ready for hookup, or that interfaces can be completed, or that subsystems and the master control are operable. Compatibility tests may include tests of components, subassemblies, assemblies, or subsystems. Such tests shall be as defined at the appropriate specification level.

(b) Operational tests - Tests of the integrated system.

Compatibility tests and operational tests at the system level shall be defined for verifications as indicated in subsection 4.3, Table 2.

4.1.3 Previous Tests. Maximum use shall be made of test data available from the subsystem research experiments, from subsystem tests and other hardware tests already completed. Where conformance to this specification can be established at less cost by analysis of such data, tests shall not be repeated.

4.2 Specific System Test Requirements

The following tests and examinations are defined herein specifically for verification of system requirements and shall be applied as necessary for the purposes of subsection 4.3, Table 2.

4.2.1 Examination of Installations. The contractor shall examine plant installations to verify before functional testing that subsystems, master control, and interfaces conform to physical requirements.

4.2.2 Operational Tests (Integrated System). Functional demonstration of the Pilot Plant system shall be performed by the contractor to the extent specified in the negotiated Pilot Plant test plan. The test plan shall include, as a minimum, the operational testing of the integrated system necessary to verify conformance to requirements identified for this method of verification in subsection 4.3, Table 2.

4.2.3 Life Tests and Analysis. One set of each major subassembly of the system design shall be subjected to extended life testing in accordance with the applicable subsystem requirements specifications.

4.3 Verification of Conformance

Verification that the requirements of Sections 3 and 5 of this specification are fulfilled shall be performed by the methods specified in Table 2. The methods of verification are defined as follows:

(a) Inspection - Examination and measurement of product.

(b) Analysis - Examination of the design and associated data, which may include relevant test information.

(c) Similarity - Demonstration or acceptable evidence of the performance of a product which is sufficiently similar to permit conformance to be inferred.

(d) Test - Functional operation or exposure under specified conditions to evaluate product performance.

(e) Demonstration - Exhibition of the product or service in its intended modes and conditions.

4.3.1 Hardware Acceptance. The contractor shall provide a method whereby conformance of hardware to the design and to the applicable detail specifications will be verified. This shall be accomplished progressively as system elements are manufactured. As the Pilot Plant system is integrated, conformance to design at that level shall be verified. For purposes of Pilot Plant acceptance, this verification of conformance includes proof-by-assembly and the examination of records as elements of inspection. Satisfactory system demonstration shall be accomplished. In addition, evidence shall be maintained of satisfactory accomplishment of inspections and tests required by codes and standards that apply for the system.

4.4 Formal Qualifications

For the Pilot Plant system, formal design qualification shall require satisfactory completion of all contractually required tests, include those specified for subsystems, and the completion of all other required verifications and the integrated system demonstration tests in the negotiated test plan.

5.0 PREPARATION FOR DELIVERY

Pilot Plant equipment shall be prepared for delivery in accordance with Section 5.0 of the appropriate detail Subsystem Requirements Specification.

Table 2

REQUIREMENT VERIFICATION MATRIX

Verification Methods	Test Categories
1. Inspection	A. Compatibility Test
2. Analysis	
3. Similarity	B. Operational Test (integrated system)
4. Test	
5. Demonstration	

N/A denotes "not applicable"

Requirement (paragraph)	Verification Method	Test Category	Remarks
3.1 Central Receiver Pilot Plant Definition	N/A	N/A	
3.1.1 General Description	N/A	N/A	
3.1.1(a) Collector Subsystem	1	N/A	
3.1.1(b) Receiver Subsystem	1	N/A	
3.1.1(c) Thermal Storage Subsystem	1	N/A	
3.1.1(d) Electrical Power Generation Subsystem	1	N/A	
3.1.1(e) Master Control	1	N/A	
3.1.2 Pilot Plant Application	N/A	N/A	
3.1.3 System Diagrams	N/A	N/A	
3.1.3.1 Central Receiver Solar Thermal Power System Diagram	N/A	N/A	

Table 2

REQUIREMENT VERIFICATION MATRIX (Continued)

Verification Methods

1. Inspection
2. Analysis
3. Similarity
4. Test
5. Demonstration

Test Categories

A. Compatibility Test

B. Operational Test (integrated system)

N/A denotes "not applicable"

Requirement (paragraph)	Verification Method	Test Category	Remarks
3.1.3.2 Functional Block Diagram	N/A	N/A	
3.1.3.3 Central Receiver Pilot Plant Layout	N/A	N/A	
3.1.4 Interface Definition	1, 2, 4	B	
3.1.4.1 Electrical Power Transmission Network/ Pilot Plant Interface	1, 2, 4, 5	B	
3.1.4.2 Pilot Plant/Site Interface	1, 2	N/A	
3.1.5 Operational and Deployment Concepts	5	B	
3.1.5.1 Power Production Mode	5	B	
3.1.5.2 Research Testing Mode	5	B	
3.1.5.2.1 Normal Startup	2, 5	B	Included as test required by 3.1.5.2
3.1.5.2.2 Normal Solar Operation	2, 5	B	Same

Table 2

REQUIREMENT VERIFICATION MATRIX (Continued)

Verification Methods

1. Inspection
2. Analysis
3. Similarity
4. Test
5. Demonstration

Test Categories

A. Compatibility Test

B. Operational Test (integrated system)

N/A denotes "not applicable"

Requirement (paragraph)	Verification Method	Test Category	Remarks
3.1.5.2.3 Low Solar Power Operation	2, 5	B	Same
3.1.5.2.4 Intermittent Cloudiness Operation	2, 5	B	Same
3.1.5.2.5 Thermal Storage Charging	2, 5	B	Same
3.1.5.2.6 Extended Operation (Stored Energy)	2, 5	B	Same
3.1.5.2.7 Fully Charged Thermal Storage	2, 5	B	Same
3.1.5.2.8 Normal Shutdown	2, 5	B	Same
3.1.5.2.9 Emergency Shutdown	2, 5	B	Verified in part by tests in the Master Control Subsystem Specification.
3.1.5.2.10 Subsystem Conditioning	2, 5	B	Turning of rotor to be demonstrated.
3.1.5.3 Deployment Concept	1, 2	N/A	Rewrite for Barstow.
3.2 Characteristics	N/A	N/A	

Table 2

REQUIREMENT VERIFICATION MATRIX (Continued)

Verification Methods	Test Categories
1. Inspection	A. Compatibility Test
2. Analysis	
3. Similarity	B. Operational Test (integrated system)
4. Test	
5. Demonstration	

N/A denotes "not applicable"

Requirement (paragraph)	Verification Method	Test Category	Remarks
3.2.1 Performance	4, 5	B	
3.2.1.1 Dynamic Performance	N/A	N/A	
3.2.1.1.1 Startup	2, 4	B	
3.2.1.1.2 Emergency Shutdown	2, 4	A	Water circulation failure may be simulated for test.
3.2.1.1.3 System Dynamic Variation	2, 4	B	Cloud effect may be simulated for test.
3.2.1.2 Endurance Capability	2, 4	→	See subsystem specifications for applicable life tests.
3.2.1.3 Other Performance Requirements	N/A	N/A	
3.2.1.3.1 Annual Power Output	2, 4	B	
3.2.1.3.2 Collector Operations	2, 4	A, B	

Table 2

REQUIREMENT VERIFICATION MATRIX (Continued)

Verification Methods	Test Categories
1. Inspection	A. Compatibility Test
2. Analysis	
3. Similarity	B. Operational Test (integrated system)
4. Test	
5. Demonstration	

N/A denotes "not applicable"

Requirement (paragraph)	Verification Method	Test Category	Remarks
3.2.2 Physical Characteristics	N/A	N/A	
3.2.2.1 System Characteristics	1,	N/A	
3.2.2.2 Collector Subsystem Characteristics	1, 2	N/A	See collector subsystem specification.
3.2.2.3 Receiver Subsystem Characteristics	1, 2	A	See receiver subsystem specification.
3.2.2.4 Thermal Storage Subsystem Characteristics	1, 2, 5	A	See receiver subsystem specification.
3.2.2.5 Electrical Power Generation Subsystem Characteristics	1, 2, 5	A	See electrical power generation subsystem specification.
3.2.2.6 Master Control	1, 2	N/A	See master control specification.
3.2.3 Reliability	1, 2, 5	B	
3.2.4 Maintainability	1, 2, 5	B	

Table 2

REQUIREMENT VERIFICATION MATRIX (Continued)

Verification Methods	Test Categories
1. Inspection	A. Compatibility Test
2. Analysis	
3. Similarity	B. Operational Test (integrated system)
4. Test	
5. Demonstration	

N/A denotes "not applicable"

Requirement (paragraph)	Verification Method	Test Category	Remarks
3.2.5 Availability	2, 5	B	
3.2.6 Environmental Conditions	2	N/A	See applicable subsystem specification.
3.2.7 Transportability	2	N/A	See applicable subsystem specification.
3.3 Design and Construction	2	N/A	See applicable subsystem specification.
3.3.1 Materials, Processes, and Parts	1, 2	N/A	See applicable subsystem specification. Inspection is to verify protective coating.
3.3.2 Electrical Transients	2, 4	A, B	
3.3.3 Electromagnetic Radiation	2	N/A	
3.3.4 Nameplate and Product Marking	1	N/A	

Table 2

REQUIREMENT VERIFICATION MATRIX (Continued)

Verification Methods	Test Categories
1. Inspection	A. Compatibility Test
2. Analysis	
3. Similarity	B. Operational Test (integrated system)
4. Test	
5. Demonstration	

N/A denotes "not applicable"

Requirement (paragraph)	Verification Method	Test Category	Remarks
3.3.5 Workmanship	1	N/A	
3.3.6 Interchangeability	1, 2	N/A	Verify by design check and approval system.
3.3.7 Safety	1, 2	N/A	
3.3.8 Human Engineering	1, 2	N/A	Design review item.
3.4 Documentation	N/A	N/A	
3.5 Logistics	N/A	N/A	
3.5.1 Maintenance	N/A	N/A	
3.5.2 Supply	1, 2	N/A	
3.6 Personnel and Training	N/A	N/A	
3.6.1 Personnel	N/A	N/A	
3.6.2 Training	N/A	N/A	

Table 2

REQUIREMENT VERIFICATION MATRIX (Continued)

Verification Methods	Test Categories
1. Inspection	A. Compatibility Test
2. Analysis	
3. Similarity	B. Operational Test (integrated system)
4. Test	
5. Demonstration	

N/A denotes "not applicable"

Requirement (paragraph)	Verification Method	Test Category	Remarks
3.7 Pilot Plant System Functional Characteristics	N/A	N/A	
3.7.1 Collector Subsystem	N/A	N/A	
3.7.1.1 Functional Modes	2, 4	B	
3.7.1.1.1 Normal Solar Operation	1, 4	B	
3.7.1.1.2 Synthetic Tracking Operation	4	B	
3.7.1.1.3 Emergency Shutdown	1, 4	B	
3.7.1.1.4 Nonoperational Modes	4	B	
3.7.1.2 Functional Interfaces	1, 2	N/A	
3.7.1.2.1 Collector Subsystem/ Receiver Unit Interface	2, 4	A	
3.7.1.2.2 Collector Subsystem/ Electrical Power Generation Subsystem Interface	1	N/A	

Table 2

REQUIREMENT VERIFICATION MATRIX (Continued)

Verification Methods

1. Inspection
2. Analysis
3. Similarity
4. Test
5. Demonstration

Test Categories

A. Compatibility Test

B. Operational Test (integrated system)

N/A denotes "not applicable"

Requirement (paragraph)	Verification Method	Test Category	Remarks
3.7.1.2.3 Collector Subsystem/ Master Control Interface	1, 2, 4, 5	A, B	
3.7.2 Receiver Subsystem	N/A	N/A	
3.7.2.1 Functional Modes	4	B	
3.7.2.1.1 Normal Solar Operation	4	B	
3.7.2.1.2 Receiver Startup	4	B	
3.7.2.1.3 Receiver Shutdown	4	B	
3.7.2.1.4 Emergency Shutdown	4	A, B	Receiver failure and overheating condition shall be simulated for test.
3.7.2.1.5 Transient Operation	4	A, B	
3.7.2.2 Functional Interfaces	1	N/A	
3.7.2.2.1 Receiver Subsystem/ Thermal Storage Subsystem Interface	1, 4	A, B	

Table 2

REQUIREMENT VERIFICATION MATRIX (Continued)

Verification Methods

1. Inspection
2. Analysis
3. Similarity
4. Test
5. Demonstration

Test Categories

A. Compatibility Test

B. Operational Test (integrated system)

N/A denotes "not applicable"

Requirement (paragraph)	Verification Method	Test Category	Remarks
3.7.2.2.2 Receiver Subsystem/ Electrical Power Generation Subsystem Interface	1, 4	B	
3.7.2.2.3 Receiver Subsystem/ Master Control Interface	1, 4	A, B	
3.7.3 Thermal Storage Subsystem	N/A	N/A	
3.7.3.1 Functional Modes	4	B	
3.7.3.1.1 Charging Operation	4	A, B	
3.7.3.1.2 Steam Generation Operation	4	A, B	
3.7.3.2 Functional Interfaces	1	N/A	
3.7.3.2.1 Thermal Storage Subsystem/Electrical Power Generation Subsystem Interface	1, 4	B	
3.7.3.2.2 Thermal Storage Subsystem/Master Control Interface	1, 4	A, B	

Table 2

REQUIREMENT VERIFICATION MATRIX (Continued)

Verification Methods	Test Categories
1. Inspection	A. Compatibility Test
2. Analysis	
3. Similarity	B. Operational Test (integrated system)
4. Test	
5. Demonstration	

N/A denotes "not applicable"

Requirement (paragraph)	Verification Method	Test Category	Remarks
3.7.4 Electrical Power Generation Subsystem	N/A	N/A	
3.7.4.1 Functional Modes	4	B	
3.7.4.1.1 Normal Solar Operation	4	B	
3.7.4.1.2 Intermittent Cloudiness Operation and Extended	4	B	
3.7.4.2 Functional Interfaces	1	N/A	
3.7.4.2.1 Electrical Power Generation Subsystem/ Master Control Interface	1, 4	A, B	
3.7.5 Master Control	N/A	N/A	
3.7.5.1 Functional Modes	4	A, B	
3.7.5.1.1 System Mode Determination	5	A, B	
3.7.5.1.2 Emergency Detection and Operation	5	A, B	

Table 2

REQUIREMENT VERIFICATION MATRIX (Continued)

Verification Methods	Test Categories
1. Inspection	A. Compatibility Test
2. Analysis	
3. Similarity	B. Operational Test (integrated system)
4. Test	
5. Demonstration	

N/A denotes "not applicable"

Requirement (paragraph)	Verification Method	Test Category	Remarks
3.7.5.1.3 Operational Information	5	A, B	
3.7.5.2 Functional Interfaces	1	A	
3.8 Environmental Impact	1, 2	N/A	
3.9 Precedence	N/A	N/A	
5.0 Preparation for Delivery	N/A	N/A	

APPENDIX B

An Analytic Evaluation of the Flux Density due to Sunlight Reflected from a Flat Mirror having a Polygonal Boundary

F. W. Lipps and M. D. Walzel
Solar Energy Laboratory, University of Houston
Houston, Texas 77004

ABSTRACT

Computer algorithms for the flux density of reflected sunlight from a heliostat become an essential part of the optical simulation problem for the solar central receiver system. An exact analytic result is available for heliostats having polygonal boundaries. An analytical method for round heliostats is given in Appendix A, which is extremely complex and requires quartic roots. A useful numerical method is given in Appendix B for helisotats of arbitrary shape. A comparison is made between the analytic method and the Hermite function method, which is much faster but less accurate. The analytic method provides a basis for evaluating all other flux density calculations.

Nomenclature

A	represents the area of the polygonal heliostat.
$\vec{b}_i$	represents the i^{th} vertex of the polygonal boundary.
B	represents the whole set of vertices and is called the boundary vector.
$F(x,y)$	is the flux density at point (x,y) of image plane.
F_H	is the flux density of a heliostat.
$\overline{F}_H$	is the flux density due to a heliostat population having guidance errors.
F_T	represents the total flux density on the receiver.
G	represents the guidance error distribution.
H	represents the reflective region of the heliostat surface (i.e., a polygonal region).
i_H	is the angle of incidence at receiver for the optic axis coming from heliostat H.
i_0	is the angle of incidence on the heliostat for a central ray from the sun.
I_i	is the i^{th} empirical coefficient of solar limb darkening.
J_i	is the i^{th} analytic flux density integral.
K_i	is the i^{th} analytic flux density integral.
ℓ	is the parameter of the heliostat boundary.
M_H	represents the flux density on the image plane of a heliostat due to a point sun having a solar constant of 1 W/m^2.
$\hat{r}$	represents a unit vector parallel to the reflected ray.
$\hat{r}_o$	represents a unit vector parallel to the optic axis and towards the receiver.
R_o	is the slant distance from the center of the heliostat to the optical center.

$R(x,y,r)$ is the irradiance/sterradian for reflected rays arriving at the point (x,y) along ray $\hat{r}$.

S represents the solar brightness distribution in W/m^2/sterradian.

$\bar{S}$ represents the effective solar brightness distribution including guidance errors.

$\hat{s}$ is the direction of the incoming sun ray.

$\hat{s}_o$ is the direction of the center of the solar disc.

t is the distance parameter for parametric ray tracing.

$\hat{n}_I$ represents the inward unit normal vector at the I^{th} receiver mode.

(u,v) represents a point in the plane of the heliostat.

$(\hat{u},\hat{v},\hat{w})$ represents an orthonormal triple of vectors attached to the heliostat, $\hat{w}$ is the upward unit normal vector.

$\hat{x}$ represents the horizontal unit vector in the image plane.

$\hat{y}$ represents the nodding vertical unit vector in the image plane.

(x_I,y_I,z_I) are coordinates of node in surface of receiver.

$(\bar{x}_I,\bar{y}_I)$ represents the projection of the receiver mode onto the image plane.

(x,y) represents a point in the image plane.

α is the polar angle measured from the center of the solar disc.

α_L is the solar limb angle (i.e. sun size parameter).

$\sigma = \pm 1$ for the orientation of an arc in the indicator function.

ρ is the net coefficient of reflectivity for sunlight on the heliostat.

$\Phi(u,v) = 0, 2\pi$ and is called the indicator function which tells us when (u,v) is inside of the closed polygon B.

ϕ is an azimuthal angle.

$\psi = \sin^2\alpha$ and is a convenient parameter for the polar angle.

$d\omega_r$ represents an element of solid angle including the ray $\hat{r}$.

$\vec{a}$ means that a is vector quantity.

$\hat{a}$ represents a unit vector in direction a.

$(a \cdot b)$ represents a scaler product of vectors a and b.

$a \times b$ represents the vector product of vectors a and b.

$a \Omega b$ represents the intersection of sets.

$a \varepsilon b$ implies that a belongs to set b.

$a * b$ represents the convolution of functions a and b.

Proj(H/I) represents the projection of heliostat H onto the image plane I.

$\pi = 3.14159.$

1. Introduction

The central receiver concept for large scale solar power systems is based on the possibility of concentrating sunlight by deploying a large number of individually guided flat mirrors, i.e. heliostats. The field of heliostats can be regarded as a fresnel reflector which tracks the sun and generates a focus as though it were a very large movable parabolic dish. A heat transfer device called a receiver is placed at the focus, which must be high above the plane of the heliostats in order to avoid interference between neighboring heliostats. Hence, the system is also called a Tower Top Concentrator.

The optical performance of the system is characterized by the flux density of reflected sunlight on the surface of the receiver. However, various receiver geometries must be dealt with and it is convenient to consider the flux density due to an individual heliostat on its own image plane. The image plane of a heliostat passes through the optical center of the system (i.e. focus) and is perpendicular to the optic axis, which is the line joining the optical center to the center of the heliostat. See Figure 1. The total flux density on the receiver, F_T, can be obtained from the individual heliostat flux densities, F_H, by projecting F_H from its image plane onto the receiver and summing over the heliostats. Each projection is parallel to the appropriate optic axis. See Nomenclature, but specifically,

$$F_T(x_I,y_I,z_I) = \sum_{H:\ \cos i_H > 0} \cos i_H F_H(\bar{x}_I,\bar{y}_I),$$

where (x_I,y_I,z_I) is a point in the surface of the receiver and $(\bar{x}_I,\bar{y}_I)$ is the corresponding point in the image plane of the heliostat H. i_H is the angle of incidence at the I^{th} point on the receiver for incoming

rays parallel to the optic axis. This formulation can be completed by introducing the following unit vectors. Let:

1) $\hat{n}_I$ represent the inward unit normal to the receiver at I,

2) $\hat{x}$ represent the horizontal unit vector in the image plane,

3) $\hat{y}$ represent the nodding vertical unit vector in the image plane, and

4) $\hat{r}_o$ represent the unit vector parallel to the optic axis and towards the receiver.

By definition the vectors $(\hat{x},\hat{y},\hat{r}_o)$ are orthonormal. See Figure 1. It follows that

$$\cos i_H = (\hat{r}_o \cdot \hat{n}_I),$$

$$\bar{x}_I = x_I\hat{x}_x + y_I\hat{x}_y + z_I\hat{x}_z, \text{ and}$$

$$\bar{y}_I = x_I\hat{y}_x + y_I\hat{y}_y + z_I\hat{y}_z.$$

Of course, this construction depends on a paraxial ray assumption which is a very good approximation because the surface of the receiver is much closer to the image plane than to the heliostat and because the solar disc is relatively small.

Hence, we see that an adequate method of calculating the flux density due to an individual heliostat can provide us with an optical simulation of the central receiver system. However, in order to be complete, we must include the effects of sun size, solar limb darkening, heliostat guidance errors, other heliostat imperfections, and the losses due to the interference of neighboring heliostats. The phenomenon of interference between neighboring helisotats is known as shading and blocking. These losses are included by introducing a boundary vector which defines the effective luminous region of the heliostat. If the

helisotats are polygonal, then the effective luminous regions will also be polygonal, and it will be sufficient to calculate the flux density due to arbitrary polygonal regions.

The effects of sun size and solar limb darkening are included by introducing the solar brightness distribution, $S(\alpha)$, in Watts/meter^2 sterradian. This function is empirically determined, but it can be given the following polynomial approximation, which permits us to proceed with an analytic evaluation of the solar flux density due to a single heliostat. Let

$$S(\alpha) = \begin{cases} I_0 + I_1 \sin^2\alpha + I_2 \sin^4\alpha + I_3\sin^6\alpha \text{ , or} \\ 0 \text{ if } \alpha \geq \alpha_L = .004660, \end{cases}$$

where α is the angle measured from the apparent center of the solar disc to the direction of the incoming ray, and α_L is the solar limb angle.

The heliostat guidance errors and other imperfections can be represented by an error distribution function G, which allows us to form a statistical estimate, $\overline{F}_H$, of the flux density via the convolution,

$$\overline{F}_H = G * F_H .$$

We have previously shown [1], that

$$F_H = S * M_H,$$

where M_H is the flux density on the image plane due to heliostat H assuming a point sun having a solar constant of 1 W/m^2. For a flat heliostat

$$M_H(x,y) = \begin{cases} \cos i_o \text{ if } (x,y) \in \text{Proj}(H/I), \text{ or} \\ 0 \text{ otherwise.} \end{cases}$$

Consequently,

$$\overline{F}_H = G * S * F_H = \overline{S} * F_H ,$$

where $\overline{S} = G * S$, which can be given a polynomial approximation of the

same kind as shown above for $S(\alpha)$. Hence, the analytic results given in this paper enable us to evaluate the effect of the error distribution G, without having to perform the costly convolution integrals.

2. The Flux Density Integral

Let $F(x,y)$ be the flux density at the point (x,y) in the image plane, and let $\tilde{R}(x,y,\hat{r})d\omega_r$ be the irradiance of the reflected rays at the point (x,y) and in the solid angle $d\omega_r$, having direction specified by the unit vector $\hat{r}$. (See Figure 1.) Consequently,

$$F(x,y) = \int_{(\hat{r}_o \cdot \hat{r}) > 0} (\hat{r}_o \cdot \hat{r})\tilde{R}(x,y,\hat{r})d\omega_r.$$

$\tilde{R}$ is determined by tracing the ray from the point (x,y) in the image plane to the point (u,v) in the plane of the heliostat. Let H denote the effective luminous region in the plane of the heliostat, and let ρ denote the coefficient of reflectivity of the heliostat for sunlight, then

$$\tilde{R}(x,y,\hat{r}) = \begin{cases} \rho S(\alpha), & \text{if } (u,v)\varepsilon H \\ 0, & \text{otherwise.} \end{cases}$$

α is determined by the law of reflection and the heliostat guidance requirement. Let $\hat{s}_o$ represent the direction towards the center of the solar disc and let $\hat{s}$ represent the direction of the sun ray which reflects into $\hat{r}$. The guidance requirement states that $\hat{s}_o$ must reflect into $\hat{r}_o$, which is the direction towards the optical center of the system. If $\hat{w}$ represents the upward normal direction of the heliostat plane, then

$$\hat{r}_o = 2(\hat{s}_o \cdot \hat{w})\hat{w} - \hat{s}_o,$$

and

$$\hat{r} = 2(\hat{s} \cdot \hat{w})\hat{w} - \hat{s},$$

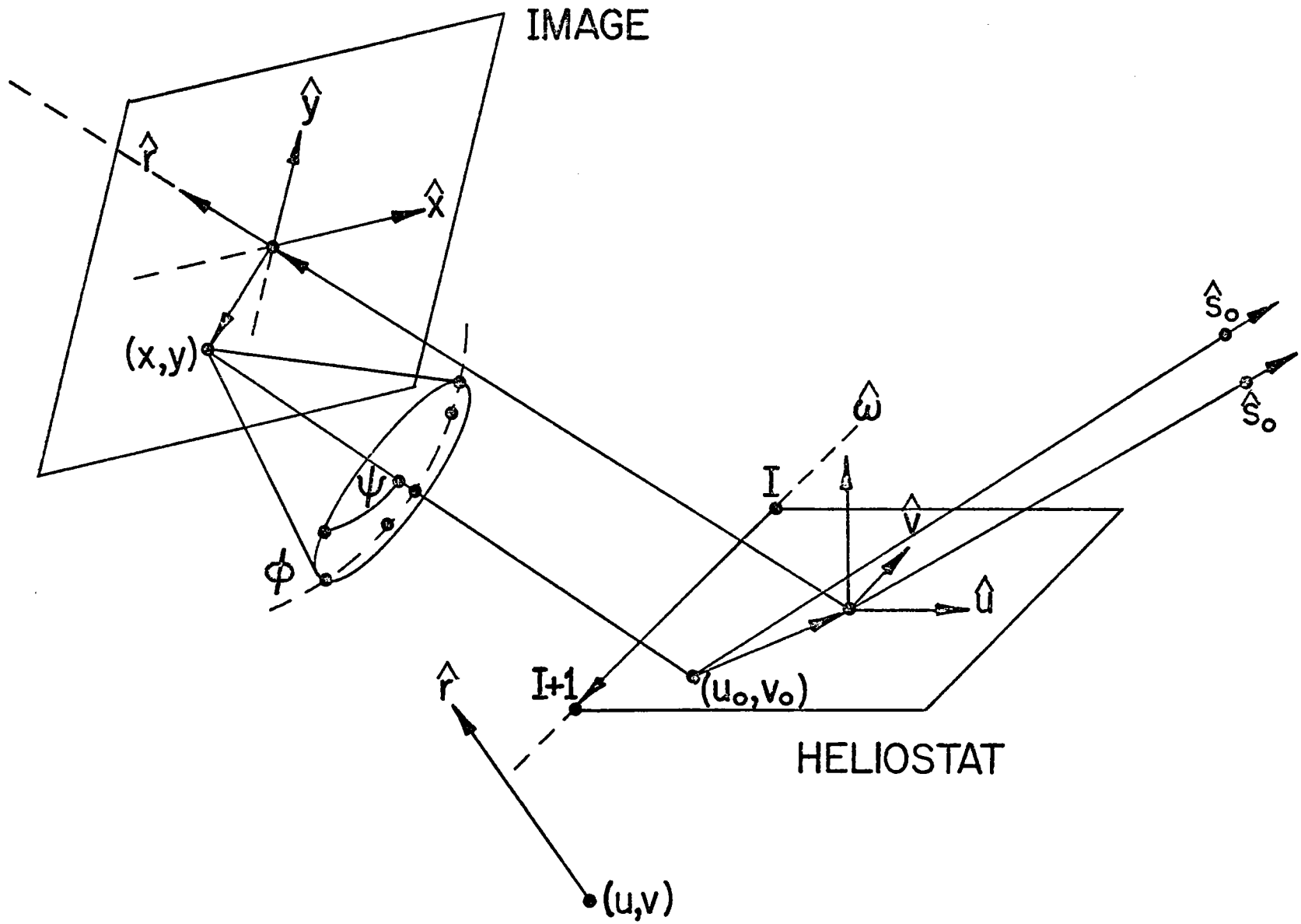

Figure 1. Shows the geometry of the image-forming process. $(\hat{u},\hat{v},\hat{w})$ is the orthonormal triple associated with the plane of the heliostat. $(\hat{x},\hat{y},\hat{r})$ is the orthonormal triple associated with the image plane. See Nomenclature for other vectors.

so that

$$(\hat{r}_o \cdot \hat{r}) = (\hat{s}_o \cdot \hat{s}) = \cos\alpha,$$

and

$$\alpha = \cos^{-1}(\hat{r}_o \cdot \hat{r}).$$

Obviously, $\hat{w}$ is determined by the guidance requirement, and

$$\hat{w} = 1/2(\hat{r}_o + \hat{s}_o)/\cos i_o,$$

with

$$\cos i_o = [\ 1/2(1 + (\hat{r}_o \cdot \hat{s}_o)\ ]^{1/2}.$$

In order to complete the explicit determination of $\tilde{R}$, it is necessary to introduce coordinates in the plane of the heliostat. Let $(\hat{u},\hat{v},\hat{w})$ be an orthonormal triple of vectors, such that $\hat{w}$ is normal to the plane of the heliostat as above, and, therefore, any vector of the form, $u\hat{u} + v\hat{v}$, lies in the plane of the heliostat. Similarly, any vector of the form $x\hat{x} + y\hat{y}$ lies in the image plane. According to Figure 1, the parametric equation of the ray from (x,y) to (u,v) along the direction $-\hat{r}$, is given by

$$\vec{x}(t) = R_o\hat{r}_o + x\hat{x} + y\hat{y} - t\hat{r},$$

where R_o is the length of the optic axis, and t is the distance from the image point (x,y) measured along the ray $-\hat{r}$. This ray pierces the plane of the heliostat, when

$$\hat{w} \cdot \vec{x}(t) = 0,$$

so that

$$t = (\hat{w}\cdot R_o\hat{r}_o + x\hat{x} + y\hat{y})/(\hat{w}\cdot\hat{r}).$$

Consequently, we can write

$$u = \hat{u}\cdot\vec{x}(t) = (u_R R_o + u_x x + u_y y)/(\hat{w}\cdot\hat{r}),$$

and

$$v = \hat{v}\cdot\vec{x}(t) = (v_R R_o + u_x x + v_y y)/(\hat{w}\cdot\hat{r}),$$

where

$$\begin{aligned} u_R/(\hat{w}\cdot\hat{r}) &= \hat{u}\cdot[\hat{r}_o - \hat{r}(\hat{w}\cdot\hat{r}_o)/(\hat{w}\cdot\hat{r})] \\ &= [(\hat{u}\cdot\hat{r}_o)(\hat{w}\cdot\hat{r}) - (\hat{u}\cdot\hat{r})(\hat{w}\cdot\hat{r}_o)]/(\hat{w}\cdot\hat{r}) \\ &= (\hat{u}\cdot\hat{w}x(\hat{r}_o x\hat{r}))/(\hat{w}\cdot\hat{r}) \\ &= -(\hat{v}\cdot\hat{r}_o x\hat{r})/(\hat{w}\cdot\hat{r}). \end{aligned}$$

In summary, we have

$$\begin{aligned} u_R &= -(\hat{v}x\hat{r}_o\cdot\hat{r}) \to 0 && \text{as } r\to r_o \\ u_x &= -(\hat{v}x\hat{x}\cdot\hat{r}) \to (\hat{v}\cdot\hat{y}) && \text{as } \hat{r}\to\hat{r}_o \\ u_y &= -(\hat{v}x\hat{y}\cdot\hat{r}) \to -(\hat{v}\cdot\hat{x}) && \text{as } \hat{r}\to\hat{r}_o \\ v_R &= (\hat{u}x\hat{r}_o\cdot\hat{r}) \to 0 && \text{as } \hat{r}\to\hat{r}_o \\ v_x &= (\hat{u}x\hat{x}\cdot\hat{r}) \to -(\hat{u}\cdot\hat{y}) && \text{as } \hat{r}\to\hat{r}_o \\ v_y &= (\hat{u}x\hat{y}\cdot\hat{r}) \to -(\hat{u}\cdot\hat{x}) && \text{as } \hat{r}\to\hat{r}_o \end{aligned}$$

It is also easy to calculate the apparent center of the solar disc. Let D_o represent the apparent center as shown in Figure 2. If

$$D_o = (u_o, v_o),$$

then

$$u_o = (\hat{v}\cdot(x\hat{y}-y\hat{x}))/\cos i_o,$$

and

$$v_o = -(\hat{u}\cdot(x\hat{y}-y\hat{x}))/\cos i_o.$$

We must now construct an analytic representation for the statement $(u,v)\varepsilon H$. For our purposes, H is polygonal, and, therefore, H is determined by its vertices. The set of u and v coordinates of the vertices is

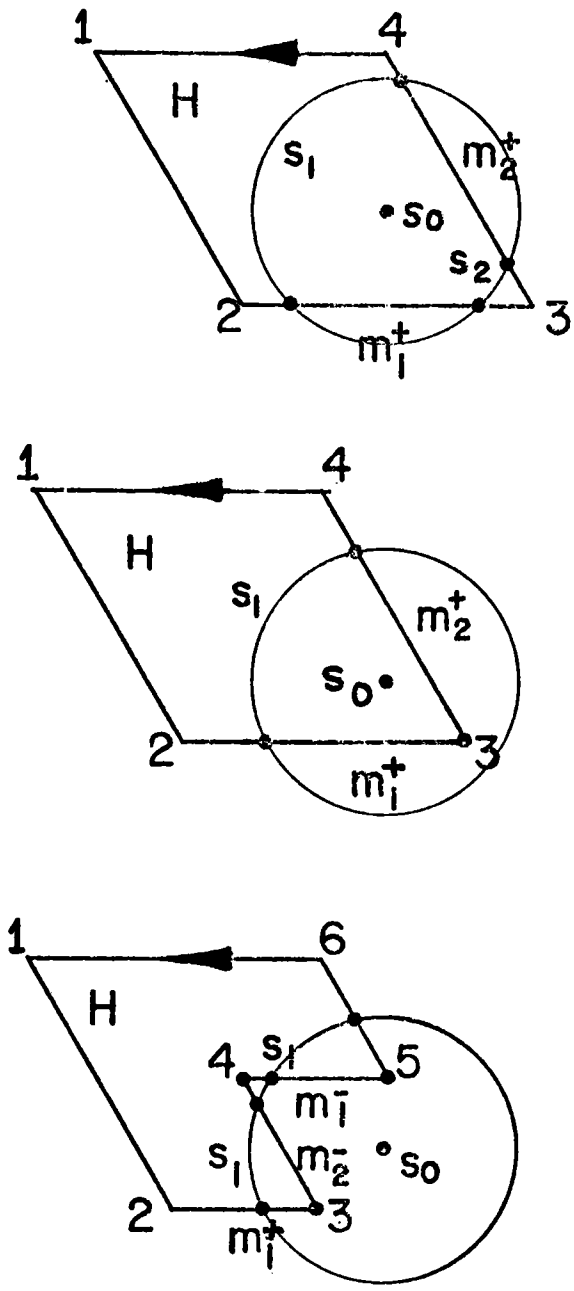

Figure 2. Shows the boundary of the heliostat in relation to the solar disc. The shaded overlapping region becomes split due to a shading event in the lower example. All essential points are dotted.

called the boundary vector of H. Specifically,

$$B = \{(u_i,v_i) \mid i = 1...N\} = \{\vec{b}_i \mid i = 1...N\} ,$$

determines H. In the absence of shading and blocking, H is the whole reflecting surface of the heliostat, and B is a constant depending only on the design of the heliostat. But if shading and/or blocking occur, then B becomes very complicated and must be input to the flux density calculation. For an illustration of the boundary vector concept, let

$$\vec{b}_i = (u_i-u,\ v_i-v,\ 0), \text{ for } i = 1...N,$$

represent the location of the i^{th} vertex with respect to an origin at (u,v). If we also assume that $\vec{b}_{N+1} = \vec{b}_1$, then

$$A(u,v) = 1/2 \sum_{i=1}^{N} (\vec{b}_i X \vec{b}_{i+1})_w$$

$$= \int_H dudv = \text{Area of H, for all } (u,v).$$

Similarly, let

$$\hat{b}_i = \vec{b}_i/|\vec{b}_i| ,$$

$$\sin\phi_i = \hat{b}_i x \hat{b}_{i+1},$$

$$\cos\phi_i = (\hat{b}_i \cdot \hat{b}_{i+1}) , \text{ and}$$

$$\sigma_i = \sin\phi_i/|\sin\phi_i| = \pm 1 ,$$

so that

$$\phi(u,v) = \sum_{i=1}^{N} \phi_i = \sum_{i=1}^{N} \sigma_i \cos^{-1}(\hat{b}_i \cdot \hat{b}_{i+1})$$

$$= \begin{cases} 2\pi \text{ if } (u,v) \epsilon H, \text{ or} \\ 0 \text{ otherwise.} \end{cases}$$

The indicator function $\phi(u,v)$ tells us whether (u,v) is inside the region H or not.

3. The Reduction to Terms

From our previous discussion, we see that

$$F(x,y) = \rho \int_{S\Omega H} d\omega_r \cos\alpha \, S(\alpha),$$

where $S\Omega H$ is the intersection of the solar disc and the solid angle subtended by the reflecting region of the heliostat as seen from (x,y). (See Figure 1.) α becomes the polar angle of an image oriented spherical polar coordinate system (α,ϕ,R), having its polar axis parallel to the optic axis $\hat{r}_o$. Consequently,

$$d\omega_r \cos\alpha = d\phi d\alpha \sin\alpha\cos\alpha,$$

which can be rewritten as

$$d\omega_r \cos\alpha = 1/2 \, d\phi d\psi,$$

if we let $\psi = \sin^2\alpha$.

We can now write

$$F(x,y) = 1/2 \, \rho \int_{S\Omega H} d\phi \int d\psi S(\psi),$$

or

$$F(x,y) = 1/2 \, \rho \sum_{i=0}^{\infty} I_i J_i(x,y)/(i+1),$$

with

$$J_i(x,y) = (i+1) \int_{S\Omega H} d\phi \int d\psi \psi^i.$$

The coefficients $(I_0,I_1,I_2,..)$ are empirical constants which depend on the sun, atmospheric effects and, possibly, also the guidance errors. The functions $(J_0,J_1,J_2,..)$ depend only on the region $S\Omega H$ and the index i.

The region $S\Omega H$ depends on the solar limb angle α_L, the orientation of the heliostat, and the boundary of the reflecting surface. In general, $S\Omega H$ may contain several disconnected regions, even if H is a

single connected region. Consequently, the boundary of SΩH may contain several cycles (i.e. closed curves), and J_i can be written

$$J_i = \sum_{i=1}^{C} \int_{(S\Omega H)_j} d\phi d\psi \, (i+1)\psi^i = \sum_{j=1}^{C} J_{ij}$$

$$= \sum_{j=1}^{C} \oint d\ell_j (d\phi/d\ell_j)\psi_j(\phi)^{i+1} \, ,$$

where $\psi_j(\phi) = \sin^2\alpha_j(\phi)$, and

$$\text{Boundary } (S\Omega H)_j = \{[\alpha_j(\ell), \phi(\ell), R=1] \mid 0 \leq \ell \leq \ell_j^*\}$$

The boundary of $(S\Omega H)_j$ consists of circular sun segments and linear heliostat segments. For a sun segment,

$$\psi_j(\phi) = \psi_L = \sin^2\alpha_L \, ,$$

and the corresponding term in J_{ij} is immediately integrable. For a linear segment, the corresponding term in J_{ij} becomes a rational function of ℓ, as we shall show later. However, it is important to reorganize J_i into a sum over segments. Let

$$J_i = \sum_{d \in D} \Delta\phi_d \psi_L^{i+1} + \sum_{m \in M} \int_{\phi_m^-}^{\phi_m^+} d\phi \psi_m(\phi)^{i+1},$$

where D is the set of sun segments and M is the set of linear segments.

Let

$$\Delta\phi_d = \begin{cases} 2\pi, \text{ or} \\ \phi_d^+ - d_d^- \end{cases}$$

so that

$$\phi \epsilon d \text{ if } \phi_d^- \leq \phi \leq \phi_d^+,$$

and

$$\phi \epsilon m \text{ if } \phi_m^- \leq \phi \leq \phi_m^+.$$

A glance at Figure 2 reveals that the set of end points $\{(\phi_m^+, \phi_m^-) \mid m \epsilon M\}$

contains the set of end points $\{(\phi_d^+,\phi_d^-)|d\epsilon D\}$ plus those vertices of H which happen to be inside the apparent solar disc. Consequently, all of the end points are determined by the equations

$$\psi_m(\phi) = \sin^2\alpha_m(\phi) = \phi_L,$$

and therefore the functions $\{\psi_m(\phi)|m\epsilon M\}$ completely detemine J_i.

In order to finish the formulation of the flux density integral, we must derive an expression for $\psi_m(\phi)$ and solve for the azimuthal angles. This can be accomplished by projecting the appropriate linear boundary segment of H onto a unit sphere surrounding the point (x,y) on the image plane as shown in Figure 1. Let

$$\vec{b}_i = u_i\hat{u} + v_i\hat{v}$$

represent the i^{th} vertex of H, so that

$$\ell_i = ((u_{i+1}-u_i)^2 + (v_{i+1}-v_i)^2)^{1/2}$$

is the length of the i^{th} linear segment. Then let

$$\vec{b}(\ell) = \vec{b}_i + (\ell/\ell_i)(\vec{b}_{i+1}-\vec{b}_i) = \vec{b}_i+\ell\hat{c}_i$$

$$\vec{R}(\ell) = R_o\hat{r}_o + x\hat{x} + y\hat{y} - \vec{b}(\ell)$$

and

$$\hat{r}(\ell) = \vec{R}(\ell)/|\vec{R}|$$

so that both $\hat{c}_i$ and $\hat{r}(\ell)$ are unit vectors and $\hat{r}(\ell)$ performs the desired mapping. Finally, we can write

$$\hat{r}(\ell) = \cos\alpha\ \hat{r}_o + \sin\alpha(\cos\phi\ \hat{x}+\sin\phi\ \hat{y}),$$

so that

$$\psi_m = \sin^2\alpha_m = (\hat{x}\cdot\hat{r})^2 + (\hat{y}\cdot\hat{r})^2$$

$$= [(x-\hat{x}\cdot\vec{b})^2 + (y-\hat{y}\cdot\vec{b})^2]/\vec{R}^2,$$

and

$$\tan\phi = (\hat{y}\cdot\hat{r})/(\hat{x}\cdot\hat{r})$$

$$= (y-\hat{y}\cdot\vec{b})/(x-\hat{x}\cdot\vec{b}).$$

Notice that

$$\vec{R}^2 = (\hat{x}\cdot\vec{R})^2 + (\hat{y}\cdot\vec{R})^2 + (\hat{r}_o\cdot\vec{R})^2$$

$$= (x-\hat{x}\cdot\vec{b})^2 + (y-\hat{y}\cdot\vec{b})^2 + (R_o-\hat{r}\cdot\vec{b})^2$$

$$\tilde{=} R_o^2,$$

but we also have

$$\vec{R}^2 = (\vec{R}_i-\hat{c}_i\ell)^2 = p^2-2q\ell+\ell^2$$

where

$$\vec{R}_i = R_o\hat{r}_o + x\hat{x} + y\hat{y} - \vec{b}_i,$$

$$p^2 = \vec{R}_i^2 = R_o^2 + x^2 + y^2 + \vec{b}_i^2 - 2\vec{b}_i\cdot(R_o\hat{r}_o + x\hat{x} + y\hat{y})$$

and

$$q = \vec{R}_i\cdot\hat{c}_i.$$

Both ψ_m and $\tan\phi$ can be developed in terms of ℓ, and then ℓ can be eliminated to give $\psi_m(\phi)$. Let

$$(\hat{x}\cdot\vec{R}) = a+b\ell = x-(\hat{x}\cdot\vec{b}_i)-(\hat{x}\cdot\hat{c}_i)\ell$$

and

$$(\hat{y}\cdot\vec{R}) = c+d\ell = y-(\hat{y}\cdot\vec{b}_i)-(\hat{y}\cdot\hat{c}_i)\ell$$

so that

$$\tan\phi = (c+d\ell)/(a+b\ell)$$

$$\ell = -(c-a\tan\phi)/(d-b\tan\phi)$$

$$\psi_m = [(a+b\ell)^2 + (c+d\ell)^2]/(p^2-2q\ell+\ell^2)$$

$$= \{[a(d-b\tan\phi) - b(c-a\tan\phi)]^2$$

$$+ [c(d-b\tan\phi) - d(c-a\tan\phi)]^2\} \times$$

$$\{p^2(d-b\tan\phi)^2+2q(d-b\tan\phi)(c-a\tan\phi)+(c-a\tan\phi)^2\}^{-1}$$

$$= \Omega^2(1+\tan^2\phi)/(T_o-2T_1\tan\phi+ T_2\tan^2\phi)$$

where

$$T_o = p^2d^2 + 2qdc + c^2$$

$$T_1 = p^2db + q(bc+ad) + ac$$

$$T_2 = p^2b^2 + 2qab + a^2$$

and

$$\Omega = ad - bc.$$

Consequently, the end point equation gives

$$\Omega^2(1+\tan^2\phi) = \psi_L(T_o-2T_1\tan\phi+T_2\tan^2\phi)$$

$$A\tan^2\phi + 2B\tan\phi + C = 0$$

and

$$\tan\phi^{\pm} = (-B\pm\sqrt{B^2-AC})/A$$

where

$$A = \Omega^2 - \psi_L T_2$$

$$B = \psi_L T_1$$

$$C = \Omega^2 - \psi_L T_o.$$

4. The Integration

The expression for J_i can be rewritten as

$$J_i = \Phi_D \psi_L^{i+1} + \sum_{m\epsilon M} K_{im}$$

where

$$\Phi_D = \sum_{d\epsilon D} \Delta\phi_d,$$

and

$$K_{im} = \int_{\phi_m^-}^{\phi_m^+} d\phi\ \psi_m(\phi)^{i+1},$$

with

$$\psi_m(\phi) = \Omega^2(1+\tan^2\phi)/(T_o-2T_1\tan\phi+T_2\tan^2\phi).$$

In a heliostat application the slant range R_o is usually so large that

$$p^2 >> q\ell >> \ell^2$$

and consequently it is useful to consider the approximation

$$\begin{aligned}\psi_m(\phi) &= (\Omega/p)^2(1+\tan^2\phi)/(d-b\tan\phi)^2 \\ &= (\Omega/p)^2/(d\cos\phi-b\sin\phi)^2 \\ &= (\Omega/p)^2/\rho^2\cos^2(\phi-\phi_o)\end{aligned}$$

where

$$\rho\cos\phi_o = d \ ,$$

$$\rho\sin\phi_o = -\ b \ ,$$

$$\rho = \sqrt{b^2+d^2} \ ,$$

and

$$\tan\phi_o = -b/d \ .$$

Consequently, we have

$$K_i = (\Omega^2/p^2\rho^2)^{i+1}\int_{\phi^-}^{\phi^+} d\phi/\cos^{2(i+1)}(\phi-\phi_o)$$

It is easy to show that

$$\int d\phi/\cos^2\phi = \tan\phi$$

$$\int d\phi/\cos^4\phi = 1/3\{\tan\phi(1+\tan^2\phi)+2\tan\phi\}$$

$$\begin{aligned}\int d\phi/\cos^6\phi &= 1/5\{\tan\phi(1+\tan^2\phi)^2 \\ &\quad + (4/3)\tan\phi(1+\tan^2\phi)+(8/3)\tan\phi\}\end{aligned}$$

and in general

$$\begin{aligned}\int d\phi/\cos^{2(i+1)}\phi &= (1/2i+1)\tan\phi/\cos^{2i}\phi \\ &\quad + (2i/2i+1)\int d\phi/\cos^{2i}\phi \\ &= (1/2i+1)\ \tan\phi\sum_{j=0}^{i} C_{ij}(1+\tan^2\phi)^j\end{aligned}$$

where the C_{ij} are given in the table below.

Table of C_{ij}

i / j	0	1	2	3	4
0	1				
1	1	2			
2	1	4/3	8/3		
3	1	6/5	8/5	16/5	
4	1	8/7	48/35	64/35	128/35

Consequently, we can write

$$K_i = (1/2i+1)(\Omega^2/p^2\rho^2)^{i+1} L_i ,$$

$$L_i = \tan(\phi-\phi_o) \sum_{j=0}^{i} C_{ij}(1+\tan^2(\phi-\phi_o))^j \Big|_{\phi^-}^{\phi^+} ,$$

where

$$\tan(\phi_\pm-\phi_o) = (\tan\phi_\pm+b/d)/(1-\tan\phi_\pm(b/d)).$$

Alternatively, we can return to the exact expression for $\psi_m(\phi)$. After multiplying numerator and denominator by $\cos^2\phi$, we have

$$\psi_m = \Omega^2/(T_o\cos^2\phi-2T_1\sin\phi\cos\phi+T_2\sin^2\phi)$$
$$= \Omega^2/(U+V\cos2(\phi-\phi_o)) ,$$

where

$$U = 1/2\ (T_o+T_2)$$

$$V\cos2\phi_o = 1/2(T_o-T_2)$$

$$V\sin2\phi_o = -T_1$$

$$V = [T_1^2 + (T_o-T_2)^2/4]^{1/2}$$

$$\tan2\phi_o = -2T_1/(T_o-T_2)$$

Hence the required integrals can be evaluated as follows:

$$K_i = \Omega^{2(i+1)} L_i$$

where

$$L_i = \int_{\phi_-}^{\phi_+} d\phi/(U+V\cos 2(\phi-\phi_0))^{i+1} = \int d\phi/\Phi^{i+1}$$

$$L_0 = (1/W)\ \tan\ [Z\tan(\phi-\phi_0)]\Big|_{\phi_-}^{\phi_+}$$

with

$$W = (U^2+V^2)^{1/2}$$

and

$$Z = [(U-V)/(U+V)]^{1/2}\ .$$

$$L_1 = \frac{V\sin 2(\phi-\phi_0)}{2W^2\Phi} - \frac{U}{2W^2}\int d\phi/\Phi$$

and for arbitrary i, we have

$$L_i = \frac{V\sin 2(\phi-\phi_0)}{2(i-2)W^2\Phi^i} + \frac{(2i-1)U}{2iW^2}\int d\phi/\Phi^i - \frac{(i-1)}{2iW^2}\int d\phi/\Phi^{i-1}$$

Notice that all of the integrals except L_0 depend on $2\phi_0$ and L_0 depends on $\tan\phi_0$. We have determined $\cos 2\phi_0$ and $\sin 2\phi_0$ which leaves ϕ_0 ambiguous by $\pm\pi$ however the integrals will be uniquely determined.

5. Conclusions

A computer simulation of the optical behavior of the solar central receiver system requires a knowledge of the flux density reflected sunlight due to each heliostat in the collector field. The problem of calculating the flux density of light reflected by a single heliostat can be formulated in various ways (see Reference 2.). However, it usually leads to a slowly converging numerical problem. We find that an efficient analytic result exists for the flux density of a flat polygonal heliostat. This formulation has been implemented by a computer program called FLASH. This program includes the effects of shading and blocking on the images. It also includes the effect of solar limb darkening up to the sixth order in the polar angle. The coefficients $\{I_i\}$ for the solar limb darkening can be generalized to include image broadening guidance errors.

Table 1 shows the appearance of the relatively nearby octagonal heliostat with a large shadow effect such as will occur when the solar elevation is low. The FLASH program is able to cope with the complexities of the reflected image by virtue of having carefully considered the relationship between the heliostat boundary and the apparent position of the solar disc as seen from the flux point in the image plane. Figures (2) and (3) show the details for typical cases.

Appendix A gives an analytic formulation of the flux density due to a round heliostat. However, in this case the algebraic complexity becomes unappetizing and a relatively slow quartic root extraction is required. Appendix B shows how to reduce the flux density problem for a heliostat of arbitrary shape to an efficient numerical integration

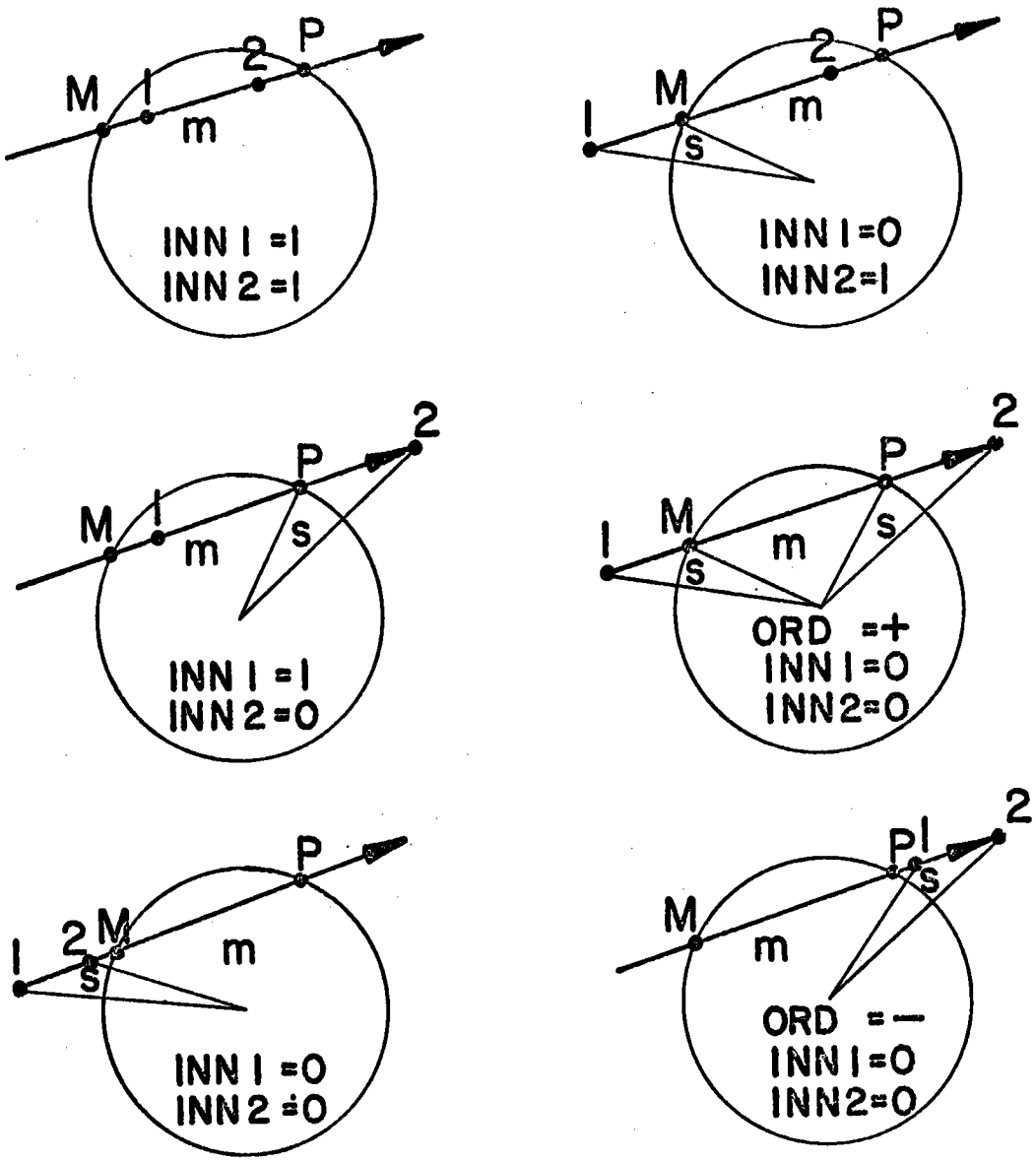

Figure 3. Shows the boundary segment (1→2) in relation to the solar disc. All six cases correspond to a positive discriminant. Points 1 and 2 are vertices of the reflecting region whereas points M and P are computed intersection points. The necessary computer control variables INN1, INN2 and ORD correspond to the various cases as shown. Mirror segments are designated by m and sun segments by s.

TABLE 1. Shows a sample heliostat image. At 5.33 hours before noon on the 162nd day after vernal equinox, the sun is almost exactly due east at an elevation of 12.87° for a site at 35° of latitude. At this early morning hour we expect a considerable amount of shading. We have selected a heliostat location one-half a tower height north of the tower. The tower height is 110 meters, the slant distance to the heliostat is 123 meters, and the heliostat is an octagon of width 6.5 meters. The tabular data is flux density in W/m^2 versus x and y coordinates in meters.

	-3.27	-2.86	-2.45	-2.05	-1.64	-1.23	-.82	-.41	0.00	+.41	.82	1.23	1.64	2.05	2.45
	.0	.0	.0	.0	.0	.0	.0	.0	.0	.0	.0	.0	.0	.0	.0
	.0	.0	.0	.0	.0	.0	.0	.0	.0	.0	.0	.0	.0	.0	.0
-3.27	.0	.0	.0	.0	80.2	174.2	187.8	162.2	137.7	99.0	25.6	.0	.0	.0	.0
-2.86	.0	.0	.0	83.2	322.7	506.6	546.9	520.1	492.5	402.2	213.8	19.5	.0	.0	.0
-2.45	.0	.0	51.8	290.6	568.6	742.5	745.6	745.6	743.0	695.5	422.1	133.0	.0	.0	.0
-2.05	.0	26.5	243.4	524.0	728.6	745.6	745.6	745.6	745.6	640.8	384.0	116.2	8.9	.0	.0
-1.64	.8	160.8	466.3	706.6	745.6	745.6	745.6	745.6	670.4	418.3	160.6	17.6	.0	.0	.0
-1.23	11.1	261.4	610.8	745.6	745.6	745.6	745.6	700.5	466.4	187.5	5.6	.0	.0	.0	.0
- .82	11.2	287.8	637.4	745.6	745.6	745.6	726.7	517.0	232.6	21.6	.0	.0	.0	.0	.0
- .41	11.2	287.8	637.4	745.6	745.6	745.6	648.9	343.9	46.3	.0	.0	.0	.0	.0	.0
0.00	11.2	287.8	637.4	745.6	745.6	745.6	608.9	257.3	2.2	.0	.0	.0	.0	.0	.0
+ .41	11.2	287.8	637.4	745.6	745.6	745.6	607.8	251.9	2.2	.0	.0	.0	.0	.0	.0
.82	11.2	269.2	621.3	745.6	745.6	745.6	607.8	251.9	2.2	.0	.0	.0	.0	.0	.0
1.23	1.9	181.4	502.4	730.5	745.6	745.6	607.8	251.9	2.2	.0	.0	.0	.0	.0	.0
1.64	.0	49.2	299.6	588.3	745.6	745.6	608.0	253.5	2.2	.0	.0	.0	.0	.0	.0
2.05	.0	.0	102.4	378.7	651.9	745.6	638.1	318.5	23.3	.0	.0	.0	.0	.0	.0
2.45	.0	.0	.0	167.5	457.6	695.5	709.5	470.0	172.5	.4	.0	.0	.0	.0	.0
2.86	.0	.0	.0	19.5	213.8	402.2	492.5	430.5	212.7	42.5	.0	.0	.0	.0	.0
3.27	.0	.0	.0	.0	25.6	99.0	137.7	162.2	98.6	19.0	.0	.0	.0	.0	.0
	.0	.0	.0	.0	.0	.0	.0	.0	.0	.0	.0	.0	.0	.0	.0
	.0	.0	.0	.0	.0	.0	.0	.0	.0	.0	.0	.0	.0	.0	.0

over one variable. We have not implemented this approach. However, it may play a useful role in the future because of its intermediate speed.

The speed of FLASH has been measured and compared to HCOEF, which impelments Walzel's Hermite function method. See References (2-5). Table 2 shows that FLASH is much slower than HCOEF but is much more accurate. Consequently, we use FLASH as a standard to test all other methods for accuracy, but in practice we use HCOEF or some other method of intermediate speed and accuracy. The comparison shown in Table 2 represents a field of octagonal heliostats with 3 mrad degrading and a sixth order approximation in both programs. The field contains 120 representative heliostats so that FLASH requires 240 seconds of computer time to generate one output of total receiver flux. Similarly, HCOEF can output a total receiver flux estimate in 2.06 seconds. The accuracy quoted for FLASH represents closure errors in the FORTRAN trigonomic functions. However, we must mention several other sources of error which can be removed if necessary.

1. If shading and blocking occur, an exact calculation requires a stereographic projection from each flux point.
2. If the reflector is nearby, the exact form of the integrals may be used. This would be suitable for a concentrating flat plate collector study.
3. The analytic fit on the solar limb darkening has some errors but for our purposes these can be ignored.

We feel that HCOEF is currently suitable for central receiver studies because we can accept 2% errors in flux density as long as the interception factors can be determined to better than 1%. Flux density

TABLE 2. Comparison of FLASH* and HCOEF† for Octagonal Heliostats with Shading and Blocking Events

	HCOEF	FLASH	RATIO
Speed (msec/image)	17.2	1995	1/116
Maximum Error in Flux (fraction of peak flux)	.02	10^{-7}	4×10^{5}
Maximum Error in Interception (fractional value)	.002	10^{-7}	2×10^{4}
Source Size (Fortran Lines)	279	118	2.36

*FLASH is the computer subroutine which implements the analytic integration described in this paper.

†HCOEF is the computer subroutine which implements the Hermite function method which is described in Reference (4).

becomes a problem only when it exceeds the maximum allowable level, but the safety margin is much greater than 2%.

Acknowledgments

This paper was prepared with the support of the U. S. Energy Research and Development Administration Grant No. E(04-3)-1108. However, any opinions, findings, conclusions, or recommendations expressed herein are those of the authors and do not necessarily reflect the views of ERDA. The concept of subroutines FLASH and HCOEF is due to F. W. Lipps. We are indebted to M. D. Walzel for the development of the Hermite function expansion [4]. Lorin Vant-Hull maintained a necessary link with applications to the Solar-Central Receiver Program.

Appendix A) Images from Round Heliostats

Although this paper is directed towards the problem of polygonal heliostats, it is also interesting to consider the images due to round heliostats. Let $\hat{w}$ represent the unit normal vector for the plane of the heliostat and let $u\hat{u} + v\hat{v}$ represent a vector in the plane of the heliostat as previously discussed. Consequently, the boundary of a round heliostat can be parameterized by the vector

$$\vec{b}(\ell) = r_H(\cos\ell\ \hat{u} + \sin\ell\ \hat{v}),$$

where r_H is the radius of the heliostat and ℓ is azimuth of $\vec{b}$. As previously, we can write

$$\psi(\ell) = \sin^2\alpha \simeq [(x-\hat{x}\cdot\vec{b})^2 + (y-\hat{y}\cdot\vec{b})^2]/R_o^2$$

$$\tan\phi(\ell) = (y-\hat{y}\cdot\vec{b})/(x-\hat{x}\cdot\vec{b})$$

and

$$K_i = \int_{\phi_-}^{\phi_+} d\phi\psi^{i+1} = \int_{\ell_-}^{\ell_+} d\ell(d\phi/d\ell)\psi^{i+1} .$$

In this case it is convenient to modify the orientations of $(\hat{u},\hat{v})$, and $(\hat{x},\hat{y})$ in their respective planes, so that $\hat{y}$ and $\hat{v}$ are normal to the plane of reflection. Specifically, let

$$\hat{y} = \hat{v} - \hat{r}_o x\hat{w}/\sin i_o$$

$$\hat{x} = \hat{y}x\hat{r} - (\hat{w} - \cos i_o \hat{r}_o)/\sin i_o$$

$$\hat{u} = \hat{v}x\hat{w} = (\cos i_o \hat{w} - \hat{r}_o)/\sin i_o$$

Consequently, $\hat{x}$ and $\hat{u}$ lie in the plane of reflection. It is easy to see that

$$\hat{x}\cdot\hat{u} = \cos i_o,$$
$$\hat{x}\cdot\hat{v} = 0,$$
$$\hat{x}\cdot\hat{w} = \sin i_o,$$

$$\hat{y}\cdot\hat{u} = 0,$$
$$\hat{y}\cdot\hat{v} = 1,$$
$$\hat{y}\cdot\hat{w} = 0,$$

$$\hat{r}\cdot\hat{u} = -\sin i_o,$$
$$\hat{r}\cdot\hat{v} = 0,$$
$$\hat{r}\cdot\hat{w} = \cos i_o,$$

and

$$\hat{r}_o\cdot\vec{b} = -r_H \sin i_o \cos\ell,$$
$$\hat{x}\cdot\vec{b} = r_H \cos i_o \cos\ell,$$
$$\hat{y}\cdot\vec{b} = r_H \sin\ell.$$

It is also convenient to introduce the dimensionless parameters

$$\xi = x/r_H,$$

$$\eta = y/r_H,$$

and

$$\Omega \quad r_H/R_o,$$

which simplify the expressions for $\psi(\ell)$ and $\phi(\ell)$.

$$\psi(\ell) = \Omega^2[(\xi-\cos i_o\cos\ell)^2+(\eta-\sin\ell)^2],$$

and

$$\tan\phi(\ell) = (\eta-\sin\ell)/(\xi-\cos i_o\cos\ell)$$

Consequently,

$$d\phi/d\ell = (1+\tan^2\phi)^{-1}d\tan\phi/d\ell,$$

$$d\tan\phi/d\ell = [-\cos(\xi-\cos i_o\cos\ell)-\cos i_o\sin\ell(\eta-\sin\ell)] \times (\xi-\cos i_o\cos\ell)^{-2}$$

$$\psi(\ell) = \Omega^2(\xi-\cos i_o\cos\ell)^2(1+\tan^2\phi),$$

and

$$d\phi/d\ell = \Omega^2[\cos i_o - \xi\cos\ell - \eta\cos i_o\sin\ell]/\psi(\ell).$$

We now have

$$K_i = \Omega^{2(i+1)} P_i$$

where

$$P_i = \int_{\ell_-}^{\ell_+} d\ell (\cos i_o + -\xi\cos\ell - \eta\cos i_o \sin\ell) Q^i(\ell)$$

and

$$Q(\ell) = (\xi - \cos i_o \cos\ell)^2 + (\eta - \sin\ell)^2$$

which can be evaluated in terms of $\ell_\pm$. The end points $\ell_\pm$ are determined by the equation,

$$\psi(\ell) = \psi_L = \sin\alpha_L ,$$

which becomes quartic in either $\cos\ell$ or $\sin\ell$. Let

$$Q(\ell) = \begin{cases} a+b\cos\ell+c\sin\ell+d\cos^2\ell, \text{ or} \\ a'+b\cos\ell+c\sin\ell-d\sin^2\ell, \text{ where} \end{cases}$$

$$a = \xi^2+\eta^2+1$$

$$b = -2\xi\cos i_o$$

$$c = -2\eta$$

$$d = \cos^2 i_o - 1$$

$$a' = \xi^2+\eta^2+\cos^2 i_o$$

so that

$$-c\sin\ell = a+b\cos\ell+d\cos^2\ell - \psi_L/\Omega^2$$

$$c^2(1-\cos^2\ell) = (a+b\cos\ell+d\cos^2\ell-\psi_L/\Omega^2)^2 ,$$

and

$$A\cos^4\ell+B\cos^3\ell+C\cos^2\ell+D\cos\ell+E = 0,$$

if

$$A = d^2$$

$$B = 2bd$$

$$C = b^2+c^2+2d(a-\psi_L/\Omega^2)$$

$$D = 2ab$$

$$E = (a-\psi_L/\Omega^2)^2-c^2 .$$

Similarly

$$-b\cos\ell = a'+c\sin\ell-\sin^2\ell-\psi_L/\Omega^2$$

$$b^2(1-\sin^2\ell) = (a'+c\sin\ell-d\sin^2\ell-\psi_L/\Omega^2)^2$$

$$A\sin^4\ell+B\sin^3\ell+C\sin^2\ell+D\sin\ell+E = 0$$

where

$$A = d^2$$
$$B = -2cd$$
$$C = b^2+c^2-2d(a'-\psi_L/\Omega^2)$$
$$D = 2a'c\ ,$$

and

$$E = (a'-\psi_L/\Omega^2)^2-b^2$$

These inevitable quartic root problems plus the complexities of evaluating the P_i make the round heliostat image unattractive for analytic calculations.

Appendix B) Images from Heliostats of Arbitrary Shape

Looking back over these notes, we see that the flux density problem is formulated as a double integral over the polar coordinates (ψ,ϕ). The integration over ψ is easy and can be performed for heliostats of arbitrary shape, but the integration over ϕ is always difficult analytically. Consequently, it is also desirable to formulate the ϕ integral as a numerical integration.

We have

$$F(x,y) = 1/2\ \rho \sum_{i=0}^{\infty} I_i J_i(x,y)/(i+1),$$

$$J_i(x,y) = \Phi_D\ \psi_L^{\,i+1} + \sum_{m\in M} K_{im},$$

and

$$K_{im} = \int_{\phi_m^-}^{\phi_m^+} d\phi\ \psi_m(\phi)^{i+1}\ ,$$

where $\psi_m(\phi)$ is a single valued branch of the boundary function. However, $\psi_m(\phi)$ will not be monotone, since

$$\psi_m(\phi_m^+) = \psi_m(\phi_m^-) = \psi_L\ .$$

The shape of the heliostat can be represented by the functions $u(\ell)$ and $v(\ell)$, so that the boundary vector

$$\vec{b}(\ell) = u(\ell)\hat{u} + v(\ell)\hat{v}$$

is known. Consequently, we can calculate $\psi(\ell)$ and $\phi(\ell)$, and it is perfectly reasonable to integrate over ℓ numerically. Let

$$K_{im} = \int_{\ell_-}^{\ell_+} d\ell\ (d\phi/d\ell)\ \psi(\ell)^{i+1}$$

$$\cong \sum_{k=0}^{N-1} \Delta\phi_k \psi(\ell_k)^{i+1}\ ,$$

where

$$\ell_k = \ell_- + k(\ell_+ - \ell_-)/N \ ,$$

and

$$\Delta\phi_k = \phi(\ell_{k+1}) - \phi(\ell_k) \quad \text{for } k = 0,1,\ldots N-1.$$

The values of $\{u(\ell_K), v(\ell_k) | k=0\ldots N-1\}$ provide all of the necessary boundary information. This approach also requires a numerical solution of the end point equation $\psi(\ell) = \psi_L$. However, it appears to be a useful numerical approach to the image problem.

Assuming that the end point equation can be dealt with satisfactorily, it may be desirable to integrate over ψ numerically. Let

$$K_{im} = \int_{\psi_o}^{\psi_L} d\psi P_m(\psi) \psi^{\,i+1} \ ,$$

where

$$P_m(\psi) = \sum_{\phi} |d\phi/d\psi_m|$$

and in general, we have

$$J_i(x,y) = \int_{\psi_o}^{\psi_L} d\psi P(\psi),$$

where

$$P(\psi) = \sum_{m} P_m(\phi) + \Phi_D \, \delta(\psi - \psi_L) \ .$$

The interesting point about this formulation is that the dependence on sun size via the parameter ψ_L is explicit, since ψ_L occurs as its upper bound of the integral and nowhere else. $P_m(\psi)$ is hard to calculate analytically and is complicated by the occurrence of singularities. However, one might want to consider several heliostats simultaneously, in order to smooth out the singularities.

REFERENCES

1. L. L. Vant-Hull and A. F. Hildebrandt, "Solar Thermal Power System Based on Optical Transmission," Solar Energy 18, 31 (1976).
2. Frederick W. Lipps, "Four Different Views of the Flux Density Integral," Solar Energy 18, 555 (1976).
3. F. W. Lipps, "An Analytic Integration of the Solar Flux Density due to Rectangular Mirrors," Paper 74-WA/SOL-10 of the ASME Winter Annual Meeting, New York, Nov. 17, 1974.
4. M. D. Walzel, F. W. Lipps, and L. L. Vant-Hull, "A Solar Flux Density Calculation for a Solar Tower Concentrator Using a Two-Dimensional Hermite Function Expansion," SEJ- .
5. M. D. Walzel, "Solar Power Density Calculation Using Two-Dimensional Hermite Ploynomials," Master's Thesis, University of Houston, May, 1976.

APPENDIX C

A Cellwise Method for the Optimization of Large Central Receiver Systems

F. W. Lipps and L. L. Vant-Hull
Solar Energy Laboratory
University of Houston, Texas 77004

Abstract

The total number of heliostats in the collector field determines the approach to the optical simulation problem. For large central receiver systems it is desirable to introduce a cell model which establishes an array of representative heliostats. See Reference [1] for central receiver systems. We now have an arsenal of computer programs which allows us to optimize the arrangement of heliostats in the collector field subject to the approximations of the cell model. Each cell contains an arbitrary regular two dimensional array of heliostats. For practical reasons we have limited our current study of the 100 MWe commercial model to four categories of heliostats arrangement, (1) radial cornfields, (2) radial staggers, (3) N-S cornfields and (4) N-S staggers.

The most important results from the 100 MWe commercial model optimization study are:

1) Staggers are better than cornfields.
2) The increased cost of the tower and receiver subsystems has moved the solution to a larger cell size and a shorter tower.
3) No panels should be deleted from the south side of the cylindrical receiver, and
4) The collector field trims to a 360 degree configuration. However, the center of the collector field is north of the tower and some compromise must be made to prevent excessive panel power asymmetry.

Nomenclature

a_c is the maximum ground coverage factor

A_c is the area of glass in cell in m^2

A_H is the area of glass/heliostat in m^2

A_L is the area of land in a cell in m^2

A_T is the total area of glass in the collector in m^2

B is a wiring geometry parameter m^{-1}

C_H is the cost of heliostats in $\$/m^2$.

C_L is the cost of land in $\$/m^2$.

C_o is fixed cost in the expression for total system cost

C_s is the total system cost in \$.

C_W is the cost of wiring in \$/m.

C_+ is the additional cost due to land and wiring.

D_c is the width of a cell in the collector model in m.

D_M is the width of the heliostat in m.

D_x is North-South heliostat spacing in m.

D_y is East-West heliostat spacing in m.

E_A is the total annual energy loss in MWHt (due to convection and reradiation)

E_c is the total energy directed towards the receiver by cell c in the collector field in MWHt

$\tilde{E}_L$ is the lagrange parameter in MWH/m^2

$E_L\ (x_c y_c)$ is the lagrangian energy function for cell c in MWH/m^2

$E_T\ (x_c y_c)$ is the transverse energy function for cell c in MWH/m^2

E_o is the total receiver output energy in MWHt.

E_T is the total energy in MWHt before losses.

f_c is the dimensionless ground coverage fraction in cell c

f_c^* is the optimum value of f_c

$\hat{f}_c$ is the alternative value of f_c defined by the coefficient of $\delta\phi_c$.

F is the figure of merit in $/MWHt

F^* is the figure of merit in $/MWHt for an ideal system having no losses

H_T is the tower heights in meters

N is the total number of cells

N_o is the number of heliostats/field controller

R_H is the dimensionless heliostat geometry factor occuring in the expression for ground coverage

S_o is the total direct beam solar energy at normal incidence over the the given time period in $MWHt/m^2$

t_c is a dimensionless parameter for the set of hyperbolae orthagonal to f_c.

$\vec{u}_f$, $(\vec{u}_t)$ is a unit vector normal to curves of constant f (or t)

W_c is length of wire required by cell c in m.

x_c is first spacing parameter for cell c in heliostat units

y_c is second spacing parameter for cell c in heliostat units

z_c is the dimensionelss fraction of glass in cell c

$\hat{\alpha}$ is the dimensionless absorptivity of the "black" receiver

α is the dimensionless relative cost of land

β is the dimensionless relative cost of wiring

γ_c is the dimensionless cell geometry factor for cell c occuring in the expression for ground coverage.

$\vec{\delta}_f$, $(\vec{\delta}_t)$ is the differential vector tangent to the curves of constant f (or t).

η_c is the receiver interception factor for energy coming from cell c.

η_{cp} is the interception fraction for receiver panel p illuminated by the reflected sunlight from cell c.

λ_c is collector efficiency for cell c

λ_T is a dimensionless measure of total energy, or equivalently a net system efficiency.

μ_c, (ν_c) is net efficiency function for cell c (with land and wiring effects included).

$\tilde{\mu}$, $(\tilde{\nu})$ is the dimensionless langrange parameter (with land and wiring effects included).

$\hat{\rho}$ is the net reflectivity of the heliostat

ρ_x is the North-South heliostat density

ρ_y is the East-West heliostat density

σ_o is the incident solar flux density in MW/m^2

τ is the time variable in hours

ϕ_c is the fraction of cell c which is covered by the heliostat array

∂ is math symbol for partial derivative

ϵ is math symbol denoting set membership

π is math symbol for 3.14159

∇ is math symbol for gradient operator

$\rightarrow$ is math symbol for a vector quantity.

The main purpose of this memo in its present form is to present the mathematical background for the cellwise optimization procedure. Re-issues are expected to clarify details of 100 MWe study.

1. Introduction

Our current view of the optical simulation model and collector field optimization problem for the large central receiver system contains the following components:

1. The Astronomical Model*
   - a) Diurnal motion of sun
   - b) Insolation model for cloudless sky:
     Air mass for round earth
     Water vapor, altitude, and turbity parameters
   - c) Sample of times for daily and annual statistics
2. The Collector Field Models
   - a) Cell model with uniformly spaced representative heliostats and variable numbers of heliostats per cell.*
   - b) Cell model with fixed number of heliostats per cell and suitably located representatives.
   - c) Individual heliostats each listed in computer storage.
3. The Heliostat Models
   - a) Square <u>with</u> or without slotting and with or <u>without</u> canting to increase concentration.*
   - b) Octagonal, etc.
   - c) Others
4. The Mounting System Models
   - a) Alt-Azimuthal*
   - b) Radial-Pitch-Roll
   - c) Azimuthal-Pitch-Roll
   - d) Polar
   - e) Receiver oriented

*The assumptions made for the current 100 MWe study are indicated by asterisks and underlining. Details will be given later.

5. The Shading and Blocking Models*
   a) Optional inclusion of remote neighbors
   b) Test for sun sensor
   c) Each segment of whole heliostat
   d) Options for greater speed and less accuracy
6. The Guidance Error Model*
7. The Image Generators
   a) Analytic model and convolution processor for guidance errors.
   b) Walzel's hermite polynomial approximation method*
8. The Focusing Strategy and Abberation Model for Canted Heliostats
9. The Receiver Models
   a) Cylindrical external*
   b) Flat panel
   c) Aperture for Cavity
10. The Aiming Strategy Models
   a) Aim at belt of cylinder
   b) Optimum two point high-low aim
   c) Three point high-low aim*
   d) Five point high-low aim
   e) Horizontal strategies
11. The Cost Model
   a) Heliostats (including guidance, etc.)*
   b) Tower*
   c) Receiver*
   d) Plumbing in tower*
   e) Land for heliostat*
   f) Wiring for heliostat*
   g) Turbine generators system, etc.
   h) Thermal storage
   i) Capacity credits
   j) Water costs
   k) Financial costs
   l) Operation and maintenance

12. The Energy Loss Model
    a) Reflection and absorption*
    b) Absorptivity versus angle of incidence*
    c) Reradiation and convection by receiver*
    d) Thermodynamic cycle efficiency
    e) Pump power and other parasitic losses
13. The Figure of Merit and Optimization Procedure*
    a) Cost model
    b) Energy model with losses
    c) External constraints
        1. Policy related choice of base time period
        2. Definition of scale, i.e. Power at Equinox Noon, etc.
        3. Mechanical for heliostats and access
        4. Flux limits for receiver
        5. Flux gradient limits for receiver

Two new programs play a role in our new optimization procedure. The LOSS program tells us how much ground space is required by a heliostat at each of the representative locations. This programs calculates the MWH/m^2 of lost energy due to a single neighbor as a function of displacement from the representative heliostat. The LOSS program provides a good sun sample for the whole year and utilizes a very efficient version of the shading and blocking processor which neglects overlapping events. Overlapping events are rare under optimized conditions. The LOSS prints provide a good starting point for the collector field optimization by estimating the heliostat spacing coordinates in each cell, for any desired type of array in that cell. See figure 1. We then proceed to the RCELL program which performs a set of variations on the geometry in each cell and outputs the optimum design. See figure 3. A summary of the optimization procedure is given below.

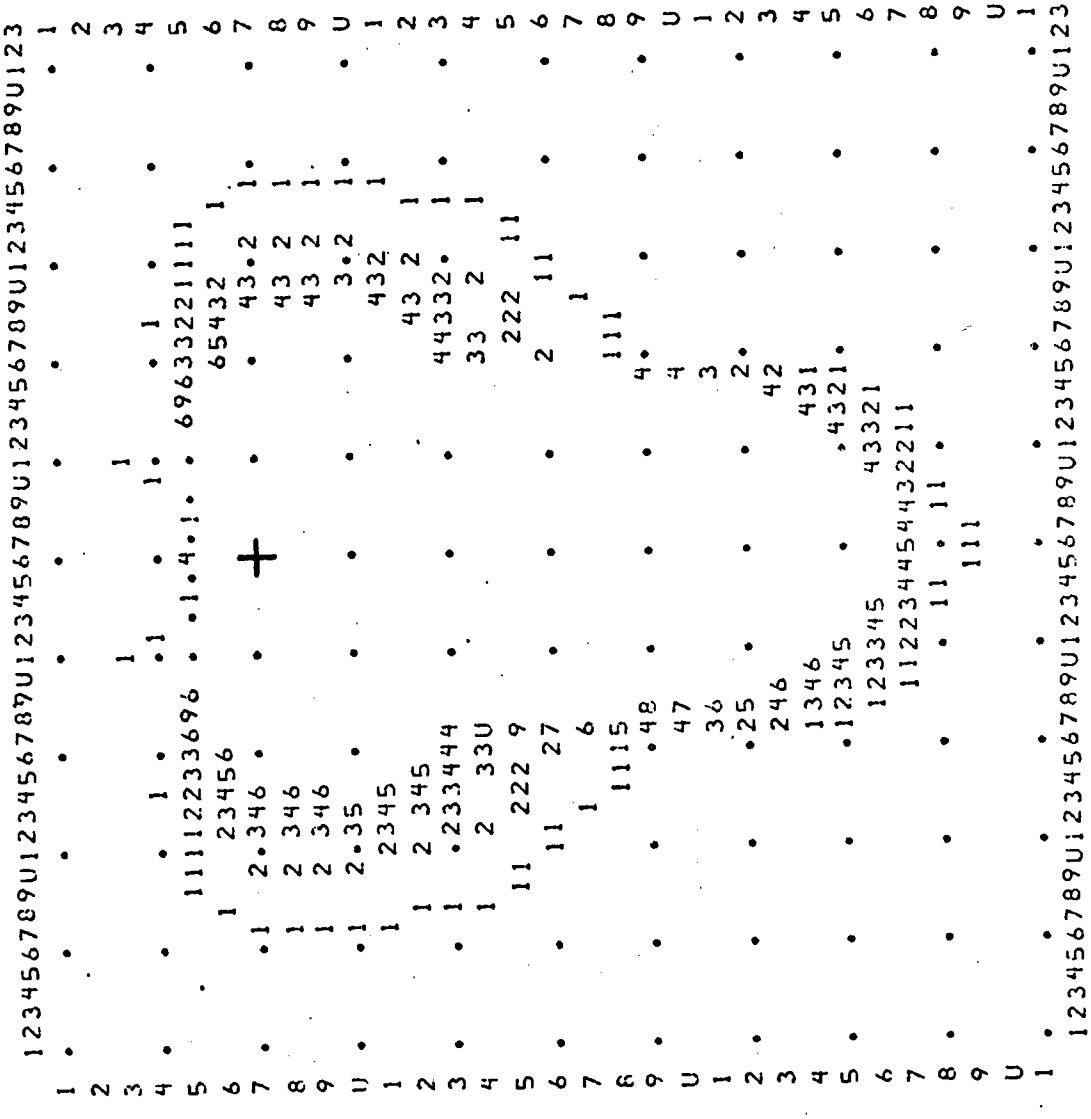

Figure 1. Contours of Percent Loss on Annual Basis. This is a LOSS print. Distance between dots is half of a heliostat width. Loss levels of 1% to 6% are shown. Displacement of the interfering heliostat is measured from the cross.

DATA FLOW SCHEMATIC FOR CELL-WISE
OPTIMIZATION PROCEDURE

The dot precedes a program and follows a data file. DATA is also enclosed by parenthesis.

The PANEL data file is generated by the scheme.

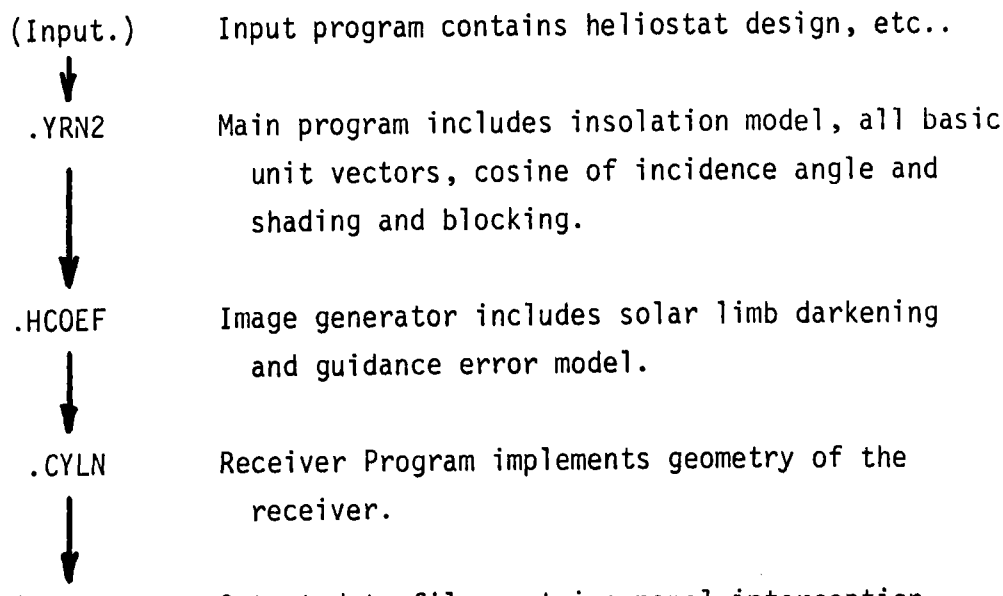

The RCELL linkage can be iterated as often as is necessary to obtain the optimization.

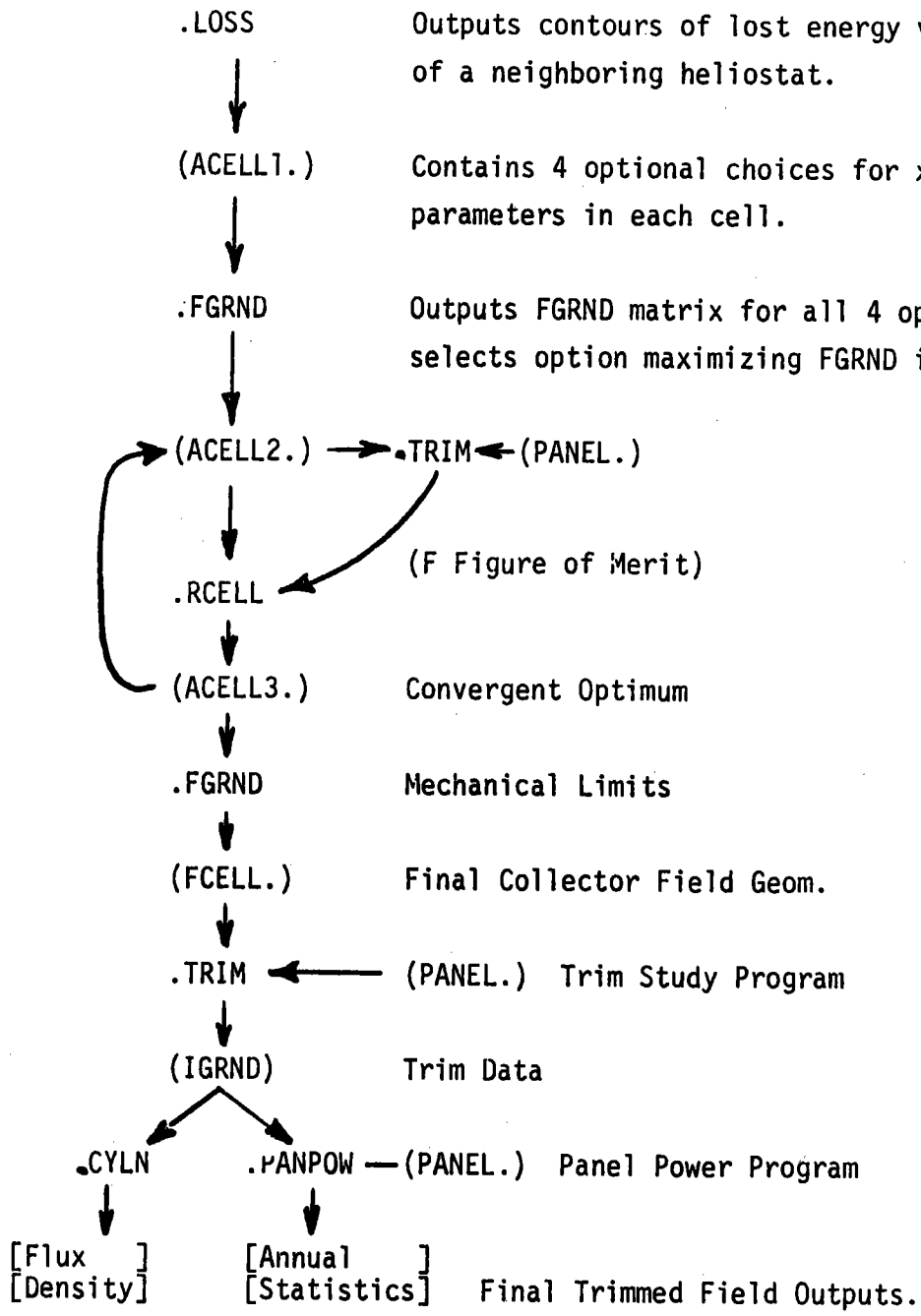

2. System Performance Model and Figure of Merit

The figure of merit F is the ratio of the total system cost C_s, to the total energy E_T, which is output by the receiver during a suitable period of time. Let

$$F = C_s/E_T = F^*/\lambda_T,$$

where

$$F^* = C_s/S_o A_T \qquad \text{in } (\$/MWH_t),$$

$$S_o = \int d\tau \sigma_\delta(\tau) \qquad \text{in } (MWH_t/m^2),$$

$$A_T = \sum_c A_c \text{ in } (m^2),$$

and

$$\lambda_T = E_T/S_o A_T = R^*/F,$$

which is the net system efficiency and is dimensionless. A_c is the total area of glass in the c^{th} cell and A_T is the total area of glass in the whole system. S_o is the total direct beam solar energy/m^2 at normal incidence over the given time period. For the present purposes, this period will be the sunlight portion of a year for which the solar elevation exceeds 15^o. F* represents the figure of merit for an ideal system with no losses and, therefore

$$\lambda_T < 1,$$

for real systems. The total energy E_T can be expressed as a sum over cells and for this purpose, we write

$$E_T = \sum_c E_c \eta_c,$$

where η_c is the receiver interception fraction for the c^{th} cell and E_c is the total energy which is redirected towards the receiver by the c^{th} cell. λ_T is a measure of the efficiency for collecting and transfering sunlight to the working fluid. We assume for simplicity that η_c is time independent and that E_c can be adequately approximated by the behaviour of a representative heliostat at the center of the cell. The

time independence of η_c is well verified for flat heliostats but is only approximately valid for focusing or canted heliostats. Let

$$E_c = \lambda_c S_o A_c,$$

and as previously

$$E_T = \lambda_T S_o A_T,$$

so that

$$\lambda_T = \sum_c \lambda_c \eta_c z_c,$$

where z_c is the fraction of glass in the c^{th} cell. Clearly, $z_c = A_c/A_T$, and

$$1 = \sum_c z_c.$$

The computer programs NCELL and RCELL output the quantity

$$g_c = E_c/A_c = \lambda_c S_o,$$

which represents the MWH/m^2 of redirected energy from each cell, versus parameters which represent various arrangements of heliostats in the cell. The CYLN program outputs the interception fraction η_c, for a McDonnell-Douglas type of external panel receiver. Actually, the panel interception fractions are determined so that η_c can be formulated for various choices of panels

$$\eta_c(P) = \sum_{p \epsilon P} \eta_{cp}$$

where P is a set of panels and η_{cp} is the interception fraction for panel p illuminated by the reflected energy from the the c^{th} cell.

The parametrization of the cell is not the same in the NCELL and the RCELL programs. For NCELL we introduce the parameters

$$\rho_x = D_M/D_x \text{ such that } 0 \leq \rho_x \leq 1,$$

$$\rho_y = D_M/D_y \text{ such that } 0 \leq \rho_y \leq 1,$$

where D_M is the heliostat width. D_x and D_y are the heliostat spacings in an assumed north-south cornfield. In this approach we can not afford the CPU-time required to average over a whole year because we require 121 samples of (ρ_x, ρ_y) covering their entire range See Reference [2]. For RCELL we consider staggers as well as cornfields and we are prepared to deal with arbitrary orientations of the cell. For the current 100 MWe study we are only interested in north-south or radial orientations. However, in RCELL we get an average over the whole year at the expense of restricting our output sample to a fraction of the range of the parameters. In this case, the parameters are

$$x = D_x/D_M = 1/\rho_x$$

and

$$y = D_y/D_M = 1/\rho_y.$$

Typically, we will output g_c and other quantities as 4 x 4 matrices.

In reality, g_c and hence λ_c depend on the heliostat location coordinates for all of the heliostats in cell c, however by assuming a cell model, we have reduced the number of independent parameters to $2N_B$, where N_B is the relevant number of neighbors surrounding the representative heliostat. For the 100MWe study, we further restrict the number of independent parameters by limiting the arrangements of neighbors to the four options:

1 Radial Oriented Cornfields,

2 Radial Oriented Staggers,

3 North-South Oriented Cornfields, and

4 North-South Oriented Staggers.

For each of these options there are two independent parameters x_c and

y_c which control the spacing between neighbors in the two independent directions for the c^{th} cell. Consequently, the area of glass in the c^{th} cell is given by

$$A_c = A_L f_c$$

where

$$f_c = A_H (\gamma_c x_c y_c D_M^2)^{-1}$$

is the ground coverage factor and A_L is the area of the cell itself. A_H is the area of the heliostat, and $\gamma_c x_c y_c D_M^2$ is the area of land required by each heliostat.

$$\gamma_c = \begin{cases} 1/2 & \text{for staggered cells, and} \\ 1 & \text{for cornfield cells.} \end{cases}$$

A "standard uniform cell" array is defined by $A_L = D_c^2$ with

$$D_c = H_T/2.$$

However, using our current model we find a need of larger cells, which are defined by

$$D_c = H_T/\sqrt{2}$$

and are called "Large Cells." In general,

$$f_c = a_c/x_c y_c$$

where

$$a_c = A_H/D_M^2 \gamma_c = R_H/\gamma_c$$

It is convenient to introduce the dimensionless parameter $R_H = A_H/D_M^2$ which corrects f_c for the shape of the heliostat. For an ideal square heliostat $R_H = 1.0$. In the present case we have a square heliostat with a central slot and 6 segments, such that $R_H = .8972$. We may also consider an octagonal heliostat for which $R_H = .8284$.

3. The Optimization

We now have expressions for λ_c or equivalently g_c as functions of (x_c,y_c). However, in order to proceed with the optimization we will need an alternative parameterization in terms f_c and t_c which form an orthogonal system of hyperbolas as shown in figure 2. Let

$$f_c = a_c/x_c y_c$$

and

$$t_c = 1/2\ (x_c^2 - y_c^2),$$

so that

$$\lambda_c(x_c,y_c) = \lambda_c(f_c,t_c).$$

We can prove that the curves of constant f_c intersect the curves of constant t_c perpendicularly by considering the variations of f_c and t_c. Let

$$\delta t_c = 0 = x_c \delta x_c - y_c \delta y_c = \vec{u}_t \cdot \vec{\delta}_t,$$

and

$$\delta f_c = 0 = \delta(x_c y_c) = y_c \delta x_c + x_c \delta y_c = \vec{u}_f \cdot \vec{\delta}_f,$$

where $\vec{\delta}_t$ is tangent to the $\delta t_c = 0$ curve and $\vec{\delta}_f$ is tangent to the $\delta f_c = 0$ curve. Clearly,

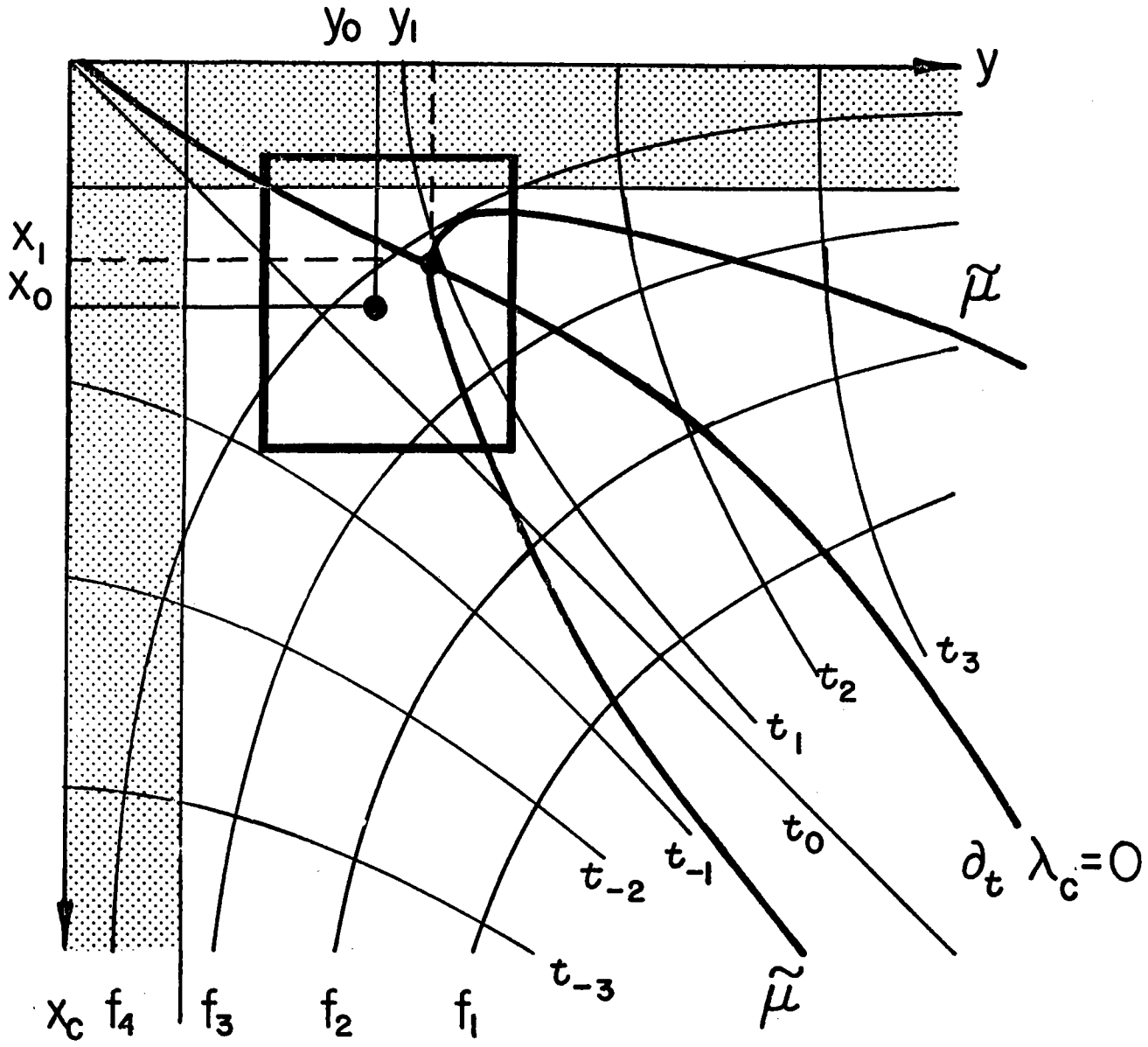

Figure 2. Parameter Space for Cell.

$$\vec{u}_t = (x_c, -y_c)\ (x_c^2 + y_c^2)^{-\frac{1}{2}},$$

and

$$\vec{u}_f = (y_c, x_c)\ (x_c^2 + y_c^2)^{-\frac{1}{2}},$$

represent unit vectors perpendicular to $\vec{\delta}_t$ and $\vec{\delta}_f$ respectively. A direct calculation gives

$$\vec{u}_t \cdot \vec{u}_f = 0.$$

and consequently,

$$\vec{\delta}_t \cdot \vec{\delta}_f = 0.$$

which proves the orthogonality of t and f. We will soon use the direction derivatives.

$$\partial_t g = \vec{u}_t \cdot \vec{\nabla}_g,$$

and

$$\partial_f g = \vec{u}_f \cdot \vec{\nabla}_g.$$

in order to solve for the optimization.

The optimization of the collector field is conveniently divided into two steps. First, we will find the conditions for an optimum having a given amount of glass A_T, and then we will vary A_T to determine its optimum value.

Assuming that C_s is a function of A_T only, then for a fixed amount of glass, $\delta C_s = 0$, and

$$\delta F = -\delta E_T C_s / E_T^2 = 0,$$

which implies that

$$\delta E_T = 0.$$

A variation of E_T, gives

$$\delta E_T = \sum_c (\lambda_c \delta A_c + A_c \delta \lambda_c)\, \eta_c S_o,$$

where

$$\delta \lambda_c = \delta f_c \partial_f \lambda_c + \delta t_c \partial_t \lambda_c,$$

and

$$0 = \sum_c \delta f_c,$$

because the total amount of glass is fixed. Each δt_c is an independent variation, so that the coefficient of δt_c in the expression for δE_T must vanish at the maximum total energy point $\{(f_c^*, t_c^*)\}$. Consequently, we have

$$\partial_t \lambda_c\, (f_c^*,\, t_c^*) = 0,$$

for all cells. We now see that

$$\delta \lambda_c = \delta f_c \partial_f \lambda_c,$$

and

$$\delta E_T = \sum_c (\lambda_c + f_c \partial_f \lambda_c)\, \eta_c \delta f_c A_L S_o.$$

The set of δf_c variables has a constraint, which must be eliminated

before the corresponding optimum condition can be determined. We can solve for any δf_N by writing

$$\delta f_N = - \sum_{c}^{N-1} \delta f_c .$$

For simplicity we define

$$\mu_c = (\lambda_c + f_c \partial_f \lambda_c)\, n_c ,$$

so that

$$\delta E_T / S_o A_L = \sum_{c}^{N-1} \mu_c \delta f_c + \mu_N \delta f_N .$$

After substituting for δf_N, we have

$$0 = \sum_{c}^{N-1} (\mu_c - \mu_N)\, \delta f_c ,$$

where the N-1 variables δf_c are independent, so that

$$\tilde{\mu} = \mu_N = \mu_c ,$$

for all cells.

Since part of the total system cost is independent of A_T and the other part is dependent on A_T, we expect to find an optimum value for A_T by considering those variations which change A_T without violating the previously established conditions for the optimum. We have

$$\tilde{\mu} = \mu_c (f_c^*, t_c^*) ,$$

and

$$\partial_t \lambda_c (f_c^*, t_c^*) = 0 .$$

A variation of the figure of merit gives

$$\delta F = 0 = \delta C_s/E_T - \delta E_T C_s/E_T^2.$$

Consequently,

$$\delta E_T/\delta A_T = (\delta C_s/\delta A_T)\ (E_T/C_s) = (\partial_A C_s)/F.$$

A variation of the total energy gives

$$\delta E_T = \left(\sum_c \mu_c \delta f_c\right)\ A_L S_o = \tilde{\mu}\delta A_T S_o,$$

so that

$$\delta E_T/\delta A_T = \tilde{\mu} S_o = (\partial_A C_s)/F,$$

and finally

$$\tilde{\mu} = (\partial_A C_s)\ (FS_o)^{-1}$$

Assuming a linear cost model, we can write

$$C_s = C_o + C_H A_T,$$

and

$$\tilde{\mu} = C_H (FS_o)^{-1}.$$

As shown in the Data Flow Schematic, the optimum value of the figure of merit F, is output by the TRIM program. Consequently, we are able to calculate the quantity

$$\tilde{E}_L = \tilde{\mu} S_o/\eta_c = C_H/(F\eta_c),$$

which we call the Lagrangian parameter in MWH/m^2 for cell c. Similarly, we can define the functions

$$E_L(x_c y_c) = S_o \mu_c / \eta_c = S_o(\lambda_c + f_c \partial_f \lambda_c),$$

and

$$E_T(x_c y_c) = S_o \partial_t \lambda_c,$$

which are output by the RCELL program for a 3 x 3 sample of the parameter space $(x_c y_c)$. The optimum point satisfies the equations

$$\tilde{E}_L = E_L(x_c y_c) \text{ and } E_T(x_c y_c) = 0.$$

Each of these equations represents a curve in the (x_c, y_c) plane. The intersection is determined by an interpolation procedure in RCELL. See figure 3.

4. The Effect of Land and Wiring Costs

Up to this point we have assumed that the system cost is a function of A_T which is the total area of glass. However, the cost of land and the cost of control wiring for the heliostats are not directly related to A_T. The following cost model is required

Input Data

C_H = 66.0 \$/m^2 for cost of heliostats and guidance devices.

C_L = 1.08 \$/m^2 for cost of land and site preparation.

C_W = 3.30 \$/m^2 for cost of wiring.

D_M = 6.502 m for width of heliostats.

Table 1: Lagrangian Parameters in MHH/m^2. Used by RCELL program to match cells of collector field.

	1	2	3	4	5	6	7	8	9	10	11
1	1.926	1.849	1.789	1.750	1.728	1.719	1.728	1.750	1.789	1.849	1.926
2	1.813	1.740	1.687	1.651	1.630	1.624	1.630	1.651	1.687	1.740	1.813
3	1.723	1.655	1.609	1.577	1.560	1.555	1.560	1.577	1.609	1.655	1.723
4	1.654	1.594	1.553	1.529	1.516	1.512	1.516	1.529	1.553	1.594	1.654
5	1.605	1.552	1.519	1.501	1.493	1.491	1.493	1.501	1.519	1.552	1.605
6	1.572	1.526	1.500	1.489	1.485	1.484	1.485	1.489	1.500	1.526	1.57?
7	1.554	1.513	1.492	1.485	1.487	1.507	1.487	1.485	1.492	1.513	1.554
8	1.548	1.508	1.489	1.484	1.509	.000	1.509	1.484	1.489	1.508	1.548
9	1.552	1.511	1.490	1.484	1.484	1.497	1.484	1.484	1.490	1.511	1.552
10	1.567	1.521	1.496	1.486	1.482	1.480	1.482	1.486	1.496	1.521	1.567
11	1.597	1.544	1.512	1.495	1.488	1.485	1.488	1.495	1.512	1.544	1.597

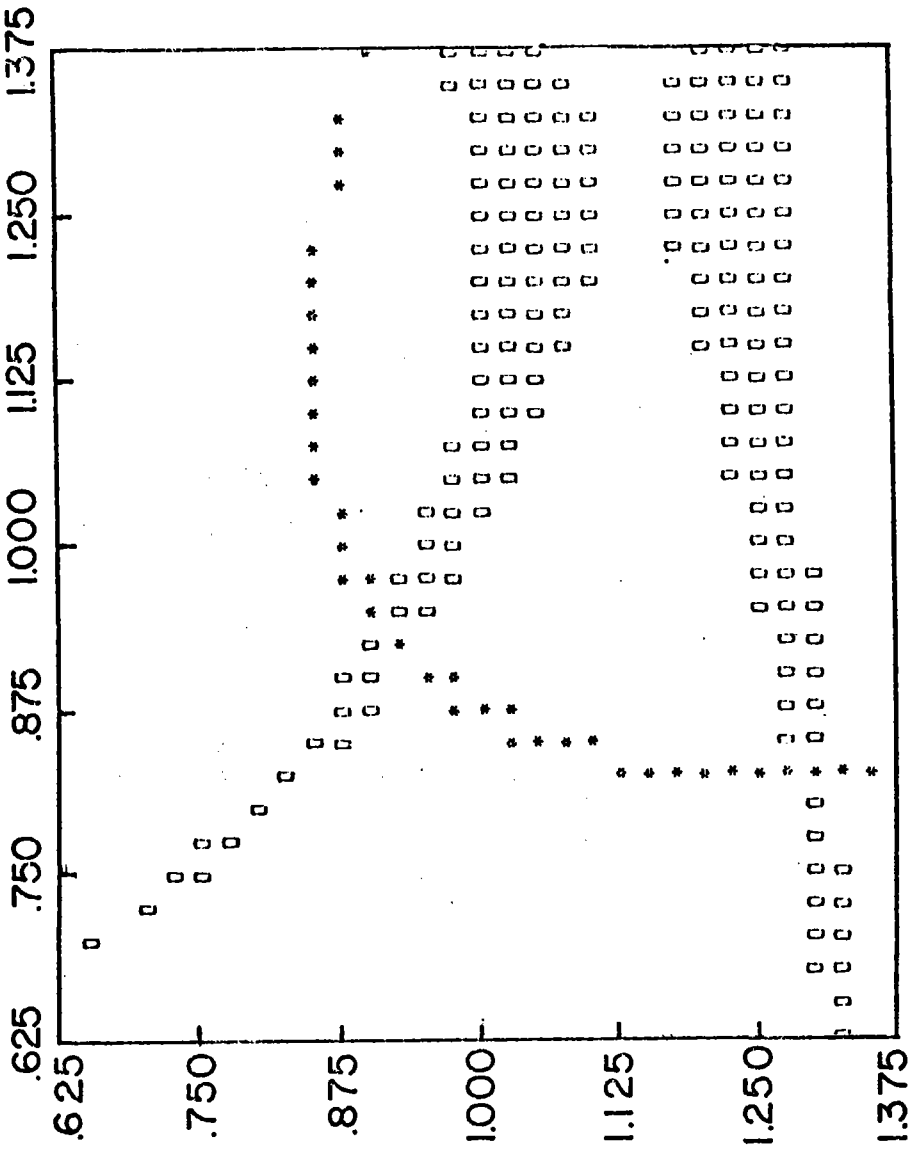

Figure 3. Locating the Optimum. This is a RCELL print. The line of stars represents the $\tilde{\mu} = \mu_c$ requirement and the line of zeros represents the $\partial_t \lambda = 0$ requirement. The intersection locates the optimum. Coordinates give ratio of output to input.

N_o = 25 = Number of Heliostats/Field Controller.

Output Requirements

$A_H = D_M^2$ = area of glass/heliostat.

$A_L = D_c^2$ = area of land/cell.

$N_H = f_c A_L / A_H$ = Number of Heliostats/cell.

$N_F = N_H / N_o$ = Number of Field Controllers/Cell.

$D_H = C_H f_c A_L$ = Cost of Heliostats/Cell.

$D_L = C_L A_L$ = Cost of Land/Cell.

$D_W = C_W W_c$ = Cost of Wiring/Cell,

where W_c is the length of wiring required for the cell. Each field controller serves N_o heliostats in a land area A_F which is given by

$$A_F = N_o A_H / f_c.$$

The mean radius of this area is given by

$$R_F = 2/3 \left(A_F/\pi \right)^{\frac{1}{2}}$$

and then W_c is given by

$$W_c = N_F N_o R_F = N_H R_F.$$

After substituting for N_F and R_F, we have

$$W_c = (f_c A_L / A_H) \cdot 2/3 \, (N_o A_H / \pi f_c)^{1/2}.$$

$$= 2/3 (N_o f_c / \pi)^{1/2} \, A_L / D_M,$$

$$= B A_L f_c^{1/2},$$

where

$$B = 2/3 \, (N_o / \pi)^{1/2} / D_M. = .289 \text{ meters}^{-1}.$$

Land costs and wiring costs both tend to increase the cost of heliostats in distant cells which must have a low density of glass because of shading and blocking requirements. Consequently, these costs can play an important role in determining the outer boundary of the collector field (i.e. the trim). Let ϕ_c be the fraction of the c^{th} cell which is covered by the array of heliostats. The covered portion of the cell has the density of coverage given by f_c, as previously. The area of glass in cell c is now given by

$$A_c = \phi_c f_c A_L = A_L a_c \phi_c / x_c y_c,$$

and ϕ_c becomes an additional parameter which must be determined by the optimization. The total system cost becomes

$$C_s = C_o + C_H A_T + C_+,$$

where

$$C_+ = C_L A_L \sum_c \phi_c + C_W B A_L \sum_c \phi_c f_c^{1/2}.$$

A variation of the cost gives

$$\delta C_s = C_H A_L \sum_c \delta(\phi_c f_c) + C_L A_L \sum_c \delta\phi_c + C_W B A_L \sum_c \delta(\phi_c f_c^{1/2}).$$

Consequently, $\delta C_s = 0$, implies that

$$0 = \sum_c [\delta f_c \phi_c (1+\tfrac{1}{2} f_c^{-\frac{1}{2}}) + \delta\phi_c (f_c+\alpha+\beta f_c^{\frac{1}{2}})]$$

where

$$\alpha = C_L/C_H = .0164,$$

and

$$\beta = C_W B/C_H = .0145.$$

A variation of the total energy gives

$$\delta E_T = \delta(\sum_c \lambda_c A_c \eta_c) S_o,$$

where

$$A_c = \phi_c f_c A_L,$$

so that

$$\delta E_T = \sum_c (\delta\lambda_c \phi_c f_c + \lambda_c \delta\phi_c f_c + \lambda_c \phi_c \delta f_c)\, \eta_c A_L S_o$$

where

$$\delta\lambda_c = \delta f_c \partial_f \lambda_c + \delta t_c \partial_t \lambda_c = \delta f_c \partial_f \lambda_c$$

as previously. We can immediately ignore the term containing δt_c since this is the only term containing δt_c and therefore, $\partial_t \lambda_c = 0$, is a condition for the optimization as before.

The first step in the optimization requires $\delta E_T = 0$ and $\delta C_s = 0$. The δE_T equation can be simplified by introducing μ_c as before.

Consequently, after cancelling the factors $A_L S_o$, the $\delta E_T = 0$ equation can be written as

$$0 = \sum_c (\mu_c \phi_c \delta f_c + \lambda_c f_c \eta_c \delta \phi_c),$$

which gives

$$\mu_N \phi_N \delta f_N = - [\sum_c^{N-1} \mu_c \phi_c \delta f_c + \sum_c^{N} \lambda_c f_c \eta_c \delta \phi_c].$$

After substituting the above expression for $\mu_N \phi_N \delta f_N$ into the $\delta C_s = 0$ equation, we have

$$0 = \sum_c^{N-1} [\mu_N \phi_N \phi_c (1+\tfrac{1}{2}\beta f_c^{\frac{1}{2}}) - \mu_c \phi_c \phi_N (1+ \tfrac{1}{2} f_N^{-\frac{1}{2}})] \delta f_c$$

$$+ \sum_c^{N} [\mu_N \phi_N (f_c+\alpha+\beta f_c^{\frac{1}{2}}) - \lambda_c f_c \eta_c \phi_N (1+\tfrac{1}{2}\beta f_N^{-\frac{1}{2}})] \delta \phi_c.$$

Each of the variations δf_c and $\delta \phi_c$ which occur in the above equation are independent and consequently their coefficients must vanish. Let

$$\tilde{\nu} = \mu_N (1+\tfrac{1}{2}\beta f_N^{-\frac{1}{2}})^{-1}, \text{ and}$$

$$\nu_c = \mu_c (1+\tfrac{1}{2}\beta f_c^{-\frac{1}{2}})^{-1}.$$

The coefficient of δf_c gives

$$\nu_c = \tilde{\nu}, \qquad \text{if } \phi_c \neq 0 \neq \phi_N,$$

and the coefficient of $\delta \phi_c$ gives

$$\lambda_c f_c \eta_c = \tilde{\nu}(f_c+\alpha+\beta f_c^{\frac{1}{2}}), \qquad \text{if } \phi_N \neq 0.$$

At first sight these equations appear to represent conflicting requirements for the ground coverage factor f_c. However, we realize

that $\phi_c \equiv 1$ for the interior cells so that the coefficient of $\delta\phi_c$ does not occur for these cells. Hence for interior cells, the one optimum requirement can be written as

$$\tilde{\nu} = \mu_N \left(1 + \tfrac{1}{2}\beta/f_N^{\frac{1}{2}}\right)^{-1} = \mu_c \left(1+ \tfrac{1}{2}\beta/f_c^{\frac{1}{2}}\right)^{-1},$$

where we have assumed that the N^{th} cell is interior, so that $\phi_N = 1$.

For an exterior cell $\phi_c \equiv 0$ and again the coefficient of $\delta\phi_c$ does not occur. A true boundary cell might have some intermediate value of ϕ_c, however this would imply a conflicting requirement for f_c, hence we conclude that $\phi_c = 0$ for boundary cells also. The remaining question is "What determines the boundary?" Let

$$\nu_c(f_c^*, t_c^*) = \tilde{\nu}$$

and let

$$\lambda_c \hat{f}_c \eta_c = \tilde{\nu} \left(\alpha + \beta \hat{f}_c^{\frac{1}{2}} + \hat{f}_c\right),$$

or equivalently,

$$\lambda_c(\hat{f}_c, t_c^*)\ \eta_c = \tilde{\nu} \left(\alpha \hat{f}_c^{-1} + \beta \hat{f}_c^{-\frac{1}{2}} + 1\right).$$

Even though the solution of the variational equation gives

$$\phi_c = 0, \text{ or } 1,$$

never-the-less we are allowed to subdivide the cells until the boundary between the interior and exterior cells becomes a smooth arc. As we go to the limit of infinitely many cells, an intermediate value of ϕ_c must occur for some very small, appropriately located cell. For this cell, we can ask, "Which value of f_c is valid?" "Is it f_c^* or $\hat{f}_c$?" The answer is, both are valid and hence

$$\hat{f}_c = f_c^* ,$$

for a boundary cell c.

For a simplified illustration let $\alpha = 0 = \beta$, so that

$$\mu_c (f_c^*, t_c^*) = \tilde{\mu},$$

and

$$\lambda_c (\hat{f}_c, t_c^*) \eta_c = \tilde{\mu},$$

which implies that

$$\lambda_c (f_c^*) + f_c^* \partial_f \lambda_c^* = \lambda_c (\hat{f}_c)$$

$$\tilde{=} \lambda_c(f_c^*) + (\hat{f}_c - f_c^*) \partial_f \lambda_c^* ,$$

and consequently, we must have either

$$\hat{f}_c \tilde{=} 2 f_c^*, \text{ or } \partial_f \lambda_c (f_c^*) \tilde{=} 0.$$

If we require $\hat{f}_c = f_c^*$, then $\partial_f \lambda_c (f_c^*) \tilde{=} 0$, which implies a no shading or blocking condition. This is the expected result, however a more accurate discussion can be made using the monotone behavior of λ_c and μ_c. See figure 4.

Proceeding to the final step of the optimization procedure, we again form δE_T and eliminate $\partial_t \lambda_c$.

$$\delta E_T \tilde{=} \sum_c (\mu_c \phi_c \delta f_c + \lambda_c f_c \eta_c \delta \phi_c) A_L S_o.$$

Using the above solutions, we have

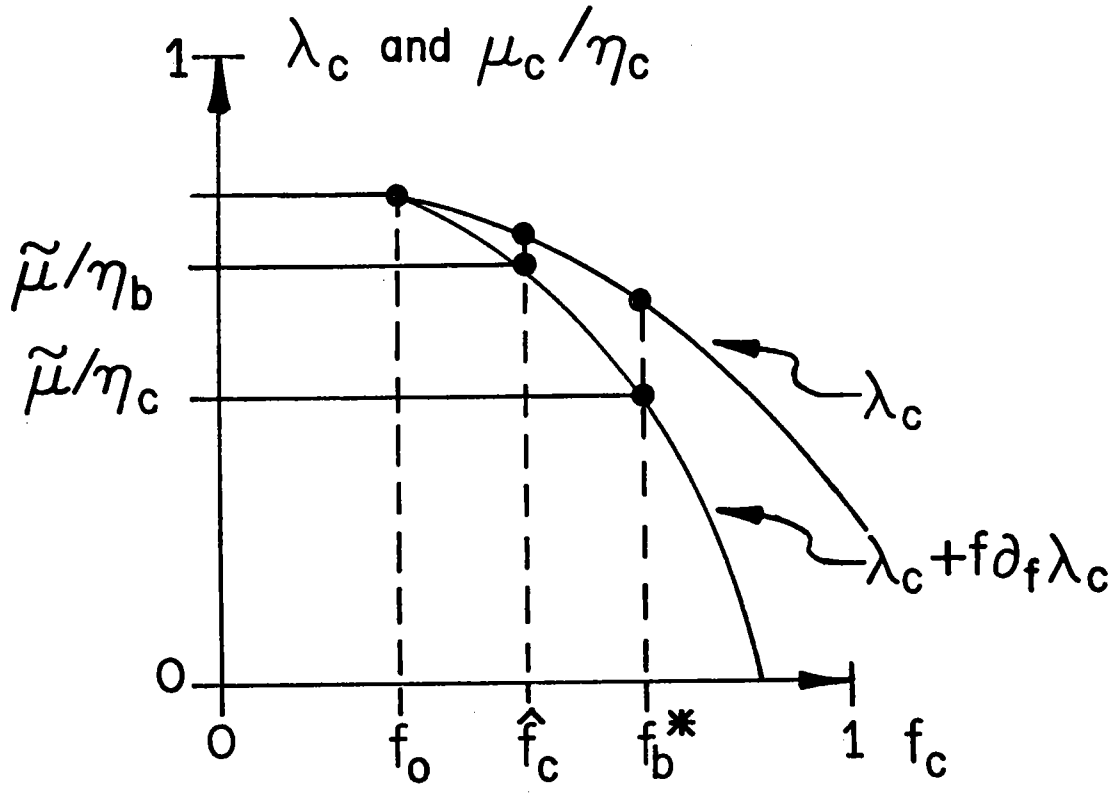

Figure 4. Cell performance versus the Ground Coverage Fraction. f_o is the maximum ground coverage possible with zero shading and blocking. f_c^* an optimum value for an interior cell. Decreasing η_c causes f_c^* to decrease. The boundary occurs when f_c^* meets $\hat{f}_b$. Notice that increasing costs α and β increase $\hat{f}_b$ so that the boundary occurs for larger η_b. For a given ground coverage f_c, the collector efficiency λ_c exceeds $\tilde{\mu}/\eta_c$.

$$\delta E_T = \tilde{\nu} \sum_c [\phi_c (1 + \tfrac{1}{2}\beta f_c^{-\frac{1}{2}})\ \delta f_c + (f_c + \alpha + \beta f_c^{\frac{1}{2}})\ \delta\phi_c]\ A_L S_o$$

$$= \tilde{\nu}\ (C_H A_L)^{-1}\ \delta C_s A_L S_o,$$

so that

$$\delta E_T / \delta C_s = \tilde{\nu}\ S_o / C_H.$$

A variation of the figure of merit gives

$$\delta F = 0 = \delta C_s / E_T - C_s \delta E_T / E_T^2,$$

so that

$$\delta E_T / \delta C_s = E_T / C_s = \tilde{\nu} S_o / C_H = 1/F,$$

and therefore,

$$\tilde{\nu} = C_H\ (S_o F)^{-1},$$

which is the same as the previous result with $\tilde{\mu} \rightarrow \tilde{\nu}$.

5. The Effect of Receiver Losses

Up to this point we have ignored losses due to reflectivity, absorptivity, convection, and reradiation. These losses can be included by expressing the total receiver output energy E_o in terms of the previously defined total energy E_T. We can write

$$E_o = \hat{\alpha}\hat{\rho}\ E_T - E_A$$

where

$$\hat{\alpha} = 0.95$$

for the absorptivity of the black receiver surface. McDonnell-Douglas currently assumes a commercial PYROMARK high temperature black.

$$\hat{\rho} = 0.91,$$

for the net reflectivity of the current McDonnell-Douglas heliostat, however a better operational value would be 10% less due to dust.

$$E_A = H_A P_L$$
$$= 3376 \text{ (HRS/YR)} \times 36.89 \text{ (MW)} = 124{,}536 \text{ (MWH}_t\text{/YR)},$$

for the estimated annual losses due to convection and reradiation for a 24 panel cylindrical receiver. The LOSS estimate depends on an assumed mean wind and the operating temperature.

The figure of merit must be redefined as

$$F = C_s/E_o$$

so that

$$\delta F = \delta C_s/E_o - \delta E_o C_s/E_o^2$$

where

$$\delta E_o = \hat{\alpha}\hat{\rho}\ \delta E_T.$$

Consequently, the first step in the optimization procedure is unchanged. (i.e. $\delta F = 0 = \delta C_s$ implies $\delta E_T = 0$ as previously). However in the second step of the optimization, $\delta F = 0$ now gives

$$\delta E_T/\delta C_s = (\hat{\alpha}\hat{\rho})^{-1}\ \delta E_o/\delta C_s = (\hat{\alpha}\hat{\rho})^{-1}\ E_o/C_s$$
$$= (\hat{\alpha}\hat{\rho}\ F)^{-1} = \tilde{\nu}\ S_o/C_H,$$

and therefore

$$\tilde{\nu} = C_H(\hat{\alpha}\hat{\rho}\ S_o F)^{-1} = C_H\ (\hat{S}_o F)^{-1},$$

where

$$\hat{S}_o = \hat{\alpha}\ \hat{\rho}\ S_o,$$

is the effective annual insolation for the central receiver system in MWH/m^2. $\hat{S}_o$ might also include factors for the expected percent of possible insolation and percent of annual usage.

It is also worth noticing that $\tilde{\nu}$ is almost independent of $\hat{\alpha}\hat{\rho}$. Substituting the definition of F into the expression for $\tilde{\nu}$, gives

$$\tilde{\nu} = C_H[\hat{\alpha}\hat{\rho}\ S_o C_s/(\hat{\alpha}\hat{\rho}E_T - E_A)]^{-1}$$

$$= (E_T - E_A/\hat{\alpha}\hat{\rho})\ C_H/(S_o C_s)$$

which becomes independent of $\hat{\alpha}\hat{\rho}$ as $E_A \to 0$.

6. Conclusions

The TRIM subroutine provides a preliminary estimate of the figure of merit which is based on a preliminary cell geometry and a sorting procedure which selects the brightest cells first. The cell sort allows us to build a collector field with an optimum selection of cells (assuming the preliminary cell geometry). The resulting value of the figure of merit F, allows us to calculate $\tilde{\mu}$, or $\tilde{\nu}$, and $\tilde{E}_L$ which are required by the RCELL optimization program. RCELL is not very sensitive to errors in F. After converging the solution for $\{(x_c,y_c)\}$ or equivalently $\{(f_c,t_c)\}$ we return to performance estimating programs as shown in the DATA FLOW SCHEMATIC.

Figure 5 shows the optimum trim resulting from the cell sort. It also shows the occurance of mechanical constraints in the near tower

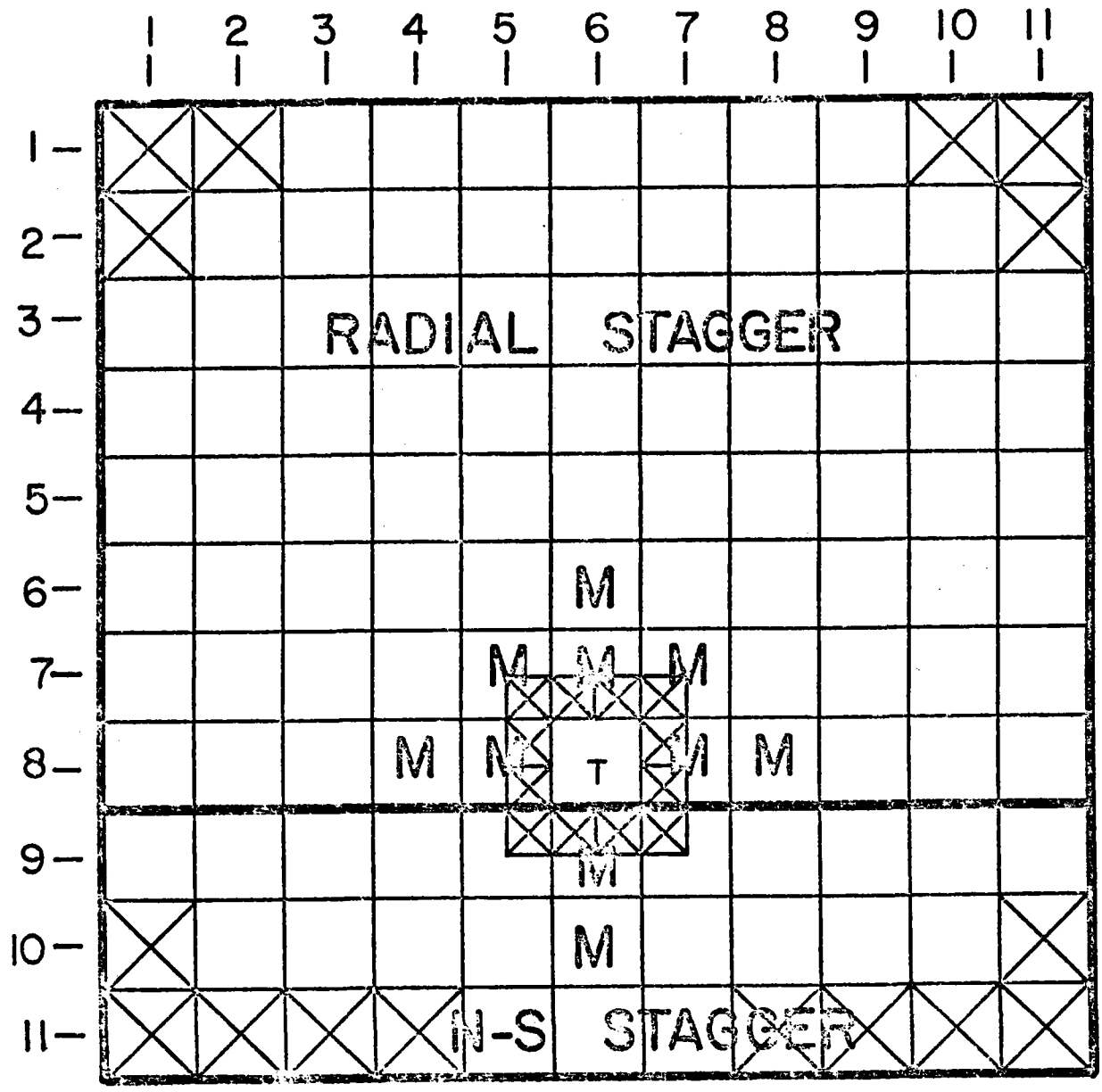

Figure 5. Optimum Trim for 100 MW Commercial Model. x marks cells deleted by TRIM. T marks the tower cell. M marks cells restricted by mechanical limits. Rows (1-8) contain a radial stagger. Rows (9-11) contain a N-S stagger.

regions. Notice the field is staggered throughout. We have N-S stagger in the southern field but a radial stagger can be used universally. This is a 360^{o} field which is suited to cylindrical receiver. Figures 6 and 7 give the heliostat spacing coordinates as a function of tower elevation angle. Figures 8 and 9 give the resulting diurnal power curves for the 100 MWe plant and the scale model pilot plant, respectively.

A previous effort to achieve an optimum collector field by the cell method is given in Reference [2]. The optimum collector field was also discussed by J. D. Hankins, Reference [3], who used a continuum approach.

Acknowledgements

This paper was prepared with the support of the US Energy Research and Development Administration Grant Nos. E(04-3)-1188 and EG-76-G-05-5178. However, any opinions, findings, conclusions, or recommendations expressed herein are those of the authors and do not necessarily reflect the views of ERDA. The authors have enjoyed working with the McDonnell-Douglas Corp and express their gratitude to the ERDA-Solar Thermal Work Group for having made it possible.

STMPO
#364

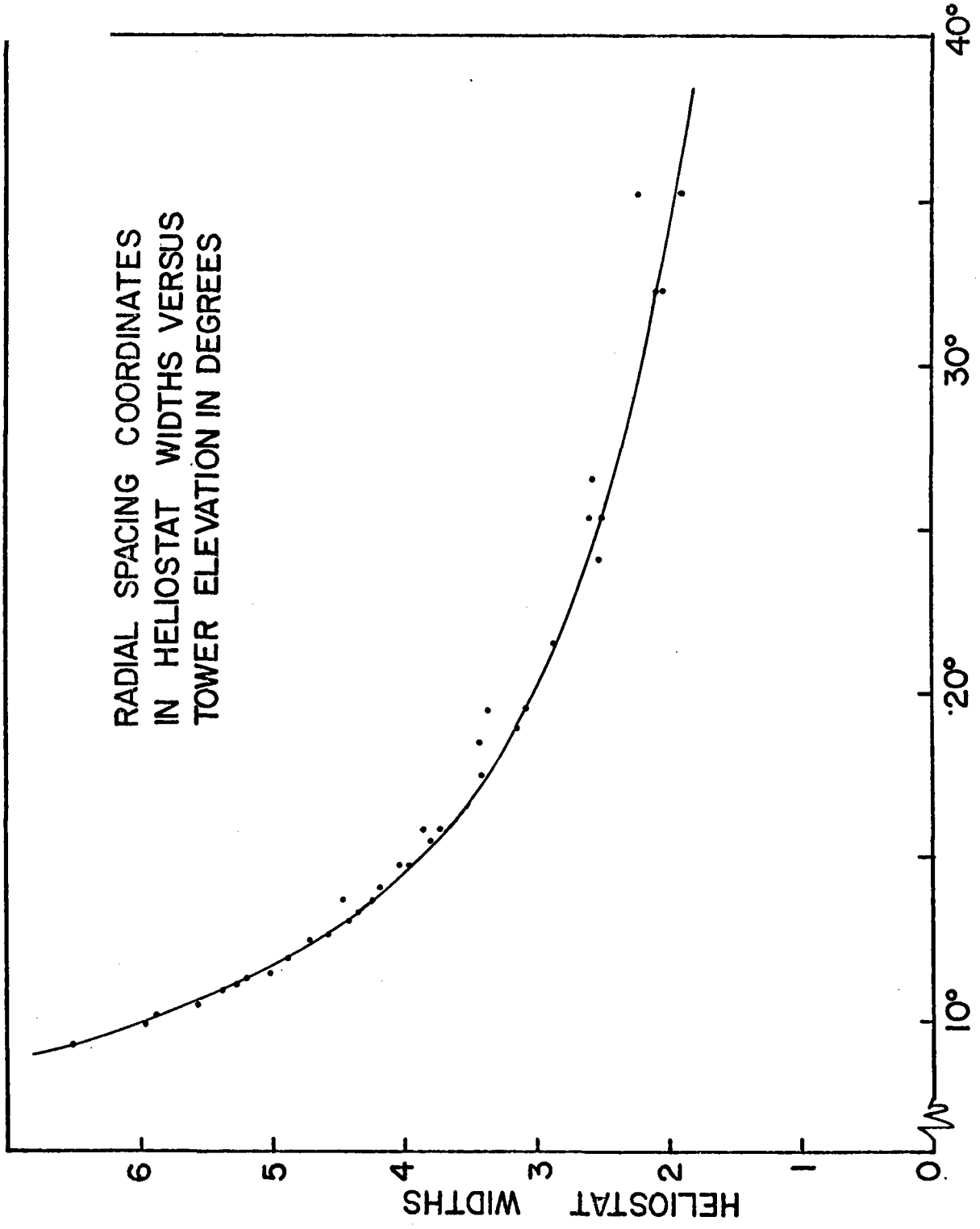

Figure 6. Radial Spacing Coordinates in Heliostat Widths versus Tower Elevation in Degrees.

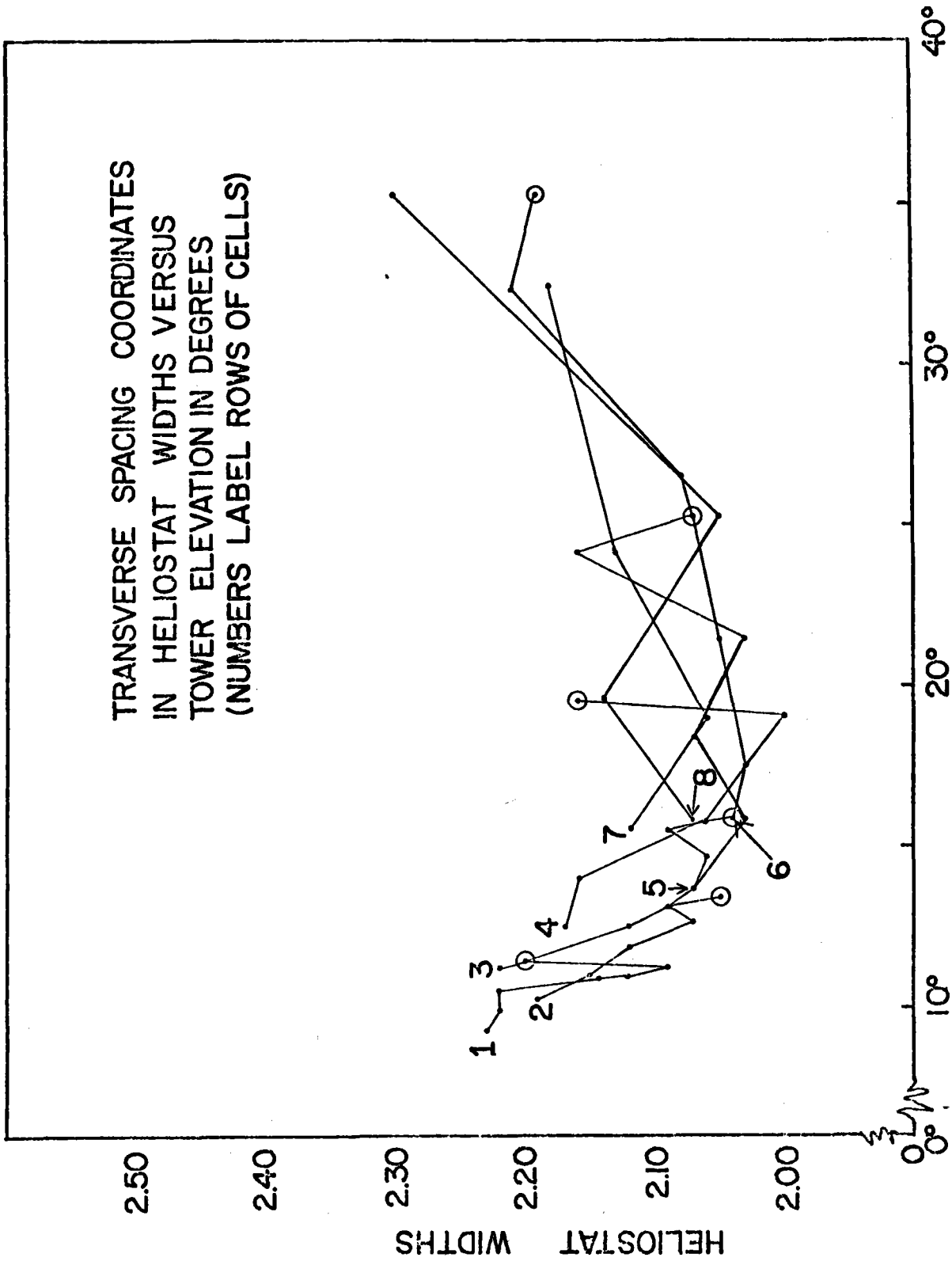

Figure 7. Transverse Spacing Coordinates in Heliostat Width versus Tower Elevations in Degrees. Note vertical scales expanded.

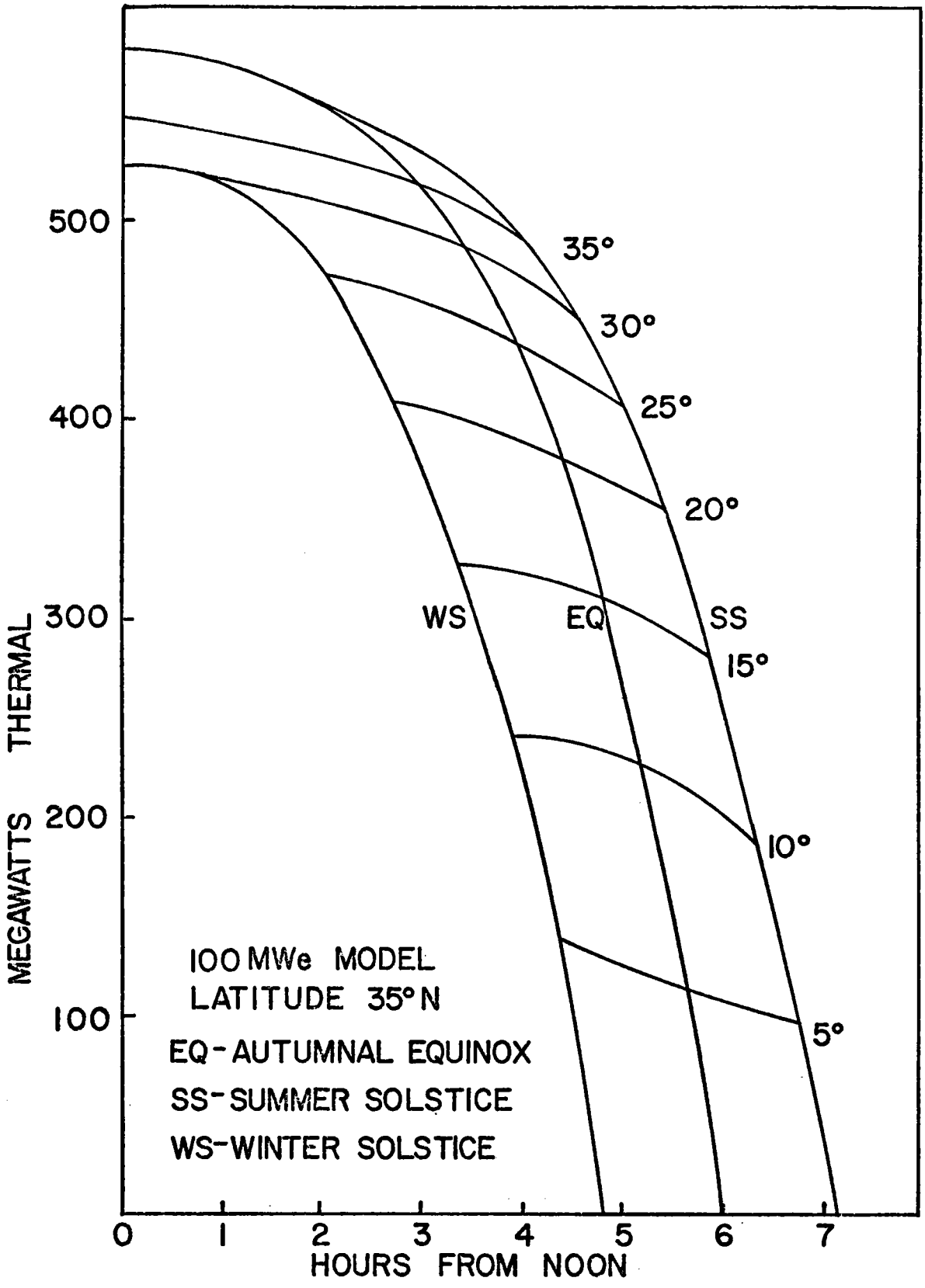

Figure 8. Diurnal Power Curves for 100 MWe Model showing power in MWt versus HRS and solar elevation in degrees. Based on nearest neighbors only.

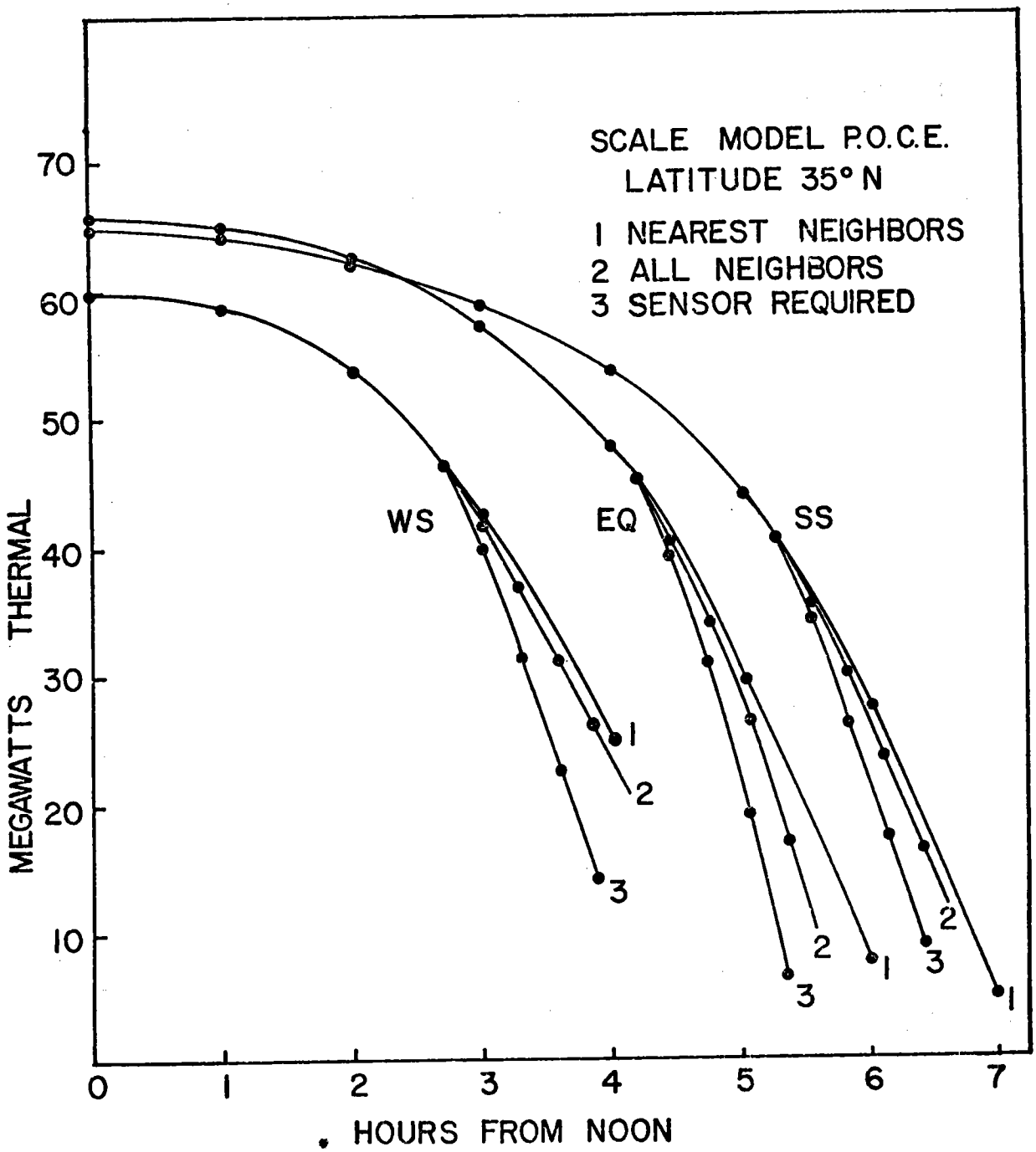

Figure 9. Diurnal Power Curves for Scale Model Pilot Plant showing startup phenomena which depend on sensor acquisition and remote neighbor interference. Losses discussed in section 5 are not included here or in Figure 8.

Table 2 Cost of Thermal Energy for Three Different Heliostat Costs

HELIOSTAT COST ($/M^2)	FIGURE OF MERIT ($/MWH/YR)	EQ. NOON ($/KW$_T$)	AVERAGE ($/KW$_T$)
66	44.6	144	151
83	52.6	169	178
100	60.7	195	205
C_H	F	F_{EQ}	F_{AV}

$F = C_S/E_T$

$F_{EQ} = C_S/P_{EQ} = (E_T/P_{EQ})F = 3.218F$

$F_{AV} = C_S/P_{AV} = (E_T/P_{AV})F = (H_{YR}/10^3)F = 3.377F$

H_{YR} = 3377 HRS/YR above 15^o Elevation

E_T/P_{EQ} = 1630 MWH/506.5 MW = 3.218

REFERENCES

1. L. L. Vant-Hull and A. F. Hildebrandt, Solar Thermal Power System Based on Optical Transmission, Solar Energy 18, 31 (1976).
2. M. S. Abdel-Monem, A. F. Hildebrandt, F. W. Lipps, and L. L. Vant-Hull, A. New Method for Collector Field Optimization, Heliotechnique and Development 1, 372 (1976), and also Proceedings of the COMPLES International Conference, Dhahran, Saudi Arabia, Nov. 2-6, 1975.
3. J. D. Hankins, Cost-Optimal Deployment of Mirrors Associated with a High-Temperature Solar Energy System, ISES paper at U. S. Section Annual Meeting, Aug. 19-23, 1974 at Colorado State University, Ft. Collins, Colorado.

☆U.S. GOVERNMENT PRINTING OFFICE: 1978-740-306/ 9355 REGION NO. 4